frontiers | Research Topics

Gut microbial response to host metabolic phenotypes, volume II

Edited by
Jie Yin, Yong Su and Hui Han

Published in
Frontiers in Nutrition

ISSN 1664-8714
ISBN 978-2-83251-603-4
DOI 10.3389/978-2-83251-603-4

About Frontiers

Frontiers is more than just an open access publisher of scholarly articles: it is a pioneering approach to the world of academia, radically improving the way scholarly research is managed. The grand vision of Frontiers is a world where all people have an equal opportunity to seek, share and generate knowledge. Frontiers provides immediate and permanent online open access to all its publications, but this alone is not enough to realize our grand goals.

Frontiers journal series

The Frontiers journal series is a multi-tier and interdisciplinary set of open-access, online journals, promising a paradigm shift from the current review, selection and dissemination processes in academic publishing. All Frontiers journals are driven by researchers for researchers; therefore, they constitute a service to the scholarly community. At the same time, the *Frontiers journal series* operates on a revolutionary invention, the tiered publishing system, initially addressing specific communities of scholars, and gradually climbing up to broader public understanding, thus serving the interests of the lay society, too.

Dedication to quality

Each Frontiers article is a landmark of the highest quality, thanks to genuinely collaborative interactions between authors and review editors, who include some of the world's best academicians. Research must be certified by peers before entering a stream of knowledge that may eventually reach the public - and shape society; therefore, Frontiers only applies the most rigorous and unbiased reviews. Frontiers revolutionizes research publishing by freely delivering the most outstanding research, evaluated with no bias from both the academic and social point of view. By applying the most advanced information technologies, Frontiers is catapulting scholarly publishing into a new generation.

What are Frontiers Research Topics?

Frontiers Research Topics are very popular trademarks of the *Frontiers journals series*: they are collections of at least ten articles, all centered on a particular subject. With their unique mix of varied contributions from Original Research to Review Articles, Frontiers Research Topics unify the most influential researchers, the latest key findings and historical advances in a hot research area.

Find out more on how to host your own Frontiers Research Topic or contribute to one as an author by contacting the Frontiers editorial office: frontiersin.org/about/contact

Gut microbial response to host metabolic phenotypes, volume II

Topic editors

Jie Yin — Hunan Agricultural University, China

Yong Su — Nanjing Agricultural University, China

Hui Han — Chinese Academy of Sciences (CAS), China

Citation

Yin, J., Su, Y., Han, H., eds. (2023). *Gut microbial response to host metabolic phenotypes, volume II*. Lausanne: Frontiers Media SA.

doi: 10.3389/978-2-83251-603-4

Table of contents

frontiers | Frontiers in Nutrition

TYPE Editorial
PUBLISHED 03 February 2023
DOI 10.3389/fnut.2023.1136510

OPEN ACCESS

EDITED AND REVIEWED BY
Christophe Lacroix,
ETH Zürich, Switzerland

*CORRESPONDENCE
Yong Su
✉ yong.su@njau.edu.cn

SPECIALTY SECTION
This article was submitted to Nutrition and Microbes, a section of the journal Frontiers in Nutrition

RECEIVED 03 January 2023
ACCEPTED 23 January 2023
PUBLISHED 03 February 2023

CITATION
Han H, Su Y and Yin J (2023) Editorial: Gut microbial response to host metabolic phenotypes, volume II. *Front. Nutr.* 10:1136510. doi: 10.3389/fnut.2023.1136510

Editorial: Gut microbial response to host metabolic phenotypes, volume II

Hui Han[1,2], Yong Su[1]* and Jie Yin[3]

[1]College of Animal Science and Technology, Nanjing Agricultural University, Nanjing, China, [2]State Key Laboratory of Animal Nutrition, Institute of Animal Science, Chinese Academy of Agricultural Sciences, Beijing, China, [3]College of Animal Science and Technology, Hunan Agricultural University, Changsha, China

KEYWORDS

gut microbiota, microbial response, host, metabolism, phenotypes

Editorial on the Research Topic
Gut microbial response to host metabolic phenotypes, volume II

Numerous studies have emphasized the importance of gut microbiota in modulating various physiological functions, including metabolism, inflammation, and neural development (1–3). Gut microbiota can not only affect the digestion and absorption of nutrients but also produce numerous metabolic bioactive signaling molecules to regulate host metabolism (4–6). A comprehensive understanding of the interaction of gut microbiota and host metabolism will create opportunities for new therapeutic approaches to the treatment of metabolic disorders.

It has been well-established that the gut microbiota is sensitive to dietary components, especially carbohydrates, fats, and proteins. In this Research Topic, dietary protein (Wang, Peng et al.) and starch (Wang, Zhou et al.) have been reported to shape microbial composition. Additionally, Hou et al. thoroughly discussed the role of gut microbiota in host metabolism, including carbohydrate, lipid, amino acid, and nucleic acid metabolism. These studies systematically interrogated the impact of diets with varying protein and starch content and illustrated the complex association between diets, gut microbiota and host metabolism. Moreover, studies have also revealed the diversity and characteristics of gut microbiota along the gastrointestinal tract (GIT) by using pig as a physiological relevant model of human metabolism. For example, Song et al. found that microbial richness and diversity gradually increased from the small to large intestine. Moreover, the bacterial composition was different between the small and large intestine, which might due to differing physiological functions as required by the host. Like bacteria, gut fungi is also an important part of the intestinal microbiota that interacts with host metabolism (7). However, studies on characterizing the gut fungal diversity and composition along the whole GIT are limited. In this Research Topic, Li et al. reported that the difference in the gut fungal diversity and composition along the GIT sections was smaller than that between batches in pigs.

Alterations of gut microbiota have been implicated in the pathogenesis of metabolic disorders. In this Research Topic, Dong et al. used metagenomic and metabolic methods to investigate the changes in gut microbiota (including bacteria, bacteriophage, and archaea) in mice with obesity and atherosclerosis. Long et al. gave a comprehensive overview regarding the association between gut microbiota-derived metabolites and pathogenesis of ischemic stroke. Building on the complex association between gut microbiota and metabolic disorders, studies have aimed to evaluate the causality of gut microbiota in host metabolism by using antibiotics and fecal microbiota transplantation (FMT). However, the effectiveness and impacts of FMT on specific bacterial strains remain unclear. Tan et al. showed that an antibiotic cocktail containing vancomycin, ampicillin, neomycin, and metronidazole in drinking water effectively eliminated

the microbial strains belonging to *Bacteroidets*, *Actinobacteria*, and *Verrucoomicrobia*, which can be restored by transplantation of microbiota from healthy control mice.

Laboratory and clinical studies have highlighted the potential to use interventions related to gut microbiota for treating metabolic disorders (8–10). For example, probiotics containing either single or multiple microorganism strains (especially strains of genera *Lactobacilli* and *Bifidobacteria*) have proven to be effective therapeutic approaches for alleviating metabolic disorders (11–13). Similarly, in this Research Topic, studies showed that some strains of *Lactobacillus* applied in asthma (Wang W. et al.) and obesity (Ma Y. et al.) were able to modify the gut microbial composition and exhibit beneficial effects on host. Additionally, Guo et al. found that dietary intervention with oropharyngeal probiotic ENT-K12 effectively reduced episodes of upper respiratory tract infections in children with recurrent respiratory tract infections during high peak season. Besides, dietary prebiotics have been demonstrated to alter gut microbiota and impart favorable metabolic benefits. In this respect, studies in this Research Topic reported that extracts from bearberry (Ma J. et al.), dark tea (Wang C. et al.), Artemisia argyi leaf (Wang, Ma et al.), Aurantii Fructus Immaturus (Chen et al.), and cannabis (Gong et al.) were able to positively alter gut microbiota and improve metabolism and inflammation. These studies may provide novel therapeutic strategies for treating metabolic diseases.

Overall, studies in this Research Topic promoted the understating of the role of gut microbiota in host metabolism, although the precise mechanism was not fully clear. Furthermore, data from the above mentioned studies offered microbiome-based strategies for alleviating metabolic diseases. However, additional studies are necessary to further shed light on the complex interaction between gut microbiota and host metabolism in order to find opportunities to alleviate metabolism-related diseases. Additionally, the evidence of concept generated in animal models need to be further translated to clinical setting.

Author contributions

All authors listed have made a substantial, direct, and intellectual contribution to the work and approved it for publication.

Funding

This study was supported by grants from the National Natural Science Foundation of China (32072688, 32272891, and 31872362).

Acknowledgments

We would like to thank all authors for their papers and the reviewers for the painstaking care taken in helping improve the clarity of the manuscript.

Conflict of interest

The authors declare that the research was conducted in the absence of any commercial or financial relationships that could be construed as a potential conflict of interest.

Publisher's note

References

1. Chakaroun RM, Olsson LM, Bäckhed F. The potential of tailoring the gut microbiome to prevent and treat cardiometabolic disease. *Nat Rev Cardiol.* (2022). doi: 10.1038/s41569-022-00771-0. [Epub ahead of print].

2. Cao Y, Oh J, Xue M, Huh WJ, Wang J, Gonzalez-Hernandez JA, et al. Commensal microbiota from patients with inflammatory bowel disease produce genotoxic metabolites. *Science.* (2022) 378:eabm3233. doi: 10.1126/science.abm3233

3. Dohnalová L, Lundgren P, Carty JRE, Goldstein N, Wenski SL, Nanudorn P, et al. A microbiome-dependent gut-brain pathway regulates motivation for exercise. *Nature.* (2022) 612:739–47. doi: 10.1038/s41586-022-05525-z

4. Cox TO, Lundgren P, Nath K, Thaiss CA. Metabolic control by the microbiome. *Genome Med.* (2022) 14:80. doi: 10.1186/s13073-022-01092-0

5. Han H, Jiang Y, Wang M, Melaku M, Liu L, Zhao Y, et al. Intestinal dysbiosis in nonalcoholic fatty liver disease (Nafld): focusing on the gut-liver axis. *Crit Rev Food Sci Nutr.* (2021) 18:1–18. doi: 10.1080/10408398.2021.1966738

6. Han H, Yi B, Zhong R, Wang M, Zhang S, Ma J, et al. From gut microbiota to host appetite: gut microbiota-derived metabolites as key regulators. *Microbiome.* (2021) 9:162. doi: 10.1186/s40168-021-01093-y

7. Guégan M, Martin E, Tran Van V, Fel B, Hay AE, Simon L, et al. Mosquito sex and mycobiota contribute to fructose metabolism in the Asian Tiger Mosquito Aedes Albopictus. *Microbiome.* (2022) 10:138. doi: 10.1186/s40168-022-01325-9

8. Liu Y, Zhong X, Lin S, Xu H, Liang X, Wang Y, et al. *Limosilactobacillus reuteri* and Caffeoylquinic Acid synergistically promote adipose browning and ameliorate obesity-associated disorders. *Microbiome.* (2022) 10:226. doi: 10.1186/s40168-022-01430-9

9. Benítez-Páez A, Hartstra AV, Nieuwdorp M, Sanz Y. Species- and strain-level assessment using rrn long-amplicons suggests donor's influence on gut microbial transference via fecal transplants in metabolic syndrome subjects. *Gut Microbes.* (2022) 14:2078621. doi: 10.1080/19490976.2022.2078621

10. Mocanu V, Zhang Z, Deehan EC, Kao DH, Hotte N, Karmali S, et al. Fecal microbial transplantation and fiber supplementation in patients with severe obesity and metabolic syndrome: a randomized double-blind, placebo-controlled phase 2 trial. *Nat Med.* (2021) 27:1272–9. doi: 10.1038/s41591-021-01399-2

11. Liang C, Zhou XH, Gong PM, Niu HY Lyu LZ, Wu YF, et al. *Lactiplantibacillus plantarum* H-87 prevents high-fat diet-induced obesity by regulating bile acid metabolism in C57bl/6j mice. *Food Funct.* (2021) 12:4315–24. doi: 10.1039/D1FO00260K

12. Rodrigues RR, Gurung M, Li Z, García-Jaramillo M, Greer R, Gaulke C, et al. Transkingdom interactions between lactobacilli and hepatic mitochondria attenuate western diet-induced diabetes. *Nat Commun.* (2021) 12:101. doi: 10.1038/s41467-020-20313-x

13. López-Moreno A, Suárez A, Avanzi C, Monteoliva-Sánchez M, Aguilera M. Probiotic strains and intervention total doses for modulating obesity-related microbiota dysbiosis: a systematic review and meta-analysis. *Nutrients.* (2020) 12:1921. doi: 10.3390/nu12071921

frontiers | Frontiers in Nutrition

CLINICAL TRIAL
published: 10 May 2022
doi: 10.3389/fnut.2022.900448

Oropharyngeal Probiotic ENT-K12 as an Effective Dietary Intervention for Children With Recurrent Respiratory Tract Infections During Cold Season

Hongyan Guo[1†], Xiaochen Xiang[2†], Xuan Lin[3], Qiang Wang[2*], Si Qin[4], Xinyan Lu[1], Jiawei Xu[1], Ying Fang[2], Yang Liu[2], Jing Cui[2] and Zhi Li[2]*

[1] Medical College, Wuhan University of Science and Technology, Wuhan, China, [2] Institute of Infection, Immunology and Tumor Microenvironment, Hubei Province Key Laboratory of Occupational Hazard Identification and Control, Medical College, Wuhan University of Science and Technology, Wuhan, China, [3] Department of Endocrinology, CR & WISCO General Hospital Affiliated to Wuhan University of Science and Technology, Wuhan, China, [4] College of Food Science and Technology, Hunan Agricultural University, Changsha, China

OPEN ACCESS

Edited by:
Hui Han,
Chinese Academy of Sciences (CAS), China

Reviewed by:
Si Jin,
Huazhong University of Science and Technology, China
Shufang Xu,
Wuhan Central Hospital, China

***Correspondence:**
Xuan Lin
854964946@qq.com
Qiang Wang
wangqiang@wust.edu.cn

[†] These authors share first authorship

Specialty section:
This article was submitted to Nutrition and Microbes, a section of the journal Frontiers in Nutrition

Received: 20 March 2022
Accepted: 28 March 2022
Published: 10 May 2022

Citation:
Guo H, Xiang X, Lin X, Wang Q, Qin S, Lu X, Xu J, Fang Y, Liu Y, Cui J and Li Z (2022) Oropharyngeal Probiotic ENT-K12 as an Effective Dietary Intervention for Children With Recurrent Respiratory Tract Infections During Cold Season. Front. Nutr. 9:900448. doi: 10.3389/fnut.2022.900448

Recurrent respiratory tract infections (RRTi) cause a high burden of disease and lead to negative impact on quality of life, frequent school/work absenteeism, and doctor visits, which remain a great challenge to pediatricians because RRTi can increase the risk of various complications including antibiotic overuse and resistance, which is one of the biggest threats to global health, and there is no confirmed effective treatment. In this study, we aimed to assess the clinical efficacy and safety of oropharyngeal probiotic ENT-K12 as a dietary intervention or a complementary treatment along with standard medical treatment during acute respiratory infections among children with RRTi during cold season. The results of this study show that when comparing to practicing of standard medical treatment only, the complementary intake of oropharyngeal probiotic ENT-K12 can effectively reduce episodes of both acute and RRTi in school children, shorten the course of respiratory symptoms onset, reduce the use of antibiotics and antiviral drugs, and reduce the absence days from both children's school and parents' work. Using oropharyngeal probiotics as a complementary dietary intervention to stabilize oropharyngeal microflora, specifically inhibiting respiratory pathogens and enhancing host immunity, could possibly be a promising approach to reduce RRTi burden and combating antibiotic resistance in long term, more clinical studies will be needed to further confirm the clinical practicing guide to ensure its clinical benefit.

Methods: A total of 100 susceptible children with RRTi aged 3–10 years, living in Wuhan, China, were selected. They were randomized to the probiotic group and control group at the beginning of the trial during the cold season. Fifty children in the probiotic group took oropharyngeal probiotic ENT-K12 for 30 days, along with standard medical treatment when there was an onset of respiratory symptoms and medical treatment was needed, and fifty children in the control group did not take oropharyngeal probiotics but only had standard medical treatment when there was an onset of respiratory symptoms and medical treatment was needed. Patients were followed up for 30 days during the cold season. The primary objective of this study is to assess the complementary dietary interventional efficacy of oropharyngeal probiotic ENT-K12 on episodes of respiratory

tract infections during the cold season, and the secondary objective is to assess the interventional efficacy of oropharyngeal probiotic on days of respiratory symptoms onset, using antiviral drugs, antibiotics, and antipyretics, days of children absent from school, and days of parents absent from work, as well as to confirm tolerability and safety judged by adverse event reporting.

Results: There were 47 children, 22 male and 25 female children, with an average age of 5.71 years (SD = 1.99) in the probiotic group finishing the study, and 50 children, 32 male and 18 female children, in the control group with an average age of 6.12 years (SD = 1.98) finishing the study. During the 30-day period of oropharyngeal probiotic intake, children in the probiotic group totally had 7 episodes of upper respiratory tract infections, while children in the control group totally had 17 episodes of upper respiratory tract infections, indicating that the incidence of upper respiratory tract infection in the probiotic group (14.89%) was significantly lower than that in the control group (34.00%) during the intervention period. The days of using antibiotics and antiviral drugs in the probiotic group were significantly lower than that in the control group, and the course of respiratory symptoms onset was shorter and more moderate in the probiotic group than that in the control group; in addition, compared with the control group, both the days of children absent from school and parents' absence from work in the probiotic group were significantly lower. Children treated with oropharyngeal probiotic ENT-K12 had excellent tolerability with no side effects reported, hence confirmed safety of applying oropharyngeal probiotic ENT-K12 as a prophylactic use or an effective dietary intervention along with standard medication during respiratory infections onset.

Conclusion: Intake of oropharyngeal probiotic ENT-K12 as a dietary intervention can effectively reduce episodes of upper respiratory tract infections in school children with RRTi during high peak season, reduce the days of using antibiotics and antiviral drugs, and reduce children's sick leave days, parents' absence days from work, and shorten the course of respiratory infections; the safety of oropharyngeal probiotic ENT-K12 has been confirmed with no side effects reported, excellent tolerability, and easy acceptance. Notably, this study opens up a new research idea in the field of microbe promoting human health by supplying direct proof to support its efficiency and safety.

Keywords: *Streptococcus salivarius* subsp. *thermophilus* ENT-K12, recurrent respiratory tract infections, oropharyngeal probiotics, children, dietary intervention

INTRODUCTION

The oropharyngeal microflora acts as a barrier against colonization of potentially respiratory pathogens and against overgrowth of already present opportunistic respiratory pathogens. A balanced and stabilized oropharyngeal microflora can help control the growth of opportunistic respiratory pathogens and coordinate with host immune system impacting human health and diseases; in contrast, host colonization with respiratory pathogens and the formation of pathogenic biofilms during childhood cause recurrent respiratory tract infections (RRTi) and chronic inflammations such as wheezing and asthma that are difficult to eradicate in later life (1), and the increased otopathogen abundance and decreased oropharyngeal/nasopharyngeal bacterial diversity that significant increased hazard ratios for allergic diseases are associated with commonly prescribed multiple classes of antibiotics and viral RRTi during infancy (2, 3), a cross-sectional survey conducted in Beijing, China, with 7,222 preschool-aged children revealed that asthma, allergy, initial use of antibiotics before 6 months, and breast feeding might exert a graded, dose-dependent effect on RRTi susceptibility, especially the significant odds of RRTi were 8.31 for asthma, which plays a leading role (4). Compared with healthy adults, infants and young children are at an increased risk of RRTi due to the relative immaturity of their immune system. According to a cohort study, children with RRTi documented a median of 113 days with respiratory symptoms, 9.6 acute respiratory infection episodes, and 6 physician visits for respiratory infection per child per year; early nasopharyngeal colonization with *Streptococcus pneumoniae*

was common in children who later developed RRTi, while asymptomatic rhinovirus infections at young age in children with recurrent infections may due to aberrant innate immune responses. Exposure to antibiotic treatment early in life may have a lasting impact on the composition of the microbiota leading to permanent replacement by resistant pathogens. The clinical sequelae of RRTi can result in long-term complications and prolonged antibiotic regimens prescribed and further contribute to the disease economic burden, which is projected to increase over the next 20 years, highlighting the importance of safe and effective prevention strategies for reducing RRTi prevalence in children (5, 6).

Pooled prevalence of Group A *Streptococcus* from pharyngeal specimens was 37% in children who present with sore throat and 12% in asymptomatic children (7), in China, *S. pneumoniae* colonization was found in 21.6% in children aged under 5 years with fever and flu-like symptoms, of which the frequency is positively correlated with the number of respiratory pathogens detected providing a strong evidence against empiric antibiotic use for treating respiratory infections (8). Comparing respiratory virome and serum cytokine profiles between children diagnosed with acute respiratory tract infections also indicates that respiratory microbe homeostasis and specific cytokines are associated with the onset of RRTi over time (9). In our experience, pediatric outpatient visits caused by RRTi are generally $\leq$10 years of age, and most are treated more frequently with antibiotics and corticosteroids to eliminate acute-onset respiratory symptoms because there is no international consensus about the best effective and safe prophylactic treatment for pediatric RRTi, even if systematic review of the efficacy and safety of immunotherapy for RRTi were reported (10, 11).

Recently, the beneficial aspects of bacteriocins, a set of miscellaneous peptide-based bacterium killers produced by microbiota commensals, have been considered as a backup plan for traditional antibiotic treatments to cure multiresistant infections and finely reshape the endogenous microbiota for prophylaxis use of RRTi (12). Bacteriocins, salivaricin A2, and salivaricin B specifically produced by oropharyngeal probiotic ENT-K12 have been reported to contribute bactericidal activities to various respiratory pathogens, including most *Streptococcus pyogenes* and *Micrococcus luteus* strains (13); the bactericidal mode of action of salivaricin B is to interfere with the cell wall peptidoglycan biosynthesis of respiratory pathogens resulting in the reduction of its cell wall thickness together with changes to cytoplasmic membrane integrity, which kill 40% of *S. pyogenes* cells after 30 min and 90% in $<$3 h of exposure; the irreversible defection of the cell envelopes leads to a failure to generate daughter cells indicating a rapid killing activity; yet no salivaricin B-resistant *S. pyogenes* strains have been reported previously, and so far no significant resistance to salivaricin B was reported (14, 15). The recent computing study has demonstrated that salivaricin B showed predicted binding affinity toward the ACE2, the binding domain of severe acute respiratory syndrome coronavirus 2 (SARS-CoV-2), with potential activity against the SARS-CoV-2 beta variant (16). The mode of action of bacteriocins is remarkably different from conventional antibiotics, and the machinery used by pathogens to develop resistance should be different. With this in mind, bacteriocins may be considered as new-age infection fighters (17).

A study using real-time PCR to monitor the persistence of oropharyngeal probiotic ENT-K12 administration in oral cavity indicates that within few days of administration, ENT-K12 typically colonizes various sites of oropharyngeal mucosal membranes including the tongue, buccal, and both sides of pharynx; its simulated bacteriocin can be detected in saliva (18), plus that the megaplasmid encoding salivaricin A2 and salivaricin B appear to be transmissible between *S. salivarius* strains with the megaplasmid having been observed to move to another *S. salivarius* strain in the oral cavity of subjects colonized with strain ENT-K12 (19), providing its beneficial effect of maintaining oropharyngeal homeostasis and as an antipharyngitis agent (20, 21), and the ability of preventing immune activation induced by oral pathogens without altering the native salivary microbiome and inflammatory markers in healthy oral cavity (22). Furthermore, oropharyngeal probiotic ENT-K12 is able to downregulate immune responses through the action on NF-κB signaling pathways elicited by pathogens, inhibit NF-κB subunit translocating into the nucleus, attenuate IL-8 secretion induced by inflammatory mediators, upregulate genes responsible for activating the interferon signaling pathways with antiviral and cytokine modulation properties, and specifically alter the expression of host genes involved in multiple innate defense pathways, epithelial layer adhesion, and homeostasis pathways, altogether stimulating an anti-inflammatory response and actively protecting the host from inflammation and apoptosis induced by pathogens (23). This study aimed to confirm the recognition that administration of oropharyngeal probiotic ENT-K12 among children with RRTi could provide complementary therapeutic effects for acute respiratory infections and inflammation, and to prevent new respiratory episodes in children with RRTi, meanwhile to reduce the needs of antibiotic courses for pediatric RRTi.

MATERIALS AND METHODS

General Information

The single-center, open, randomized controlled trial was conducted in Wuhan CR & WISCO General Hospital from January to March 2021 according to the criteria set by the Declaration of Helsinki and with the approval of the local ethics committee, the Ethics Committee of CR & WISCO General Hospital Affiliated to Wuhan University of Science and Technology (registration number HRWGZYY20210003). The parents and their children who participated in the trial were informed of the trial methods and signed the consent.

To be considered legible for enrollment into the study, subjects met the following criteria: (1) children aged 3–10 years who attend school; (2) children who experienced 3 or more episodes of upper respiratory infections in the previous year; and (3) parents/legal guardians who were familiar with and agree to the study and signed informed consent. Subjects were excluded from the study if they met the following exclusion criteria: (1) children with immunological insufficiency or defects; (2) children who underwent tonsillectomy or adenotonsillectomy;

(3) children who were suffering from bronchospasm, asthma, allergic rhinitis, adenoid hypertrophy, or chronic sinusitis; (4) children who were allergic to milk protein; (5) children who were suffering from systemic disease, such as diabetes, kidney disease, gastrointestinal diseases, or rheumatology; (6) children who were suffering from infectious diseases such as measles, mumps, or rubella; (7) children who had been taking antibiotics and immunosuppressive drugs in the past week; and (8) children who had on-site symptoms of respiratory tract infections such as sore throat, other upper respiratory infections, or suspected/confirmed respiratory infections.

Study Material

The study product, Bactoblis oropharyngeal probiotic formula, is formulated in the form of slowly dissolving oral lozenges by Probionet GmbH (Herisau, Switzerland); the preparation of this formula used in the clinical trial contained no <1 billion colony-forming units (CFUs)/lozenges of *Streptococcus salivarius* ENT-K12 (also known as *Streptococcus salivarius* subsp. *thermophilus* ENT-K12) over shelf life.

All children enrolled in this study underwent a general clinical examination and were randomized to receive oropharyngeal probiotic for 30 days in the probiotic group or no intervention in the control group. Parents/guardians were asked to instruct their children to take one lozenge before bed after brushing their teeth every evening and suck the lozenge until it is fully dissolved (∼4–5 min) to ensure that the child does not chew or swallow the lozenges directly. The children were suggested not to drink or swallow any substance for at least 1 h after the administration of the study product.

During the entire study period, if any symptoms of respiratory tract infections are present, the parents of children are required to contact the research practitioner and visit the hospital for further medical examination and medical treatment prescribed if needed; if there was evidence of respiratory tract infections, the enrolled children in both groups were asked to record the variety and duration of drug treatment and continue complementarily taking the study product throughout the study period in case of antibiotic or other medical treatment was required. The participated subjects were required to return for final visits after 30 days and return any unused study product. Compliance will be assessed by counting unused lozenges at the final visit; compliance criteria judged at 90% of dispensed lozenges consumed.

Objectives

During the study, at least five visits over a 2-month period were involved, namely, screening visit on day 0 (Visit 1), routine visit on days 7 and 14 (Visit 2 and 3), final visit on day 30 (Visit 4), and follow-up visit on day 60 (Visit 5). Additional visits took place if the enrolled children experienced symptoms of respiratory tract infections, so a diagnosis could be confirmed and if necessary, a prescription provided. The primary objective was to access efficacy of oropharyngeal probiotic ENT-K12 on reducing incidence of respiratory tract infections among children with RRTi during cold season. The secondary objective was to assess the efficacy of oropharyngeal probiotic ENR-K12 on the reduced number of days of respiratory symptoms onset, the reduced number of days under treatment with antibiotics, antiviral drugs, antipyretics, and steroids, the reduced number of days the children were absent from school and their parents were absent from work, and to confirm safety judged by adverse events reported. The episodes of upper respiratory tract infections are confirmed after clinically diagnosed according to a child's medical history and symptoms on site.

Statistical Method

SPSS 26.0 statistical software was used to process the data, and the data were expressed as mean ± standard deviation (X ± S). The chi-square test and Wilcoxon rank sum test were used to compare the general data (i.e., age and gender), and the Wilcoxon rank sum test was used to compare the different clinical outcomes between two groups, and $P < 0.05$ was considered statistically significant. Kaplan–Meier statistics were used to evaluate the level of protection of oropharyngeal probiotics against respiratory tract infections over time. The survival analysis was used to determine the differences in cumulative incidence of patients under different conditions during clinical observation.

RESULTS

A total of 100 children were selected to participate in this trial. A total of 50 children received oropharyngeal probiotic ENT-K12 every day before bed for 30 days as the probiotic group, and the other 50 children did not receive oropharyngeal probiotics served as the control group. Two children in the probiotic group dropped out of the study for personal reasons at the beginning of the trial; one child in the probiotic group was removed from the trial due to irregular use of oropharyngeal probiotic, and the data were not included in the statistical study. Finally, 47 children in the probiotics group completed the experiment, and 50 children in the control group completed the experiment.

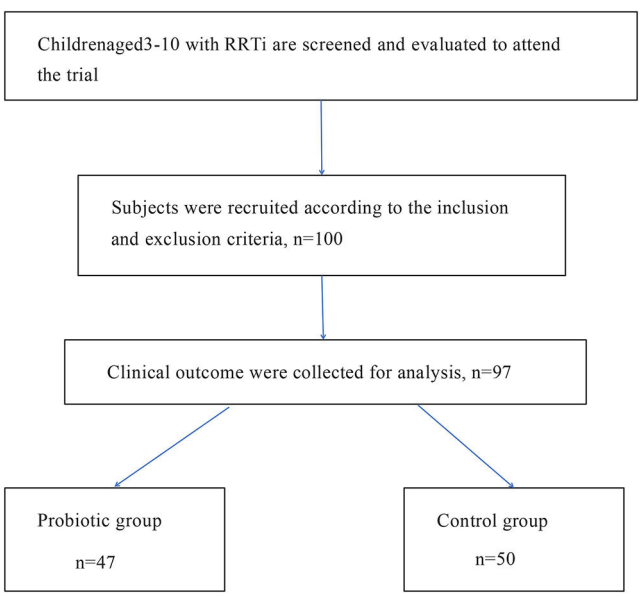

TABLE 1 | The baseline characteristics of children with recurrent respiratory tract infections (RRTi).

	Probiotic group ($n = 47$)	Control group ($n = 50$)	*P*-value
Gender			0.228
Male	22	32	
Female	25	18	
Age	5.71 ± 1.99	6.12 ± 1.98	0.301
Numbers of respiratory tract infections in the past year	3.37 ± 0.53	3.58 ± 0.92	0.536
Pneumococcal vaccination			1
No	47	50	
Yes	0	0	
Influenza vaccination			1
No	47	50	
Yes	0	0	

X ± S is used to describe the average level and variability of the data.

TABLE 2-1 | The clinical outcomes during the 30 days of oropharyngeal probiotic intervention among children with RRTi in cold season.

	Probiotic group ($n = 47$)	Control group ($n = 50$)	*P*-value
Incidence of respiratory tract infections	7/47 (14.89%)	17/50 (34.00%)	0.045
Respiratory symptoms onset (days)	20	65	
Sick days (days/person)	0.42 ± 1.05	1.30 ± 2.22	0.030
Duration of each episode (days/episode)	2.85 ± 0.69	3.93 ± 2.11	0.034
Absence from school (days/person)	0.26 ± 0.65	1.32 ± 2.33	0.040
Absence from work (days/person)	0.02 ± 0.14	0.60 ± 1.55	0.016
Taking antibiotics (days/person)	0.02 ± 0.14	0.64 ± 1.93	0.052
Taking anti-viral drug (days/person)	0.06 ± 0.32	0.60 ± 1.55	0.045
Taking antipyretics drug (days/person)	0	0.18 ± 0.82	0.086

X ± S is used to describe the average level and variability of the data.

As shown in **Table 1**, there was no difference in basic characteristics between the two groups. The probiotic group consisted of 22 male and 25 female children, while the control group consisted of 32 male and 18 female children. There was no difference in gender, mean age, the episode numbers of respiratory infections in the past year, pneumococcal vaccination, and influenza vaccination between the two groups ($P > 0.05$).

Table 2-1 shows the clinical outcomes of oropharyngeal probiotic administration among children with RRTi during the 30 days intervention in cold season; oropharyngeal probiotic ENT-K12 administration significantly reduced the episodes of respiratory tract infections by 56% ($P < 0.05$) comparing with the control group, of which, 7 episodes of respiratory tract infections were observed in the group of 47 children with RRTi treated with oropharyngeal probiotic and 17 episodes were observed in the group of 50 non-treated children with RRTi. By comparison with the control group, children with RRTi in the probiotic group experienced a significantly fewer days of respiratory symptoms onset (by 68%, $P < 0.05$), of which a total of 20 days (0.42 days/person) of respiratory symptoms onset observed in the probiotic group, whereas a total of 65 days (1.3 days/person) was observed in the control group. Meanwhile, complementary treatment with oropharyngeal probiotics during the acute respiratory infections along with the standard medication further resulted in a significantly shorter (by 27%, $P < 0.05$) average duration of each respiratory episodes (2.85 days/episode) compared with the control group (3.93 days/episode). Due to the reduction in incidence and duration of each episode, children with RRTi treated with oropharyngeal probiotic had significantly fewer days absent from school by 80% ($P < 0.05$), whereas children treated with oropharyngeal probiotics had averagely 0.26 days/person absence from school and 1.32 days/person was reported in the control group. Apart from children's school attendance, parents' work attendance affected by their children's sickness was also recorded, and the parents of children treated with oropharyngeal probiotic had significantly less days absent from work by 97% ($P < 0.05$); of which 0.02 days/person of absence from work was reported for the probiotic group and 0.6 days/person were reported for the control group. During the study period, when there was evidence of a respiratory tract infection, the enrolled children in both groups were asked to record the variety and duration of medication including antibiotic treatment prescribed by the study practitioner, and continue taking oropharyngeal probiotic ENT-K12 throughout the study period. Our data reveal that children in the probiotic group had significantly less medication compared with those in control group. The number of days taking antibiotics complementarily treated with oropharyngeal probiotics was observed to be reduced by 97% ($P = 0.05$); it is reported that totally 1 day (0.02 days/person) of medication history on antibiotics was observed in the probiotic group compared with totally 32 days (0.64 days/person) observed in the control group; moreover, number of days taking antiviral drugs complementarily treated with oropharyngeal probiotics was observed to be reduced by 90% ($P < 0.05$); it is reported that totally 3 days (0.06 days/person) of medication history on antiviral drugs was observed in the probiotic group compared with totally 30 days (0.6 days/person) observed in the control group; furthermore, no record of antipyretics/steroid intake was observed in the probiotic group compared with 9 days (0.18 days/person) that observed in the control group ($P = 0.086$).

Table 2-2 shows the clinical outcomes of oropharyngeal probiotic administration during the 30 days follow-up period in cold season. During the follow-up period, there were no observed episodes of respiratory tract infections among 47 children with RRTi treated with oropharyngeal probiotic, and 6 episodes (incidence 12%, $P < 0.05$) of upper respiratory tract infections observed in 50 children with RRTi of the control group. Similarly, there were no observed respiratory symptoms onset, absence from school or work, and no need for taking standard medication in 47 children with RRTi treated with oropharyngeal probiotic, while 23 days (0.46 days/person, $P < 0.05$) of respiratory symptoms onset, resulting in average 4.2 days per respiratory episodes ($P < 0.05$), 0.46 days per child absence from school ($P < 0.05$), 0.3 days per parent absence from work

($P < 0.05$), 0.16 days per child taking antibiotics ($P < 0.5$), 0.14 days per child taking antiviral drug ($P < 0.5$), and 0.06 days per child taking antipyretics drug ($P < 0.5$) among children with RRTi were observed in control group during the 30 days follow-up period.

X ± S is used to describe the average level and variability of the data.

Furthermore, the Kaplan–Meier statistical analysis was used to estimate the level of protection effect of oropharyngeal probiotic over time; as shown in **Figure 1**, the Kaplan–Meier curve of probability not having any episodes of respiratory tract infections decreased gradually from 1 on the first day approaching to a flat at 0.83 on day 12, while the flat lasted until day 60 when this study ended, as per the control group, the probability not having any episodes of respiratory infections continuously decreased to 0.54 at the end of this study ($P = 0.002$). As shown in **Figure 2**, the Kaplan–Meier statistic is used to estimate the needs of medical treatment including antibiotics and antiviral drugs over time; the probability of not having any courses of antibiotic and antiviral drugs treatment decreased gradually from 1 on the first day approaching to a flat at 0.94 on day 6, while the flat lasted until day 60, the end of this study; in contrast, the probability of not having any courses of antibiotic and antiviral drugs treatment continuously decreased approaching to 0.64 until the end of this study in the control group ($P = 0.001$). Notably, children in the probiotic group experienced sustained protection from respiratory tract infections; hence, the needs for medical treatment were reduced within 2 weeks of oropharyngeal probiotic administration resulting in an extremely lower incidence rate of acute or RRTi and treatment courses comparing with the control group.

TABLE 2-2 | The clinical outcomes during the 30 days of follow-up period.

	Probiotic group ($n = 47$)	Control group ($n = 50$)	*P*-value
Incidence of respiratory tract infections	0	6/50 (12.00%)	0.025
Respiratory symptoms onset (days)	0	23	
Sick days (days/person)	0	0.46 ± 1.43	0.027
Duration of each episode (days/episode)	0	4.20 ± 1.64	0.027
Absence from school (days/person)	0	0.46 ± 1.29	0.014
Absence from work (days/person)	0	0.30 ± 0.90	0.025
Taking antibiotics (days/person)	0	0.16 ± 0.81	0.164
Taking anti-viral drug (days/person)	0	0.14 ± 0.70	0.164
Taking antipyretics drug (days/person)	0	0.06 ± 0.42	0.327

Table 3 shows the tolerance and side effects reported by children treated with oropharyngeal probiotic ENT-K12. There is a very high profile in terms of tolerability as 46 out of 47 children had an "excellent feeling" about taking oropharyngeal probiotic ENT-K12 lozenges and another 1 had a "good feeling" about taking oropharyngeal probiotic ENT-K12 lozenges,

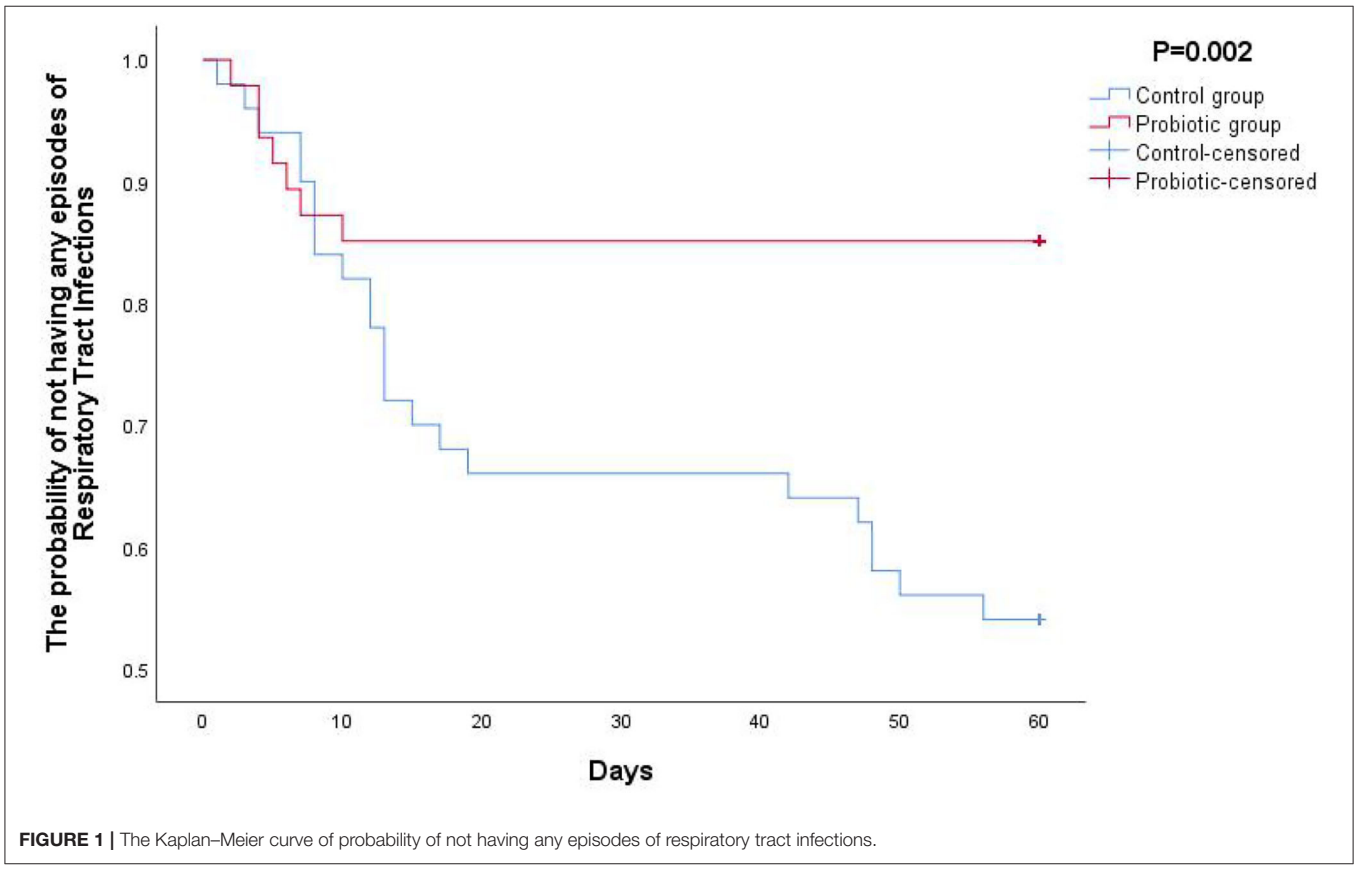

FIGURE 1 | The Kaplan–Meier curve of probability of not having any episodes of respiratory tract infections.

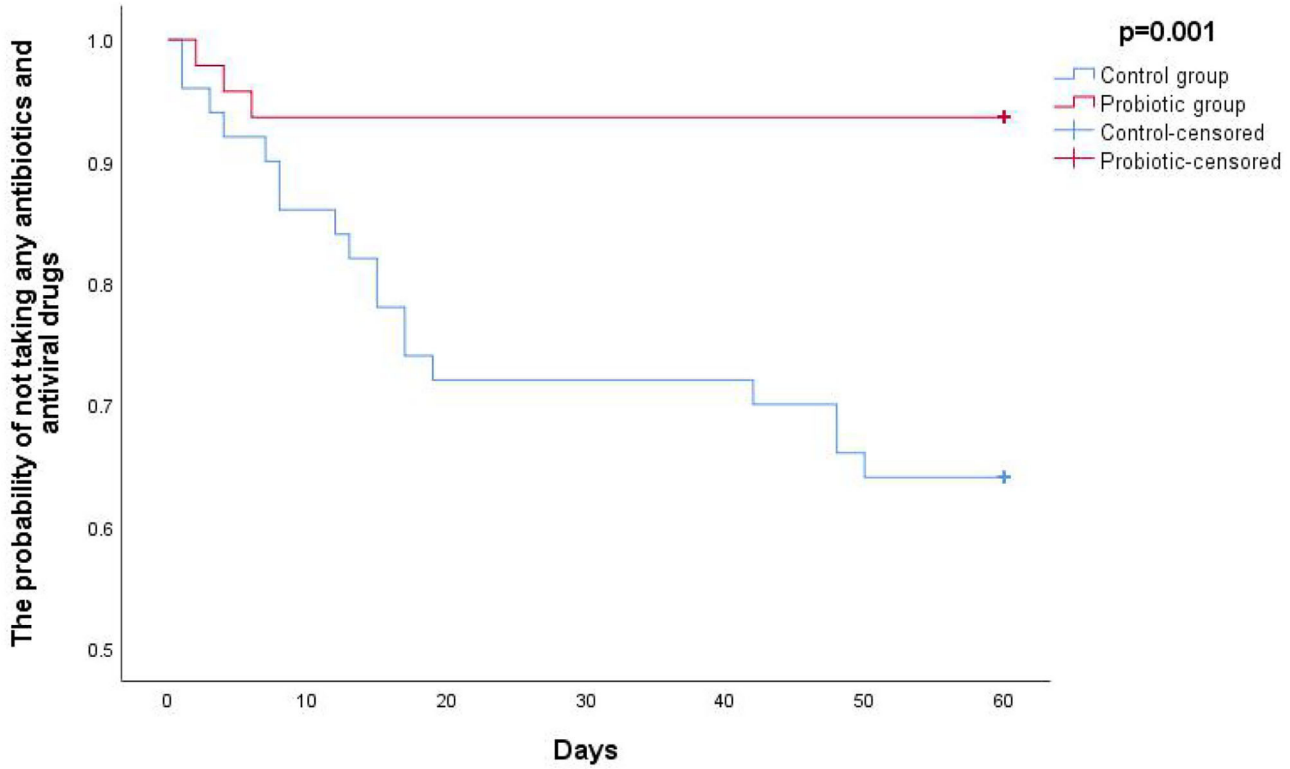

FIGURE 2 | The Kaplan–Meier curve of probability of not taking any antibiotics and antiviral drugs.

TABLE 3 | Tolerance and side effects reported by children treated with oropharyngeal probiotics ($n = 47$).

Results	Tolerability	Side-effects
Excellent, *n*	46	None
Good, *n*	1	None
General, *n*	0	None
Non-qualified, *n*	0	None

while there were no side effects reported during the whole study period.

DISCUSSION

Largely assessed data have shown that certain gut probiotic strains may carry a potential to modify the incidence of respiratory infections or duration of each episode (24–27), and in favor of the probiotic groups regarding to incidence of respiratory infections, severity of symptoms, incidence of antibiotic use, and absent days of school having been reported; however, the beneficial levels of those gut probiotics in preventing new respiratory episodes in children with RRTi were limited due to low-quality evidence, and many of the said clinical trials showed no statistically significant difference of illness episodes between intervention and control groups (28, 29). Due to colonization at the interfaces between the environment and both respiratory tract and digestive tract, alone with performing various mode of actions, administration of oropharyngeal probiotics can provide a much greater level of beneficial effects to protect host from respiratory infections comparing to gut probiotics; it was suggested that the oropharyngeal probiotic strain ENT-K12 should be incorporated in future trials of bacteriotherapy of RRTi as it showed outstanding positive influences on human ear-nose-throat health during short-term administration and great safety profile (30–32). Key symptoms of the respiratory tract infections observed during this study include sneezing, fatigue, sore/itchy throat, cough, low fever, nasal congestion, running nose, and dizziness, and there were 3 children who experienced high fever $>38^{\circ}$C in the control group during the intervention period, while no children experienced high fever in the probiotic group (data not shown). Considering that most children extremely resist and are scared by the hospital blood collection process, while unnecessary serological diagnosis and etiological examination are not required for commonly happened respiratory infections and common cold, serological diagnosis and etiological examination were not conducted for all the children during this study. In this study, incidence of respiratory infections among children with RRTi reduced 56% during the cold season during the 30 days intervention; if counting on the follow-up period together, the reduction rate would be 68% during the whole study period

of 60 days, this is a consistent result with earlier research that oropharyngeal probiotic ENT-K12 treatment in children with a history of recurrent pharyngotonsillitis significantly reduced not only their new episodes by >90% in 3 months compared to the previous year (33) but also during the following 9 months of follow-up period (34), reduced the incidence of both pharyngotonsillitis and acute otitis media in children (35), and significantly reduced the incidence of both upper and lower respiratory tract infections such as tonsillopharyngitis, tracheitis, rhinitis, laryngitis, and otitis media among young children (36). It is worth to mention that during the middle of this study, there was a coronavirus disease 2019 (COVID-19) endemic in Wuhan and the short-term influence was reflected in the incidence of respiratory infections during that time, which can be observed in both Kaplan–Meier curves, an obvious flat exists before day 20 lasting until around day 40; according to the epidemic prevention policy in Wuhan, many communities including the families of the children participated in this study should spontaneously or passively be quarantined for 14 days while people paid much more attention wearing masks at all times in the public in order to stop the spread of COVID-19 endemic ensuring the public health. This evidence prove that not only keeping social distance and wearing masks could effectively protect people from respiratory infections that transmitted *via* droplets and aerosols (37), but also maintaining a balanced oropharyngeal microflora *via* administration of oropharyngeal probiotics could further keep children from various kinds of respiratory infections including SARS-CoV-2 (38), and the said oropharyngeal homeostatic could effectively prevent respiratory infections on occupational health including first-line medical personnel who are in close contact with patients hospitalized for COVID-19 during pandemic (39).

This study may offer some fresh insights into the relationship between the duration of oropharyngeal homeostatic and the incidence of pediatric respiratory infections that reflected the children's immunity status; in this study, the accumulated incident rate of respiratory infections dramatically slowed down since day 12 among children with RRTi treated with oropharyngeal probiotics while it kept increased among children with RRTi in the control group; this phenomenon could possibly explain the colonization of oropharyngeal probiotics in oral cavity, 12 days are estimated for an efficient colonization at the dose of taking 1 lozenge per day, hence providing a better oropharyngeal homeostatic that could probably last for at least 30 days after stop consuming oropharyngeal probiotics; similar phenomenon was also been observed in the previous study among frontline medical staff who fight against COVID-19, without been observed in the control group, medical staff treated with 2 lozenge/day of oropharyngeal probiotic ENT-K12 were effectively been benefited by the oropharyngeal homeostatic since day 10 lasting until the end of study, indicating an effective colonization at dose of 2 lozenges per day (40). Another study also shown that the abundance of otopathogens, *Moraxella*, was lower in the nasopharynx and abundance of oral commensal bacteria, *S. salivarius*, was higher in saliva in young children after taking oropharyngeal probiotic ENT-K12 for 1 month (41), indicating the alteration of oropharyngeal/ nasopharyngeal microflora after oropharyngeal probiotic intervention.

In this study, a total of 7 episodes were observed in the probiotic group during the first 12 days, and only 3 courses of medical treatment were prescribed by the research practitioner during the first 6 days, which indicates that since 1 week after administration, children with RRTi only had minor respiratory symptoms onset while their immune system was able to recover themselves without antibiotic or antiviral drug intervention. This phenomenon was not observed in the control group, while 18 courses of medication were prescribed along with 23 episodes throughout the entire study period; this further explains the fact that a balanced oropharyngeal/nasopharyngeal homeostatic could provide host a better tolerance to respiratory infections, and the upper respiratory microbiome landscape could be considered to be used for medical diagnostics and as a target for therapy (42).

In this study, repeated episodes were not observed in children treated with oropharyngeal probiotic ENT-K12, while 3 repeated episodes (all the repeated episodes were observed during the follow-up period for all 3 children) were observed in the control group, as the number of study subjects and RRTi episodes were small, statistic data are not shown, and it would be interesting to see the difference in new repeated episodes incidence among children with RRTi when conducting a longer period study with a larger sample size.

Previous studies have shown that treatment with oropharyngeal probiotic reduced the exacerbation frequency of chronic adenoiditis and the requirement for medication (43). A similar beneficial effect of oropharyngeal complementary treatment was observed in our study, during intervention period; when acute respiratory symptoms onset, children complementary treated with oropharyngeal ENT-K12 in combination with medication (3 courses in total; 1 took antibiotics for 1 day and 2 took antiviral drugs for 1 and 2 days, respectively) or without medication further shortened the duration of respiratory symptoms onset compared to those treated with only medication in control group (14 courses in total; prescribed with antibiotics, antiviral drugs or antipyretics for various period of time from 1 to 10 days). This complementary beneficial effect was also been demonstrated in previous study that oropharyngeal probiotic treatment among pediatric patients with recurrent pharyngotonsillitis of whom the pharmacological approach was no longer effective thus referred to tonsillectomy surgery could effectively prevent new episodes and reduced the needs for antibiotic treatment and tonsillectomy by 72% comparing to control group (44). It further explains that oropharyngeal administration may improve homeostasis, which plays an important role in host susceptibility to respiratory infections.

Up to date, the international consensus of the available approaches for the prevention of RRTi in children is immunotherapy, while probiotic treatment has not been suggested yet because it is not clear which bacteria strain,

dosage, and administration schedule can offer the best results (45). The perspective of "new-age" immunotherapy, such as checkpoint inhibition triggering the immunopathology events or cytokine therapies modulating inflammation development, has been raised to reduce the burden of infectious diseases threatened by antibiotic resistance (46). The recent meta-analysis has shown that the immunostimulants, OM-85 BV and pidotimod, which have been widely used and suggested by pediatricians in the prevention and treatment of RRTi in susceptible children, can reduce the incidence of respiratory tract infections by 0.21 and 0.19 per month, respectively (47); however, long-term use of the said drugs is challenging for children and their families. Actually, probiotics do have great potential as the "new-age" immunotherapy, as several *in vitro*/*in vivo* studies have summarized the strain-specific immunomodulatory effects and the stimulation of interferon (IFN) pathways to antagonize viral respiratory infections due to that microbiome has co-evolved with the eukaryotic genome of its host (26, 48). While waiting for new knowledge, more clinical trials should be conducted to help us having more insights regarding to the clinical benefit of oropharyngeal probiotics administration, alone or complementary use with medication, which could be an effective and safe immunotherapy for children with RRTi in the near future.

The limitations of this study include the lack of oropharyngeal microflora analysis data before and after the intervention of oropharyngeal probiotics as we have limited experiences in oropharyngeal microbiome study methodology. Furthermore, the size of this study was not big enough, and duration was not long enough for us to conduct a statistic analysis on the reduction of RRTi incidence in children treated with oropharyngeal probiotics; however, an obvious trend of RRTi incidence reduction could already been observed in only 30 days and lasted for another 30 follow-up days in this study. Finally, there might be influences on the data of children and parents absent from school and work cause Chinese New Year national holiday was overlapping the later period of this study, and the leave days could have been increased in the control group if it was normal working days; however, a trend already could be observed that 0.07 days of work leave taken was corresponded to each school leave day of children in probiotic group, while 0.45 days of work leave taken was corresponded to each school leave day of children in control group during the intervention period (statistical data not shown), which might further indicate that the days of parents absent from work might associated with the severity of pediatric respiratory symptoms onset.

CONCLUSION

There are growing interests in the microbiome-based therapeutics, which provide exciting opportunities for decreasing susceptibility to infections and enhancing resistance to a range of diseases (49); economic studies showed that compared to non-probiotic consumption, generalized probiotic intake in the United States and Canada population would have allowed cost savings for the healthcare, averting respiratory illness sick days and antibiotic prescriptions (50, 51). To develop an effective approach that can be used alone or in combination with antibiotics reducing the dose required for activity is of the upmost importance. Oropharyngeal probiotic ENT-K12 lozenge as a delivery carrier for both innate immune modulator fighting viral infections and bacteriocins showing multiple modes of action by inhibiting cell wall biosynthesis of respiratory pathogens stimulated by ENT-K12 strain, treatment of oropharyngeal probiotic ENT-K12 can effectively prevent new episodes of acute and RRTi in school children with RRTi during cold season, shorten the duration and decrease the severity of respiratory symptoms onset when complementary treated with medication, reduce the use of antibiotics and antiviral drugs, and the absence days from both children's school and parents' work. Using oropharyngeal probiotics as a complementary treatment to stabilize oropharyngeal microflora, specifically inhibiting respiratory pathogens, could possibly be a promising approach to reduce RRTi burden and combating antibiotic resistance in long term, more clinical researches are needed to further confirm the optimized clinical practices.

DATA AVAILABILITY STATEMENT

The raw data supporting the conclusions of this article will be made available by the authors, without undue reservation.

ETHICS STATEMENT

The studies involving human participants were reviewed and approved by CR & WISCO General Hospital Affiliated to Wuhan University of Science and Technology. Written informed consent to participate in this study was provided by the participants' legal guardian/next of kin.

AUTHOR CONTRIBUTIONS

XLI, QW, and SQ guided and completed the whole experimental design. XLU and JX involved in the data collection. HG and XX were responsible for the arrangement of data and analyzing the data. YF, YL, JC, and ZL participated in the interpretation of the results. HG and XX wrote the initial draft with all authors providing critical feedback and edits to subsequent revisions. HG and XX have contributed equally to this work and share first authorship. XLI and QW reviewed and revised the manuscript before submission, they are co-corresponding authors.

FUNDING

This research is a self-funded project.

REFERENCES

1. Esposito S, Soto-Martinez ME, Feleszko W, Jones MH, Shen KL, Schaad UB. Nonspecific immunomodulators for recurrent respiratory tract infections, wheezing and asthma in children: a systematic review of mechanistic and clinical evidence. *Curr Opin Allergy Clin Immunol.* (2018) 18:198–209. doi: 10.1097/ACI.0000000000000433
2. Zven SE, Susi A, Mitre E, Nylund CM. Association between use of multiple classes of antibiotic in infancy and allergic disease in childhood. *JAMA Pediatr.* (2020) 174:199–200. doi: 10.1001/jamapediatrics.2019.4794
3. Chonmaitree T, Jennings K, Golovko G, Khanipov K, Pimenova M, Patel JA, et al. Nasopharyngeal microbiota in infants and changes during viral upper respiratory tract infection and acute otitis media. *PLoS ONE.* (2017) 12:e0180630. doi: 10.1371/journal.pone.0180630
4. Zhou B, Niu W, Liu F, Yuan Y, Wang K, Zhang J, et al. Risk factors for recurrent respiratory tract infection in preschool-aged children. *Pediatr Res.* (2021) 90:223–31. doi: 10.1038/s41390-020-01233-4
5. Toivonen L, Karppinen S, Schuez-Havupalo L, Teros-Jaakkola T, Vuononvirta J, Mertsola J, et al. Burden of recurrent respiratory tract infections in children: a prospective cohort study. *Pediatr Infect Dis J.* (2016) 35:e362–9. doi: 10.1097/INF.0000000000001304
6. Schaad UB, Esposito S, Razi CH. Diagnosis and management of recurrent respiratory tract infections in children: a practical guide. *Arch Pediatr Infect Dis.* (2015) 4:e31039. doi: 10.5812/pedinfect.31039
7. Shaikh N, Leonard E, Martin JM. Prevalence of streptococcal pharyngitis and streptococcal carriage in children: a meta-analysis. *Pediatrics.* (2010) 126:e557–64. doi: 10.1542/peds.2009-2648
8. Tang J, Chen J, He T, Jiang Z, Zhou J, Hu B, et al. Diversity of upper respiratory tract infections and prevalence of Streptococcus pneumoniae colonization among patients with fever and flu-like symptoms. *BMC Infect Dis.* (2019) 19:24. doi: 10.1186/s12879-018-3662-z
9. Li Y, Fu X, Ma J, Zhang J, Hu Y, Dong W, et al. Altered respiratory virome and serum cytokine profile associated with recurrent respiratory tract infections in children. *Nat Commun.* (2019) 10:2288. doi: 10.1038/s41467-019-10294-x
10. Niu H, Wang R, Jia YT, Cai Y. Pidotimod, an immunostimulant in pediatric recurrent respiratory tract infections: a meta-analysis of randomized controlled trials. *Int Immunopharmacol.* (2019) 67:35–45. doi: 10.1016/j.intimp.2018.11.043
11. Yin J, Xu B, Zeng X, Shen K. Broncho-Vaxom in pediatric recurrent respiratory tract infections: a systematic review and meta-analysis. *Int Immunopharmacol.* (2018) 54:198–209. doi: 10.1016/j.intimp.2017.10.032
12. Hols P, Ledesma-Garcia L, Gabant P, Mignolet J. Mobilization of microbiota commensals and their bacteriocins for therapeutics. *Trends Microbiol.* (2019) 27:690–702. doi: 10.1016/j.tim.2019.03.007
13. Wescombe PA, Upton M, Dierksen KP, Ragland NL, Sivabalan S, Wirawan RE, et al. Production of the lantibiotic salivaricin A and its variants by oral streptococci and use of a specific induction assay to detect their presence in human saliva. *Appl Environ Microbiol.* (2006) 72:1459–66. doi: 10.1128/AEM.72.2.1459-1466.2006
14. Barbour A, Tagg J, Abou-Zied OK, Philip K. New insights into the mode of action of the lantibiotic salivaricin B. *Sci Rep.* (2016) 6:31749. doi: 10.1038/srep31749
15. Barbour A, Wescombe P, Smith L. Evolution of lantibiotic salivaricins: new weapons to fight infectious diseases. *Trends Microbiol.* (2020) 28:578–93. doi: 10.1016/j.tim.2020.03.001
16. Erol I, Kotil SE, Fidan O, Yetiman AE, Durdagi S, Ortakci F. *In silico* analysis of bacteriocins from lactic acid bacteria against SARS-CoV-2. *Probiotics Antimicrob Proteins*. (2021) 1–13. doi: 10.1007/s12602-021-09879-0
17. Dicks LMT, Dreyer L, Smith C, Van Staden AD. A review: the fate of bacteriocins in the human gastro-intestinal tract: do they cross the gut-blood barrier? *Front Microbiol.* (2018) 9:2297. doi: 10.3389/fmicb.2018.02297
18. Horz HP, Meinelt A, Houben B, Conrads G. Distribution and persistence of probiotic *Streptococcus salivarius* K12 in the human oral cavity as determined by real-time quantitative polymerase chain reaction. *Oral Microbiol Immunol.* (2007) 22:126–30. doi: 10.1111/j.1399-302X.2007.00334.x
19. Wescombe PA, Heng NC, Burton JP, Chilcott CN, Tagg JR. Streptococcal bacteriocins and the case for *Streptococcus salivarius* as model oral probiotics. *Fut Microbiol.* (2009) 4:819–35. doi: 10.2217/fmb.09.61
20. Macdonald KW. The role of *Streptococcus salivarius* as a modulator of homeostasis in the oral cavity Electronic Thesis and Dissertation Repository. (2015). Available online at: https://ir.lib.uwo.ca/etd/2816
21. Jansen PM, Abdelbary MMH, Conrads G. A concerted probiotic activity to inhibit periodontitis-associated bacteria. *PLoS ONE.* (2021) 16:e0248308. doi: 10.1371/journal.pone.0248308
22. Macdonald KW, Chanyi RM, Macklaim JM, Cadieux PA, Reid G, Burton JP. Streptococcus salivarius inhibits immune activation by periodontal disease pathogens. *BMC Oral Health.* (2021) 21:245. doi: 10.1186/s12903-021-01606-z
23. Cosseau C, Devine DA, Dullaghan E, Gardy JL, Chikatamarla A, Gellatly S, et al. The commensal Streptococcus salivarius K12 downregulates the innate immune responses of human epithelial cells and promotes host-microbe homeostasis. *Infect Immun.* (2008) 76:4163–75. doi: 10.1128/IAI.00188-08
24. Esposito S, Rigante D, Principi N. Do children's upper respiratory tract infections benefit from probiotics? *BMC Infect Dis.* (2014) 14:194. doi: 10.1186/1471-2334-14-194
25. Zolnikova O, Komkova I, Potskherashvili N, Trukhmanov A, Ivashkin V. Application of probiotics for acute respiratory tract infections. *Italian J Med.* (2018) 12:32. doi: 10.4081/itjm.2018.931
26. Lehtoranta L, Latvala S, Lehtinen MJ. Role of probiotics in stimulating the immune system in viral respiratory tract infections: a narrative review. *Nutrients.* (2020) 12:3163. doi: 10.3390/nu12103163
27. Laursen RP, Hojsak I. Probiotics for respiratory tract infections in children attending day care centers-a systematic review. *Eur J Pediatr.* (2018) 177:979–94. doi: 10.1007/s00431-018-3167-1
28. Wang Y, Li X, Ge T, Xiao Y, Liao Y, Cui Y, et al. Probiotics for prevention and treatment of respiratory tract infections in children: a systematic review and meta-analysis of randomized controlled trials. *Medicine.* (2016) 95:e4509. doi: 10.1097/MD.0000000000004509
29. Li L, Hong K, Sun Q, Xiao H, Lai L, Ming M, et al. Probiotics for preventing upper respiratory tract infections in adults: a systematic review and meta-analysis of randomized controlled trials. *Evid Based Complement Alternat Med.* (2020) 2020:8734140. doi: 10.1155/2020/8734140
30. Power DA, Burton JP, Chilcott CN, Dawes PJ, Tagg JR. Preliminary investigations of the colonisation of upper respiratory tract tissues of infants using a paediatric formulation of the oral probiotic Streptococcus salivarius K12. *Eur J Clin Microbiol Infect Dis.* (2008) 27:1261–3. doi: 10.1007/s10096-008-0569-4
31. Zupancic K, Kriksic V, Kovacevic I, Kovacevic D. Influence of oral probiotic *Streptococcus salivarius* K12 on ear and oral cavity health in humans: systematic review. *Probiotics Antimicrob Proteins.* (2017) 9:102–10. doi: 10.1007/s12602-017-9261-2
32. Di Pierro F. Assessment of efficacy of BLIS-producing probiotic K12 for the prevention of group a Streptococcus pharyngitis: a short communication. *Probiotics Antimicrob Proteins.* (2019) 11:332–4. doi: 10.1007/s12602-018-9398-7
33. Di Pierro F, Colombo M, Zanvit A, Risso P, Rottoli AS. Use of *Streptococcus salivarius* K12 in the prevention of streptococcal and viral pharyngotonsillitis in children. *Drug Healthc Patient Saf.* (2014) 6:15–20. doi: 10.2147/DHPS.S59665
34. Gregori G, Righi O, Risso P, Boiardi G, Demuru G, Ferzetti A, et al. Reduction of group A beta-hemolytic streptococcus pharyngo-tonsillar infections associated with use of the oral probiotic Streptococcus salivarius K12: a retrospective observational study. *Ther Clin Risk Manag.* (2016) 12:87–92. doi: 10.2147/TCRM.S96134
35. Di Pierro F, Risso P, Poggi E, Timitilli A, Bolloli S, Bruno M, et al. Use of *Streptococcus salivarius* K12 to reduce the incidence of pharyngo-tonsillitis and acute otitis media in children: a retrospective analysis in not-recurrent pediatric subjects. *Minerva Pediatr.* (2018) 70:240–45. doi: 10.23736/S0026-4946.18.05182-4
36. Kryuchko T, Tkachenko OY. An open-label study to evaluate the effects of Streptococcus salivarius K12 given as a powder formula to prevent respiratory infections in young children, *Nutrafoods*. (2021) 1:246–53. doi: 10.17470/NF-021-0032
37. Leung NHL. Transmissibility and transmission of respiratory viruses. *Nat Rev Microbiol.* (2021) 19:528–45. doi: 10.1038/s41579-021-00535-6

38. Pierro FD, Colombo M. The administration of *S. salivarius* K12 to children may reduce the rate of SARS-CoV-2 infection. *Minerva Med.* (2021) 112:514–16. doi: 10.23736/S0026-4806.21.07487-5
39. Pico-Monllor JA, Ruzafa-Costas B, Nunez-Delegido E, Sanchez-Pellicer P, Peris-Berraco J, Navarro-Lopez V. Selection of probiotics in the prevention of respiratory tract infections and their impact on occupational health: scoping review. *Nutrients*. (2021) 13:4419. doi: 10.3390/nu13124419
40. Wang Q, Lin X, Xiang X, Liu W, Fang Y, Chen H, et al. Oropharyngeal probiotic ENT-K12 prevents respiratory tract infections among frontline medical staff fighting against COVID-19: a pilot study. *Front Bioeng Biotechnol.* (2021) 9:646184. doi: 10.3389/fbioe.2021.646184
41. Sarlin S, Tejesvi MV, Turunen J, Vanni P, Pokka T, Renko M, et al. Impact of *Streptococcus salivarius* K12 on nasopharyngeal and saliva microbiome: a randomized controlled trial. *Pediatr Infect Dis J.* (2021) 40:394–402. doi: 10.1097/INF.0000000000003016
42. Kumpitsch C, Koskinen K, Schopf V, Moissl-Eichinger C. The microbiome of the upper respiratory tract in health and disease. *BMC Biol.* (2019) 17:87. doi: 10.1186/s12915-019-0703-z
43. Karpova EP, Karpycheva IE, Tulupov DA. [Prophylaxis of chronic adenoiditis in the children]. *Vestn Otorinolaringol.* (2015) 80:43–45. doi: 10.17116/otorino201580643-45
44. Marini G, Sitzia E, Panatta ML, De Vincentiis GC. Pilot study to explore the prophylactic efficacy of oral probiotic *Streptococcus salivarius* K12 in preventing recurrent pharyngo-tonsillar episodes in pediatric patients. *Int J Gen Med.* (2019) 12:213–17. doi: 10.2147/IJGM.S168209
45. Esposito S, Jones MH, Feleszko W, Martell JAO, Falup-Pecurariu O, Geppe N, et al. Prevention of new respiratory episodes in children with recurrent respiratory infections: an expert consensus statement. *Microorganisms*. (2020) 8:1810. doi: 10.3390/microorganisms8111810
46. Mcculloch TR, Wells TJ, Souza-Fonseca-Guimaraes F. Towards efficient immunotherapy for bacterial infection. *Trends Microbiol.* (2022) 30:158–69. doi: 10.1016/j.tim.2021.05.005
47. Zhang W, Huang J, Liu H, Wen X, Zheng Q, Li L. Whether immunostimulants are effective in susceptible children suffering from recurrent respiratory tract infections: a modeling analysis based on literature aggregate data. *J Clin Pharmacol.* (2022) 62:245–53. doi: 10.1002/jcph.1969
48. Levy M, Kolodziejczyk AA, Thaiss CA, Elinav E. Dysbiosis and the immune system. *Nat Rev Immunol.* (2017) 17:219–32. doi: 10.1038/nri.2017.7
49. Sorbara MT, Pamer EG. Microbiome-based therapeutics. *Nat Rev Microbiol.* (2022) 1–16. doi: 10.1038/s41579-021-00667-9
50. Lenoir-Wijnkoop I, Merenstein D, Korchagina D, Broholm C, Sanders ME, Tancredi D. Probiotics reduce health care cost and societal impact of flu-like respiratory tract infections in the usa: an economic modeling study. *Front Pharmacol.* (2019) 10:980. doi: 10.3389/fphar.2019.00980
51. Lenoir-Wijnkoop I, Gerlier L, Roy D, Reid G. The clinical and economic impact of probiotics consumption on respiratory tract infections: projections for Canada. *PLoS ONE.* (2016) 11:e0166232. doi: 10.1371/journal.pone.0166232

Conflict of Interest: The authors declare that the research was conducted in the absence of any commercial or financial relationships that could be construed as a potential conflict of interest.

Publisher's Note: All claims expressed in this article are solely those of the authors and do not necessarily represent those of their affiliated organizations, or those of the publisher, the editors and the reviewers. Any product that may be evaluated in this article, or claim that may be made by its manufacturer, is not guaranteed or endorsed by the publisher.

frontiers | Frontiers in Nutrition

ORIGINAL RESEARCH
published: 03 June 2022
doi: 10.3389/fnut.2022.918098

Evaluation of an Antibiotic Cocktail for Fecal Microbiota Transplantation in Mouse

Jijun Tan, Jiatai Gong, Fengcheng Liu, Baizhen Li, Zhanfeng Li, Jiaming You, Jianhua He and Shusong Wu**

Hunan Collaborative Innovation Center for Utilization of Botanical Functional Ingredients, College of Animal Science and Technology, Hunan Agricultural University, Changsha, China

Objective: This study aimed to evaluate the effect of an antibiotic cocktail on gut microbiota and provide a reference for establishing an available mouse model for fecal microbiota transplantation (FMT) of specific microbes.

Design: C57BL/6J mice (n = 24) had free access to an antibiotic cocktail containing vancomycin (0.5 g/L), ampicillin (1 g/L), neomycin (1 g/L), and metronidazole (1 g/L) in drinking water for 3 weeks. Fecal microbiota was characterized by 16S rDNA gene sequencing at the beginning, 1st week, and 3rd week, respectively. The mice were then treated with fecal microbiota from normal mice for 1 week to verify the efficiency of FMT.

Results: The diversity of microbiota including chao1, observed species, phylogenetic diversity (PD) whole tree, and Shannon index were decreased significantly ($P < 0.05$) after being treated with the antibiotic cocktail for 1 or 3 weeks. The relative abundance of *Bacteroidetes*, *Actinobacteria*, and *Verrucomicrobia* was decreased by 99.94, 92.09, and 100%, respectively, while *Firmicutes* dominated the microbiota at the phylum level after 3 weeks of treatment. Meanwhile, *Lactococcus*, a genus belonging to the phylum of *Firmicutes* dominated the microbiota at the genus level with a relative abundance of 80.63%. Further FMT experiment indicated that the fecal microbiota from the receptor mice had a similar composition to the donor mice after 1 week.

Conclusion: The antibiotic cocktail containing vancomycin, ampicillin, neomycin, and metronidazole eliminates microbes belonging to *Bacteroidetes*, *Actinobacteria*, and *Verrucomicrobia*, which can be recovered by FMT in mice.

Keywords: antibiotic cocktail, pretreatment, gut microbiota, mouse model, fecal microbiota transplantation

OPEN ACCESS

Edited by:
Hui Han,
Chinese Academy of Sciences (CAS), China

Reviewed by:
Zhouzheng Ren,
Northwest A&F University, China
Na Dong,
Northeast Agricultural University, China
Baichuan Deng,
South China Agricultural University, China

****Correspondence:***
Jianhua He
jianhuahy@hunau.net
Shusong Wu
wush688@huanu.edu.cn

Specialty section:
This article was submitted to Nutrition and Microbes, a section of the journal Frontiers in Nutrition

Received: *12 April 2022*
Accepted: *04 May 2022*
Published: *03 June 2022*

Citation:
Tan J, Gong J, Liu F, Li B, Li Z, You J, He J and Wu S (2022) Evaluation of an Antibiotic Cocktail for Fecal Microbiota Transplantation in Mouse. Front. Nutr. 9:918098. doi: 10.3389/fnut.2022.918098

INTRODUCTION

Fecal microbiota transplantation (FMT) has been widely used as an intervention method in the reconstruction of receptor gut microbiota in mice-model experiments against various diseases, such as obesity (1), colitis (2), *clostridium difficile* infection (3) and spinal cord injury (4). However, donor-derived microbiota transplanted into receptor guts is not easy to achieve colonization since indigenous microbiota is dominant and stable (5). Hence, suitable intestinal preparation is vital in the pretreatment of FMT to attain a susceptible microbiota environment. Antibiotic treatments for mice are more fundamental and economical than for germ-free (GF) mice because GF mice may induce global developmental

changes in receptor guts, which can mask disease-specific attributes of donor material (6). However, methods of antibiotic treatments before FMT have been formed diversely, such as composition of antibiotics (7), administration time (8), and concentrations (9).

The antibiotic cocktail containing vancomycin, ampicillin, neomycin, and metronidazole have been adopted widely in mice (10–12). Vancomycin belonging to glycopeptide antibiotics, ampicillin belonging to beta-lactam antibiotics, neomycin belonging to aminoglycoside antibiotics, and metronidazole belonging to nitroimidazoles antibiotics constitute the most common classes of antibiotics against gram-positive bacteria, aerobes or anaerobes (13). The underlying antibacterial mechanisms of these single categories of antibiotics have been well studied (14, 15). However, studies that aim to assess the influence of antibiotic cocktails on different specific microbes are rare, although the antibiotic cocktail may lead to loss of diversity and changes in microbes' composition (16, 17). Importantly, pieces of evidence are needed to understand the characteristics of microbes after treatment with the antibiotic cocktail to ensure the availability of the antibiotic cocktail and establish an FMT-based non-specific microbe mouse model. Consequently, this study aimed to evaluate the effect of an antibiotic cocktail containing vancomycin, ampicillin, neomycin, and metronidazole in drinking water on the composition of gut microbiota, and further verify the effectiveness of FMT.

MATERIALS AND METHODS

Diets and Reagents

Mouse feed (D12450J) was purchased from Research Diets Inc. (New Brunswick, NJ, United States), and the diet composition was shown in **Supplementary Table 1**. Antibiotics including vancomycin, ampicillin, neomycin, and metronidazole were purchased from Shanghai Yuanye Bio-Technology Co., Ltd. (Shanghai, China).

Mouse Model and Experimental Design

The experimental procedures were approved by the Hunan Agricultural University Institutional Animal Care and Use Committee (Permission No. 2020A34). Mice and sterilized poplar bedding were purchased from Hunan Slake Jingda Laboratory Animal Co., Ltd. (License No. SCXK-Xiang 2019-0004, Changsha, Hunan, China). Mice were housed separately in cages with a sterile environment under controlled temperature (23.5°C) and light (12 h light/day) and had free access to feed, drinking water, or an antibiotic cocktail containing vancomycin (0.5 g/L), ampicillin (1 g/L), neomycin (1 g/L), and metronidazole in drinking water.

A total of twenty-four C57BL/6J mice (SPF class, male, and 4 weeks of age) were raised separately with free access to an antibiotic cocktail containing vancomycin (0.5 g/L), ampicillin (1 g/L), neomycin (1 g/L), and metronidazole (1 g/L) in drinking water for consecutive 3 weeks. Then, mice were treated with clean drinking water for 3 days to avoid the interference of antibiotic cocktails on FMT, followed by FMT for 1 week. FMT experiment was conducted with a modified method based on Gong et al. (12). Briefly, fecal samples were collected sterilely through mild stimulation of the anus in mice, and resuspended in sterile phosphate buffer solution (PBS) at 0.125 g/ml, followed by low-speed (800 × *g*) centrifugation (Low-Speed Bench Centrifuge, TD4 angle rotor, Hunan Michael Laboratory Instrument Co., Ltd., Changsha, China) for 10 min. Ultimately, 0.15 ml of that supernatant was administered to mice by oral gavage once a day for up to consecutive 7 days. Feces of mice at the beginning of the experiment (0 W), the first week (1 W), the third week (3 W), as well as feces from donor mice (dM) and receptor mice (rM) were collected for characterization of microbiota (**Figure 1A**).

Analysis of Gut Microbiota

Total DNA of feces was extracted by using a Stool DNA Isolation Kit (Tiangen Biotech Co., Ltd., Beijing, China). DNA quality was detected and controlled by Nanodrop (Thermo Fisher Scientific Inc., Rockford, IL, United States), and then 30 ng DNA was used for PCR amplification. The V4 hypervariable region of the bacterial 16S rRNA gene was amplified by PCR, where the forward primer was 515a: 5′–GTGCCAGCMGCCGCGGTAA-3′ and the reverse primer was 806: 5′-GGACTACHVGGGTWTCTAAT-3′. For each sample, a 10-digit barcode sequence was added to the 5′ end of the forward and reverse primers (provided by Allwegene Technology Inc., Beijing, China), and each sample was carried out by three same replications to mitigate reaction-level PCR biases. The volume of PCR reaction was 25 μL, containing 12.5 μL of 2xTaq PCR MasterMix, 1 μL of forward and 1 μL of reverse primers at the concentration of 5 μM, respectively, 3 μL BSA at the concentration of 2 ng/μL, 3 μL DNA samples (30 ng), and 4.5 μL double-distilled H_2O (ddH_2O). Cycling parameters were 95°C for 5 min, followed by 25 cycles at 95°C for 45 s, 50°C for 50 s, and 72°C for 45 s, and a final extension at 72°C for 10 min. Detection parameters of agarose gel electrophoresis were referred to as follows: concentration of gel with 1%, voltage with 170V, and electrophoretic time of 30 min. Three PCR products from the same sample were mixed in equidensity ratios and purified with a GeneJET Gel Extraction Kit (Thermo Fisher Scientific Inc., Rockford, IL, United States), quantified using real-time PCR, and sequenced at Allwegene Technology Inc. (Beijing, China).

Statistical Analysis

Results are expressed as means ± *SD*. Significant differences between groups were determined using one-way ANOVA tests, followed by Fisher's least significant difference (LSD) and Duncan's Multiple Range test (SPSS21, IBM Corp., Armonk, NY, United States). A probability of $P < 0.05$ was considered significant.

RESULTS

The Effect of Antibiotic Cocktail on a Cluster of Fecal Microbiota

As shown in **Figure 1B**, treatment with the antibiotic cocktail for 1 or 3 weeks induced obvious changes in microbiota clusters, and

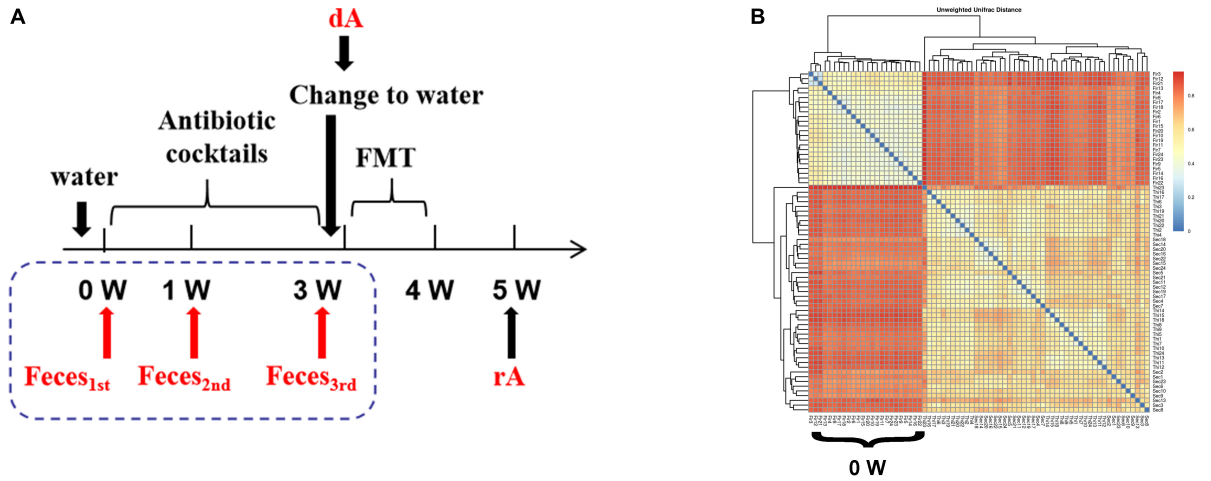

FIGURE 1 | The cluster of fecal microbiota. **(A)** Experimental design drawing. Receptor mice had free access to antibiotic cocktails containing vancomycin (0.5 g/L), ampicillin (1 g/L), neomycin (1 g/L), and metronidazole (1 g/L) in drinking water. Feces were collected on the first day of the experiment (0 W), the first week of the experiment (1 W), the third week of the experiment (3W), as well as feces from donor mice (dM) fed with normal diet and feces from receptor mice (rM) when FMT ended over another 1 week. All mice were fed a normal diet. **(B)** β-diversity indices of unweighted_unifrac_distance. The redder color is, the farther distance is. dM, donor mice fed with a normal diet; FMT, fecal microbiota transplantation; PLS-DA, partial least squares discriminant analysis; rM, receptor mice transplanted with microbiota from dM.

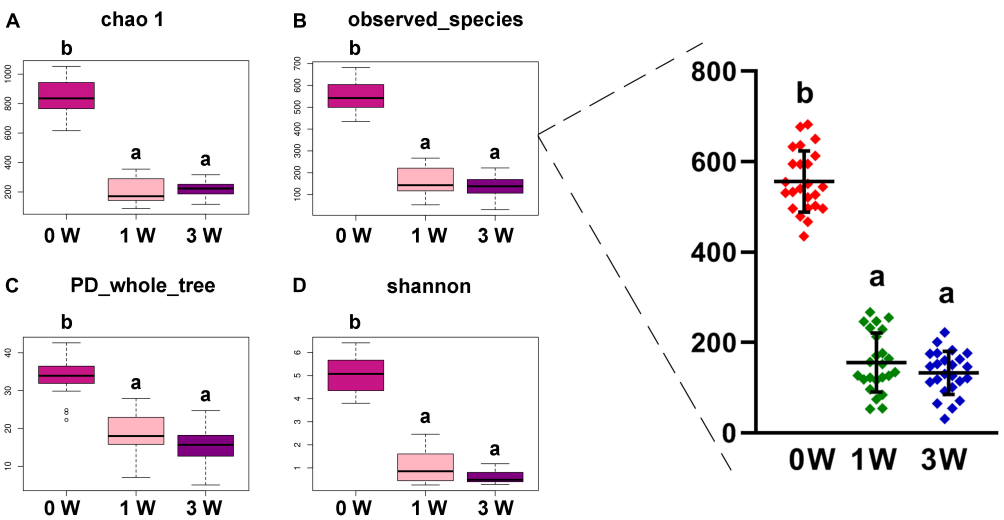

FIGURE 2 | The α diversity of fecal microbiota. **(A)** Chao 1. **(B)** Observed species. **(C)** PD whole tree. **(D)** Shannon. Data represented as mean ± SD (n = 24). Bars with different letters differ significantly ($P < 0.05$). Chao1, observed species, and PD whole tree are species richness indices, and the Shannon index reflects the diversity of gut microbiota. PD, phylogenetic diversity.

the evolutionary tree between 1 and 3 weeks suggested a similar sample composition.

The Effect of Antibiotic Cocktail on α Diversity of Microbiota

The abundance of gut microbiota is associated with the stability of the micro-ecological environment. As shown in **Figure 2**, the antibiotic cocktail led to a significant decrease in α diversity of the microbiota, including Chao 1 (A), observed species (B), phylogenetic diversity (PD) whole tree (C), and Shannon index (D). Especially, observed species were decreased by 71.94% (556 to 156) and 76.08% (556 to 133) by administration with the antibiotic cocktail for 1 or 3 weeks ($P < 0.05$), respectively.

The Effect of Antibiotic Cocktail on Microbiota Composition at the Phylum Level

To make an insight into the alteration of gut microbiota after treatment with an antibiotic cocktail, the relative abundance of microbes at the phylum level in different periods was

analyzed. The relative abundance of 3 kinds of phyla including *Bacteroidetes*, *Actinobacteria*, and *Verrucomicrobia* was decreased significantly by the antibiotic cocktail ($P < 0.05$). In detail, Bacteroidetes was decreased by 98.75 and 99.94%, *Actinobacteria* was decreased by 38.05 and 92.09%, while *Verrucomicrobia* was decreased by 99.71 and 100%, respectively, after treatment with the cocktail for 1 or 3 weeks (**Figure 3A**). *Firmicutes* dominated the gut microbiota, and the ratio of *Firmicutes* to *Bacteroidetes* was increased by the antibiotic cocktail in a dose-dependent manner (**Figure 3B**).

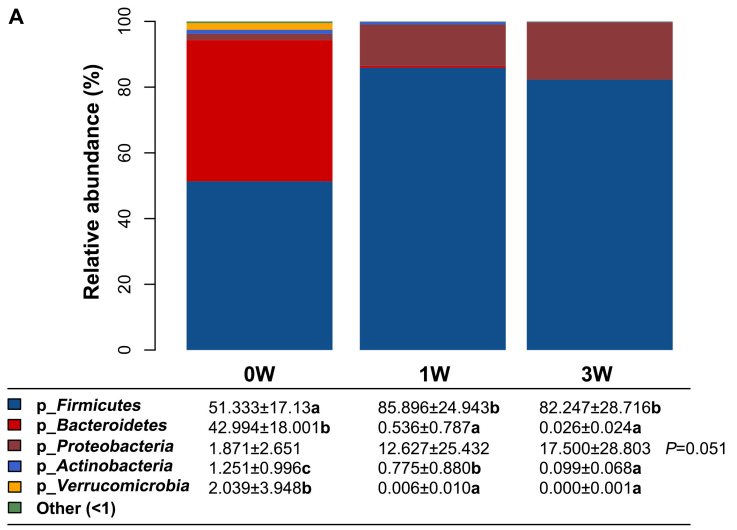

	0W	1W	3W	
p_*Firmicutes*	51.333±17.13**a**	85.896±24.943**b**	82.247±28.716**b**	
p_*Bacteroidetes*	42.994±18.001**b**	0.536±0.787**a**	0.026±0.024**a**	
p_*Proteobacteria*	1.871±2.651	12.627±25.432	17.500±28.803	*P*=0.051
p_*Actinobacteria*	1.251±0.996**c**	0.775±0.880**b**	0.099±0.068**a**	
p_*Verrucomicrobia*	2.039±3.948**b**	0.006±0.010**a**	0.000±0.001**a**	
Other (<1)				

FIGURE 3 | The relative abundance of fecal microbiota at the phylum level. **(A)** The relative abundance of microbes. **(B)** The ratio of Firmicutes to Bacteroidetes. Data represented as mean ± SD ($n = 24$). Bars with different letters differ significantly ($P < 0.05$). p_ represents microbial phylum.

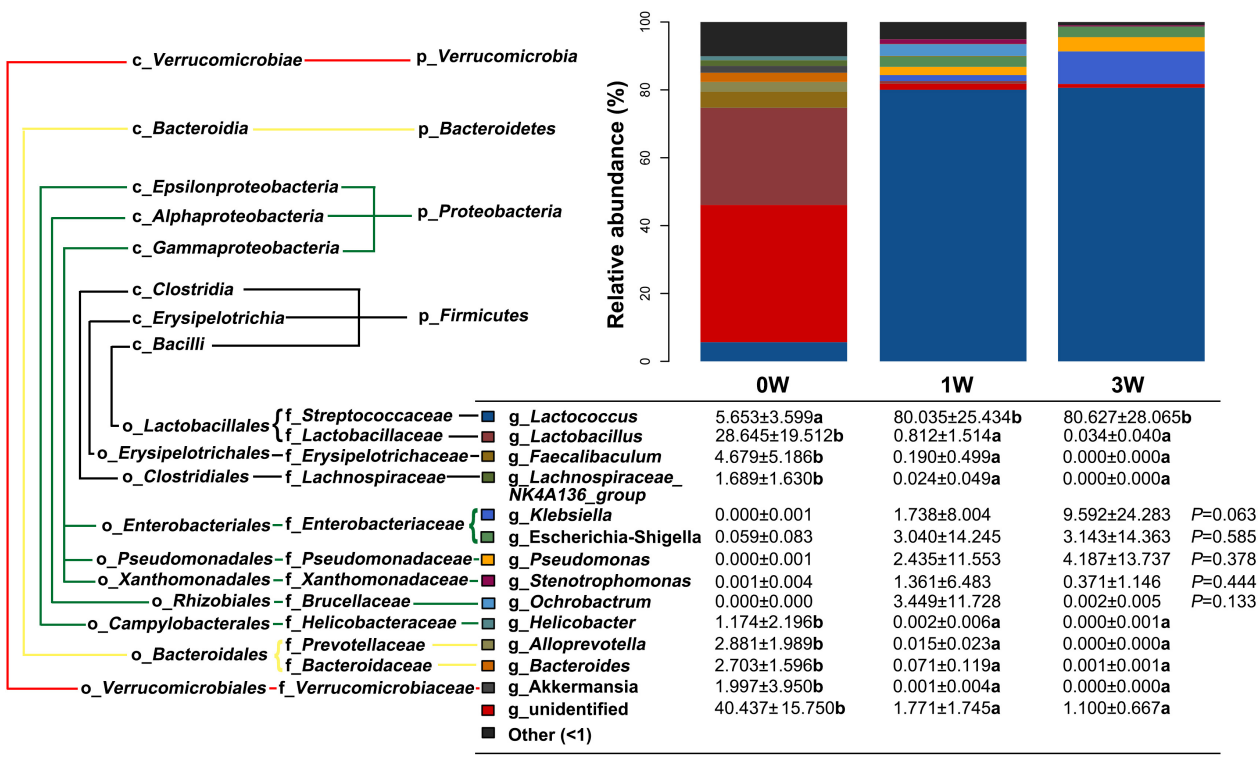

	0W	1W	3W	
g_*Lactococcus*	5.653±3.599**a**	80.035±25.434**b**	80.627±28.065**b**	
g_*Lactobacillus*	28.645±19.512**b**	0.812±1.514**a**	0.034±0.040**a**	
g_*Faecalibaculum*	4.679±5.186**b**	0.190±0.499**a**	0.000±0.000**a**	
g_*Lachnospiraceae_NK4A136_group*	1.689±1.630**b**	0.024±0.049**a**	0.000±0.000**a**	
g_*Klebsiella*	0.000±0.001	1.738±8.004	9.592±24.283	*P*=0.063
g_Escherichia-Shigella	0.059±0.083	3.040±14.245	3.143±14.363	*P*=0.585
g_*Pseudomonas*	0.000±0.001	2.435±11.553	4.187±13.737	*P*=0.378
g_*Stenotrophomonas*	0.001±0.004	1.361±6.483	0.371±1.146	*P*=0.444
g_*Ochrobactrum*	0.000±0.000	3.449±11.728	0.002±0.005	*P*=0.133
g_*Helicobacter*	1.174±2.196**b**	0.002±0.006**a**	0.000±0.001**a**	
g_*Alloprevotella*	2.881±1.989**b**	0.015±0.023**a**	0.000±0.000**a**	
g_*Bacteroides*	2.703±1.596**b**	0.071±0.119**a**	0.001±0.001**a**	
g_Akkermansia	1.997±3.950**b**	0.001±0.004**a**	0.000±0.000**a**	
g_unidentified	40.437±15.750**b**	1.771±1.745**a**	1.100±0.667**a**	
Other (<1)				

FIGURE 4 | The relative abundance of fecal microbiota at the genus level. Data represented as mean ± SD ($n = 24$). Bars with different letters differ significantly ($P < 0.05$). g_ represents microbial genus.

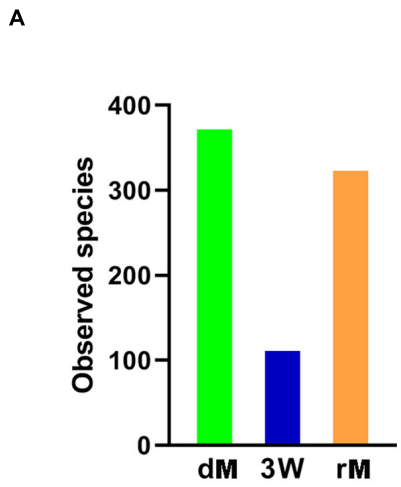

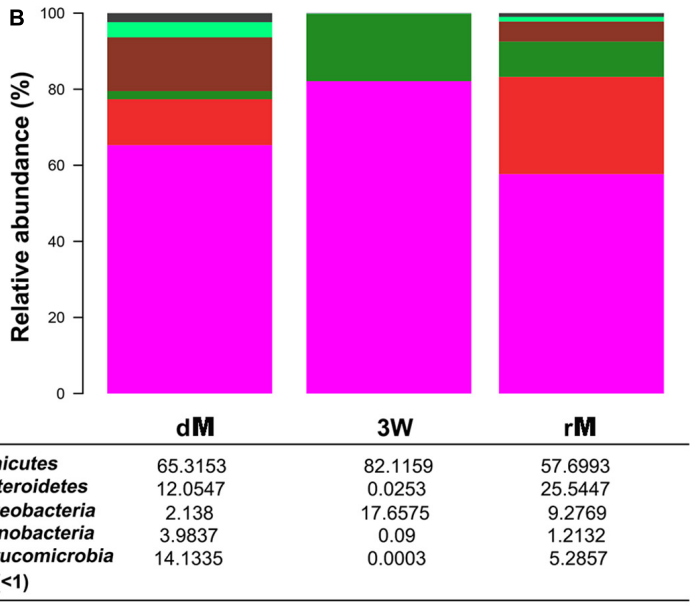

	dM	3W	rM
p_*Firmicutes*	65.3153	82.1159	57.6993
p_*Bacteroidetes*	12.0547	0.0253	25.5447
p_*Proteobacteria*	2.138	17.6575	9.2769
p_*Actinobacteria*	3.9837	0.09	1.2132
p_*Verrucomicrobia*	14.1335	0.0003	5.2857
Other (<1)			

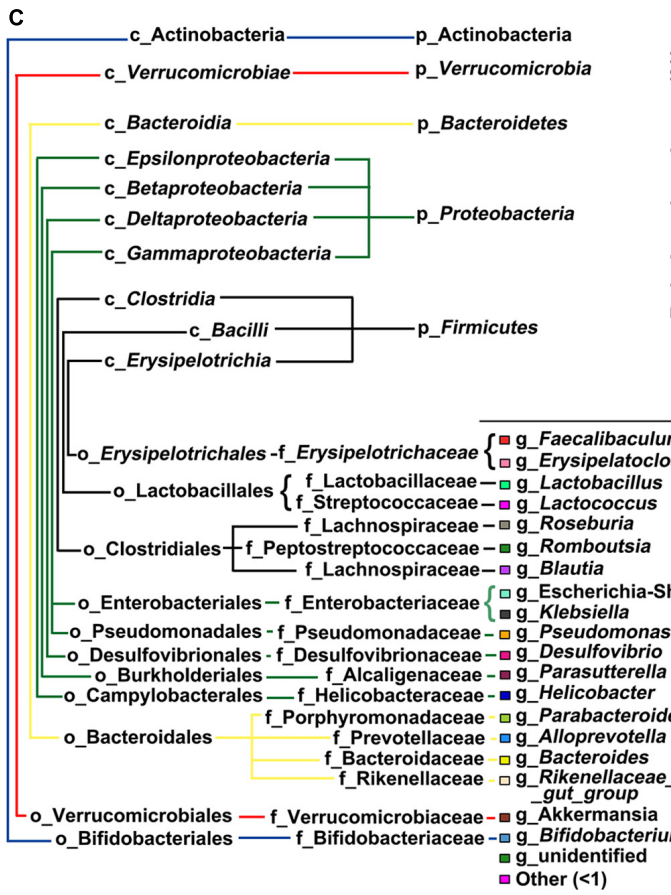

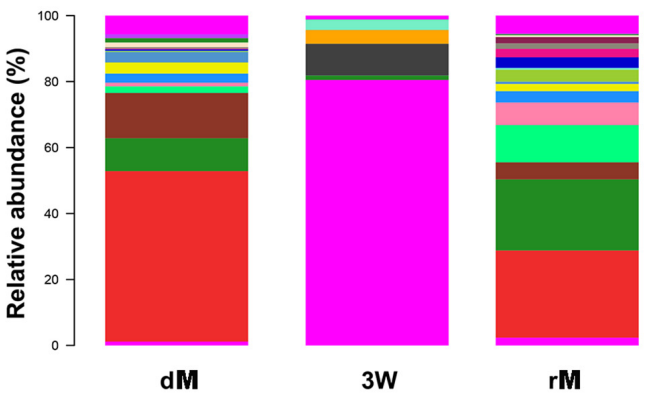

	dM	3W	rM
g_*Faecalibaculum*	51.6701	0	26.4213
g_*Erysipelatoclostridium*	1.1208	0	6.7986
g_*Lactobacillus*	2.0048	0.0348	11.2891
g_*Lactococcus*	1.1763	80.5	2.371
g_*Roseburia*	0.3995	0	1.6645
g_*Romboutsia*	1.3168	0.0354	0.3144
g_*Blautia*	1.1615	0.0143	0.2219
g_Escherichia-Shigella	0.1036	3.14	0.5437
g_*Klebsiella*	0	9.63	0.0333
g_*Pseudomonas*	0	4.18	0
g_*Desulfovibrio*	0.2219	0.0003	2.5596
g_*Parasutterella*	0.037	0	1.9308
g_*Helicobacter*	0.4735	0.0003	3.2328
g_*Parabacteroides*	0.2145	0.0006	3.5916
g_*Alloprevotella*	2.7742	0.0002	3.4474
g_*Bacteroides*	3.3401	0.0006	2.1713
g_*Rikenellaceae_RC9_gut_group*	1.413	0.0019	0.54
g_*Akkermansia*	13.7082	0	5.1785
g_*Bifidobacterium*	3.2107	0.0042	0.7176
g_unidentified	9.9834	1.29	21.5609
Other (<1)			

FIGURE 5 | The diversity and relative abundance of fecal microbiota after FMT. **(A)** Observed species of fecal microbiota among donor mice (dM), mice treated with the antibiotic cocktail for 3 weeks (3W), and receptor mice (rM). **(B)** Effect of FMT on the relative abundance of fecal microbiota at the phylum level. **(C)** Effect of FMT on the relative abundance of fecal microbiota at the genus level. dM: donor mice fed with normal diet; FMT, fecal microbiota transplantation; rM, receptor mice with FMT from dM; p_ represents microbial phylum, g_ represents microbial genus.

The Effect of Antibiotic Cocktail on Microbiota Composition at the Genus Level

Further analysis of the relative abundance of microbes at the genus level revealed that *Lactococcus*, a genus belonging to the phylum of *Firmicutes*, was increased significantly after being treated with the antibiotic cocktail for 1 or 3 weeks ($P < 0.05$), and became the dominant genus (80.63%) in the microbial community (**Figure 4**). On the other hand, *Lactobacillus*, *Faecalibaculum,* and *Lachnospiraceae_ NK4A136_group* belonging to the phylum of *Firmicutes*, *Helicobacter* belonging to the phylum of *Proteobacteria*, *Alloprevotella*, and *Bacteroides* belonging to the phylum of *Bacteroidetes*, and *Akkermansia* belonging to the phylum of *Verrucomicrobia* were decreased significantly by the antibiotic cocktail ($P < 0.05$).

Efficiency of Fecal Microbiota Transplantation on Antibiotics-Pretreated Mice

To verify whether the pretreatment of the antibiotic cocktail is effective, a further FMT experiment was conducted. As shown in **Figure 5**, the observed species in receptor mice (rM) were elevated obviously as compared with antibiotics-pretreated mice at the 3rd week (3 W). Meanwhile, the number of observed species in rM was similar to that in donor mice (dM) (**Figure 5A**). Further analysis of the composition of relative gut microbiota at phylum or genus level revealed that FMT reversed relative gut microbiota composition, with more abundant taxon as well as similar relative gut microbiota composition to dM (**Figures 5B,C**).

DISCUSSION

Driven by its amenable property, the antibiotic cocktail serves as the conventionally applicable method to deplete indigenous microbiota to make receptors obtain a susceptible status. In the present study, an antibiotic cocktail containing vancomycin (0.5 g/L), ampicillin (1 g/L), neomycin (1 g/L), and metronidazole (1 g/L) was used in the mouse model for FMT. Vancomycin and ampicillin mainly suppress gram-positive bacteria by inhibiting the synthesis of cell walls (18). Neomycin can inhibit the synthesis of protein in aerobes (19), and metronidazole can inhibit the synthesis of DNA in anaerobes (20). In this study, the observed species of indigenous microbiota were depleted by 71.94% (from 556 to 156) and 76.08% (from 556 to 133), mainly including *Bacteroidetes*, *Actinobacteria,* and *Verrucomicrobia*, after being treated with the antibiotic cocktail for 1 and 3 weeks, respectively, but recovered by the subsequent FMT with fecal microbiota from normal mice. Moreover, treatment with the cocktail increased significantly the ratio of *Firmicutes* to *Bacteroidetes*, which was similar to the results of an antibiotic cocktail containing ampicillin (1 g/L) and neomycin (0.5 g/L) for 2 weeks (21). Unexpectedly, *Lactococcus*, a genus belonging to the phylum of *Firmicutes*, dominated the gut microbiota of mice at the genus level after treating with the antibiotic cocktail either for 1 or 3 weeks. The relative abundance of *Lactobacillus* and *Akkermansia* were also decreased significantly by administrating with the antibiotic cocktail for 1 or 3 weeks, which was in accordance with previous studies (14, 22). However, the relative abundance of Proteobacteria had large individual differences in this study, while another study reported that the alpha subclass of Proteobacteria can be decreased significantly by the antibiotic cocktail (23).

Antibiotics directly target antibiotic-sensitive bacterial species and then affect other microbes owing to the dysbiosis (24). Recent studies have suggested that *Lactococcus* (such as *Lactococcus lactis subsp. lactis*) may act as the predator bacterial to exert their antibacterial property *via* the generation of bacteriocins (25), and an antibiotic cocktail of ciprofloxacin and metronidazole in drinking water *ad libitum* to mice for 2 weeks can enhance the relative abundance of *Lactococcus lactis* (26). Potentially, the antibiotic cocktail containing vancomycin, ampicillin, neomycin, and metronidazole may cause a relative increase in predators bacterial such as *Lactococcus* (25) and pro-inflammatory bacteria such as *Escherichia-Shigella* and *Klebsiella* (27), but decrease the relative abundance of anti-inflammatory bacteria such as *Akkermansia* (28) and autoimmunity-driven bacteria such as *Lactobacillus* (29), which further affect the capability of microbiota in controlling intestinal inflammation and immunity (30), with a susceptible micro-environment (31) ready for FMT.

Collectively, the antibiotic cocktail effectively depleted indigenous microbiota, and is available for the pretreatment of FMT. Nevertheless, considering the dominant genus *Lactococcus* after treatment with the antibiotic cocktail, extra data in different situations are needed to ensure disease-specific attributes of donors.

CONCLUSION

Treatment with an antibiotic cocktail containing vancomycin (0.5 g/L), ampicillin (1 g/L), neomycin (1 g/L), and metronidazole (1 g/L) in drinking water for 3 weeks eliminated microbes belonging to *Bacteroidetes*, *Actinobacteria*, and *Verrucomicrobia* in the gut microbiota of mice, and those microbes can be recovered by FMT.

DATA AVAILABILITY STATEMENT

The datasets presented in this study can be found in online repositories. The names of the repository/repositories and accession number(s) can be found in the article/ **Supplementary Material**.

ETHICS STATEMENT

The animal study was reviewed and approved by the Hunan Agricultural University Institutional Animal Care and Use Committee.

AUTHOR CONTRIBUTIONS

JT, JG, FL, BL, ZL, and JY: experimental execution. JT and SW: writing – original draft preparation. SW and JH: writing – review and editing and supervision. All authors contributed to the article and approved the submitted version.

FUNDING

We gratefully acknowledge the support from the National Natural Science Foundation of China (32102578), Key R&D Program of Hunan Province (2021NK2010), and Fellowship of China Postdoctoral Science Foundation (2021T140715 and 2021M703545), and Huxiang High-Level Talent Gathering Project of HUNAN Province (2019RS1053).

SUPPLEMENTARY MATERIAL

The Supplementary Material for this article can be found online at: https://www.frontiersin.org/articles/10.3389/fnut.2022.918098/full#supplementary-material

Supplementary Table 1 | Diet composition of mouse feed.

REFERENCES

1. Zhang XY, Chen J, Yi K, Peng L, Xie J, Gou X, et al. Phlorizin ameliorates obesity-associated endotoxemia and insulin resistance in high-fat diet-fed mice by targeting the gut microbiota and intestinal barrier integrity. *Gut Microbes.* (2020) 12:1–18. doi: 10.1080/19490976.2020.1842990
2. Zhang L, Ma X, Liu P, Ge W, Hu L, Zuo Z, et al. Treatment and mechanism of fecal microbiota transplantation in mice with experimentally induced ulcerative colitis. *Exp Biol Med.* (2021) 246:1563–75. doi: 10.1177/15353702211006044
3. Littmann ER, Lee JJ, Denny JE, Alam Z, Maslanka JR, Zarin I, et al. Host immunity modulates the efficacy of microbiota transplantation for treatment of Clostridioides difficile infection. *Nat Commun.* (2021) 12:755. doi: 10.1038/s41467-020-20793-x
4. Jing Y, Yu Y, Bai F, Wang L, Yang D, Zhang C, et al. Effect of fecal microbiota transplantation on neurological restoration in a spinal cord injury mouse model: involvement of brain-gut axis. *Microbiome.* (2021) 9:59. doi: 10.1186/s40168-021-01007-y
5. Liu L, Kirst ME, Zhao L, Li E, Wang GP. Microbiome resilience despite a profound loss of minority microbiota following clindamycin challenge in humanized gnotobiotic mice. *Microbiol Spectr.* (2022) 10:e0196021. doi: 10.1128/spectrum.01960-21
6. Staley C, Kaiser T, Beura LK, Hamilton MJ, Weingarden AR, Bobr A, et al. Stable engraftment of human microbiota into mice with a single oral gavage following antibiotic conditioning. *Microbiome.* (2017) 5:87. doi: 10.1186/s40168-017-0306-2
7. Xu J, Xu H, Peng Y, Zhao C, Zhao H, Huang W, et al. The effect of different combinations of antibiotic cocktails on mice and selection of animal models for further microbiota research. *Appl Microbiol Biotechnol.* (2021) 105:1669–81. doi: 10.1007/s00253-021-11131-2
8. Huang CE, Feng SY, Huo FJ, Liu HL. Effects of four antibiotics on the diversity of the intestinal microbiota. *Microbiol Spectr.* (2022) 10:e0190421. doi: 10.1128/spectrum.01904-21
9. Liu J, Miyake H, Zhu H, Li B, Alganabi M, Lee C, et al. Fecal microbiota transplantation by enema reduces intestinal injury in experimental necrotizing enterocolitis. *J Pediatr Surg.* (2020) 55:1094–8. doi: 10.1016/j.jpedsurg.2020.02.035
10. Luna M, Guss JD, Vasquez-Bolanos LS, Castaneda M, Rojas MV, Strong JM, et al. Components of the gut microbiome that influence bone tissue-level strength. *J Bone Miner Res.* (2021) 36:1823–34. doi: 10.1002/jbmr.4341
11. Su H, Liu J, Wu G, Long Z, Fan J, Xu Z, et al. Homeostasis of gut microbiota protects against polychlorinated biphenyl 126-induced metabolic dysfunction in liver of mice. *Sci Total Environ.* (2020) 720:137597. doi: 10.1016/j.scitotenv.2020.137597
12. Gong S, Yan Z, Liu Z, Niu M, Fang H, Li N, et al. Intestinal microbiota mediates the susceptibility to polymicrobial sepsis-induced liver injury by granisetron generation in mice. *Hepatology.* (2019) 69:1751–67. doi: 10.1002/hep.30361
13. Duan H, Yu L, Tian F, Zhai Q, Fan L, Chen W. Antibiotic-induced gut dysbiosis and barrier disruption and the potential protective strategies. *Crit Rev Food Sci Nutr.* (2020) 62:1427–52. doi: 10.1080/10408398.2020.1843396
14. Shi Y, Kellingray L, Zhai Q, Gall GL, Narbad A, Zhao J, et al. Structural and functional alterations in the microbial community and immunological consequences in a mouse model of antibiotic-induced dysbiosis. *Front Microbiol.* (2018) 9:1948. doi: 10.3389/fmicb.2018.01948
15. Isaac S, Scher JU, Djukovic A, Jimenez N, Littman DR, Abramson SB, et al. Short- and long-term effects of oral vancomycin on the human intestinal microbiota. *J Antimicrob Chemother.* (2017) 72:128–36. doi: 10.1093/jac/dkw383
16. Saxena A, Moran RRM, Bullard MR, Bondy EO, Smith MF, Morris L, et al. Sex differences in the fecal microbiome and hippocampal glial morphology following diet and antibiotic treatment. *PLoS One.* (2022) 17:e0265850. doi: 10.1371/journal.pone.0265850
17. Wu Q, Xu ZY, Song SY, Zhang H, Zhang WY, Liu LP, et al. Gut microbiota modulates stress-induced hypertension through the HPA axis. *Brain Res Bull.* (2020) 162:49–58. doi: 10.1016/j.brainresbull.2020.05.014
18. Antonoplis A, Zang X, Wegner T, Wender PA, Cegelski LA. Vancomycin-arginine conjugate inhibits growth of carbapenem-resistant e. coli and targets cell-wall synthesis. *ACS Chem Biol.* (2019) 14:2065–70. doi: 10.1021/acschembio.9b00565
19. Zuo PX, Yu PF, Alvarez Pedro JJ. Aminoglycosides antagonize bacteriophage proliferation, attenuating phage suppression of bacterial growth, biofilm formation, and antibiotic resistance. *Appl Environ Microbiol.* (2021) 87:e0046821. doi: 10.1128/AEM.00468-21
20. Meng L, Yin J, Yuan Y, Xu N. Near-infrared fluorescence probe: BSA-protected gold nanoclusters for the detection of metronidazole and related nitroimidazole derivatives. *Anal Methods.* (2017) 9:768-73. doi: 10.1039/C6AY03280J
21. Schepper JD, Collins FL, Rios-Arce ND, Raehtz S, Schaefer L, Gardinier JD, et al. Probiotic *Lactobacillus reuteri* prevents postantibiotic bone loss by reducing intestinal dysbiosis and preventing barrier disruption. *J Bone Miner Res.* (2019) 34:681–98. doi: 10.1002/jbmr.3635
22. Yin J, Wang PM, Liao SSX, Peng X, He Y, Chen YR, et al. Different dynamic patterns of b-lactams, quinolones, glycopeptides and macrolides on mouse gut microbial diversity. *PLoS One.* (2015) 10:e0126712. doi: 10.1371/journal.pone.0126712
23. Morgun A, Dzutsev A, Dong X, Greer RL, Sexton DJ, Ravel J, et al. Uncovering effects of antibiotics on the host and microbiota using transkingdom gene networks. *Gut.* (2015) 64:1732–43. doi: 10.1136/gutjnl-2014-308820
24. Croswell A, Amir E, Teggatz P, Barman M, Salzman NH. Prolonged impact of antibiotics on intestinal microbial ecology and susceptibility to enteric Salmonella infection. *Infect Immun.* (2009) 77:2741–53. doi: 10.1128/iai.00006-09
25. Juturu V, Wu JC. Microbial production of bacteriocins: latest research development and applications. *Biotechnol Adv.* (2018) 36:2187–200. doi: 10.1016/j.biotechadv.2018.10.007
26. Suez J, Zmora N, Zilberman-Schapira G, Mor U, Dori-Bachash M, Bashiardes S, et al. Post-antibiotic gut mucosal microbiome reconstitution is impaired by probiotics and improved by autologous FMT. *Cell.* (2018) 174:1406.e–23.e. doi: 10.1016/j.cell.2018.08.047
27. Trevejo-Nuñez G, Lin B, Fan L, Aggor FEY, Biswas PS, Chen K, et al. Regnase-1 deficiency restrains *Klebsiella pneumoniae* infection by regulation of a type i interferon response. *mBio.* (2022) 13:e0379221. doi: 10.1128/mbio.03792-21

28. Grajeda-Iglesias C, Durand S, Daillère R, Iribarren K, Lemaitre F, Derosa L, et al. Oral administration of *Akkermansia muciniphila* elevates systemic antiaging and anticancer metabolites. *Aging.* (2021) 13:6375–405. doi: 10.18632/aging.202739
29. Zegarra-Ruiz DF, ElBeidaq A, Iniguez AJ, Lubrano Di Ricco M, Manfredo Vieira S, Ruff WE, et al. A diet-sensitive commensal *Lactobacillus* strain mediates TLR7-dependent systemic autoimmunity. *Cell Host Microbe.* (2019) 25:113.e–27.e. doi: 10.1016/j.chom.2018.11.009
30. Strati F, Pujolassos M, Burrello C, Giuffre MR, Lattanzi G, Caprioli F, et al. Antibiotic-associated dysbiosis affects the ability of the gut microbiota to control intestinal inflammation upon fecal microbiota transplantation in experimental colitis models. *Microbiome.* (2021) 9:39. doi: 10.1186/s40168-020-00991-x
31. Shang L, Yu H, Liu H, Chen M, Zeng X, Qiao S. Recombinant antimicrobial peptide microcin J25 alleviates DSS-induced colitis via regulating intestinal barrier function and modifying gut microbiota. *Biomed Pharmacother.* (2021) 139:111127. doi: 10.1016/j.biopha.2020.111127

Conflict of Interest: The authors declare that the research was conducted in the absence of any commercial or financial relationships that could be construed as a potential conflict of interest.

frontiers | Frontiers in Nutrition

ORIGINAL RESEARCH
published: 15 June 2022
doi: 10.3389/fnut.2022.940217

Effects of Diets With Different Protein Levels on Lipid Metabolism and Gut Microbes in the Host of Different Genders

*Kaijun Wang[1,2], Xiaomin Peng[1], Anqi Yang[1], Yiqin Huang[1], Yuxiao Tan[1], Yajing Qian[1], Feifei Lv[1] and Hongbin Si[1]**

[1] State Key Laboratory for Conservation and Utilization of Subtropical Agro-bioresources, College of Animal Science and Technology, Guangxi University, Nanning, China, [2] Animal Nutritional Genome and Germplasm Innovation Research Center, College of Animal Science and Technology, Hunan Agricultural University, Changsha, China

OPEN ACCESS

Edited by:
Hui Han,
Chinese Academy of Sciences (CAS), China

Reviewed by:
Yuying Li,
Institute of Subtropical Agriculture (CAS), China
Jing Gao,
Institute of Subtropical Agriculture (CAS), China

***Correspondence:**
Hongbin Si
shb2009@gxu.edu.cn

Specialty section:
This article was submitted to Nutrition and Microbes, a section of the journal Frontiers in Nutrition

Received: 10 May 2022
Accepted: 30 May 2022
Published: 15 June 2022

Citation:
Wang K, Peng X, Yang A, Huang Y, Tan Y, Qian Y, Lv F and Si H (2022) Effects of Diets With Different Protein Levels on Lipid Metabolism and Gut Microbes in the Host of Different Genders. Front. Nutr. 9:940217. doi: 10.3389/fnut.2022.940217

The purpose of this experiment was to investigate the effects of different protein levels on lipid metabolism and gut microbes in mice of different genders. A total of 60 mice (30 female and 30 male) were randomly assigned to six groups and fed female mice with low protein diet (FLP), basal protein diet (FBD), and high protein diet (FHP). Similarly, the male mice fed with low protein diet (MLP), basal protein diet (MBD), and high protein diet (MHP). The low protein diet contained 14% CP, the basal diet contained 20% CP, and the high protein diet contained 26% CP. The results of the study showed that both basal and high protein diets significantly reduced the perirenal adipose tissues (PEAT) index in male mice compared to low protein diet ($p < 0.05$). For the gut, the FHP significantly increased the relative gut weight compared to the FBD and FLP ($p < 0.05$). At the same time, the FHP also significantly increased the relative gut length compared with the FBD and FLP ($p < 0.05$). The MHP significantly increased TC concentration compared with the MLP ($p < 0.05$), and the MBD tended to increase TC concentration compared with the MLP in serum ($p = 0.084$). The histomorphology result of the jejunum and ileum showed that a low protein diet was beneficial to the digestion and absorption of nutrients in the small intestine of mice. While different protein levels had no effect on the total number of fecal microbial species in mice, different protein levels had a significant effect on certain fecal microbes in mice, the absolute abundance of *Verrucomicrobia* in the feces of male mice was significantly higher in both high and basal protein diets than in the low protein diet ($p < 0.05$). The high protein diet significantly reduced the absolute abundance of *Patescibacteria* in the feces of female mice compared to both the basal and low protein diets ($p < 0.05$). The absolute abundance of *Patescibacteria* in male feces was not affected by dietary protein levels ($p > 0.05$). Taken together, our results suggest that a low protein diet can alter fat deposition and lipid metabolism in mice, and that it benefited small intestinal epithelial structure and microbes.

Keywords: protein, lipid, gut, bacterial community, microbiota

INTRODUCTION

Nutrients are essential elements for maintaining health in all living organisms. Various nutrient regulatory systems exist between different organisms in order to correctly sense the nutrient environment in which they live (1). Normally, when a shortage/excess of each nutrient is detected in body tissues, some specific signaling pathways are activated, and then responsive metabolic responses are triggered (1). Protein is one of the most important nutrients, as nearly half of the dry weight of the mammalian body is made up of proteins with an incredible variety of biological functions (2). Obesity has become a major public health problem in China. In the most recent national survey, more than half of Chinese adults were overweight or obese, according to criteria for the Chinese population (3). Overweight and obesity were responsible for 11.1% of non-communicable disease (NCDs) related deaths in 2019, an increase of 5.7% from 1990 (4). These circumstances also lead to substantial health expenditures by countries to manage NCDs (5). While overweight and obesity are rapidly increasing, China has also undergone social, economic and environmental transformations. Lifestyle factors such as eating habits and physical activity have changed dramatically (6, 7). Weight loss is a major goal of reducing the risk of diabetes in humans (8). One study suggested a low-fat diet and energy restriction for obesity prevention and weight loss, but a high-protein diet is a popular alternative (9). Traditional weight loss strategies typically advise overweight and obese individuals to reduce fat intake to reduce energy intake by 500–750 calories (10). However, a high protein diet can firstly increase the body's satiety and also increase energy expenditure, so it has become an alternative to energy restriction for weight loss (11–13).

It should be noted that the long-term effects of high protein diet, especially when combined with high fat diet, remain controversial (14). The results of systematic reviews and meta-analyses suggest that the long-term efficiency of high protein diet to induce weight loss in humans is uncertain unless dietary intervention is combined with energy restriction (15–17). While human trials have examined the ability of the high protein diet to induce weight loss in obese patients, the effects of the high protein diet in rodents were primarily conducted in preventing the development of obesity. In order to study the complex relationship between host and microbes in general, it is crucial to better understand the interactions between host and gut microbes. This can be achieved by measuring the molecules that contribute to this interaction, especially the metabolites formed by the microbiota that are available for uptake by the host. Gut microbes play key roles in animal health, including digestion of food, metabolism, regulation of immunity, and defense against invading pathogens (18–20). Many animal experiments have reported that high fat/high protein diet can effectively reduce or even prevent the development of obesity (21–26), but the ability of high protein diet to reverse obesity in rodents and its effects on fat metabolism and changes in gut microbes are far from clear. The current global obesity epidemic requires effective weight loss strategies in addition to effective methods to prevent weight gain.

The low protein diet is critical for addressing environmental concerns and conserving protein resources, but their impact on the gut microenvironment is not fully understood. Given the popularity of high protein diet, we here aimed to investigate whether diets with different protein levels can affect lipid metabolism in mice. Furthermore, we explored whether the improvement of lipid metabolism at different protein levels also affected gut microbes. Using mice as a model, it is possible to systematically study the importance of different protein levels on fat metabolism in mice, and to evaluate the possible harmful or beneficial effects of diets with different protein levels on intestinal tissue structure.

MATERIALS AND METHODS

Animals and Dietary Treatments

The studies were approved by the Laboratory Animal Welfare and Animal Experimental Ethical Inspection Committee at the Guangxi University (Nanning, China).

Four-week-old male C57 mice (specific pathogen-free) were purchased from SLAC Laboratory Animal Central (Changsha, China). After a 1-week adaptation period, the mice were housed in a controlled environment (temperature: 25 ± 2°C, relative humidity: 45–60%, and a 12-h light–dark cycle), with free access to food and drinking water during the experiment. The diet of mice was mainly composed of corn, soybean meal, beer yeast, casein and lard. The low protein diet contained 14% CP, the basal diet contained 20% CP, and the high protein diet contained 26% CP. A total of 30 male mice of similar weight were randomly grouped into the low protein diet (MLP), basic diet (MBD), and high protein diet (MHP). Similarly, 30 female mice of similar weight were randomly grouped into the low protein diet (FLP), basic diet (FBD), and high protein diet (FHP). Throughout the experiment, the body weight of mice was measured weekly for 4 weeks. Fecal samples were collected and stored at −80°C until further analysis. At the end of the experiment, all mice were fasted overnight and killed by cervical dislocation with sodium pentobarbital anesthesia, and all efforts were made to minimize suffering. After killing, blood, subcutaneous adipose tissues (SAT), abdominal adipose tissues (AAT), perirenal adipose tissues (PEAT), liver, jejunum, ileum, and fecal contents were collected for further analyses.

Analysis of Biochemical Parameters in Blood Samples

Serum samples were separated after centrifugation at 3,000 rpm for 10 min at 4°C. An automatic biochemistry analyzer was used to test serum biochemical parameters (27), including total cholesterol (TC, 2021061K), high density lipoprotein (HDL, 2021061K), low density lipoprotein (LDL, 2021061K) and triglycerides (TG, 2021051K).

Histology Analysis

The jejunal and ileal tissues were removed and fixed in 4% formaldehyde solution, after which the fixed tissues were

paraffin-embedded and the jejunal and ileal tissues blocks were cut into 5 μm sections, and stained with hematoxylin and eosin. In the present study, we used the pre-defined method which was reported to define the lesion (28). In each section, villus height (VH) and crypt depth (CD) were measured using a light microscope with a computer-assisted morphometric system. VH was defined as the distance from the villus tip to the crypt mouth, and CD from the crypt mouth to the base.

Microbiota Analysis

Total genome DNA from fecal samples was extracted for amplification using a specific primer with a barcode (16S V3–V4). Sequencing libraries were generated and analyzed according to our previous study (29).

Statistical Analyses

Statistical analyses between the means of each group were analyzed by using one-way ANOVA (one-way analysis of variance) followed by Duncan comparison range tests through SPSS 22.0. Statistical significance was set at $p < 0.05$.

RESULTS

Body, Adipose Tissue, and Gut Weight or Length

As shown in **Figure 1**, the three different ratios of protein had no significant effect on the final body weight of male mice ($p > 0.05$). At the same time, the different levels of protein had no significant effect on body weight of female mice ($p > 0.05$). Although different ratios of protein had no significant effect on SAT and AAT indexes in female and male mice, both MBD and MHP significantly reduced the PEAT index compared to MLP ($p < 0.05$). There was no significant effect on liver index of female and male mice by protein ratios ($p > 0.05$). For the gut, the high protein diet significantly increased the relative gut weight of female mice compared to the basal and low protein diets ($p < 0.05$). At the same time, the high protein diet also significantly increased the relative gut length of female mice compared with the basal and low protein diets ($p < 0.05$). However, different levels of protein concentration diet had no significant effect on the relative weight and relative length of gut to male mice. Furthermore, there was no significant difference in gut length between female and male mice between diets with different protein levels ($p > 0.05$).

Lipid Metabolism Index in Serum

As shown in **Figure 2**, the FHP tended to increase serum TC concentration compared with the FLP ($p = 0.083$). However, the MHP significantly increased TC concentration compared with the MLP ($p < 0.05$), and the MBD tended to increase TC concentration compared with the MLP in serum ($p = 0.084$). Although diets with different protein levels in female mice had no significant effect on serum TG concentrations ($p > 0.05$), however, the MBD significantly increased the content of TG in serum compared with the MLP ($p < 0.05$). The FLP resulted in significantly higher serum HDL than the FBD and FHP ($p < 0.05$), whereas both the FHP and FBD significantly increased serum LDL level in female mice ($p < 0.05$). Different levels of protein diets did not significantly alter serum HDL and LDL levels in male mice ($p > 0.05$).

Histomorphological Analysis of Small Intestine

The jejunal tissue morphology under three different dietary treatments to female and male mice was shown in **Figure 3**. According to our study, jejunal villus length decreased with increasing dietary protein levels in both male and female mice, and a high protein diet resulted in a significantly lower jejunal villus length than a low protein diet ($p < 0.05$). In female mice, both the basal diet and the high protein diet significantly increased CD in the jejunum ($p < 0.05$), while the three dietary treatments had no effect on CD in male mice ($p > 0.05$). With the increase of dietary protein level, the ratio of jejunal villus length to CD (L/D) decreased in female mice, and the L/D ratio of basal diet and high protein diet was significantly lower than that of low protein diet ($p < 0.05$). The results for male mice showed that increased protein levels led to a decrease in jejunal L/D, but the difference was not significant ($p > 0.05$). The jejunal villus width of the FLP was significantly lower than that of the FBD ($p < 0.001$) and the FBD was significantly higher than that of the FHP ($p < 0.05$), and the protein concentration had no effect on the villus width of the male mice ($p > 0.05$). The number of jejunal goblet cells on the FBD was significantly lower than that on the FLP and FHP ($p < 0.05$), and the number of jejunal goblet cells in male mice also tended to be higher on the low protein diet than on the basal diet ($p = 0.082$). The high protein diet resulted in significantly lower jejunal villus area in female mice than on the basal diet ($p < 0.05$), while the high protein diet in male mice resulted in significantly lower jejunal villus area than the low protein diet ($p < 0.05$).

The ileal tissue morphology under three different dietary treatments to female and male mice was shown in **Figure 4**. In this study, the ileal villus length significantly decreased in high protein diet than low protein diet for male mice ($p < 0.05$), and three protein diets had no significantly difference on villus length of female mice ($p > 0.05$). In female mice, the FBD significantly increased CD in the ileum compared with the FLP ($p < 0.05$), while the MBD tended to decreased CD than MLP in the ileum of male mice ($p = 0.079$). With the increase of dietary protein level, the ratio of ileal L/D decreased in female mice, and the L/D ratio of basal diet and high protein diet was significantly lower than that of low protein diet ($p < 0.05$). The results for male mice showed that various protein level diets had no significant difference on ileal L/D ($p > 0.05$). The ileal villus width of the MBD was significantly higher than that of the MLP ($p < 0.05$), and the MBD tended to increase the ileal villus width than that of the MHP in male mice ($p = 0.054$). The protein concentration had no effect on the ileal villus width of the female mice ($p > 0.05$). The number of ileal goblet cells on the FBD was significantly higher than that on the FLP ($p < 0.05$), and the number of ileal goblet cells in male mice had no significant difference between the

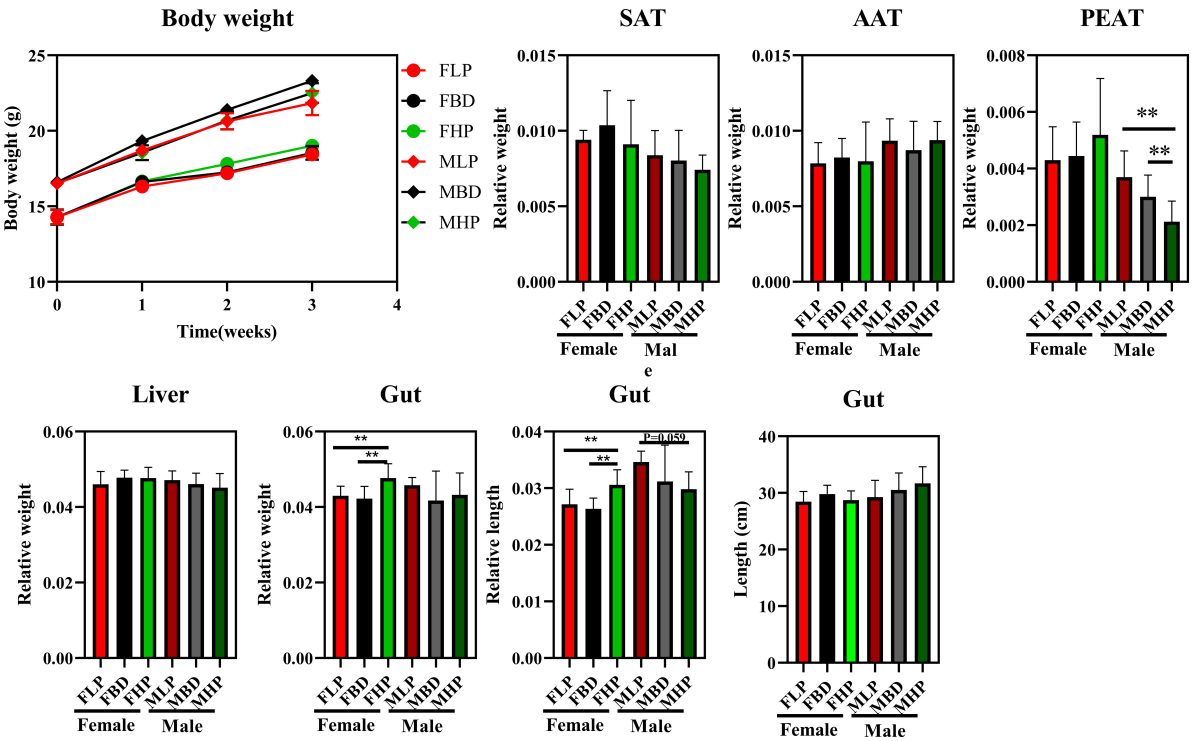

FIGURE 1 | Effects of diets with different protein levels on body weight, lipid accumulation, liver weight and gut appearance in mice.

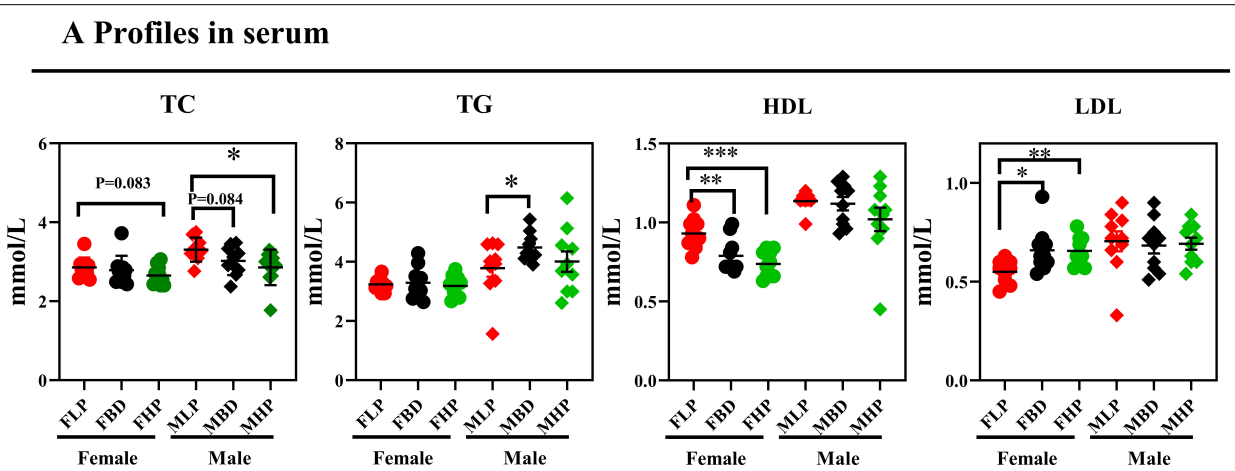

FIGURE 2 | Effects of diets with different protein levels on serum lipid levels in mice.

low and high protein diet in female mice ($p > 0.05$). Meanwhile, different levels of protein diet had no effect on the number of goblet cells in the ileum of male mice ($p > 0.05$). Finally, different levels of protein diet had no significant effect on ileal villus area in both female and male mice ($p > 0.05$).

Fecal Bacterial α and β Diversity

The fecal bacterial α diversity in male and female mice with different levels of protein diets was shown in **Figure 5A**. The results showed that the FBD tended to reduce observed species compared to the FLP ($p = 0.068$), while no significant difference was found between the high protein diet and the other two groups ($p > 0.05$). There were no significant differences in fecal observed species in male mice fed the diets of the three protein levels ($p > 0.05$). The low protein diet significantly increased the Shannon index compared with the basal diet in female mice ($p < 0.05$), while the high protein diet did not produce significant differences with the other two groups on Shannon index in female mice ($p > 0.05$). In the fecal bacteria of male mice, the MLP significantly increased the

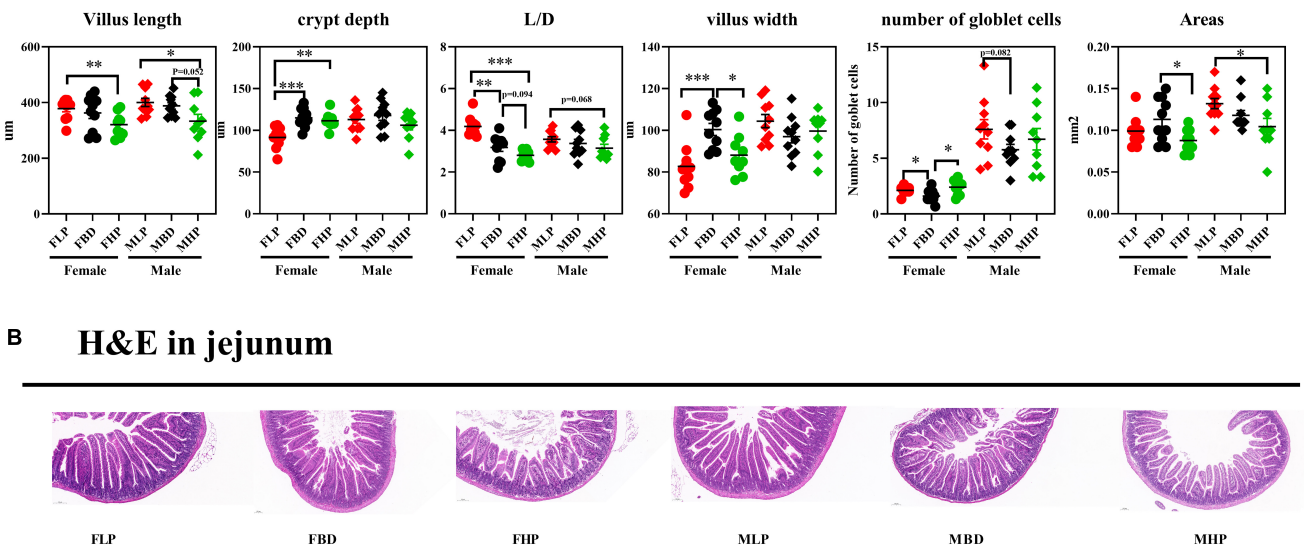

FIGURE 3 | Effects of diets with different protein levels on the morphology of jejunal epithelial tissue in mice. **(A)** The structure of the jejunal epithelial tissue. **(B)** Light microscopy cross-section of jejunal tissue.

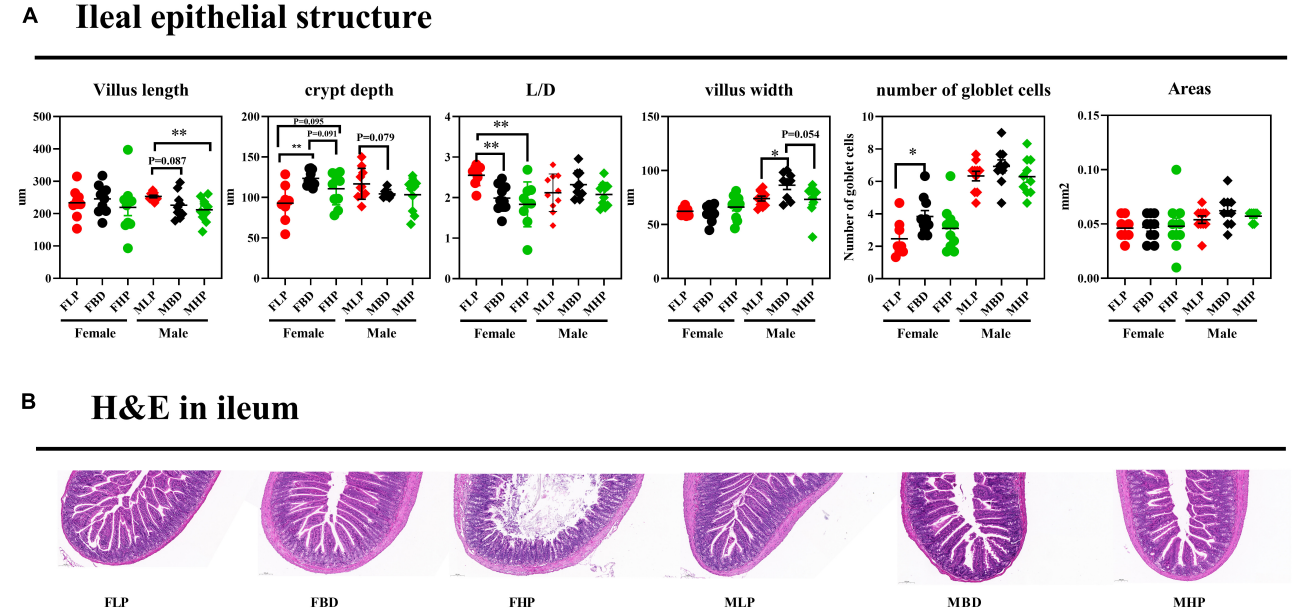

FIGURE 4 | Effects of diets with different protein levels on the morphology of ileal epithelial tissue in mice. **(A)** The structure of the ileal epithelial tissue. **(B)** Light microscopy cross-section of ileal tissue.

Shannon index of bacteria compared to the MBD ($p < 0.05$), while the MHP showed a trend to increase the Shannon index compared to the MBD ($p = 0.055$). The high protein diet significantly improved Simpson index over basal diet in female mice ($p < 0.05$), whereas high protein diets over basal diets tended to increase Simpson index in male mice ($p = 0.051$). At the same time, the low protein diet also significantly improved the Simpson index in male mice compared to the basal diet ($p < 0.05$). There were no significant differences in the fecal bacterial chao1 index and PD_whole_tree between the three diets in either female or male mice ($p > 0.05$). As shown in **Figure 5B**, the principal components of female mice were similar between the different protein levels and did not produce significant separation. In male mice, however, there was a

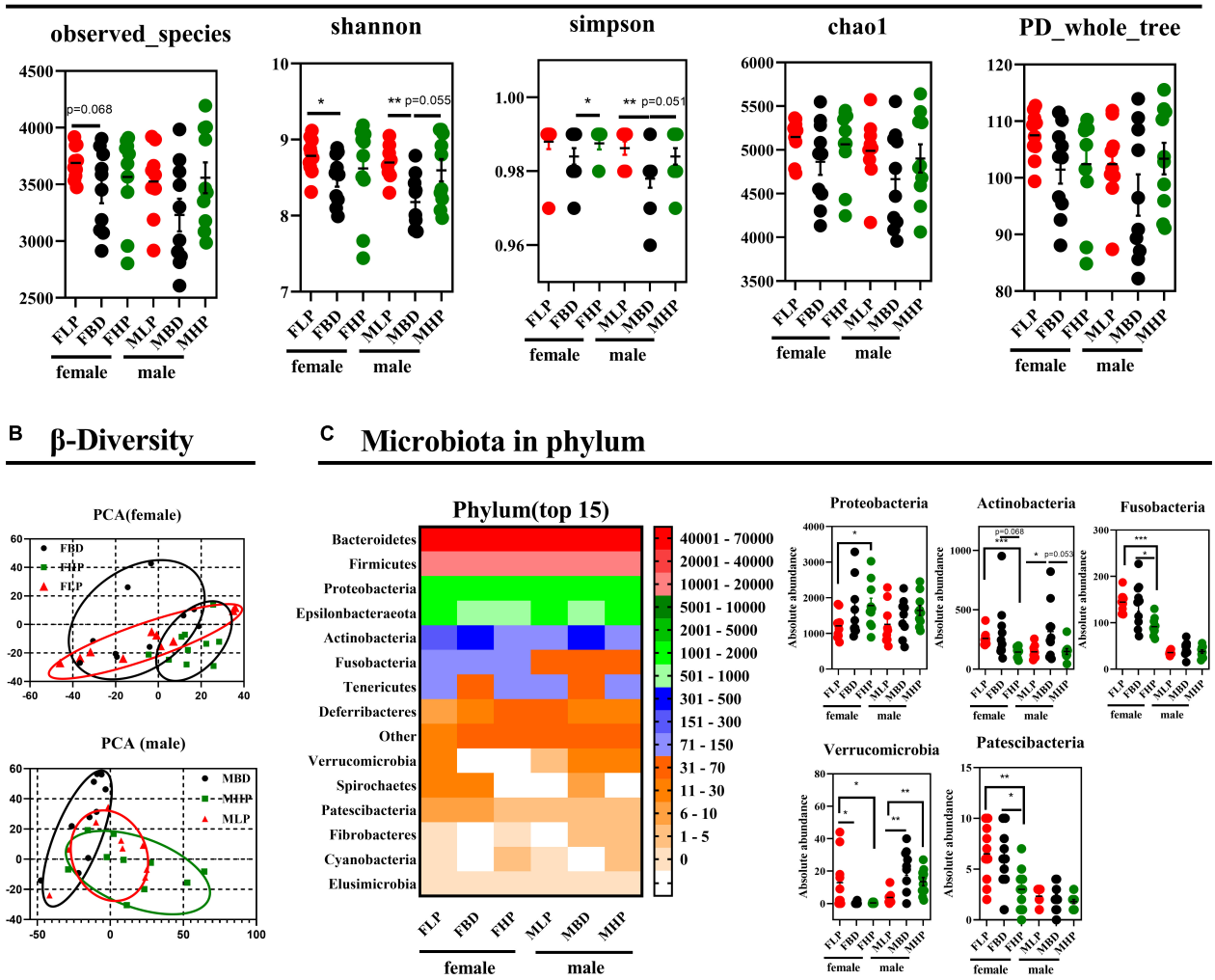

FIGURE 5 | Effects of diets with different protein levels on **(A)** α diversity, **(B)** β diversity, and **(C)** phylum-level bacteria in the fecal microbiota of mice.

distinctly different cluster of microbiomes between the basal and high protein diets.

Diets With Different Protein Levels Affect Fecal Microbiota Composition

The bacterial effects of different protein levels on the top 15 bacteria at the phylum level of the fecal microbiota of male and female mice were shown in **Figure 5C**. The high protein diet significantly increased the absolute abundance of *Proteobacteria* in the feces of female mice compared to the low protein diet ($p < 0.05$). The abundance of *Proteobacteria* did not make a difference in male feces ($p > 0.05$). In contrast, the high protein diet significantly reduced the absolute abundance of *Actinobacteria* in the feces of female mice compared to the low protein diet ($p < 0.05$). The abundance of *Actinobacteria* in the feces of female mice tended to decrease in the high protein diet compared with the basal protein diet ($p = 0.068$). Furthermore, the high protein diet significantly reduced the absolute abundance of *Fusobacteria* in the feces of female mice compared to the low and basal protein diet ($p < 0.05$). The absolute abundance of *Fusobacteria* in male mice was not affected by dietary protein levels ($p > 0.05$). In addition, both high protein and basal protein diets significantly reduced the absolute abundance of *Verrucomicrobia* in the feces of female mice compared to low protein diets ($p < 0.05$). Conversely, the absolute abundance of *Verrucomicrobia* in the feces of male mice was significantly higher in both high and basal protein diets than in the low protein diet ($p < 0.05$). The high protein diet significantly reduced the absolute abundance of *Patescibacteria* in the feces of female mice compared to both the basal and low protein diets ($p < 0.05$). The absolute abundance of *Patescibacteria* in male feces was not affected by dietary protein levels ($p > 0.05$).

Downward to species level (**Figure 6**), we found that 17 out of 30 species were markedly changed throughout the entire stage.

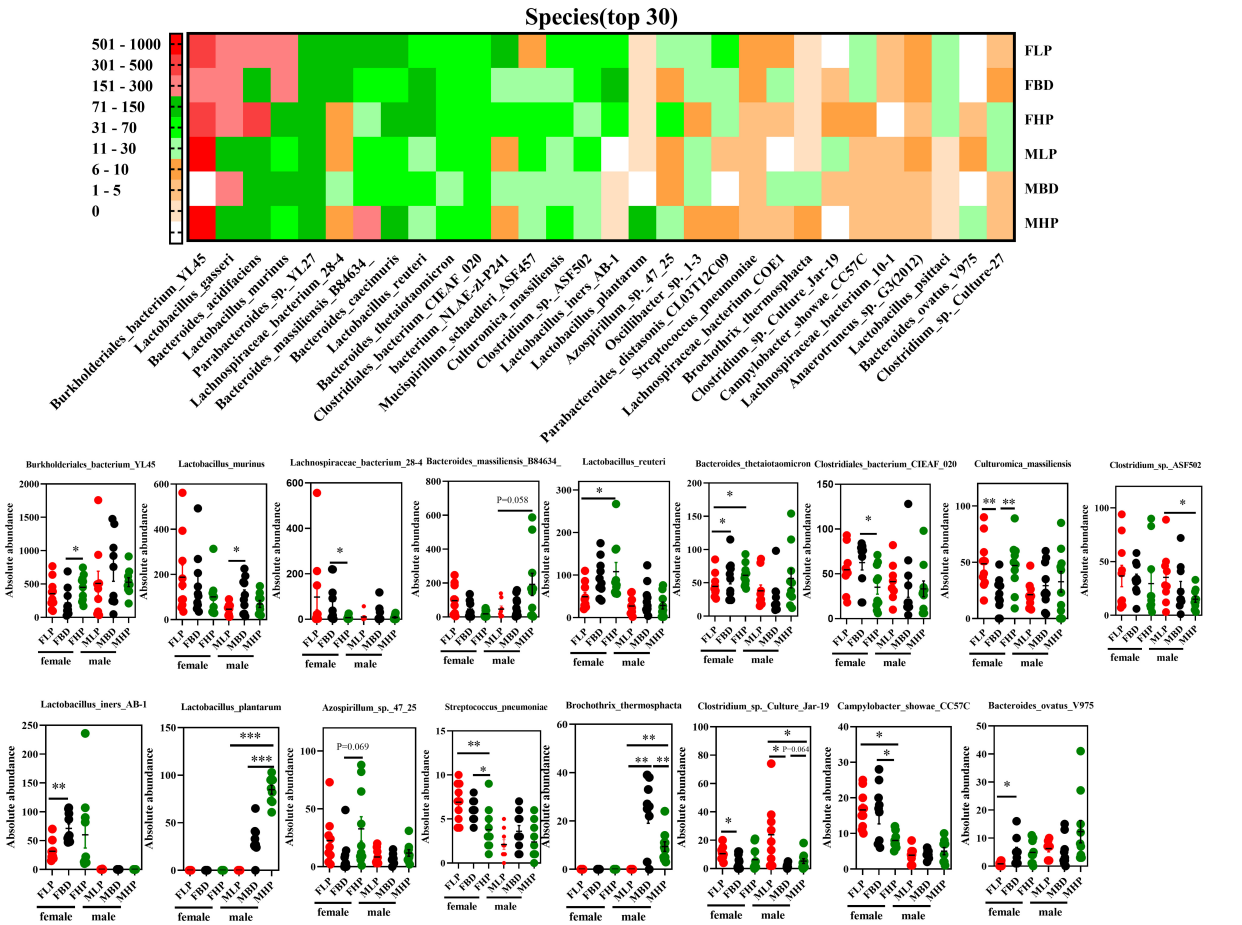

FIGURE 6 | Effects of diets with different protein levels on species-level bacteria in the fecal microbiota of mice.

The high protein diet of female mice significantly increased the absolute abundances of *Burkholderiales_bacterium*_YL45 and *Culturomica_massiliensis* ($p < 0.05$), but significantly decreased the absolute abundances of *Lachnospiraceae_bacterium*_28-4, *Clostridiales_bacterium_CIEAF*_020, *Streptococcus_pneumoniae* and *Campylobacter_showae*_CC57C compared with the basal diet ($p < 0.05$). At the same time, the abundance of *Azospirillum_sp.*_47_25 has an upward trend in the high protein diet compared with the basal diet in the feces of female mice ($p = 0.069$). However, the abundances of *Lactobacillus_murinus*, *Bacteroides_massiliensis*_B84634_, *Clostridium_sp.*_ASF502, *Lactobacillus_plantarum* and *Brochothrix_thermosphacta* in female mice feces were not affected by protein levels ($p > 0.05$). In the fecal microbiota of male mice, a high protein diet significantly increased the absolute abundances of *Lactobacillus_plantarum* and *Brochothrix_thermosphacta* ($p < 0.05$), but significantly decreased the absolute abundances of *Clostridium_sp.*_ASF502 and *Clostridium_sp._Culture*_Jar-19 compared with a low protein diet ($p < 0.05$). In addition, the high protein diet tended to increase *Clostridium_sp._Culture*_Jar-19 abundance in male mice feces compared to basal protein diet ($p = 0.064$). And in male mice fecal microbiota, the absolute abundances of *Burkholderiales_bacterium*_YL45, *Lachnospiraceae_bacterium*_28-4, *Lactobacillus_reuteri*, *Bacteroides_thetaiotaomicron*, *Clostridiales_bacterium_CIEAF*_020, *Culturomica_massiliensis*, *Lactobacillus_iners_AB*-1, *Azospirillum_sp.*_47_25, *Streptococcus_pneumoniae*, *Campylobacter_ showae*_CC57C, and *Bacteroides_ovatus*_V975 were not affected by dietary protein levels ($p > 0.05$).

DISCUSSION

In this study, female and male mice were used as experimental models to investigate the effects of different levels of protein diets on fat deposition, fecal microbiota, and small intestinal tissue structure in mice. Studies have shown that dietary protein played a role in regulating lipid biological synthesis. In some rodents' research, genes participating in new fat production and lipid storage such as PPARγ (21), ACC (21, 30), FASN (21, 30),

SCD1 (31), and SREBP1c (31, 32) were reduced by intake of HP diet. Compared with LP diet, the HP diet fat intake and lipid biological synthetic genes were lower. The HP diet reduces liver fat more effectively than the LP diet (33). For example, in mice and human research, the HP diet has proven to increase energy consumption, reduce blood glucose levels, promote fat oxidation, thereby supporting weight loss, and reducing liver fat (34–37). The HP diet may inhibit liver fat production at the molecular level to reduce liver fat (21, 22, 38). The relatively lower carbohydrate content in the HP diet may also be part of the cause of new fat production and reduced intrahepatic fat. In addition, compared with fat-generating genes, in several rats' research, dietary protein intake has not changed the expression of genes related to lipid oxidation or substrate oxidation (30, 32). Our results showed that the HP diet is significantly reduced in the perirenal fat more than the LP and the basic diet. The reason may be that the fat intake and lipid biological synthesis may be inhibited.

The biochemical indicators of the body's blood can not only feedback the health of the host and the strength of immune function, but also reveal the biological characteristics of different hosts (39). When the level of TC in the host's blood rises, hypertrophymia will occur. Compared with LDL, HDL level may lead to this situation (40). Some researchers have compared the influence of LP and HP diets on obesity and their related diseases. One of the main discoveries in the system summary was that the HP solution has a favorable impact on TG and HDL (16). This was consistent with the results of the HP diet in our research reduced the HDL in the female blood. The HP diet reduced TC and HDL, but LDL has increased, indicating that the lipid metabolism in the blood has changed. These data are very important for preventing hyperlipidemia and heart and liver disease (41).

Different parts of the digestive tract assume different responsibilities. The small intestine was the key place for the host to absorb nutrients. The height of villi and the depth of crypts in the small intestine were important indicators to evaluate its digestion and absorption function. The CD reflects the speed of cell formation, while shallower crypts indicate that the cell maturity was accelerated and the secretion function is enhanced. The VH and CD could fully reflect the functional state of the small intestine (42). In the present study, jejunal villus length decreased and CD increased after mice were fed the HP diet, suggesting that the HP diet may have a potential adverse effect on jejunal function. Since the small intestine surface area (represented by the tight villus packing and long villus protrusions) showed the maximum nutrient absorption allowed (43), the reduced ratio of VH to CD in the jejunum and ileum of the HP group diet indicated nutrient absorption reduce. Crypts were where ISCs were synthesized and amplifying cells were transported, and CD could also reflect the proliferation of intestinal epithelial cells. In the present study, an increase in jejunal CD with increasing protein levels in the diet showed the possibility of intestinal epithelial proliferation, whereas an increase in epithelial proliferation with increasing protein levels in the ileum occurred only in the FLP and FBD groups. The intestinal epithelial barrier in animals was initiated by the ISC niche, which develops differentiated cell types, including Paneth cells and goblet cells (44). The increase in goblet cells in the FBD group indicated the possibility of ISC proliferation in the ileum. Thus, the microbiota in the FBD group than in the FLP group may have stimulated ISCs, improved ileal barrier function, and was supported by an increase in Lactobacillus, which has been reported to stimulate intestinal epithelial cell proliferation through Nox-mediated reactive oxygen species production (45).

Dietary protein was an essential nutrient for animals and it was necessary for the physiological functions of organs. The structural integrity of the gut and the homeostasis of the gut microbiota ensure the chemical induction and digestive functions of the gut, which were prerequisites for nutrient absorption, metabolism, and deposition. The gut microbiota was considered a key factor in maintaining gut function (46, 47), it was a complex ecosystem with nearly 100 trillion microorganisms, most of which were bacteria (48). Many factors influenced gut microbiota composition and activity, including diet, environment, and age; of these, diet was the most important (49–51). Diet played a crucial role in shaping the composition of animal gut microbiota and the state of immune responses mediated by gut microbiota (52). We explored the effect of diets with different protein levels on fecal microbial diversity in mice. In the present study, it can be concluded that the fecal community diversity of mice on a low protein diet was higher than that on a basal diet and a high protein diet, but it was observed that different protein levels had no effect on the total fecal microbial population in mice. The microbiome consists of trillions of microbial cells with high inter- and intra-species variability, so it was difficult to define a healthy gut microbiome based on the species in the gut (53, 54). However, the variability of microbial functional genes and metabolites may be low (54, 55). An increased ratio of *Firmicutes* to *Bacteroides* has been reported in obese animals (56) and was associated with host energy intake (57, 58). Some researchers have shown that the composition of different microbial communities in the digestive tract of animals was different, and the diversity and density of microbial communities gradually increased from the stomach to the hindgut (59). For the ileal microbiota, the reduced *Enterobacteriaceae* within the *Proteobacteria* phylum were thought to contain many pathogenic bacteria when dietary protein decreased by 3 percentage points (60), suggesting the potential for pathogen suppression by moderate dietary protein restriction. The *Streptococcus* and *Escherichia-Shigella* can cause a variety of infections and diseases, such as scarlet fever and bacillary dysentery (61, 62). In this study, different protein level diets had no difference in *Escherichia-Shigella* of female and male mice. Research by NEIS et al. showed that when the concentration of diet protein is reduced by 3 percentage points, the number of *Streptococcus* and *Escherichia-Shigella* declined in the ileum, and the *Streptococcus* participated in the use of amino acids (63). Therefore, the decline of link bacteria such as *Streptococcus_pneumoniae* in feces of FHP diet, it can be explained as insufficient protein substrates required for fermentation, which was consistent with previous research (64, 65). The *Lactobacillus* bacteria in the intestine could ferment the carbohydrates in the diet into lactic acid and improved the intestinal environment (66, 67). The elevation of *Lactobacillus_plantarum* and *Lactobacillus_reuteri* in the high

protein diet in this study fitted this situation. An increasing on *Lactobacillus_murinus* and *Lactobacillus_iners*_AB-1 in the basal diet compared to the low protein diet may be because the carbohydrates in the basal diet were higher than the low protein diet, but the two bacteria were decreased in the high protein diet. It may be that the high protein diet weakened the intestinal barrier function. Chen et al. used pigs as an experimental model to show that the abundance of *Lachnospiraceae*, which was saccharolytic and can degrade cellulose, was increased in low protein diet (68). This was consistent with our findings that the high protein diet reduced *Lachnospiraceae_bacterium*_28-4 in the feces of female mice compared to the basal diet. Therefore, according to the results of this study, a low protein diet was more beneficial to the gut microbiome.

CONCLUSION

In conclusion, this study demonstrated that diets with different protein levels can affect lipid deposition and lipid metabolism in mice. At the same time, a high protein diet weakened the small intestinal barrier structure, which weakened the host's ability to digest and absorb nutrients. Although different protein levels had no effect on the total number of fecal microbial species in mice, different protein levels had significant effects on the structure of some fecal microbiota in mice. The reduction of *Lactobacillus_murinus* and *Lactobacillus_iners*_AB-1 on the low protein diet due to higher carbohydrates in the basal diet than the low protein diet. Besides, the high protein diet reduced *Lachnospiraceae_bacterium*_28-4 in the feces of female mice compared to the basal diet. Our study provided a more comprehensive understanding of lipid metabolism, gut barrier and fecal microbial response to diets at different protein levels in female and male mice.

DATA AVAILABILITY STATEMENT

The original contributions presented in the study are included in the article/supplementary material, further inquiries can be directed to the corresponding author.

ETHICS STATEMENT

The studies were approved by the Laboratory Animal Welfare and Animal Experimental Ethical Inspection Committee at the Guangxi University (Nanning, China).

AUTHOR CONTRIBUTIONS

KW and HS designed the experiment. KW conducted the experiment and wrote the manuscript. KW, XP, AY, YH, YT, YQ, and FL collected and analyzed the data. HS revised the manuscript. All authors contributed to the article and approved the submitted version.

FUNDING

This research was supported by a grant from the Science and Technology Major Project of Guangxi (China) (No. AA17204057) and the Key Research and Development Plan of Guangxi (China) (No. AB19245037).

REFERENCES

1. Chantranupong L, Wolfson RL, Sabatini DM. Nutrient-sensing mechanisms across evolution. *Cell.* (2015) 161:67–83. doi: 10.1016/j.cell.2015.02.041
2. Forbes RM, Cooper AR, Mitchell HH. The composition of the adult human body as determined by chemical analysis. *J Biol Chem.* (1953) 203:359–66.
3. The State Council Information Office of the People's Republic of China. *Press briefing for the Report on Chinese Residents' Chronic Diseases and Nutrition 2020*. (2020). Available online at: http://www.gov.cn/xinwen/2020-12/24/content_5572983.htm (accessed December 26, 2020).
4. Institute for Health Metrics and Evaluation. *Global Health Data Exchange. GBD Results Tool.* (2021). Available online at: http://ghdx.healthdata.org/gbd-results-tool (accessed January 10, 2021).
5. Qin X, Pan J. The medical cost attributable to obesity and overweight in China: estimation based on longitudinal surveys. *Health Econom.* (2016) 25:1291–311. doi: 10.1002/hec.3217
6. Popkin BM. Synthesis and implications: China's nutrition transition in the context of changes across other low- and middle-income countries. *Obes Rev.* (2014) 15:60–7. doi: 10.1111/obr.12120
7. Du SF, Wang HJ, Zhang B, Zhai FY, Popkin BM. China in the period of transition from scarcity and extensive undernutrition to emerging nutrition-related non-communicable diseases, 1949-1992. *Obes Rev.* (2014) 15:8–15. doi: 10.1111/obr.12122
8. Hamman RF, Wing RR, Edelstein SL, Lachin JM, Bray GA, Delahanty L, et al. Effect of weight loss with lifestyle intervention on risk of diabetes. *Diab Care.* (2006) 29:2102–7. doi: 10.2337/dc06-0560
9. Myrmel LS, Fauske KR, Fjære E, Bernhard A, Liisberg U, Hasselberg AE, et al. The impact of different animal-derived protein sources on adiposity and glucose homeostasis during ad libitum feeding and energy restriction in already obese mice. *Nutrients.* (2019) 11:11051153. doi: 10.3390/nu11051153
10. Koliaki C, Spinos T, Spinou M, Brinia ME, Mitsopoulou D, Katsilambros N. Defining the optimal dietary approach for safe, effective and sustainable weight loss in overweight and obese adults. *Healthcare.* (2018) 6:73. doi: 10.3390/healthcare6030073
11. Madsen L, Myrmel LS, Fjære E, Øyen J, Kristiansen K. Dietary proteins, brown fat, and adiposity. *Front Physiol.* (2018) 9:1792. doi: 10.3389/fphys.2018.01792
12. Pesta DH, Samuel VT. A high-protein diet for reducing body fat: mechanisms and possible caveats. *Nutrit Metabol.* (2014) 11:53. doi: 10.1186/1743-7075-11-53
13. Westerterp-Plantenga MS. Protein intake and energy balance. *Regulat Peptides.* (2008) 149:67–9. doi: 10.1016/j.regpep.2007.08.026
14. Cuenca-Sánchez M, Navas-Carrillo D, Orenes-Piñero E. Controversies surrounding high-protein diet intake: satiating effect and kidney and bone health. *Adv Nutrit.* (2015) 6:260–6. doi: 10.3945/an.114.007716
15. Lepe M, Bacardí Gascón M, Jiménez Cruz A. Long-term efficacy of high-protein diets: a systematic review. *Nutric Hospital.* (2011) 26:1256–9. doi: 10.1590/s0212-16112011000600010
16. Santesso N, Akl EA, Bianchi M, Mente A, Mustafa R, Heels-Ansdell D, et al. Effects of higher-versus lower-protein diets on health outcomes: a systematic review and meta-analysis. *Eur J Clin Nutrit.* (2012) 66:780–8. doi: 10.1038/ejcn.2012.37

17. Wycherley TP, Moran LJ, Clifton PM, Noakes M, Brinkworth GD. Effects of energy-restricted high-protein, low-fat compared with standard-protein, low-fat diets: a meta-analysis of randomized controlled trials. *Am J Clin Nutrit.* (2012) 96:1281–98. doi: 10.3945/ajcn.112.044321
18. Wang K, Peng X, Lv F, Zheng M, Long D, Mao H, et al. Microbiome-metabolites analysis reveals unhealthy alterations in the gut microbiota but improved meat quality with a high-rice diet challenge in a small ruminant model. *Animals.* (2021) 11:2306. doi: 10.3390/ani11082306
19. Sun J, Wang K, Xu B, Peng X, Chai B, Nong S, et al. Use of hydrolyzed Chinese gallnut tannic acid in weaned piglets as an alternative to zinc oxide: overview on the gut microbiota. *Animals.* (2021) 11:2000. doi: 10.3390/ani11072000
20. Cani PD, Delzenne NM. The role of the gut microbiota in energy metabolism and metabolic disease. *Curr Pharmaceut Design.* (2009) 15:1546–58. doi: 10.2174/138161209788168164
21. Freudenberg A, Petzke KJ, Klaus S. Comparison of high-protein diets and leucine supplementation in the prevention of metabolic syndrome and related disorders in mice. *J Nutrit Biochem.* (2012) 23:1524–30. doi: 10.1016/j.jnutbio.2011.10.005
22. Freudenberg A, Petzke KJ, Klaus S. Dietary l-leucine and l-alanine supplementation have similar acute effects in the prevention of high-fat diet-induced obesity. *Amino Acids.* (2013) 44:519–28. doi: 10.1007/s00726-012-1363-2
23. Kiilerich P, Myrmel LS, Fjære E, Hao Q, Hugenholtz F, Sonne SB, et al. Effect of a long-term high-protein diet on survival, obesity development, and gut microbiota in mice. *Am J Physiol Endocrinol Metab.* (2016) 310:E886–99. doi: 10.1152/ajpendo.00363.2015
24. Marsset-Baglieri A, Fromentin G, Tomé D, Bensaid A, Makkarios L, Even PC. Increasing the protein content in a carbohydrate-free diet enhances fat loss during 35% but not 75% energy restriction in rats. *J Nutrit.* (2004) 134:2646–52. doi: 10.1093/jn/134.10.2646
25. McAllan L, Skuse P, Cotter PD, O'Connor P, Cryan JF, Ross RP, et al. Protein quality and the protein to carbohydrate ratio within a high fat diet influences energy balance and the gut microbiota in C57BL/6J mice. *PLoS One.* (2014) 9:e88904. doi: 10.1371/journal.pone.0088904
26. Pichon L, Huneau JF, Fromentin G, Tomé D. A high-protein, high-fat, carbohydrate-free diet reduces energy intake, hepatic lipogenesis, and adiposity in rats. *J Nutrit.* (2006) 136:1256–60. doi: 10.1093/jn/136.5.1256
27. Gao J, Ma L, Yin J, Liu G, Ma J, Xia S, et al. Camellia (Camellia oleifera bel.) seed oil reprograms gut microbiota and alleviates lipid accumulation in high fat-fed mice through the mTOR pathway. *Food Funct.* (2022) 13:4977–92. doi: 10.1039/d1fo04075h
28. Wang KJ, Yan QX, Ren A, Zheng ML, Zhang PH, Tan ZL, et al. Novel linkages between bacterial composition of hindgut and host metabolic responses to sara induced by high-paddy diet in young goats. *Front Vet Sci.* (2022) 8:791482. doi: 10.3389/fvets.2021.791482
29. Yin J, Han H, Li Y, Liu Z, Zhao Y, Fang R, et al. Lysine restriction affects feed intake and amino acid metabolism via gut microbiome in piglets. *Cell Physiol Biochem.* (2017) 44:1749–61. doi: 10.1159/000485782
30. Stepien M, Gaudichon C, Fromentin G, Even P, Tomé D, Azzout-Marniche D. Increasing protein at the expense of carbohydrate in the diet down-regulates glucose utilization as glucose sparing effect in rats. *PLoS One.* (2011) 6:e14664. doi: 10.1371/journal.pone.0014664
31. Noguchi Y, Nishikata N, Shikata N, Kimura Y, Aleman JO, Young JD, et al. Ketogenic essential amino acids modulate lipid synthetic pathways and prevent hepatic steatosis in mice. *PLoS One.* (2010) 5:e12057. doi: 10.1371/journal.pone.0012057
32. Chaumontet C, Even PC, Schwarz J, Simonin-Foucault A, Piedcoq J, Fromentin G, et al. High dietary protein decreases fat deposition induced by high-fat and high-sucrose diet in rats. *Br J Nutrit.* (2015) 114:1132–42. doi: 10.1017/s000711451500238x
33. Xu C, Markova M, Seebeck N, Loft A, Hornemann S, Gantert T, et al. High-protein diet more effectively reduces hepatic fat than low-protein diet despite lower autophagy and FGF21 levels. *Liver Int.* (2020) 40:2982–97. doi: 10.1111/liv.14596
34. Markova M, Pivovarova O, Hornemann S, Sucher S, Frahnow T, Wegner K, et al. Isocaloric diets high in animal or plant protein reduce liver fat and inflammation in individuals with type 2 diabetes. *Gastroenterology.* (2017) 152:571.e–85.e. doi: 10.1053/j.gastro.2016.10.007
35. Benjaminov O, Beglaibter N, Gindy L, Spivak H, Singer P, Wienberg M, et al. The effect of a low-carbohydrate diet on the nonalcoholic fatty liver in morbidly obese patients before bariatric surgery. *Surg Endosc.* (2007) 21:1423–7. doi: 10.1007/s00464-006-9182-8
36. Bortolotti M, Maiolo E, Corazza M, Van Dijke E, Schneiter P, Boss A, et al. Effects of a whey protein supplementation on intrahepatocellular lipids in obese female patients. *Clin Nutrit.* (2011) 30:494–8. doi: 10.1016/j.clnu.2011.01.006
37. Arslanow A, Teutsch M, Walle H, Grünhage F, Lammert F, Stokes CS. Short-term hypocaloric high-fiber and high-protein diet improves hepatic steatosis assessed by controlled attenuation parameter. *Clin Transl Gastroenterol.* (2016) 7:e176. doi: 10.1038/ctg.2016.28
38. Petzke KJ, Freudenberg A, Klaus S. Beyond the role of dietary protein and amino acids in the prevention of diet-induced obesity. *Int J Mol Sci.* (2014) 15:1374–91. doi: 10.3390/ijms15011374
39. Chen C, Yang B, Zeng Z, Yang H, Liu C, Ren J, et al. Genetic dissection of blood lipid traits by integrating genome-wide association study and gene expression profiling in a porcine model. *BMC Genom.* (2013) 14:848. doi: 10.1186/1471-2164-14-848
40. Abd El-Gawad IA, El-Sayed EM, Hafez SA, El-Zeini HM, Saleh FA. The hypocholesterolaemic effect of milk yoghurt and soy-yoghurt containing bifidobacteria in rats fed on a cholesterol-enriched diet. *Int Dairy J.* (2005) 15:37–44. doi: 10.1016/j.idairyj.2004.06.001
41. Abdel-Maksoud M, Sazonov V, Gutkin SW, Hokanson JE. Effects of modifying triglycerides and triglyceride-rich lipoproteins on cardiovascular outcomes. *J Cardiovasc Pharmacol.* (2008) 51:331–51. doi: 10.1097/FJC.0b013e318165e2e7
42. Rieger J, Janczyk P, Hünigen H, Neumann K, Plendl J. Intraepithelial lymphocyte numbers and histomorphological parameters in the porcine gut after Enterococcus faecium NCIMB 10415 feeding in a *Salmonella* Typhimurium challenge. *Vet Immunol Immunopathol.* (2015) 164:40–50. doi: 10.1016/j.vetimm.2014.12.013
43. Shyer AE, Huycke TR, Lee CH, Mahadevan L, Tabin CJ. Bending gradients: how the intestinal stem cell gets its home. *Cell.* (2015) 161:569–80. doi: 10.1016/j.cell.2015.03.041
44. Peterson LW, Artis D. Intestinal epithelial cells: regulators of barrier function and immune homeostasis. *Nat Rev Immunol.* (2014) 14:141–53. doi: 10.1038/nri3608
45. Jones RM, Luo L, Ardita CS, Richardson AN, Kwon YM, Mercante JW, et al. Symbiotic lactobacilli stimulate gut epithelial proliferation via Nox-mediated generation of reactive oxygen species. *Embo J.* (2013) 32:3017–28. doi: 10.1038/emboj.2013.224
46. Sczesnak A, Segata N, Qin X, Gevers D, Petrosino JF, Huttenhower C, et al. The genome of Th17 cell-inducing segmented filamentous bacteria reveals extensive auxotrophy and adaptations to the intestinal environment. *Cell Host Microbe.* (2011) 10:260–72. doi: 10.1016/j.chom.2011.08.005
47. Chen J, Li Y, Tian Y, Huang C, Li D, Zhong Q, et al. interaction between microbes and host intestinal health: modulation by dietary nutrients and gut-brain-endocrine-immune axis. *Curr Protein Pept Sci.* (2015) 16:592–603. doi: 10.2174/1389203716666150630135720
48. Collins SM, Surette M, Bercik P. The interplay between the intestinal microbiota and the brain. *Nat Rev Microbiol.* (2012) 10:735–42. doi: 10.1038/nrmicro2876
49. Fan P, Li L, Rezaei A, Eslamfam S, Che D, Ma X. Metabolites of dietary protein and peptides by intestinal microbes and their impacts on gut. *Curr Protein Pept Sci.* (2015) 16:646–54. doi: 10.2174/1389203716666150630133657
50. Sonnenburg ED, Smits SA, Tikhonov M, Higginbottom SK, Wingreen NS, Sonnenburg JL. Diet-induced extinctions in the gut microbiota compound over generations. *Nature.* (2016) 529:212–5. doi: 10.1038/nature16504
51. Ma N, Tian Y, Wu Y, Ma X. Contributions of the interaction between dietary protein and gut microbiota to intestinal health. *Curr Protein Pept Sci.* (2017) 18:795–808. doi: 10.2174/1389203718666170216153505
52. Saresella M, Mendozzi L, Rossi V, Mazzali F, Piancone F, LaRosa F, et al. Immunological and clinical effect of diet modulation of the gut microbiome in multiple sclerosis patients: a pilot study. *Front Immunol.* (2017) 8:1391. doi: 10.3389/fimmu.2017.01391
53. Nguyen TL, Vieira-Silva S, Liston A, Raes J. How informative is the mouse for human gut microbiota research? *Dis Models Mechanisms.* (2015) 8:1–16. doi: 10.1242/dmm.017400

54. Sender R, Fuchs S, Milo R. Revised estimates for the number of human and bacteria cells in the body. *PLoS Biol.* (2016) 14:e1002533. doi: 10.1371/journal.pbio.1002533
55. McCoy KD, Geuking MB, Ronchi F. Gut microbiome standardization in control and experimental mice. *Curr Protoc Immunol.* (2017) 117:21–3. doi: 10.1002/cpim.25
56. Bäckhed F, Ding H, Wang T, Lora VH, Gou YK, Nagy A, et al. The gut microbiota as an environmental factor that regulates fat storage. *PNAS.* (2004) 101:15718–23. doi: 10.1073/pnas.0407076101
57. Cottenie K. Integrating environmental and spatial processes in ecological community dynamics. *Ecol Lett.* (2005) 8:1175–82. doi: 10.1111/j.1461-0248.2005.00820.x
58. Ley RE, Turnbaugh PJ, Lein SK, Gordon JI. Human gut microbes associated with obesity. *Nature.* (2006) 444:1022–3. doi: 10.1038/4441022a
59. Hooper LV, Wong MH, Thelin A, Hansson L, Falk PG, Gordon JI. Molecular analysis of commensal host-microbial relationships in the intestine. *Science.* (2001) 291:881–4. doi: 10.1126/science.291.5505.881
60. Lv LX, Fang DQ, Shi D, Chen DY, Yan R, Zhu YX, et al. Alterations and correlations of the gut microbiome, metabolism and immunity in patients with primary biliary cirrhosis. *Environ Microbiol.* (2016) 18:2272–86. doi: 10.1111/1462-2920.13401
61. Davies MR, Holden MT, Coupland P, Chen JHK, Venturini C, Barnett TC, et al. Emergence of scarlet fever Streptococcus pyogenes emm12 clones in Hong Kong is associated with toxin acquisition and multidrug resistance. *Nat Genet.* (2015) 47:84–7. doi: 10.1038/ng.3147
62. Pop M, Walker AW, Paulson J, Lindsay B, Antonio M, Hossain MA, et al. Diarrhea in young children from low-income countries leads to large-scale alterations in intestinal microbiota composition. *Genome Biol.* (2014) 15:R76. doi: 10.1186/gb-2014-15-6-r76
63. Neis E, Dejong C, Rensen S. The role of microbial amino acid metabolism in host metabolism. *Nutrients.* (2015) 7:7042930. doi: 10.3390/nu7042930
64. Zhou LP, Fang LD, Sun Y, Su Y, Zhu WY. Effects of the dietary protein level on the microbial composition and metabolomic profile in the hindgut of the pig. *Anaerobe.* (2016) 38:61–9. doi: 10.1016/j.anaerobe.2015.12.009
65. Fan PX, Liu P, Song PX, Chen XY, Ma X. Moderate dietary protein restriction alters the composition of gut microbiota and improves ileal barrier function in adult pig model. *Sci Rep.* (2017) 7:43412. doi: 10.1038/srep43412
66. Kleerebezem M, Boekhorst J, van Kranenburg R, Molenaar D, Oscar PK, Leer R, et al. Complete genome sequence of Lactobacillus plantarum WCFS1. *PNAS.* (2003) 100:1990–5. doi: 10.1073/pnas.0337704100
67. Fukuda S, Toh H, Hase K, Oshima K, Nakanishi Y, Yoshimura K, et al. Bifidobacteria can protect from enteropathogenic infection through production of acetate. *Nature.* (2011) 469:543–7. doi: 10.1038/nature09646
68. Chen XY, Song PX, Fan PX, He T, Jacobs D, Levesque CL, et al. Moderate dietary protein restriction optimized gut microbiota and mucosal barrier in growing pig model. *Front Cell Infect Microbiol.* (2018) 8:246. doi: 10.3389/fcimb.2018.00246

Conflict of Interest: The authors declare that the research was conducted in the absence of any commercial or financial relationships that could be construed as a potential conflict of interest.

frontiers | Frontiers in Nutrition

ORIGINAL RESEARCH
published: 30 June 2022
doi: 10.3389/fnut.2022.947367

Lactobacillus plantarum Alleviates Obesity by Altering the Composition of the Gut Microbiota in High-Fat Diet-Fed Mice

*Yong Ma, Yanquan Fei, Xuebing Han, Gang Liu and Jun Fang**

Hunan Provincial Engineering Research Center of Applied Microbial Resources Development for Livestock and Poultry, College of Bioscience and Biotechnology, Hunan Agricultural University, Changsha, China

Metabolic disorders and intestinal flora imbalance usually accompany obesity. Due to its diverse biological activities, *Lactobacillus plantarum* is widely used to alleviate various diseases as a probiotic. Here, we show that *L. plantarum* can reduce the body weight of mice fed high-fat diets, reduce fat accumulation, and enhance mice glucose tolerance. Our results show that *L. plantarum* can significantly reduce the expression of DGAT1 and DGAT2, increase the expression of Cpt1a, and promote the process of lipid metabolism. Further data show that *L. plantarum* can increase the SCFA content in the colon and reverse the intestinal flora disorder caused by HFD, increase the abundance of *Bacteroides*, and *Bifidobacteriales*, and reduce the abundance of *Firmicutes* and *Clostridiales*. Finally, through Pearson correlation analysis, we found that *Bacteroides* and SCFAs are positively correlated, while *Clostridiales* are negatively correlated with SCFAs. Therefore, we believe that *L. plantarum* can regulate the structure of the intestinal microbial community, increase the production of SCFAs and thus regulate lipid metabolism.

Keywords: high fat diet, *Lactobacillus plantarum*, SCFA, fat metabolism, intestinal microbes

OPEN ACCESS

Edited by:
Yong Su,
Nanjing Agricultural University, China

Reviewed by:
Shunqing Liang,
University of Massachusetts Medical School, United States
Shuwei Xie,
University of Nebraska Medical Center, United States

****Correspondence:***
Jun Fang
fangjun1973@hunau.edu.cn

Specialty section:
This article was submitted to Nutrition and Microbes, a section of the journal Frontiers in Nutrition

Received: *18 May 2022*
Accepted: *10 June 2022*
Published: *30 June 2022*

Citation:
Ma Y, Fei Y, Han X, Liu G and Fang J (2022) Lactobacillus plantarum Alleviates Obesity by Altering the Composition of the Gut Microbiota in High-Fat Diet-Fed Mice. Front. Nutr. 9:947367. doi: 10.3389/fnut.2022.947367

INTRODUCTION

Accumulating evidence points a high-fat diet will increase the potential risk of metabolic diseases (1). Long-term excessive intake of high-energy foods can lead to the accumulation of fat, which can lead to obesity. Obesity and the development of metabolic disorders have caused great troubles for the world health security authorities. According to the World Health Organization, over the past 30 years, more than 9 million children have been considered overweight in the world (https://www.who.int/zh). According to the U.S. Centers for Disease Control and Prevention, the national obesity rate from 2017 to 2018 was 42.4% (https://www.cdc.gov/obesity/data/adult.html). The obesity caused by this long-term high-fat diet will further cause metabolic diseases such as diabetes and non-alcoholic fatty liver (2, 3). Most importantly, HFD-induced obesity is usually accompanied by changes in the structure of the gut microbial community (4), and gut microbes are a vital part of the host's energy intake (5). This reduction in gut microbial diversity and changes in the abundance of specific microorganisms may be determinants of lipid metabolism and obesity. Intestinal microbes are involved in the process from lipid synthesis and absorption to lipid metabolism in obesity (6).

This also causes obesity to be accompanied by changes in the intestinal microbial community. The dominance of *Bacteroides* in normal individuals is caused by the fact that *Bacteroides* can ferment the dietary fiber that the host cannot digest and absorb for energy. However, when fat accumulates, this microorganism community will change, and the abundance of *Firmicutes* will increase significantly in obese hosts (7). Changes in the community structure of intestinal microbes can alter the secretion of intestinal hormones, including peptide YY, GLP-1, leptin, and weaken their effects of inhibiting gastric emptying, reducing appetite, and increasing satiety (8).

With a deep understanding of intestinal microbes, the mechanism of action of probiotics and host flora has been well known by people. Probiotics can produce anti-pathogenic microbial products, which are biologically compatible with the host or interact directly with the host's immune cells, regulate host metabolism, etc. (9). As a probiotic, *Lactobacillus plantarum* has been used to treat and alleviate various diseases due to its diversified functions (10). Through genome-wide association analysis and non-targeted metabolomics analysis, Mao et al. found that *L. plantarum* and its metabolites can significantly increase the level of the neurotransmitter γ-aminobutyric acid in the hippocampus (11). *L. plantarum* has shown an irreplaceable role in intestinal health. *L. plantarum* can activate PPAR-α and restore the structure of mitochondria and ultimately repair the intestinal barrier (12). Further studies have found that bacteriocin, a metabolite of *L. plantarum*, can prevent the loss of Caco-2 cell transcellular permeability and inhibit the expression of inflammatory factors (13). Salomé-Desnoulez et al. developed fluorescent *L. plantarum* strains to track and monitor its dynamic role in intestinal inflammation and found that *L. plantarum* mainly colonizes the intestinal lumen and mucous layer and directly acts on damaged epithelial cells (14). Recent experiments have shown that most of the probiotics acting on the intestine can inhibit obesity, so we suspect that *L. plantarum*, with multiple biological activities, plays an essential role in lipid metabolism.

MATERIALS AND METHODS

Animal and Experimental Design

This animal experiment completely follows the Guidelines for Care and Use of Laboratory Animals of Hunan Agricultural University. Twenty-four 8-week-old C57BL/6J mice [purchased from Hunan Sileike Jingda Co (Changsha, China)] with an average weight of 18 g were acclimated for 7 days in a sterile environment. They were divided into three groups with 8 mice in each group by completely random allocation. The first group was treated with the basal diet (CON), the second group was treated with high-fat diet (HFD), and the third group was treated with *L. plantarum* and high-fat diet (HFD-LP). During the experiment, mice can drink and eat freely. In 1–4 weeks, the HFD group and HFD-LP group were fed with high-fat diets. We administered *L. plantarum* (1×10^8 cfu) to mice in the HFD-LP group for 5–8 weeks, and the other two groups were administered the same dose of normal saline (**Figure 1A**). Collection of mice epididymal adipose tissue: the mouse testis was found in the lower abdomen and lifted with tweezers. The white fat attached to it was epididymal fat and stripped along the vas deferens to the end of the testis. Inguinal fat: Inguinal fat was cut bluntly between the skin and muscle of the hind limb of mice with ophthalmic scissors, and the skin was capped at the tip of the scissors to avoid cutting off subcutaneous fat. Then the skin was longitudinally cut to expose the inguinal fat, the inguinal lymph nodes were stripped, and the adipose tissue was cut off. Perirenal fat: The kidney was lifted with tweezers and all adipose tissues were cut off along the surface of the renal fascia. All adipose tissues were weighed using a one-tenth balance. Serum samples were collected for serologic analysis. Liver tissue, intestinal contents, and mouse faces were collected and immediately snap-frozen in liquid nitrogen, then transferred and stored in a −80° refrigerator.

Glucose and Insulin Tolerance Tests

The intraperitoneal glucose tolerance test (IPGTT) was performed after the mice were fasted for 6 h. Each mouse was injected intraperitoneally with glucose (2 g/kg body weight), and the blood glucose of the mice tail vein was measured with a blood glucose meter for the next 0, 15, 30, 60, and 120 min. The insulin tolerance test (ITT) was performed after the mice were fasted for 6 h. Each mouse was injected intraperitoneally with insulin (0.75 U/kg body weight), and the blood glucose of the mice tail vein was measured with a blood glucose meter for the next 0, 15, 30, 60, and 120 min.

Fat Histopathology

Use gradient concentration of xylene and ethanol solution to dehydrate and transparent adipose tissue. Embed the tissue block with melted paraffin, slice the wax block and stain it with Hematoxylin and Eosin, finally use alcohol for dehydration, and add neutral gum to mount the slide.

Serologic Analysis

The content of alanine aminotransferase, aspartate aminotransferase, blood glucose, and triglyceride, high-density lipoprotein and low-density lipoprotein (n=8) was measured using kits and a microplate reader (14041717, VT, United States).

Real-Time Fluorescence-Based Quantitative PCR

Take the liver tissue and grind it with liquid nitrogen, grind it into powder, transfer it into a 1.5 ml EP tube and mix with 1 ml Trizol, and centrifuge at 12,000 g for 10 min at 4°C. Add 120 ul of chloroform to the supernatant, centrifuge for 15 min at 4°C and 1,200 r, take 300 ul of supernatant into another centrifuge tube, add an equal volume of isopropanol to the supernatant, centrifuge at 4°C, 1,000 r for 10 min, remove the supernatant, add 600 ul of 75% ethanol to wash the precipitate, centrifuge at 8,000 r, 4°C for 10 min, remove the ethanol, add an appropriate amount of DNAase Free Water, and use a reverse transcription kit (gDNA Eraser) for reverse transcription. The resulting cDNA was analyzed by conducting the real-time quantitative polymerase chain reaction with a SuperReal PreMix Plus (SYBR Green) reagent kit (TIANGEN, Beijing, China) with various primers (**Table 1**).

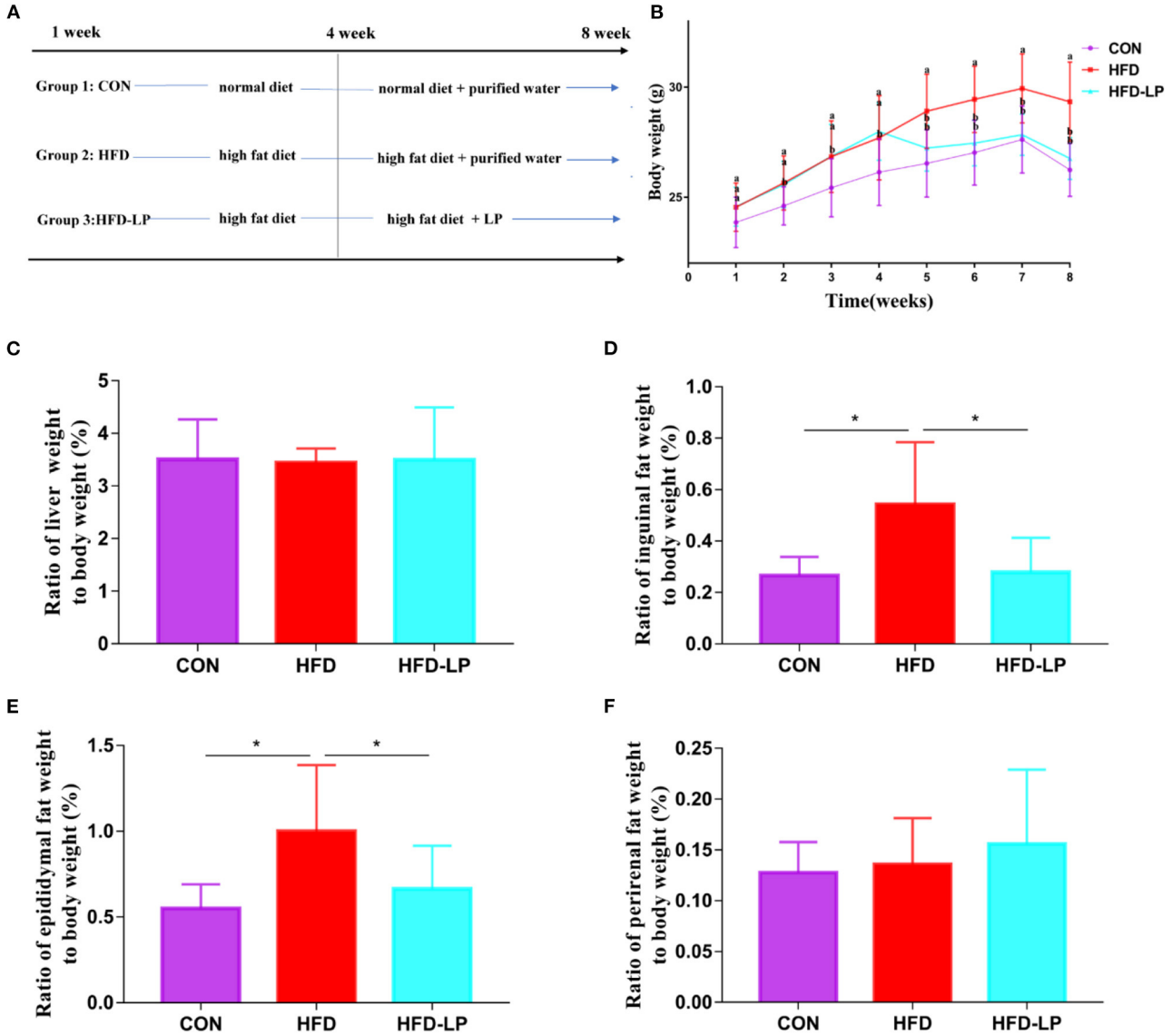

FIGURE 1 | Effect of *Lactobacillus plantarum* on body weight, fat and internal organs of obese mice. **(A)** the experimental process; **(B)** the body weight; **(C)** the ratio of liver weight to body weight; **(D)** the ratio of Inguinal fat weight to body weight; **(E)** the ratio of Epididymis fat weight to body weight; **(F)** the ratio of perirenal fat weight to body weight. Data are mean ± SD ($n = 8$) and analyzed by one-way ANOVA. $^*p < 0.05$.

SCFA Content in Feces

The analysis was performed using HP7890B gas chromatograph (Agilent) equipped with flame ionization detector and DB-FF capillary column (internal diameter 0.25 mm, length 30 m, film thickness 0.5 μm; temperature 40–250°C; Agilent Technologies, USA). The temperature of the injector and detector are 200 and 270°C, respectively. The carrier gas uses high-purity and high-purity nitrogen with a flow rate of 40 ml/min. Heating program: the initial temperature is 80°C, hold for 0.5 min, 5°C/min rise to 130°C, hold for 2 min, and then rise at 20–240°C/min, hold for 1 min. Confirm the types of short-chain fatty acids and calculate the content of short-chain fatty acids by comparing the retention time and peak area of the sample and the standard. The content of short-chain fatty acids is expressed in μg/g chyme.

16S Ribosomal RNA Amplicon Sequencing

Stool samples were extracted from microbial DNA using QIAamp DNA Stool Mini Kit (QIAGEN, Hilden, Germany). The sequence of the extracted DNA V3-V4 region was analyzed by high-throughput sequencing technology. First, the purified DNA was used as a template, and the universal primers 357F 5'-ACTCCTACGGRAGGCAGCAG-3' and 806R 5'-GGACTACHVGGGTWTCTAAT-3' primers were used for PCR amplification, and these primers were also fused with part of Miseq sequencing primers. The amplified products were

TABLE 1 | Primers for this study.

Primers	Nucleotide sequence of primers (5'−3')
β-actin	F: TGTCCACCTTCCAGCAGATGT
	R: AGCTCAGTAACAGTCCGCCTAGA
DGAT 2	F: AGTGGCAATGCTATCATCATCGT
	R: TCTTCTGGACCCATCGGCCCCAGGA
DGAT 1	F: TTCCGCCTCTGGGCATT
	R: AGAATCGGCCCACAATCCA
Cpt1a	F: CAGTCGACTCACCTTTCCTG
	R: CATCATGGCTTGTCTCAAGTG
TNF-α	F: ATGAGAAGTTCCCAAATGGC
	R: CTCCACTTGGTGGTTTGCTA
IL-6	F: CCTCTCTGCAAGAGACTTCCAT
	R: AGTCTCCTCTCCGGACTTGT
IL-1β	F: TGCCACCTTTTGACAGTGATG
	R: AAGGTCCACGGGAAAGACAC

subjected to 1.2% agarose gel electrophoresis, the samples with good results were run on 2% agarose gel, and the electrophoresis bands were cut and recovered, and the recovered product was used as a template for PCR amplification (8 cycles). Add adapters, sequencing primers, and tag sequences required for sequencing on the Illumina platform at both ends of the target fragment. Use AxyPrepDNA gel recovery kit (AXYGEN company) to recover all PCR products, and use FTC-3000TM Real-Time PCR instrument for fluorescence quantification, complete library construction after equal molar ratio mixing, and computer sequencing (illumina miseq PE300). Analyze the offline data, use mothur (Version 1.33.3) to analyze α diversity and β diversity, and use R language to map the species composition at the level of the phyla, the family, the genera and the species, and the species differences between groups.

Data Analysis

All data in this study were analyzed using SPSS 22.0, expressed as mean ± standard error of the mean (SEM). The difference between the means of the groups was analyzed using a one-way ANOVA pair and evaluated using Tukey multiple comparisons. $P < 0.05$ was regarded as a significant difference.

RESULTS

Lactobacillus plantarum Can Reduce HFD-Induced Body Weight and Fat Gain

Starting from the second week, the weight of the mice in the HFD and HFD-LP groups fed with high-fat diets was significantly higher than that in the CON group fed with ordinary diets, and the gap reached the largest in the fourth. From the fifth week, we gave the HFD-LP group an intragastric administration of *L. plantarum*. The bodyweight of the HFD-LP group was significantly lower than that of the HFD group and dropped to the same level as the CON group (**Figure 1B**). There was no significant difference in the ratio of the liver (**Figure 1C**) and perirenal fat weight (**Figure 1F**) to body weight (%) between the three groups. Compared with the HFD group, the ratio of inguinal fat (**Figure 1D**) and epididymal fat (**Figure 1E**) weight to body weight (%) of the CON and HFD-LP groups was significantly reduced.

Lactobacillus plantarum Can Enhance Glucose Tolerance, Insulin Resistance and Reduce Adipocyte Size in Obese Mice

In the intraperitoneal glucose tolerance test, we found that all mice had a significant increase in blood glucose after 15 min of intraperitoneal injection of glucose, but within 30–120 min, compared with the HFD group, the mice blood glucose of CON group and the HFD-LP group decreased significantly (**Figure 2A**). The area under the glucose curve (AUC) of the HFD group mice was significantly larger than that of the CON group and HFD-LP group (**Figure 2B**). In the insulin tolerance test, we found that compared with the CON group and the CON-LP group, the initial blood glucose of the HFD group mice was significantly increased, and the insulin sensitivity was significantly reduced (**Figure 2C**). The area under the glucose curve (AUC) of the HFD group mice was significantly larger than that of the CON group and HFD-LP group (**Figure 2D**).

We performed HE staining sections on epididymal fat and inguinal fat of mice and found that compared with the CON group and the CON-LP group, the size of the adipocytes in the epididymal fat of the HFD group increased significantly (**Figure 2E**). The size of the adipocytes in the inguinal fat of the CON group was significantly smaller than that of the HFD group and HFD-LP group, while the size of the adipocytes in the inguinal fat of the HFD-LP group was significantly smaller than that of the HFD group (**Figure 2F**).

Lactobacillus plantarum Can Improve the Biochemical Indexes of Obese Mice

The mouse serum biochemical indicators showed that the serum levels of alanine aminotransferase, blood glucose, and triglyceride in the HFD group were significantly higher than those in the CON group and the HFD-LP group (**Figures 3A,C,D**). There was no significant difference in the content of aspartate aminotransferase in mouse serum among the three groups (**Figure 3B**). The HFD group and HFD-LP group mice serum high-density lipoprotein and low-density lipoprotein levels were significantly higher than those in the CON group (**Figures 3E,F**).

Lactobacillus plantarum Can Improve Gene Expression and Substance Content in the Liver

In order to explore the alleviating effect of *L. plantarum* on chronic liver damage caused by obesity, we measured the expression of inflammatory factors and fat metabolism genes in liver tissues. The results show that compared with the CON and HFD-LP groups, DGAT1, DGAT2, TNF-α, IL-6, and IL-1β mRNA expression in the liver of the HFD group increased significantly (**Figures 4A,B,D–F**). The expression of Cpt1a in the liver of the HFD-LP group was significantly higher than

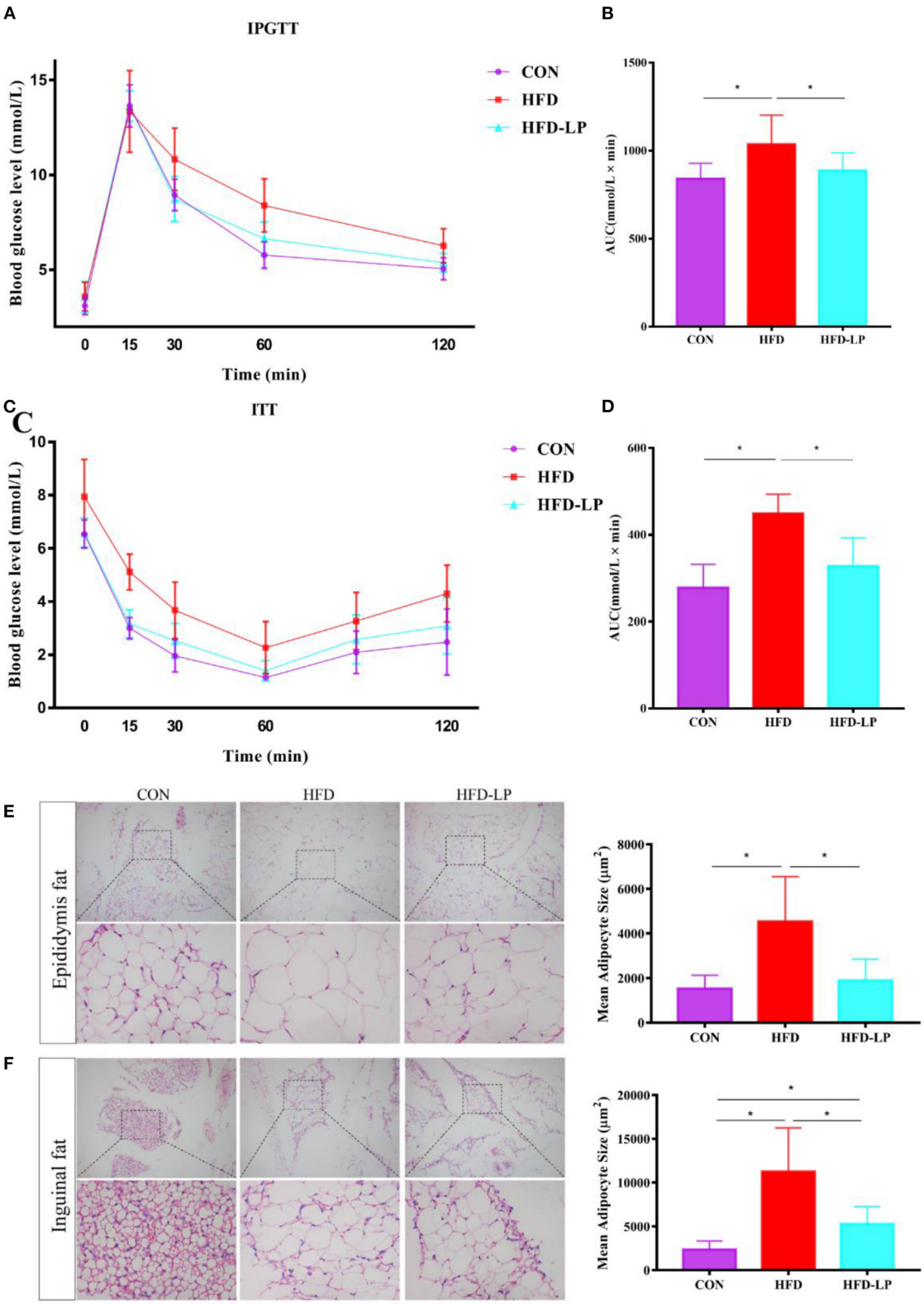

FIGURE 2 | Effect of *Lactobacillus plantarum* on glucose tolerance, insulin resistance and fat morphology in obese mice. **(A)** Plasma glucose level in mouse glucose tolerance test; **(B)** The area under the glucose curve (AUC) using the trapezoidal rule; **(C)** Plasma glucose level in mouse insulin tolerance test; **(D)** The area under the glucose curve (AUC) using the trapezoidal rule. **(E)** H&E staining on epididymal fat depots. Representative sections from inguinal fat depots of all groups (400×). Histological analysis of mean adipose cell size. **(F)** H&E staining on inguinal fat depots. Representative sections from inguinal fat depots of all groups (400×). Histological analysis of mean adipose cell size. Data are mean ± SD ($n = 8$) and analyzed by one-way ANOVA. *$p < 0.05$.

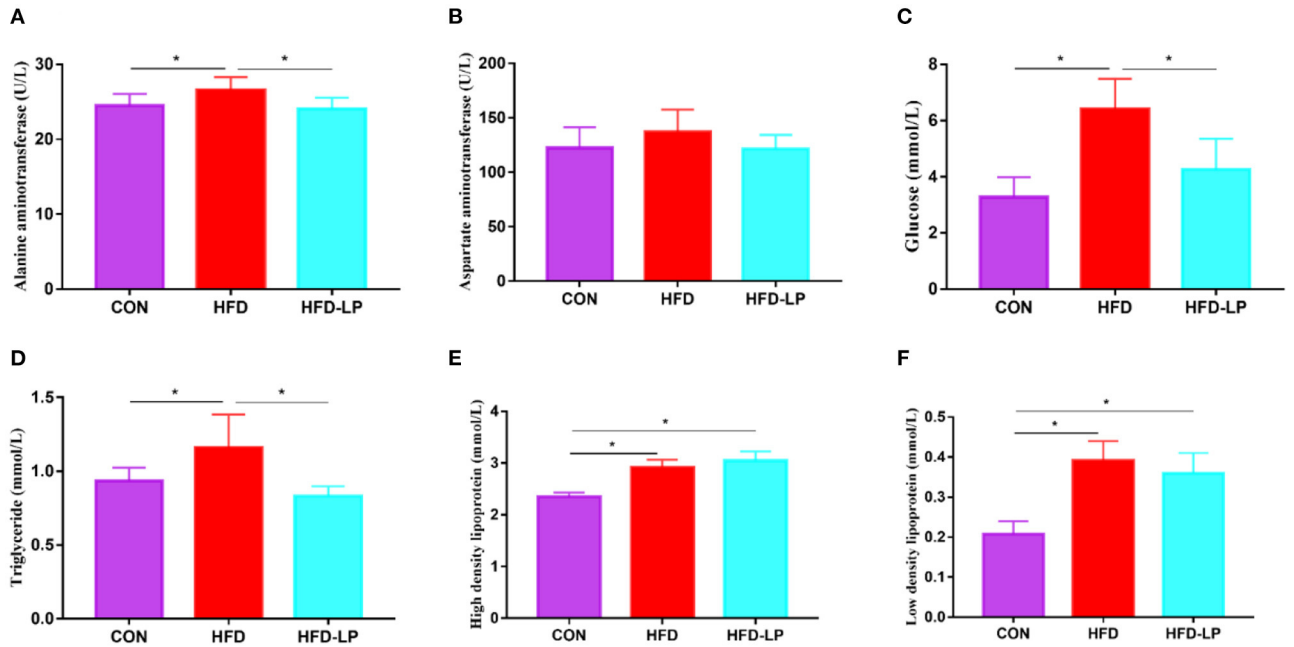

FIGURE 3 | Effects of *Lactobacillus plantarum* on the biochemical indexes of obese mice **(A)** the content of alanine aminotransferase in serum; **(B)** the content of aspartate aminotransferase in serum; **(C)** the Blood glucose level; **(D)** the content of triglyceride in serum; **(E)** the content of high-density lipoprotein in serum; **(F)** the content of low-density lipoprotein. Data are mean ± SD ($n = 8$) and analyzed by one-way ANOVA. *$p < 0.05$.

that in the HFD group (**Figure 4C**). We also further explored the effect of *L. plantarum* on the ability of the liver to resist oxidative stress. The results showed that high-fat diets significantly increased the levels of triglyceride, total cholesterol, and MDA in the liver tissues of mice. The intragastric treatment of *L. plantarum* significantly reduced the content of these substances and improved the ability of mice to resist oxidative stress (**Figures 4G–I**).

Lactobacillus plantarum Can Improve SCFAs Content in Mouse Feces

As we all know, short-chain fatty acids can regulate the body's metabolism. Therefore, we determined the SCFAs content in feces and explored the regulation effect of *L. plantarum* on host intestinal metabolism. Compared with the CON group, the contents of acetic acid, propionic acid, isobutyric acid, butyric acid, valeric acid and total SCFA in the feces of the HFD group were significantly reduced (**Figures 5A–E,G**). But compared with the HFD group, the levels of acetic acid, propionic acid, valeric acid, isovaleric acid and total SCFA in the feces of the HFD-LP group increased significantly (**Figures 5A,B,E–G**).

Lactobacillus plantarum Can Change the Colonic Microbial Composition of Obese Mice

Finally, we determined the structure of the colonic microbial community to explore the effect of *L. plantarum* on the homeostasis of the mouse intestinal microenvironment. The major bacteria in the colon are *Bacteroidetes*, *Firmicutes* and *Verrucomicrobia* in the Phylum, accounting for over 97%. The proportion of *Bacteroidetes* is 57.25, 54.39, and 63.28%, that of *Firmicutes* is 30.56, 43.37, and 33.97%, that of *Verrucomicrobia* is 12.50, 1.21, and 0.66% in the CON group, HFD group and HFD-LP group, respectively (**Figure 6A**). Compared with the CON group, the expression abundance of *Firmicutes* in the colon of the HFD group increased significantly, while the expression abundance of *Verrucomicrobia* decreased significantly ($p < 0.05$). Compared with the HFD group, the expression abundance of *Bacteroidetes* in the colon of the HFD-LP group increased significantly, while the expression abundance of *Firmicutes* decreased significantly ($p < 0.05$). The expression abundance of *Verrucomicrobia* in the colon of the HFD-LP group was significantly lower than that of the CON group ($p < 0.05$).

The top ten bacteria at Class were showed in **Figure 6B**. The most colonic bacterial are *Bacteroidia*, *Clostridia* and *Verrucomicrobiae*, accounting for more than 90%. The proportion of *Bacteroidia* is 57.25, 54.29, and 63.27%, that of *Clostridia* is 26.45, 39.92, and 29.49%, that of *Verrucomicrobiae* is 9.37, 0.91, and 0.49% in the CON group, HFD group and HFD-LP group, respectively (**Figure 6B**). Compared with the CON group, the expression abundance of *Clostridia* and *Bacillli* in the colon of the HFD group increased significantly ($p < 0.05$). Compared with the HFD group, the expression abundance of *Bacteroidetes* in the colon of the HFD-LP group increased significantly, while the expression abundance of *Clostridia* and *Bacillli* decreased significantly ($p < 0.05$).

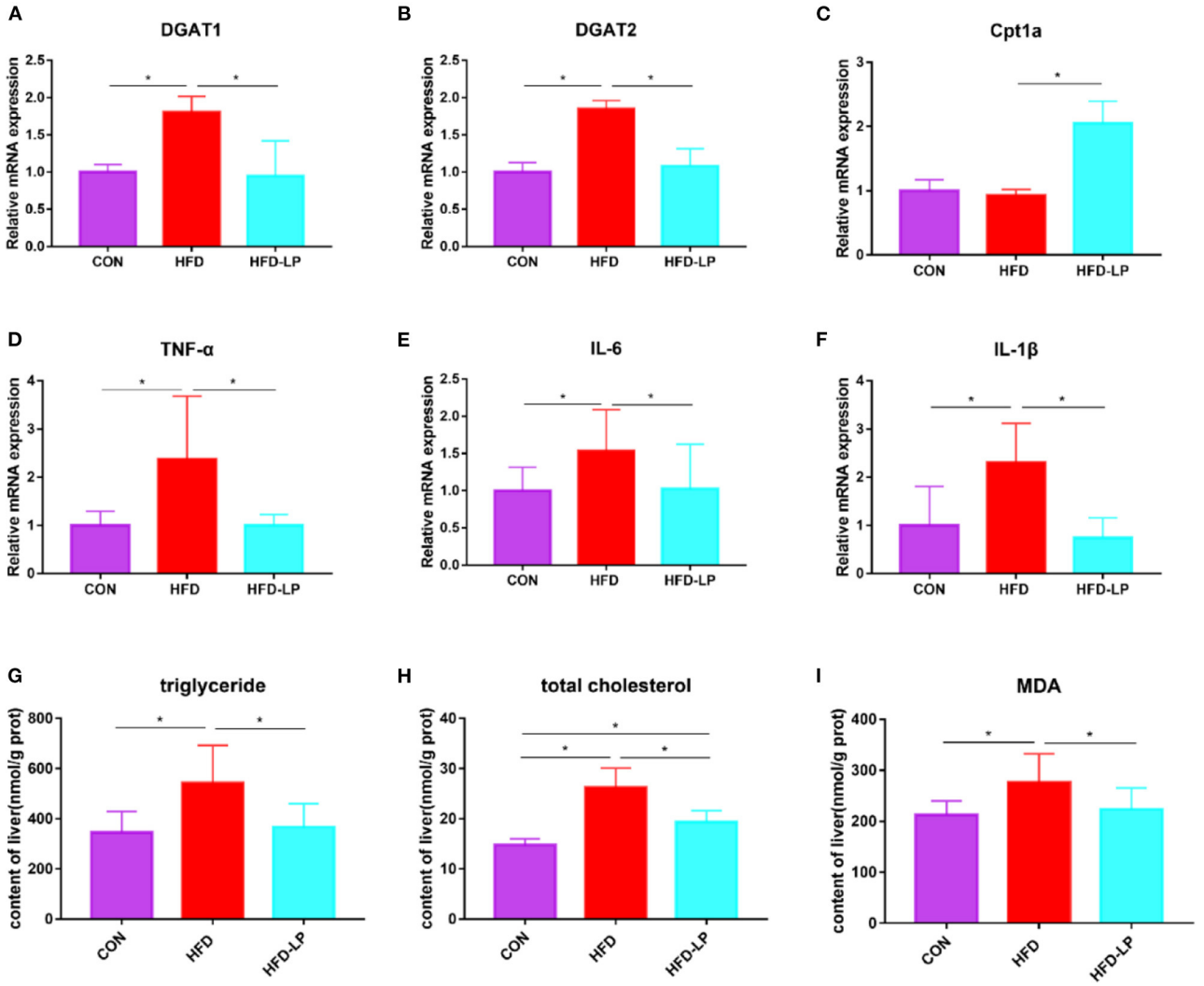

FIGURE 4 | Effects of *Lactobacillus plantarum* on inflammatory factors and lipid metabolism-related genes in obese mice **(A)** relative mRNA expression of DGAT1 in colon tissue; **(B)** relative mRNA expression of DGAT2 in colon tissue; **(C)** relative mRNA expression of Cpt1a in colon tissue; **(D)** relative mRNA expression of TNF-α in colon tissue; **(E)** relative mRNA expression of IL-6 in colon tissue; **(F)** relative mRNA expression of IL-1β in colon tissue; **(G)** the content of triglyceride in liver tissue; **(H)** the content of total cholesterol in liver tissue; **(I)** the content of MDA in liver tissue. Data are mean ± SD ($n = 8$) and analyzed by one-way ANOVA. *$p < 0.05$.

The top ten bacterial at the Order were selected and made into bar percentages for analysis. The first three were *Bacteroidales, Clostridiales*, and *Verrucomicrobiales*. The proportion of *Bacteroidales* is 57.25, 54.29, and 63.27%, that of *Clostridiales* is 26.45, 39.92, and 24.49%, that of *Verrucomicrobiales* is 9.37, 0.91, and 0.49% in the CON group, HFD group and HFD-LP group, respectively (**Figure 6C**). Compared with the CON group, the expression abundance of *Clostridiales* in the colon of the HFD group increased significantly ($p < 0.05$). Compared with the HFD group, the expression abundance of *Bacteroidales* and *Bifidobacteriales* in the colon of the HFD-LP group increased significantly, while the expression abundance of *Clostridiales* decreased significantly ($p < 0.05$).

Through LEfSe analysis, we found that *Bifidobacterium* at the Genus level, *Bifidobacteriaceae* at Family level, and *Bacillales* at Order level were significantly enriched in the HFD-LP group, and had significant effects on differences between groups (**Figure 7B**, $P \leq 0.05$). LEfSe then used linear discriminant analysis (LDA) to estimate the magnitude of the effect of species abundance on the effect of differences in each group. We have screened for differential species with LDA scores > 2 as shown in **Figure 7A**. Finally, we analyzed the correlation between gut microbes and SCFAs, fat metabolism genes and found *Bacteroidia* is positively correlated with all short-chain fatty acids, while *Clostridia* is negatively correlated with five SCFAs, including acetic acid, propionic acid, and isobutyric acid. *Bacteroidia* also showed a positive correlation with Cpt1a (**Figure 7C**).

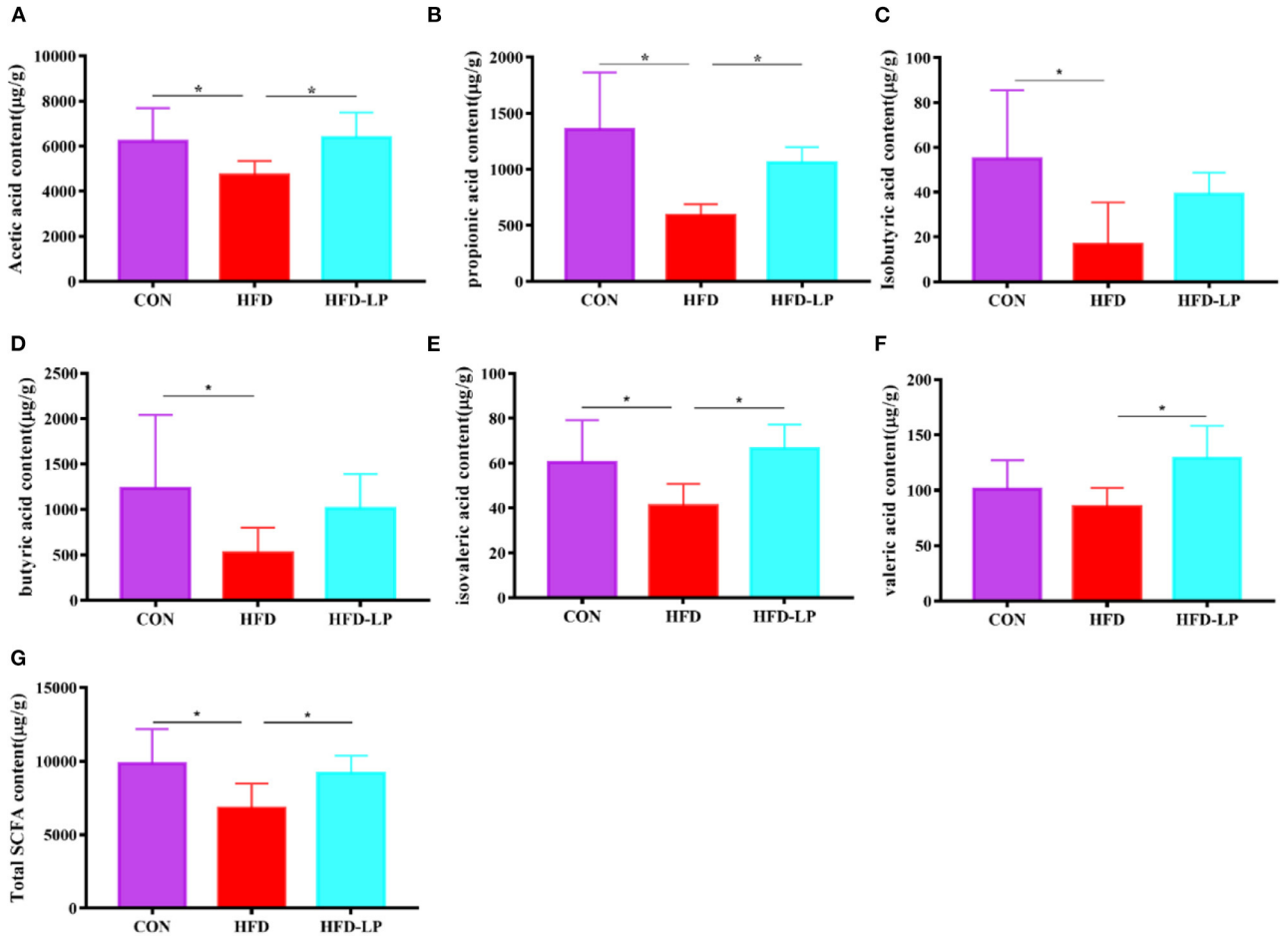

FIGURE 5 | Effect of *Lactobacillus plantarum* on SCFA in obese mice **(A)** the content of acetic acid; **(B)** the content of propionic acid; **(C)** the content of isobutyric acid; **(D)** the content of butyric acid; **(E)** the content of isovaleric acid; **(F)** the content of valeric acid; **(G)** the content of total SCFA. Data are mean ± SD ($n = 8$) and analyzed by one-way ANOVA. *$p < 0.05$.

DISCUSSION

Obesity and the chronic metabolic diseases caused by it pose a threat to human health on a large scale in the world (15). We need to find a safe and effective way of treatment and relief, and probiotics are a very effective choice. This is because probiotics have a vital role in gastrointestinal health and the regulation of metabolism (16). In this experiment, we selected a strain of *L. plantarum* with excellent activity and function to explore its effect on lipid metabolism in obese mice. We found that *L. plantarum* can significantly reduce the body weight, fat content, and fat cell size of obese mice. In addition, *L. plantarum* also improves mice's glucose tolerance, insulin resistance, and anti-inflammatory and antioxidant capacity. The most important thing is that it increases the expression of lipid metabolism genes and regulates the morphology of the intestinal microbial community.

Blood glucose is involved in many regulatory processes in lipid metabolism. For example, when glucose concentration in the blood increases, it activates lipid synthetic enzymes, including fatty acid synthase and acetyl-CoA carboxylase, ultimately leading to glucose storage in lipid form in adipocytes (17). In our experiments, obese mice treated with *L. plantarum* gavage showed a significant decrease in blood glucose levels 30 min after receiving intraperitoneal glucose injections, exhibiting the same ability to regulate blood glucose in normal mice. It indicates that obese mice treated with *L. plantarum* gavage can effectively reduce the abnormal increase in blood glucose values and the accumulation of group glucose in the form of fat. On the other hand, insulin can prevent the liver from producing and releasing glucose through glycogenolysis and inhibition of gluconeogenesis. In our experiment, obese mice did not show the hypoglycemic ability of insulin, but mice treated with *L. plantarum* gavage recovered the hypoglycemic function of insulin (18).

Our study is the first to demonstrate that *L. plantarum* can reduce DGAT gene expression in the intestinal tissues of obese mice. The N-terminal region of DGAT1 and the hydrophobic layer form a dimer. The acyl acceptor lipid

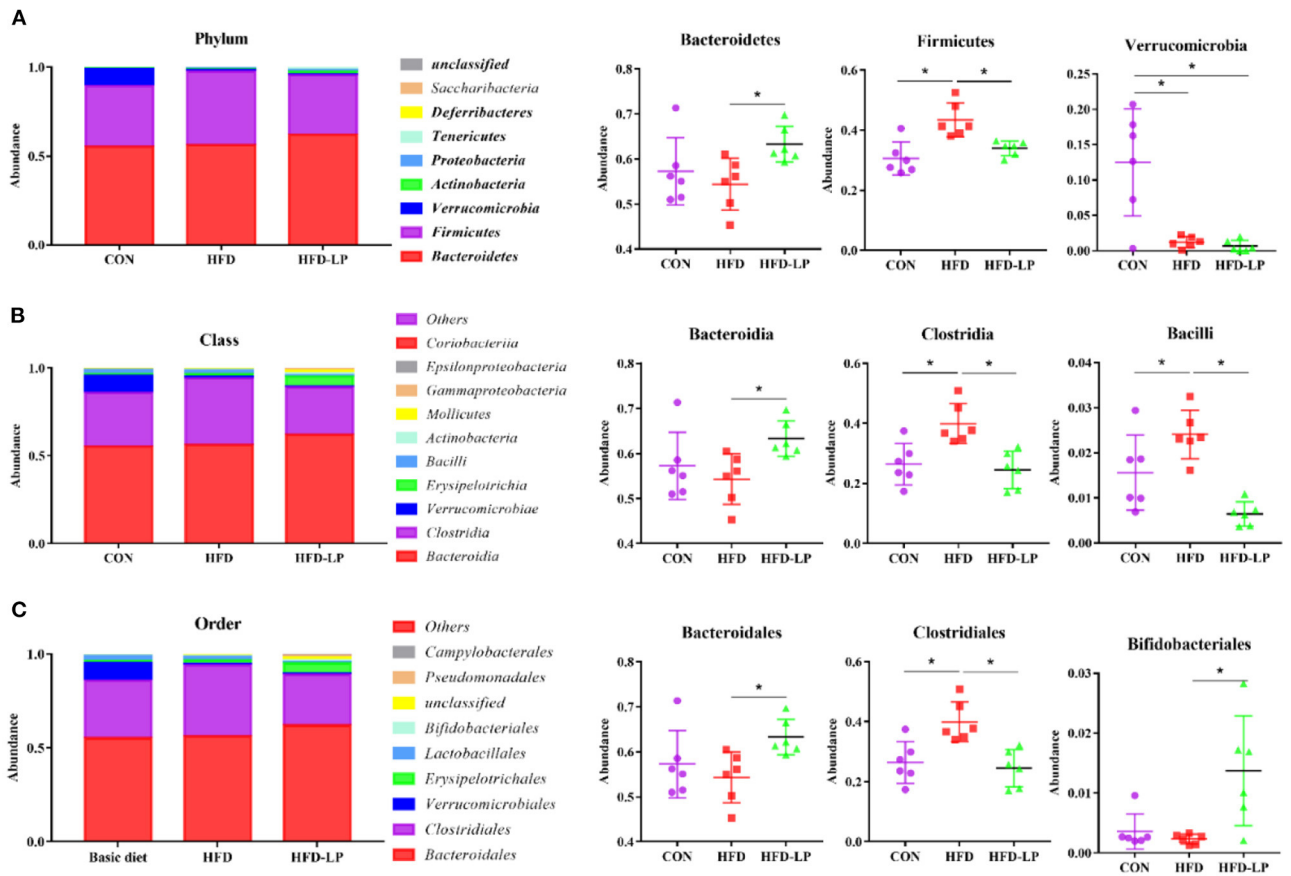

FIGURE 6 | Effect of *Lactobacillus plantarum* on the gut microflora in obese mice **(A)** Microorganism composition structure at phylum level and the specific percentages of *Bacteroidetes*, *Firmicutes*, and *Verrucomicrobia*; **(B)** Microorganism composition structure at Class level and the specific percentages of *Bacteroidia*, *Clostridia*, and *Bacilli*; **(C)** Microorganism composition structure at Order level and the specific percentages of *Bacteroidales*, *Clostridiales*, and *Bifidobacteriales*. Data are mean ± SD ($n = 6$) and analyzed by one-way ANOVA. *$p < 0.05$.

substrate like DAG enters the lipid bilayer from the water transport channel. The acyl chain of acyl *CoA* is transferred to the receptor, ultimately producing TG (19). Pharmacological manipulations have revealed that DGAT1 activity acts mainly on the gastrointestinal system. The deficiency of DGAT1 in organisms promotes intestinal insulin release and alters lipid absorption, thus improving obesity and its adverse effects (20). And DGAT2 can act synergistically with DGAT1 on TG secretion in hepatocytes (21). Abnormal and excessive accumulation of TGs in organisms can lead to obesity and increase the risk of metabolism-related diseases (22). In our experiments, gavage treatment with *L. plantarum* significantly reduced the abnormal expression of DGAT1 and DGAT2 genes in the intestinal tissues of obese mice and reduced the lipid metabolism-related diseases caused by excessive TG accumulation. Notably, it has been shown that downregulation of the DGAT gene significantly promotes the expression of the CPT1A protein (23), a critical mitochondrial β-oxidation regulatory enzyme involved in long-chain fatty acids, which can dramatically inhibit fat accumulation (24). CPT1A in the outer mitochondrial membrane can catalyze the reverse transport of acyl-coenzyme A groups to L-carnitine to form acyl-carnitine esters (25). In our experiments, gavage treatment with *L. plantarum* significantly increased CPT1A gene expression, promoted fatty acid oxidation, and reduced fat accumulation.

Previous studies have emphasized the important role of SCFA in microbial regulation of intestinal health (26, 27). SCFA is produced by intestinal *Bacteroides* fermenting polysaccharides and some carbohydrates that are difficult for the host to absorb and digest (28). The percentage abundance of *Bacteroides* in the intestine is also increased by the gavage of *L. plantarum*, and as reported in previous experiments, with the increase of the expression level of *Bacteroides*, the gavage treatment of *L. plantarum* also increased the content of SCFA in the content. Acetic acid can promote the oxidation of fatty acids, increase the energy consumption of the host, and ultimately reduce fat (29). The study of Barbara et al. showed that acetic acid activates the 5′-AMP-activated protein kinase in the intestine, thereby mediating adipokines to regulate lipid metabolism and maintain glucose homeostasis (30). On the other hand, SCFA

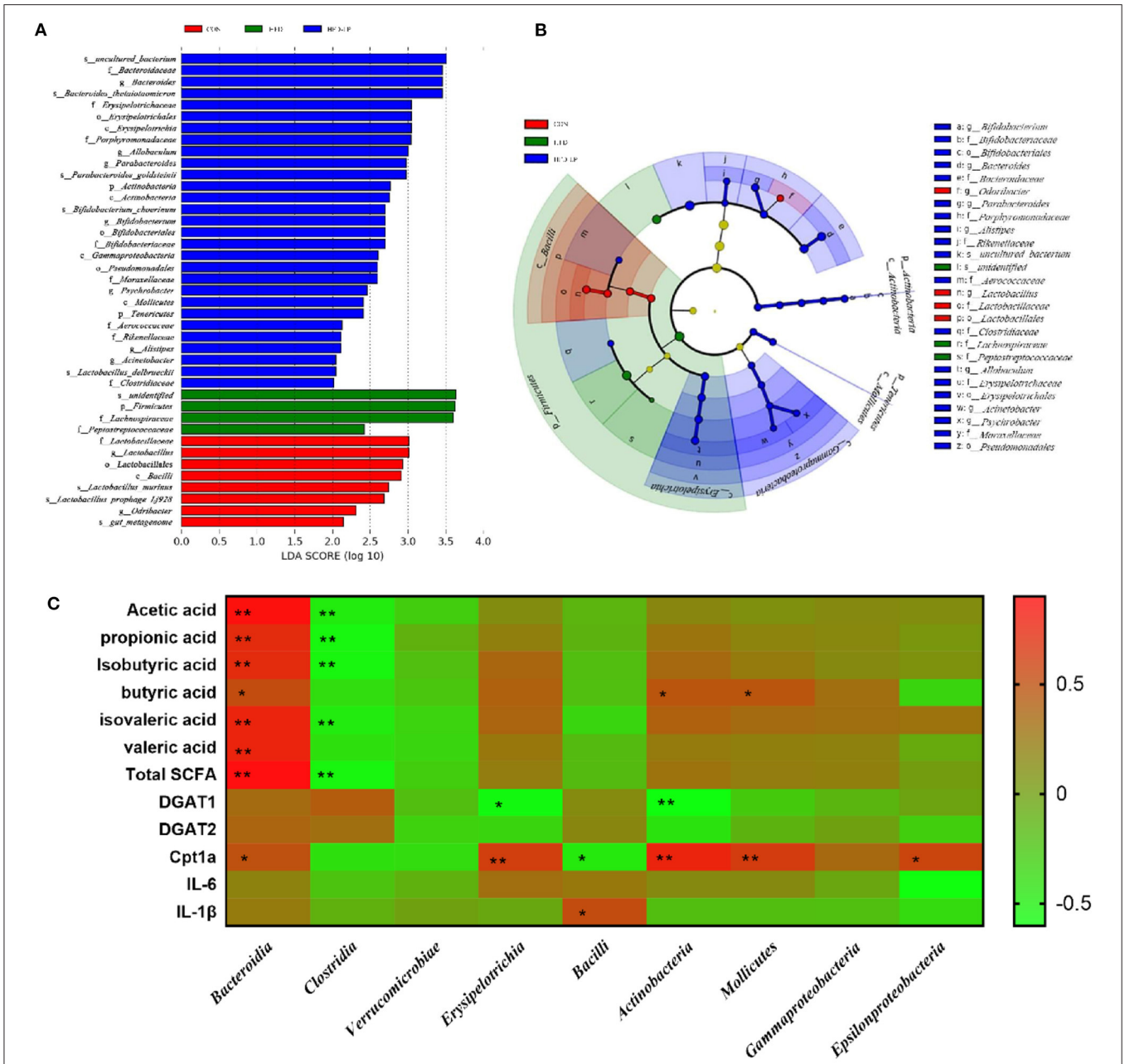

FIGURE 7 | Characteristic of mouse colon microorganisms determined by intragastric administration of *Lactobacillus plantarum*. **(A)** LDA score, an LDA score higher than 2 was considered to be an important contributor to the model; **(B)** LEfSe taxonomic cladogram, different colors suggest enrichment of certain taxa in the control group (red), HFD group (blue) and HFD-LP group (green). **(C)** Analysis of correlations between SCFAs levels, lipid metabolism-related genus level and intestinal microbe abundance.

can also enhance the organism's sense of fullness, because acetic acid promotes the circulating levels of GLP-1 and PYY in the body (31).

We have observed that *L. plantarum* can significantly regulate the intestinal microbial community structure of obese mice. It is well known that obese mice fed by HFD have decreased intestinal *Bacteroides* abundance and *Firmicutes* abundance increased (32, 33). However, the ratio of *Firmicutes* to *Bacteroides* returned to normal levels after intragastric treatment with *L. plantarum*. In addition, we found that the gavage treatment of *L. plantarum* also reduced the expression of *Clostridia* in the HFD group. The high abundance of *Clostridia* can metabolize and produce excess fecal deoxycholic acid (DCA) (34). This ecological disorder further reduces the uncoupling of bile acids (35). DCA can stimulate the expression of S1PR2, regulate the protein kinase (ERK) signali pathway, and induce the activation

of NLRP3 inflammasomes (36), which is one of the causes of chronic inflammation caused by obesity. This also verified that the gavage treatment of *L. plantarum* can significantly reduce the expression of pro-inflammatory factors in colon tissue. Surprisingly, the gavage of *L. plantarum* significantly improved the expression of *Bifidobacteriales*, and previous studies also showed that it can alleviate obesity (37, 38). *Bifidobacterium* strains can bind to mucin, stimulate the production of colonic mucus, and interact with the intestinal probiotic flora (39). The increased abundance of *bifidobacteria* also prevents the physiological damage of colon mucus and enhances the host body's metabolism (40).

DATA AVAILABILITY STATEMENT

The datasets presented in this study can be found in online repositories. The names of the repository/repositories and accession number(s) can be found below: https://www.ncbi.nlm.nih.gov/, PRJNA832208.

ETHICS STATEMENT

The animal study was reviewed and approved by the Hunan Agricultural University's Animal Ethics Committee.

AUTHOR CONTRIBUTIONS

GL and JF guided and completed the whole experimental design and reviewed and revised the manuscript before submission. YF was involved in the data collection. XH was responsible for the arrangement of data and analyzing the data. YM participated in interpreting the results and wrote the initial draft with all authors providing critical feedback and edits to subsequent revisions. All authors contributed to the article and approved the submitted version.

FUNDING

This study was supported by National Natural Science Foundation of China (Nos. 31772642 and 31672457), Ministry of Agricultural of the People's Republic of China (2015-Z64, 2016-X47), Hunan Provincial Science and Technology Department (2021JJ30008, 2019TP2004, 2017NK2322, 2016WK2008, and 2016TP2005), Double First-class Construction project of Hunan Agricultural University (SYL201802003), China Postdoctoral Science Foundation (2018M632963 and 2019T120705), Postgraduate Scientific Research Innovation Project of Hunan Province (CX20210654), and Science and Technology Innovation and Entrepreneurship Project for University Students of Hunan Province (2021RC1004).

REFERENCES

1. O'Neill S, O'Driscoll L. Metabolic syndrome: a closer look at the growing epidemic and its associated pathologies. *Obes Rev.* (2015) 16:1–12. doi: 10.1111/obr.12229
2. Tong M, Saito T, Zhai P, Oka SI, Mizushima W, Nakamura M, et al. Mitophagy is essential for maintaining cardiac function during high fat diet-induced diabetic cardiomyopathy. *Circ Res.* (2019) 124:1360–71. doi: 10.1161/CIRCRESAHA.118.314607
3. Hwang S, He Y, Xiang X, Seo W, Kim SJ, Ma J, et al. Interleukin-22 ameliorates neutrophil-driven nonalcoholic steatohepatitis through multiple targets. *Hepatology.* (2020) 72:412–29. doi: 10.1002/hep.31031
4. Miyamoto J, Igarashi M, Watanabe K, Karaki SI, Mukouyama H, Kishino S, et al. Gut microbiota confers host resistance to obesity by metabolizing dietary polyunsaturated fatty acids. *Nat Commun.* (2019) 10:4007. doi: 10.1038/s41467-019-11978-0
5. Dalby MJ, Ross AW, Walker AW, Morgan PJ. Dietary uncoupling of gut microbiota and energy harvesting from obesity and glucose tolerance in mice. *Cell Rep.* (2017) 21:1521–33. doi: 10.1016/j.celrep.2017.10.056
6. Gomes AC, Hoffmann C, Mota JF. The human gut microbiota: Metabolism and perspective in obesity. *Gut Microbes.* (2018) 9:308–25. doi: 10.1080/19490976.2018.1465157
7. Torres-Fuentes C, Schellekens H, Dinan TG, Cryan JF. The microbiota-gut-brain axis in obesity. *Lancet Gastroenterol Hepatol.* (2017) 2:747–56. doi: 10.1016/S2468-1253(17)30147-4
8. Nøhr MK, Pedersen MH, Gille A, Egerod KL, Engelstoft MS, Husted AS, et al. GPR41/FFAR3 and GPR43/FFAR2 as cosensors for short-chain fatty acids in enteroendocrine cells vs FFAR3 in enteric neurons and FFAR2 in enteric leukocytes. *Endocrinology.* (2013) 154:3552–64. doi: 10.1210/en.2013-1142
9. Sanders ME, Merenstein DJ, Reid G, Gibson GR, Rastall RA. Probiotics and prebiotics in intestinal health and disease: from biology to the clinic. *Nat Rev Gastroenterol Hepatol.* (2019) 16:605–16. doi: 10.1038/s41575-019-0173-3
10. Seddik HA, Bendali F, Gancel F, Fliss I, Spano G, Drider D. *Lactobacillus plantarum* and its probiotic and food potentialities. *Probiotics Antimicrob Proteins.* (2017) 9:111–22. doi: 10.1007/s12602-017-9264-z
11. Mao JH, Kim YM, Zhou YX, Hu D, Zhong C, Chang H, et al. Genetic and metabolic links between the murine microbiome and memory. *Microbiome.* (2020) 8:53. doi: 10.1186/s40168-020-00817-w
12. Crakes KR, Santos Rocha C, Grishina I, Hirao LA, Napoli E, Gaulke CA, et al. PPARα-targeted mitochondrial bioenergetics mediate repair of intestinal barriers at the host-microbe intersection during SIV infection. *Proc Natl Acad Sci USA.* (2019) 116:24819–29. doi: 10.1073/pnas.1908977116
13. Heeney DD, Zhai Z, Bendiks Z, Barouei J, Martinic A, Slupsky C, et al. Lactobacillus plantarum bacteriocin is associated with intestinal and systemic improvements in diet-induced obese mice and maintains epithelial barrier integrity in vitro. *Gut Microbes.* (2019) 10:382–97. doi: 10.1080/19490976.2018.1534513
14. Salomé-Desnoulez S, Poiret S, Foligné B, Muharram G, Peucelle V, Lafont F, et al. Persistence and dynamics of fluorescent *Lactobacillus plantarum* in the healthy versus inflamed gut. *Gut Microbes.* (2021) 13:1–16. doi: 10.1080/19490976.2021.1897374
15. Schulze MB. Metabolic health in normal-weight and obese individuals. *Diabetologia.* (2019) 62:558–66. doi: 10.1007/s00125-018-4787-8
16. Quigley EMM. Prebiotics and probiotics in digestive health. *Clin Gastroenterol Hepatol.* (2019) 17:333–44. doi: 10.1016/j.cgh.2018.09.028
17. Saltiel AR, Kahn CR. Insulin signalling and the regulation of glucose and lipid metabolism. *Nature.* (2001) 414:799–806. doi: 10.1038/414799a
18. Paranjape SA, Chan O, Zhu W, Horblitt AM, McNay EC, Cresswell JA, et al. Influence of insulin in the ventromedial hypothalamus on pancreatic glucagon secretion in vivo. *Diabetes.* (2010) 59:1521–7. doi: 10.2337/db10-0014
19. Sui X, Wang K, Gluchowski NL, Elliott SD, Liao M, Walther TC, et al. Structure and catalytic mechanism of a human triacylglycerol-synthesis enzyme. *Nature.* (2020) 581:323–8. doi: 10.1038/s41586-020-2289-6
20. Liu J, Gorski JN, Gold SJ, Chen D, Chen S, Forrest G, et al. Pharmacological inhibition of diacylglycerol acyltransferase 1 reduces body weight and modulates gut peptide release–potential insight into mechanism of action. *Obesity.* (2013) 21:1406–15. doi: 10.1002/oby.20193
21. McLaren DG, Han S, Murphy BA, Wilsie L, Stout SJ, Zhou H, et al. DGAT2 Inhibition alters aspects of triglyceride metabolism in rodents but not in non-human primates. *Cell Metab.* (2018) 27:1236–48.e1236. doi: 10.1016/j.cmet.2018.04.004

22. Zhou B, Liu C, Xu L, Yuan Y, Zhao J, Zhao W, et al. N -Methyladenosine reader protein YT521-B homology domain-containing 2 suppresses liver steatosis by regulation of mRNA stability of lipogenic genes. *Hepatology.* (2021) 73:91–103. doi: 10.1002/hep.31220
23. Cheng X, Geng F, Pan M, Wu X, Zhong Y, Wang C, et al. Targeting DGAT1 ameliorates glioblastoma by increasing fat catabolism and oxidative stress. *Cell Metab.* (2020) 32:229–42.e228. doi: 10.1016/j.cmet.2020.06.002
24. Nakamura MT, Yudell BE, Loor JJ. Regulation of energy metabolism by long-chain fatty acids. *Prog Lipid Res.* (2014) 53:124–44. doi: 10.1016/j.plipres.2013.12.001
25. Schlaepfer IR, Joshi M. CPT1A-mediated fat oxidation, mechanisms, and therapeutic potential. *Endocrinology.* (2020) 161:bqz046. doi: 10.1210/endocr/bqz046
26. Sonnenburg ED, Zheng H, Joglekar P, Higginbottom SK, Firbank SJ, Bolam DN, et al. Specificity of polysaccharide use in intestinal bacteroides species determines diet-induced microbiota alterations. *Cell.* (2010) 141:1241–52. doi: 10.1016/j.cell.2010.05.005
27. Neyrinck AM, Possemiers S, Druart C, Van de Wiele T, De Backer F, Cani PD, et al. Prebiotic effects of wheat arabinoxylan related to the increase in bifidobacteria, Roseburia and Bacteroides/Prevotella in diet-induced obese mice. *PLoS ONE.* (2011) 6:e20944. doi: 10.1371/journal.pone.0020944
28. Daniele G, Guardado Mendoza R, Winnier D, Fiorentino TV, Pengou Z, Cornell J, et al. The inflammatory status score including IL-6, TNF-α, osteopontin, fractalkine, MCP-1 and adiponectin underlies whole-body insulin resistance and hyperglycemia in type 2 diabetes mellitus. *Acta Diabetol.* (2014) 51:123–31. doi: 10.1007/s00592-013-0543-1
29. Suzuki T, Yoshida S, Hara H. Physiological concentrations of short-chain fatty acids immediately suppress colonic epithelial permeability. *Br J Nutr.* (2008) 100:297–305. doi: 10.1017/S0007114508888733
30. Kahn BB, Alquier T, Carling D, Hardie DG. AMP-activated protein kinase: ancient energy gauge provides clues to modern understanding of metabolism. *Cell Metab.* (2005) 1:15–25. doi: 10.1016/j.cmet.2004.12.003
31. Saad MJ, Santos A, Prada PO. Linking gut microbiota and inflammation to obesity and insulin resistance. *Physiology.* (2016) 31:283–93. doi: 10.1152/physiol.00041.2015
32. Rastmanesh R. High polyphenol, low probiotic diet for weight loss because of intestinal microbiota interaction. *Chem Biol Interact.* (2011) 189:1–8. doi: 10.1016/j.cbi.2010.10.002
33. Chang CJ, Lin CS, Lu CC, Martel J, Ko YF, Ojcius DM, et al. Ganoderma lucidum reduces obesity in mice by modulating the composition of the gut microbiota. *Nat Commun.* (2015) 6:7489. doi: 10.1038/ncomms8489
34. Wang L, Gong Z, Zhang X, Zhu F, Liu Y, Jin C, et al. Gut microbial bile acid metabolite skews macrophage polarization and contributes to high-fat diet-induced colonic inflammation. *Gut Microbes.* (2020) 12:1–20. doi: 10.1080/19490976.2020.1819155
35. Xu M, Cen M, Shen Y, Zhu Y, Cheng F, Tang L, et al. Deoxycholic acid-induced gut dysbiosis disrupts bile acid enterohepatic circulation and promotes intestinal inflammation. *Dig Dis Sci.* (2021) 66:568–76. doi: 10.1007/s10620-020-06208-3
36. Zhao S, Gong Z, Du X, Tian C, Wang L, Zhou J, et al. Deoxycholic acid-mediated sphingosine-1-phosphate receptor 2 signaling exacerbates DSS-induced colitis through promoting cathepsin B release. *J Immunol Res.* (2018) 2018:2481418. doi: 10.1155/2018/2481418
37. Parnell JA, Reimer RA. Prebiotic fiber modulation of the gut microbiota improves risk factors for obesity and the metabolic syndrome. *Gut Microbes.* (2012) 3:29–34. doi: 10.4161/gmic.19246
38. Everard A, Belzer C, Geurts L, Ouwerkerk JP, Druart C, Bindels LB, et al. Cross-talk between Akkermansia muciniphila and intestinal epithelium controls diet-induced obesity. *Proc Natl Acad Sci USA.* (2013) 110:9066–71. doi: 10.1073/pnas.1219451110
39. He F, Ouwehan AC, Hashimoto H, Isolauri E, Benno Y, Salminen S. Adhesion of Bifidobacterium spp. to human intestinal mucus. *Microbiol Immunol.* (2001) 45:259–62. doi: 10.1111/j.1348-0421.2001.tb02615.x
40. Everard A, Lazarevic V, Derrien M, Girard M, Muccioli GG, Neyrinck AM, et al. Responses of gut microbiota and glucose and lipid metabolism to prebiotics in genetic obese and diet-induced leptin-resistant mice. *Diabetes.* (2011) 60:2775–86. doi: 10.2337/db11-0227

Conflict of Interest: The authors declare that the research was conducted in the absence of any commercial or financial relationships that could be construed as a potential conflict of interest.

frontiers | Frontiers in Nutrition

ORIGINAL RESEARCH
published: 30 June 2022
doi: 10.3389/fnut.2022.921758

Liver Transcriptome and Gut Microbiome Analysis Reveals the Effects of High Fructose Corn Syrup in Mice

Yu Shen[1,2†], Yangying Sun[1†], Xiaoli Wang[2], Yingping Xiao[2], Lingyan Ma[2], Wentao Lyu[2], Zibin Zheng[2], Wen Wang[2] and Jinjun Li[3*]*

[1] State Key Laboratory for Managing Biotic and Chemical Threats to the Quality and Safety of Agro-products, College of Food and Pharmaceutical Sciences, Ningbo University, Ningbo, China, [2] Institute of Agro-product Safety and Nutrition, Zhejiang Academy of Agricultural Sciences, Hangzhou, China, [3] Institute of Food Sciences, Zhejiang Academy of Agricultural Sciences, Hangzhou, China

OPEN ACCESS

Edited by:
Jie Yin,
Hunan Agricultural University, China

Reviewed by:
Shimeng Huang,
China Agricultural University, China
Daxi Ren,
Zhejiang University, China

***Correspondence:**
Wen Wang
ww_hi1018@163.com
Jinjun Li
lijinjun@zaas.ac.cn

[†] *These authors have contributed equally to this work*

Specialty section:
This article was submitted to Nutrition and Microbes, a section of the journal Frontiers in Nutrition

Received: *16 April 2022*
Accepted: *01 June 2022*
Published: *30 June 2022*

Citation:
Shen Y, Sun Y, Wang X, Xiao Y, Ma L, Lyu W, Zheng Z, Wang W and Li J (2022) Liver Transcriptome and Gut Microbiome Analysis Reveals the Effects of High Fructose Corn Syrup in Mice. Front. Nutr. 9:921758. doi: 10.3389/fnut.2022.921758

High fructose corn syrup (HFCS) is a viscous mixture of glucose and fructose that is used primarily as a food additive. This article explored the effect of HFCS on lipid metabolism-expressed genes and the mouse gut microbiome. In total, ten 3-week-old male C57BL/6J mice were randomly divided into two groups, including the control group, given purified water (Group C) and 30% HFCS in water (Group H) for 16 weeks. Liver and colonic content were collected for transcriptome sequencing and 16S rRNA gene sequencing, respectively. HFCS significantly increased body weight, epididymal, perirenal fat weight in mice ($p < 0.05$), and the proportion of lipid droplets in liver tissue. The expression of the ELOVL fatty acid elongase 3 (Elovl3) gene *was* reduced, while Stearoyl-Coenzyme A desaturase 1 (*Scd1*), peroxisome proliferator activated receptor gamma (*Pparg)*, fatty acid desaturase 2 (*Fads2*), acyl-CoA thioesterase 2 (*Acot2*), acyl-CoA thioesterase 2 (*Acot3*), acyl-CoA thioesterase 4 (*Acot4*), and fatty acid binding protein 2 (*Fabp2*) was increased in Group H. Compared with Group C, the abundance of Firmicutes was decreased in Group H, while the abundance of Bacteroidetes was increased, and the ratio of Firmicutes/Bacteroidetes was obviously decreased. At the genus level, the relative abundance of *Bifidobacterium*, *Lactobacillus*, *Faecalibaculum*, *Erysipelatoclostridium,* and *Parasutterella* was increased in Group H, whereas that of *Staphylococcus*, *Peptococcus*, *Parabacteroides*, *Donghicola,* and *Turicibacter was* reduced in Group H. *Pparg*, *Acot2*, *Acot3,* and *Scd1* were positively correlated with *Erysipelatoclostridium* and negatively correlated with *Parabacteroides*, *Staphylococcus,* and *Turicibacter*. *Bifidobacterium* was negatively correlated with *Elovl3*. Overall, HFCS affects body lipid metabolism by affecting the expression of lipid metabolism genes in the liver through the gut microbiome.

Keywords: gut microbiota, hepatic lipid metabolism, high fructose corn syrup, transcriptome analysis, mouse

INTRODUCTION

High fructose corn syrup (HFCS) is a viscous mixture of glucose and fructose. In recent years, due to the rising price of sugar, the low price and better taste of HFCS have been favored by the food industry, especially in beverage production, and it is also a key ingredient in baked goods, desserts, and juices (1). Fructose in the diet may contribute to increased energy intake and weight gain, which can lead to problems, such as obesity (2). Furthermore, an HFCS diet significantly alters the community structure of the gut microbiome and lipid metabolism (3, 4).

The liver is primarily the site of fructose metabolism, which is an essential organ in the body related to lipid metabolism (5, 6) and plays an important role in regulating appetite and body weight (7). Li et al. found that most of the changes in the liver transcriptome level of laying hens are closely related to fat metabolism by performing transcriptome analysis on the liver of young and laying hens (8). It was shown that peroxisome proliferator activated receptor gamma (*Pparg*) is a key factor in lipid formation and can be combined with specific substances to reduce lipid formation (9). Studies on broilers of the same breed and different body weights showed that the expression of *LIPG* and *CPT1A* genes is related to lipid metabolism (10, 11). Emmanuelle (12) adipose regulation in animals of different body sizes is related to the regulation of genes involved in adipogenesis. Furthermore, the expression of different genes in the organism may lead to differences in fat deposition (13).

The gut microbiome affects host lipid metabolism and plays an important role in the development of metabolic diseases through interaction with the diet (14, 15). The human gut contains a diverse and complex microbial community that plays an important role in energy and lipid metabolism (16). The gut microbiome is colonized by 10^{14} macroorganisms of numerous species, which are important components of the human gut microbiome ecosystem (17). The microbiome in the gastrointestinal tract of mice consists mainly of Firmicutes (74%) and Bacteroidetes (23%) at the phylum level (18). A high-fructose diet altered the Firmicutes/Bacteroidetes ratio and the abundance of *Parasutterella*, *Lactobacillus*, *Bifidobacteriaceae,* and *Alistipes* (19, 20). Crescenzo et al. (21) indicated that a fructose diet alters the mouse gut microbiome, which contributes to the dysregulation of liver metabolism.

Thus, to better understand the effects of HFCS intake on mouse metabolism, this study is aimed to determine the effects of HFCS intake on the gene expression of liver lipid metabolism and the community structure and function of the gut microbiome in mice and the association between the gene expression and the gut microbiome.

MATERIALS AND METHODS

Ethics Statement

The study was conducted at the Laboratory Animal Center of Zhejiang Academy of Agricultural Sciences (Animal Experimentation License No. 286868667) and was approved by the Zhejiang Provincial Ethics Committee for Laboratory Animals (Ethical Approval No. 78865576). All methods were conducted following the relevant guidelines and regulations.

Preparation of Animal and Liver Tissue Samples

Male C57BL/6J mice of 3-week-old were purchased from Shanghai Slack Company. After all mice were adaptively fed for 1 week, they were randomly divided into two groups, the control group (Group C) and the HFCS group (Group H), which were fed drinking water containing 30% HFCS. All mice were fed at room temperature and relative humidity of 50–70%. Each group was exposed to light for 12 h a day, and the mice were free to eat and drink. After 16 weeks of intervention, water was removed without fasting for 12 h. The mice were weighed, and the liver, epididymal fat, and perirenal fat were quickly weighed. To analyze the liver, the left leaf was placed in 4% paraformaldehyde, and the right leaf was stored at −80°C. Data were recorded in time for all operations. The liver samples for examination were fixed with 4% paraformaldehyde. After the fixed state was achieved, the samples were pruned, dehydrated, embedded, sectioned, stained, and sealed in strict accordance with the standard operating procedure (SOP) of the unit for pathological experiment detection and finally qualified for microscopic examination. The whole intestine was separated from the abdominal cavity of the mice, and the content of the colon was removed and stored on dry ice.

RNA Extraction

Total RNA was isolated from the liver tissues of 10 mice. TRIzol (Invitrogen, USA) was used to purify the extract, and the purity of RNA (ratio of OD260/280 and OD260/230) was detected by a Nano Spectrophotometer (Implen, Maryland, CA, USA). An Agilent 2100 Bioanalyzer (Agilent Technologies, Santa Clara, CA, USA) was used to accurately detect the integrity and total amount of RNA.

Library Construction and Sequencing

According to the manufacturer's suggestion, the kit used to build the library was the NEBNext® Ultra™ RNA Library Prep Kit for illumination. After the library was built, Qubit 2.0 Fluorometer was used for preliminary quantification, and the library was diluted to 1.5 ng/μl. Then, an Agilent 2100 Bioanalyzer was used to detect the insert size of the library. After the insert size met the expectation, quantitative real-time PCR (qRT-PCR) accurately quantified the effective concentration of the library (the effective concentration of the library was higher than 2 nM) to ensure the quality of the library. After library inspection was qualified, different libraries were pooled according to the requirements of effective concentration and target off-board data volume. Then, Illumina sequencing was performed, and a 150 bp paired-end reading was generated.

Differential Gene Expression Analysis

DESeq2 software (1.20.0) was used to analyze the differential expression between the two comparison combinations. DESeq2 provides statistical procedures for determining differential expression in digital gene expression data using a model based

TABLE 1 | Primers for RT-qPCR.

Gene	Size (bp)	Annealing (°C)	Forward (5′ to 3′)	Reword (5'to3')
GAPDH	127	60	GAAGGTCGGTGTGAACGGATTTG	CATGTAGACCATGTAGTTGAGGTCA
Scd1	110	60	GCAAGCTCTACACCTGCCTCTTC	CAGCCGTGCCTTGTAAGTTCTG
Pparg	133	60	CCAAGAATACCAAAGTGCGATCA	CCCACAGACTCGGCACTCAAT
Elovl3	91	60	GTAAGCGTCCACTCATCTTTGTC	CCCGAAGGCACTTTGTTCTTGTAT
Fads2	86	60	CGACATTTCCAACACCATGCCAA	CACTCGCCAAGGACAAACAC
Acot2	97	60	GACAGGGTTTCTCTGTGTACC	GTGGCTTTACTCCCAGCACTT
Acot3	121	60	CTGCTACATCCCTGGAGTTC	CCCTTAACTGCTGAGCCATCTTT
Acot4	178	60	GCCTGTAACAGACATGGTAGATTC	CTGTAACAAGCACAGGCTGGTA
Fabp2	73	60	CTGATTGCTGTCCGAGAGGTT	GCTTGGCCTCAACTCCTTCATAT

on a negative binomial distribution. Benjamini and Hochberg's method was used to adjust the p-value to control the error detection rate. Genes with an adjusted $p < 0.05$ found by DESeq2 were called differentially expressed genes (DEGs).

DEGs of Gene Oncology (GO) and Kyoto Encyclopedia Gene and Genome (KEGG) Enrichment Analyses

Gene Oncology enrichment analysis of DEGs was realized by Cluster Profiler (3.4.4) software, in which the gene length bias was corrected, and GO terms with corrected p-values <0.05 were significantly enriched by DEGs. We used Cluster Profiler (3.4.4) software analysis of DEGs in KEGG pathway enrichment after using a local version of the GSEA tool http://www.broadinstitute.org/gsea/index. jsp, GO to the species, KEGG GSEA datasets. The KEGG (http://www.genome.jp/KEGG/) (22) information from the molecular level, especially the genome sequencing high flux experimental technology of large-scale molecular datasets, understands cells, biological, ecological system, the advanced features of biological systems, and the utility of the database resources. In this study, KOBAS (23) software was used to test the statistical enrichment of DEGs in the KEGG pathway.

RT-QPCR Analysis

To confirm the reproducibility and accuracy of the RNA sequencing (RNA-Seq) gene expression data obtained from mouse liver libraries, RT-qPCR analysis was performed. The RT-qPCR system (20 μl) was as follows: Power SYBR® Green Master Mix, 10 μl; gene-specific upstream and downstream primers (10 μmol/L), 0.5 μl; sterile water, 8 μl; and cDNA template, 1 μl. The reaction conditions were as follows: 95°C for 1 min, followed by 40 cycles of 95°C for 15 s and 63°C for 25 s (for collecting fluorescence data). The relative expression level of each gene was determined by the 2^{-Ct} method using GAPDH as the internal reference gene, and the reaction was repeated three times for each sample. The primers used for quantification in the study were designed using the Primer-Basic Local Alignment Search Tool (BLAST) on the NCBI website (https://www.ncbi.nlm.nih.gov/tools/primer-blast/). Gene information for RT-PCR is shown in **Table 1**.

Histological Staining

The histological morphology of the liver was observed using hematoxylin-eosin staining. After fixation with 4% paraformaldehyde and in good condition, the samples were pruned, dehydrated, embedded, sectioned, stained, and sealed in strict accordance with the procedures of the unit's pathological experiment detection SOP and finally qualified for microscopic examination. Steatosis of liver tissue in mice treated with 30% HFCS was observed.

DNA Extraction and Sequencing

According to the instructions of the manufacturer, microbial genomic DNA was obtained from each intestinal content (QIAamp DNA Stool Mini Kit QIAGEN, CA, USA). The barcode-specific primers 515 F 5′-barcode-GTGCCAGCMGCCGCGG-3′ and 907 R 5′-CCGTCAATTCMTTTRAGTTT-3′ were synthesized to amplify the V4+V5 region of 16S rRNA gene sequencing (24). The PCRs were performed in triplicate using a 20 μl mixture that contained 4 μl of 5 × FastPfu Buffer, 2 μl of 2.5 mM deoxynucleotide triphosphates (dNTPs), 0.8 μl of forward primer (5 μM), 0.8 μl of reverse primer (5 μM), 0.4 μl of FastPfu Polymerase, 0.2 μl of bovine serum albumin (BSA), 10 ng of template DNA, and ddH_2O was added to 20 μl. Amplicons were extracted from 2% agarose gels and purified using the AxyPrep DNA Gel Extraction Kit (Axygen Biosciences, Union City, CA, USA) according to the manufacturer's instructions and quantified using a QuantiFluorTM-ST (Promega, USA) Bioinformatics Analysis Illumina paired reads that were multiplexed, and clean reads were screened in the Quantitative Analysis of Microbial Ecology (QIIME) quality filter (25), combined into labels using FLASH (26), and then allocated a unique barcode to each sample. After removing redundancy, the labels of each sample were analyzed, and UPARSE and UCHIME were used to assign unique labels with sequence similarity ≥97% to the same operational taxonomic unit (OTU). Selected OTUs were annotated with taxonomic information using the Ribosomal Database Project (RDP) classifier (27). Alpha diversity and beta diversity were calculated and visualized in GraphPad Prism 8.0.2 (San Diego, CA, USA).

Statistical Analysis

All the data were statistically analyzed by SPSS version 23 software using one-way ANOVA. The mean ± standard deviation (SD; $x \pm s$) is indicated, and $p < 0.05$ was considered statistically significant.

RESULTS

Body Weight and Fat Deposition in Mice

The average body weight of mice in Group C was 29.060 ± 0.446 g and that in Group H was 38.220 ± 1.515 g, and the difference between the two groups was extremely significant ($p < 0.001$; **Figure 1A**). The average weight of epididymal fat showed a significant increase in the H group, which was 1.886 ± 0.216 g, while the weight of epididymal fat in Group C was 0.762 ± 0.098 g ($p < 0.001$; **Figure 1B**). By comparing the perirenal fat of mice in the two groups, we found that the difference between the two groups was extremely significant, 0.284 ± 0.020 g in Group C and 0.732 ± 0.123 g in Group H ($p < 0.001$; **Figure 1C**). The results showed that the liver weight of mice in Group H was increased but not significantly different as compared to Group C, while the average liver weight of Group C was 1.152 ± 0.031 g and that of Group H was 1.364 ± 0.100 g ($p = 0.0778$; **Figure 1D**). Round vacuoles of varying sizes were observed in the cytoplasm, and larger areas of lipid droplets were observed in Group H than in Group C. As shown in **Figures 1E–H**, it

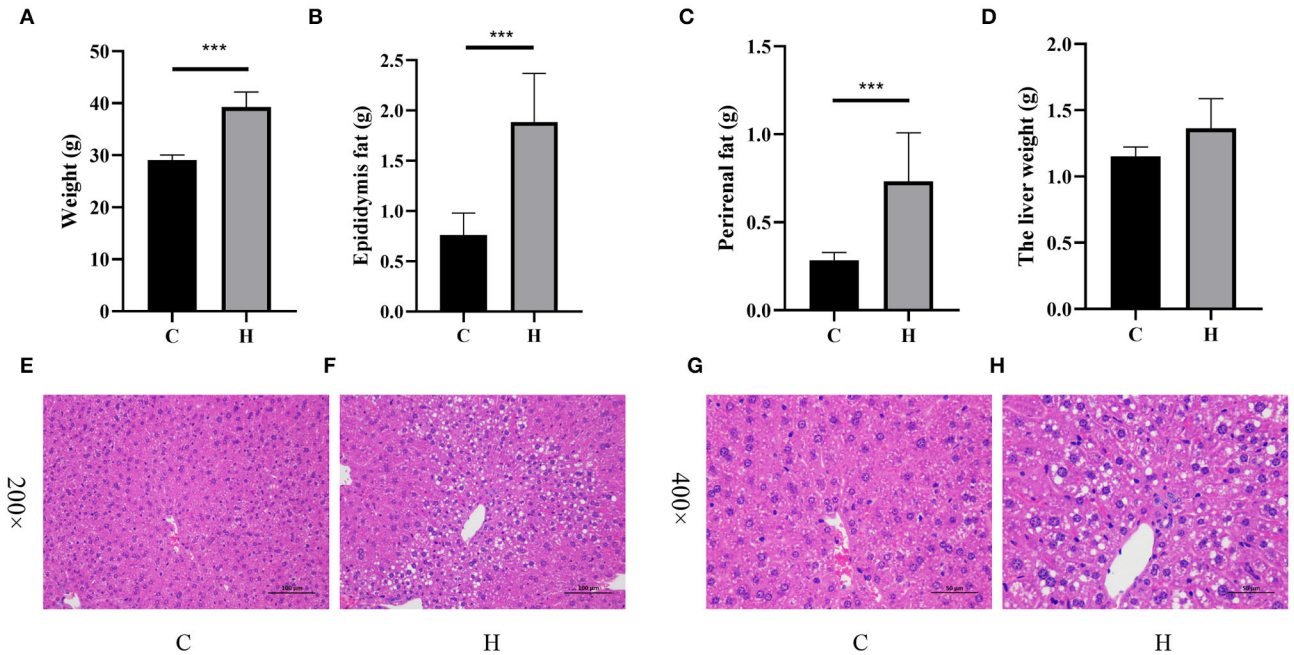

FIGURE 1 | High fructose corn syrup (HFCS) treatment affects body weight and fat deposition in mice. **(A)** Body weight of each group during the intervention period; **(B)** epididymal fat content in each group during the intervention period; **(C)** perirenal fat content in each group during the intervention period; **(D)** liver weight in each group during the intervention period; **(E)** the liver section was enlarged to 200× in Group C; and **(F)** the liver section was enlarged to 200× in Group H. **(G)** The liver section was enlarged to 400× in Group C and **(H)** the liver section was enlarged to 400× in Group H. ***$p < 0.001$.

TABLE 2 | Summary of the original data, clean data, sequencing error rate, clean read rate, and clean Q30 and Q20 base rate of the ordered samples.

Sample	raw_reads	clean_reads	clean_bases	Clean Q30 bases rate (%)	Mapped ratio (%)
C1	47,303,062	46,303,274	6.95G	94.80	94.06
C2	47,089,510	46,136,604	6.92G	94.13	93.48
C3	44,272,672	43,279,174	6.49G	94.43	93.85
C4	41,283,960	40,213,348	6.03G	94.40	92.99
C5	46,466,272	45,560,390	6.83G	94.69	93.80
H1	45,602,948	44,095,038	6.61G	94.75	93.34
H2	47,022,136	45,853,632	6.88G	94.56	95.24
H3	46,125,854	44,628,824	6.69G	94.67	93.72
H4	47,664,476	46,361,598	6.95G	94.62	95.05
H5	43,186,314	41,922,528	6.29G	94.67	93.84

was clear that the liver fat content in Group H was higher than that in Group C.

Differential Gene Expression Analysis

The Illumina HiSeq library was sequenced using the Illumina HiSeq platform to produce a paired-end reading of 150 bp. All sequencing data have been submitted to the NCBI Comprehensive Gene Expression Database with the registration number PRJNA731593. RNA from 10 samples was used, and the quality control method was mainly used to accurately detect RNA integrity with an Agilent 2100 Bioanalyzer. The results showed that the concentration and total amount of 10 samples met the requirements of sequencing. Ten samples were sequenced using the Hiseq 2500 high-throughput sequencing platform, and the average original reading of the 10 samples was 45,601,720. After removing the sequencing fitting and primer sequences, filtering the low-quality value data, and sequencing quality control, a total of 66.64 GB of clean

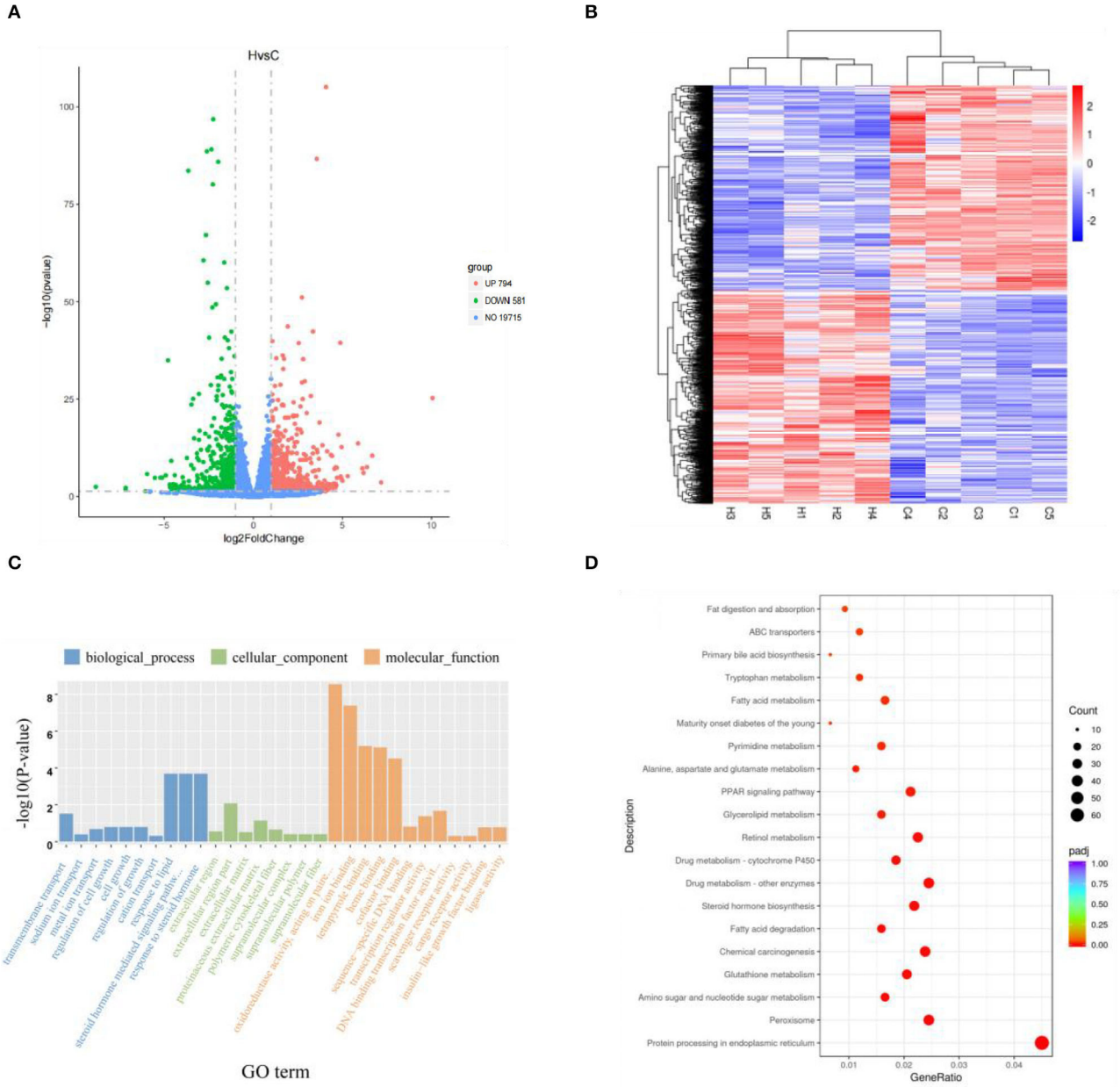

FIGURE 2 | Volcano map of total gene expression of Groups C and H. Red dots represent upregulated genes, green dots represent downregulated genes, and blue dots represent non-differentially expressed genes **(A)**. Expression profiles of 1,375 differentially expressed genes in liver tissue. Red represents upregulated genes, and blue represents downregulated genes **(B)**. Gee Oncology (GO) term enrichment analysis of differentially expressed genes **(C)**. KEGG pathway enrichment analysis of the first 20 differentially expressed genes obtained by Kyoto Encyclopedia of Genes and Genomes (KEGG) enrichment **(D)**.

data were obtained, and the average clean reading of the 10 samples was 44,435,441. In the clean data, Q30 is the percentage of the base with a recognition accuracy of over 99.9%; the reading proportion of the mass value over 30 (Q30) ranges from 94.13 to 94.8%; in the library, the content of gas chromatography ranges from 48.44 to 50.41% (**Table 2**), indicating good sequencing results.

A total of 21,090 genes were expressed in Groups C and H, with $p < 0.05$ and |log-2-fold change|> 1 as the threshold, and 1,375 DEGs were found. There were 794 upregulated genes and 581 downregulated genes in Group H when compared with Group C (**Figure 2A**). The DEG expression patterns of each sample were clustered on the basis of the log2 (fold change) values of their expression ratios, which exhibited good repeatability of samples in the two groups (**Figure 2B**).

To further elucidate the functional role of 1,375 DEGs, the GO and KEGG pathways were enriched to search for significant overabundance categories. GO terms were divided into three categories: biological processes, cell components, and molecular functions, and 47 terms ($p < 0.05$) were significantly enriched in the three categories. The first 30 terms were obtained through GO enrichment (that included 10 biological process terms, 8 molecular function terms, and 12 cellular component terms). Further analysis was performed to determine the relevant regulatory function (**Figure 2C**). Five terms were found to be related to lipid metabolism, including response to lipid (GO: 0033993), cellular response to lipid (GO: 0071396), response to steroid hormone (GO: 0048545), cellular response to steroid hormone stimulus (GO: 0071383), and steroid hormone-mediated signaling pathway (GO: 0043401). Five of these terms all belong to biological processes (**Table 3**).

A total of 1,375 DEGs were also integrated into the KEGG pathway database, and 32 pathways ($p < 0.05$) were significantly enriched. **Figure 2D** shows the first 20 significantly enriched pathways. Lipid metabolism and deposition involve five pathways, i.e., biosynthesis of unsaturated fatty acids pathway (mmu01040), steroid hormone biosynthesis (mmu00140) with 9 genes and 14 genes, 13 genes in peroxisome proliferator-activated receptors (PPAR) signaling pathway (mmu03320) and fatty acid elongation pathway (mmu00062) of 6 genes, tyrosine metabolism pathway (mmu00350) with 6 genes, and primary bile acid biosynthesis pathway (mmu00120) of 4 genes (**Table 4**). Combining GO and KEGG analysis, we screened 12 genes related to lipid metabolism (**Table 5**).

RT-QPCR Validation

To verify the RNA-Seq expression results, we further determined the expression level of 8 lipid-related genes in the liver of mice from Groups C and H, i.e., Stearoyl-Coenzyme A desaturase 1 (*Scd1*), *Pparg*, ELOVL Fatty Acid Elongase 3 (*Elovl3*), fatty acid desaturase 2 (*Fads2*), acyl-CoA thioesterase 2 (*Acot2*), acyl-CoA thioesterase 3 (*Acot3*), acyl-CoA thioesterase 4 (*Acot4*), and fatty acid binding protein 2 (*Fabp2*), of the eight genes. Only one was downregulated, and all the others were upregulated, using RT-qPCR analysis. These 8 genes related to growth metabolism were selected from the KEGG pathways and the GO terms that were significantly enriched in relation to lipid metabolism. Interestingly, these DEGs were all upregulated. Although the expression levels of these 8 determined genes in the liver were higher in Group C than in Group H, *Fabp2* was not significantly different ($p = 0.071$), and *Scd1*, *Pparg*, *Elovl3*, *Fads2*, *Acot2*, *Acot3*, and *Acot4* were genes that showed a significant ($p < 0.05$) difference between Groups C and H (**Figure 3**).

Differences in the Diversity and Composition of the Colon Microbiome in Mice

After 16SrRNA gene sequencing of colonic contents, the alpha diversity analysis structure indicated that Chao1 index, Shannon index and Simpson index indices were not significantly different ($P > 0.05$). It was shown that HFCS had no significant effect on the abundance of gut microbiota components in mice (**Figures 4A–C**). Beta diversity indicated that there was a large separation between Group C and Group H, indicating a considerable difference in gut microbial composition between the two groups (**Figure 4D**). To further investigate the effect of HFCS on intestinal microorganisms, we analyzed the microbial composition in the colon of mice in Groups C and H. Analysis of differences at the phylum level of the gut microbiome showed that when compared to Group C, the abundance of Proteobacteria and Actinobacteria was reduced in Group H. The abundance of Firmicutes was significantly reduced and Bacteroidetes was significantly increased in Group H. Analysis of differences at the genus level of the gut microbiome revealed that the abundances of *Allobaculum* and *Faecalibaculum* were significantly reduced, and the abundance of *Erysipelotrichaceae_uncultured*, *Parabacteroides,* and *Staphylococcus* was increased in Group H (**Figure 4E**).

Linear Discriminant Analysis Effect Size (LEfSe) Identified Different Bacteria Between Groups C and H

To further investigate the differences in the structure and abundance of mouse colonic bacteria at the level of 100 genera, heatmap analysis was performed on the differential genera obtained from LEfSe analysis. The results showed that there were obvious intergeneric differences in the colonic microbiome of mice. Under HFCS intervention, the relative abundance of *Bifidobacterium*, *Lactobacillus*, *Faecalibaculum*, *Erysipelatoclostridium,* and *Parasutterella* was increased in Group H, whereas the relative abundance of *Staphylococcus*, *Peptococcus*, *Parabacteroides*, *Donghicola,* and *Turicibacter* was reduced in Group H (**Figure 5**).

Correlation Analysis of Differentially Abundant Genera and Lipid Metabolism-Related Genes in Mice

Correlation analysis was performed to reveal the association between the gut microbiome and lipid metabolism-related genes. Through Spearman's correlation analysis, *Pparg*, *Acot2*, *Acot3,* and *Scd1* were positively correlated with *Erysipelatoclostridium* and negatively correlated with *Parabacteroides*, *Staphylococcus,*

TABLE 3 | The significantly enriched terms associated with lipid metabolism.

Term ID	Description	*p*-value	Gene number	Gene name
GO:0033993	response to lipid	0.035791763	6	*Rorc/Pparg/Nr3c2/Esrrg/Rxrg/Nr4a1*
GO:0043401	cellular response to lipid	0.035791763	6	*Rorc/Pparg/Nr3c2/Esrrg/Rxrg/Nr4a1*
GO:0048545	response to steroid hormone	0.035791763	6	*Rorc/Pparg/Nr3c2/Esrrg/Rxrg/Nr4a1*
GO:0071383	cellular response to steroid hormone stimulus	0.035791763	6	*Rorc/Pparg/Nr3c2/Esrrg/Rxrg/Nr4a1*
GO:0071396	steroid hormone mediated signaling pathway	0.035791763	6	*Rorc/Pparg/Nr3c2/Esrrg/Rxrg/Nr4a1*

TABLE 4 | The significantly enriched pathways associated with lipid metabolism.

Pathway ID	Description	*P* value	Gene number	Gene name
mmu01040	Biosynthesis of unsaturated fatty acids	0.000321506	9	*Elovl3/Fads2/Acot4/Acot3/Scd1/Acot2/Acnat2/Gm40474/Acot5*
mmu00140	Steroid hormone biosynthesis	0.00033063	14	*Cyp17a1/Cyp2b9/Cyp2c54/Ugt2b1/Cyp2c70/Cyp2c37/Ugt1a9/Gm41857/Cyp2c38/Cyp2b13/Cyp7b1/Cyp2c39/Hsd3b5/Ugt2b38*
mmu03320	PPAR signaling pathway	0.001733084	13	*Ubc/Fads2/Cd36/Pparg/Fabp2/Cyp27a1/Pck2/Cyp4a31/Scd1/Rxrg/Cyp4a14/Cyp4a12b/Plin1*
mmu00062	Fatty acid elongation	0.014560226	6	*Elovl3/Acot4/Acot3/Acot2/Gm40474/Acot5*
mmu00350	Tyrosine metabolism	0.019064803	6	*Got1/Aox3/Ddc/Adh7/Adh6-ps1/Aldh3a1*
mmu00120	Primary bile acid biosynthesis	0.020084289	4	*Cyp27a1/Cyp46a1/Acnat2/Cyp7b1*

TABLE 5 | Information of 12 differentially expressed genes associated with lipid metabolism.

Gene name	Gene ID	log2FoldChange	C readcount	H readcount	*P*-value	Descriptions
Pparg	19016	1.49	108.59	304.67	2.31E−15	peroxisome proliferator activated receptor gamma
Scd1	20249	1.19	64,638.17	147,212.05	1.09E−08	stearoyl-Coenzyme A desaturase 1
Rorc	19885	1.31	400.22	990.88	2.20E−14	RAR-related orphan receptor gamma
Fads2	56473	1.03	8,223.41	16,791.25	1.24E−22	fatty acid desaturase 2
Acot2	171210	1.93	307.2	1,170.6	1.96E−08	acyl-CoA thioesterase 2
Acot4	171282	1.41	631.39	1,674.93	2.05E−16	acyl-CoA thioesterase 4
Fabp2	14079	1.19	88.6	167.69	2.66E−13	fatty acid binding protein 2
Apoa4	11808	4.08	5,675.48	95,974.87	7.93E−106	apolipoprotein A-IV
Cyp46a1	13116	1.63	24.96	77.45	9.04E−09	cytochrome P450, family 46, subfamily a, polypeptide 1
Cyp27a1	104086	−1.01	5,987.95	2,970.2	5.74E−12	cytochrome P450 family 27 subfamily A member 1
Cyp7b1	13123	−1.43	4,090.27	1,520.04	0.0006842	cytochrome P450, family 7, subfamily b, polypeptide 1
Plin1	103968	−3.39	4.16	0.42	0.0419683	perilipin 1
Acot3	171281	2.12	386.94	1,682.7	2.120216	Acyl-CoA Thioesterase 3
Elovl3	12686	−2.61	9,921.82	1,628.4	2.71E−89	ELOVL Fatty Acid Elongase 3

Log2-foldchange of readcount by Group C (C readcount) vs. Group H (H readcount), of which 9 genes upregulated expression (log2-foldchange > 0) and 3 genes downregulated expression (log2-foldchange < 0).

and *Turicibacter*. *Bifidobacterium* was negatively correlated with *Elovl3* (**Figure 6**).

DISCUSSION

High fructose corn syrup is a syrupy mixture of glucose and fructose. In recent years, HFCS has been widely used in the food industry and has mostly replaced sucrose with the advantages of low price and better taste. Bocarsly (28) showed that a short-term intake of 8% HFCS increased body weight, along with increased abdominal fat in mice. These results suggest that HFCSs may have profound negative impacts on the liver and adipose tissue. HFCS alters body metabolism (3), and we found that HFCS intake affects intestinal microbes in a previous study (29). In the present study, we found that HFCS intake resulted in a significant increase in body weight and epididymal and perirenal fat in mice ($p < 0.001$). Although there was no significant difference in liver weight, observation of liver sections revealed that the proportion of lipid droplet area in liver tissue was greater in Group H than in Group C. Collectively, we thoroughly investigated mouse colonic microbes by 16S rRNA gene sequencing and analyzed changes in the abundance and

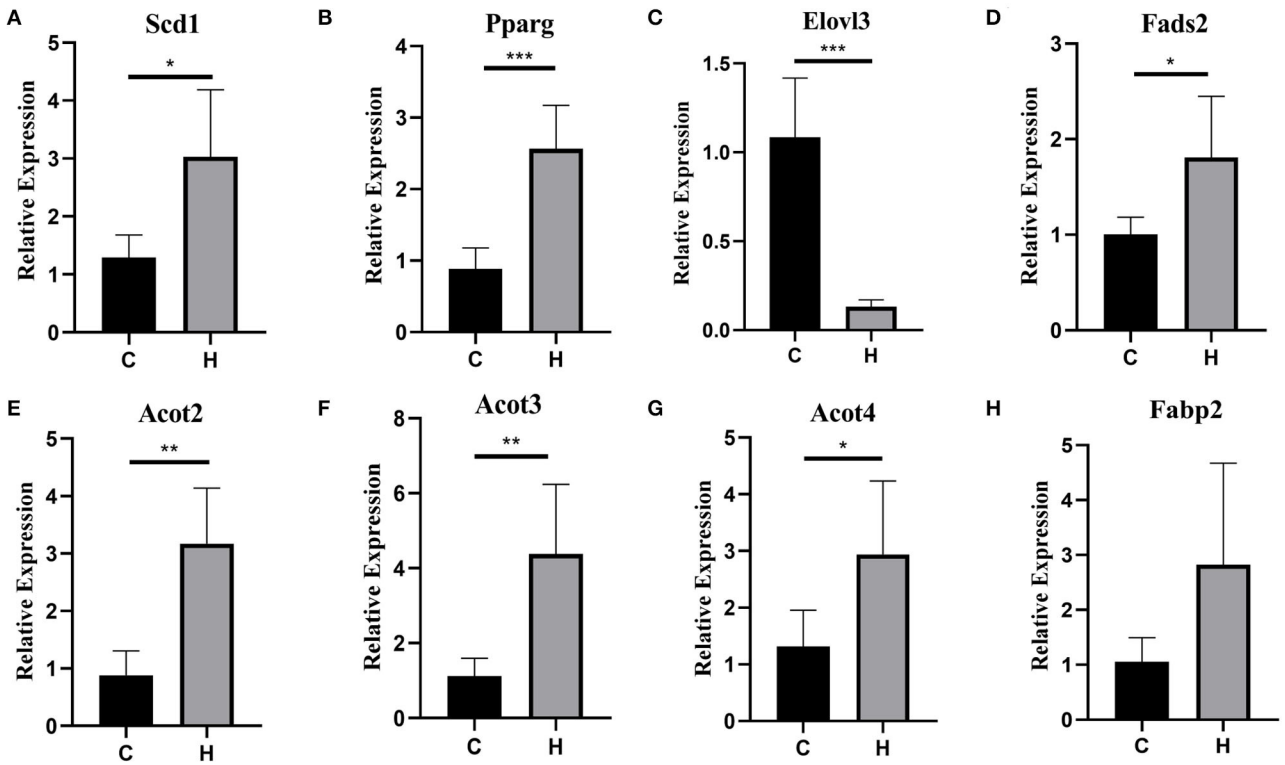

FIGURE 3 | (A–H) Validation of 8 differentially expressed genes (DEGs) between the groups C and H mice by RT-qPCR. The x-axis denotes the group, and the y-axis denotes the log2-fold change derived from RT-qPCR. $^{*}p < 0.05$, $^{**}p < 0.01$, $^{***}p < 0.001$.

structure of mouse colonic microbes after HFCS intervention. Not surprisingly, various bacteria existed in the mouse colon, with the dominant phyla being Bacteroidetes and Firmicutes, giving a result similar to other studies. Furthermore, we identified a total of 1,375 DEGs in the two groups by transcriptome analysis. Compared with Group C, we found 794 upregulated and 581 downregulated genes in Group H and found pathways related to lipid metabolism and inflammation. In addition, RT-PCR results showed that the expression of the *Elovl3* gene was reduced, while the other genes, such as *Scd1, Pparg, Fads2, Acot2, Acot3, Acot4, and Fabp2,* were all upregulated in Group H. Finally, this study shows that HFCS induces abnormalities in hepatic lipid metabolism and alters the structural abundance of the gut microbiome.

The liver is an important metabolic organ in the body that plays a role in deoxidation, storage of liver sugar, and synthesis of secreted proteins (30). Past studies have shown that one of the causes of obesity is the accumulation of individual lipids, which leads to a series of diseases (31). HFCS is considered to be more lipogenic than sucrose, which increases the risk for non-alcoholic fatty liver disease (NAFLD) and dyslipidemia (32). Similarly, in the present study, we found that the administration of HFCS induced higher liver fat infiltration and the most extensive fat blisters as compared to controls.

To better understand the mechanism by which HFCSs regulate hepatic lipid accumulation, further transcriptome sequencing was performed. There were 794 upregulated and 581 downregulated genes between the two groups, which were enriched in lipid metabolic pathways. In particular, the most significant difference observed regards the "biosynthesis of unsaturated fatty acids," which play multiple roles in human health (33). Functional analysis showed that the *Fabp2* and *Acot2* genes were related to liver regulation of lipid metabolism and IR through a series of biological processes (34). In the present study, the expression of *Acot2*, *Acot3*, and *Acot4* was significantly increased by HFCS treatment, suggesting that these three genes could promote adipocyte differentiation. *Elovl3* is known to promote fatty acid synthesis (lipogenesis), and RT-PCR results showed that the expression of the *Elovl3* gene was reduced. It was shown that the periodic expression of *Elovl3* in the liver may be controlled by the biological clock, related hormones, and transcription factors and confirmed that *Elovl3* has high and rhythmic expression in male mice (35). We speculate that the external environment may be a contributing factor in this phenomenon.

Peroxisome proliferator activated receptor gamma can control the peroxisome beta-oxidation pathway of fatty acids. Tontonoz et al. (36) reported that *Pparg* regulates adipocyte differentiation. The RT-PCR results showed that the expression of the *Pparg* gene was upregulated in Group H, and it is speculated that HFCS treatment increases the expression of *Pparg* and promotes

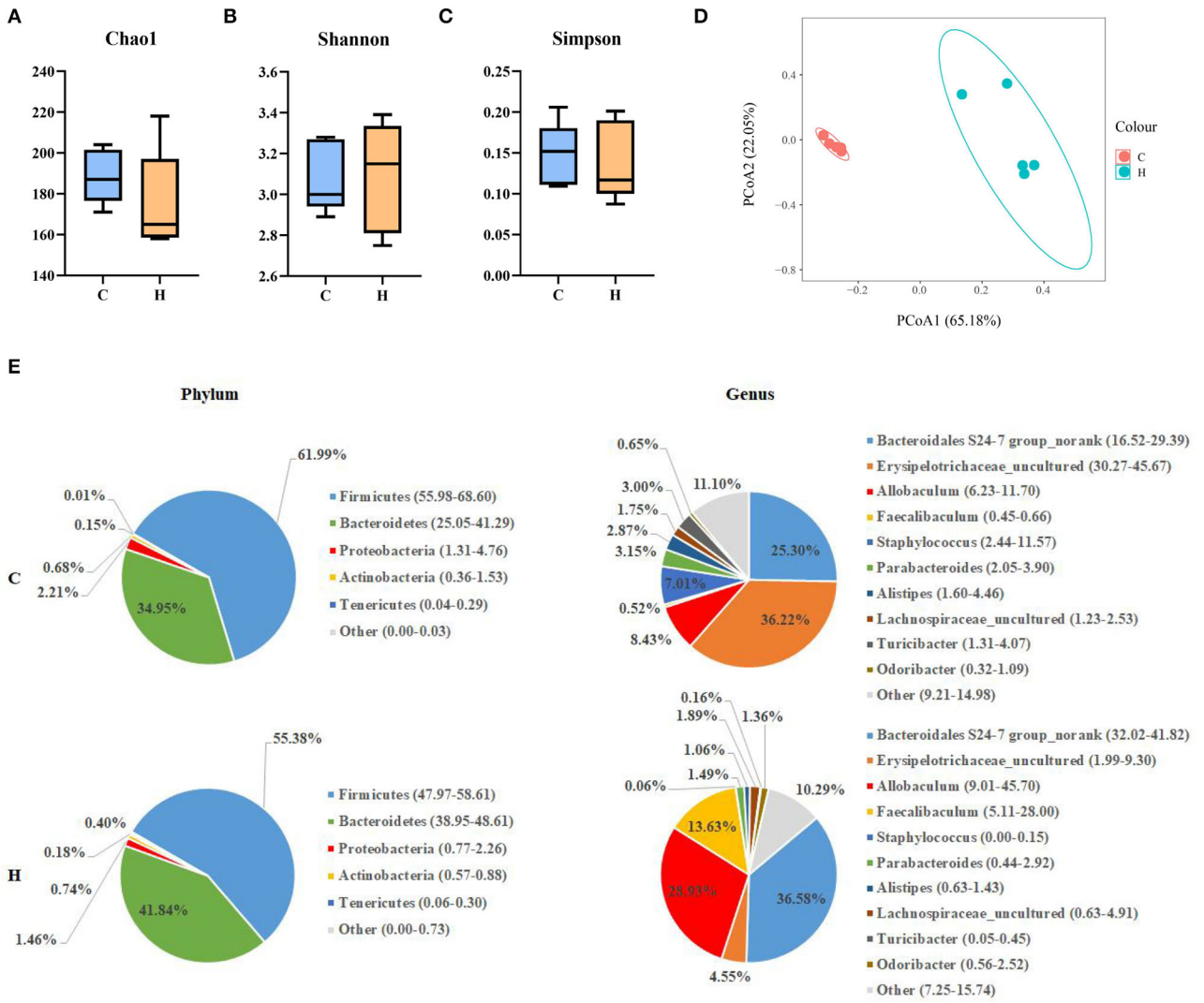

FIGURE 4 | Alpha diversity, including the Chao1 index, Shannon index, and Simpson index **(A–C)**. Principal coordinates analysis (PCoA) of the difference in the microbial community composition of 10 colons in mice. The percentages present the relative contribution of the 2 principal coordinates (PC1–PC2) **(D)**; phylum- and genus-level pie charts of the microbial composition in the colon of Groups C and H mice **(E)**.

the differentiation of adipocytes, which leads to the occurrence or aggravation of the individual obesity. Research shows that perilipin 1 (*Plin1*) expression is decreased in obese participants as compared to healthy controls (37). These findings demonstrate a novel role for *Plin* expression in adipose tissue metabolism and obesity regulation (38). *Fabp2* can help to maintain energy homeostasis by acting as a lipid sensor. *Fabp2* is a key factor in lipogenesis and lipid transport (34). In this study, we found that the *Fabp2* gene was enriched in the PPAR signaling pathway and that its expression was upregulated in Group H. Collectively, our findings suggested a functional role for *Pparg* and *Fabp2* in the regulation of HFCS-mediated hepatic lipid metabolism.

On the other hand, *Scd1* plays key roles in lipid storage, liposome homeostasis, and energy metabolism (39). The study of the *Scd1* gene mutant mouse strain provides evidence that *Scd1* is an important control point of lipid metabolism (40). Scd1-deficient mice had decreased liver fat content, suggesting the lack of *Scd1* protected mice from fat accumulation in the liver (41). This experiment revealed that the expression of *Scd1* was increased in the liver of mice by HFCS intervention, thus regulating the process of lipid metabolism, which is consistent with previous findings. In this study, Cytochrome P450 Family 27 Subfamily A Member 1 (*Cyp27a1*) and Cytochrome P450, Family 7, Subfamily b, Polypeptide 1 (*Cyp7b1*) were found to be reduced by HFCS intervention. Other studies have reported that Cyp27A1$^{-/-}$ mice have an enlarged liver and kidneys and increased triglyceride levels and fatty acid synthesis, and cholesterol absorption and synthesis (42). Furthermore, *Cyp7b1* has broad substrate specificity, is widely distributed in most organs, and plays important roles in the regulation of lipid

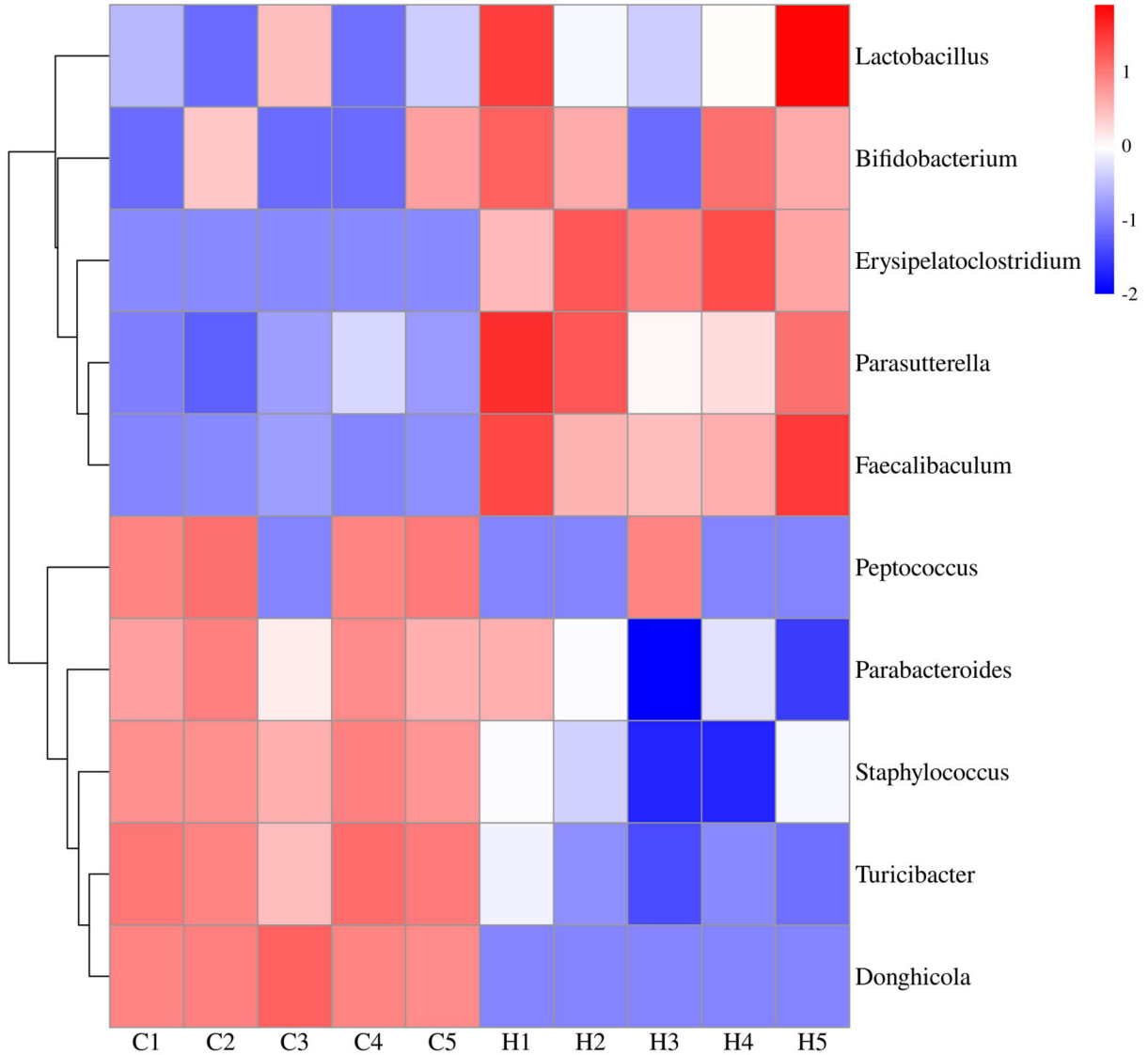

FIGURE 5 | Expression profiles of 10 differentially expressed bacteria in colonic contents. The vertical axis represents the genus clusters, and one row represents one genus. The color scale represents the expression abundance of the genera; red represents increased abundance, and blue represents decreased abundance.

metabolism (43). Overall, alterations in gene expression levels can affect lipid metabolism.

Many studies have shown that the gut microbiome plays an important role in determining body weight (44). PCoA representation of the bacterial genera composition of all samples revealed that HFCS intervention altered the mouse colon microbiome when compared with Group C. Our expectation was confirmed that specific bacteria would exist in the mouse colon, with the dominant phyla being Bacteroidetes and Firmicutes, a result consistent with other studies (45). In the present study, mice in Group H had a lower relative abundance of the Firmicutes phylum and a higher relative abundance of the Bacteroidetes phylum than mice in Group C. This result was confirmed by Mastrocola et al. (19), who found that the ratio of Firmicutes/Bacteroidetes and abundance of Firmicutes were decreased in mice fed fructose (20), which is consistent with our findings. In the present study, the relative abundance of *Bifidobacterium*, *Lactobacillus*, *Faecalibaculum*, *Erysipelatoclostridium,* and *Parasutterella* was increased after the HFCS diet as compared to the normal diet, as shown by the genus level of the heatmap, in contrast to the decrease in the relative abundance of *Staphylococcus*, *Peptococcus*, *Parabacteroides*, *Donghicola,* and *Turicibacter*. *Lactobacillus* remained tightly attached in the intestinal epithelium (46), and the abundance of *Lactobacillus* was increased with sugar intake (20). *Bifidobacterium* was increased only in mice fed the Western-style diet (WSD) + fructose diet, which is consistent with our findings. *Lactobacillus* and *Bifidobacterium*

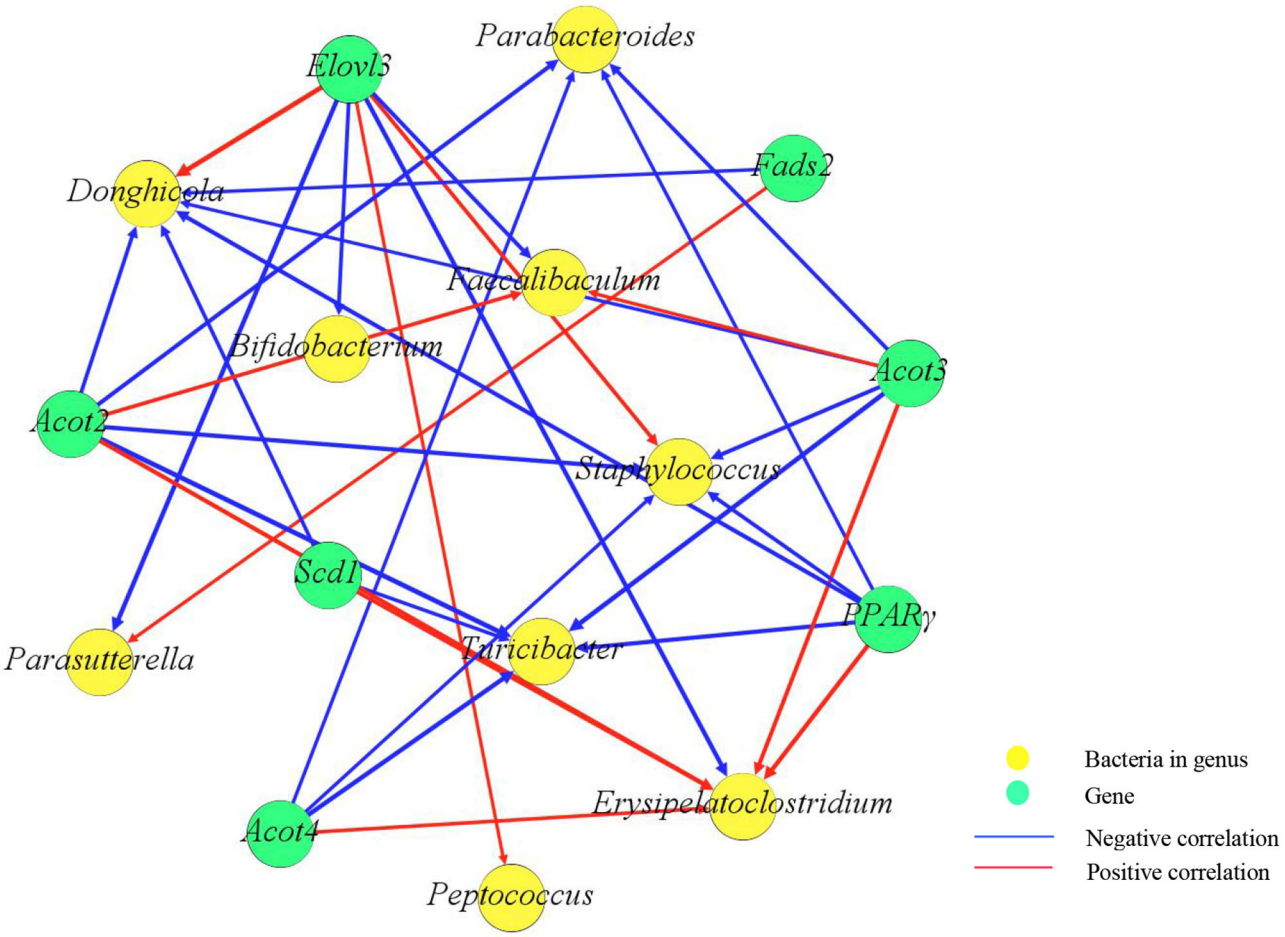

FIGURE 6 | Correlation network diagram between genes and the gut microbiome. Yellow spots represent bacteria, and green spots represent genes. Red lines represent positive correlations, and blue lines represent negative correlations. The weight of the lines represents the strength of the correlation, and the thicker the line is, the greater the absolute value of the correlation. The number of spots represents the number of correlated objects.

are considered to have health benefits, but some studies have found harmful effects on physical health (47, 48). *Parabacteroides* have an anti-obesity effect, Julia Beisner et al. found that they decreased after a high-fructose diet (19). Wang B et al. observed changes in intestinal microorganisms in mice through different diets and found that some studies showed a lower abundance of *Turicibacter* and *Pediococcus* in fructose diets than in controls (49).

Some studies have shown that the gut microbiome affects energy metabolism by regulating key genes (50). Erysipelotrichaceae has a positive correlation with obesity (51), and *Turicibacter* has been closely associated with abnormal lipid metabolism (52). *Parabacteroides* have an anti-obesity effect (45). *Pparg*, *Acot2,* and *Acot3* can promote adipocyte differentiation. It has been shown that the knockdown of Scd1 inhibits adipogenesis (53). *Scd1* can play a vital role in lipid metabolism, and its product oleic acid (OA) can promote lipolysis by upregulating lipase (54, 55). In this study, we found that *Pparg, Acot2, Acot3, and Scd1* were positively correlated with *Erysipelatoclostridium* and negatively correlated with *Turicibacter* and *Parabacteroides. Bifidobacterium* can suppress fat accumulation and regulate obesity and related metabolic diseases by affecting lipid metabolism (56–58). Elovl3 deletion may lead to reduced lipid accumulation in the liver (59). Our results showed that *Bifidobacterium* was positively correlated with *Pparg* and *Acot3* and negatively correlated with *Elovl3.* Overall, gut microbes can regulate related genes to influence lipid metabolism.

CONCLUSION

Our study demonstrated that HFCS intake resulted in a significant increase in body weight, epididymal and perirenal fat content, and an increase in the proportion of lipid droplet area in the liver, suggesting that HFCS may affect liver lipid metabolism in mice, leading to a lipid deposition. GO and KEGG analysis showed that *Pparg*, *Scd1*, RAR Related Orphan ReceptorC (*Rorc*), *Fads2*, *Acot2*, *Acot4*, *Fabp2*, apolipoprotein A-IV

(*Apoa4*), cytochrome P450, family 46, subfamily a,polypeptide1 (*Cyp46a1*), *Cyp27a1*, *Cyp7b1*, and *Plin1*, 12 genes were screened and found to display keyregulatory roles in lipidmetabolism. The PCR results contributed to elucidating the metabolic effect of HFCS in reducing the expression of *Elovl3* and increasing the expression of *Scd1, Pparg, Fads2, Acot2, Acot3, Acot4, and Fabp2* in sthe liver. At the phylum level, the HFCS diet increased the abundance of the Firmicutes phylum while decreasing the abundance of the Bacteroidetes phylum. Obviously, the Firmicutes/Bacteroidetes ratio also was reduced. At the genus level, the relative abundance of *Bifidobacterium*, *Lactobacillus*, *Faecalibaculum*, *Erysipelatoclostridium,* and *Parasutterella* was increased; in contrast, the relative abundance of *Staphylococcus*, *Peptococcus*, *Parabacteroides*, *Donghicola,* and *Turicibacter* was reduced by the HFCS diet. Correlation analysis indicated that *Pparg*, *Acot2*, *Acot3, and Scd1* were positively correlated with *Erysipelatoclostridium* and negatively correlated with *Turicibacter*. We conclude that HFCS has a significant impact on genes related to lipid metabolism in the liver and changes the structure and function of the colonic microbiome in mice; in particular, it decreases the abundance of bacteria with anti-obesity effects, which suggests that it may lead to disruption of intestinal function and thus affect the body's metabolism. In general, HFCS regulates the expression of lipid metabolism genes in the liver by affecting the gut microbiome, thereby influencing organismal metabolism.

DATA AVAILABILITY STATEMENT

The data presented in the study are deposited in the NCBI (National Center for Biotechnology Information) repository, accession numbers: PRJNA731593 and PRJNA826752.

ETHICS STATEMENT

The animal study was reviewed and approved by Zhejiang Provincial Ethics Committee for Laboratory Animals (Ethical Approval No.78865576).

AUTHOR CONTRIBUTIONS

YSh: methodology, review and editing, and data curation. YSu: methodology and review and editing. XW: methodology. YX: visualization. LM: supervision. WL: validation. ZZ: software. WW: funding acquisition, project administration, and resources. JL: conceptualization and investigation. All authors contributed to the article and approved the submitted version.

FUNDING

This research was supported by the State Key Laboratory for Managing Biotic and Chemical Threats to the Quality and Safety of Agroproducts, Grant/Award Number: 2010DS700124-ZZ2017.

ACKNOWLEDGMENTS

The authors would like to thank all members of the lab for their advice and technical assistance.

SUPPLEMENTARY MATERIAL

The Supplementary Material for this article can be found online at: https://www.frontiersin.org/articles/10.3389/fnut.2022.921758/full#supplementary-material

REFERENCES

1. Hanover LM, White JS. Manufacturing, composition, and applications of fructose. *Am J Clin Nutr.* (1993) 58:724S−32S. doi: 10.1093/ajcn/58.5.724S
2. Bray GA, Nielsen SJ, Popkin BM. Consumption of high-fructose corn syrup in beverages may play a role in the epidemic of obesity. *Am J Clin Nutr.* (2004) 79:537–43. doi: 10.1093/ajcn/79.4.537
3. Bhat SF, Pinney SE, Kennedy KM, McCourt CR, Mundy MA, Surette MG, et al. Exposure to high fructose corn syrup during adolescence in the mouse alters hepatic metabolism and the microbiome in a sex-specific manner. *J Physiol.* (2021) 599:1487–511. doi: 10.1113/JP280034
4. Diana CH, Mónica ST, Francisco LV. Miriam, Héctor L, Ricardo C, et al. Modulation of gut microbiota by Mantequilla and Melipona honeys decrease low-grade inflammation caused by high fructose corn syrup or sucrose in rats. *Food Res Int.* (2022) 151:110856. doi: 10.1016/j.foodres.2021.110856
5. Schultz A, Neil D, Aguila MB. Mandarim-de-Lacerda CA. Hepatic Adverse Effects of Fructose Consumption Independent of Overweight/Obesity. *Int J Mol Sci.* (2013) 14:21873–86. doi: 10.3390/ijms141121873
6. Reccia I, Kumar J, Akladios C, Virdis F, Pai M, Habib N, et al. Non-alcoholic fatty liver disease: a sign of systemic disease. *Metabolism.* (2017) 72:94–108. doi: 10.1016/j.metabol.2017.04.011
7. Fam BC, Joannides CN, Andrikopoulos S. The liver: Key in regulating appetite and body weight. *Adipocyte.* (2012) 1:259–64. doi: 10.4161/adip.21448
8. Li H, Wang T, Xu C, Wang D, Ren J, Li Y, et al. Transcriptome profile of liver at different physiological stages reveals potential mode for lipid metabolism in laying hens. *BMC Genom.* (2015) 16:763. doi: 10.1186/s12864-015-1943-0
9. Chon KS, Hoon KY, Wook SS, EunYi M, Suhkneung P, Hee US. Corrigendum to "Fisetin induces Sirt1 expression while inhibiting early adipogenesis in 3T3-L1 cells" [Biochem. Biophys. Res. Commun. 467(4) (2015) 638-644]. *Biochem Biophys Res Commun.* (2018) 506:306. doi: 10.1016/j.bbrc.2018.10.068
10. Pirany N, Balani AB, Hassanpour H, Mehraban H. Differential expression of genes implicated in liver lipid metabolism in broiler chickens differing in weight. *Br Poult Sci.* (2019) 61:10–6. doi: 10.1080/00071668.2019.1680802
11. Xu YY, Xu YS, Wang Y, Qin W, Shi JS. Dendrobium nobile Lindl. alkaloids regulate metabolism gene expression in livers of mice. *J Pharm Pharmacol.* (2017) 69:1409–17. doi: 10.1111/jphp.12778
12. Bourneuf E, Hérault F, Chicault C, Carré W, Assaf S, Monnier A, et al. Microarray analysis of differential gene expression in the liver of lean and fat chickens. *J Anim Sci Biotechnol.* (2006) 372:162–70. doi: 10.1016/j.gene.2005.12.028
13. D'Andre H, Paul W, Xu S, Jia X, Zhang R, Sun L, et al. Identification and characterization of genes that control fat deposition in chickens. *J Anim Sci Biotechnol.* (2014) 4:43. doi: 10.1186/2049-1891-4-43
14. Schoeler M, Caesar RJRiE, Disorders M. Dietary lipids, gut microbiota and lipid metabolism. *Rev Endocr Metab Disord.* (2019) 20:461–72. doi: 10.1007/s11154-019-09512-0

15. Velagapudi VR, Hezaveh R, Reigstad CS, Gopalacharyulu P, Yetukuri L, Islam S, et al. The gut microbiota modulates host energy and lipid metabolism in mice. *J Lipid Res*. (2010) 51:1101–12. doi: 10.1194/jlr.M002774
16. Sonnenburg JL, Bäckhed F. Diet–microbiota interactions as moderators of human metabolism. *Nature*. (2016) 535:56–64. doi: 10.1038/nature18846
17. Zhang YJ Li S, Gan RY, Zhou T, Xu DP Li HB. Impacts of Gut Bacteria on Human Health and Diseases. *Int J Mol Sci*. (2015) 16:7493–519. doi: 10.3390/ijms16047493
18. Xiao L, Estellé J, Kiilerich P, Ramayo-Caldas Y, Xia Z, Feng Q, et al. A reference gene catalogue of the pig gut microbiome. *Nat Microbiol*. (2016) 1:16161. doi: 10.1038/nmicrobiol.2016.161
19. Mastrocola R, Ferrocino I, Liberto E, Chiazza F, Cento AS, Collotta D, et al. Fructose liquid and solid formulations differently affect gut integrity, microbiota composition and related liver toxicity: a comparative in vivo study. *J Nutr Biochem*. (2018) 55:185–99. doi: 10.1016/j.jnutbio.2018.02.003
20. Noble EE, Hsu TM, Jones RB, Fodor AA. Kanoski SE. Early-Life Sugar Consumption Affects the Rat Microbiome Independently of Obesity. *J Nutr*. (2017) 147:20–8. doi: 10.3945/jn.116.238816
21. Crescenzo R, Mazzoli A, Luccia BD, Bianco F, Cancelliere R, Cigliano L, et al. Dietary fructose causes defective insulin signalling and ceramide accumulation in the liver that can be reversed by gut microbiota modulation. *Food Nutr Res*. (2017) 61:1331657. doi: 10.1080/16546628.2017.1331657
22. Minoru K, Michihiro A, Susumu G, Masahiro H, Mika H, Masumi I, et al. KEGG for linking genomes to life and the environment. *Nucleic Acids Res*. (2008) 36:D480–4. doi: 10.1093/nar/gkm882
23. Mao X, Tao C, Olyarchuk JG, Wei L. Automated genome annotation and pathway identification using the KEGG Orthology (KO) as a controlled vocabulary. *Bioinformatics*. (2005) 21:3787–93. doi: 10.1093/bioinformatics/bti430
24. Zheng Z, Xiao Y, Ma L, Lyu W, Peng H, Wang X, et al. Low dose of sucralose alter gut microbiome in mice. *Front Nutr*. (2022) 9:848392. doi: 10.3389/fnut.2022.848392
25. Lawley B, Tannock GW. Analysis of 16S rRNA gene amplicon sequences using the QIIME software package. *Methods Mol Biol*. (2017) 1537:153–63. doi: 10.1007/978-1-4939-6685-1_9
26. Magoč T, Salzberg SL. FLASH: fast length adjustment of short reads to improve genome assemblies. *Bioinformatics*. (2011) 27:2957–963. doi: 10.1093/bioinformatics/btr507
27. Wang Q. Naive Bayesian classifier for rapid assignment of rRNA sequences into the new bacterial taxonomy. *Appl Environ Microbiol*. (2007) 73:5261–7. doi: 10.1128/AEM.00062-07
28. Bocarsly ME. High-fructose corn syrup causes characteristics of obesity in rats: increased body weight, body fat and triglyceride levels. *Pharmacol Biochem Behav*. (2010) 97:101–6. doi: 10.1016/j.pbb.2010.02.012
29. Han X, Feng Z, Chen Y, Zhu L, Li X, Wang X, et al. Effects of high-fructose corn syrup on bone health and gastrointestinal microbiota in growing male mice. *Front Nutr*. (2022) 9:829396. doi: 10.3389/fnut.2022.829396
30. Sahini N, Borlak J. Recent insights into the molecular pathophysiology of lipid droplet formation in hepatocytes. *Prog Lipid Res*. (2014) 54:86–112. doi: 10.1016/j.plipres.2014.02.002
31. Sipka S, Bruckner G. The Immunomodulatory Role of Bile Acids. *Int Arch Allergy Immunol*. (2014) 165:1–8. doi: 10.1159/000366100
32. Mock K, Lateef S, Benedito VA, Tou JC. High-fructose corn syrup-55 consumption alters hepatic lipid metabolism and promotes triglyceride accumulation. *J Nutr Biochem*. (2017) 39:32–9. doi: 10.1016/j.jnutbio.2016.09.010
33. Brenner, Rodolfo R. Antagonism between Type 1 and Type 2 diabetes in unsaturated fatty acid biosynthesis. *Future Lipidol*. (2006) 1:631–40. doi: 10.2217/17460875.1.5.631
34. Hu G, Wang S, Tian J, Chu L, Li H. Epistatic effect between ACACA and FABP2 gene on abdominal fat traits in broilers - ScienceDirect. *J Genet Genomics*. (2010) 37:505–12. doi: 10.1016/S1673-8527(09)60070-9
35. Chen H, Lei G, Dan Y, Xiao Y, Jin Y. Coordination between the circadian clock and androgen signaling is required to sustain rhythmic expression of Elovl3 in mouse liver. *J Biol Chem*. (2019) 294:7046–56. doi: 10.1074/jbc.RA118.005950
36. Tontonoz P, Hu E, Spiegelman BM. Stimulation of adipogenesis in fibroblasts by PPAR gamma 2, a lipid-activated transcription factor. *Cell*. (1994) 79:1147–56. doi: 10.1016/0092-8674(94)90006-X
37. Ylmaz EG, Bozkurt H. Ndad za A, Thomford NE, Dandara C. Childhood Obesity Risk in Relationship to Perilipin 1 (PLIN1) Gene Regulation by Circulating microRNAs. *OMICS*. (2020) 24:43–50. doi: 10.1089/omi.2019.0150
38. Miyoshi H, Souza SC, Endo M, Sawada T, Perfield JW, Shimizu C, et al. Perilipin overexpression in mice protects against diet-induced obesity. *J Lipid Res*. (2010) 51:975–82. doi: 10.1194/jlr.M002352
39. Thumser AE, Moore JB, Plant NJ. Fatty acid binding proteins: tissue-specific functions in health and disease. *Curr Opin Clin Nutr Metab Care*. (2014) 17:124–9. doi: 10.1097/MCO.0000000000000031
40. Dobrzyn A, Ntambi JM. The role of stearoyl-CoA desaturase in the control of metabolism. *Prostaglandins Leukot Essent Fatty Acids*. (2005) 73:35–41. doi: 10.1016/j.plefa.2005.04.011
41. Cohen P. Role for Stearoyl-CoA Desaturase-1 in Leptin-Mediated Weight Loss. *Science*. (2002) 297:240–3. doi: 10.1126/science.1071527
42. Repa JJ, Lund EG, Horton JD, Leitersdorf E, Russell DW, Dietschy JM, et al. Disruption of the Sterol 27-Hydroxylase Gene in Mice Results in Hepatomegaly and Hypertriglyceridemia: Reversal by cholic acid feeding. *J Biol Chem*. (2000) 275:39685–92. doi: 10.1074/jbc.M007653200
43. Chiang JYL. Regulation of bile acid synthesis: pathways, nuclear receptors, and mechanisms. *J Hepatol*. (2004) 40:539–51. doi: 10.1016/j.jhep.2003.11.006
44. Cardinelli CS, Sala PC, Alves CC, Torrinhas RS, Waitzberg DL. Influence of intestinal microbiota on body weight gain: a narrative review of the literature. *Obes Surg*. (2015) 25:346–53. doi: 10.1007/s11695-014-1525-2
45. Beisner J, Gonzalezgranda A, Basrai M, Dammsmachado A, Bischoff SC. Fructose-induced intestinal microbiota shift following two types of short-term high-fructose dietary phases. *Nutrients*. (2020) 12:3444. doi: 10.3390/nu12113444
46. Karczewski J, Troost FJ, Konings I, Dekker J, Wells JM. Regulation of human epithelial tight junction proteins by Lactobacillus plantarum in vivo and protective effects on the epithelial barrier. *Am J Physiol Gastrointest Liver Physiol*. (2010) 298:G851–9. doi: 10.1152/ajpgi.00327.2009
47. Gois M, Sinha T, Spreckels JE, Vila AV, Kurilshikov A. Role of the gut microbiome in mediating lactose intolerance symptoms. *Gut*. (2022) 71:215–7. doi: 10.1136/gutjnl-2020-323911
48. Pararajasingam A, Uwagwu J. Lactobacillus: the not so friendly bacteria. *BMJ Case Rep*. (2017) 2017:bcr2016218423. doi: 10.1136/bcr-2016-218423
49. Wang B, Gao R, Wu Z, Yu Z. Functional Analysis of Sugars in Modulating Bacterial Communities and Metabolomics Profiles of Medicago sativa Silage. *Front Microbiol*. (2020) 11:641. doi: 10.3389/fmicb.2020.00641
50. Backhed F, Ding H, Wang T, Hooper LV, Koh GY, Nagy A, et al. The gut microbiota as an environmental factor that regulates fat storage. *Proc Natl Acad Sci USA*. (2004) 101:15718–23. doi: 10.1073/pnas.0407076101
51. Ye J, Zhao Y, Chen X, Zhou H, Xiao M. Pu-erh tea ameliorates obesity and modulates gut microbiota in high fat diet fed mice. *Food Res Int*. (2021) 144:110360. doi: 10.1016/j.foodres.2021.110360
52. Li C, Zhang Y, Ge Y, Qiu B. Tao H. Comparative transcriptome and microbiota analyses provide new insights into the adverse effects of industrial trans fatty acids on the small intestine of C57BL/6 mice. *Eur J Nutr*. (2021) 60:975–87. doi: 10.1007/s00394-020-02297-y
53. Ntambi JM, Miyazaki M, Stoehr JP, Lan H, Kendziorski CM, Yandell BS, et al. Loss of stearoyl-CoA desaturase-1 function protects mice against adiposity. *Proc Natl Acad Sci USA*. (2002) 99:11482–6. doi: 10.1073/pnas.132384699

54. Zou Y, Wang YN, Ma H, He ZH, Tang Y, Guo L. et al. SCD1 promotes lipid mobilization in subcutaneous white adipose tissue. *J Lipid Res.* (2020) 61:1589–604. doi: 10.1194/jlr.RA120000869
55. Ravaut G, Légiot A, Bergeron KF, Mounier C. Monounsaturated fatty acids in obesity-related inflammation. *Int J Mol Sci.* (2020) 22:330. doi: 10.3390/ijms22010330
56. Yamamura R, Okubo R, Katsumata N, Odamaki T, Hashimoto N, Kusumi I, et al. Lipid and energy metabolism of the gut microbiota is associated with the response to probiotic bifidobacterium breve strain for anxiety and depressive symptoms in schizophrenia. *J Pers Med.* (2021) 11:987. doi: 10.3390/jpm11100987
57. Kikuchi K, Ben Othman M, Sakamoto K. Sterilized bifidobacteria suppressed fat accumulation and blood glucose level. *Biochem Biophys Res Commun*. (2018) 501:1041–7. doi: 10.1016/j.bbrc.2018.05.105
58. Sun Y, Tang Y, Hou X, Wang H, Science YBJFiV. Novel Lactobacillus reuteri HI120 Affects Lipid Metabolism in C57BL/6 Obese Mice. *Front Vet Sci.* (2020) 7:560241. doi: 10.3389/fvets.2020.560241
59. Zadravec D, Brolinson A, Fisher RM, Carneheim C, Csikasz RI, Bertrand-Michel J, et al. Ablation of the very-long-chain fatty acid elongase ELOVL3 in mice leads to constrained lipid storage and resistance to diet-induced obesity. *FASEB J.* (2010) 24:4366–77. doi: 10.1096/fj.09-152298

Conflict of Interest: The authors declare that the research was conducted in the absence of any commercial or financial relationships that could be construed as a potential conflict of interest.

Publisher's Note: All claims expressed in this article are solely those of the authors and do not necessarily represent those of their affiliated organizations, or those of the publisher, the editors and the reviewers. Any product that may be evaluated in this article, or claim that may be made by its manufacturer, is not guaranteed or endorsed by the publisher.

frontiers | Frontiers in Nutrition

ORIGINAL RESEARCH
published: 14 July 2022
doi: 10.3389/fnut.2022.931427

Lactobacillus fermentum CECT5716 Alleviates the Inflammatory Response in Asthma by Regulating TLR2/TLR4 Expression

Weifang Wang[1], Yunfeng Li[2], Guojing Han[1], Aimin Li[3] and Xiaomei Kong[3]**

[1] Department of Respiratory and Critical Care Medicine, The Eighth Medical Center of the PLA General Hospital, Beijing, China, [2] Hebei Key Laboratory of Chinese Medicine Research on Cardio-Cerebrovascular Disease, Hebei University of Chinese Medicine, Shijiazhuang, China, [3] NHC Key Laboratory of Pneumoconiosis, Shanxi Key Laboratory of Respiratory Diseases, Department of Pulmonary and Critical Care Medicine, The First Hospital of Shanxi Medical University, Taiyuan, China

Background: Asthma is a chronic disease, which is harmful to the health of the body and the quality of life. Supplementation of *Lactobacillus* can affect the immune environment of the lungs through the gut-lung axis. This study aimed to explore the potential regulatory targets of *Lactobacillus* to relieve inflammation in asthma and determine a new approach for improving asthma.

Methods: A mouse ovalbumin (OVA)-induced model was constructed. OVA mice were supplemented with *Lactobacillus fermentum* CECT5716 by gavage. The gut microbiota composition of normal and OVA mice was analyzed using 16S ribosomal DNA identification. BALF, serum, lung tissues, and duodenal tissues were collected. Wright's staining was performed to determine the cell content of the alveolar lavage fluid. Hematoxylin-eosin staining, Masson staining, and periodic acid-Schiff staining were performed to observe the improvement in the lungs of OVA mice supplemented with *Lactobacillus*. Immunofluorescence was performed to measure the severity of the intestinal barrier leakage. Enzyme-linked immunosorbent assay was carried out to determine the expression levels of inflammatory cell factors, while quantitative reverse transcription-polymerase chain reaction and western blotting were performed to detect the levels of toll-like receptor 2 (TLR2)/TLR4 expression and cell adhesion factors.

Results: Compared with Control mice, OVA mice exhibited malignant conditions, such as intestinal leakage and lung edema. After supplementation with *Lactobacillus*, the inflammatory cell content in the bronchoalveolar lavage fluid decreased, and the inflammatory response was alleviated. The level of TLR2/TLR4 expression was reduced. The inflammatory cell infiltration in the airway mucosa of OVA mice was improved, alveolar swelling was reduced and the basement membrane appeared thinner.

Conclusion: The *Lactobacillus* inhibited the TLR2/TLR4 expression in OVA mice. Supplementation with *Lactobacillus* can alleviate the inflammatory response in OVA mice, inhibit pulmonary fibrosis, and treat asthma.

Keywords: asthma, *Lactobacillus fermentum* CECT5716, gut microbiota, TLR2, TLR4, lung

OPEN ACCESS

Edited by:
Jie Yin,
Hunan Agricultural University, China

Reviewed by:
Ann Catherine Archer,
JSS Academy of Higher Education and Research, India
Yaoyao Xia,
South China Agricultural University, China

****Correspondence:***
Aimin Li
dcliaim@163.com
Xiaomei Kong
sunnydr99@163.com

Specialty section:
This article was submitted to Nutrition and Microbes, a section of the journal Frontiers in Nutrition

Received: *29 April 2022*
Accepted: *20 June 2022*
Published: *14 July 2022*

Citation:
Wang W, Li Y, Han G, Li A and Kong X (2022) Lactobacillus fermentum CECT5716 Alleviates the Inflammatory Response in Asthma by Regulating TLR2/TLR4 Expression. Front. Nutr. 9:931427. doi: 10.3389/fnut.2022.931427

INTRODUCTION

Asthma is a chronic bronchial inflammatory disease involving various cells and cytokines (1). The clinical manifestations are mainly wheezing, shortness of breath, chest tightness, cough and other symptoms, and are affected by environmental stimuli and genetic factors (2). The currently available treatment options alleviate the symptoms of asthma and other allergic diseases, but do not provide a complete cure. Most people with asthma tend to boost their immunity by taking specific microbial food supplements or probiotics that can potentially prevent or treat allergic diseases (3). It is widely recognized that commensal microorganisms are relevant for human and animal health, participating in several important biological functions, including nutrient digestion, vitamin synthesis, and pathogens inhibition (4, 5). Probiotics have anti-inflammatory effects and anti-cancer effects, induce beneficial bacterial proliferation, suppress harmful bacteria, improve intestinal health, reduce blood cholesterol levels, and suppress endogenous infections (6). Lactic acid bacteria are a probiotic that prevents the early development of allergic diseases in children and mouse asthma models (7). In many studies, the oral administration of probiotics such as *Lactobacillus rhamnosus* GG, *Lactobacillus gasseri, Lactobacillus fermentum* NWS29, *Lactobacillus casei* NWP08, *Lactobacillus rhamnosus* NWP13, and *Lactobacillus salivarius* PM-A0006 have shown significant benefits in mouse models of allergic asthma (8). In different experimental models, *Lactobacillus fermentum* CECT5716 has shown anti-inflammatory effects and capacity to modulate microbiota composition (9). It suggests a potential use of *Lactobacillus fermentum* CECT5716 in clinical practice. However, no association between *Lactobacillus fermentum* CECT5716 and asthma has been reported yet. This study was conducted to investigate the effects of *Lactobacillus fermentum* CECT5716 on asthma prevention using a murine model of asthma.

Well-documented examples of probiotic-effector molecules in *Lactobacillus* and *Bifidobacterium* strains include surface-localized molecules such as specific pili, S-layer proteins, extracellular polysaccharides, polypeptides; more broadly produced metabolites such as tryptophan-associated and histamine-associated metabolites; CpG-rich DNA; and various enzymes (such as lactase and bile salt hydrolases) (10). The gut microbiota is an important stimulator of the development and function of the immune system and plays an important role in regulating immune responses. The composition and metabolites of the microbiota of allergic individuals are different from those of healthy individuals (11). In addition, asthma involves disturbances in the gut microbiota and is associated with metabolic dysfunction. Manipulation of the gut microbiota using oral probiotics or high-fiber dietary supplements that increase the synthesis of short-chain fatty acids contributes to the affinitive local and distal mucosal immunity in mice (12). Therefore, modulating the gut microbiota using probiotics and through dietary changes is a reasonable treatment to prevent asthma and other allergic diseases (13). In this study, we focused on improving the gut microbiota using *Lactobacillus fermentum* CECT5716 as the direction of research.

Gut microbiota can help maintain the normal functioning of the human body through specific signaling pathways. Toll-like receptors (TLRs) expressed by antigen presenting cells (macrophages, dendritic cells) and other various cells (e.g., airway epithelial cells) are innate immune sensors, which recognize microbial pathogen-associated molecular patterns (bacteria, fungi, and virus structures) as well as endogenous danger molecules from host cells (14). It reported that TLR2 and TLR4 is a key protein in OVA-induced exacerbation of murine lung eosinophilia by Asian sand dust (15). Pharmacological and probiotic methods for specific toll-like receptor 2 (TLR2) signaling processes can be developed to treat colonic motility diseases related to the use of antibiotics or other factors (16). rs3804099 in TLR2 and rs4986791 in TLR4 are significantly associated with an increased risk of asthma. The polymorphism of TLRs plays an important role in the occurrence of asthma (17). The TLR2, TLR4, and MyD88 have important and complex roles in promoting the development of OVA-induced antibiotic-associated diarrhea. Therefore, the activation of TLR signaling may be required for developing and suppressing asthma induced by *Streptococcus pneumoniae* and establishing other potential immunomodulatory therapies (18). After *Streptococcus pneumoniae* infection, the accumulation of eosinophils in the bronchoalveolar lavage fluid (BALF) and blood, the release of Th2 cytokines from the mediastinal lymph nodes, spleen cells, and aryl hydrocarbon receptor (AHR) was observed (19). Previous studies have shown that TLR2/TLR4 can promote the expression of inflammatory factors in the Th17 cells, including interleukin (IL)-4, IL-5, and IL-17 (20). In induced sputum, asthma patients with higher total serum immunoglobulin (IgE) levels showed increased macrophage expression of TLR4. This result may be due to the relationship between innate immunity and the IgE-mediated adaptive immune response in asthma. The TLR4 is a potential therapeutic target (21). To study the relationship between the gut microbiota and the TLR2/TLR4 expression, we constructed an OVA mouse model to observe the pathological improvement.

Previous studies have shown that the gut microbiota may affect the signaling pathway to improve asthma. We found that the gut microbiota of asthmatic mice was disturbed. We explored whether the administration of *Lactobacillus fermentum* CECT5716 could reduce the TLR2/TLR4 expression, inhibit the production of inflammatory factors by inflammatory cells, decrease intestinal leakage and pneumonia, and treat asthma. These findings provide a good basis for the treatment of asthma.

MATERIALS AND METHODS

Strain Preparation

Lactobacillus fermentum CECT5716 was provided from Hangzhou Hongsai Biotechnology Co., Ltd. Lactobacilli strains were grown in Mann–Rogosa–Sharpe Agar (MRS) (CM1153R, Thermo, China) at 37°C. After overnight growth, bacteria were transferred to MRS broth and cultured at 37°C until the stationary phase. Afterwards, the bacteria were pelleted (3000 × g

for 10 min), washed twice with phosphate-buffered saline (PBS) and suspended in specific media for *in vivo* or *in vitro* assays.

Experimental Design

Eight-week-old C57BL/6 mice weighing 22 ± 2 g were purchased from SiPeiFu Biotechnology Co., Ltd. During the experiment, the care and use of laboratory animals complied with the "Guiding Opinions on the Good Treatment of Laboratory Animals" issued by the Ministry of Science and Technology in 2006. The asthmatic mice were sensitized by intraperitoneally injecting 0.2 mL of PBS containing 20 μg OVA (O1641, Sigma-Aldrich, Shanghai) and 2 mg alum on the 1st and 5th days and then exposing them to 1% OVA using a nebulizer on the 12th and 13th days of atomization (w/v) for 40 min. The mice in the control group were injected with 200 uL PBS at the same time. After 24 h, BALF serum, lung tissues, and duodenal tissues were collected for subsequent testing. Each of the following groups consisted of five mice: Control group (normal mice injected with 200 uL PBS), OVA group (asthma model mice injected with 200 uL PBS), and OVA + probiotics group. Twenty-four hours after the second sensitization, 10^{10} CFU (200 uL of PBS) of *Lactobacillus fermentum* CECT5716 was administered to the OVA group by gavage once a day for 4 weeks (22). For euthanasia, mice were anesthetized with isoflurane (4%) and then inoculated with an intraperitoneal injection of pentobarbital (0.5 mL per mouse). Mice were sacrificed on day 56. Blood for total IgE, bronchoalveolar lavage fluid (BALF), lung tissues and duodenal tissues for cytokine analysis were collected and subsequently analyzed as previously described (23).

Hematoxylin-Eosin Staining

Lung tissues from different groups of mice were used for Hematoxylin-eosin staining. The lung tissues were fixed in 4% paraformaldehyde for 24 h and embedded in paraffin. Then, the tissues were cut into slices. The slices were then placed in xylene for 15 min three times; immersed in 100, 100, 95, 85, and 75% ethanol for 5 min; and soaked in distilled water for 5 min. The sections were stained with hematoxylin (H301933, Aladdin, China) for 3 min and washed with distilled water. Next, the sections were stained with eosin (E196384, Aladdin, China) for 5 s, dehydrated with gradient alcohol (95–100%) for 5 min, and then removed and placed twice in xylene for 10 min. Finally, the sections were sealed with a neutral gum and observed under a microscope (BA210T, Motic, China).

Masson Staining

The whole tissue was covered with an appropriate amount of nuclear staining solution and stained for 3–5 min. The staining solution was rinsed with tap water. The slices (AY89-2, Yuantai, China) were soaked in distilled water. The sections were soaked in weak alkaline solvents such as PBS or ammonia for 5–10 min until the nuclei appeared blue. The slices were separated with a color separation solution for 30 s and rinsed with absolute alcohol until they appeared transparent, blow-dried, and sealed.

Quantitative Reverse Transcription-Polymerase Chain Reaction

Subsequently, qRT-PCR was performed on a fluorescence qPCR instrument (QuantStudio1, Thermo, United States) using an UltraSYBR Mixture (CW2601, CWBIO, China). The following reaction conditions were used: pre-denaturation at 95°C for 10 min, 40 cycles of denaturation at 94°C for 15 s, and annealing at 60°C for 30s. β-actin was used as an internal reference primer; the primer sequences are shown in **Table 1**. The relative quantitative method ($2^{-\triangle\ \triangle\ Ct}$ method) was used to calculate the relative transcription level of the target gene: △△Ct = △ experimental group – △ control group, △Ct = Ct (target gene) – Ct (β -actin).

Western Blot

The protein was separated by sodium dodecyl sulphate–polyacrylamide gel electrophoresis using 10% gel and transferred to the NC membrane by electrotransfer. The membrane was blocked with 5% skimmed milk for 2 h at room temperature to allow it to bind non-specifically and incubated with the primary antibody overnight at 4°C. The primary antibodies used were rabbit anti-TLR2 (1:2000, 66645-1-Ig, Proteintech), rabbit anti-TLR4 (1:500, 19811-1-AP, Proteintech), rabbit anti-E-cad (1:5000, 20874-1-AP, Proteintech), rabbit anti-Occludin (1:3000, 27260-1-AP, Proteintech), rabbit anti-ZO-1 (1:8000, 21773-1-AP, Proteintech), rabbit anti-Claudin-2 (1:800, ab204049, Abcam), and rabbit anti-β-actin (1:5000, 60008-1-Ig, Proteintech). The membrane was washed three times with TBST for 10 min. Next, the HRP-labeled HRP goat anti-mouse IgG (1:5000, SA00001-1, Proteintech) was incubated. The film was immersed in SuperECL Plus (K-12045-D50, Advansta, United States) to observe for luminescence. β-actin was used as the internal reference. The target band was analyzed using ImageJ software.

16S Ribosomal RNA Identification

We sent the collection of fecal samples to the Apexbio (Shanghai, China) for 16S rDNA analysis. The Qiime 2 software was used to calculate the alpha diversity index of each sample, draw the rank-abundance curve based on OTU, and create the dilution curve based on alpha diversity. Meanwhile, the R software was used to draw the relative abundance histograms of species (R ggplot2 package), genus-level abundance heat maps (R reshape2/ggplot2 package), box plots of the differences in alpha diversity between groups based on the Wilcoxon test (between two groups) (R

TABLE 1 | Primer sequences.

Gene	Sequences (5′-3′)
TLR4	F: AGACACTTTATTCAGAGCCGTTG
	R: AAGGCGATACAATTCCACC
TLR2	F: CTCTTCAGCAAACGCTGTTCT
	R: GGCGTCTCCCTCTATTGTATTG
β-actin	F: ACATCCGTAAAGACCTCTATGCC
	R: TACTCCTGCTTGCTGATCCAC

phyloseq package), PCA dimensionality reduction analysis map based on the Bray-Curtis distance (phyloseq/vegan package), sample clustering tree based on the Euclidean distance (R built-in function), and ANOSIM of bacterial abundance difference map (R DESeq2 package). In addition, web analysis tools were utilized to create the Venn diagram and perform the Lefse analysis, picrust2 function prediction, and Krona species composition analysis.

Immunofluorescence

All the duodenum tissues were fixed in 4% paraformaldehyde overnight and embedded in paraffin with standard techniques. Then, the tissues were cut into slices. The slices were placed in xylene for 20 min; immersed in 100, 95, 85, and 75% ethanol sequentially for 5 min at each level; and then immersed in 0.01 M citrate buffer (pH 6.0). After continuously boiling the slices for 20 min, they were removed after cooling for 20 min and cooled to room temperature. Appropriately diluted primary antibodies against E-cadherin (1:50, ab15098, Abcam), Occludin (1:50, 20874-1-AP, PTG), ZO-1 (1:50, 27260-1-AP, PTG), and Claudin-2 (1:50, 21779-1-AP, PTG) were added to the slices. Approximately 50–100 uL of anti-rabbit-IgG-labeled fluorescent antibody were also added on the slices and incubated at 37°C for 90 min. A DAPI working solution was used to stain the nucleus for 10 min at 37°C. Finally, the results were observed under a fluorescence microscope.

Wright's Staining

A total of 50 μL of Ray Dahl staining reagent (D010-1-2, Jiancheng, China) was added to 2 μL of suspended cell smear; the tissue section was stained for 1 min. Then, 100 μL of differentiation solution was directly added to the smear. The glass slide was shaken gently until the dye was completely mixed with the sample, and then the sample was dyed for 5 min. The smear was placed twice on xylene for 10 min. The cytoplasm of monocytes appeared grayish blue, while that of lymphocytes appeared light blue.

Enzyme-Linked Immunosorbent Assay

After blood collection, the chest was opened, the complete trachea, bronchus and lung tissue were isolated, the right main bronchus was ligated, and 2 mL of normal saline was injected into the left lung lobe through the left bronchus with a lavage device connected to a syringe, and slowly aspirated three times. Then suck it out with negative pressure and repeat twice. After centrifuging the lavage solution at 3,000 rpm × 10 min, 0.5 mL of the supernatant lavage solution was lyophilized. The IL-4 (CSB-E04634M), IL-5 (CSB-E04637M), IL-13 (CSB-E04602M), IL-12 (CSB-E04600M), IFN-γ (CSB-E04578M), and IgE (CSB-E07983m) kits (Wuhan Huamei Biological Engineering Co., Ltd.) were used for the experiments (24). We removed a standard from the kit and centrifuged it at 6,000-10,000 rpm for 30 s. The concentrated washing solution was diluted 1:25 with deionized water. Biotin-labeled antibody solution was diluted 1:100 times with biotin-labeled antibody diluent. Standard and sample wells were separately set and tested; then, 100 μL of standard or sample was added to each well, the sample was shaken gently in order to mix, the plate was covered with stickers, and the sample was incubated at 37°C for 2 h. Then, 100 μL of biotin-labeled antibody working solution was added to each well. Each hole was covered with a new board. The kit was incubated at 37°C for 1 h. Approximately 100 μL of horseradish peroxidase-labeled avidin working solution was added to each well. Next, 90% substrate solution was added to each well, and then the sample was incubated at 37°C for 15–30 min. Finally, 50 μL of stop solution was added to each hole in sequence. Five minutes after terminating the reaction, the optical density of each pore was measured using a microplate at 450 nm.

Periodic Acid-Schiff Staining

First, the slices were immersed twice in xylene for 10 min; placed in 100, 95, 85, and 75% ethanol for 5 min; and then soaked in distilled water for 5 min. Next, 50 ul of periodate was added to the slices and allowed to stand for 10 min. The slices were washed with tap water for 10 min, stained with Schiff's solution (S378685, Aladdin, China) for 10 minutes, and then stained with hematoxylin for 5–10 min. Finally, the sections were observed under a microscope.

Statistical Analysis

All data were analyzed using GraphPad Prism 8.0 software (GraphPad Software, San Diego, California, United States). The measurement data were expressed as mean ± standard deviation (SD). The two sets of data conforming to the normal distribution were used unpaired T test. The multiple sets of data conforming to the normal distribution adopt one-way analysis of variance, and then perform Tukey's *post hoc* test. A P value of < 0.05 was considered significant.

RESULTS

The Expression of TLR2/TLR4 Protein Was Activated in the Ovalbumin Group

We constructed an OVA model to assess the pathological conditions of mice with asthma. In order to observe whether the OVA model was successful, HE staining and Masson staining were performed on the lung tissues of mice. The results are displayed in **Figures 1A,B**. OVA group compared with the control group, lung tissue had increased inflammatory cell infiltration. The base membrane was thickened. Deposition of collagen was seen not only in the basement membrane of bronchial epithelia and blood vessels, but also in lung parenchyma. These findings showed that the OVA mice were successfully established. Compared with the control group, TLR2/TLR4 expression in the lung and duodenum tissues of OVA-induced murine asthma model was increased (**Figures 1C–H**). In summary, the TLR2/TLR4 expression was activated in the OVA mice.

Asthma Led to Gut Dysmicrobiota

The above results indicated that the TLR2/TLR4 expression in the duodenum interfered with the pathology of asthma. Therefore,

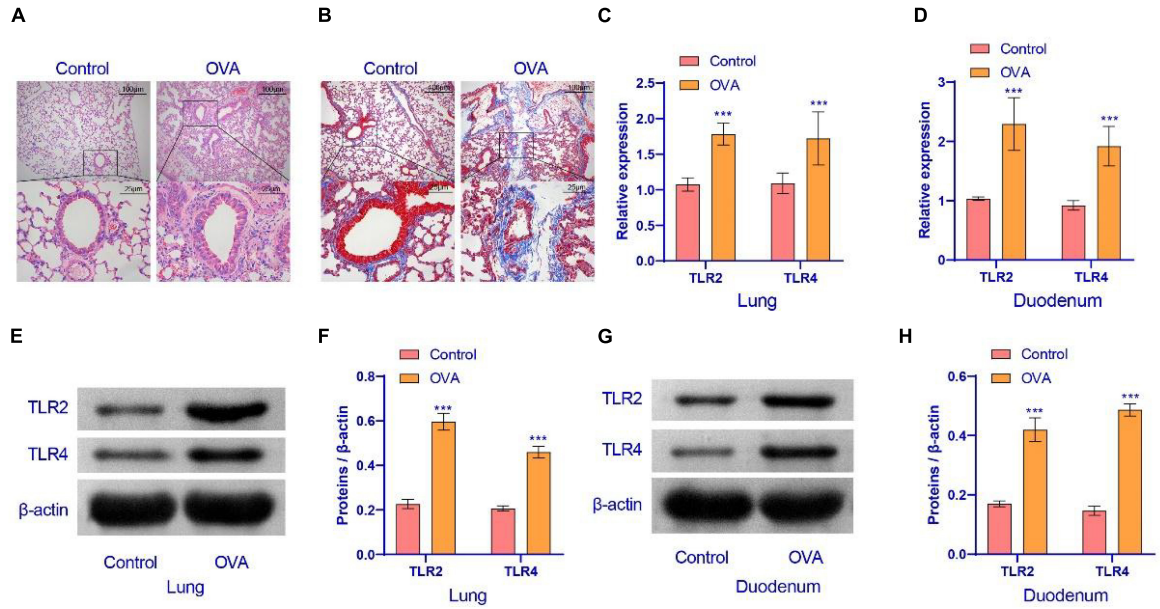

FIGURE 1 | Airway inflammation and TLR2/TLR4 expression in the lung of asthma mice. **(A)** HE staining were performed on the lung tissues of mice. **(B)** Masson staining was performed on the lung tissues of mice. **(C,D)** qRT-PCR was used to detect the expression of mRNA. The level of TLR2/TLR4 mRNA was suppressed in the OVA group. **(E–H)** Western blot was used to measure the expression of proteins. The expression of TLR2/TLR4 protein was raised in the OVA group. up: × 100, scale bar = 100 μm; down: × 400, scale bar = 25 μm. ***Compared with the control group, $P < 0.001$. Unpaired *t*-test was utilized for the comparison between two groups. $n = 5$ for each group.

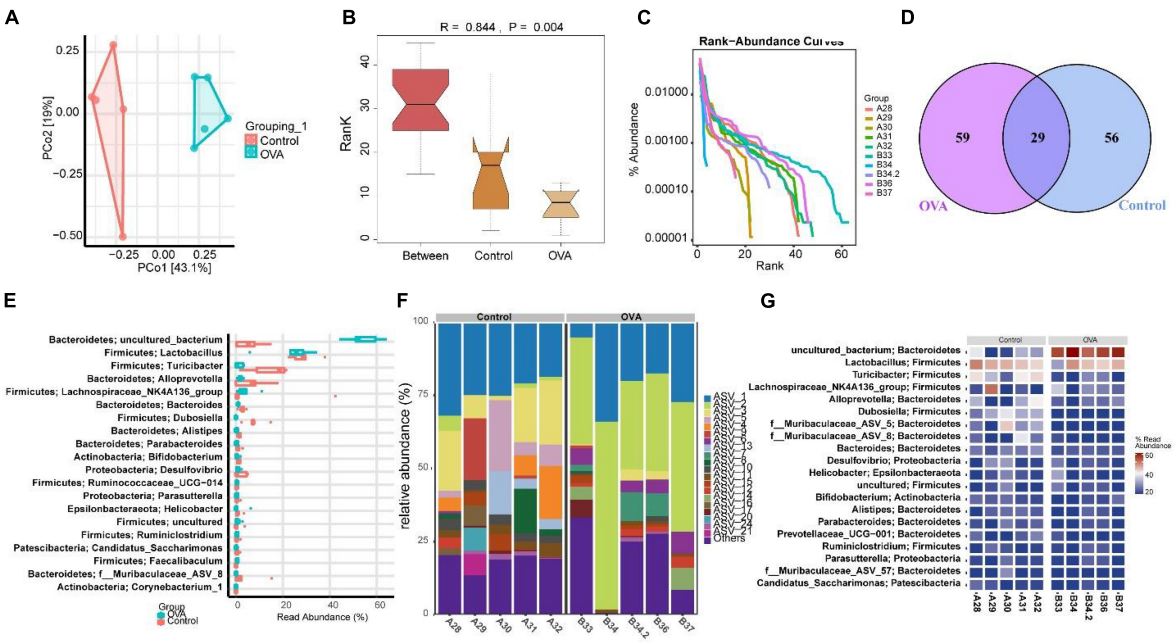

FIGURE 2 | Asthma could cause gut dysmicrobiota. **(A)** PCA was performed to analyze the similarity of samples. **(B)** ANOSIM was used to analyze the difference between two samples. **(C)** Rank abundance. **(D)** OUT Venn diagram. **(E)** Box diagram of phylum. **(F)** Phylum distribution histogram. **(G)** Heat map of the phylum distribution.

we explored whether asthma affected the gut microbiota of mice. Principal component analysis (PCA) showed that the microbial community structure between the control and OVA groups was less similar (**Figure 2A**). The analysis of similarities (ANOSIM) obtained an R value of 0.844, showing that the between-group variance was larger than the within-group variance (**Figure 2B**).

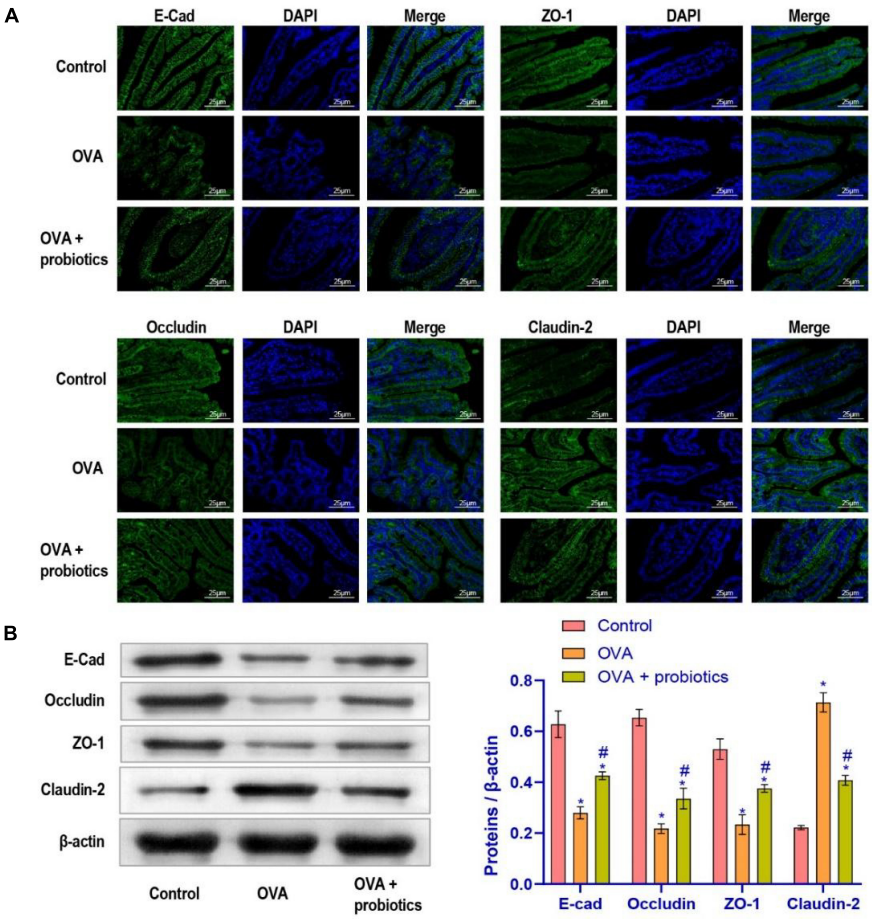

FIGURE 3 | The leakage of intestinal barrier was alleviated after supplementation of Lactobacillus fermentum CECT5716. **(A)** Immunofluorescence imaging of E-cad, ZO-1, Occludin, and Claudin-2 (× 400, scale bar = 25 μm). **(B)** Western blot was used to measure the expression of proteins. Protein expression levels of E-cad, ZO-1, Occludin, and Claudin-2 in each group. *Compared with the control group, $P < 0.05$. #Compared with the OVA group, $P < 0.05$. One-way ANOVA was used among multiple groups. $n = 5$ for each group.

The rank-abundance curve showed that the OVA group curve had a larger range on the horizontal axis and a higher species richness (**Figure 2C**). The OUT Venn diagram showed that the control group had 56 unique OTU numbers, while the OVA group had 59 OTUs (**Figure 2D**). The results suggested significant differences in *Bacteroidetes* and *Firmicutes* between the control and OVA groups (**Figure 2E**). The heat map and the abundance bar graph showed substantial differences in the phylum composition between the control and OVA groups (**Figures 2F,G**). These results suggest that the gut microbiota of asthmatic mice is imbalanced.

Lactobacillus fermentum CECT5716 Supplementation Could Reduce the Intestinal Barrier Leakage

The above experiments showed that asthma could cause gut dysmicrobiota and that the TLR2/TLR4 expression were disturbed. We examined whether *Lactobacillus* supplementation could improve the intestinal barrier leakage caused by disruption of the gut microbiota. Therefore, *Lactobacillus fermentum* CECT5716 was administered to evaluate its effect in the duodenal function of OVA mice. Immunofluorescence was performed to evaluate the expression levels of E-cadherin, ZO-1, Occludin, and Claudin-2 in the duodenum. Results showed that the duodenum of mice supplemented with was repaired (**Figure 3A**). Then, we examined the expression levels of adhesion link proteins. Compared with the OVA group, the E-cad, ZO-1, and Occludin protein expression levels in the OVA + probiotics group increased, while and the Claudin-2 protein level significantly decreased (**Figure 3B**). In short, results indicated that *Lactobacillus* supplementation could reduce the intestinal barrier leakage.

Lactobacillus fermentum CECT5716 Could Inhibit the Level of Pro-inflammatory Factors in BALF

We explored further whether the lung function could be improved by supplementation with *Lactobacillus*. We extracted

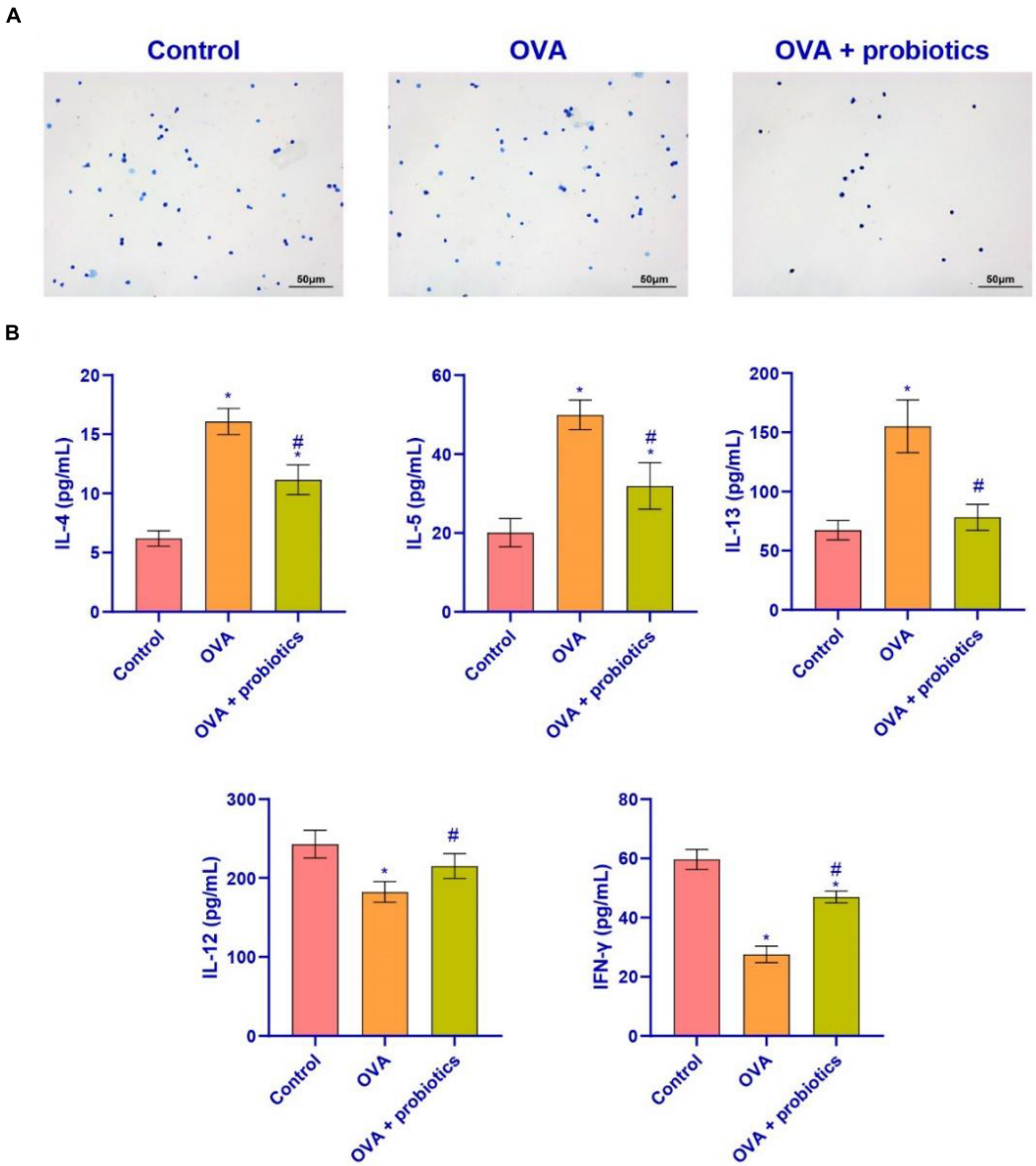

FIGURE 4 | *Lactobacillus ferokay smentum* CECT5716 might inhibit the level of pro-inflammatory factors in BALF. **(A)** Wright's staining (× 200, scale bar = 50 μm). **(B)** ELISA was used to measure the level of inflammatory factors. Expression levels of inflammatory factors (IL-4, IL-5, IL-13, IL-12, and IFN-γ). *Compared with the control group, $P < 0.05$. #Compared with the OVA group, $P < 0.05$. One-way ANOVA was used among multiple groups. $n = 5$ for each group.

BALF from mice for the follow-up experiments. Wright's staining was performed to detect the number of inflammatory cells in the BALF. The data suggested that the number of inflammatory cells decreased in the OVA + probiotics group. *Lactobacillus* supplementation inhibited the production of inflammatory cells (**Figure 4A**). ELISA was carried out to analyze the levels of pro-inflammatory and anti-inflammatory factors in Th2 cells found in the BALF. Compared with the OVA group, the levels of pro-inflammatory factors (IL-4, IL-5, and IL-13) in the OVA + probiotics group significantly decreased. Meanwhile, the levels of anti-inflammatory factors (IL-12 and interferon gamma [IFN-γ]) were significantly increased (**Figure 4B**). The above data showed that supplementation with *Lactobacillus* reduced the level of pro-inflammatory factors.

Lactobacillus fermentum CECT5716 Could Inhibit the Expression of TLR2/TLR4

The above experimental results indicated that *Lactobacillus* could alleviate asthmatic mice' inflammation in the duodenum and lungs. We studied the effect of *Lactobacillus* on the TLR2/TLR4 expression in the duodenum and lungs of mice.

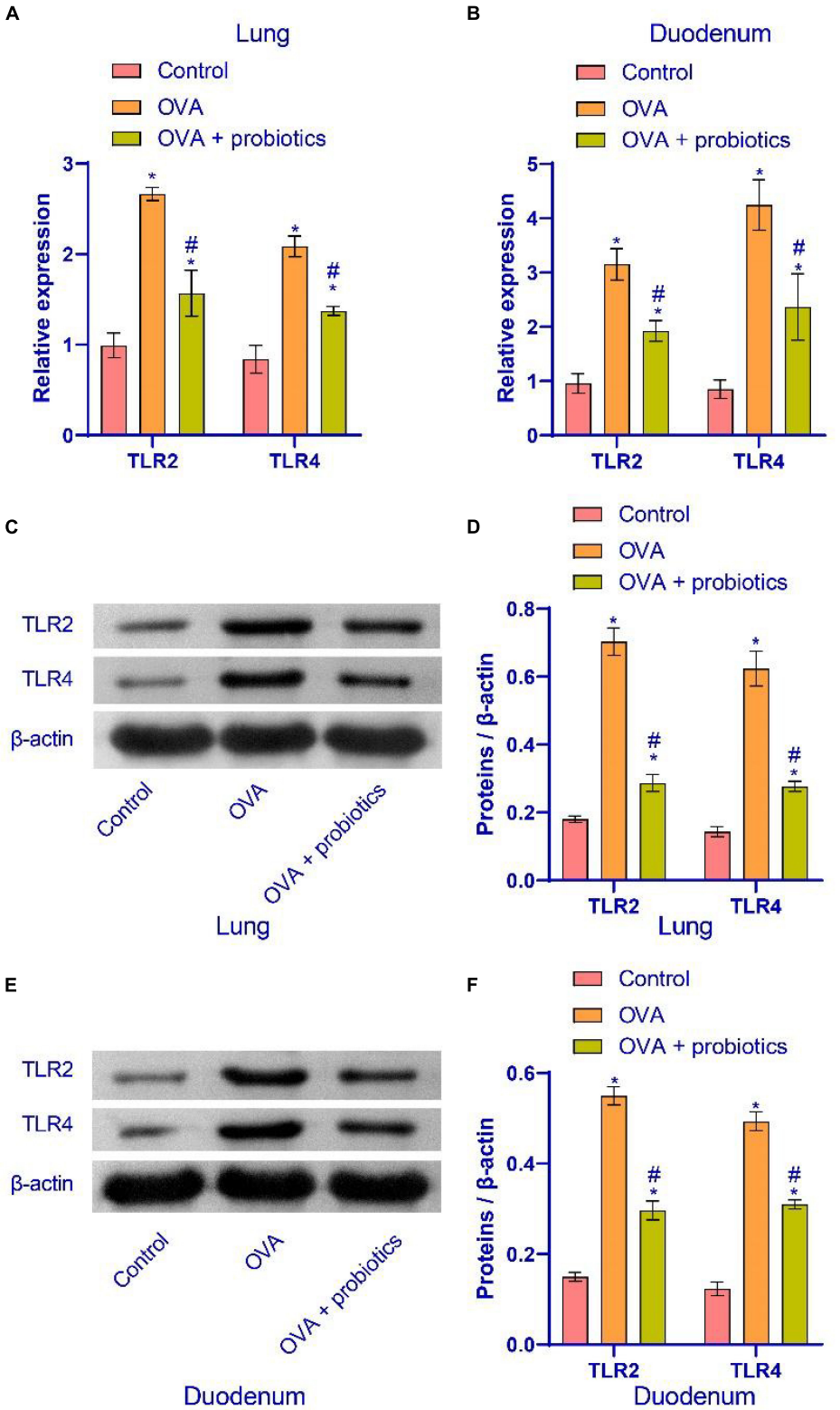

FIGURE 5 | Supplementation with Lactobacillus fermentum CECT5716 could inhibit the TLR2/TLR4 expression. **(A,B)** qRT-PCR was used to detect the expression of mRNA. Lactobacillus supplementation could reduce the mRNA expression of TLR2 and TLR4. **(C–F)** Western blot was used to measure the expression of proteins. Lactobacillus supplementation could inhibit the protein expression of TLR2 and TLR4. *Compared with the control group, $P < 0.05$. #Compared with the OVA group, $P < 0.05$. One-way ANOVA was used among multiple groups. $n = 5$ for each group.

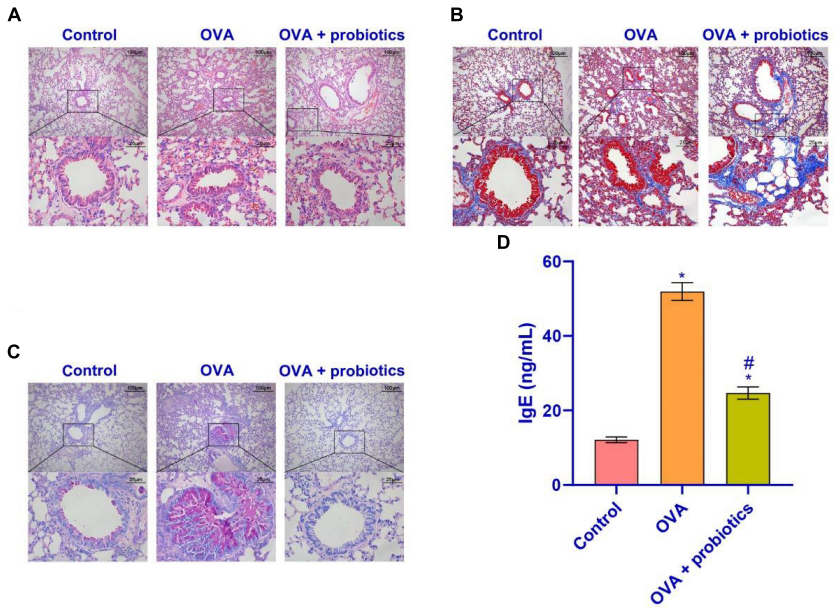

FIGURE 6 | *Lactobacillus fermentum* CECT5716 could relieve the inflammatory cell infiltration. **(A)** HE staining was performed to determine the pathological changes in the lung tissue. **(B)** The degree of lung fibrosis was analyzed by Masson staining. **(C)** PAS staining was utilized to observe the proliferation of tracheal goblet cells in the lung tissues of each group. **(D)** Level of IgE in the serum. Up: × 100, scale bar = 100 μm; down: × 400, scale bar = 25 μm. *Compared with the control group, $P < 0.05$. #Compared with the OVA group, $P < 0.05$. One-way ANOVA was used among multiple groups. $n = 5$ for each group.

qRT-PCR and western blotting were performed to detect the expression of TLR2/TLR4. In the OVA + probiotics group, the mRNA expression of TLR2 and TLR4 in the lungs of mice was downregulated. The protein expression of TLR2 and TLR4 reduced. The protein expression of TLR2 and TLR4 also decreased. Similar results were observed in the duodenum of this group (**Figure 5**). The results showed that *Lactobacillus* did not affect the expression of TLR2 and TLR4 in normal mice. This finding showed that the TLR2/TLR4 expression in OVA mice was decreased.

Lactobacillus fermentum CECT5716 Could Reduce the Inflammatory Cell Infiltration

The above results showed that supplementation with *Lactobacillus* could increase the TLR2/TLR4 expression. We observed the pathological conditions of the mice's lungs. Hematoxylin-eosin (HE) staining, Masson staining, and PAS staining were used to observe the lungs of mice supplemented with *Lactobacillus*. **Figures 6A–C** shows that compared with the OVA group, the inflammatory cell infiltration in the airway mucosa in the OVA + probiotics group improved, the alveolar swelling was reduced, and basement membrane thinning. Finally, ELISA was used to detect the IgE content. **Figure 6D** shows that supplementation with *Lactobacillus* significantly inhibited the production of IgE. Overall, *Lactobacillus* supplementation can relieve lung inflammation.

DISCUSSION

This study aimed to determine whether *Lactobacillus fermentum* CECT5716 supplementation could improve the intestines and lungs of asthmatic mice. The TLR2/TLR4 expression may affect the secretion of inflammatory factors by the inflammatory cells, which regulate the target of asthma progression. *Lactobacillus* supplementation could regulate the gut microbiota composition by inhibiting the TLR2/TLR4 expression, thus relieving duodenal leakage and pulmonary inflammatory symptoms.

Asthma remains an important medical emergency, the most common cause of acute hospital admissions in children, and the most common chronic respiratory disease in adults (25). Anti-inflammatory and bronchodilator therapies are the main treatments for asthma (26). Chrysanthemum improved the OVA-induced allergic asthma by inhibiting the activation of pro-inflammatory cytokines and their upstream TLR/NF-κB/NLRP3 pathways (27). The oral administration of probiotics led to the suppression of serum OVA-specific IgE production through the TLR2 pathway. This enhances the production of IFN-γ in spleen cells that respond to OVA (28). Supplementation with *Lactobacillus fermentum* CECT5716 differentially modulates the immune response of IECs triggered by TLR4 activation through the regulation of the expression of negative TLR regulators (29). ILR mediates the secretion of cytokines by immune cells. In skin diseases, an increase in IL-4 and IL-13 levels is caused by abnormalities in TLR-mediated processes (30). In systemic inflammation, regulation of TLR could help improve the cell barrier function. The main reason for this is that the function of Occludin in cells is destroyed (31). The above research objects

include active ingredients in plants and probiotics, which can improve asthma by affecting TLR2 or TLR4 pathway *in vivo*. Our choice of research objects are also probiotics. Firstly, we constructed OVA model mice. The results of HE and Masson staining showed that the infiltration of inflammatory cells in the lung tissue of OVA mice increased. The abnormal expression of TLR2/TLR4 in asthmatic mice is consistent with previous studies. The TLR2/TLR4 expression of OVA mice was activated and the intestinal flora was disordered. After that, we observed whether asthma was improved by supplementing OVA mice with *Lactobacillus fermentum* CECT5716. However, we did not elucidate the association between Lactobacillus fermentum and intestinal microbiota. This provided direction for the next step in our research program.

Lactobacillus is one of the most widely known probiotics (32, 33). Probiotics can reduce the autoimmune response of patients with rheumatoid arthritis by improving inflammation and disease activity (34). In addition, probiotics reduce the risk of islet autoimmunity in children with the highest genetic risk of type 1 diabetes (35). In ulcerative colitis, probiotics induce and maintain remission (36). However, little is known about the interactions between probiotics and host cells or how to manipulate these interactions to obtain a stronger regulatory response (37). In this sense, the sensor of innate immunity is the target of probiotics and plays an important role in the expression of TLRs (38). TLR4 was an important immune pattern recognition receptor, which can control the innate and adaptive immune responses, and played an important role in the initiation and regulation of airway inflammation (39). A few studies reported on the role of *Lactobacillus* in the treatment of asthma (8, 40). We conducted experiments to verify these findings and found that *Lactobacillus* species can provide basic beneficial effects, inhibit the inflammatory response in asthmatic mice, and inhibit the progression of lung fibrosis in mice. Studies have shown that asthma improves by repairing the gut barrier (41). Our results are consistent with those of previous studies. *Lactobacillus* supplementation in OVA mice up-regulated the expression of E-cad, ZO-1 and Occludin. It inhibited the expression of Claudin-2 protein to improve the intestinal barrier leakage caused by intestinal microecological disorder. TLR2 gene knockout in asthmatic mice can alleviate the airway inflammation, whose mechanism may be that the allergic airway inflammation of asthmatic mice is alleviated (42). Our results of pro-inflammatory factors (IL-4, IL-5, and IL-13) were significantly decreased in OVA mice supplemented with *Lactobacillus*, while the levels of anti-inflammatory factors (IL-12, IFN-γ) were significantly increased. *Lactobacillus fermentum* CECT5716 can inhibit the production of IgE in OVA mice. The TLR2/TLR4 expression in OVA mice was inhibited. However, we have not studied TLR2/TLR4 at the clinical level. We will conduct more in-depth research on TLR2/TLR4 in future research, and hope to make some clinical research progress.

In conclusion, this study found that in asthmatic mice, *Lactobacillus fermentum* CECT5716 could protect the intestines and lungs. We verified that the risk of intestinal leakage was curbed. The TLR2/TLR4 expression was inhibited, and the levels of inflammatory factors secreted by inflammatory cells in mice were reduced. The cavitation in the lungs was relieved. Results of our study clarified that *Lactobacillus fermentum* CECT5716 can inhibit the TLR2/TLR4 expression to relieve lung inflammation in asthmatic mice.

DATA AVAILABILITY STATEMENT

The datasets presented in this study can be found in online repositories. The names of the repository/repositories and accession number(s) can be found below: https://www.ncbi.nlm.nih.gov/, PRJNA739083.

ETHICS STATEMENT

This study was approved by the Animal Experiment Ethics Committee of Hebei University of Chinese Medicine (No. DWLL2020077) and conducted in strict accordance with the national institutes of health guidelines for the care and use of experimental animals.

AUTHOR CONTRIBUTIONS

WW, YL, and GH had data collection and analysis, and manuscript preparation. AL and XK supervised the whole study, data analysis, and manuscript preparation. All authors contributed to the article and approved the submitted version.

FUNDING

This work was supported by Hebei Provincial Department of Human Resources and Social Secruity Fund (C20210358) and Wu Jieping Medical Foundation.

ACKNOWLEDGMENTS

We thank the Chinese PLA General Hospital, Hebei University of Chinese Medicine and the First Hospital of Shanxi Medical University for all the supports.

REFERENCES

1. Chapman DG. Mechanisms of airway hyperresponsiveness in asthma: the past, present and yet to Come. *Clin Exp Allergy.* (2016) 45:706–19. doi: 10.1111/cea.12506
2. Spacova I, Beeck WV. *Lactobacillus rhamnosus* probiotic prevents airway function deterioration and promotes gut microbiome resilience in a murine asthma model. *Gut Microbes.* (2020) 11:1729–44. doi: 10.1080/19490976.2020.1766345
3. Forsberg A, West CE. Pre- and probiotics for allergy prevention: time to revisit recommendations. *Clin Exp Allergy.* (2016) 46:1506–21.
4. Dicks LMT, Geldenhuys J. Our gut microbiota: a long walk to homeostasis. *Benef Microbes.* (2018) 9:3–20. doi: 10.3920/BM2017.0066

5. Sánchez B, Delgado S. Probiotics, gut microbiota, and their influence on host health and disease. *Mol Nutr Food Res.* (2017) 61:doi: 10.1002/mnfr.201600240
6. Jin SW, Lee GH. Lactic acid bacteria ameliorate diesel exhaust particulate matter-exacerbated allergic inflammation in a murine model of asthma. *Life (Basel).* (2020) 10:260. doi: 10.3390/life10110260
7. Żukiewicz-Sobczak W, Wróblewska P. Probiotic lactic acid bacteria and their potential in the prevention and treatment of allergic diseases. *Cent Eur J Immunol.* (2014) 39:104–8. doi: 10.5114/ceji.2014.42134
8. Wu C-T, Lin F-H. Effect of *Lactobacillus rhamnosus* GG immunopathologic changes in chronic mouse asthma model. *J Microbiol Immunol Infect.* (2019) 52:911–9. doi: 10.1016/j.jmii.2019.03.002
9. Molina-Tijeras JA, Diez-Echave P, Vezza T, Hidalgo-García L, Ruiz-Malagón AJ, Rodríguez-Sojo MJ, et al. *Lactobacillus fermentum* CECT5716 ameliorates high fat diet-induced obesity in mice through modulation of gut microbiota dysbiosis. *Pharmacol Res.* (2021) 167:105471. doi: 10.1016/j.phrs.2021.105471
10. Lebeer S, Bron PA. Identification of probiotic effector molecules: present state and future perspectives. *Curr Opin Biotechnol.* (2018) 49:217–23. doi: 10.1016/j.copbio.2017.10.007
11. Zimmermann P, Messina N. Association between the intestinal microbiota and allergic sensitization, eczema, and asthma: a systematic review. *J Allergy Clin Immunol.* (2019) 143:467–85. doi: 10.1016/j.jaci.2018.09.025
12. Fonseca W, Lucey K. *Lactobacillus johnsonii* supplementation attenuates respiratory viral infection via metabolic reprogramming and immune cell modulation. *Mucosal Immunol.* (2017) 10:1569–80. doi: 10.1038/mi.2017.13
13. Thorburn AN, McKenzie CI. Evidence that asthma is a developmental origin disease influenced by maternal diet and bacterial metabolites. *Nat Commun.* (2015) 6:7320. doi: 10.1038/ncomms8320
14. He M, Ichinose T, Yoshida Y, Arashidani K, Yoshida S, Takano H, et al. Urban PM2.5 exacerbates allergic inflammation in the murine lung via a TLR2/TLR4/MyD88-signaling pathway. *Sci Rep.* (2017) 7:11027. doi: 10.1038/s41598-017-11471-y
15. He M, Ichinose T, Song Y, Yoshida Y, Bekki K, Arashidani K, et al. Desert dust induces TLR signaling to trigger Th2-dominant lung allergic inflammation via a MyD88-dependent signaling pathway. *Toxicol Appl Pharmacol.* (2016) 296:61–72. doi: 10.1016/j.taap.2016.02.011
16. Yarandi SS, Kulkarni S. Intestinal bacteria maintain adult enteric nervous system and nitrergic neurons via toll-like receptor 2-induced neurogenesis in mice. *Gastroenterology.* (2020) 159:200–13. doi: 10.1053/j.gastro.2020.03.050
17. Zhao J. Association of polymorphisms in TLR2 and TLR4 with asthma risk: an update meta-analysis. *Medicine (Baltimore).* (2017) 96:e7909. doi: 10.1097/MD.0000000000007909
18. Thorburn AN, Tseng HY. TLR2, TLR4 AND MyD88 mediate allergic airway disease (AAD) and *Streptococcus pneumoniae*-induced suppression of AAD. *PLoS One.* (2016) 11:e0156402. doi: 10.1371/journal.pone.0156402
19. Ps P, Jf K. Neonatal exposure to pneumococcal phosphorylcholine modulates the development of house dust mite allergy during adult life. *J Immunol Res.* (2015) 194:5838–50. doi: 10.4049/jimmunol.1500251
20. Li P, Wang J. A novel inhibitory role of microRNA-224 in particulate matter 2.5-induced asthmatic mice by inhibiting TLR2. *J Cell Mol Med.* (2020) 24:3040–52. doi: 10.1111/jcmm.14940
21. Crespo-Lessmann A. Expression of toll-like receptors 2 and 4 in subjects with asthma by total serum IgE level. *Respir Res.* (2016) 17:41. doi: 10.1186/s12931-016-0355-2
22. Spacova I, Van Beeck W, Seys S, Devos F, Vanoirbeek J, Vanderleyden J, et al. *Lactobacillus rhamnosus* probiotic prevents airway function deterioration and promotes gut microbiome resilience in a murine asthma model. *Gut Microbes.* (2020) 11:1729–44. doi: 10.1080/19490976.2020.1766345
23. Spacova I, Petrova MI, Fremau A, Pollaris L, Vanoirbeek J, Ceuppens JL, et al. Intranasal administration of probiotic *Lactobacillus rhamnosus* GG prevents birch pollen-induced allergic asthma in a murine model. *Allergy.* (2019) 74:100–10. doi: 10.1111/all.13502
24. Zhu Y, Xiong Y. Chiropractic therapy modulated gut microbiota and attenuated allergic airway inflammation in an immature rat model. *Med Sci Monit.* (2020) 26:e926039. doi: 10.12659/MSM.926039
25. Ramsahai JM, Hansbro PM, Wark PAB. Mechanisms and management of asthma exacerbations. *Am J Respir Crit Care Med.* (2019) 199:423–32. doi: 10.1164/rccm.201810-1931CI
26. Papi A, Brightling C, Pedersen SE, Reddel HK. Asthma. *Lancet.* (2018) 391:783–800. doi: 10.1016/s0140-6736(17)33311-1
27. Roy S, Manna K, Jha T, Saha KD. Chrysin-loaded PLGA attenuates OVA-induced allergic asthma by modulating TLR/NF-κB/NLRP3 axis. *Nanomedicine.* (2020) 30:102292. doi: 10.1016/j.nano.2020.102292
28. Kawashima T, Hayashi K, Kosaka A, Kawashima M, Igarashi T, Tsutsui H, et al. *Lactobacillus plantarum* strain YU from fermented foods activates Th1 and protective immune responses. *Int Immunopharmacol.* (2011) 11:2017–24. doi: 10.1016/j.intimp.2011.08.013
29. Garcia-Castillo V, Komatsu R, Clua P, Indo Y, Takagi M, Salva S, et al. Evaluation of the immunomodulatory activities of the probiotic strain *Lactobacillus fermentum* UCO-979C. *Front Immunol.* (2019) 10:1376. doi: 10.3389/fimmu.2019.01376
30. Bon LV. Distinct evolution of TLR-mediated dendritic cell cytokine secretion in patients with limited and diffuse cutaneous systemic sclerosis. *Ann Rheum Dis.* (2010) 69:1539–47. doi: 10.1136/ard.2009.128207
31. Terheyden L, Roider J. Basolateral activation with TLR agonists induces polarized cytokine release and reduces barrier function in RPE in vitro. *Graefes Arch Clin Exp Ophthalmol.* (2021) 259:413–24. doi: 10.1007/s00417-020-04930-2
32. Håkansson Å, Aronsson CA. Effects of *Lactobacillus plantarum* and *Lactobacillus paracasei* on the peripheral immune response in children with celiac disease autoimmunity: a randomized, double-blind, placebo-controlled clinical trial. *Nutrients.* (2019) 11:1925. doi: 10.3390/nu11081925
33. Anatriello E, Cunha M. Oral feeding of *Lactobacillus bulgaricus* N45.10 inhibits the lung inflammation and airway remodeling in murine allergic asthma: relevance to the Th1/Th2 cytokines and STAT6/T-bet. *Cell Immunol.* (2019) 341:103928. doi: 10.1016/j.cellimm.2019.103928
34. Alipour B. Effects of *Lactobacillus casei* supplementation on disease activity and inflammatory cytokines in rheumatoid arthritis patients: a randomized double-blind clinical trial. *Int J Rheum Dis.* (2014) 17:519–27. doi: 10.1111/1756-185X.12333
35. Uusitalo U, Liu X. Association of early exposure of probiotics and islet autoimmunity in the TEDDY study. *JAMA Pediatr.* (2016) 170:20–8. doi: 10.1001/jamapediatrics.2015.2757
36. Miele E. Effect of a probiotic preparation (VSL#3) on induction and maintenance of remission in children with ulcerative colitis. *Am J Gastroenterol.* (2009) 104:437–43. doi: 10.1038/ajg.2008.118
37. Sharma G. Probiotics as a potential immunomodulating pharmabiotics in allergic diseases: current status and future prospects. *Allergy Asthma Immunol Res.* (2018) 10:575–90. doi: 10.4168/aair.2018.10.6.575
38. Hu X, Yu Y. The role of acetylation in TLR4-mediated innate immune responses. *Immunol Cell Biol.* (2013) 91:611–4. doi: 10.1038/icb.2013.56
39. Pascual M. Role of TLR4 in ethanol effects on innate and adaptive immune responses in peritoneal macrophages. *Immunol Cell Biol.* (2011) 89:716–27. doi: 10.1038/icb.2010.163
40. Lin C-H. Administration of *Lactobacillus paracasei* HB89 mitigates PM2.5-induced enhancement of inflammation and allergic airway response in murine asthma model. *PLoS One.* (2020) 15:e0243062. doi: 10.1371/journal.pone.0243062
41. Zhang L, He X. Transcriptome-wide profiling discover: PM2.5 aggravates airway dysfunction through epithelial barrier damage regulated by Stanniocalcin 2 in an OVA-induced model. *Ecotoxicol Environ Saf.* (2021) 220:112408. doi: 10.1016/j.ecoenv.2021.112408

42. Ma S-Q, Wei H-L. TLR2 regulates allergic airway inflammation through NF-κB and MAPK signaling pathways in asthmatic mice. *Eur Rev Med Pharmacol Sci.* (2018) 22:3138–46. doi: 10.26355/eurrev_201805_15073

Conflict of Interest: The authors declare that the research was conducted in the absence of any commercial or financial relationships that could be construed as a potential conflict of interest.

Publisher's Note: All claims expressed in this article are solely those of the authors and do not necessarily represent those of their affiliated organizations, or those of the publisher, the editors and the reviewers. Any product that may be evaluated in this article, or claim that may be made by its manufacturer, is not guaranteed or endorsed by the publisher.

frontiers | Frontiers in Nutrition

TYPE Original Research
PUBLISHED 02 September 2022
DOI 10.3389/fnut.2022.927363

OPEN ACCESS

EDITED BY
Hui Han,
Chinese Academy of Sciences (CAS), China

REVIEWED BY
Waranya Chatuphonprasert, Mahasarakham University, Thailand
Severine Navarro, The University of Queensland, Australia

*CORRESPONDENCE
Hongmei Jiang
jhmndcn@hunau.edu.cn
Jun Fang
fangjun1973@hunau.edu.cn

SPECIALTY SECTION
This article was submitted to Nutrition and Microbes, a section of the journal Frontiers in Nutrition

RECEIVED 24 April 2022
ACCEPTED 29 July 2022
PUBLISHED 02 September 2022

CITATION
Chai Y, Ding S, Jiang L, Wang S, Yuan X, Jiang H and Fang J (2022) The mitigative effect of ovotransferrin-derived peptide IQW on DSS-induced colitis via alleviating intestinal injury and reprogramming intestinal microbes.
Front. Nutr. 9:927363.
doi: 10.3389/fnut.2022.927363

The mitigative effect of ovotransferrin-derived peptide IQW on DSS-induced colitis via alleviating intestinal injury and reprogramming intestinal microbes

Yajuan Chai[1], Sujuan Ding[1], Lihong Jiang[1], Shuangshuang Wang[2], Xiangnan Yuan[3], Hongmei Jiang[1]* and Jun Fang[1]*

[1]College of Bioscience and Biotechnology, Hunan Agricultural University, Changsha, China, [2]Department of Cardiology, Wenling First People's Hospital (The Affiliated Wenling Hospital of Wenzhou Medical University), Wenling, China, [3]Department of Rehabilitation, Shengjing Hospital of China Medical University, Shenyang, China

Inflammatory bowel disease (IBD) is a chronic disease with multiple complications during its development, and it is difficult to cure. The aim of this study was to evaluate the alleviating effect of different concentrations of the bioactive peptide IQW (Ile-Gln-Trp) on dextran sodium sulfate (DSS)-induced colitis in mice. For this study, we randomly divided 56 ICR mice into seven groups: the (I) control (CON), (II) dextran sodium sulfate treatment (2.5% DSS), (III) IQW-DSS (20 μg/ml) treatment, (IV) IQW-DSS (40 μg/ml) treatment, (V) IQW-DSS (60 μg/ml) treatment, (VI) IQW-DSS (80 μg/ml) treatment, and (VII) IQW-DSS (100 μg/ml) groups. The results showed that IQW at 60 μg/ml alleviated body weight loss, improved the liver index ($p < 0.05$), and improved histomorphological and pathological changes in the colon compared to the DSS-treated group. IQW at 60 μg/ml and IQW at 80 μg/ml modified intestinal microbial disorders. In addition, IQW at 60 μg/ml significantly increased butyric acid levels and decreased valeric acid levels, while IQW at 80 μg/ml significantly increased isobutyric acid and isovaleric acid levels. Hence, IQW at a concentration of 60 μg/ml alleviates DSS-induced colitis by enhancing the body's anti-inflammatory ability and regulating intestinal flora and metabolic changes. In the above context, IQW at 60 μg/ml could be a potential candidate for IBD prevention and treatment.

KEYWORDS

Ile-Gln-Trp, colitis, sodium dextran sulfate, intestinal flora, short-chain fatty acids (SCFA)

Introduction

The global prevalence of IBD, a complex inflammatory disease of the gastrointestinal tract, continues to grow (1, 2). Its main forms include two different chronic recurrent inflammatory diseases, Crohn's disease (CD) and ulcerative colitis (UC) (3). The inflammation of the intestine caused by CD has chronic intermittent symptoms and can affect all segments of the bowel, most commonly the terminal ileum and colon, showing segmental, asymmetrical, and transmural aspects with a variety of complications (4). UC is an inflammatory disease confined to the colonic mucosa, with the disease usually extending from the rectum to the proximal colon and showing alternating symptoms of deterioration and remission (5). The etiology of IBD is unclear, but previous studies have demonstrated that the pathogenesis of IBD is driven by genetic, environmental, immune, and intestinal flora factors (1). Dysbiosis of the gut flora, tissue damage, and metabolic abnormalities are all common symptoms of IBD.

In a healthy state, homeostasis of gut microbes plays an important role in maintaining the host's metabolic balance, immune response, and other physiological stability (6), while during IBD, gut microbial dysbiosis is thought to be partly responsible for IBD, and the composition of the microbiota can regulate the balance between inflammation and homeostasis in the gut (7). Firmicutes show a decrease in abundance, and Proteobacteria show an increase in abundance in the presence of IBD. Some pathogens also show an increase in abundance, such as adherent invasive *Escherichia coli* (*E. coli*) (8, 9). Moreover, bile acid derivatives, short-chain fatty acids (SCFAs), and tryptophan metabolites, all of which are produced from microbial metabolisms, have been linked to gut immunological and inflammatory damages (10). SCFAs, i.e., can be a source of energy for the intestinal epithelium and have an anti-inflammatory activity, which is important for maintaining intestinal homeostasis and maintaining the intestinal barrier and has an impact on changes in the host's body mass index during IBD (11). Hence, prevention and treatment of colitis are particularly important by regulation of changes in gut microbes and their metabolites.

Bioactive peptides are short chains of biologically active amino acids that regulate immune, cardiovascular, neurological, and gastrointestinal physiological responses (12), and they are recognized as an excellent candidate in the development of drugs for treatment of IBD (13). Research has shown that an ovotransferrin-derived peptide, which is the ovalbumin extracted from eggs, has antioxidant activity and antiviral and immunological effects, and it has been used in treatment of diseases (14, 15). Ma Yong et al. found that addition of IQW to diet helped to regulate serum amino acid levels and the expression of inflammatory factors, and to reduce damage to the intestinal barrier (16). Liu et al. investigated the use of bioactive peptides made from egg whites to improve antioxidant effects and maintain intestinal flora balance during treatment of DSS-induced colitis (17). Yutaro Kobayashi et al.'s study showed that oral egg white ovotransferrin can be used as a preventive drug against IBD to maintain intestinal health (18). However, there are only a few studies on the efficacy of different concentrations of IQW in the therapy of DSS-induced colitis. Therefore, this study was conducted to identify an effective treatment for IBD by evaluating the effect of different dietary concentrations of the egg bioactive peptide IQW on dextran sodium sulfate (DSS)-induced colitis in mice.

Materials and methods

Animal husbandry and sample collection

Six-week-old female C57BL/6J mice were housed in a rearing room at a room temperature of 22 ± 2°C and a light period of 12 h and were free to drink and eat. After 1 week of acclimatization, 56 mice were randomly divided into 7 groups with 8 mice in each, and IQW was dissolved in drinking water at concentration gradients of 20 μg/ml (20 IQW-DSS), 40 μg/ml (40 IQW-DSS), 60 μg/ml (60 IQW-DSS), 80 μg/ml (80 IQW-DSS), and 100 μg/ml (100 IQW-DSS) for 1 week. The control group and DSS-induced model group were fed pure water for 1 week. The drinking water was then changed to 2.5% DSS (DSS:water/2.5:100) (Mw: 36,000–50,000 Da) for 1 week for the DSS group and the IQW feeding group at different concentrations. The mice were induced with colitis and killed after 3 days of normal feeding with drinking water. Colon tissues and contents were collected to detect colon damage, intestinal microbes, and short-chain fatty acid content in feces. All the experimental animal protocols comply with Chinese animal welfare guidelines. The Hunan Agricultural University Animal Care and Use Committee approved the experiments.

Immune organ index determination

On the 24th day, the mice were killed. The liver and spleen were dissected and weighed to calculate the immune organ index.

The calculation formula of the immune organ index is as follows:

$$\text{Immune organ index} = \frac{\text{Target organ weight (g)}}{\text{Body weight (kg)}}$$

Hemoglobin level determination

Wet feces (5 g/100 ml distilled water) were put into a mixer for homogenization, and then 0.5 ml feces homogenates were put into a centrifuge tube for 10 min in a boiling water bath

to inactivate the plant oxidase. After the sample was cooled, 30 ml of 30% acetic acid was added and mixed evenly; the above mixture was left to stand for two minutes and then 4.5 ml of ethyl acetate was added and shaken gently for 2 min, and centrifuge at 2000 rmp for 3 min to separate the organic phase and the aqueous phase. One ml of the upper solution was removed, 1 ml of TMB (tetramethylaniline) working solution was added and was mixed well; 0.5 mL of 30 ml /L H_2O_2 solution was added and was mixed to start the oxidize the reaction.

We observed the absorbance at A660 for 1 min and recorded it at 30 and 60 s to calculate the hemoglobin content. The hemoglobin standard curve (0.1–1 mg HB) was used to calculate the concentration of fecal hemoglobin with a content of 4–40 mg/g. Samples containing feces with hemoglobin more than 40 mg/g can be diluted with additional distilled water, and the determination results shall be multiplied by the appropriate dilution factor.

The hemoglobin content calculation formula is as follows:

$$\frac{\text{mg Hb}}{\text{g feces}} = \frac{[\text{mg Hb}(30\text{ s}) + \text{mg Hb}(60\text{ s})]/2}{0.025\text{ g feces}}$$

Intestinal histopathological analysis

The middle section of the intestine of about 2 cm was taken and fixed in a 10% neutral formalin (4% paraformaldehyde) solution. The contents could be removed by changing the fixative 2–3 times within a week after the sample had been taken. The intestinal fixative was washed off with pre-cooled saline, blotted on filter paper, placed in a 10% neutral formalin solution for 72 h, removed, washed 3 times with alcohol, and dehydrated with a gradient of alcohol (75 → 85 → 95 → 100 → 100% II). A microscopic observation of the hematoxylin-stained tissue was then performed. Histological scores were determined according to the severity of inflammation. Grading criteria included (19): (1) inflammation severity scores 0, 1, 2, and 3, respectively, represent none, mild, moderate, and severe; (2) inflammatory cell infiltration scores 0, 1, 2, and 3, respectively, represent normal, mucosal, submucosal, and transmural infiltration; (3) epithelial lesion scores 0, 1, 2, and 3, respectively, represent integrity, crypt structure deformation, erosion, and ulcer; (4) score of lesion degrees 0, 1, 2, and 3, respectively, represent no lesion, point lesion, multifocal lesion, and diffuse lesion; (5) edema scores of 0, 1, 2, and 3, respectively, represent no edema of the mucosa, mild edema, submucosal edema, and edema of the whole colon wall. The results of the histological analysis of the colon were expressed by the sum of scores obtained at all levels.

16S rDNA pyrophosphate sequencing

Total DNA was extracted from the microbial genome of each mouse's intestinal segment using the QIAamp Genome Extraction Kit (Qiagen, Hilden, Germany) according to instructions. DNA purity was determined, and DNA concentration was adjusted. The purified DNA was used as a template for PCR amplification using fused primers of the universal primers 357F 5′-ACTCCTACGGRAGGCAGCAG-3′ and 806R 5′-GGACTACHVGGGTWTCTAAT-3′ in the V3–V4 region of 16S rDNA and some Miseq sequencing primers. The PCR products were detected by 1.2% agarose gel electrophoresis. Samples with good detection results were recovered by 2% agarose gel electrophoresis. The recovered products were used as a template for one-time PCR amplification for 8 cycles. An Illumina platform sequencing connector, a sequencing primer, and a tag sequence were added to both ends of the target fragment. All the PCR products were recovered using an AxyPrepDNA gel recovery kit (AXYGEN), and fluorescence quantification was performed using a FTC-3000TM Real-Time PCR instrument. The library was constructed after being mixed with an equal molar ratio. The Illumina Miseq regent V3 kit was used to complete the sequencing of Illumina Miseq PE300 in Microbiotech (Shanghai) Co., Ltd.

The reads of each sample were assigned to the original data with a barcode, and the effective sequences of each sample were obtained. The Trimmomatic software was used to remove the low-quality sequences at the end of the sequencing. According to the overlap relationship between PE reads, the Flash software was used to splice paired reads into a sequence, and the mothur software was used to control and filter the quality of the sequence. The ambiguous bases, homologous regions of single bases, long and short sequences, and some chimeras generated in the PCR process were removed to obtain the optimized sequences. Operational taxonomic unit (OUT) clustering (UPARSE software) was performed, and the OTU representative sequences were compared with the SILVA 128 database for species information annotation. Based on taxonomic information, a statistical analysis of the community structure was carried out at the phylum, class, order, family, genus, and species classification levels. Based on the above analysis, a series of statistical and visual analyses of community structure and phylogeny was carried out. An alpha diversity analysis was performed using mothur (version 1.33.3) (Chao, Ace, Shannon, Simpson, etc.). Based on the OTU analysis of sequence similarity clustering, coverage, sobs, Chao, ACE, Shannon, Simpson, PD whole tree, and other indexes were calculated to obtain alpha diversity, which was used to reflect the abundance and diversity of microbial communities.

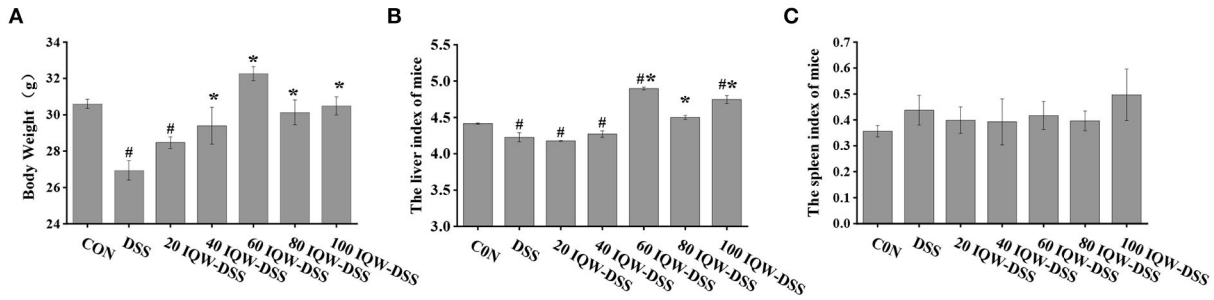

FIGURE 1
Evaluation of **(A)** body weight and **(B,C)** immune organs affected by egg protein transferrin-derived peptide IQW in the progression of colitis. CON: control group, DSS: mice treated with 2.5% DSS, 20 IQW-DSS: 20 μg/ml IQW and 2.5% DSS-treated mice, 40 IQW-DSS: 40 μg/ml IQW and 2.5% DSS-treated mice, 60 IQW-DSS: 60 μg/ml IQW and 2.5% DSS-treated mice, 80 IQW-DSS: 80 μg/ml IQW and 2.5% DSS-treated mice, and 100 IQW-DSS: 100 μg/ml IQW and 2.5% DSS treated mice; $n = 8$. Note: the results are given as mean ± SEM. $^{\#}p < 0.05$ vs. control group, $^{*}p < 0.05$ vs. the DSS group.

Short-chain fatty acid determination

Sample pre-treatment: we weighed 1 g of the fresh sample accurately and recorded the mass of each sample (0.5 g of dry sample, take care not to get the sample on the cap as much as possible to avoid shaking it off later) and then added 5 ml of ultra-pure water. (1) The vortex was vibrated for 30 min, stored at 4°C overnight, and then centrifuged for 10 min at 1,000 revolutions. The supernatant was transferred, and 4 ml of ultra-pure water was added to the precipitate. It was then shaken for another 30 min and mixed. After centrifugation, the supernatant was merged into a 10-ml coloration dish for constant volume. (2) It was then shaken and mixed for 30 min and centrifuged for 10 min to the transfer supernatant. Two ml of ultrapure water was added; the mixture was shaken and mixed for 30 min and centrifuged, and then the supernatant was transferred. The previous step was then repeated, the supernatant was combined, and the volume was fixed to a 10-mL cuvette. After achieving a constant volume, the liquid was transferred into a 10-ml centrifuge tube and centrifuged at 12,000 rpm for 15 min before mixing it with the supernatant. The supernatant and 25% metaphosphoric acid were added into a 2-ml centrifuge tube at a volume ratio of 9:1 and mixed well, and it was then let to stand and react at room temperature for 3–4 h. After the standing reaction, the mixture was centrifuged, filtered under 45 μm of a microporous membrane, and added to a machine bottle (above 600 μl) for testing. The chromatographic column was DB-FFAP with a specification of 30 m*250 μm*0.25 μm. High-purity nitrogen and hydrogen (99.999%) were used for the carrier and auxiliary gases, respectively, with a detector FID temperature of 280°C, an inlet temperature of 250 °C, a split ratio of 50:1, and an injection volume of 1 μl. Programmed temperature: the primary temperature was 60°C, and the temperature was increased to 220°C at a rate of 20°C/min for 1 min.

Data analysis

The experimental data were collated using Excel 2010, and then a one-way ANOVA and Duncan's test were performed on the differences between the groups using the SPSS 16.0 statistical software. The results were expressed as mean ± SEM ($p < 0.05$) and plotted with Origin 8.0. A Pearson correlation analysis was performed using GraphPad prism 8.4 to determine the relationship between different microorganisms and different short-chain fatty acids in the development of DSS-induced inflammation.

Results

Effect of different concentration gradients of IQW on the body weight and immune organ index during the development of colitis induced by DSS

In this study, the evaluation of body weight and immune organs that were affected by egg protein transferrin-derived peptide IQW in the progression of colitis are shown in Figure 1. The results showed that DSS had a negative effect on the body weight of the mice ($p < 0.05$), that IQW (40, 60,80 and 100 μg/ml) could alleviate the effect of DSS on body weight loss ($p < 0.05$), and that 20 μg/ml IQW had no effect on body weight loss ($p > 0.05$) (Figure 1A). Compared with the CON group, the liver weight of the DSS, 20, and 40 μg/ml IQW groups was significantly decreased, while that of the 60 and 100 μg/ml groups was significantly increased ($p < 0.05$). The liver weight of mice in the 60, 80, and 100 μg/ml IQW groups was significantly higher than that of the DSS group ($p < 0.05$) (Figure 1B). There was no significant difference in spleen index among the groups ($p > 0.05$) (Figure 1C).

Different concentration gradients of IQW treatment can alleviate colitis induced by DSS

The effects of egg protein transferrin-derived peptides IQW on colitis are shown in Figure 2. The pathological observation of colonic tissues and feces hemoglobin detection revealed that DSS and IQW-DSS treatment resulted in a significant increase in fetal hemoglobin levels and histological scores, and that IQW-DSS treatment with different concentration gradients significantly reduced feces hemoglobin levels and histological scores compared to the DSS-treated group ($p < 0.05$) (Figures 2A,B). In addition, the results of mice colon sections after HE staining showed that DSS caused the colon tissues to have multiple erosive lesions and extensive inflammatory cell infiltration, and that IQW alleviated the degree of colonic erosion (Figure 2C). The colonic length of the mice treated with different concentration gradients of IQW-DSS was also increased compared to the DSS group (Figure 2D).

Effect of different concentration gradients of egg active peptide IQW on intestinal microorganisms during the development of colitis induced by DSS

Based on the 16S rDNA high-throughput sequencing of colonic contents analyzed with the alpha diversity index, the results showed no significant differences in alpha diversity indices among the groups (Figures 3, 4). The analysis of the microbiota at the phylum level revealed Firmicutes, Bacteroidetes, and Proteobacteria as the dominant phyla, and DSS induction increased Bacteroidetes and Proteobacteria compared to the control group. Compared with the CON group, 80 μg/ml IQW significantly decreased the abundance of Bacteroidetes (Figure 4A1), Firmicutes were significantly increased at 20 and 80 μg/ml IQW, and were significantly decreased at 40 μg/ml IQW (Figure 4A2); 20, 40, and 60μg/ml IQW significantly increased Proteobacteria abundance (Figure 4A3). Compared with the DSS group, the abundance of Bacteroidetes in the colon of mice in the 20, 60, 80, and 100 μg/ml IQW groups was significantly decreased ($p < 0.05$). Compared with the DSS group, the abundance of Firmicutes in the colon of the 20, 60, and 80 μg/ml IQW groups was significantly increased. The abundance of Firmicutes in the colon of the 40 μg/ml IQW group was significantly decreased ($p < 0.05$). Compared with the DSS group, the abundance of Proteobacteria in the colon of mice in the 20 and 40 μg/ml IQW groups was significantly increased, while in the colon of the 80 and 100 μg/ml IQW groups it was decreased considerably ($p < 0.05$) (Figure 4A).

After the analysis at the genus level, the dominant bacteria were found to be *Bacteroides*, *Lactobacillus*, and *Staphylococcus*, which accounted for 11-32%. In the control group, the relative abundances were 7.8% *Bacteroides*, 3.88% *Lactobacillus*, and 2.47% *Staphylococcus*. In the DSS group, the relative abundances were 10.51% *Bacteroides*, 1.2% *Lactobacillus*, and 0.08% *Staphylococcus*. In the 20 μg/ml IQW-DSS group, the relative abundances were 8.3% *Bacteroides*, 4% *Lactobacillus*, and 0.41% *Staphylococcus*. In the 40 μg/ml IQW-DSS group, the relative abundances were 15.12% *Bacteroides*, 1.72% *Lactobacillus*, and 1.52% *Staphylococcus*; In the 60 μg/ml IQW-DSS group, the relative abundances were 16.6% *Bacteroides*, 11.49% *Lactobacillus*, and 4.06% *Staphylococcus*. In the 80 μg/ml IQW-DSS group, the relative abundances were 4.5% *Bacteroides*, 16.6% *Lactobacillus*, and 6.78% *Staphylococcus*. In the 100 μg/ml IQW group, the relative abundances were 10.31% *Bacteroides*, 2.35% *Lactobacillus*, and 1.13% *Staphylococcus*. Compared with the CON group, the abundance of *Bacteroides* in the colon of the DSS group was increased significantly, and the abundance of *Staphylococcus* was decreased significantly ($p < 0.05$). Compared with the CON group, the abundances of *Lactobacillus* and *Staphylococcus* at 60 and 80 μg/ml IQW were significantly increased (Figures 4B2,B3). Compared with the DSS group, the abundance of *Bacteroides* in the colon of the 40 and 60 μg/ml IQW groups was increased significantly, while that of the 80 μg/ml IQW group was decreased significantly ($p < 0.05$). Compared with the DSS group, the abundance of *Lactobacillus* and *Staphylococcus* in the colon of the 60 and 80 μg/ml IQW groups was increased significantly ($p < 0.05$) (Figure 4B).

Effect of different concentration gradients of egg active peptide IQW on volatile fatty acids of intestinal metabolites during the development of colitis induced by DSS

The effects of egg protein transferrin-derived peptide IQW on the level of short-chain fatty acids during the development of DSS-induced colitis are shown in Figure 5. Compared with the CON group, the contents of acetic acid, isobutyric acid, butyric acid, isovalerate, and total SCFAs in the feces of mice in the DSS group were significantly decreased ($p < 0.05$) (Figures 5A,C–E,G). Compared with the CON group, the levels of total short-chain fatty acids, acetic acid, propionic acid, and isovaleric acid were significantly reduced in the IQW-DSS treatment groups at different concentrations (Figures 5A,B,E,G). The levels of isobutyric acid and valeric acid were significantly reduced in the 20, 40, 60, and 100 μg/ml IQW groups (Figures 5C,F), and the level of butyric acid was significantly

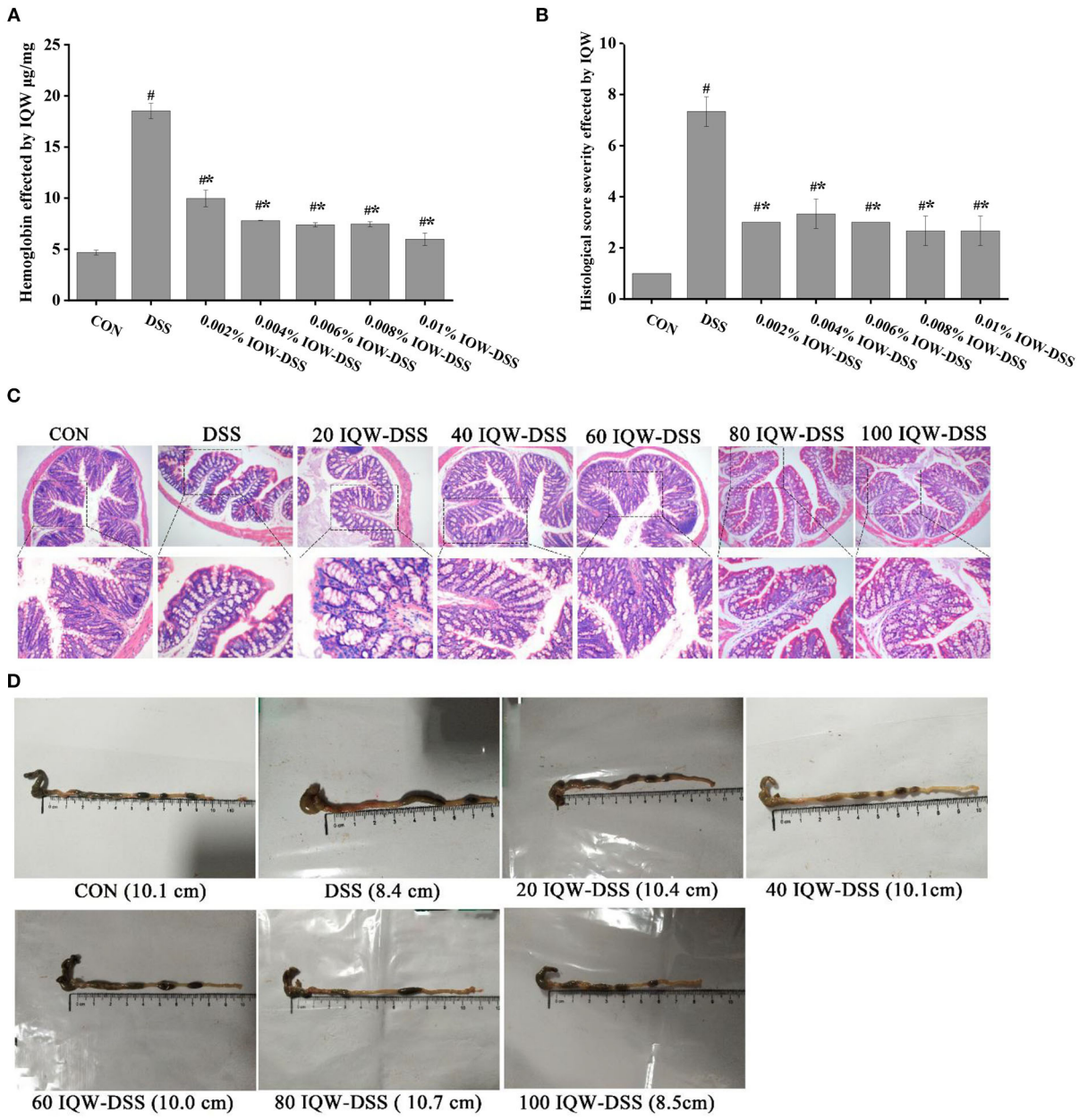

FIGURE 2
Effects of egg protein transferrin-derived peptide IQW on colitis. **(A)** Hemoglobin levels, **(B)** histological score severity, **(C)** micrograph of H and E-stained colon tissue section (×100 and ×200 magnification), and **(D)** length of the colon. CON: control group, DSS: mice treated with 2.5% DSS, 20 IQW-DSS: 20 μg/ml IQW and 2.5% DSS-treated mice, 40 IQW-DSS: 40 μg/ml IQW and 2.5% DSS-treated mice, 60 IQW-DSS: 60 μg/ml IQW and 2.5% DSS-treated mice, 80 IQW-DSS: 80 μg/ml IQW and 2.5% DSS-treated mice, and 100 IQW-DSS: 100 μg/ml IQW and 2.5% DSS-treated mice. The results are given as mean ± SEM. $^{\#}p < 0.05$ vs. the control group, $^{*}p < 0.05$ vs. the DSS group.

reduced in the 100 μg/ml IQW-treated group (Figure 5D). Compared with the DSS group, the acetic acid content in the feces of mice in the 20 and 100 μg/ml IQW groups was significantly decreased, and the propionate content in the feces of mice in the 20 and 60 μg/ml IQW groups was considerably reduced ($p < 0.05$) (Figures 5A,B). Compared with the DSS group, the contents of isobutyric acid and isovaleric acid in the feces of the 80 μg/ml IQW group were significantly increased, while those of the 100 μg/ml IQW group were significantly decreased ($p < 0.05$) (Figures 5C,E). Compared with the DSS group, the butyric acid in the feces of mice in the 60 μg/ml IQW group was increased ($p < 0.05$) (Figure 5D). Compared with the

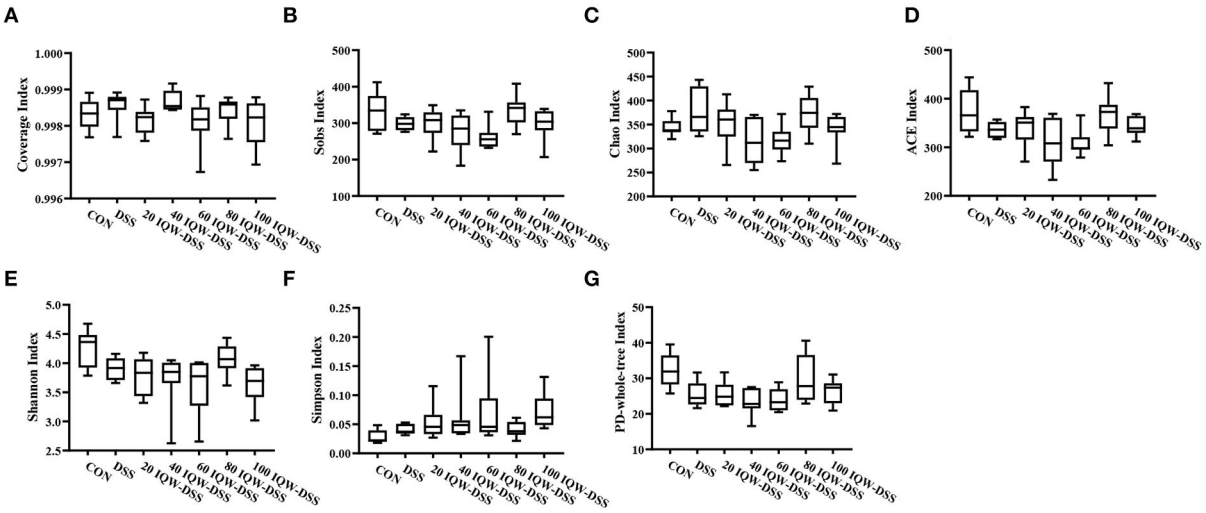

FIGURE 3
Diversity indexes of microbiota in mouse colon. **(A)** Coverage index, **(B)** Sobs index, **(C)** Chao index, **(D)** ACE index, **(E)** Shannon index, **(F)** Simpson index, and **(G)** PD-whole-tree index. CON1: control group, DSS1: mice treated with 2.5% DSS, 20 IQW-DSS: 20 μg/ml IQW and 2.5% DSS-treated mice, 40 IQW-DSS: 40 μg/ml IQW and 2.5% DSS-treated mice, 60 IQW-DSS: 60 μg/ml IQW and 2.5% DSS-treated mice, 80 IQW-DSS: 80 μg/ml IQW and 2.5% DSS-treated mice, and 100 IQW-DSS1: 100 μg/ml IQW and 2.5% DSS-treated mice; $n = 8$.

DSS group, the valeric acid in the feces of mice in the 40, 60, and 100 μg/ml IQW groups was decreased significantly ($p < 0.05$) (Figure 5F). Compared with the DSS group, the total SCFAs in mice feces in the 20 and 100 μg/ml IQW groups was significantly decreased ($p < 0.05$) (Figure 5G).

Effect of intestinal microflora on volatile fatty acid levels in intestinal metabolites

The correlation analysis of microflora and volatile fatty acids in the gut revealed that the butyrate levels were correlated positively with the abundance of *Lactobacillus* ($p = 0.002$) and Firmicutes ($p = 0.0045$) and negatively with the abundance of *Staphylococcus* ($p = 0.0349$) and Bacteroidetes ($p = 0.0057$) (Figures 6A–D), the valerate levels were negatively correlated with *Staphylococcus* abundance ($p = 0.0128$) (Figure 6E), and the isobutyrate levels were positively correlated with the abundance of Firmicutes ($p = 0.0301$) (Figure 6F).

Discussion

IBD is a multifactorial disease with multiple complications, which make the diagnosis and treatment of IBD a major challenge. The DSS-induced mouse colitis model has similar clinical symptoms of colitis, such as weight loss, metabolic disorders, and intestinal flora disorders (20–22). In this study, the effects and possible mechanisms for the relief of colitis were investigated by administering different concentration gradients of IQW in the context of DSS induction.

Ovotransferrin can bind to metal ions to enhance its antioxidant properties in addition to its antibacterial activity (23). In the present study, we found that the administration of 2.5% DSS induced weight loss, bloody stools, shortened colon length, and impaired colon histomorphology in mice, and that IQW treatment alleviated the negative effects of DSS and improved weight loss, shortened colon length, and colonic erosion. In addition, in the presence of DSS, the concentration of 60 μg/ml IQW significantly alleviated DSS-induced colitis in the mice. This may be related to amino acids that comprise IQW (15). Tryptophan is involved in the kynurenine, indole, and 5-hydroxytryptamine pathways, and it is essential for regulation of IBD by acting on immune cells, pro- or anti-inflammatory cytokines, and the microbial composition of the gut (24). Glutamine, a critical respiratory substrate for intestinal cells, maintains and restores intestinal function during enteritis by inducing MKP-1 kinase (25).

Progression of IBD is associated with microbial ecological dysbiosis, so controlling gut microbial dysbiosis can be conducted to treat IBD (26). Changes in the gut microbiome are responsible for many inflammatory diseases, including colitis, and when the microbiome is dysregulated, it induces inflammatory responses and immune-induced diseases (27). *Bacteroides*, *Lactobacillus*, *Prevotella*, and *Ruminococcus* are florae associated with IBD (28). The microbial diversity of the gut and its functions are altered in patients with IBD compared to the healthy gut, and examples include Firmicutes, Bacteroidetes, and Proteobacteria. There is evidence that the

10.3389/fnut.2022.927363

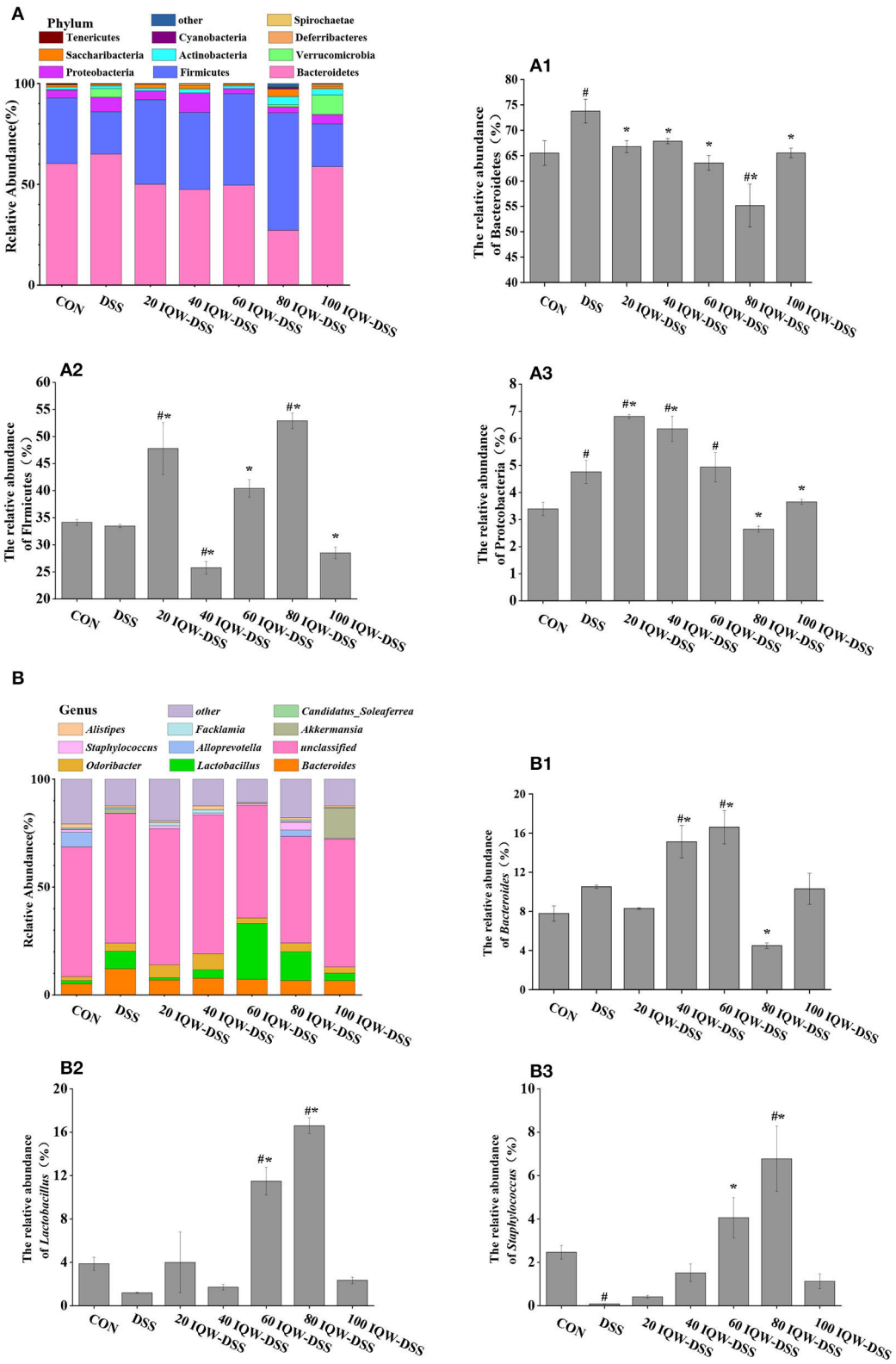

FIGURE 4
Analysis of microbial composition in the progression of colitis. **(A)** Changes in colonic microorganisms at the phylum level: **(A1)** Bacteroidetes, **(A2)** Firmicutes, and **(A3)** Proteobacteria. **(B)** Changes in colonic microorganisms at the genus level: **(B1)** *Bacteroides*, **(B2)** *Lactobacillus*, and **(B3)** *Staphylococcus*. CON: control group, DSS: mice treated with 2.5% DSS, 20 IQW-DSS: 20 μg/ml IQW and 2.5% DSS-treated mice, 40 IQW-DSS: 40 μg/ml IQW and 2.5% DSS-treated mice, 60 IQW-DSS: 60 μg/ml IQW and 2.5% DSS-treated mice, 80 IQW-DSS: 80 μg/ml IQW and 2.5% DSS-treated mice, and 100 IQW-DSS: 100 μg/ml IQW and 2.5% DSS-treated mice; $n = 8$. The results are given as mean ± SEM. $^{\#}p < 0.05$ vs. the control group, $^{*}p < 0.05$ vs. the DSS group.

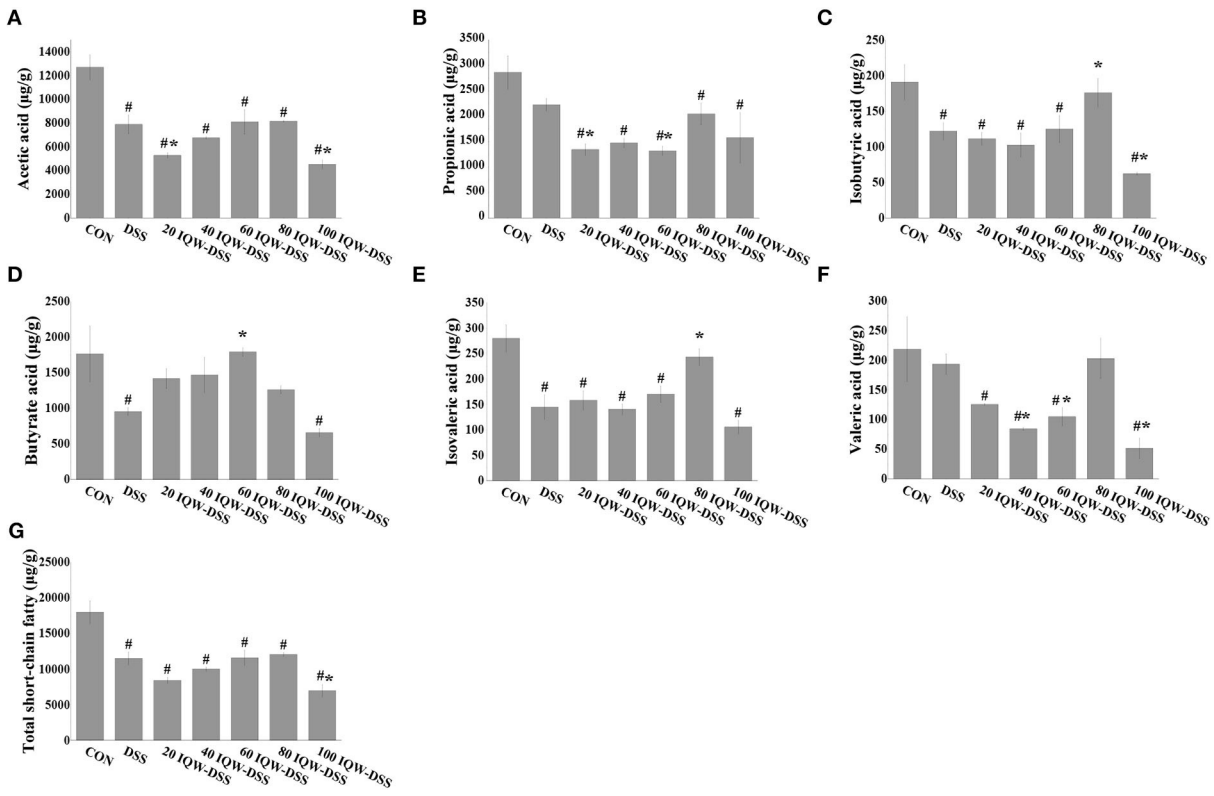

FIGURE 5
Effects of egg protein transferrin-derived peptide IQW on level of short-chain fatty acids during the development of DSS-induced colitis. **(A)** Acetic acid, **(B)** propionic acid, **(C)** isobutyric acid, **(D)** butyrate, **(E)** isovaleric acid, **(F)** valeric acid, and **(G)** total short-chain fatty acids. CON: control group, DSS: mice treated with 2.5% DSS, 20 IQW-DSS: 20 μg/ml IQW and 2.5% DSS-treated mice, 40 IQW-DSS: 40 μg/ml IQW and 2.5% DSS-treated mice, 60 IQW-DSS: 60 μg/ml IQW and 2.5% DSS-treated mice, 80 IQW-DSS: 80 μg/ml IQW and 2.5% DSS-treated mice, and 100 IQW-DSS: 100 μg/ml IQW and 2.5% DSS-treated mice; $n = 8$. The results are given as mean ± SEM. $^{\#}p < 0.05$ vs. the control group, $^{*}p < 0.05$ vs. the DSS group.

abundance of anti-inflammatory florae, such as *Bifidobacterium* and *Bacteroides*, is decreased during inflammation (7, 29). In this test, the alpha diversity index of microorganisms has no significant change, which may be due to the poor homogeneity among the mice. However, by the analysis of the dominant species at the phylum and genus levels, it was found that compared with the DSS-induced group, the IQW treatment group had increased abundance of Firmicutes and decreased abundance of Bacteroidetes at the phylum level; At the genus level, IQW treatment showed an increasing trend for *Lactobacillus* and *Staphylococcus* and a decreasing trend for *Bacteroides*. Liu et al. found in their research with an IBD model that the level of Bacteroides was restored during IQW treatment (17). Liu et al. also found that IQW reversed the change in intestinal dominant flora abundance in the treatment of ETEC-induced inflammation in a model (30). Ma Yong et al. (31). reported that IQW treatment could restore the levels of Firmicutes, Bacteroidetes and *Lactobacillus*, but that it had no significant impact on intestinal microbial diversity, which was consistent with the results of this test. These results suggest that IQW treatment can reprogram the intestinal microbial community. To some extent, it can restore the intestinal flora disorder induced by inflammation.

In addition, IQW can improve colitis through microbial metabolic pathways. SCFAs, produced by digestion of complex dietary fiber by microorganisms, are important energy and signal molecules that affect the physiological health of the host and have the characteristics of resisting inflammation, protecting the intestinal barrier, and maintaining intestinal homeostasis (6, 11). The results of this study showed that although there was no significant effect of IQW therapy on total SCFAs under DSS induction, the levels of SCFAs were lowered in the DSS group, 60 μg/ml IQW increased butyric acid and reduced valeric acid levels, and 80 μg/ml IQW increased the branched-chain fatty acids isobutyric and isovaleric acids. This may be related to changes in microbial diversity. For example, Firmicutes are the main microbial species producing butyrate in the colon, and the lactic acid produced by *Lactobacillus* can promote the production of butyrate (32, 33), while its abundance changes after IQW treatment. Thus, IQW treatment of colitis

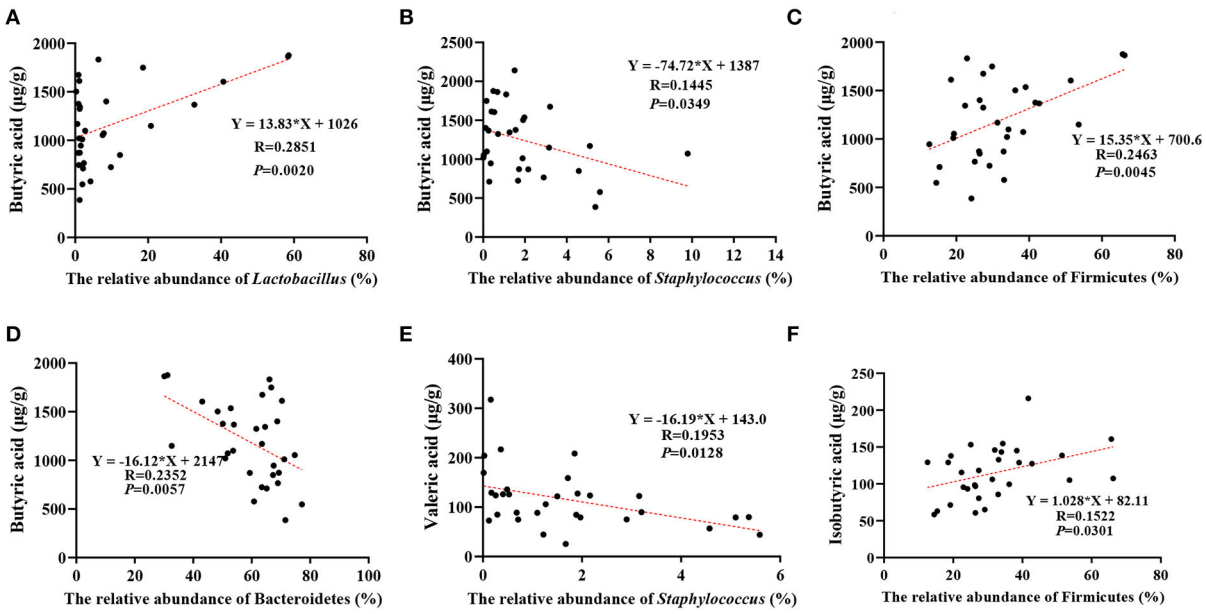

FIGURE 6
Correlation between different microorganisms and different short-chain fatty acids in the development of DSS-induced inflammation. **(A)** Effect of relative abundance of *Lactobacillus* on butyrate acid, **(B)** effect of relative abundance of *Staphylococcus* on butyrate acid, **(C)** effect of relative abundance of Firmicutes on butyrate acid, **(D)** effect of relative abundance of Bacteroidetes on butyrate acid, **(E)** effect of relative abundance of *Staphylococcus* on valeric acid, and **(F)** effect of relative abundance of Firmicutes on Isobutyric acid. The results are given as mean ± SEM ($n = 31$), $p < 0.05$.

can be achieved by regulating microorganisms and their metabolism. However, branched-chain fatty acids are generally considered to be harmful to the colon, as the fermentation of proteins to produce branched-chain fatty acids is accompanied by fermentation products, such as ammonia, phenol, p-formic acid, and hydrogen sulfide, which may affect the epithelial cells of the colon (34). Moreover, studies have proved that isovaleric acid can directly affect the longitudinal smooth muscle cells of the colon of mice, activate the protein kinase A (PKA) signal, and cause relaxation of the smooth muscle of the colon (35). It is therefore particularly important that the appropriate concentration is chosen for the treatment of colitis with IQW.

We suggest that IQW can alleviate DSS-induced weight loss, fecal occult blood, and histological damage. At the same time, egg active peptide IQW can also regulate the intestinal microbial community structure in mice, alleviate DSS-induced colon microbial disorder, and increase the abundance of probiotics, such as *Lactobacillus*. Overall, egg-active peptide IQW can alleviate DSS-induced colitis.

Data availability statement

The datasets presented in this study can be found in online repositories. The name of the repository and accession number can be found below: National Center for Biotechnology Information (NCBI) BioProject, https://www.ncbi.nlm.nih.gov/bioproject/, PRJNA832929.

Ethics statement

The animal study was reviewed and approved by the Hunan Agricultural University Animal Care and Use Committee.

Author contributions

YC: writing (original draft preparation). SD: study protocol. LJ, SW, and XY: index detection. HJ and JF: writing (review and editing). All authors contributed to manuscript revision, and read and approved the submitted version.

Funding

This research was supported by the National Key Research and Development Program of China (2021YFD1300205-2), the National Natural Science Foundation of China (81902297 and 81900441), Natural Science Foundation of Zhejiang Province (LQ19H020002), Hunan Provincial Science and Technology Department (2020NK2004, 2019TP2004, 2018WK4025, and 2020ZL2004), Local Science and Technology

Development Project Guided by The Central Government (YDZX20184300002303 and 2018CT5002), Scientific Research Fund of Hunan Provincial Education Department (2020JGYB112), and Double FirstClass Construction Project of Hunan Agricultural University (SYL201802003, YB2018007, CX20190497, and CX20190524).

Conflict of interest

The authors declare that the research was conducted in the absence of any commercial or financial relationships that could be construed as a potential conflict of interest.

Publisher's note

All claims expressed in this article are solely those of the authors and do not necessarily represent those of their affiliated organizations, or those of the publisher, the editors and the reviewers. Any product that may be evaluated in this article, or claim that may be made by its manufacturer, is not guaranteed or endorsed by the publisher.

References

1. Seyed Tabib NS, Madgwick M, Sudhakar P, Verstockt B, Korcsmaros T, Vermeire S. Big Data in Ibd: Big Progress for Clinical Practice. *Gut.* (2020) 69:1520–32. doi: 10.1136/gutjnl-2019-320065

2. Windsor JW, Kaplan GG. Evolving epidemiology of Ibd. *Curr Gastroenterol Rep.* (2019) 21:40. doi: 10.1007/s11894-019-0705-6

3. Zhang YZ Li YY. Inflammatory bowel disease: pathogenesis. *World J Gastroenterol.* (2014) 20:91–9. doi: 10.3748/wjg.v20.i1.91

4. Torres J, Mehandru S, Colombel J-F, Peyrin-Biroulet L. Crohn's disease. *Lancet.* (2017) 389:1741–55. doi: 10.1016/S0140-6736(16)31711-1

5. Ordás I, Eckmann L, Talamini M, Baumgart DC, Sandborn WJ. Ulcerative colitis. *Lancet.* (2012) 380:1606–19. doi: 10.1016/S0140-6736(12)60150-0

6. Koh A, De Vadder F, Kovatcheva-Datchary P, Backhed F. From dietary fiber to host physiology: short-chain fatty acids as key bacterial metabolites. *Cell.* (2016) 165:1332–45. doi: 10.1016/j.cell.2016.05.041

7. Glassner KL, Abraham BP, Quigley EMM. The microbiome and inflammatory bowel disease. *J Allergy Clin Immunol.* (2020) 145:16–27. doi: 10.1016/j.jaci.2019.11.003

8. Ahlawat S, Kumar P, Mohan H, Goyal S, Sharma KK. Inflammatory bowel disease: tri-directional relationship between microbiota, immune system and intestinal epithelium. *Crit Rev Microbiol.* (2021) 47:254–73. doi: 10.1080/1040841X.2021.1876631

9. Matsuoka K, Kanai T. The gut microbiota and inflammatory bowel disease. *Semin Immunopathol.* (2015) 37:47–55. doi: 10.1007/s00281-014-0454-4

10. Lavelle A, Sokol H. Gut microbiota-derived metabolites as key actors in inflammatory bowel disease. *Nat Rev Gastroenterol Hepatol.* (2020) 17:223–37. doi: 10.1038/s41575-019-0258-z

11. Dabek-Drobny A, Kaczmarczyk O, Wozniakiewicz M, Pasko P, Dobrowolska-Iwanek J, Wozniakiewicz A, et al. Association between fecal short-chain fatty acid levels, diet, and body mass index in patients with inflammatory bowel disease. *Biology (Basel).* (2022) 11:108. doi: 10.3390/biology11010108

12. Qiao Q, Chen L, Li X, Lu X, Xu Q. Roles of dietary bioactive peptides in redox balance and metabolic disorders. *Oxid Med Cell Longev.* (2021) 2021:5582245. doi: 10.1155/2021/5582245

13. Ma Y, Yan W, Ding S, Fei Y, Liu G, Fang J. Effects of bioactive peptide on inflammatory bowel disease, focus on signal transduction and intestinal microbiota. *Curr Pharm Des.* (2018) 24:2782–8. doi: 10.2174/1381612824666180829103945

14. Chen S, Jiang H, Peng H, Wu X, Fang J. The utility of ovotransferrin and ovotransferrin-derived peptides as possible candidates in the clinical treatment of cardiovascular diseases. *Oxid Med Cell Longev.* (2017) 2017:6504518. doi: 10.1155/2017/6504518

15. Majumder K, Chakrabarti S, Davidge ST, Wu J. Structure and activity study of egg protein ovotransferrin derived peptides (Irw and Iqw) on endothelial inflammatory response and oxidative stress. *J Agric Food Chem.* (2013) 61:2120–9. doi: 10.1021/jf3046076

16. Ma Y, Jiang H, Fang J, Liu G. Irw and Iqw reduce colitis-associated cancer risk by alleviating dss-induced colonic inflammation. *Biomed Res Int.* (2019) 2019:6429845. doi: 10.1155/2019/6429845

17. Liu G, Yan W, Ding S, Jiang H, Ma Y, Wang H, et al. Effects of Irw and Iqw on oxidative stress and gut microbiota in dextran sodium sulfate-induced colitis. *Cell Physiol Biochem.* (2018) 51:441–51. doi: 10.1159/000495240

18. Kobayashi Y, Rupa P, Kovacs-Nolan J, Turner PV, Matsui T, Mine Y. Oral administration of hen egg white ovotransferrin attenuates the development of colitis induced by dextran sodium sulfate in mice. *J Agric Food Chem.* (2015) 63:1532–9. doi: 10.1021/jf505248n

19. Ding S, Yan W, Fang J, Jiang H, Liu G. Potential role of lactobacillus plantarum in colitis induced by dextran sulfate sodium through altering gut microbiota and host metabolism in murine model. *Sci China Life Sci.* (2021) 64:1906–16. doi: 10.1007/s11427-020-1835-4

20. Kiesler P, Fuss IJ, Strober W. Experimental models of inflammatory bowel diseases. *Cell Mol Gastroenterol Hepatol.* (2015) 1:154–70. doi: 10.1016/j.jcmgh.2015.01.006

21. Kim JJ, Shajib MS, Manocha MM, Khan WI. Investigating intestinal inflammation in Dss-induced model of Ibd. *J Vis Exp.* 11:108 (2012). doi: 10.3791/3678

22. Xu H, Cai F, Li P, Wang X, Yao Y, Chang X, et al. Characterization and analysis of the temporal and spatial dynamic of several enteritis modeling methodologies. *Front Immunol.* (2021) 12:727664. doi: 10.3389/fimmu.2021.727664

23. Benede S, Molina E. Chicken egg proteins and derived peptides with antioxidant properties. *Foods.* (2020) 9:735. doi: 10.3390/foods9060735

24. Li X, Zhang ZH, Zabed HM, Yun J, Zhang G, Qi X. An insight into the roles of dietary tryptophan and its metabolites in intestinal inflammation and inflammatory bowel disease. *Mol Nutr Food Res.* (2021) 65:e2000461. doi: 10.1002/mnfr.202000461

25. Jeong SY, Im YN, Youm JY, Lee HK, Im SY. L-Glutamine Attenuates Dss-Induced Colitis Via Induction of Mapk Phosphatase-1. *Nutrients.* (2018) 10:288. doi: 10.3390/nu10030288

26. Alshehri D, Saadah O, Mosli M, Edris S, Alhindi R, Bahieldin A. Dysbiosis of gut microbiota in inflammatory bowel disease: current therapies and potential for microbiota-modulating therapeutic approaches. *Bosn J Basic Med Sci.* (2021) 21:270–83. doi: 10.17305/bjbms.2020.5016

27. Round JL, Mazmanian SK. The gut microbiota shapes intestinal immune responses during health and disease. *Nat Rev Immunol.* (2009) 9:313–23. doi: 10.1038/nri2515

28. Jandhyala SM, Talukdar R, Subramanyam C, Vuyyuru H, Sasikala M, Nageshwar Reddy D. Role of the normal gut microbiota. *World J Gastroenterol.* (2015) 21:8787–803. doi: 10.3748/wjg.v21.i29.8787

29. Wright EK, Kamm MA, Teo SM, Inouye M, Wagner J, Kirkwood CD. Recent advances in characterizing the gastrointestinal microbiome in Crohn's disease: a systematic review. *Inflamm Bowel Dis.* (2015) 21:1219–28. doi: 10.1097/MIB.0000000000000382

30. Liu N, Zhou L, Fang J, Jiang H, Liu G. Effects of Iqw and Irw on inflammation and gut microbiota in etec-induced diarrhea. *Mediators Inflamm.* (2021) 2021:2752265. doi: 10.1155/2021/2752265

31. Ma Y, Ding S, Liu G, Fang J, Yan W, Duraipandiyan V, et al. Egg protein transferrin-derived peptides irw and iqw regulate citrobacter rodentium-induced,

inflammation-related microbial and metabolomic profiles. *Front Microbiol.* (2019) 10:643. doi: 10.3389/fmicb.2019.00643

32. Munoz-Tamayo R, Laroche B, Walter E, Dore J, Duncan SH, Flint HJ, et al. Kinetic modelling of lactate utilization and butyrate production by key human colonic bacterial species. *FEMS Microbiol Ecol.* (2011) 76:615–24. doi: 10.1111/j.1574-6941.2011.01085.x

33. Zhang W, Zou G, Li B, Du X, Sun Z, Sun Y, et al. Fecal microbiota transplantation (Fmt) alleviates experimental colitis in mice by gut microbiota regulation. *J Microbiol Biotechnol.* (2020) 30:1132–41. doi: 10.4014/jmb.2002.02044

34. Aguirre M, Eck A, Koenen ME, Savelkoul PH, Budding AE, Venema K. Diet drives quick changes in the metabolic activity and composition of human gut microbiota in a validated in vitro gut model. *Res Microbiol.* (2016) 167:114–25. doi: 10.1016/j.resmic.2015.09.006

35. Blakeney BA, Crowe MS, Mahavadi S, Murthy KS, Grider JR. Branched short-chain fatty acid isovaleric acid causes colonic smooth muscle relaxation via camp/Pka pathway. *Dig Dis Sci.* (2018) 64:1171–81. doi: 10.1007/s10620-018-5417-5

frontiers | Frontiers in Nutrition

TYPE Original Research
PUBLISHED 08 September 2022
DOI 10.3389/fnut.2022.1006517

OPEN ACCESS

EDITED BY
Yong Su,
Nanjing Agricultural University, China

REVIEWED BY
Yongsheng Chen,
Jinan University, China
Wuquan Deng,
Chongqing Emergency Medical Center, China

*CORRESPONDENCE
Meng Shi
shimeng@hunau.edu.cn
Chaoxi Zeng
chaoxizeng@hunau.edu.cn
Chenghao Lv
1756790187@qq.com

†These authors have contributed equally to this work and share first authorship

SPECIALTY SECTION
This article was submitted to Nutrition and Microbes, a section of the journal Frontiers in Nutrition

RECEIVED 29 July 2022
ACCEPTED 17 August 2022
PUBLISHED 08 September 2022

CITATION
Wang C, Hu M, Yi Y, Wen X, Lv C, Shi M and Zeng C (2022) Multiomic analysis of dark tea extract on glycolipid metabolic disorders in db/db mice. *Front. Nutr.* 9:1006517. doi: 10.3389/fnut.2022.1006517

Multiomic analysis of dark tea extract on glycolipid metabolic disorders in db/db mice

Caiqiong Wang[1†], Minghai Hu[2†], Yuhang Yi[1], Xinnian Wen[1], Chenghao Lv[1,3*], Meng Shi[1*] and Chaoxi Zeng[1*]

[1]Laboratory of Food Function and Nutrigenomics, College of Food Science and Technology, Hunan Agricultural University, Changsha, China, [2]Department of Neurobiology and Human Anatomy, School of Basic Medical Science, Central South University, Changsha, China, [3]College of Bioscience and Biotechnology, Hunan Agricultural University, Changsha, Hunan, China

Glycolipid metabolic disorder is a serious threat to human health. Dark tea is a kind of traditional Chinese tea, which may regulate the glycolipid metabolic disorders. Dark tea extract (DTE) is the water extraction obtained from dark tea. Compared with traditional dark tea, DTE has the benefits of convenient consumption and greater potential for promoting health. However, the regulation of DTE on glycolipid metabolism and its molecular mechanism is rarely investigated. In our study, DTE was used as raw material to study the effect and molecular mechanism of its intervention on the glycolipid metabolic in db/db diabetic mice by using multiomics analysis and modern biological techniques. (1) DTE could significantly reduce fasting glucose in diabetic db/db mice, and the higher dose group has a better effect. Histopathological examination showed that DTE slightly improve the number of islets and decrease the number of islet β cells in the pancreatic tissue in db/db mice. (2) RNA-Seq was used to analyze the gene expression in liver tissue. In terms of biological processes, DTE mainly affected the inflammation and fatty acid metabolism. In terms of cell components, the lipoprotein and respiratory chain are mainly affected. In the aspect of molecular function, DTE mainly affected the redox related enzyme activity, iron ion binding and glutathione transferase. Arachidonic acid metabolism pathway, glutathione metabolism and PPAR signaling pathway were enriched by DTE with the results of KEGG pathway enrichment. In addition, real-time PCR results confirmed that DTE could significantly activate key genes of PPAR signaling pathway like *Fabp1*, *Cyp4a1*, *Ehhadh*, *Cyp4a32*, *Aqp7* and *Me1*. (3) 16s rDNA showed that DTE could significantly decrease the ratio of *Firmicutes/Bacteroidetes* and the abundance of *Proteobacteria*, and increased the relative abundance of *Verrucomicrobia* at the phylum level. At the genus level, the relative abundance of *Akkermansia*, *Prevotellaceae*, *Bacteroides* and *Alloprevotella* was significantly increased after DTE treatment. This study provides multiomics molecular evidence for the intervention effect of DTE on abnormal glucose and lipid metabolism and the application of precise nutritional diet intervention of dark tea extract.

KEYWORDS

dark tea, glycolipid metabolism, gene expression, gut microbiota, multiple omics

Introduction

Glucolipid metabolism disorder is a metabolic disorder that seriously threatens human health and affects the quality of life. Glucolipid metabolism disorders mainly take insulin resistance, oxidative stress, chronic inflammation, and intestinal flora imbalance as their core pathologies, resulting in systemic multi-tissue organ dysfunction and multi-system damage, which need to be comprehensively prevented and controlled from the whole body (1). Insulin-related signaling pathways such as IRS/PI3K/AKT/GLUT4, IRS/PI3K/GSK, MAPK/ERK, and PI3K/Akt/GSK play important roles in the development of metabolic syndrome associated with abnormal glucolipid metabolism. In addition, insulin resistance induces heterotopical lipid deposition and reduces mitochondrial function, which in turn leads to storms of inflammatory factors and induces oxidative imbalance in the body. Oxidative stress state destroys antioxidant enzymes, and ultimately leads to abnormal glucolipid metabolism (2, 3). The NF-κB signaling pathway is an important link between inflammation and glucolipid metabolism disorder (4). PPARγ can inhibit the activity of NF-κB DNA and reduce the expression of NF-κB mediated inflammatory mediators, finally exerting the anti-inflammatory effect (5). Concurrently, PPARγ can regulate the expression of various adipokines, inflammatory factors in adipocytes, insulin signal transduction, and regulate the regular balance of insulin and glucolipid metabolism. After investigating the intestinal flora of obese and normal people, it is found that the risk of metabolic diseases such as diabetes and nonalcoholic fatty liver disease will be increased in people with low microbial abundance (6). According to a study on the intestinal flora of 345 Chinese patients with T2DM, the abundance of *Firmicutes* and *Clostridium* in the intestinal flora of patients with diabetes mellitus tended to decrease (7).

Dark tea is one of the six major teas in China and belongs to post-fermented teas. Depending on its origin and different fermentation method, it includes ripe Pu'er Tea, Fuzhuan Brick Tea, Liupao Tea, Qing Brick Tea and Kang Brick Tea (8). Dark tea is rich in bioactive components, such as alkaloids, flavonoids, free amino acids, polyphenols, polysaccharides and volatile compounds, etc. A large number of research reports have confirmed that, dark tea and its extracts had significant effects in regulating abnormal glucolipid metabolism (9, 10). Many studies have shown that dark tea can significantly inhibit the absorption rate of glucose and enhance the insulin resistance (11). A study reported that Qingzhuan tea extracts exerted potent inhibitory effects against α-glucosidase (12). Instant dark tea with high levels of theabrownines showed antioxidant ability and inhibitory activities of α-glucosidase and pancreatic lipase (13). A series of *in vivo* studies also found that dark tea affected abnormal glucose metabolism by decreasing insulin resistance. Fuzhuan Brick Tea significantly antagonized HFD-induced insulin resistance with elevations in serum leptin, TC, TG, LDL-C, blood urea nitrogen, uric acid, and creatinine levels. Furthermore, Fuzhuan brick tea alleviated insulin resistance through down-regulation of SIRP-α expression and activation of the insulin signaling Akt/GLUT4, FoxO1, and mTOR/S6K1 pathways in skeletal muscle (14). Pu'er Tea extract improve the insulin sensitivity and glucose tolerance by increasing the expression of GLUT4 in adipose tissues, maintaining insulin signal transduction and reducing the expression of gluconeogenesis-related genes in the liver (15). Moreover, studies have shown that black tea can improve the oxidation and catabolism of fatty acids, while inhibiting the generation and accumulation of fat. Fuzhuan Brick Tea polysaccharides could up-regulate the expression of genes related to fatty acid decomposition in rats and down-regulate the expression of genes related to lipogenesis (16). A randomized, double-blind, placebo-controlled study showed that consumption of Pu'er Tea extract was associated with improvements to lipid profile, including a mild reduction in cholesterol and the cholesterol: high-density lipoprotein ratio after only 4 weeks, as well as a reduction in triglycerides and very small-density lipoproteins (17). Pu'er Tea also ameliorates hepatic lipid metabolism, inflammation, and insulin resistance in mice with HFD-induced nonalcoholic steatohepatitis, presumably by modulating hepatic IL-6/STAT3 signaling (18). In conclusion, dark tea or its extracts may affect abnormal glucolipid metabolism by reducing blood glucose levels, reducing insulin resistance, affecting the metabolism of fatty acid, and improving the related inflammation factors.

Multi-Omics combines two or more omics research methods, such as genomics, transcriptomics, microbiology, proteomics or metabolomics, to conduct systematic research on biological samples, and integrate and analyze the data of each omics to deeply mine the biological data. In recent years, a large number of studies have unveiled the molecular mechanisms of abnormal glucolipid metabolism using multi-omics technology, as well as precision nutritional intervention based on transcriptomics. Currently, relevant studies have explored the effects of black tea on gene expression regulators and intestinal microecological balance based on multiomic technology. Study on that utilization of microbiological technology, Fuzhuan Brick Tea-induced increase in abundances of beneficial bacteria *Clostridiaceae*, *Bacteroidales*, and *Lachnospiraceae* and decreases in harmful *Ruminococcaceae, Peptococcaceae*, *Peptostreptococcaceae*, and *Erysipelotrichaceae* were causal antecedents for Fuzhuan Brick Tea to reduce obesity and improve metabolic disorders (19).

In this study, the extract of dark tea was used to investigate the effects of blood glucose and lipid levels in diabetic mice. Then, RNA-Seq sequencing was performed on the liver of the mice to analyze the gene expression differences in the liver, screen the differentially expressed genes, perform Gene Ontology (GO) functional annotation and enrichment analysis on the differentially expressed genes, and further perform

Kyoto Encyclopedia of Genes and Genomes (KEGG) signaling pathway annotation and enrichment analysis on the differential genes. Finally, 16s rDNA sequencing was conducted on mouse droppings to preliminary analyze structure, abundance, diversity, the differential species at the genus level and the significantly differential species of intestinal micro-organisms in mice. This study will provide new foundations and insights for precision nutritional intervention and the action mechanism of dark tea in metabolic syndrome.

Materials and methods

Materials and chemicals

Dark tea extract (DTE) was provided by Hunan Tea Industry Group Co. Ltd. (Changsha, China). Metformin hydrochloride (MET) was purchased from Beijing Jingfeng Pharmaceutical Group Co., Ltd. (Beijing, China).

Animals and models

There were 40 male diabetic db/db mice and 10 C57BL/6 mice (8 weeks old, specific pathogen free grade) were obtained from Hunan Jingda Experimental Animal Co., Ltd. (SCXK (Xiang) 2019-0004) and raised in the barrier environment of Hunan Drug Safety Evaluation Research Center (SYXK (Xiang) 2015-0016). SPF male db/db mice were fasted for 12 h, and their fasting blood glucose was detected. Forty animals with fasting blood glucose higher than 11.1 mmol/L and body weight ranging from 28.9 to 36.0 g were randomly divided into control group, MET group (0.26 g/kg), low-dose DTE group (DTE-L, 0.78 g/kg) and high-dose DTE group (DTE-H, 1.56 g/kg), with 10 animals in each group. Another 10 male C57BL/6 mice of SPF were taken as the normal control group, with blood sugar values of 3.1–7.2 mmol/L and body weight of 19.3 23.1 g. Each dose group was given the corresponding drugs by gavage of 20 ml/kg once a day for 11 weeks, while the normal control group and the model control group were given the same volume by gavage. During the experiment, the weight and blood glucose of animals were monitored regularly every week. At the end of 11th week intervention, the mice were sacrificed by cervical vertebra after ether anesthesia. Then, serum was obtained from mouse eyes after centrifugation. Afterwards, liver and pancreas were collected and stored at-80 for further use.

Serum parameters analysis

The serum were used to evaluate triglyceride (TG), total cholesterol (CHO), high-density lipoprotein cholesterol (HDL), low-density lipoprotein cholesterol (LDL) (Wako Pure Chemical Industries, Ltd., Chuo-ku, Japan). Blood glucose level was measured using blood glucose test strip (Sinocare Inc Co. Ltd, Changsha, China). Insulin detection kit from Jiangsu MEIMIAN Biological Industry Co., Ltd. (Yancheng, China).

IRI and histopathology analysis

IRI = fasting blood glucose (mmol/L) × fasting insulin (mIU/L)/22.5. Histological Analysis and Morphometry Part of the liver tissue was fixed with 4% paraformaldehyde. After 24 h, the livers were embedded in paraffin wax. Then, the liver samples were processed using cryostat (CM1950, Leica, Germany) and stained with haematoxylin–eosin (H&E). Finally, these slices were observed using the Olympus light microscope.

Total RNA extraction and sequencing

The extraction and detection of total RNA of mice in each experimental group were completed by Beijing Novogene Technology Co., Ltd. (Beijing, China). RNA from the total sample was isolated and purified using Trizol (Invitrogen, USA). The quantity and purity of total RNA were then controlled by NanoDrop ND-1000, RNA integrity was tested by Bioanalyzer 2100, and RNA concentration was quantified by agarose electrophoresis. MRNAs with polyadenylation (PolyA) were purified by using oligo (dT) magnetic beads for specific capture, and the captured mRNA was fragmented by using a magnesium ion disruption kit at 94°C for 5–7 min under a high temperature condition, and the obtained fragmented RNA was reverse transcribed into cDNA by reverse transcriptase action. *E. coli* DNA polymerase I and RNase H were used to convert the compound double chains of these DNA and RNA into DNA double chains, and dUTP Solution was added into the two chains to fill the ends of the double-stranded DNA into flat ends and add an A base at each end to enable it to connect with the linker with T base at the end. Their fragment sizes were subsequently screened and purified using oligo(dT) magnetic beads. To be maintained at 95°Cfor 3 min by PCR-predenaturation, 98°C for a total of eight cycles of 15 s each, annealing to 60°C for 15 s, extension at 72°C for 30 s, and finally extension at 72°C for 5 min to form a library with a fragment size of 300 ± 50 bp. Finally, it was double-ended sequenced using Illumina NovaSeq™ 6,000 according to standard operations in sequencing mode PE150.

qRT-PCR analysis

To measure the expression of *Fabp1*, *Cyp4a1*, *Ehhadh*, *Cyp4a32*, *Aqp7* and *Me1* in the liver, total RNA of the liver was extracted using Omega total RNA Kit. RNA was reversely

transcribed using PrimeScript RT Master Mix. QPCR primers were designed by Biological Engineering Co., Ltd. (Shanghai, China) based on the cDNA sequence. Real-time quantitative reverse transcription PCR (qRT PCR) was performed using SYBR GreenMaster Mix and QuantStudio 3 Flex according to the manufacturer's guidelines. The experiments were performed on a flat plate, three in each group in parallel, and using the $2^{-\Delta\Delta Ct}$ method. The reaction procedure was as follows: 95°C for 10 min using a three-step cycle using the Rotor-Gene Q6200 real-time PCR system followed by 40 cycles of 95°C for 10 s, 60°C for 20 s and 72°C for 20 s. The reaction mixture (20 μl) consisted of 2 μl cDNA solution, 10 μl IQTM SYBRR Green Supermix, and 6 μl primers. Three for each group were parallel and the results were averaged. β-actin was used as a reference gene. The comparative cycle threshold method was used to evaluate the relative expression level of genes.

DNA extraction and 16S gene sequencing

DNA from different samples was extracted using the EZNA tool DNA Kit (D4015, Omega, Inc., USA) according to the manufacturer's instructions. The reagent that was designed to uncover DNA from trace amounts of the sample has been shown to be effective for the preparation of DNA of most bacteria. Nuclear-free water was used for blank. The total DNA was eluted in 50 μL of elution buffer and stored at −80°C until PCR measurement.

Statistical analysis

Results were expressed as mean ± SD. The significant differences between groups were analyzed by the One-way ANOVA followed Tukey's multiple comparison post-test, and by using the LSD procedure of SPSS 26, and different statistical significance were accepted at $p < 0.05$. The correlation between gut microbiota, serum index and metabolites were analyzed by SPSS statistical program. Statistical significance was set at $p < 0.05$.

Results

Effects of DTE on metabolic parameters including serum lipid and blood glucose levels in db/db mice

As shown in Figure 1, compared with the normal group, the fasting blood glucose of mice in the control group was significantly increased ($p < 0.01$). Compared with the control group, there is no significant hypoglycemic effect was observed in the DTE-L and DTE-H group at the levels of D0, D7, D14, D21, D28, D35, D42, D49, and D56. The fasting blood glucose of db/db diabetic mice in the DTE-L and DTE-H group was significantly reduced ($p < 0.05$ or $p < 0.01$) when D63, D70, and D77 were given. Besides, the reducing effects of the DTE-H group of fasting blood glucose in dB/dB diabetic mice were better than the DTE-L group in D49, D56, D63, D70, and D77. The fasting blood glucose of db/db mice in the MET was significantly reduced ($p < 0.05$ or $p < 0.01$) after administration of D21, D28, D35, D42, D49, D56, D63, D70, and D77.

HDL of the DTE-L and DTE-H groups showed an upward trend with no statistical difference with respect to the normal group. The content of TG of the control group, DTE-L group and DTE-H group tended to be decreased, but there was no statistical difference. The CHO level in the DTE-L group and DTE-H group was lower than that that of control group, but there was no statistical difference. Relative to the control group, the LDL level of the MET group increased significantly ($p < 0.05$) (Table 1).

Effect of DTE on serum insulin level and IRI of db/db mice

Compared with the normal group, serum insulin of db/db diabetic mice in the control group tended to decrease, and the IRI was significantly increased ($p < 0.01$). Compared with the control group, the serum insulin levels of db/db diabetic mice in the DTE-H group were significantly increased. The IRI of db/db diabetic mice in the MET group was decreased significantly ($p < 0.01$) (Table 2).

Effect of DTE on morphology of pancreas tissue in mice

As shown in Figure 2, the islets were spherical cell masses composed of endocrine cells, and each islet was composed of many cells, with a clear islet boundary in the normal control group. Compared to the normal group, the pathological score of pancreatic tissue hyperplasia in db/db diabetic mice was significantly increased ($p < 0.01$). In the control group, the islets of langerhans were seriously damaged, and the number of islets was significantly reduced, with the result that the islets became smaller, and the boundary was fuzzy. The number of β cells in the islets was significantly reduced, which was disorganized, with partial cell necrosis and unclear cell boundary. Compared to the control group, the pathological scores of pancreatic tissues in db/db diabetic mice in the MET group tended to decrease, but there was no statistical difference. The DTE-H group and MET group could slightly improve the damage of pancreatic tissue, vague islet boundary, and disordered arrangement of islet β cells in diabetic mice.

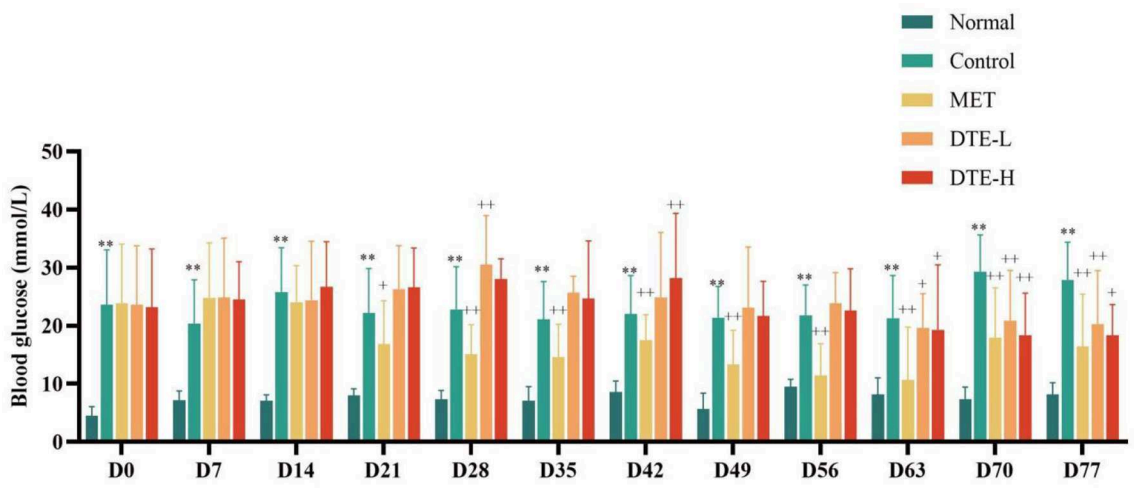

FIGURE 1
The effect of DTE on fasting blood glucose of db/db diabetic mice. Control, MET, DTE-L, DTE-H vs. Normal, $^{**}p < 0.01$; MET, DTE-L, DTE-H vs. Control, $^{+}p < 0.05$, $^{++}p < 0.01$.

Effect of DTE on gene expression in liver of db/db mice

Data quality control required Q20> 90%, Q30> 85%, and GC content of 40–50% after filtration to indicate no abnormalities during sequencing. The minimum values of Q20 and Q30 for the samples were 96.75 and 91.30%, respectively, and the GC content was within the range of 46.49–49.86%, indicating that the sequencing quality was preferable. Principal component analysis (PCA) was also frequently used to assess inter-group differences and sample repetition within groups. Regarding the PCA data of the DTE group, we previously performed three sets of DTE, but only one set of experimental data was valid, and the experimental data showed significant differences between the DTE group, MET group, and control group. As shown in Figure 3, PC1 accounted for 41.55%, and it could significantly distinguish between the control group and other treatment groups, indicating that the other treatment groups had significant differences in liver transcriptional expression. PC2 accounted for 17.42%, significantly differentiating the MET group from the DTE group, indicating that DTE was able to regulate mouse gene expression at the transcriptome level.

The data of gene transcriptional expression levels of the control, MET and DTE group obtained by RNA-Seq sequencing are shown in Figure 4. Compare to the Control group, DTE group had 1,506 differential genes, including 617 up-regulated genes and 889 down-regulated genes; Compare to the Control group, there were 777 differential genes in the MET group, including 441 down-regulated genes and 336 up-regulated genes; Compare to the DTE group, there were 336 differential genes in the MET group, including 233 down-regulated genes and 103 up-regulated genes.

Compare to the DTE group, the GO functional classification and enrichment analysis of differentially expressed genes in the control group were shown in Figure 5A. A total of 6,574 items were screened out, and a total of 423 items with significant statistical significance were screened out, including

TABLE 1 The effect of DTEon blood lipid levels.

	TG (mmol/L)	CHO (mmol/L)	HDL (mmol/L)	LDL (mmol/L)
Normal	0.45 ± 0.19	2.80 ± 0.35	2.25 ± 0.25	0.26 ± 0.12
Control	0.37 ± 0.29	3.38 ± 0.44	2.95 ± 0.45	0.26 ± 0.09
MET	0.72 ± 0.55	4.65 ± 1.54^{+}	3.75 ± 0.71	0.61 ± 0.82^{+}
DTE-L	0.38 ± 0.12	3.15 ± 1.49	3.20 ± 4.50	0.23 ± 0.17
DTE-H	0.32 ± 0.27	3.24 ± 1.61	2.99 ± 1.14	0.38 ± 0.25

MET, DTE-L, DTE-H vs. Control, $^{+}p < 0.05$.

TABLE 2 The effect of DTE on insulin and insulin resistance index (IRI).

	Insulin (mIU/L)	IRI
Normal	48.08 ± 2.74	16.13 ± 3.96
Control	43.80 ± 4.00	47.57 ± 15.89**
MET	48.56 ± 2.76	26.87 ± 14.46^{++}
DTE-L	46.25 ± 3.19	43.84 ± 11.20
DTE-H	48.63 ± 4.72	40.31 ± 12.62

Control, MET, DTE-L, DTE-H vs. Normal, $^{**}p < 0.01$; MET, DTE-L, DTE-H vs. Control, $^{++}p<0.01$.

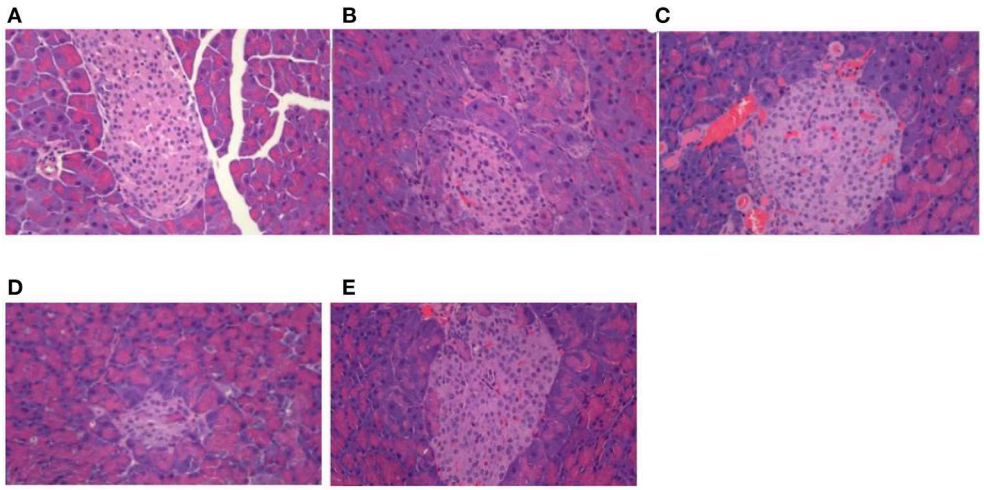

FIGURE 2
Effect of DTE on morphology of pancreas tissue in mice. **(A)** Normal group; **(B)** Control group; **(C)** MET group; **(D)** DTE-L group; **(E)** DTE-H group.

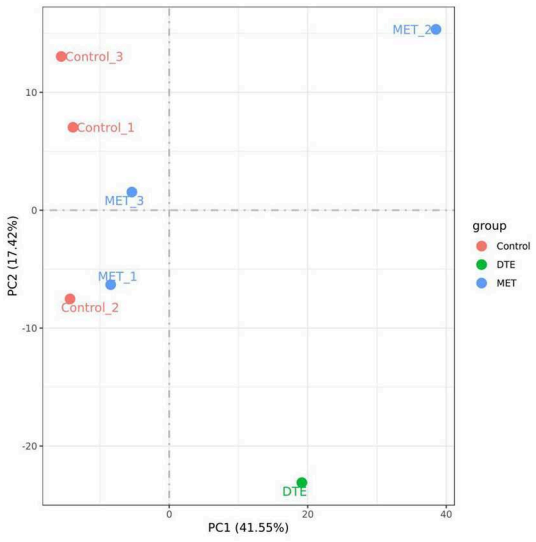

FIGURE 3
The PCA of the samples. The experimental data showed significant differences between the DTE group, MET group, and control group.

294 items concerning biological processes (BP), 49 items concerning cellular components (CC) and 80 items concerning molecular functional processes (MF). In biological processes, the most significant 10 items were: response to stilbenoid, acute inflammatory response, response to bacterium, humoral immune response, fatty acid metabolic process, protein activation cascade, reactive oxygen species metabolic process, leukocyte migration involved in inflammatory response, positive regulation of response to external stimulu, and leukocyte migration. In cellular component, the most significant 10 items were: plasma lipoprotein particle, lipoprotein particle, extracellular matrix, protein-lipid complex, external side of plasma membrane, side of membrane, respiratory chain, collagen-containing extracellular matrix, respiratory chain complex, and high-density lipoprotein particle. In the molecular functional process, the most significant 10 items were: iron ion binding, heme binding, tetrapyrrole binding, monooxygenase activity, cofactor binding, glutathione transferase activity, arachidonic acid monooxygenase activity, oxidoreductase activity, peptidase regulator activity, and arachidonic acid epoxygenase activity. The biological effects of DTE are mainly concentrated on anti-inflammation, anti-oxidation, anti-bacteria, and fatty acid metabolism. In terms of cell composition, DTE mainly affects its lipoprotein and respiratory chain. In terms of molecular functional process, DTE mainly affects the activity of redox-related enzymes, iron ion binding and glutathione transferase, etc. Thus, DTE showed a regulatory effect on lipid metabolism, inflammation, and redox as compared with the control group.

Compare to the MET group, the GO functional classification and enrichment analysis of differentially expressed genes in the control group are shown in Figure 5B. A total of 5,168 items were screened out, and a total of 248 items with significant statistical significance were screened out, including 191 items on biological process, 24 items on cellular component and 33 items on molecular functional process. In biological process, the most 10 significant items are: acute infectious response, humoral immune response, defense response to bacterium, acute-phase response, protein activation cascade, response to interferon-gamma, defense response to other organism, positive

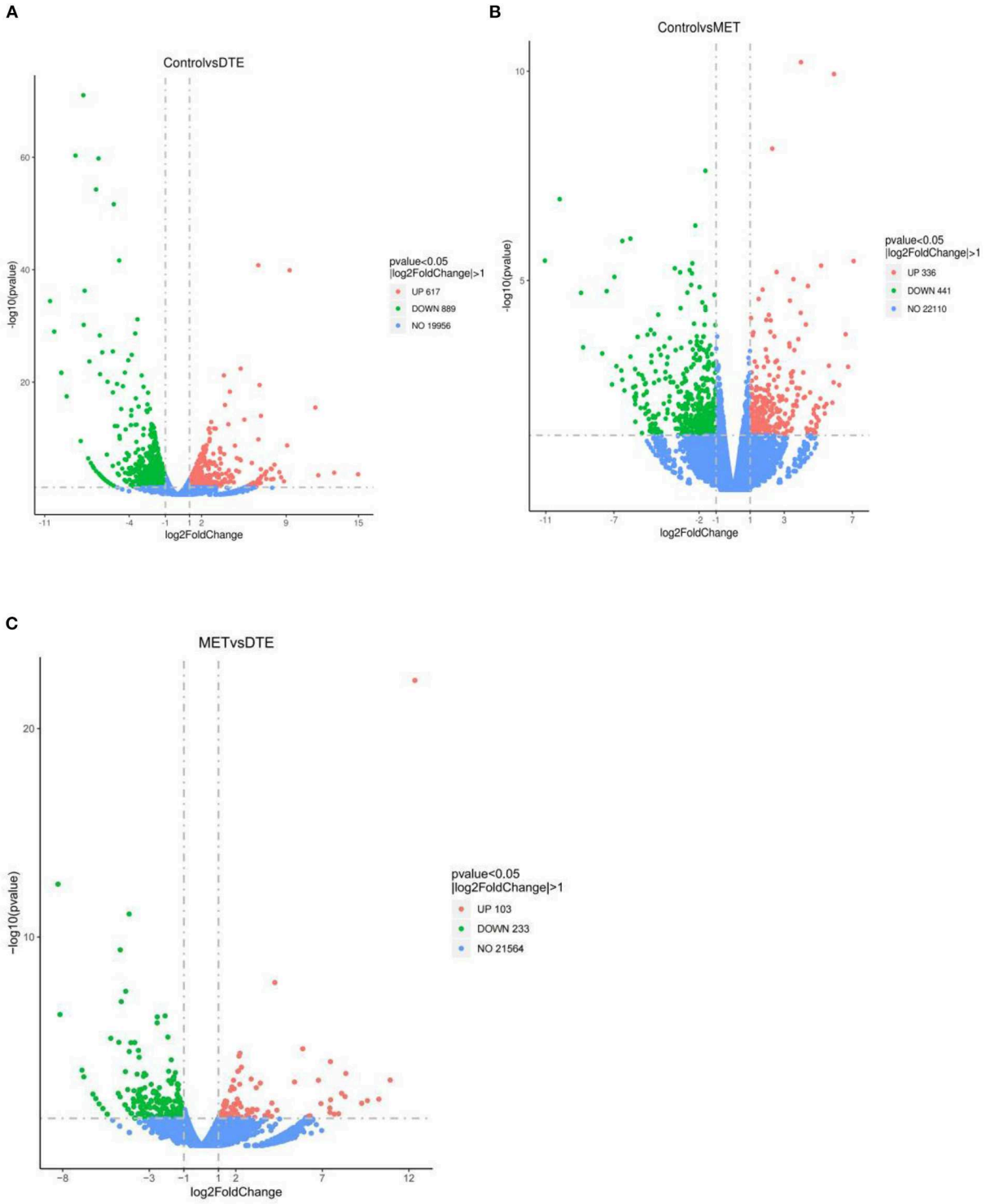

FIGURE 4
Volcanic map of difference gene expression between groups. **(A)** Control vs. DTE; **(B)** Control vs. MET; **(C)** MET vs. DTE.

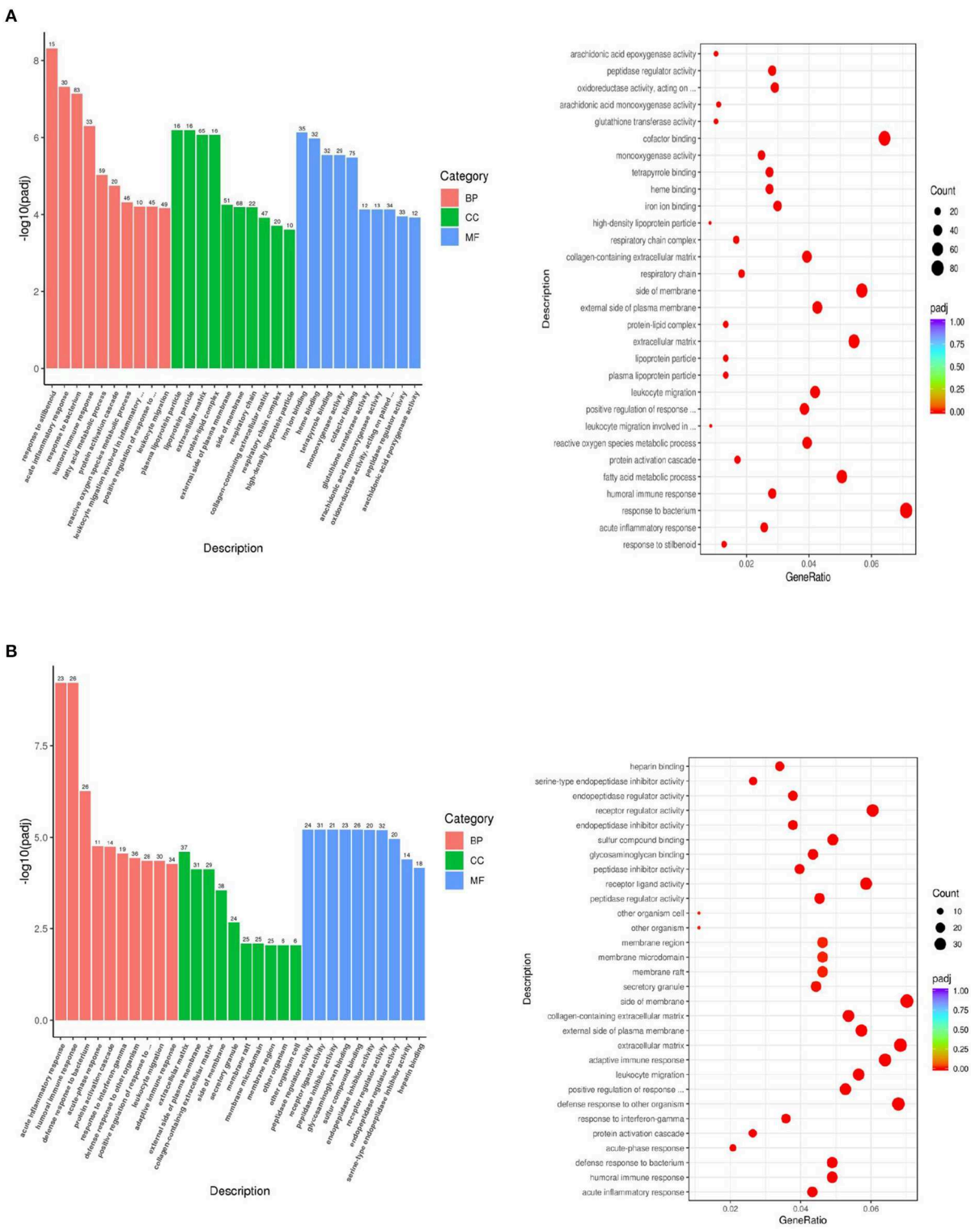

FIGURE 5
GO function analysis of difference gene expression. **(A)** Control vs. DTE; **(B)** Control vs. MET.

regulation of response to external stimulus, leukocyte migration, and adaptive immune response. In cellular component, the most 10 significant items are: extracellular matrix, externally side of plasma membrane, collagen-containing extracellular matrix, side of membrane, secretory grand, membrane raft, membrane microdomain, membrane region, other organism cell, and other organism cell. In items of molecular function, the most 10 significant entries were: peptidase regulator activity, receptor ligand activity, peptidase inhibitor activity, glycosaminoglycan binding, sulfur compound binding, endopeptidase inhibitor activity, receptor regulator activity, endopeptidase regulator activity, serine-type endopeptidase inhibitor activity, and heparin binding.

KEGG pathway analysis

As shown in Figure 6A, the KEGG biological pathways significantly enriched in the DTE group were as follows: Retinol metabolism, Chemical carcinogenesis, Arachidonic acid metabolism, PPAR signaling pathway, Drug metabolism enzymes, Staphylococcus aureus infection, Drug metabolism-cytochrome P450, Complement and coagulation cascades, Amoebiasis, atherosclerosis, Glutathione metabolism, and Oxidative phosphorylation. As shown in Figure 6B, the KEGG biological pathways significantly enriched in the MET group were as follows: Complement and coagulation cascades, *Staphylococcus aureus* infection, Cytokine-cytokine receptor interaction, Hematopoietic cell lineage, Systemic lupus erythematosus, Cell adhesion molecule, Amoebiasis, IL-17 signaling pathway, Chemokine signaling pathway, Glutathione metabolism, Primary immunodeficiency, Arachidonic acid metabolism.

In the comparison between DTE group and MET group, we found that two common signal pathways: Arachidonic acid metabolism pathway and Glutathione metabolism were significantly enriched. As shown in Figure 7A, in the arachidonic acid metabolism signaling pathway, the cytochrome P450 (CYPs) such as *CYP2*, *CYP4A*, and *CYP4A11* are significantly upregulated. As shown in Figure 7B, in the glutathione metabolic pathway, *Cyp4f18*, *Cyp2b13*, *Ltc4s*, *Pla2g4f*, *Alox15*, and *Cyp2c40* genes were significantly upregulated. In the comparison between the DTE group and the control group, we found that the PPAR signaling pathway also exhibited significant enrichment. As shown in Figure 7C, in the PPAR signaling pathway, the *Cyp4a12a*, *Cyp4a1*, *Acaa1b*, *Cyp4a10*, *Pltp*, *Plin4*, *Scd1*, *Cyp4a1*, *Apoa2*, *Pparg*, *Lpl*, *Cyp8b1*, *Fabp2*, *Adipoq*, *Cyp7a1*, *Me1*, *Cyp4a32*, *Ubc/Acsl1* genes were up-regulated, and the *Ehhadh*, *Fabp1*, *FABP3*, *FABP4* and *Aqp7* genes were down-regulated, all of which were closely related to glycolipid metabolism.

qRT-PCR analysis

To verify the effect of DTE on PPAR signaling pathway, qRT-PCR technology was used to analyze the genes related to glucolipid metabolism of *Cyp4a1*, *Cyp4a32*, *Me1*, *Fabp1*, *Ehhadh,* and *Aqp7* in PPAR signaling pathway. The results of qRT-PCR were shown in Figure 8. Compared with the control group, the expressions of *Cyp4a1*, *Cyp4a32*, and *Me1* genes involved in glycolipid metabolism were significantly up-regulated in DTE group, and the expressions of *Fabp1*, *Ehhadh,* and *Aqp7* were significantly decreased ($p < 0.05$), suggesting that the extract of DTE could significantly activate key genes of PPAR signaling pathway, and the transcriptome sequencing result was credible.

Effects of DTE on composition of gut microbiota

As shown in Table 3, compare to the normal group, the community diversity, total number of species and abundance in the control, MET and DTE groups were decreased. Compare to the control group, the community diversity, total number of species and abundance in the MET group were decreased, while the community diversity in the DTE group was decreased, but the total number of species and abundance were increased without significant difference ($p > 0.05$). Compare to the MET group, the community diversity of the DTE group was decreased, and the total number and abundance of species were increased, but there was no significant difference ($p > 0.05$).

To study how the intestinal microflora of mice changed, we compared different groups of OTUs (Figure 9). There are 131 differences in normal group, 70 differences in control group, 45 differences in MET group and 72 differences in DTE group, which indicates that the abundance of intestinal microorganisms in each group is different. In addition, there are 252 identical OTUs in the four comparison groups, and the OTUs in the control group are more abundant than those in other groups.

At the phylum level, as shown in Figure 9B, the relative abundance of *Bacteroidetes* and *Firmicutes* is higher in MET group and DTE group. Among the four groups, the relatively abundant ones are: *Bacteroidetes, Firmicutes*, *Verrucomicrobia*, *Desulfobacterota*, *Proteobacteria*, *Actinobacteriota*, *Campilobacterota*, *Cyanobacteria*, and *Deferribacter*. In normal group, control group, MET group and DTE group, the ratio of F/B was 0.89, 1.05, 0.94, 0.48, and 0.29, respectively. Compare to the normal group, the relative abundance of *Proteobacteria* in control group increased. In addition, compared with control group, DTE group significantly increased the relative abundance of *Verrucomicrobia*.

At the genus level, as shown in Figure 9C, the relative abundance of beneficial bacteria such as *Bacteroide*,

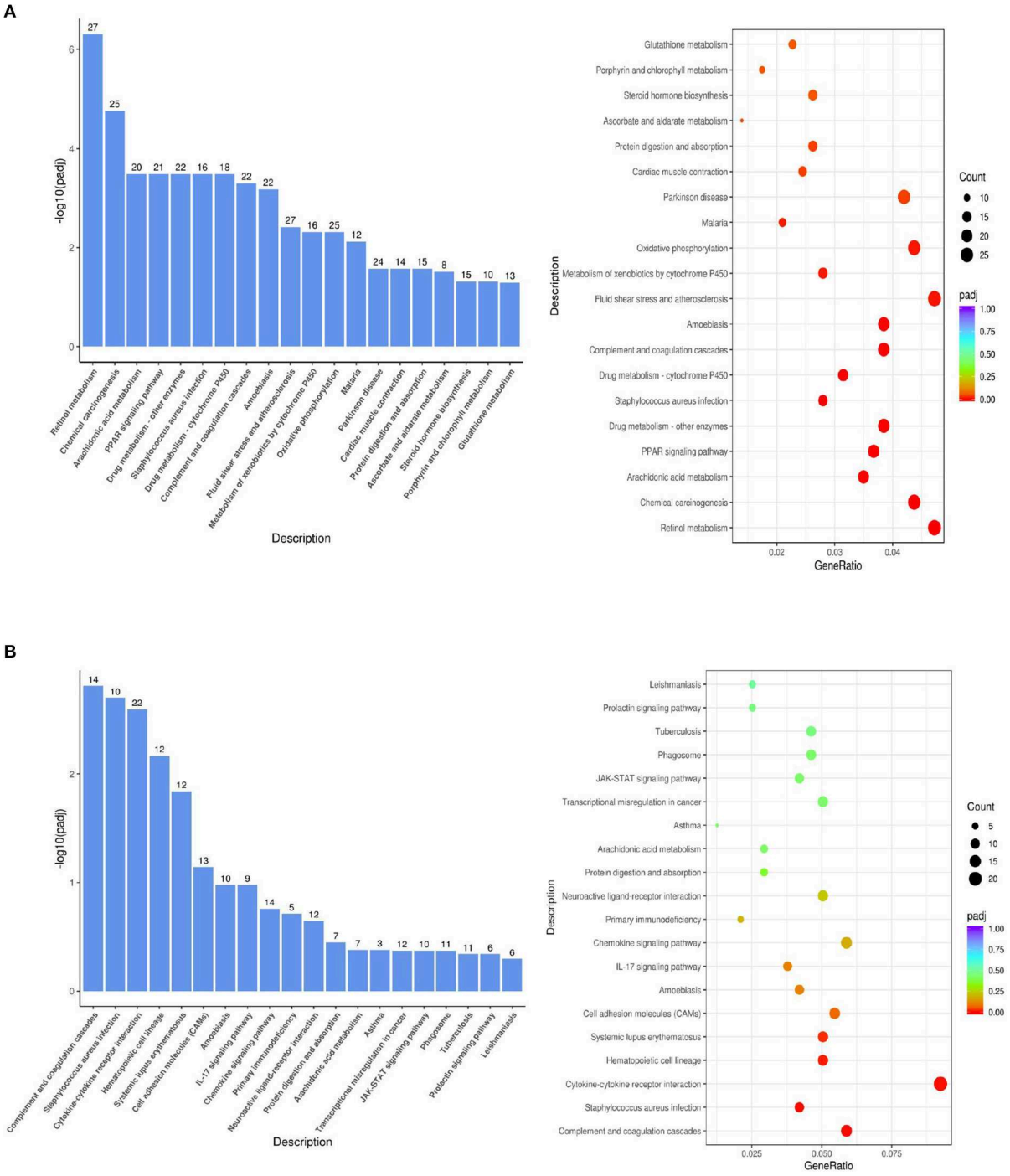

FIGURE 6
KEGG pathway analysis of the difference gene expression. **(A)** DTE vs. Control; **(B)** MET vs. Control.

Akkermansia, and *Alloprevotella* was decreased in the control group. The MET group significantly increased the relative abundance of *Lachnospiraceae NK4A136*, *Alloprevotella,* and *Escherichia shigella*. The DTE group significantly increased the relative abundance of *Akkermansia*, *Prevotella*, *Bacteroides*, and *Alloprevotella*.

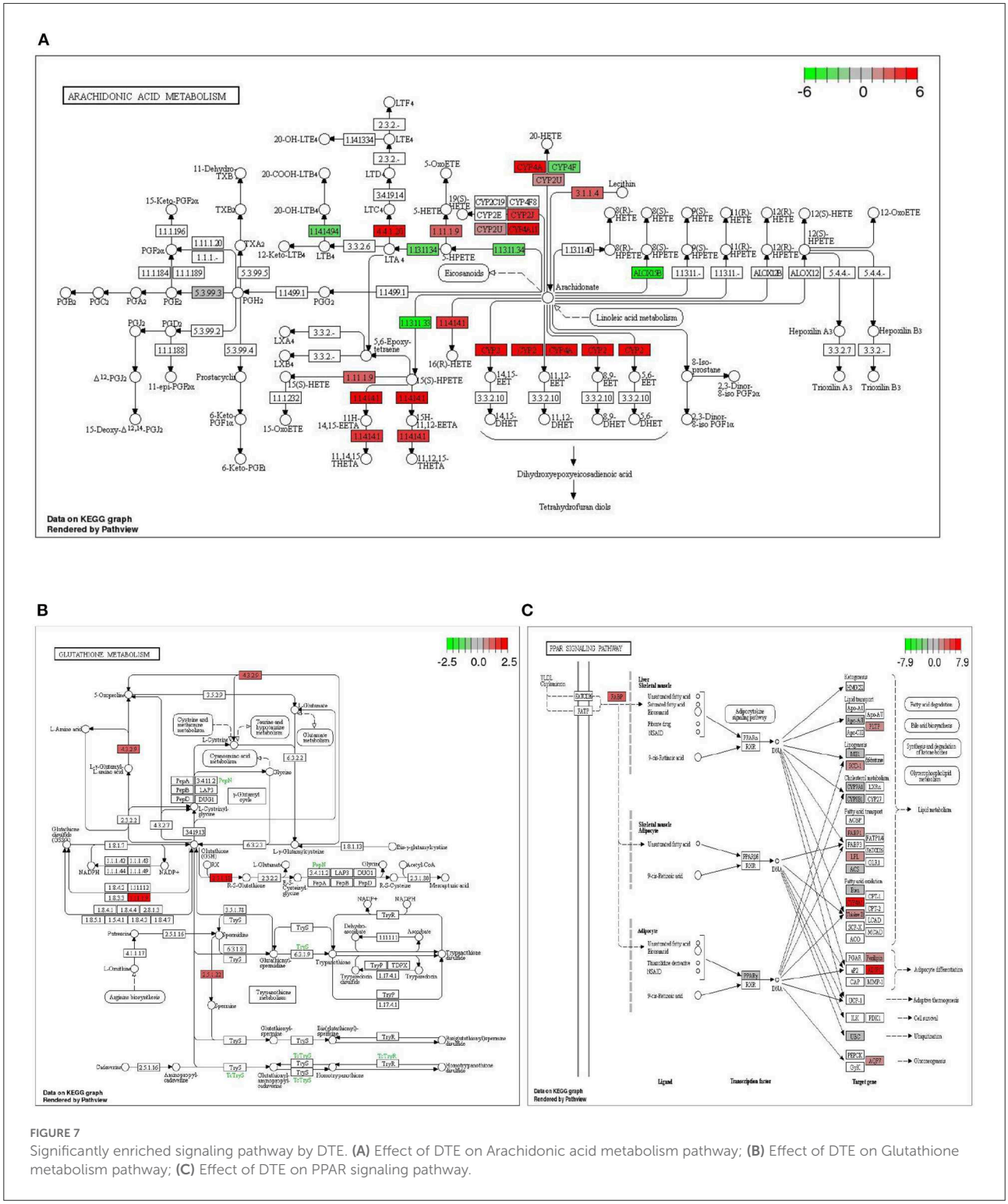

FIGURE 7
Significantly enriched signaling pathway by DTE. **(A)** Effect of DTE on Arachidonic acid metabolism pathway; **(B)** Effect of DTE on Glutathione metabolism pathway; **(C)** Effect of DTE on PPAR signaling pathway.

Discussion

With the changes in diet structure, lifestyle and the increasingly serious aging trend, the incidence of metabolic syndrome, with glycolipid metabolic disorders as the core, is showing a rapidly rising trend worldwide (20). How to efficiently restore mitochondrial function, regulate oxidative stress and inflammatory signaling pathways is the goal of improving

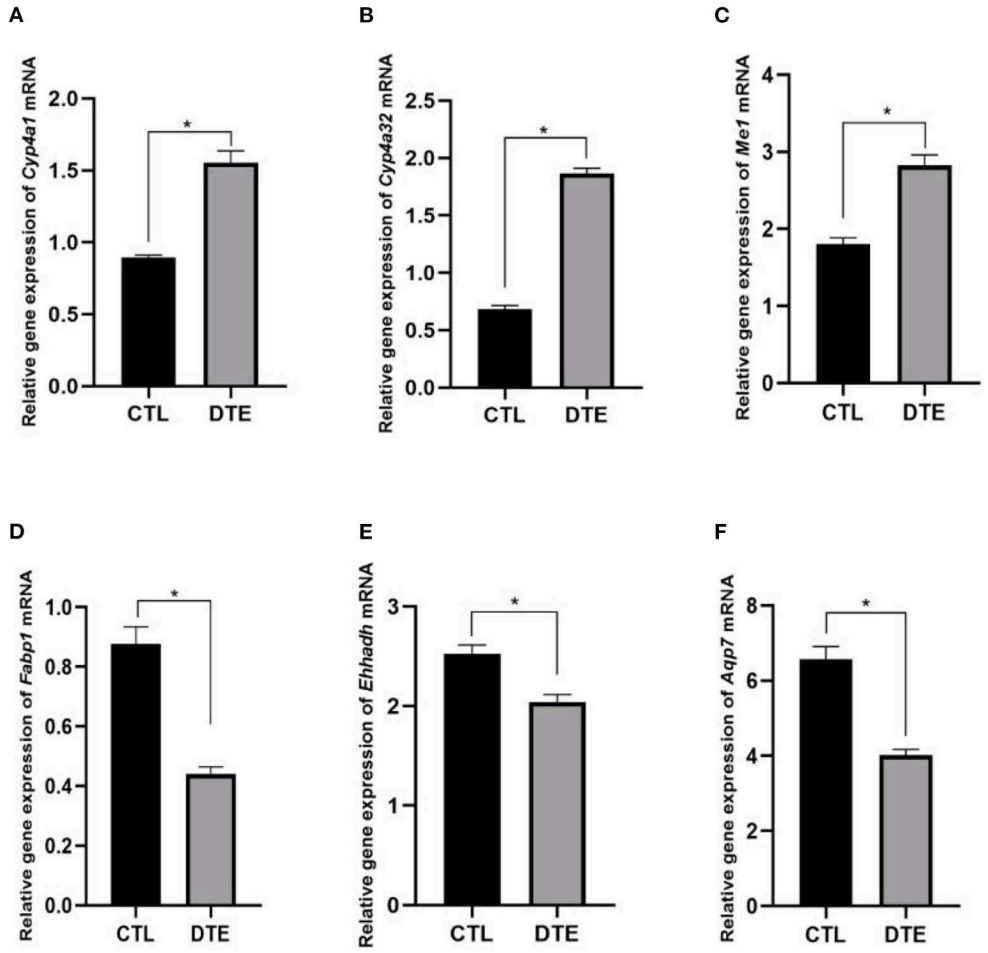

FIGURE 8
Effects of DTE on expression of PPAR signaling pathway related genes by qRT-PCR. **(A)** *Cyp4a*; **(B)** *Cyp4a32*; **(C)** *Me1*; **(D)** *Fabp1*; **(E)** *Ehhadh*; **(F)** *Aqp7*; DTE vs. Control, *$p < 0.05$; **$p < 0.01$.

TABLE 3 Effect of DTE on intestinal microbial diversity db/db diabetic mice.

Sample name	Observed_ species	Shannon	Chao 1	ACE
Normal	473.67 ± 25.15	5.89 ± 0.36	536.15 ± 47.53	535.36 ± 41.24
Control	415 ± 62.04	5.45 ± 0.25	461.54 ± 71.88	470.8 ± 70.52
MET	304.67 ± 13.64	4.56 ± 0.63	348.44 ± 28.88	358.89 ± 33
DTE	451 ± 25.83	4.420 ± 0.29	493.873 ± 36.47	503.556 ± 40.52

Compare to the normal group, the community diversity, total number of species and abundance in the control, MET and DTE groups were decreased.

disorders of glucolipidic metabolism (21). The natural food active ingredient has remarkable effect on regulate glycolipid metabolism disorder. Cellular, animal, and clinical studies have shown that dark tea has a variety of physiological functions and health benefits, including anti-oxidant (22), anti-inflammatory (23), anti-cancer (24), anti-diabetes (25), prevent cardiovascular disease (26), and regulation of intestinal microbiota (27). However, effects of DTE on glucolipid metabolism by multi-omic strategy have been rarely studied. Thus, in this study, 16S rDNA and metabonomic approach were applied to comprehensively investigate the effects of DTE on glucolipid metabolism. Serum parameters indicated that DTE could regulate blood glucose and lipid levels. 16S rDNA sequencing and metabolomics showed significant effects on the composition of the intestinal microbiota and liver metabolites.

Our study showed that DTE may ameliorate metabolic disorders in db/db diabetic mice by significantly lowering blood glucose, serum insulin level, TC, TG, LDL, and lightly improve the islet damage. Dark tea has been reported to play an important role in reducing blood lipid and blood glucose. Fuzhuan brick tea water extracts could significantly suppress

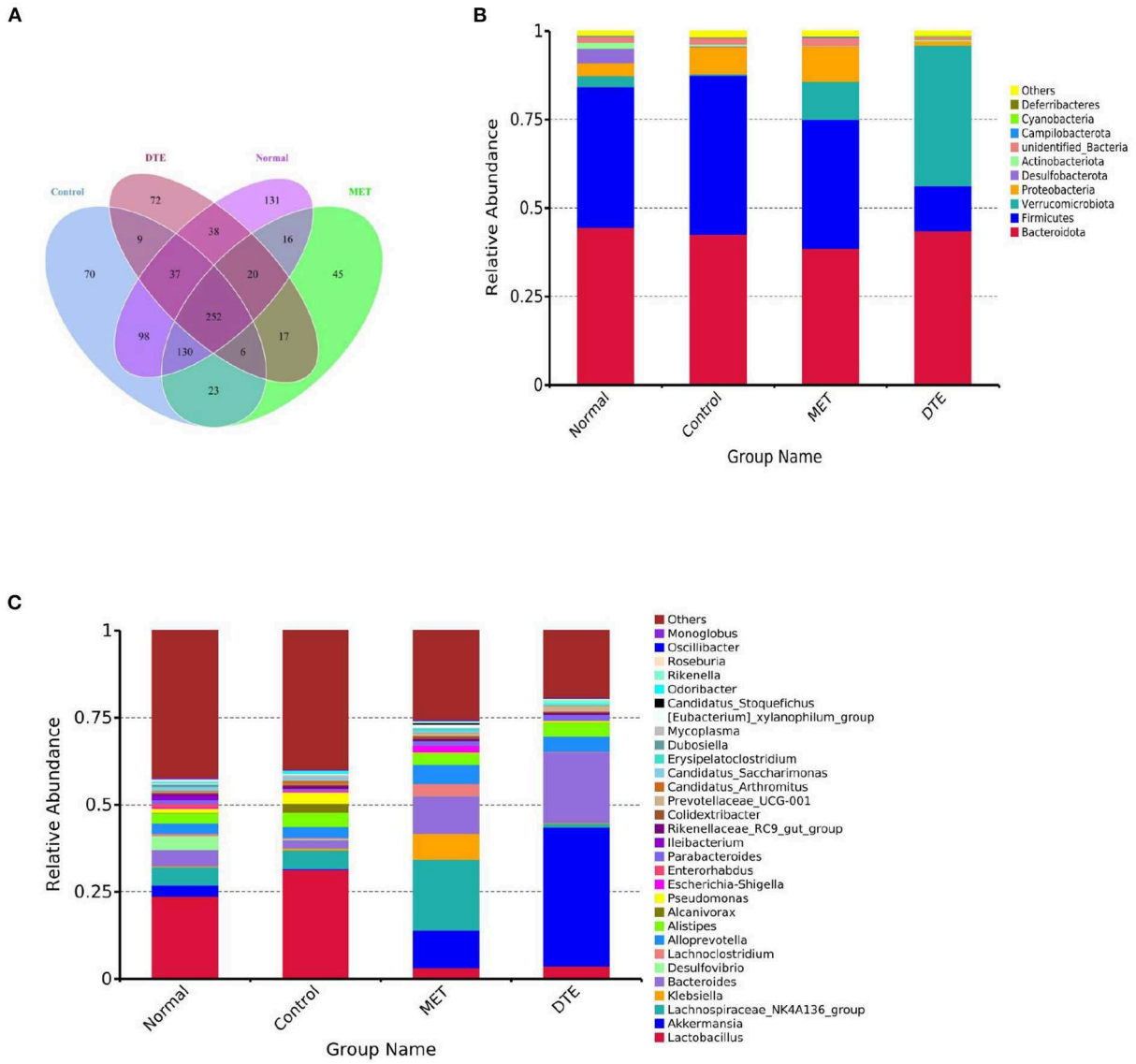

FIGURE 9
Effect of DTE on intestinal microbial community of diabetic mice. **(A)** Venn diagram based on OTU; **(B)** Effect of DTE on intestinal microbial community of diabetic mice at phylum species level; **(C)** Effect of DTE on intestinal microbial community of diabetic mice at genus level.

the increase of body weight and accumulation of adipose tissue, and reduced the level of serum triacylglycerol, total cholesterol and low-density lipoprotein (LDL) cholesterol in obese rats fed a high-fat diet (28). Qing Brick Tea exerted remarkable functions on decreasing the level of serum triglyceride and preventing hepatic fat accumulation (29). Pu'er Tea was found to have anti-hyperglycemic effects *via* inhibition on alpha-amylase and alpha-glucosidase (30). The above studies are consistent with our experimental results that DTE can regulate blood glucose and blood lipid.

RNA-Seq technique was used to preliminarily analyze the gene expression of mouse liver, and the potential differential metabolites and related metabolic pathways were analyzed from the perspective of metabonomics, which could reveal the effect of DTE on metabolic reaction of life system from the overall and dynamic perspective. Through GO functional classification and enrichment analysis, we found that DTE effects on biological processes mainly focused on anti-inflammatory, antioxidant, antibacterial and fatty acid metabolism. In terms of cell components, DTE mainly affects lipoprotein and respiratory chain. In terms of molecular functional process, DTE mainly affects its redox-related enzyme activity, iron binding and glutathione transferase. MET has been recognized as an effective drug to regulate glycolipid metabolism and

reduce blood glucose (31). Compared with MET group, DTE group has some similarities in BP, CC, and MF. We speculate that DTE may have potential biological functions such as regulating glucose and lipid metabolism and improving inflammatory response.

By analyzing the enrichment results of KEGG pathway, we found that three typical signal pathways: Arachidonic acid metabolism pathway, Glutathione metabolism and PPAR pathway were significantly enriched. Arachidonic acid plays an important role in blood, liver, muscle and other organ systems as phospholipid-bound structural lipid. Cytochrome P450 (CYP) is a kind of protein with iron porphyrin as the auxiliary group, also known as monooxygenase, which mainly exists in the endoplasmic reticulum of liver cells. This enzyme can promote the metabolism of drugs, so it is also known as liver drug enzyme. Arachidonic acid is a bioactive substance of many circulating eicosanoic acid derivatives, such as prostaglandin E2 (PGE2), prostacyclin (PGI2), thromboxane A2 (TXA2), leukotrienes and C4 (LTC4), which plays an important role in regulating lipid protein metabolism, vascular elasticity, leukocyte function and platelet activation (32). In the signal pathway of arachidonic acid metabolism, CYP such as *CYP2*, *CYP4A*, *CYP4A11* are significantly up-regulated. It was found that the extract of Chenopodium album can reduce the activity of cytochrome P4502E1 (*CYP2E1*), enhance the activity of catalase and improve the histological structure of rat liver to reduce the oxidative stress (33). We speculate that DTE may intervene the abnormal metabolism of glucose and lipid in the liver of diabetic mice through arachidonic acid metabolism.

Glutathione (GSH) is the most abundant antioxidant and a major detoxification agent in cells. It is synthesized through two-enzyme reaction catalyzed by glutamate cysteine ligase and glutathione synthetase, and its level is well regulated in response to redox change. Accumulating evidence suggests that GSH may play important roles in cell signaling (34). As shown in the effect of DTE on the glutathione metabolic pathway, *Cyp4f18*, *Cyp2b13*, *Ltc4s*, *Pla2g4f*, *Alox15*, and *Cyp2c40* genes were significantly up-regulated. We speculated that DTE might intervene in glucolipid metabolism by regulating oxidative stress through the glutathione metabolic pathway.

PPAR is a core factor in the anti-inflammatory response pathway and participates in the formation of inflammatory and metabolic signal regulatory networks by different pathways, thus significantly affecting the regulation of glucolipid metabolism. PPARγ also can reduce the expression of NF-κB-mediated inflammatory mediators and exert its anti-inflammatory effect (35). PPARγ regulate the expression of many fat and inflammatory factors such as TNFα and regulate the glucolipid metabolism process (36). In the PPAR signaling pathway, *Cyp4a12a*, *Cyp4a1*, *Acaa1b*, *Cyp4a10*, *Pltp*, *Plin4*, *Scd1*, *Cyp4a1*, *Apoa2*, *Pparg*, *Lpl*, *Cyp8b1*, *Fabp2*, *Adipoq*, *Cyp7a1*, *Me1*, *Cyp4a32*, and *Ubc/Acsl1* genes were up-regulated, and *Ehhadh*, *Fabp1*, *FABP3*, *FABP4*, and *Aqp7* genes were down-regulated, all of which were closely related to glycolipid metabolism. The increased expression of *FABP1* is mainly related to the occurrence of insulin resistance and the promotion of fatty acid transport (37). *AQP7* also showed a significant correlation with glucolipid metabolism indicators (38). Since DTE may significantly up-regulate the genes expression of PPAR signaling pathway, we speculate that DTE may have the potential to regulate inflammatory factors, glycolipid metabolism, and promote fatty acid transport.

Intestinal microflora plays an important role in host health, the change of intestinal microflora may induce intestinal oxidative stress, and lead to glycolipid metabolism disorder (39). The ratio of *Firmicutes/Bacteroidetes* is widely believed to be important for maintaining the homeostasis of the intestinal environment. Reduction of the F/B value leads to T2D (40). After treatment with DTE, the value of F/B was decreased, indicating DTE positively regulated the gut microbiota. *Bacteroidetes*, *Firmicutes*, *Proteobacteria* and *Verrucomicrobia* can regulate glycolipid metabolism and improve insulin resistance (40). After treatment with DTE, the relative abundance of *Proteobacteria* was decreased, and the relative abundance of *Verrucomicrobia* was increased. These results indicated that DTE could regulate the structural composition of the intestinal flora to improve the intestinal environment and reduce the risks of diabetes and obesity.

At the genus level, treatment with DTE significantly increased the relative abundance of *Akkermansia*, *Prevotellaceae*, *Bacteroides,* and *Alloprevotella*. *Akkermansia* can regulate immune response, lipid metabolism, inhibit inflammation, and improve the disorder of intestinal flora. The decrease in abundance is closely related to the development of inflammatory intestinal diseases, T2D and cardiovascular diseases (41). As shown in Figure 9C, the proportion of *Akkermansia* in control group is 0.34%, and that in DTE group is 35.76%. The results showed that DTE could significantly increase the relative abundance of *Akkermansia*, improve the intestinal microenvironment, and then regulate the abnormal of glucose and lipid metabolism.

Conclusion

In the present study, multi-omics precision nutrition method was applied to carry out multi-dimensional health big data detection and analysis at the animal level from the aspects of the microbiome and RNA sequencing. We found that DTE could significantly reduce the blood glucose in db/db diabetic mice, improve the blood lipid to a certain extent, slightly repair the pancreatic injury, and promote the insulin secretion. According to GO analysis, DTE mainly affected the inflammation, fatty acid metabolism, and redox-related enzyme activities. 16S rDNA sequencing showed that DTE significantly reduced the ratio

of F/B and increased the relative abundances of *Akkermansia*, *Prevotellaceae*, *Bacteroides*, and *Alloprevotella*. Besides, real-time qPCR was performed to verify the regulatory effect of DTE on PPAR signaling pathway, which provides us with direct and comprehensive molecular evidence for the beneficial effect of DTE on metabolic disorders.

Data availability statement

The data presented in the study are deposited in the GSA repository: https://ngdc.cncb.ac.cn/gsub/, accession number CRA007923.

Ethics statement

The animal study was reviewed and approved by Hunan Drug Safety Evaluation Research Center.

Author contributions

CL and MH wrote the original draft. CL, MH, and CW performed the experiments and collected the samples. CL, YY, and XW contributed to methodology and data analysis. MS and CZ participated in supervision. CL, MS, and CZ contributed to project administration and conceptualization, writing, reviewing, and editing. All authors listed have made a substantial, direct, and intellectual contribution to the work and approved it for publication.

Funding

This work was partially supported by the National Key Research and Development Program of China (2019YFC1604903) and the Hunan Province Innovative Postdoctoral Project (2021RC2080).

Conflict of interest

The authors declare that the research was conducted in the absence of any commercial or financial relationships that could be construed as a potential conflict of interest.

Publisher's note

All claims expressed in this article are solely those of the authors and do not necessarily represent those of their affiliated organizations, or those of the publisher, the editors and the reviewers. Any product that may be evaluated in this article, or claim that may be made by its manufacturer, is not guaranteed or endorsed by the publisher.

References

1. Guo J. Research progress on prevention and treatment of glucolipid metabolic disease with integrated traditional Chinese and western medicine. *Chin J Integr Med.* (2017) 23:403–9. doi: 10.1007/s11655-017-2811-3

2. You M, Matsumoto M, Pacold CM, Cho WK, Crabb DW. The role of Amp-activated protein kinase in the action of ethanol in the liver. *Gastroenterology.* (2004) 127:1798–808. doi: 10.1053/j.gastro.2004.09.049

3. Hou L, Jiang F, Huang B, Zheng W, Jiang Y, Cai G, et al. Dihydromyricetin ameliorates inflammation-induced insulin resistance *via* phospholipase C-Camkk-Ampk signal pathway. *Oxid Med Cell Longev.* (2021) 2021:8542809. doi: 10.1155/2021/8542809

4. Barazzoni R, Gortan Cappellari G, Ragni M, Nisoli E. Insulin resistance in obesity: an overview of fundamental alterations. *Eat Weight Disord.* (2018) 23:149–57. doi: 10.1007/s40519-018-0481-6

5. Zhao Y, Li Z, Lu E, Sheng Q, Zhao Y. Berberine exerts neuroprotective activities against cerebral ischemia/reperfusion injury through up-regulating ppar-Γ to suppress Nf-Kb-mediated pyroptosis. *Brain Res Bull.* (2021) 177:22–30. doi: 10.1016/j.brainresbull.2021.09.005

6. Le Chatelier E, Nielsen T, Qin J, Prifti E, Hildebrand F, Falony G, et al. Richness of human gut microbiome correlates with metabolic markers. *Nature.* (2013) 500:541–6. doi: 10.1038/nature12506

7. Qin J, Li Y, Cai Z, Li S, Zhu J, Zhang F, et al. A metagenome-wide association study of gut microbiota in type 2 diabetes. *Nature.* (2012) 490:55–60. doi: 10.1038/nature11450

8. Zhu M-z, Li N, Zhou F, Ouyang J, Lu D-m, Xu W, et al. Microbial bioconversion of the chemical components in dark tea. *Food Chemistry.* (2020) 312:126043. doi: 10.1016/j.foodchem.2019.126043

9. Zhu J, Yu C, Zhou H, Wei X, Wang Y. Comparative evaluation for phytochemical composition and regulation of blood glucose, hepatic oxidative stress and insulin resistance in mice and Hepg2 models of four typical Chinese dark teas. *J Sci Food Agric.* (2021) 101:6563–77. doi: 10.1002/jsfa.11328

10. Wu Y, Sun H, Yi R, Tan F, Zhao X. Anti-obesity effect of liupao tea extract by modulating lipid metabolism and oxidative stress in high-fat-diet-induced obese mice. *J Food Sci.* (2021) 86:215–27. doi: 10.1111/1750-3841.15551

11. Wang PC, Zhao S, Yang BY, Wang QH, Kuang HX. Anti-diabetic polysaccharides from natural sources: a review. *Carbohydr Polym.* (2016) 148:86–97. doi: 10.1016/j.carbpol.2016.02.060

12. Liu S, Yu Z, Zhu H, Zhang W, Chen Y. *In vitro* alpha-glucosidase inhibitory activity of isolated fractions from water extract of qingzhuan dark tea. *BMC Complement Altern Med.* (2016) 16:378. doi: 10.1186/s12906-016-1361-0

13. Wang Y, Zhang M, Zhang Z, Lu H, Gao X, Yue P. High-theabrownins instant dark tea product by aspergillus niger via submerged fermentation: A-glucosidase and pancreatic lipase inhibition and antioxidant activity. *J Sci Food Agric.* (2017) 97:5100–6. doi: 10.1002/jsfa.8387

14. Du H, Wang Q, Yang X. Fu Brick tea alleviates chronic kidney disease of rats with high fat diet consumption through attenuating insulin resistance in skeletal muscle. *J Agric Food Chem.* (2019) 67:2839–47. doi: 10.1021/acs.jafc.8b06927

15. Cai X, Hayashi S, Fang C, Hao S, Wang X, Nishiguchi S, et al. Pu'erh tea extract-mediated protection against hepatosteatosis and insulin resistance in mice with diet-induced obesity is associated with the induction of *de novo* lipogenesis in visceral adipose tissue. *J Gastroenterol.* (2017) 52:1240–51. doi: 10.1007/s00535-017-1332-3

16. Chen G, Xie M, Wan P, Chen D, Dai Z, Ye H, et al. Fuzhuan brick tea polysaccharides attenuate metabolic syndrome in high-fat diet induced mice in association with modulation in the gut microbiota. *J Agric Food Chem.* (2018) 66:2783–95. doi: 10.1021/acs.jafc.8b00296

17. Jensen GS, Beaman JL, He Y, Guo Z, Sun H. Reduction of body fat and improved lipid profile associated with daily consumption of a puer tea extract in a hyperlipidemic population: a randomized placebo-controlled trial. *Clin Interv Aging.* (2016) 11:367–76. doi: 10.2147/CIA.S94881

18. Cai X, Fang C, Hayashi S, Hao S, Zhao M, Tsutsui H, et al. Pu-Erh tea extract ameliorates high-fat diet-induced nonalcoholic steatohepatitis and insulin resistance by modulating hepatic Il-6/Stat3 signaling in mice. *J Gastroenterol.* (2016) 51:819–29. doi: 10.1007/s00535-015-1154-0

19. Liu D, Huang J, Luo Y, Wen B, Wu W, Zeng H, et al. Fuzhuan brick tea attenuates high-fat diet-induced obesity and associated metabolic disorders by shaping gut microbiota. *J Agric Food Chem.* (2019) 67:13589–604. doi: 10.1021/acs.jafc.9b05833

20. Zhou Y-J, Xu N, Zhang X-C, Zhu Y-Y, Liu S-W, Chang Y-N. Chrysin improves glucose and lipid metabolism disorders by regulating the Ampk/Pi3k/Akt signaling pathway in insulin-resistant Hepg2 cells and Hfd/Stz-induced C57bl/6j mice. *J Agric Food Chem.* (2021) 69:5618–27. doi: 10.1021/acs.jafc.1c01109

21. Arnold SE, Arvanitakis Z, Macauley-Rambach SL, Koenig AM, Wang H-Y, Ahima RS, et al. Brain insulin resistance in type 2 diabetes and alzheimer disease: concepts and conundrums. *Nature Reviews Neurology.* (2018) 14:168–81. doi: 10.1038/nrneurol.2017.185

22. Zhao P, Alam MB, Lee S-H. Protection of Uvb-induced photoaging by fuzhuan-brick tea aqueous extract *via* Mapks/Nrf2-mediated down-regulation of Mmp-1. *Nutrients.* (2019) 11:60. doi: 10.3390/nu11010060

23. Zhang X, Wu Q, Zhao Y, Aimy A, Yang X. Consumption of post-fermented Jing-Wei Fuzhuan brick tea alleviates liver dysfunction and intestinal microbiota dysbiosis in high fructose diet-fed mice. *RSC Adv.* (2019) 9:17501–13. doi: 10.1039/C9RA02473E

24. Zheng K, Zhao Q, Chen Q, Xiao W, Jiang Y, Jiang Y. The synergic inhibitory effects of dark tea (*Camellia sinensis*) extract and p38 inhibition on the growth of pancreatic cancer cells. *J Cancer.* (2019) 10:6557–69. doi: 10.7150/jca.34637

25. Gao W, Xiao C, Hu J, Chen B, Wang C, Cui B, et al. Qing Brick Tea (Qbt) aqueous extract protects monosodium glutamate-induced obese mice against metabolic syndrome and involves up-regulation transcription factor nuclear factor-erythroid 2-related factor 2 (Nrf2) antioxidant pathway. *Biomed Pharmacother.* (2018) 103:637–44. doi: 10.1016/j.biopha.2018.04.043

26. Liu Y, Luo L, Luo Y, Zhang J, Wang X, Sun K, et al. Prebiotic properties of green and dark tea contribute to protective effects in chemical-induced colitis in mice: a fecal microbiota transplantation study. *J Agric Food Chem.* (2020) 68:6368–80. doi: 10.1021/acs.jafc.0c02336

27. Chen G, Xie M, Wan P, Chen D, Ye H, Chen L, et al. Digestion under Saliva, simulated gastric and small intestinal conditions and fermentation *in vitro* by human intestinal microbiota of polysaccharides from Fuzhuan brick tea. *Food Chem.* (2018) 244:331–9. doi: 10.1016/j.foodchem.2017.10.074

28. Li Q, Liu Z, Huang J, Luo G, Liang Q, Wang D, et al. Anti-obesity and hypolipidemic effects of Fuzhuan brick tea water extract in high-fat diet-induced obese rats. *J Sci Food Agric.* (2013) 93:1310–6. doi: 10.1002/jsfa.5887

29. Mao QQ, Li BY, Meng JM, Gan RY, Xu XY, Gu YY, et al. Effects of several tea extracts on nonalcoholic fatty liver disease in mice fed with a high-fat diet. *Food Sci Nutr.* (2021) 9:2954–67. doi: 10.1002/fsn3.2255

30. Yang C-Y, Yen Y-Y, Hung K-C, Hsu S-W, Lan S-J, Lin H-C. Inhibitory effects of Pu-Erh tea on alpha glucosidase and alpha amylase: a systemic review. *Nutr Diabetes.* (2019) 9:23. doi: 10.1038/s41387-019-0092-y

31. Sanchez-Rangel E, Inzucchi SE. Metformin: clinical use in type 2 diabetes. *Diabetologia.* (2017) 60:1586–93. doi: 10.1007/s00125-017-4336-x

32. Wang B, Wu L, Chen J, Dong L, Chen C, Wen Z, et al. Metabolism pathways of arachidonic acids: mechanisms and potential therapeutic targets. *Signal Transduct Target Ther.* (2021) 6:94. doi: 10.1038/s41392-020-00443-w

33. Duh PD, Chen SY, Chu CC, Chyau CC, Fu ZH. Effect of Water Extract of Djulis (Chenopodium Formosaneum) and Its Bioactive Compounds on Alcohol-Induced Liver Damage in Rats. *International J of Food and Nutritional Sci.* (2018) 5:55–63. doi: 10.15436/2377-0619.18.1816

34. Zhang H, Forman HJ. Glutathione synthesis and its role in redox signaling. *Semin Cell Dev Biol.* (2012) 23:722–8. doi: 10.1016/j.semcdb.2012.03.017

35. Kong L, Chen J, Ji X, Qin Q, Yang H, Liu D, et al. Alcoholic fatty liver disease inhibited the co-expression of Fmo5 and Pparα to activate the Nf-Kb signaling pathway, thereby reducing liver injury *via* inducing gut microbiota disturbance. *J Exp Clin Cancer Res.* (2021) 40:18. doi: 10.1186/s13046-020-01782-w

36. Guilherme A, Virbasius JV, Puri V, Czech MP. Adipocyte dysfunctions linking obesity to insulin resistance and type 2 diabetes. *Nat Rev Mol Cell Biol.* (2008) 9:367–77. doi: 10.1038/nrm2391

37. Tsai IT, Wu C-C, Hung W-C, Lee T-L, Hsuan C-F, Wei C-T, et al. Fabp1 and Fabp2 as markers of diabetic nephropathy. *Int J Med Sci.* (2020) 17:2338–45. doi: 10.7150/ijms.49078

38. Shen FX, Gu X, Pan W, Li WP, Li W, Ye J, et al. Over-expression of Aqp7 contributes to improve insulin resistance in adipocytes. *Exp Cell Res.* (2012) 318:2377–84. doi: 10.1016/j.yexcr.2012.07.016

39. Cani PD, Amar J, Iglesias MA, Poggi M, Knauf C, Bastelica D, et al. Metabolic endotoxemia initiates obesity and insulin resistance. *Diabetes.* (2007) 56:1761–72. doi: 10.2337/db06-1491

40. Abenavoli L, Scarpellini E, Colica C, Boccuto L, Salehi B, Sharifi-Rad J, et al. Gut microbiota and obesity: a role for probiotics. *Nutrients.* (2019) 11:2690. doi: 10.3390/nu11112690

41. Xu Y, Wang N, Tan H-Y, Li S, Zhang C, Feng Y. Function of akkermansia muciniphila in obesity: interactions with lipid metabolism, immune response and gut systems. *Front Microbiol.* (2020) 11:219. doi: 10.3389/fmicb.2020.00219

frontiers | Frontiers in Nutrition

TYPE Original Research
PUBLISHED 09 September 2022
DOI 10.3389/fnut.2022.948573

OPEN ACCESS

EDITED BY
Yong Su,
Nanjing Agricultural University, China

REVIEWED BY
Hao Zhong,
Zhejiang University of Technology, China
Shunfen Zhang,
State Key Laboratory of Animal Nutrition, Institute of Animal Sciences (CAAS), China

*CORRESPONDENCE
Zehe Song
zehesong111@163.com

SPECIALTY SECTION
This article was submitted to Nutrition and Microbes, a section of the journal Frontiers in Nutrition

RECEIVED 20 May 2022
ACCEPTED 02 August 2022
PUBLISHED 09 September 2022

CITATION
Ma J, Chen S, Li Y, Wu X and Song Z (2022) Arbutin improves gut development and serum lipids *via Lactobacillus intestinalis*. *Front. Nutr.* 9:948573. doi: 10.3389/fnut.2022.948573

Arbutin improves gut development and serum lipids *via Lactobacillus intestinalis*

Jie Ma[1], Shuai Chen[2], Yuying Li[3], Xin Wu[1] and Zehe Song[1]*

[1]Animal Nutritional Genome and Germplasm Innovation Research Center, College of Animal Science and Technology, Hunan Agricultural University, Changsha, China, [2]Key Laboratory of Systems Health Science of Zhejiang Province, School of Life Sciences, Hangzhou Institute for Advanced Study, University of Chinese Academy of Sciences, Hangzhou, China, [3]Institute of Bast Fiber Crops, Chinese Academy of Agricultural Sciences, Changsha, China

Arbutin has been widely studied in whitening, anti-inflammatory, and antioxidant. However, the interaction between arbutin and intestinal microbes has been rarely studied. Thus, mice were treated with arbutin concentrations of 0, 0.1, 0.2, 0.4, and 1 mg/ml. We found that arbutin promoted gut development such as villus length, villus areas, and villus length/crypt depth (L/D). Total cholesterol (TC), high-density lipoprotein (HDL), and low-density lipoprotein (LDL) were significantly reduced by low concentrations of arbutin. Importantly, we analyzed the microbial composition in the control and 0.4 mg/ml arbutin group and found that the abundance of *Lactobacillus intestinalis* (*L. intestinalis*) was highest and enhanced in arbutin. Further, mice were fed with oral antibiotics and antibiotics + 0.4 mg/ml arbutin and then we transplanted fecal microbes from oral 0.4 mg/ml arbutin mice to mice pretreated with antibiotics. Our results showed that arbutin improves gut development, such as villus width, villus length, L/D, and villus areas. In addition, *L. intestinalis* monocolonization was carried out after a week of oral antibiotics and increased villus length, crypt depth, and villus areas. Finally, *in vitro* arbutin and *L. intestinalis* co-culture showed that arbutin promoted the growth and proliferation of *L. intestinalis*. Taken together, our results suggest that arbutin improves gut development and health of *L. intestinalis*. Future studies are needed to explore the function and mechanism of *L. intestinalis* affecting gut development.

KEYWORDS

arbutin, gut development, gut microbiota, fecal microflora transplantation, *Lactobacillus intestinalis*

Introduction

Arbutin is a natural phytochemical active substance, which is extracted from the bearberry leaves of *Ericaceae* and *Saxifragaceae* families (1, 2). It inhibits the activity of tyrosinase to reduce the production of melanin in the host (3), thereby lowering the deposition of melanin (4, 5). Meanwhile, arbutin is also associated with antioxidant

(6, 7) and anti-inflammatory (8, 9). Additionally, arbutin has been widely studied for its role in protecting against nerve injury or other diseases caused by nerve injury (10, 11). However, arbutin regulation of gut development and host metabolism through gut microbiota has rarely been reported. The intestinal villi were directly contacted with nutrients and absorbed small molecules into the blood (12, 13), whereas the crypt was genetically regulated to shrink and invaginate (14), which was not conducive to nutrient absorption. Goblet cells secrete mucins and mucopolysaccharides to form the mucous system and were the site of colonization by gut microbes (15). Arbutin was rarely absorbed by the small intestine, but the majority was used by gut microbiota. Numerous studies reported that the role of phytochemicals was weakened by low bioavailability (16). Arbutin is a β-glucoside derived from hydroquinone (HQ) (1,4-dihydroxybenzene) (2, 3), its bioactivity and bioavailability were altered by gut microbes secreting glycoside hydrolase (17), and gut microbes have been identified as closely related to host metabolic disorders and diseases (18, 19).

Whether arbutin regulates gut development and host metabolism by altering gut microbes is unclear. Thus, we speculated that the interaction between arbutin and intestinal microbiome influences the pathological status and development of the gastrointestinal tract. Our results indicated that arbutin directly affects the composition of gut microbiota and development; further, *Lactobacillus intestinalis* (*L. intestinalis*) may serve as the potential mechanism.

Materials and methods

Bacterial strains

The *L. intestinalis* (ATCC49335) used in this study was purchased by Beijing Beina Chuanglian Biotechnology Research Institute (Beijing, China). Unless otherwise stated, bacterial strains were grown in MRS Broth (MRSB) (Qingdao Hope Biotechnology Corporation Ltd.) or on MRS Agar (MRSA) plates at 37°C.

Animal studies

Fifty female C57BL/6 mice (aged 6 weeks, 17 ± 0.5 g and aged 4 weeks, 14 ± 0.5 g) were randomly divided into 5 groups with arbutin solution of 0, 0.1, 0.2, 0.4, and 1 mg/ml (20) and fed maintenance diet lasted 3 weeks. We found that arbutin 0.4 mg/ml was most effective in improving intestinal index; thus, twenty mice were treated with antibiotics and antibiotics + 0.4 mg/ml arbutin for 3 weeks. Then, we transplanted fecal microbes from oral 0.4 mg/ml arbutin mice to mice pretreated with antibiotics for 1 week and then normal feeding for 2 weeks. Finally, twenty mice were pretreated with antibiotics for a week, 1.3×10^9 colony-forming unit (CFU)/ml *L. intestinalis* was intragastric to mice for 1 week, and then normal feeding for 2 weeks. All the animals were purchased from Hunan SJA Laboratory Animal Corporation Ltd. (Changsha, China) and used in this study. All the experimental animals were allowed free access to food and drinking water, and subjected to 12-h light-dark cycles, controlled temperature (23 ± 2°C), and humidity (45–60%) during the experiment. The basic diet was described in our previous study (21).

Hematoxylin and eosin staining

Intestinal HE staining was performed. The jejunal and ileal segments were fixed in 4% paraformaldehyde solution. The sections were first treated with xylene and ethanol solution for 15 and 5 min, respectively, then stained with hematoxylin for 5 min, rinsed with water for 5 min, then stained with eosin solution for 1–3 min, and then washed with ethanol and sealed. Finally, the villi, and crypt morphology were observed under a microscope.

Serum biochemical parameters

Serum samples were separated after centrifugation at 1,500 × *g* for 10 min at 4°C and 100 μl serum was transferred into another tube. Serum biochemical parameters were determined using an Automatic Biochemistry Analyzer (Cobas c 311, Roche).

Antibiotic treatment and fecal microflora transplantation

To eradicate commensal bacteria, filter-sterilized drinking water was supplemented with ampicillin (0.5 mg/ml, Meilunbio), gentamicin (0.5 mg/ml, Meilunbio), metronidazole (0.5 mg/ml, Meilunbio), neomycin (0.5 mg/ml, Meilunbio), and vancomycin (0.25 mg/ml, Meilunbio) for 1 week. Antibiotics were purchased from Dalian Meilun Biotechnology Corporation Ltd. (Dalian, China). Before fecal microbiota transplantation, the native gut microbiota in one group of C57 female mice (n = 10 biologically independent animals per group) was deleted by administering drinking water containing a cocktail of antibiotics for 1 week. Fecal samples of ∼200 mg were then collected from arbutin (0.4 mg/ml)-fed mice and resuspended in 2.0 ml normal saline. Fecal samples were mixed and centrifuged at 1,000 × *g*, and the microbiota supernatants were transplanted into the microbiota-depleted mice by gavaging with 0.2 ml per mice for 1 week. After transplantation, two groups of mice were administrated with a standard diet and regular water.

Gut microbiota profiling

Total genome DNA from ileal chyme and mucosa was extracted using cetyltrimethylammonium bromide (CTAB) method. DNA concentration and purity were monitored on 1% agarose gels. According to the concentration, DNA was diluted to 1 ng/μl using sterile water. 16S rDNA genes of distinct regions (16S V3-V4) were amplified using a specific primer (515F-806R) with the barcode. All the PCR reactions were carried out with 15 μl of the Phusion® High-Fidelity PCR Master Mix (New England Biolabs), 2 μM of forward and reverse primers, and about 10 ng of template DNA. Sequencing libraries were generated using the TruSeq® DNA PCR-Free Sample Preparation Kit (Illumina, United States) following the manufacturer's recommendations and index codes were added according to our previous study (22). Microbial communities were investigated by iTag sequencing of 16S rDNA genes (23, 24).

Statistical analysis

All the statistical analyses were performed using the one-way ANOVA and *t*-test analysis in SPSS version 20.0 software (SPSS Incorporation, Chicago, IL, United States). The data are expressed as the means ± SEM). $P < 0.05$ was considered statistically significant. All the figures in this study were drawn using GraphPad Prism version 8.0.

Results

Arbutin administration improves gut development

Final body weight was not obviously changed (**Figure 1A**), but the relative weight and weight/length of the intestine were significantly increased by arbutin administration at 0.2 and 0.4 mg/ml ($P < 0.05$) (**Figures 1B,D**), and arbutin did not alter the intestinal length, villus width and crypt depth (**Figures 1C,F,H**). Thus, we continued to investigate the intestinal pathology section; the results showed that the villus length was increased by 0.4 and 1.0 mg/ml arbutin, villus area was enhanced by 0.2 and 0.4 mg/ml arbutin, and villus length/crypt depth (L/D) was higher at 0.4 mg/ml arbutin ($P < 0.05$) (**Figures 1E,G,I,J**).

Effects of arbutin on serum biochemical parameters

To further understand the role of arbutin, lipid parameters in serum were determined (**Figures 2A–F**). Arbutin at 0.4 mg/ml significantly enhanced the content of serum glucose (Glu) ($P < 0.05$) (**Figure 2A**). Nevertheless, arbutin at 0.2 mg/ml lowered the content of total cholesterol (TC) and high-density lipoprotein (HDL) ($P < 0.05$) (**Figures 2C,D**), and low-density lipoprotein (LDL) was lowered at 0.1 and 0.2 mg/ml ($P < 0.05$) (**Figure 2E**). These results suggested that arbutin can improve intestinal development and serum lipid parameters.

Arbutin alters the composition of gut microbiota

To investigate the effects of arbutin on gut microbes, we determined the microbiome by 16S rDNA sequencing at 0.4 mg/ml (**Figures 3**, **4**). Venn diagram showed that 597 and 111 different operational taxonomic units (OTUs) were found in the control and arbutin groups and contained the same 540 OTUs (**Figure 3A**), rarefaction curve indicated that the sample capacity and sample depth were reasonable (**Figure 4B**). Arbutin significantly decreased the α-diversity index [observed species, Shannon index, phylogenetic diversity (PD), Simpson index, Chao1, and abundance-based coverage estimator (ACE)] ($P < 0.05$) (**Figures 3B–D**, **4A,C–E**). Meanwhile, the β-diversity index was reduced ($P < 0.05$) (**Figure 3E**), and principal component analysis showed that there were different zones of intestinal microflora between the control group and arbutin (**Figure 3F**). At the phylum level, the relative abundance of *Actinobacteria* and *Proteobacteria* was clearly lowered by arbutin ($P < 0.05$) (**Figure 3G**). At the species level, 0.4 mg/ml arbutin markedly increased the abundance of *Lactobacillus intestinalis* ($P < 0.05$) (**Figures 3H**, **4F**), while the abundance of *Bifidobacterium animalis*, *Bacillus velezensis*, *Lachnospiraceae bacterium_M18-1*, *Eubacterium* sp_*14-2*, *Helicobacter ganmani*, *Lachnospiraceae bacterium_10-1*, *Lachnospiraceae bacterium_615*, *Planoglabratella opercularis*, *Pseudoflavonifractor* sp_*Marseille-P3106*, *Clostridium leptum*, *Clostridium* sp_*ASF356*, *Dubosiella newyorkensis*, *Burkholderiales bacterium_YL145*, *Desulfovibrio* sp_*ABHU2SB*, *Firmicutes_bacterium CAG_194_44_15*, *Clostridium* sp_*Culture-27*, and *Ruminiclostridium* sp_*KB18* was lowered compared to control ($P < 0.05$) (**Figures 3H**, **4F**).

Arbutin improves gut development with an antibiotics cocktail and fecal microflora transplantation

The intestinal microbiota has been shown to regulate intestinal development (25) and host metabolism (18). To further determine the role of intestinal microbiota, 4 weeks mice were given an antibiotics cocktail for 1 week with oral arbutin solution (0.4 mg/ml). Predictably, arbutin significantly enriched the villi width compared to the antibiotics group in the jejunum ($P < 0.05$) (**Figures 5A,C**), but villus length, villus area, crypt depth, L/D were not changed (**Figure 5B,D–F**), and there

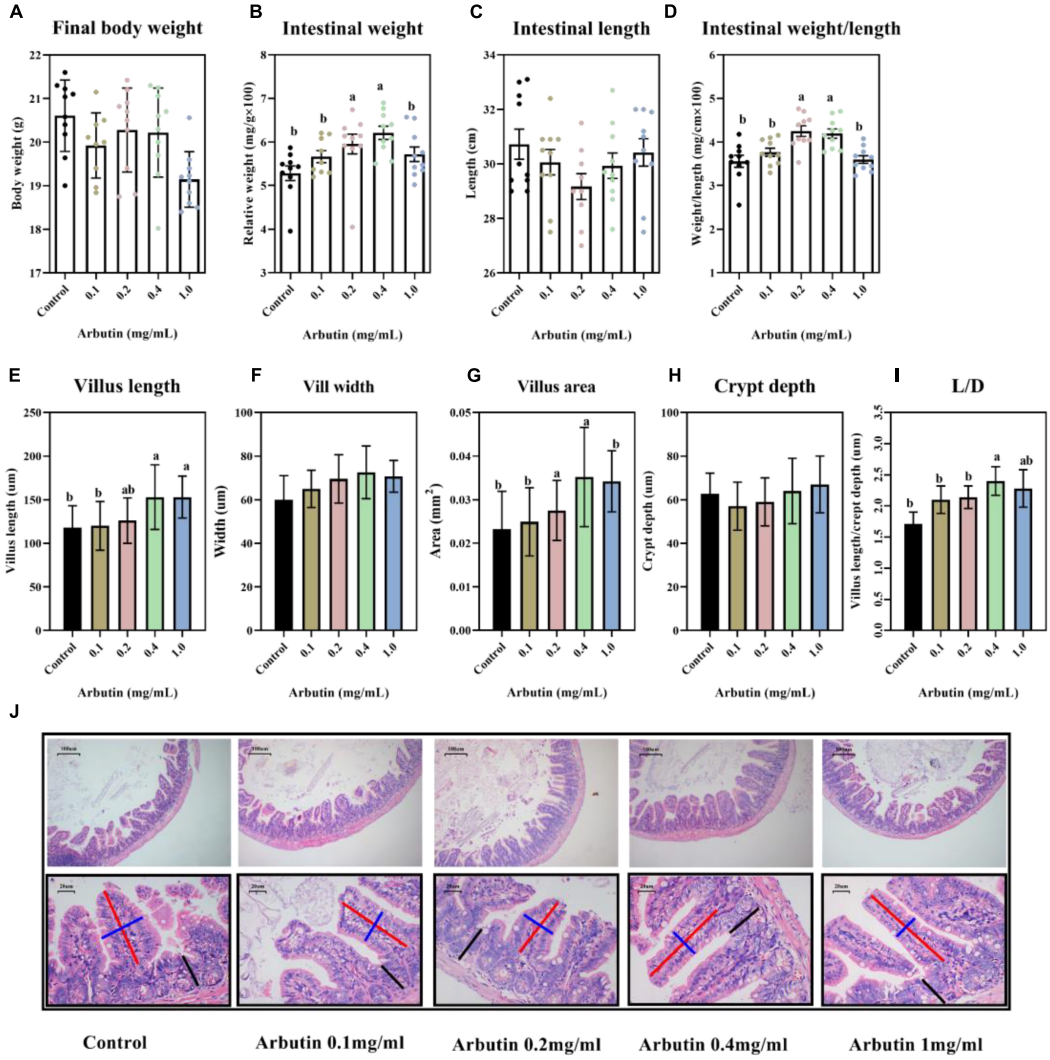

FIGURE 1
Oral arbutin improves gut development. Final body weight **(A)**, relative intestinal weight **(B)**, intestinal length **(C)**, intestinal weight/length **(D)**, villus length **(E)**, villus width **(F)**, villus areas **(G)**, crypt depth **(H)**, L/D **(I)**, and HE staining of jejunum and ileum **(J)**. Values are presented as the means ± SEMs. Differences were assessed by one-way ANOVA and denoted as follows: a and b indicate significant differences in each group.

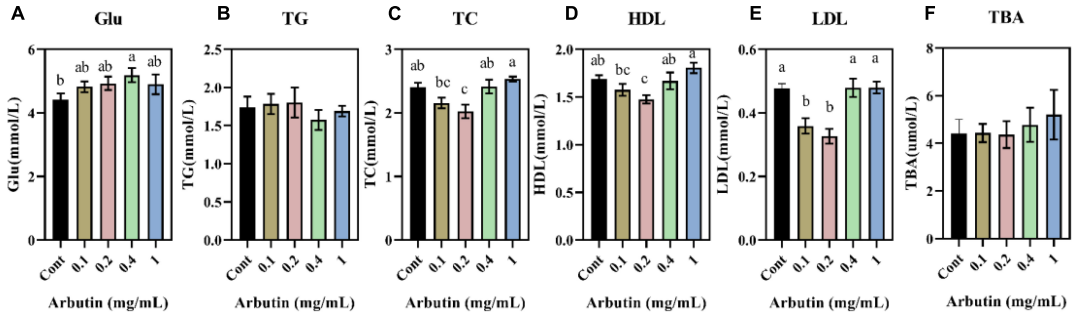

FIGURE 2
Effects of oral arbutin on serum lipids. Glucose **(A)**, total triglycerides **(B)**, total cholesterol **(C)**, high-density lipoprotein **(D)**, low-density lipoprotein **(E)**, and total bile acid **(F)** (n = 10). Values are presented as the means ± SEMs. Differences were assessed by one-way ANOVA and denoted as follows: a and b indicate significant differences in each group.

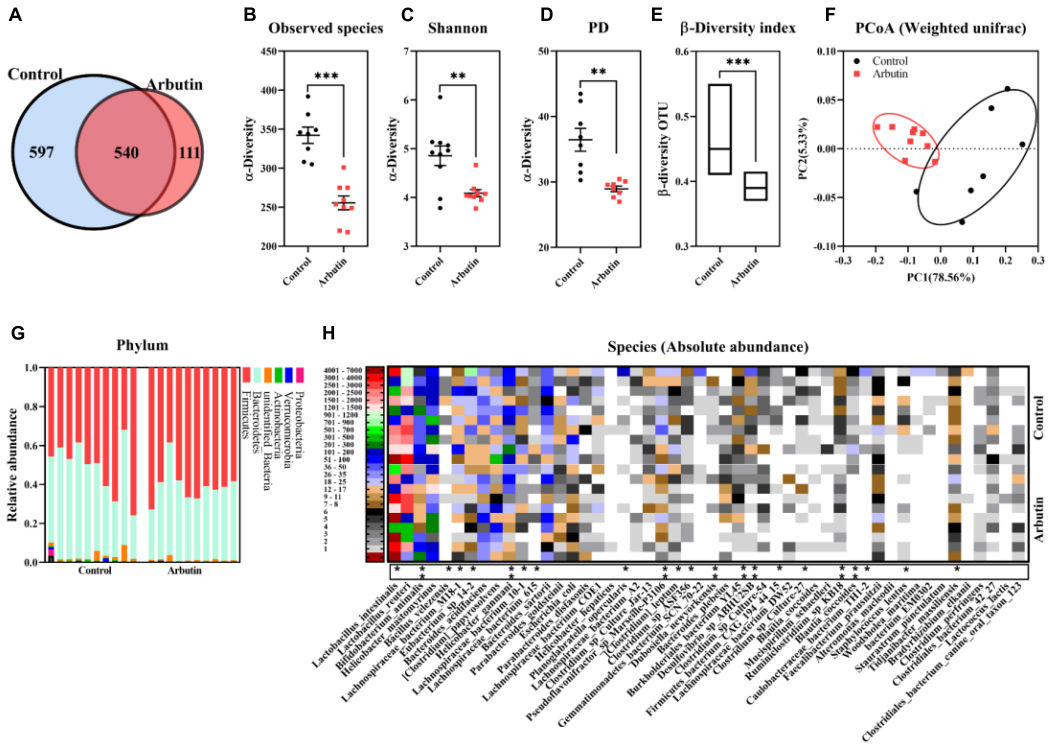

FIGURE 3
Arbutin alters the gut microbiota. Venn diagram **(A)**, observed species **(B)**, Shannon index **(C)**, PD_whole_tree **(D)**, β-diversity index **(E)**, principal component analysis **(F)**, phylum **(G)**, and species **(H)** were analyzed at 0.4 mg/ml. Differences were assessed by *t*-test and denoted as follows: $^{*}P < 0.05$, $^{**}P < 0.01$, $^{***}P < 0.001$.

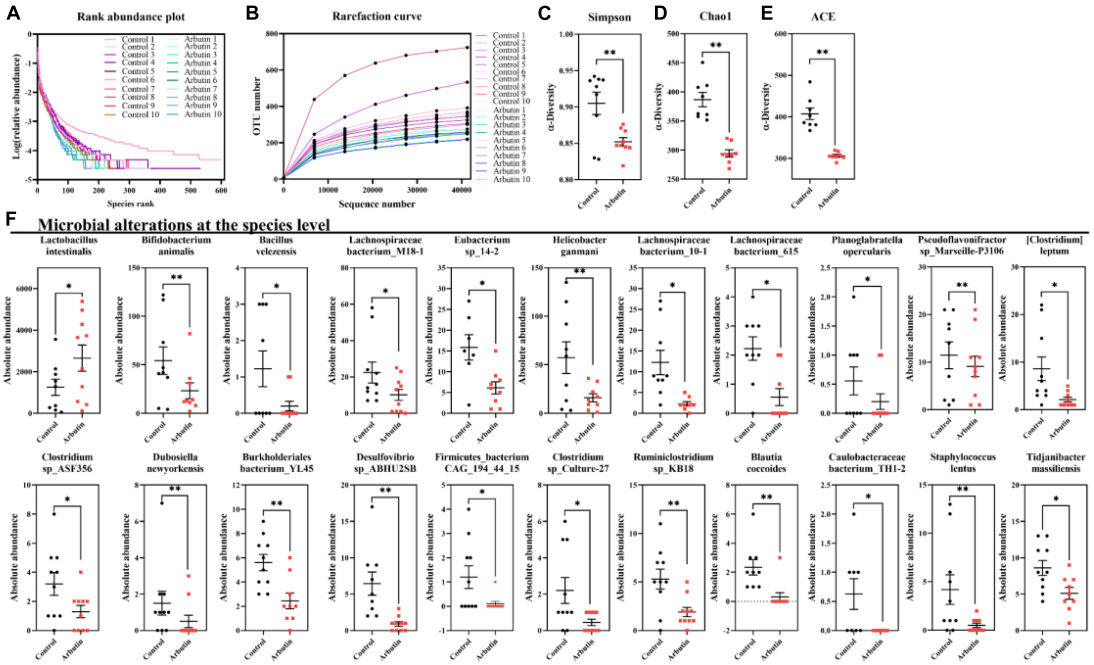

FIGURE 4
Arbutin alters the gut microbiota. Rank abundance plot **(A)**, rarefaction curve **(B)**, Simpson index **(C)**, Chao1 **(D)**, ACE **(E)**, and species **(F)** were analyzed at 0.4 mg/ml. Differences were assessed by *t*-test and denoted as follows: $^{*}P < 0.05$, $^{**}P < 0.01$.

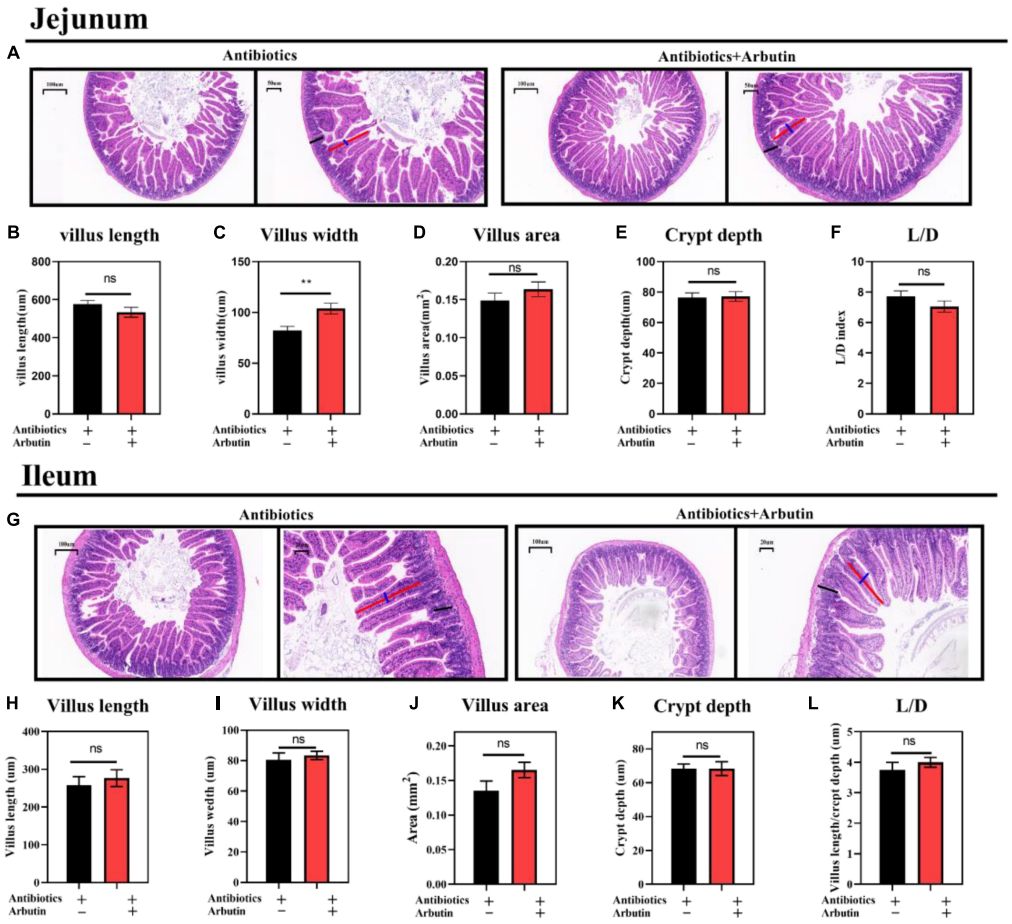

FIGURE 5
Arbutin administration improved jejunal and ileal gut development after oral cocktails. HE staining of the jejunum **(A)**, villus length in the jejunum **(B)**, villus width in the jejunum **(C)**, villus areas in the jejunum **(D)**, crypt depth in the jejunum **(E)**, L/D in the jejunum **(F)**, HE staining of the ileum **(G)**, villus length in the ileum **(H)**, villus width in the ileum **(I)**, villus areas in the ileum **(J)**, crypt depth in the ileum **(K)**, and L/D in the ileum **(L)** (n = 10). Differences were assessed by t-test and denoted as follows: $^{**}P < 0.01$.

was a tendency to enhance the ileal villi index (Figures 5G–L). Then, we further collected feces from mice administered with arbutin 0.4 mg/ml and transplanted them to mice with an antibiotics cocktail. Fecal microflora transplantation significantly improved intestinal pathologies, such as jejunal villus length (Figures 6A,B), jejunal villus length/villus width (L/D) (Figures 6A,F), and ieal villus areas (Figure 6J). But jejunal villus width, jejunal villus area, jejunal crypt depth, ileal villus legth, ileal villus width, ileal crypt depth and ileal L/D were uninfluential (Figures 6C–E,H,I,K,L). In summary, gut microbes contributed improving intestinal development.

Lactobacillus intestinalis colonization reduces gut damage after an antibiotics cocktail

We have found that the abundance of *L. intestinalis (Lin)* was markedly enhanced by arbutin and was the most abundant bacterium in the gut (Figures 3H, 4F). *L. intestinalis* was often found in the gut of the host, which was treated for various diseases (26–28) and metabolic disorders (29, 30), but the effect of *L. intestinalis* on gut development and host lipid metabolism was unclear. Thus, we investigated the role of *Lin* on intestinal pathology and used *Lin* monocolonization (31) with an antibiotics cocktail for 1 week. Interestingly, after an antibiotics cocktail for 1 week, *Lin* monocolonization clearly increased the villus length, crypt depth, and villus areas (Figures 7A–C,E), and there was a tendency to elevate the number of goblet cells (Figures 7A,G). Whereas villus width and L/D were not changed by *L. intestinalis* (Figures 7D,F).

Arbutin promotes the growth of *Lactobacillus intestinalis in vitro*

In order to verify the previous results, we co-cultured arbutin and *L. intestinalis* to investigate the growth of

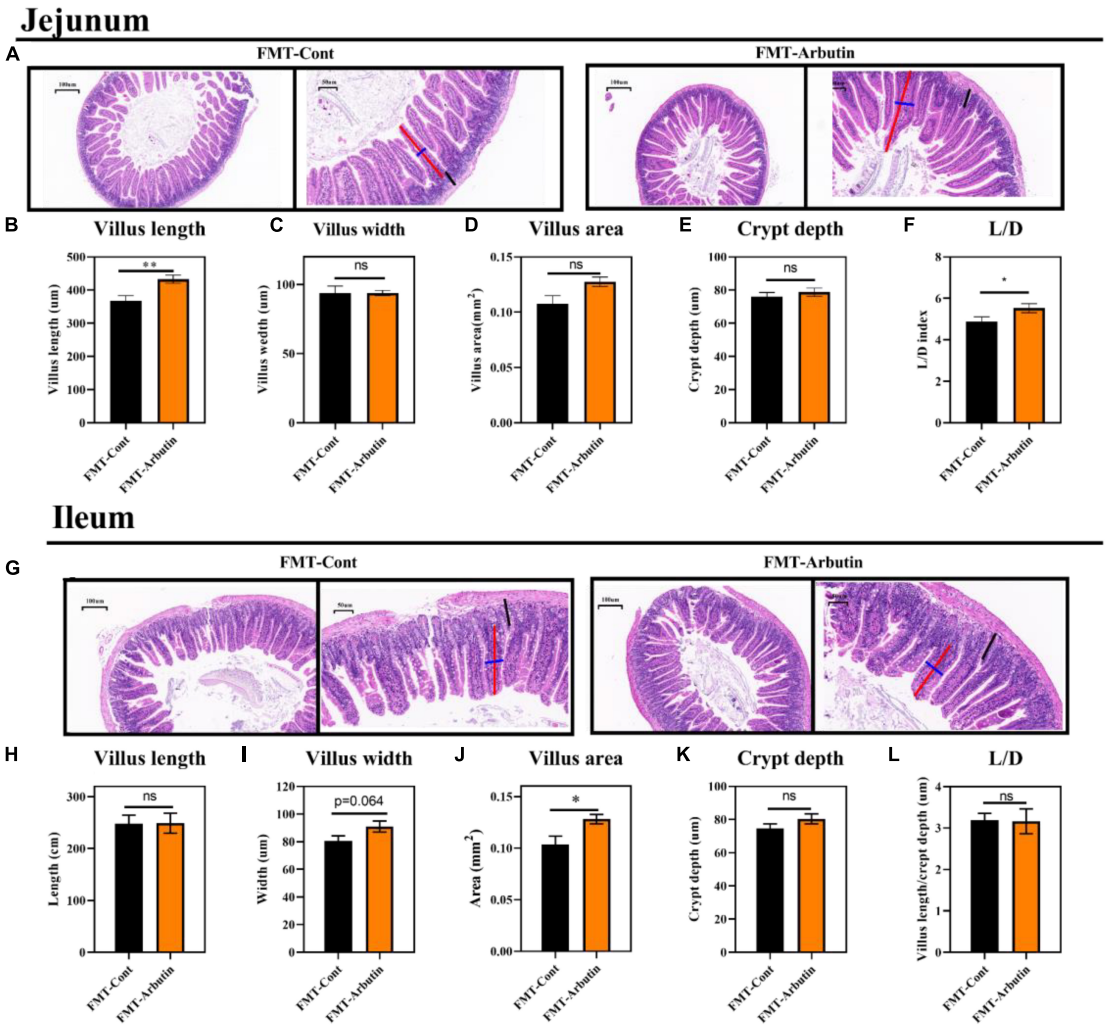

FIGURE 6
Fecal microflora transplantation improved gut development in mice. HE staining of the jejunum **(A)**, villus length in the jejunum **(B)**, villus width in the jejunum **(C)**, villus areas in the jejunum **(D)**, crypt depth in the jejunum **(E)**, L/D in the jejunum **(F)**, HE staining of the ileum **(G)**, villus length in the ileum **(H)**, villus width in the ileum **(I)**, villus areas in the ileum **(J)**, crypt depth in the ileum **(K)**, and L/D in the ileum **(L)** (n = 10). Differences were assessed by t-test and denoted as follows: $^{*}P < 0.05$, $^{**}P < 0.01$.

L. intestinalis in vitro. The results showed that arbutin significantly promotes the growth of *L. intestinalis* ($P < 0.05$) (Figure 8).

Discussion

In recent years, arbutin has often been extensively studied that it inhibited tyrosinase activity to reduce melanin deposition in the cosmetic industry (32). Meanwhile, arbutin is often used to treat various diseases, such as types of cancers, central nervous system disorders, osteoporosis, diabetes, and so on (20). Arbutin, as a phytochemical active substance, is low bioavailability in the gut, and incompletely played a beneficial role (33). Further, they are degraded by microbes to increase their biological activity (34). However, the potential of arbutin has rarely been reported about promoting intestinal health. Thus, we explored the effects of arbutin on gut health in the common condition, oral antibiotic cocktails, fecal microflora transplantation, and *Lin* monocolonization.

We investigated the effects of different concentrations of arbutin on gut health and serum lipids in mice in normal conditions. We found that low concentrations of arbutin reduced serum lipids, whereas reversed at high concentrations. Previous studies have shown that arbutin significantly reduced adipocyte differentiation and promoted fatty acid uptake in 3T3-L1 adipocytes (35). The polyjuice decoction containing arbutin decreased the total cholesterol, triglyceride, VLDL, and LDL in diabetic rats (36). Importantly, we found that arbutin plays an important role in promoting intestinal development.

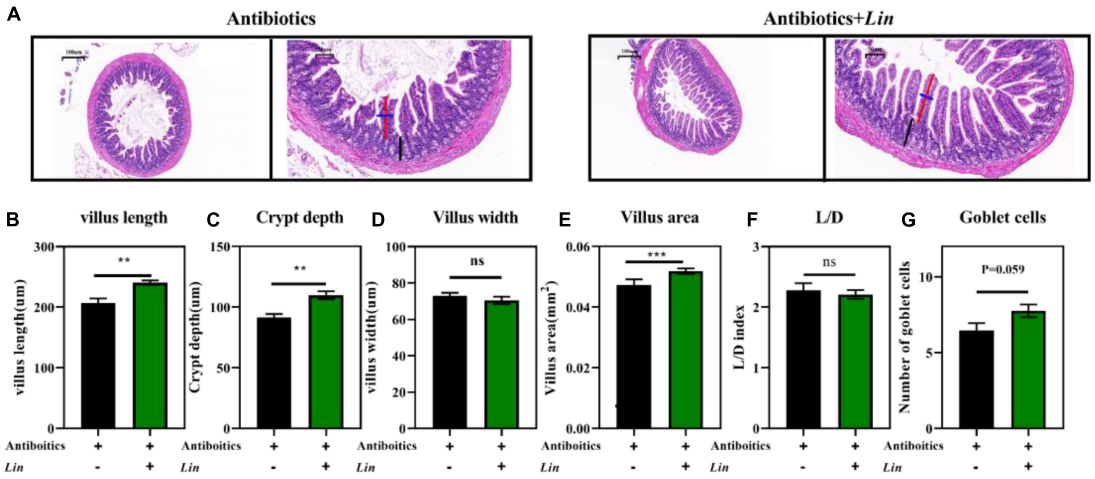

FIGURE 7
Lactobacillus intestinalis colonization improved intestinal development in mice. HE staining the ileum **(A)**, villus length in the ileum **(B)**, villus width in the ileum **(C)**, villus areas in the ileum **(D)**, crypt depth in the ileum **(E)**, L/D in the ileum **(F)**, and the number of goblet cells **(G)** (n = 10). Differences were assessed by t-test and denoted as follows: $^{**}P < 0.01$, $^{***}P < 0.001$.

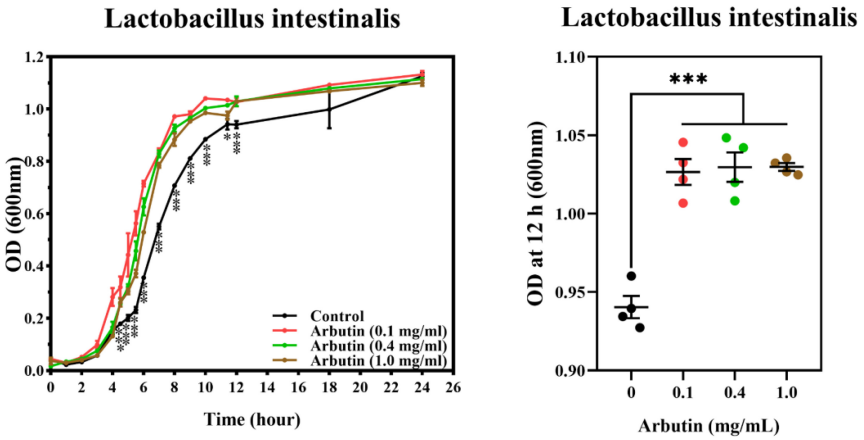

FIGURE 8
Arbutin promotes the growth of *Lactobacillus intestinalis in vitro*. Arbutin and *L. intestinalis* were co-cultured and determined the OD value at 0–24 h. Differences were assessed by t-test and denoted as follows: $^{*}P < 0.05$, $^{***}P < 0.001$.

In this trial, 0.4 and 1.0 mg/kg arbutin markedly enhanced the villus length, villus areas, and L/D compared to control. Villus index was highly associated with nutrient absorption and gut health (37); thus, the increased villus length, villus areas, and L/D indicated a positive role of arbutin in gut nutrient absorption. The gut microbiota may be an important reason for this result. Arbutin, as a natural phytochemical, is a β-glucoside derived from hydroquinone (2, 3) whose bioactivity and bioavailability can be modified by glycoside hydrolase activity of gut microbiota through the release of acylglycines (38). Microorganisms are associated with the absorption and metabolism of arbutin, a novel *Janthinobacterium* strain (SNU WT3), isolated from the kidney of rainbow trout showed that different biochemical details such as arbutin compared to its close relatives identified (39). Further, *Bifidobacterium* was proved to degrade arbutin (containing glycosides) to elevate bioavailability by secreting β-glucosidase (38). We found that *L. intestinalis* was significantly increased by arbutin, which played an important role in gut health and metabolic disorders (26, 29, 40). However, the abundance of another 21 species of bacteria (such as *Bifidobacterium animalis*, *Bacillus velezensis*, *Lachnospiraceae bacterium_M18-1*, *Eubacterium* sp_*14-2*, and *Helicobacter ganmani*) was significantly reduced. Interestingly, arbutin was reported to reduce colitis symptoms and inhibit lipopolysaccharide-induced inflammation (41), and there were significant negative correlations between arbutin contents

and the enriched gut microbiota (e.g., *Eubacterium* and *Ruminococcus*) (42), suggesting that there was bactericidal ability about arbutin.

Gut damage is often associated with drugs, environmental stress, and lifestyle (43). Especially, antibiotics are considered only beneficial, but also potentially harmful drugs, as their abuse appears to play a role in the pathogenesis of several disorders associated with microbiota impairment (44). In this trial, we demonstrated the beneficial effects of arbutin in improving gut health with antibiotics cocktail and fecal microflora transplantation. The result was attributed to arbutin administration altering the gut microflora, such as *L. intestinalis*. Fecal microflora transplantation is a common technique for the treatment of host metabolic disorders and diseases (45, 46). The gut microbiota development of cesarean section infants was rapidly restored by orally derived fecal microflora transplantation (47). Fecal microflora transplantation played beneficial effects on gastrointestinal transport and intestinal barrier dysfunction (48), which were related to intestinal permeability and pathology (49), such as villus length, villus areas, and L/D. Furthermore, the monocolonization technique improves the gut microbiota structure and metabolic process of the host (50, 51) and is also one of the measures to investigate bacterial function. For example, probiotic colonization improved intestinal barrier function and intestinal health, newly identified health-associated bacteria, such as *Faecalibacterium prausnitzii*, *Akkermansia muciniphila*, *Ruminococcus bromii*, and *Roseburia* species (52, 53). Our results showed that *L. intestinalis* monocolonization reduced intestinal damage after an antibiotics cocktail, such as villus length, crypt depth, villus areas, and the number of goblet cells.

To prove the effect of arbutin on *L. intestinalis* growth, we used the co-culture method of arbutin and *L. intestinalis*. Previous studies have found that Bifidobacterium degraded β-glucosidase to enhance the activity of glycoside by secreting β-glucosidase (38). Liu et al. identified a glycoside hydrolase, which is very important for the growth of type I rhamnogalacturonan acid by commensal bacteroides (54). We found that arbutin significantly promoted the proliferation of *L. intestinalis*, suggesting the potential of arbutin on *L. intestinalis* proliferation and utilizing arbutin to increase biological activity.

Conclusion

Arbutin, as a phytochemical, has been widely studied in whitening, anti-inflammatory, and antioxidant, while the interaction between arbutin and intestinal microbes has been rarely studied. In this trial, we focused on the effects of arbutin on intestinal development and microbes. Predictably, arbutin played a positive role in the gut, such as improving the pathological state of the jejunum and ileum and altering the intestinal microbial structure. In addition, we demonstrated the beneficial effects of arbutin on intestinal development through fecal microflora transplantation and *L. intestinalis* monocolonization by antibiotic cocktail therapy. However, the specific mechanisms of *L. intestinalis* in intestinal development need to be further explored.

Data availability statement

The datasets presented in this study can be found in online repositories. The names of the repository/repositories and accession number(s) can be found in the article/supplementary material. The data presented in the study are deposited in the NCBI (https://dataview.ncbi.nlm.nih.gov/object/PRJNA839245) repository, accession number: PRJNA839245.

Ethics statement

The animal model and experimental procedures used in this experiment were approved by the Hunan Agricultural University Institutional Animal Care and Use Committee (202005).

Author contributions

JM was the primary investigator in this study. SC participated in the animal experiments. YL performed the statistical data analysis. XW participated in the sample analysis. ZS examined the manuscript. All authors contributed to the article and approved the submitted version.

Funding

This study was supported by the National Natural Science Foundation of China (Grant No: 31902171).

Acknowledgments

We thank the College of Animal Science and Technology, Hunan Agricultural University, Animal Nutrition Genome, and Germplasm Innovation Research Center for their support.

Conflict of interest

The authors declare that the research was conducted in the absence of any commercial or financial relationships that could be construed as a potential conflict of interest.

Publisher's note

References

1. Shang Y, Wei W, Zhang P, Ye BC. Engineering *Yarrowia lipolytica* for enhanced production of arbutin. *J Agric Food Chem.* (2020) 68:1364–72. doi: 10.1021/acs.jafc.9b07151

2. Zhou H, Zhao J, Li A, Reetz MT. Chemical and biocatalytic routes to arbutin (dagger). *Molecules.* (2019) 24:3303. doi: 10.3390/molecules24183303

3. Zhu X, Tian Y, Zhang W, Zhang T, Guang C, Mu W. Recent progress on biological production of alpha-arbutin. *Appl Microbiol Biotechnol.* (2018) 102:8145–52. doi: 10.1007/s00253-018-9241-9

4. Park JJ, Hwang SJ, Kang YS, Jung J, Park S, Hong JE, et al. Synthesis of arbutin-gold nanoparticle complexes and their enhanced performance for whitening. *Arch Pharm Res.* (2019) 42:977–89. doi: 10.1007/s12272-019-01164-7

5. Zaid AN, Al Ramahi R. Depigmentation and anti-aging treatment by natural molecules. *Curr Pharm Des.* (2019) 25:2292–312. doi: 10.2174/1381612825666190703153730

6. Bonifacio MA, Cerqueni G, Cometa S, Licini C, Sabbatini L, Mattioli-Belmonte M, et al. Insights into arbutin effects on bone cells: Towards the development of antioxidant titanium implants. *Antioxidants.* (2020) 9:579. doi: 10.3390/antiox9070579

7. Boo YC. Arbutin as a skin depigmenting agent with antimelanogenic and antioxidant properties. *Antioxidants.* (2021) 10:1129. doi: 10.3390/antiox10071129

8. Hazman O, Sariova A, Bozkurt MF, Cigerci IH. The anticarcinogen activity of beta-arbutin on MCF-7 cells: Stimulation of apoptosis through estrogen receptor-alpha signal pathway, inflammation and genotoxicity. *Mol Cell Biochem.* (2021) 476:349–60. doi: 10.1007/s11010-020-03911-7

9. Ahmadian SR, Ghasemi-Kasman M, Pouramir M, Sadeghi F. Arbutin attenuates cognitive impairment and inflammatory response in pentylenetetrazol-induced kindling model of epilepsy. *Neuropharmacology.* (2019) 146:117–27. doi: 10.1016/j.neuropharm.2018.11.038

10. Ebrahim-Tabar F, Nazari A, Pouramir M, Ashrafpour M, Pourabdolhossein F. Arbutin improves functional recovery and attenuates glial activation in lysolecethin-induced demyelination model in rat optic chiasm. *Mol Neurobiol.* (2020) 57:3228–42. doi: 10.1007/s12035-020-01962-x

11. Ding Y, Kong D, Zhou T, Yang ND, Xin C, Xu J, et al. alpha-arbutin protects against Parkinson's disease-associated mitochondrial dysfunction *in vitro* and *in vivo*. *Neuromolecular Med.* (2020) 22:56–67. doi: 10.1007/s12017-019-08562-6

12. Bernier-Latmani J, Mauri C, Marcone R, Renevey F, Durot S, He L, et al. ADAMTS18(+) villus tip telocytes maintain a polarized VEGFA signaling domain and fenestrations in nutrient-absorbing intestinal blood vessels. *Nat Commun.* (2022) 13:3983. doi: 10.1038/s41467-022-31571-2

13. Short K, Derrickson EM. Compensatory changes in villus morphology of lactating Mus musculus in response to insufficient dietary protein. *J Exp Biol.* (2020) 223:jeb210823. doi: 10.1242/jeb.210823

14. Sumigray KD, Terwilliger M, Lechler T. Morphogenesis and compartmentalization of the intestinal crypt. *Dev cell.* (2018) 45:183.e–97.e. doi: 10.1016/j.devcel.2018.03.024

15. Cai R, Cheng C, Chen J, Xu X, Ding C, Gu B. Interactions of commensal and pathogenic microorganisms with the mucus layer in the colon. *Gut Microbes.* (2020) 11:680–90. doi: 10.1080/19490976.2020.1735606

16. Martel J, Ojcius DM, Ko YF, Young JD. Phytochemicals as prebiotics and biological stress inducers. *Trends Biochem Sci.* (2020) 45:462–71. doi: 10.1016/j.tibs.2020.02.008

17. Dey P. Gut microbiota in phytopharmacology: A comprehensive overview of concepts, reciprocal interactions, biotransformations and mode of actions. *Pharmacol Res.* (2019) 147:104367. doi: 10.1016/j.phrs.2019.104367

18. Fan Y, Pedersen O. Gut microbiota in human metabolic health and disease. *Nat Rev Microbiol.* (2021) 19:55–71. doi: 10.1038/s41579-020-0433-9

19. Morais LH, Schreiber HLt, Mazmanian SK. The gut microbiota-brain axis in behaviour and brain disorders. *Nat Rev Microbiol.* (2021) 19:241–55. doi: 10.1038/s41579-020-00460-0

20. Saeedi M, Khezri K, Seyed Zakaryaei A, Mohammadamini H. A comprehensive review of the therapeutic potential of alpha-arbutin. *Phytother Res.* (2021) 35:4136–54. doi: 10.1002/ptr.7076

21. Yin J, Li Y, Han H, Chen S, Gao J, Liu G, et al. Melatonin reprogramming of gut microbiota improves lipid dysmetabolism in high-fat diet-fed mice. *J Pineal Res.* (2018) 65:e12524. doi: 10.1111/jpi.12524

22. Yin J, Li Y, Han H, Ma J, Liu G, Wu X, et al. Administration of Exogenous Melatonin Improves the Diurnal Rhythms of the Gut Microbiota in Mice Fed a High-Fat Diet. *mSystems.* (2020) 5:e2–20. doi: 10.1128/mSystems.00002-20

23. Tsou AM, Olesen SW, Alm EJ, Snapper SB. 16S rRNA sequencing analysis: The devil is in the details. *Gut Microbes.* (2020) 11:1139–42. doi: 10.1080/19490976.2020.1747336

24. Church DL, Cerutti L, Gurtler A, Griener T, Zelazny A, Emler S. Performance and application of 16S rRNA gene cycle sequencing for routine identification of bacteria in the clinical microbiology laboratory. *Clin Microbiol Rev.* (2020) 33:e53–19. doi: 10.1128/CMR.00053-19

25. Larabi A, Barnich N, Nguyen HTT. New insights into the interplay between autophagy, gut microbiota and inflammatory responses in IBD. *Autophagy.* (2020) 16:38–51. doi: 10.1080/15548627.2019.1635384

26. Wang S, Ishima T, Zhang J, Qu Y, Chang L, Pu Y, et al. Ingestion of *Lactobacillus intestinalis* and *Lactobacillus reuteri* causes depression- and anhedonia-like phenotypes in antibiotic-treated mice *via* the vagus nerve. *J Neuroinflammation.* (2020) 17:241. doi: 10.1186/s12974-020-01916-z

27. Lim EY, Song EJ, Kim JG, Jung SY, Lee SY, Shin HS, et al. *Lactobacillus intestinalis* YT2 restores the gut microbiota and improves menopausal symptoms in ovariectomized rats. *Benef Microbes.* (2021) 12:503–16. doi: 10.3920/BM2020.0217

28. Wang N, Wu T, Du D, Mei J, Luo H, Liu Z, et al. Transcriptome and gut microbiota profiling revealed the protective effect of tibetan tea on ulcerative colitis in mice. *Front Microbiol.* (2021) 12:748594. doi: 10.3389/fmicb.2021.748594

29. Wang Y, Ouyang M, Gao X, Wang S, Fu C, Zeng J, et al. Phocea, pseudoflavonifractor and *Lactobacillus intestinalis*: Three potential biomarkers of gut microbiota that affect progression and complications of obesity-induced type 2 diabetes mellitus. *Diabetes Metab Syndr Obes.* (2020) 13:835–50. doi: 10.2147/DMSO.S240728

30. Lu X, Jing Y, Li Y, Zhang N, Zhang W, Cao Y. The differential modulatory effects of *Eurotium cristatum* on the gut microbiota of obese dogs and mice are associated with improvements in metabolic disturbances. *Food Funct.* (2021) 12:12812–25. doi: 10.1039/d1fo02886c

31. Ang QY, Alexander M, Newman JC, Tian Y, Cai J, Upadhyay V, et al. Ketogenic diets alter the gut microbiome resulting in decreased intestinal Th17 cells. *Cell.* (2020) 181:1263.e–75.e. doi: 10.1016/j.cell.2020.04.027

32. Jin YH, Jeon AR, Mah JH. Tyrosinase inhibitory activity of soybeans fermented with *Bacillus subtilis* capable of producing a phenolic glycoside, arbutin. *Antioxidants.* (2020) 9:1301. doi: 10.3390/antiox9121301

33. Wan MLY, Co VA, El-Nezami H. Dietary polyphenol impact on gut health and microbiota. *Crit Rev Food Sci Nutr.* (2021) 61:690–711. doi: 10.1080/10408398.2020.1744512

34. Luca SV, Macovei I, Bujor A, Miron A, Skalicka-Wozniak K, Aprotosoaie AC, et al. Bioactivity of dietary polyphenols: The role of metabolites. *Crit Rev Food Sci Nutr.* (2020) 60:626–59. doi: 10.1080/10408398.2018.1546669

35. Bedi O, Aggarwal S, Trehanpati N, Ramakrishna G, Grewal AS, Krishan P. *In vitro* targeted screening and molecular docking of stilbene, quinones, and flavonoid on 3T3-L1 pre-adipocytes for anti-adipogenic actions. *Naunyn Schmiedebergs Arch Pharmacol.* (2020) 393:2093–106. doi: 10.1007/s00210-020-01919-w

36. Madic V, Petrovic A, Juskovic M, Jugovic D, Djordjevic L, Stojanovic G, et al. Polyherbal mixture ameliorates hyperglycemia, hyperlipidemia and histopathological changes of pancreas, kidney and liver in a rat model of type 1 diabetes. *J Ethnopharmacol.* (2021) 265:113210. doi: 10.1016/j.jep.2020.113210

37. Moor AE, Harnik Y, Ben-Moshe S, Massasa EE, Rozenberg M, Eilam R, et al. Spatial reconstruction of single enterocytes uncovers broad zonation along the intestinal villus axis. *Cell.* (2018) 175:1156.e–67.e. doi: 10.1016/j.cell.2018.08.063

38. Modrackova N, Vlkova E, Tejnecky V, Schwab C, Neuzil-Bunesova V. Bifidobacterium beta-glucosidase activity and fermentation of dietary plant glucosides is species and strain specific. *Microorganisms.* (2020) 8:839. doi: 10.3390/microorganisms8060839

39. Jung WJ, Kim SW, Giri SS, Kim HJ, Kim SG, Kang JW, et al. *Janthinobacterium tructae* sp. nov., isolated from kidney of rainbow trout (*Oncorhynchus mykiss*). *Pathogens.* (2021) 10:229. doi: 10.3390/pathogens10020229

40. Lan J, Wang K, Chen G, Cao G, Yang C. Effects of inulin and isomalto-oligosaccharide on diphenoxylate-induced constipation, gastrointestinal motility-related hormones, short-chain fatty acids, and the intestinal flora in rats. *Food Funct.* (2020) 11:9216–25. doi: 10.1039/d0fo00865f

41. Wang L, Feng Y, Wang J, Luo T, Wang X, Wu M, et al. Arbutin ameliorates murine colitis by inhibiting JAK2 signaling pathway. *Front Pharmacol.* (2021) 12:683818. doi: 10.3389/fphar.2021.683818

42. Fang X, Wu H, Wang X, Lian F, Li M, Miao R, et al. Modulation of gut microbiota and metabolites by berberine in treating mice with disturbances in glucose and lipid metabolism. *Front Pharmacol.* (2022) 13:870407. doi: 10.3389/fphar.2022.870407

43. Fassarella M, Blaak EE, Penders J, Nauta A, Smidt H, Zoetendal EG. Gut microbiome stability and resilience: Elucidating the response to perturbations in order to modulate gut health. *Gut.* (2021) 70:595–605. doi: 10.1136/gutjnl-2020-321747

44. Ianiro G, Tilg H, Gasbarrini A. Antibiotics as deep modulators of gut microbiota: Between good and evil. *Gut.* (2016) 65:1906–15. doi: 10.1136/gutjnl-2016-312297

45. Weingarden AR, Vaughn BP. Intestinal microbiota, fecal microbiota transplantation, and inflammatory bowel disease. *Gut Microbes.* (2017) 8:238–52. doi: 10.1080/19490976.2017.1290757

46. de Groot PF, Frissen MN, de Clercq NC, Nieuwdorp M. Fecal microbiota transplantation in metabolic syndrome: History, present and future. *Gut Microbes.* (2017) 8:253–67. doi: 10.1080/19490976.2017.1293224

47. Korpela K, Helve O, Kolho KL, Saisto T, Skogberg K, Dikareva E, et al. Maternal fecal microbiota transplantation in cesarean-born infants rapidly restores normal gut microbial development: A proof-of-concept study. *Cell.* (2020) 183:324.e–34.e. doi: 10.1016/j.cell.2020.08.047

48. Palma GD, Lynch MDJ, Lu J, Dang VT, Deng Y, Jury J, et al. Transplantation of fecal microbiota from patients with irritable bowel syndrome alters gut function and behavior in recipient mice. *Sci Transl Med.* (2017) 9:eaaf6397. doi: 10.1126/scitranslmed.aaf6397

49. Craven L, Rahman A, Nair Parvathy S, Beaton M, Silverman J, Qumosani K, et al. Allogenic fecal microbiota transplantation in patients with nonalcoholic fatty liver disease improves abnormal small intestinal permeability: A randomized control trial. *Am J Gastroenterol.* (2020) 115:1055–65. doi: 10.14309/ajg.0000000000000661

50. Koch BEV, Yang S, Lamers G, Stougaard J, Spaink HP. Intestinal microbiome adjusts the innate immune setpoint during colonization through negative regulation of MyD88. *Nat Commun.* (2018) 9:4099. doi: 10.1038/s41467-018-06658-4

51. Schretter CE, Vielmetter J, Bartos I, Marka Z, Marka S, Argade S, et al. A gut microbial factor modulates locomotor behaviour in *Drosophila*. *Nature.* (2018) 563:402–6. doi: 10.1038/s41586-018-0634-9

52. Lordan C, Thapa D, Ross RP, Cotter PD. Potential for enriching next-generation health-promoting gut bacteria through prebiotics and other dietary components. *Gut Microbes.* (2020) 11:1–20. doi: 10.1080/19490976.2019.1613124

53. Sanders ME, Merenstein DJ, Reid G, Gibson GR, Rastall RA. Probiotics and prebiotics in intestinal health and disease: From biology to the clinic. *Nat Rev Gastroenterol Hepatol.* (2019) 16:605–16. doi: 10.1038/s41575-019-0173-3

54. Liu H, Shiver AL, Price MN, Carlson HK, Trotter VV, Chen Y, et al. Functional genetics of human gut commensal *Bacteroides thetaiotaomicron* reveals metabolic requirements for growth across environments. *Cell Rep.* (2021) 34:108789. doi: 10.1016/j.celrep.2021.108789

frontiers | Frontiers in Nutrition

TYPE Original Research
PUBLISHED 26 September 2022
DOI 10.3389/fnut.2022.1003763

OPEN ACCESS

EDITED BY
Jie Yin,
Hunan Agricultural University, China

REVIEWED BY
Gong Yujie,
Henan Agricultural University, China
Tiantian Li,
Academy of State Administration of Grain, China

*CORRESPONDENCE
Yingping Xiao
xiaoyp@zaas.ac.cn

SPECIALTY SECTION
This article was submitted to Nutrition and Microbes, a section of the journal Frontiers in Nutrition

RECEIVED 26 July 2022
ACCEPTED 01 September 2022
PUBLISHED 26 September 2022

CITATION
Song Y, Chen K, Lv L, Xiang Y, Du X, Zhang X, Zhao G and Xiao Y (2022) Uncovering the biogeography of the microbial commmunity and its association with nutrient metabolism in the intestinal tract using a pig model. *Front. Nutr.* 9:1003763. doi: 10.3389/fnut.2022.1003763

Uncovering the biogeography of the microbial commmunity and its association with nutrient metabolism in the intestinal tract using a pig model

Yuanyuan Song[1,2], Kai Chen[3], Lu Lv[1], Yun Xiang[4], Xizhong Du[4], Xiaojun Zhang[4], Guangmin Zhao[1] and Yingping Xiao[1]*

[1]State Key Laboratory for Managing Biotic and Chemical Threats to the Quality and Safety of Agro-products, Institute of Agro-product Safety and Nutrition, Zhejiang Academy of Agricultural Sciences, Hangzhou, China, [2]Key Laboratory of Vector Biology and Pathogen Control of Zhejiang Province, School of Life Sciences, Huzhou University, Huzhou, China, [3]Quality and Safety of Animal Products Group, Zhejiang Center of Animal Disease Control, Hangzhou, China, [4]Institute of Animal Husbandry and Veterinary Medicine, Jinhua Academy of Agricultural Sciences, Jinhua, China

The gut microbiota is a complex ecosystem that is essential for the metabolism, immunity and health of the host. The gut microbiota also plays a critical role in nutrient absorption and metabolism, and nutrients can influence the growth and composition of the gut microbiota. To gain a better understanding of the relationship between the gut microbial composition and nutrient metabolism, we used a pig model by collecting the contents of the different intestinal locations from six pigs to investigate microbial composition in different intestinal locations based on 16S rRNA gene sequencing and the concentrations of short-chain fatty acids (SCFAs), amino acids, fat, and crude ash in different intestinal locations using gas chromatography and chemical analysis. The results showed that the richness and diversity of intestinal microbial communities gradually increased from the small intestine to the large intestine. The relative abundance of Proteobacteria was higher in the jejunum and ileum, whereas the proportion of Firmicutes was higher in the cecum and colon. The concentrations of SCFAs were higher in the cecum and colon ($P < 0.05$). The concentrations of amino acids were higher in the small intestine than in the large intestine, while the amino acid content was significantly higher in the ascending colon than in the transverse colon and descending colon. The correlation analysis revealed that *Ruminococcaceae UCG-005*, *Coriobacteriaceae_uncultured*, *[Eubacterium] hallii* group, *Mogibacterium* and *Lachnospiraceae AC2044* group had a higher positive correlation with SCFAs, crude ash and fat but had a negative correlation with amino acids in different gut locations of pigs. These findings may serve as fundamental data for using nutrient metabolism to regulate human and animal gut microbes and health and provide guidance for exploring host-microbe bidirectional interaction mechanisms and driving pathways.

KEYWORDS

gut microbiota, short-chain fatty acids, nutrients, amino acid, intestinal tract

Introduction

The gastrointestinal tract (GIT) is the largest interface between the external and internal environments and contains the largest amount and the greatest diversity of microorganisms. Humans and mammals are colonized with a vast and complex microbial community, which is known to play an important role in host metabolism, including digestion and absorption of nutrients, energy acquisition, carbohydrate metabolism and the immune system (1–4). Along the longitudinal axis of the intestinal lumen, distinct microhabitats selectively harbor characteristic microbes (5, 6).

The gut microbiota can directly affect the utilization and absorption of nutrients, including carbohydrates, lipids, proteins and minerals, and are also regulated by the host nutrition (6–9). SCFAs are produced by gut saccharolytic microbes through fermenting and degrading indigestible carbohydrate (10, 11), which can provide energy for intestinal epithelial cells and serve as an energy source for the growth of anaerobic bacteria (12, 13). *Lachnospiraceae_uncultured* may be a potential beneficial bacterium involved in the metabolism of a variety of carbohydrates, and the fermentation product acetic acid is the main source of bacteria that provides energy for the host. The fermentation metabolites of *Ruminococcaceae* (*CG-004*, *05*, *013*, *014*) are mainly acetic acid and formic acid, and bacteria in the Prevotella-dominated enterotype mainly absorb monosaccharides and degrade mucins to obtain energy (14, 15). Some species of the genus *[Eubacterium] rectale* group can ferment carbohydrates in food and produce large amounts of acetic acid and butyric acid (16). In addition, acetate produced by *Bacteroides*, *Bifidobacterium*, *Prausnitzii*, and *Ruminococcus* acts on the brain through the blood–brain barrier (17). The gut microbiota may play important roles in the host amino acid balance and health through multiple pathways (18, 19). Bacteria have various metabolic pathways for amino acid metabolism, such as the synthesis of cellular proteins and amino acid catabolism (20). Studies have shown that small intestinal bacteria may mainly utilize amino acids for the synthesis of bacterial proteins, while large intestinal bacteria mainly use them for catabolism (21). Bacteria in the rumen and large intestine of animals and humans can degrade amino acids in large quantities. *Clostridium* can degrade amino acids through the Stickland reaction, and the main metabolites are branched-chain fatty acids and ammonia (22). Some studies have shown that amino acid metabolism by intestinal bacteria is ultimately performed for their survival and growth in the complex intestinal environment. For example, Lactobacillus can synthesize bacterial proteins by utilizing exogenous amino acids, which have an important role in host nutrition and physiology (23). The gut microbiota also synthesizes many essential amino acids, such as lysine, threonine, and arginine. For example, some intestinal microorganisms are able to bind NH_3 from the breakdown of amino acids and resynthesize essential amino acids or proteins (24).

In recent years, numerous studies have shown a correlation between the gut microbiota and host metabolism (25–30), but the impact of the gut microbiota on nutrient metabolism remains unclear, and few studies have examined the metabolic compartmentalization of nutrients in different locations of the intestinal tract. Pigs are very similar to humans in terms of gastrointestinal tract development, physiology, digestive function and composition, the gut microbiota of pigs is 96% similar to humans in functional pathway (31–34). The minimum nutritional requirement of pigs is equivalent to the daily nutritional requirement of humans and the common physiological structure leads to a similar digestive tract transit time and nutrient absorption process, the pigs also can collect repeated measurement data (35). So pigs are an ideal model for studying human gut microbiota and nutrient metabolism. Herein, we investigated the intestinal microbiota structure in different parts of pigs and analyzed its association with the concentrations of SCFAs, amino acids, fat, and crude ash in different intestinal locations. The present findings could provide insights into the association between the microbial community and nutrient metabolism with gut homeostasis and whole-body health in humans and mammals.

Materials and methods

Ethics statement

All animal experiments were approved by the Institutional Animal Care of the Zhejiang Academy of Agricultural Sciences in accordance with the relevant rules and regulations (ZAAS-2017-009).

Animal experiments and sample collection

Six female Jinhua pigs were randomly selected from the pig farm of Jinhua Academy of Agricultural Sciences, reared in the same environment and fed the same diet daily and water *ad libitum*. The detailed ingredients and nutrient contents of the diet are presented in Table 1. The pigs (71.90 ± 0.82 kg) were killed at the age of 250 days under anesthesia, and then the contents of the jejunum, ileum, cecum, ascending colon, transverse colon, and intermediate descending colon were collected immediately. We collected samples in sterile tubes and quickly frozen them in liquid nitrogen, and then transferred to a refrigerator at−80 °C for future chemical and microbial analyses.

TABLE 1 Composition and nutrient levels of basal diet.

Items	Content		
	D 45∼90	D 91∼150	D 151∼250
Ingredient (%)			
Corn	63.30	63.00	60.94
Soybean meal	28.44	20.99	20.50
Wheat bran	3.90	11.75	13.50
$CaHPO_4$	0.30	1.20	1.20
Limestone	2.00	1.50	1.10
NaCl	0.26	0.26	0.26
Zeolite powder	0.50	1.40	1.40
L-Lysine HCL	0.30	0.20	0.10
Premix[a]	1.00	1.00	1.00
Total	100	100	100
Nutrient level[b] (%)			
Digestible energy/(MJ·kg^{-1})	13.59	13.22	13.21
Crude protein	19.38	16.74	15.15
Calcium	0.87	0.85	0.85
Phosphorus	0.69	0.61	0.58
Lysine	1.12	0.80	0.96
Methionine + Cystine	0.56	0.54	0.57
Threonine	0.75	0.64	0.56
Tryptophan	0.23	0.20	0.18

[a]45 ∼ 90 d The premix included (per kg of the diet): Cu 4.40 mg, Fe 70 mg, Mn 2.44 mg, Zn 67.10 mg, I 0.15 mg, Se 0.3 mg, VA 1 500 IU, VD_3 171.6 IU, VE 10 IU, VK_3 0.8 mg, VB_1 5 mg, VB_2 3.6 mg, VB_6 1.5 mg, VB_{12} 10 mg, pantothenic acid 10 mg, nicotinic acid 30 mg, folic acid 300 mg, biotin 50 mg; 91 ∼ 150 d: Cu 3.80 mg, Fe 55 mg, Mn 2.14 mg, Zn 58.10 mg, I 0.14 mg, Se 0.23 mg, VA 1 300 IU, VD_3 158.6 IU, VE 8 IU, VK_3 0.8 mg, VB_1 5 mg, VB_2 3.6 mg, VB_6 1.5 mg, VB_{12} 10 mg, pantothenic acid 7.49 mg, nicotinic acid 20 mg, folica cid 280 mg, biotin 50 mg; 151 ∼ 250 d:Cu 3.40 mg, Fe 9940 mg, Mn 1.44 mg, Zn 55.10 mg, I 0.14 mg, Se 0.17 mg, VA 1 286 IU, VD_3 149.5 IU, VE 7 IU, VK_3 0.8 mg, VB_1 5 mg, VB_2 3.6 mg, VB_6 1.5 mg, VB_{12} 10 mg, folic acid 260 mg, pantothenic acid 7.11 mg, nicotinic acid 10 mg, biotin 50 mg.

[b]DE, CP, Ca, TP, Lys and Met + Cys were calculated values.

DNA extraction, sequencing, and data analysis

The CTAB/SDS method was used to extract genomic DNA from 36 samples. DNA concentration and purity were monitored on a 1% agarose gel and DNA was diluted to 1 ng/μl using sterile water according to the concentration. The 16S rRNA gene V4-V5 region was amplified using primers (515F: 5′- GTGCCAGCMGCCGCGGTAA-3′; 907R: 5′-CCGTCAATTCCTTTGAGTTT-3′) with barcodes. All PCRs were conducted in 30 μL reactions with 15 μL of Phusion® High-Fidelity PCR Master Mix (New England Biolabs), 0.2 μM forward and reverse primers, and approximately 10 ng of template DNA. Initially, the samples were denaturated at 98 °C for 1 min, followed by 30 cycles of denaturation at 98 °C for 10 s, annealing at 50 °C for 30 s, elongation at 72 °C for 60 s and finally 72 °C for 5 min. We used A GeneJET Gel Extraction Kit (Thermo Scientific) to purify the PCR mixture and NEB Next® Ultra™ DNA Library Prep Kit for Illumina (NEB, Ipswich, MA, USA) to prepare sequencing libraries following the manufacturer's recommendations, and index codes were added. The Illumina paired-end reads were filtered and demultiplexed (36), merged into tags using FLASH, and assorted to each sample according to the attached barcode (37).

The RDP classifier was used to performs taxonomy assignment of the OTUs (38). We calculated and visualized the alpha diversity (Chao 1 estimator, Shannon, and Simpson indices) using GraphPad Prism 8 (GraphPad software, San Diego, CA, USA). The differences in microbial communities in different intestinal segments using principal coordinate analysis (PCoA). An analysis of linear discriminant analysis (LDA) coupled with effect size (LEfSe) were carried out to identify differentially abundant features between groups (39).

SCFA measurement

As described in our previous study, the concentrations of SCFAs in intestinal contents were detected by gas chromatography (40, 41). Briefly, 0.1 g intestinal contents of each bowel segment were weighed into a 1.5–mL centrifuge tube and suspended in Milli-Q water (9 volumes). After centrifugation (12 000 rpm, 10 min), the supernatant (0.5 mL) was collected and mixed with 0.1 mL of 25% (w/v) metaphosphoric acid and crotonic acid solution and stored at −20 °C overnight. The samples were filtered with a microporous membrane (0.22 μm), and the continuous filtrate was collected for analysis. The levels of SCFAs in each bowel content were determined using gas chromatography (GC) (Shimadzu, Kyoto, Japan), and the chromatographic column was a capillary column (InertCap FAPF). The chromatographic conditions were as follows: FID detector operating at 180 °C, column at 110 °C, vaporization chamber at 180 °C, and carrier gas nitrogen at 0.06 MPa, while the auxiliary gas consisted of hydrogen and air at pressure of 0.05 MPa and 0.05 MPa, respectively.

Chemical analysis

Samples of intestinal contents were freeze-dried. The procedure set by the Association of Official Analytical Chemists (AOAC, 2000) was used to determine the concentrations of moisture, crude fat and crude ash. We used a Hitachi L-8900 amino acid analyzer (Hitachi, Tokyo, Japan) to determine the contents of all the amino acids following acid hydrolysis as described by AOAC (2000) (42).

Co-occurrence network analysis

Based on Spearman's correlation matrices, correlation networks were analyzed between the relative abundance of bacterial abundance at the genus level and the content of SCFAs, amino acids, fat, crush ash, and moisture at different gut locations in pigs. An analysis of network structures was performed using Gephi v0.9.2 software (43).

Data analysis

We used GraphPad Prism 8 software to perform one-way analysis of variance (ANOVA). Data were expressed as means ± standard deviations (SD), and a P value < 0.05 was set as the level of statistical significance.

Results

Bacterial diversity

A total of 1,492,547 high-quality reads were generated from the 36 samples and were classified into 16,191 bacterial OTUs. Alpha diversity was observed in different gut locations. The samples from the large intestine (cecum and colon) had significantly higher Chao and Shannon indices than samples from the small intestine (jejunum and ileum) (Table 2, $P < 0.05$), suggesting that the richness and diversity of intestinal microbiota communities in pigs gradually increased from the small intestine to the large intestine in the digestive tract.

To measure the similarity between microbiota communities, a principal coordinate analysis (PCoA) was performed and revealed distinct clustering of the microbiota compositions of the different gut locations in pig (Figure 1). The community structures observed in the large intestine were significantly different from those detected in the small intestine.

Microbial community composition in different intestinal locations

To reveal the microbial composition in different intestinal locations, we calculated the abundances of the top 6 phyla and the top 10 genera in all pig samples. The dominant phyla were Firmicutes, Bacteroidetes, and Proteobacteria. Firmicutes was the most dominant phylum in different intestinal segments, representing 64.36 to 82.81% of the total microbial population in pigs (Figure 2). However, the abundance of Firmicutes (64.36%) in the jejunum was lower than that in other intestinal segments of pigs (> 70%). Firmicutes and Tenericutes were predominant in the cecum and colon of pigs and made up a smaller percentage in the jejunum and ileum. Otherwise, the abundance of Proteobacteria in the small intestine was significantly higher, ranging from 13.62 to 16.32% in the jejunum and ileum. At the genus level, the most abundant genera appeared to be very diverse in different guts. *Lactobacillus*, *Clostridium sensu stricto1*, *Bacteroidales S24-7* group norank, and *Ruminococcaceae UCG-005* were the dominant genera. *Lactobacillus* was present at higher levels in the small intestine than in the large intestine, and *Ruminococcaceae UCG-005* and *Mollicutes RF9_norank* were more abundant in the large intestine. The ileum had a higher abundance of *Lactobacillus* (46.30%) than the jejunum, cecum and colon.

A clustered heatmap based on the 50 most dominant genera is shown in Figure 3. The most abundant genera in the jejunum were *Sarcina*, *Bacteroides*, and *Faecalibacterium*, and the proportions of *Escherichia-Shigella*, *Lactobacillus*, and *Veillonella* were notably increased in the ileum. *Alloprevotella* and *Prevotellaceae* were the predominant genera in the cecum. For the different colon segments, the genera *Prevotellaceae NK3B31* group and *Prevotella 1* were considerably more abundant in the ascending colon; *Blautia, Marvinbryantia,* and *Mogibacterium* were enriched in the transverse colon; and *Christensenellaceae R-7* group, *Coriobacteriaceae_uncultured*, and *Ruminococcaceae UCG-013* had a relatively high relative abundance of bacteria in the descending colon.

To further explore the specificity of the distribution of microflora in each intestinal segment, LEfSe analysis was used to identify the genera with a differential abundance between the small and large intestine, and then the analysis identified differentially abundant genera in different colon segments. In the large intestine, a total of 57 genera were significantly enriched, while only 22 genera were enriched in the small intestine (Figure 4A). The relative abundances of *Acetobacter*, *Veillonella*, *Bacteroides*, *Erysipelotrichaceae_uncultured*, *Xylella* and *Faecalibaculum* were more abundant in the small intestine, while the abundances of *Ruminococcaceae UCG-005*, *Mollicutes RF9*_norank, *Christensenellaceae R-7* group, *Lachnospiraceae XPB1014* group, *Streptococcus*, *Terrisporobacter* and *Ruminococcaceae UCG-014* were significantly higher in the large intestine. Concerning the different colon segments, the descending colon had higher proportions of *Ruminococcaceae UCG-005*, whereas *Terrisporobacter*, *Clostridium sensu stricto 1*, *Romboutsia*, *Turicibacter*, *Ruminococcaceae UCG-008*, *Coprococcus 1*, and *Lachnospiraceae AC2044* group were enriched in the transverse colon. In addition, *Prevotellaceae NK3B31* group, *Treponema 2*, *Ruminiclostridium 5*, *Prevotellaceae UCG-001*, *Bacteroides*, and *Prevotella 1* were more abundant in the ascending colon (Figure 4B).

TABLE 2 Diversity of sequencing data of pig intestinal contents from different intestinal segments.

Sample ID	Reads	OTU	Chao	Shannon	Simpson
Jejunum	38 050 ± 2 228	420 ± 100^{bc}	420 ± 100.31^{bc}	3.88 ± 0.429^{b}	0.08 ± 0.021 2^{b}
Ileum	42 087 ± 3 873	243 ± 35^{c}	243 ± 35.31^{c}	2.75 ± 0.276^{c}	0.22 ± 0.071 7^{a}
Cecum	39 370 ± 2 771	434 ± 35^{ab}	434 ± 35.22^{ab}	4.41 ± 0.229^{ab}	0.05 ± 0.015 1^{b}
Ascending colon	46 195 ± 2 939	607 ± 30^{a}	607 ± 29.96^{a}	4.91 ± 0.158^{a}	0.03 ± 0.006 9^{b}
Transverse colon	41 266 ± 4 233	501 ± 38^{ab}	501 ± 37.70^{ab}	4.62 ± 0.146^{ab}	0.04 ± 0.009 1^{b}
Descending colon	41 790 ± 3 545	495 ± 39^{ab}	495 ± 38.53^{ab}	4.57 ± 0.189^{ab}	0.04 ± 0.010 7^{b}

All data are presented as the mean ± standard deviation (*SD*, $n = 6$). The same letters in each column indicate no significant difference ($p > 0.05$).

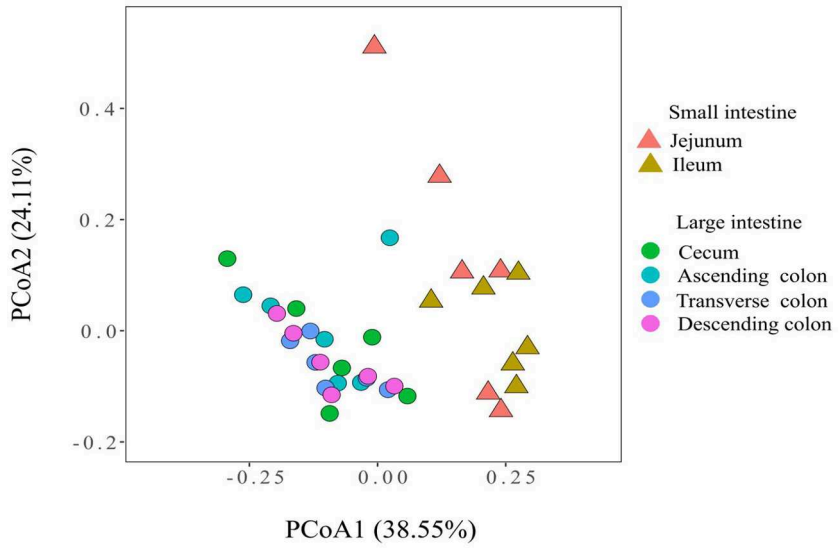

FIGURE 1
Principal coordinate analysis of the microbial communities based on the weighted UniFrac distance.

SCFAs in different intestinal locations and their correlation with the microbial community

The total levels of SCFAs were significantly higher in the cecum and colon (Figure 5) ($P < 0.05$), and acetic acid, propionic acid, and butyric acid were the main metabolic products of the microbiota. To better understand the interaction between the microbiota and SCFAs, Spearman's correlation analysis was used to assess the association between the top 100 genera and SCFAs in different intestinal segments (Figure 6). The genera *[Eubacterium] hallii* group, *Mogibacterium*, *Ruminococcaceae UCG-005*, *Ruminococcaceae UCG-004*, *Pseudobutyrivibrio*, *Marvinbryantia*, *Catenisphaera*, *[Eubacterium] coprostanoligenes* group, and *Lachnospiraceae AC2044* group were positively correlated with a variety of SCFAs. The genera *Ruminococcaceae UCG-014*, *Ruminococcaceae UCG-013* and *Coriobacteriaceae_uncultured* also had a positive correlation with valeric acid, isovaleric acid, isobutyric acid, butyric acid, and propionic acid. Furthermore, *Brevundimonas and Pandoraea* showed a negative correlation with the contents of all kinds of SCFAs.

Nutrients in different intestinal locations and their correlation with the microbial community

The proportion of crude ash in the large intestine was significantly greater than that in the small intestine, and the colon had the highest content of crude ash (Figure 7) ($P < 0.05$). Additionally, the colon had a lower moisture content and approximately the same fat content in each intestinal segment. Next, we performed a network correlation (Figure 8) to analyze the association of the top 100 genera with nutrients in different intestinal segments of pigs. The genera *[Eubacterium] hallii* group, *Lachnospiraceae AC2044* group,

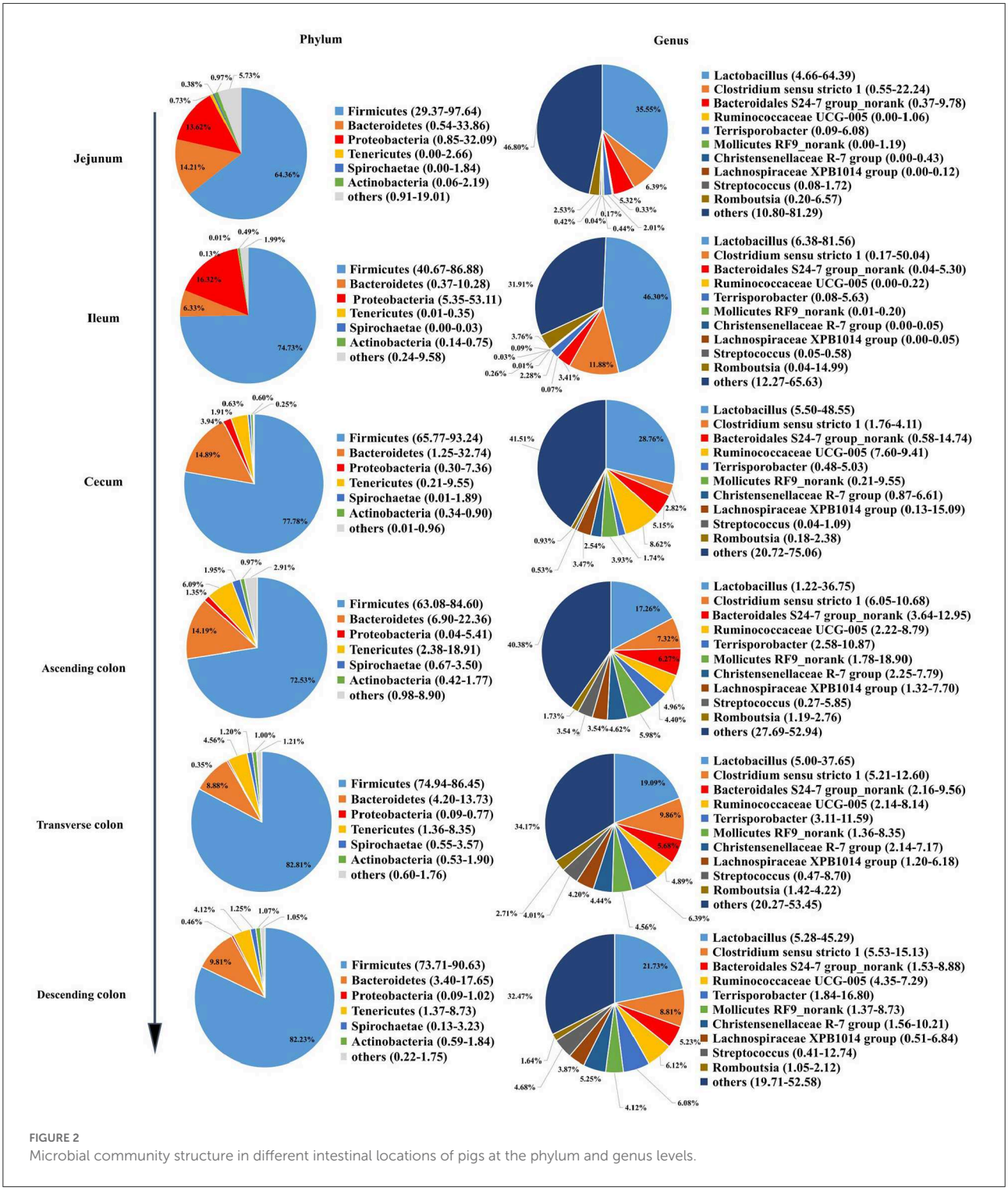

FIGURE 2
Microbial community structure in different intestinal locations of pigs at the phylum and genus levels.

Ruminococcaceae UCG-005, *Coriobacteriaceae_uncultured*, *Mogibacterium*, *Ruminococcaceae UCG-013*, *Terrisporobacter*, *Lachnospiraceae NK4A136* group, *Peptococcus*, *Turicibacter*, *Subdoligranulum and Marvinbryantia* showed a positive correlation with the contents of fat and crude ash, whereas the genera *Brevundimonas*, *Veillonella*, and *Rhodobacter* had a negative correlation.

The amino acid content in the small intestine was higher than that in the large intestine, while the amino acid content in the ascending colon was significantly higher than that

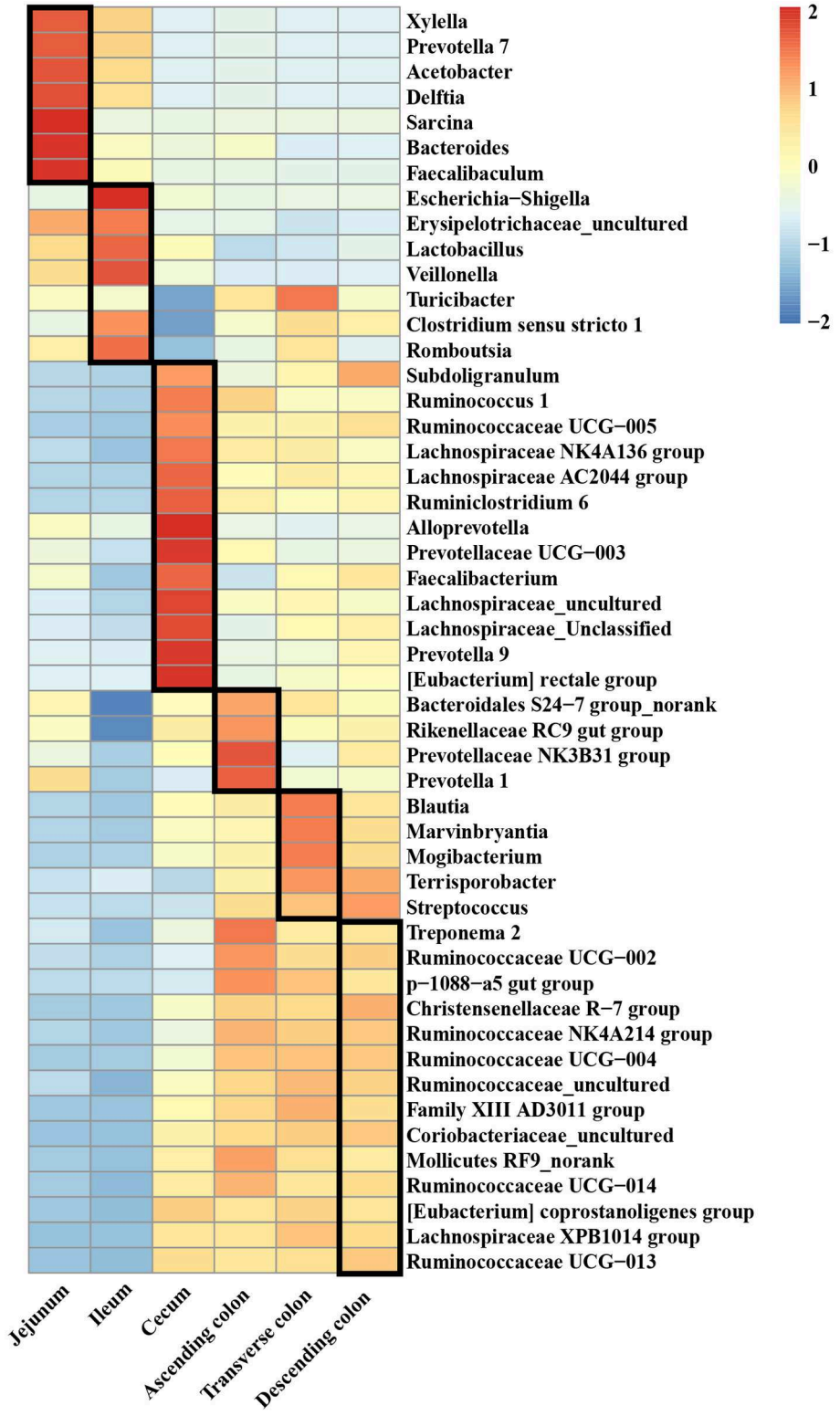

FIGURE 3
The top 50 genera in different intestinal locations of pigs.

FIGURE 4
Differentially represented genera in different intestinal locations of pigs identified by LEFSe using an LDA score threshold of > 2.5. **(A)** plots the discriminative genera enriched in the small and large intestine, **(B)** plots the discriminative genera enriched in different colon segments. The vertical axis represents the names of different genera, and the colors correspond to different intestinal locations.

in the transverse colon and descending colon (Figure 9) ($P < 0.05$). Then, a network correlation (Figure 10) was used to analyze the association of the top 100 genera with amino acids in the colon. The genera *Dorea*, *Marvinbryantia*, *Terrisporobacter*, *Romboutsia*, *[Eubacterium] rectale* group, and *[Eubacterium] hallii* group showed a negative correlation

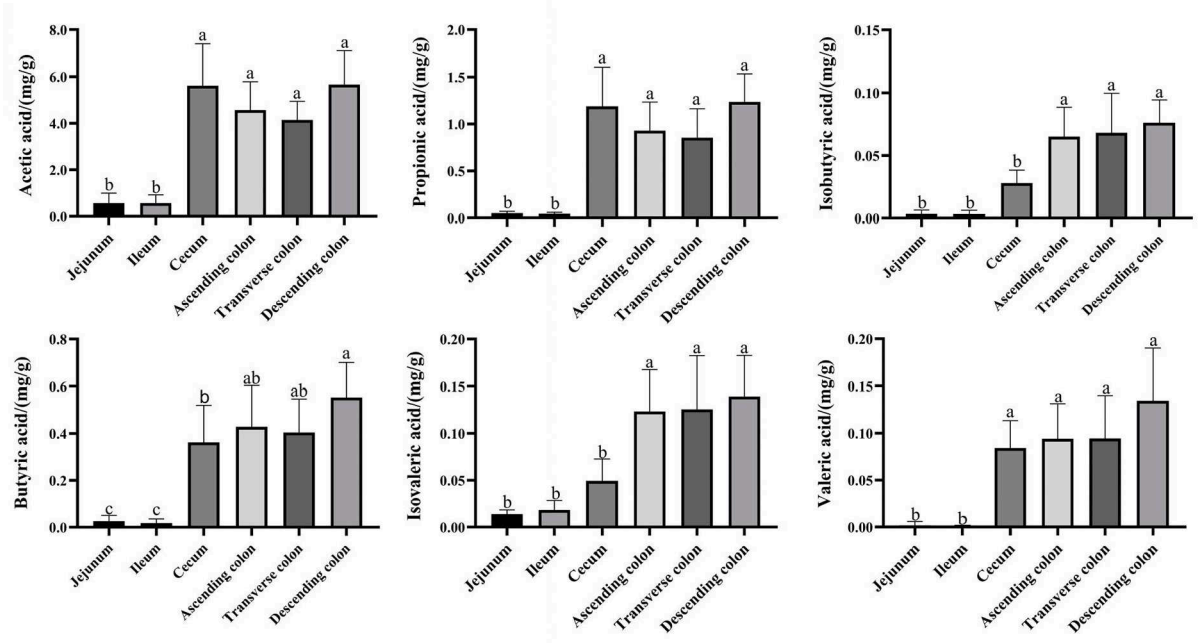

FIGURE 5
Concentrations of SCFA in different intestinal locations of pigs. Data are shown as mean ± *SD* ($n = 6$). The same letter within each column indicates no significant difference ($p > 0.05$).

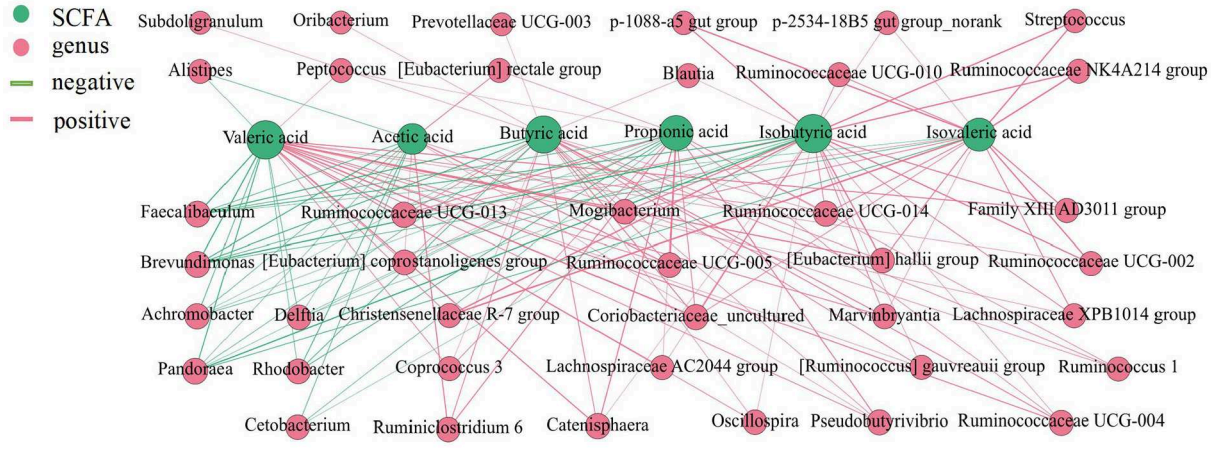

FIGURE 6
Correlation analysis between the microbial community and the concentrations of SCFAs in the intestine of pigs. The association between the top 100 genera and SCFAs were analyzed using Spearman's correlation method. The node size is proportional to the number of connections.

with the content of a variety of amino acids, indicating a robust contribution to the synthesis of amino acids. The genus *Ruminococcaceae UCG-005* was negatively correlated with histidine, *Lachnospiraceae AC2044* group, *Coriobacteriaceae_uncultured* and *Mogibacterium* and had a negative correlation with isoleucine and phenylalanine. The genera *Lachnoclostridium*, *Vibrio*, *Parabacteroides*, and *Treponema 2* showed a positive correlation with the contents of various amino acids.

The genera *Ruminococcaceae UCG-005*, *[Eubacterium] hallii* group, *Lachnospiraceae AC2044* group, *Coriobacteriaceae_uncultured* and *Mogibacterium* clearly showed a positive correlation with the contents of SCFA, fat, and crude ash and a negative correlation with amino

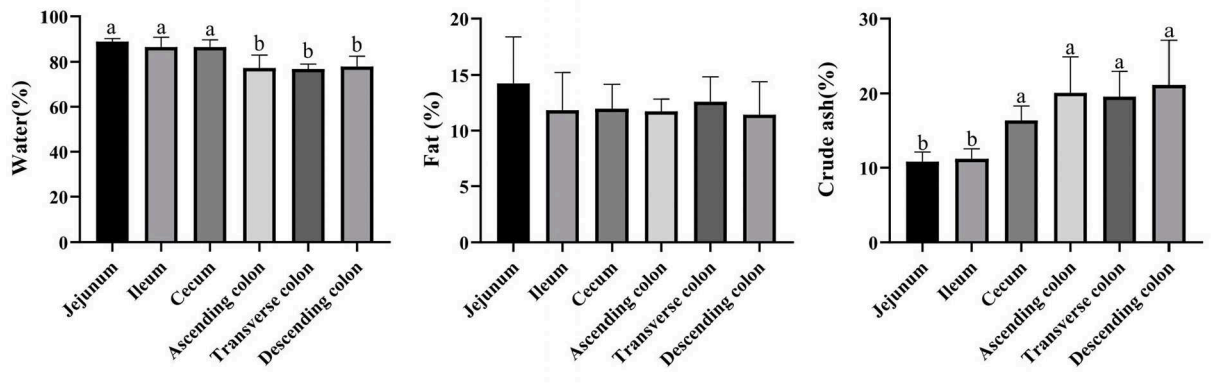

FIGURE 7
Concentrations of moisture, fat, and crude ash in different intestinal locations of pigs. The concentration of fat and crude ash was based on the dry matter of the intestinal contents. Data are shown as mean ± *SD* ($n = 6$). The same letter within each column indicates no significant difference ($p > 0.05$).

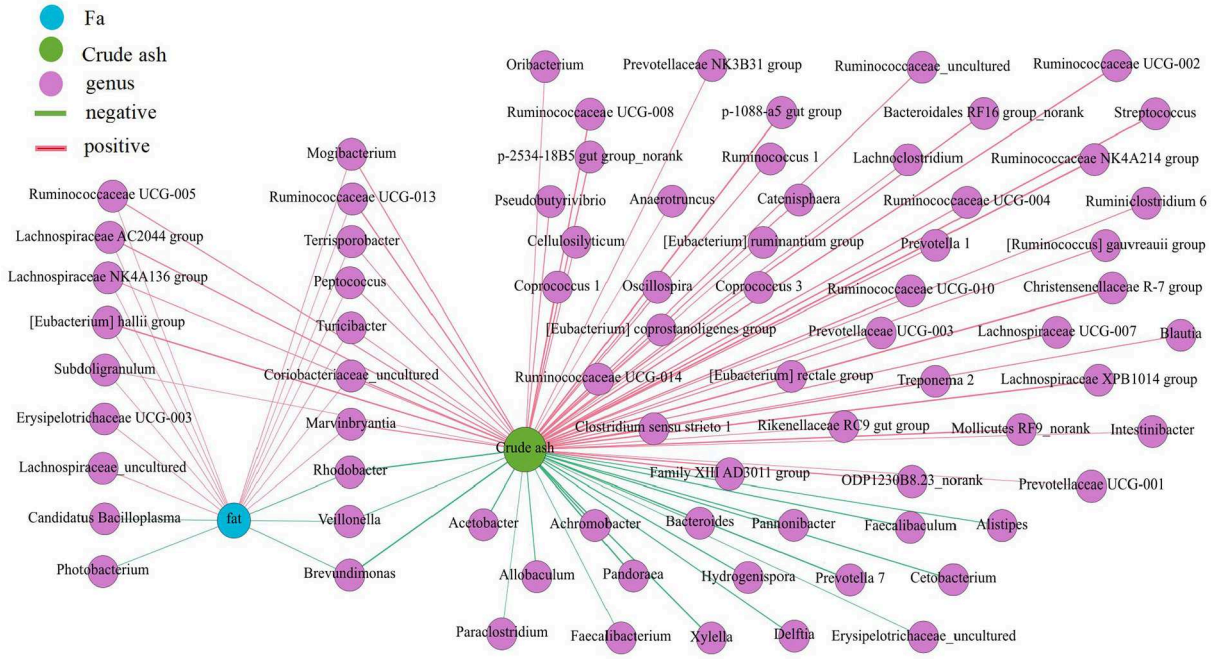

FIGURE 8
Correlation analysis between the microbial community and the concentration of fat and crude ash in intestine of pigs. The association between the top 100 genera and the fat and crude ash were analyzed using Spearman's correlation method. The node size is proportional to the number of connections.

acids. Then, we analyzed the relative abundance of these genera in different intestinal locations. The results showed that *Ruminococcaceae UCG-005*, *[Eubacterium] hallii* group, *Lachnospiraceae AC2044* group, *Coriobacteriaceae_uncultured* and *Mogibacterium* were more abundant in the colon and cecum than in the jejunum and ileum (Figure 11) ($P < 0.05$).

Discussion

The intestinal tract of humans and mammals is colonized by a dense and highly complex microbial community composed mainly of bacteria, which form a relatively dynamic and stable microecosystem in the intestinal environment and play an important role in the growth and health of the host (44–46).

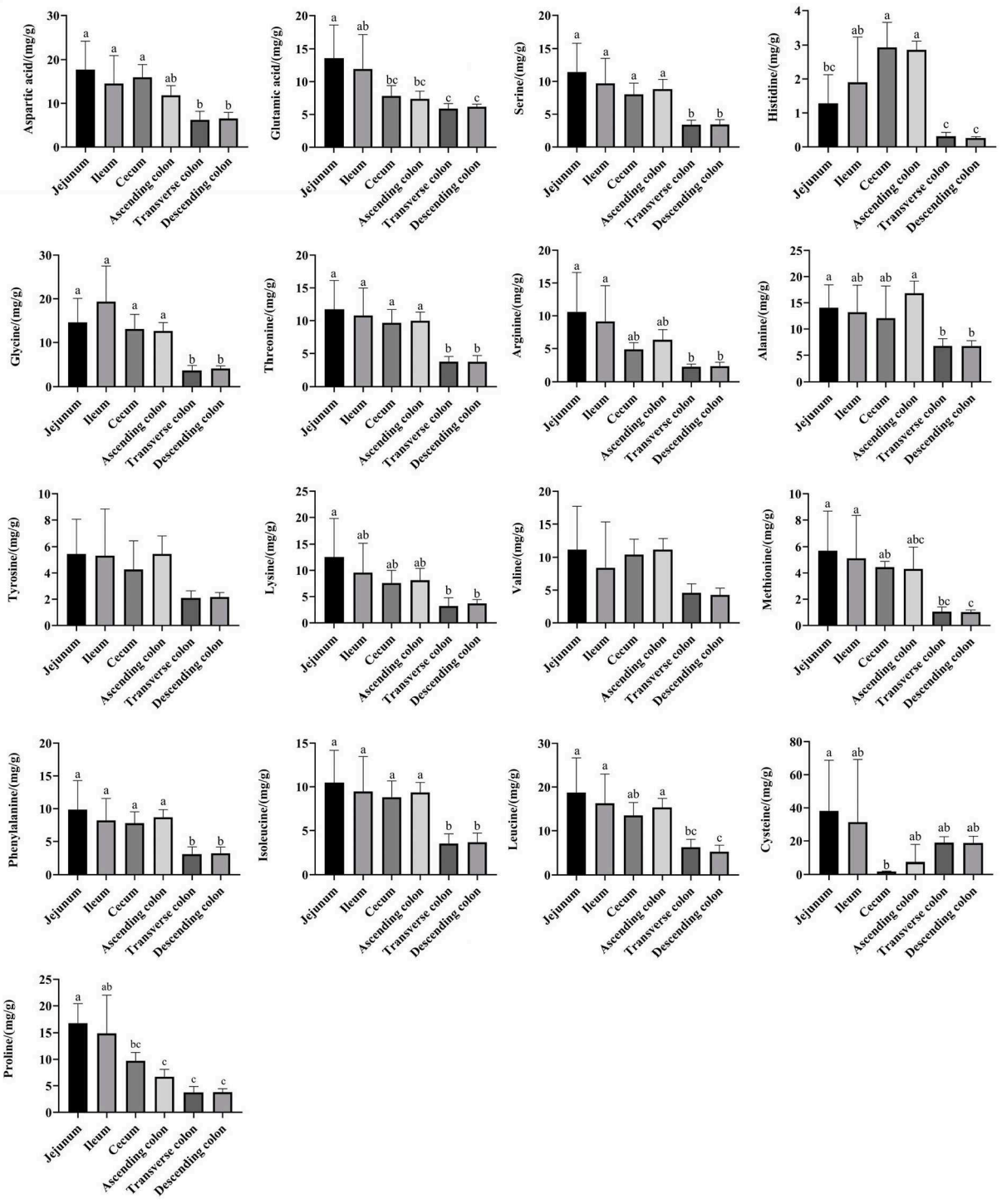

FIGURE 9
The concentrations of amino acids in different intestinal locations of pigs. The concentration was based on the dry matter of the intestinal contents. Data are shown as mean ± *SD* ($n = 6$). The same letter within each column indicates no significant difference ($p > 0.05$).

The intestinal microbiota is involved in nutrient absorption, metabolism and storage (47). Previous studies have shown that the intestinal microbiota contribute a lot in regulating the nutrient metabolism of hosts and maintaining energy balance (28, 48, 49). Due to the similarity between the human and pig microbiota and the knowledge that approximately 96%

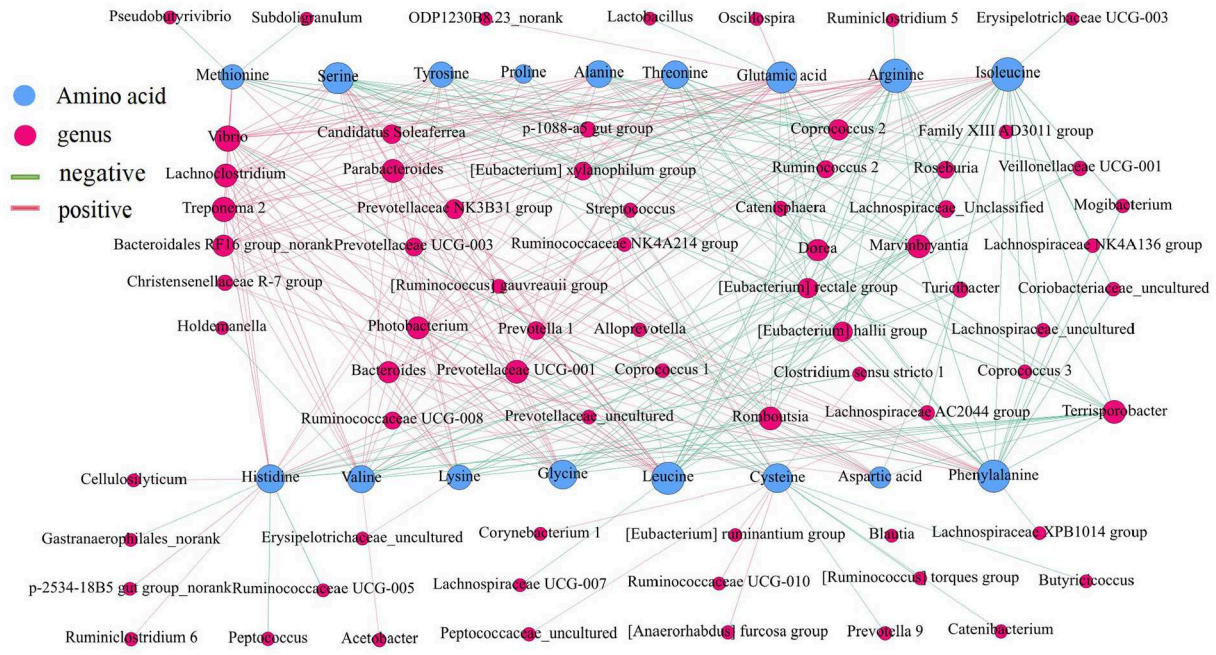

FIGURE 10
Correlation analysis between the microbial community and the concentrations of amino acids in the intestine of pigs. The association between the top 100 genera in the colon and the amino acids was analyzed using Spearman's correlation method. The node size is proportional to the number of connections.

similarity of the functional pathways between the human and pig gut microbiota (34, 50), in this study, we used the pig as a model to analyze the microbial composition and contents of SCFA, amino acids, fat, and crude ash in different intestinal locations to explore the correlation between the intestinal microbiota and the metabolism and absorption of nutrients.

The diversity and abundance of the microbiota were higher in the large intestine than in the small intestine; simultaneously, the microbiota in the colon was the richest and the most diverse, which was consistent with the results of a previous study showing that the richness and diversity of the microbiota gradually increased along the digestive tract from the duodenum to the colon (51). PCoA showed that the microbiota in the small intestine clearly differed from that in the large intestine, which might be closely related to the physiological functions of each intestinal segment. Additionally, each region harbor specific microbial community (52). Proteobacteria were predominant in the jejunum and ileum and made up a smaller percentage in the cecum and colon, whereas the proportion of Firmicutes was higher than in the cecum and colon, which was consistent with the findings of several previous studies on the distribution of different intestinal microbiota in pigs (1) (53, 54). In contrast, the relative abundance of *Acetobacter*, *Veillonella*, *Bacteroides*, *Erysipelotrichaceae_uncultured*, *Xylella* and *Faecalibaculum* were higher in the small intestine of pigs, while *[Eubacterium]*, *Ruminococcaceae*, *Mollicutes*, *Christensenellaceae*, *Lachnospiraceae*, *Streptococcus*, *Terrisporobacter* and *Ruminococcaceae* were enriched in the large intestine. The main reason for the unique microbiota in the difficult intestine is that from the proximal small intestine to the large intestine, a strong pH gradient and a large oxygen gradient can be observed (55, 56). The small intestine is a harsh microenvironment formicrobial life because of the shorter transit time and lower pH values and there is an increased proportion of aerobic or facultative anaerobic bacteria. In contrast, the large intestine dominantly hosts a number of anaerobic bacteria (57). Moreover, within the same intestinal segment, the distribution of bacteria in different spaces was also distinct. In this study, diversity of the microbial composition was found in different colonic locations, with the descending colon containing higher proportions of the *Ruminococcaceae UCG-005* while the transverse colon was enriched with *Terrisporobacter*, *Clostridium sensu stricto 1*, *Romboutsia* and *Turicibacter*, and the ascending colon had greater abundances of *Prevotellaceae NK3B31* group, *Treponema 2*, *Ruminiclostridium 5*. Numerous investigations have been conducted to examine the intestinal microbiota in different human intestinal segments and have shown that the jejunum is mainly composed of gram-positive aerobic bacteria, including *Lactobacillus*, *Streptococcus* and *Staphylococcus*; the number of ileal anaerobic bacteria exceeds aerobic bacteria; and more than

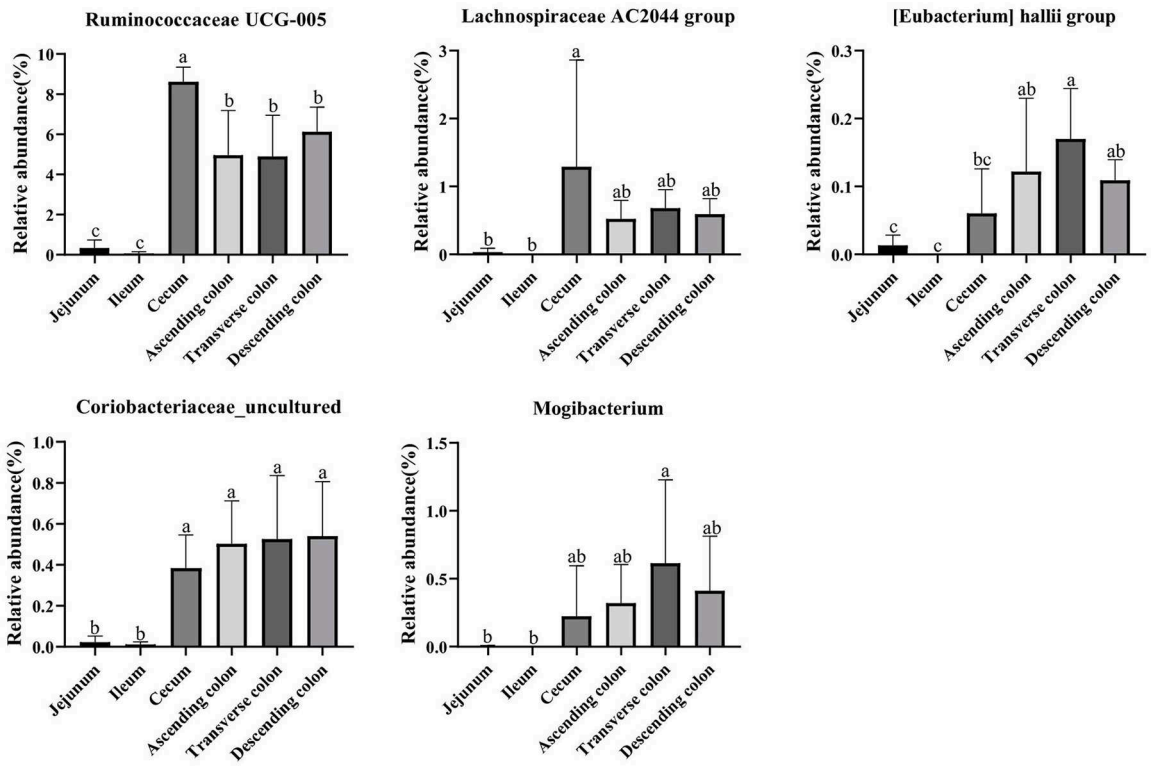

FIGURE 11
The relative abundance of *Ruminococcaceae UCG-005*, *[Eubacterium] hallii* group, *Lachnospiraceae AC2044* group, *Coriobacteriaceae_uncultured* and *Mogibacterium* in different intestinal locations of pigs. Data are shown as mean ± *SD* ($n = 6$). The same letter within each column indicates no significant difference ($p > 0.05$).

98% of the colon contains obligate anaerobic bacteria, mainly *Bacteroides*, *Bifidobacterium*, and *Eubacterium* (56, 58, 59). The similarity of bacterial structure leads to the similar nutrient absorption process between pigs and human sand the colon is the main place of bacterial fermentation between pigs and humans (35, 60), therefore the application of pigs in human nutrition model models is increasingly gaining traction.

SCFAs are considered indirect microbial metabolism substrates and involved in the regulation of energy metabolism, immunity, adipose tissue expansion and modulation of cancer cell development (61, 62). In our study, the concentrations of SCFA were higher in the large intestine than in the small intestine due to the slower rate of flow in the large intestine and metabolism favoring fermentation of indigestible carbohydrates; additionally, the anaerobic state of the colon provides an ideal environment for anaerobic digestion (56, 63). Previous studies have reported that anaerobic bacteria in the colon ferment undigested carbohydrates from the small intestine to produce SCFAs. Propionic acid is the main product of Bacteroidetes fermentation, and butyric acid is mainly produced by the metabolism of Firmicutes (64), in accordance with our findings. The genera *Ruminococcaceae* (*UCG-004*, *UCG-005*, *UCG-014*, *UCG-013*), *Coriobacteriaceae_uncultured*, *[Eubacterium]* (*hallii* group, *coprostanoligenes* group), *Mogibacterium*, *Pseudobutyrivibrio*, *Marvinbryantia*, *Catenisphaera*, and *Lachnospiraceae AC2044* group had a positive correlation with a variety of SCFAs based on the network analysis. Simultaneously, these genera were enriched in the large intestine, which suggested that the large intestine was the main region of SCFA production and that these genera were the core bacteria of fiber fermentation.

The crude ash and fat are important indicators to reflect nutrients. The content of crude ash is related to the absorption and utilization of minerals, the gut microbiota can affect the host mineral metabolism and participate in the metabolism of calcium, iron, magnesium, selenium, copper, and zinc (65–67). The fat content is involved in metabolism and body energy reserves and is an important index affecting human health (1, 68). Due to different digestive enzymes in the jejunum, ileum, cecum and colon, there are differences in digestion, absorption and utilization of nutrients in different intestinal locations (45, 56, 69). In our study, the proportion of crude ash in the large intestine was significantly greater than that in the small intestine. The genera *[Eubacterium] hallii* group, *Lachnospiraceae AC2044* group, *Ruminococcaceae UCG-005*,

Coriobacteriaceae_uncultured, and *Mogibacterium* showed a positive correlation with fat and crude ash. The utilization of amino acids is widely distributed among bacteria residing in the digestive tract of humans and animals (18, 70), and the microbial community structure in different intestinal segments affects compartmentalized amino acid metabolism (54). In our study, the amino acid content was higher in the small intestine than the large intestine, while it was significantly higher in the ascending colon than in the transverse colon and descending colon, which is consistent with a previous study showing faster transit and a preference for amino acid metabolism in the small intestine, where the community primarily consisted of rapidly dividing facultative anaerobes such as Proteobacteria and Lactobacillales (71). In contrast, bacteria in the large intestine use amino acids mainly for catabolism. Bacteria in the large intestine of humans and animals can degrade a large number of amino acids, and the products of fermented amino acids, including short-chain and branched-chain fatty acids, can also participate in the energy metabolism of the host (72). The genera *Dorea*, *Marvinbryantia*, *Terrisporobacter*, *Romboutsia*, *[Eubacterium] rectale* group, *[Eubacterium] hallii* group, *Ruminococcaceae UCG-005*, *Lachnospiraceae AC2044* group, *Coriobacteriaceae_uncultured*, and *Mogibacterium* showed a negative correlation with the contents of a variety of amino acids in the colon. Moreover, most of these bacteria were enriched in the transverse colon and descending colon, making a robust contribution to the degradation of amino acids. The genera *Ruminococcaceae UCG-005*, *[Eubacterium] hallii* group, *Lachnospiraceae AC2044* group, *Coriobacteriaceae_uncultured* and *Mogibacterium* showed a positive correlation with the contents of SCFA, fat, and crude ash and a negative correlation with amino acids and these genera were mainly distributed in the colon and cecum.

Conclusion

This work presents the first overview of the microbial community and nutrient metabolism in different intestinal locations using a pig model. The richness and diversity of intestinal microbial communities gradually increased from the small intestine to the large intestine. The concentrations of SCFA were higher in the large intestine than in the small intestine, and the concentrations of amino acids in the small intestine were higher than in the large intestine, while the amino acid content in the ascending colon was significantly higher than those in the transverse colon and descending colon. The *Ruminococcaceae UCG-005*, *Coriobacteriaceae_uncultured*, *[Eubacterium] hallii*, *Mogibacterium*, and *Lachnospiraceae AC2044* group had a positive correlation with the contents of SCFA, fat, and crude ash and a negative correlation with amino acids in different gut locations of pigs. Collectively, these correlation outcomes prompted us to further understand the relationship between the microbiota and nutrient metabolism in different gut environments, which is important for gut health and whole-body homeostasis.

Accession number

The sequencedata of this study have been submitted to the NCBI Sequence Read Archive (SRA) database under the study accession number: PRJNA853391.

Data availability statement

The datasets presented in this study can be found in online repositories. The names of the repository/repositories and accession number(s) can be found below: https://www.ncbi.nlm.nih.gov/, PRJNA853391.

Ethics statement

The animal study was reviewed and approved by (ZAAS-2017-009).

Author contributions

Experiment design: KC, LL, YX, and YS. Animal experiments: YS, XZ, and GZ. Data analysis and visualization: YS, XD, and YX. Roles, writing—original draft, writing—review and editing: YS and YX. All authors contributed to the article and approved the submitted the manuscript.

Funding

This work was supported by the National Natural Science Foundation of China (31972999), Development Center of Animial Husbandry and Agricultural Machinery in Jinhua City (OBANG2021-FW030-ZFCG0321), State Key Laboratory for Managing Biotic and Chemical Threats to the Quality and Safety of Agro-products, Zhejiang Academy of Agricultural Sciences (2010DS700124-ZZ1905).

Conflict of interest

The authors declare that the research was conducted in the absence of any commercial or financial relationships that could be construed as a potential conflict of interest.

Publisher's note

References

1. Armet A, Deehan E, O'Sullivan A, Mota J, Field C, Prado C, et al. Rethinking healthy eating in light of the gut microbiome. *Cell Host Microbe.* (2022) 30:764–85. doi: 10.1016/j.chom.2022.04.016

2. Li M, Zhou H, Pan X, Xu T, Zhang Z, Zi X, et al. Corrigendum: cassava foliage affects the microbial diversity of Chinese indigenous geese caecum using 16s Rrna Sequencing. *Sci Rep.* (2017) 7:46837. doi: 10.1038/srep46837

3. Miao Z, Du W, Xiao C, Su C, Gou W, Shen L, et al. Gut microbiota signatures of long-term and short-term plant-based dietary pattern and cardiometabolic health: a prospective cohort study. *BMC Med.* (2022) 20:204. doi: 10.1186/s12916-022-02402-4

4. Corrigan A, Leeuw Mde, Penaud-Frézet S, Dimova D, Murphy RA. Phylogenetic and functional alterations in bacterial community compositions in broiler ceca as a result of mannan oligosaccharide supplementation. *Applied Environ Microbiol.* (2015) 81:3460–70. doi: 10.1128/AEM.04194-14

5. Yang H, Wu J, Huang X, Zhou Y, Zhang Y, Liu M, et al. Abo genotype alters the gut microbiota by regulating galnac levels in pigs. *Nature.* (2022) 606:358–67. doi: 10.1038/s41586-022-04769-z

6. Forgie A, Drall K, Bourque S, Field C, Kozyrskyj A, Willing B. The impact of maternal and early life malnutrition on health: a diet-microbe perspective. *BMC Med.* (2020) 18:135. doi: 10.1186/s12916-020-01584-z

7. Murakami M, Tognini P, Liu Y, Eckel-Mahan K, Baldi P, Sassone-Corsi P. Gut Microbiota directs Pparγ-driven reprogramming of the liver circadian clock by nutritional challenge. *EMBO Rep.* (2016) 17:1292–303. doi: 10.15252/embr.201642463

8. Pifer R, Russell R, Kumar A, Curtis M, Sperandio V. Redox, amino acid, and fatty acid metabolism intersect with bacterial virulence in the gut. *Proc Natl Acad Sci U S A.* (2018) 115:E10712–E9. doi: 10.1073/pnas.1813451115

9. Hua Y, Yun X, Robinson K, Wang J, Xiao Y. Gut microbiota is a major contributor to adiposity in pigs. *Front Microbiol.* (2018) 9:3045. doi: 10.3389/fmicb.2018.03045

10. Alou MT, Lagier JC, Raoult D. Diet influence on the gut microbiota and dysbiosis related to nutritional disorders. *Human Microbiome J.* (2016) 1:3–11. doi: 10.1016/j.humic.2016.09.001

11. Yao Y, Cai X, Fei W, Ye Y, Zhao M, Zheng C. The role of short-chain fatty acids in immunity, inflammation and metabolism. *Critical Rev Food Sci Nutr.* (2022) 62:1–12. doi: 10.1080/10408398.2020.1854675

12. Stinson L, Geddes D. Microbial metabolites: the next frontier in human milk. *Trends Microbiol.* (2022) 30:408–10. doi: 10.1016/j.tim.2022.02.007

13. Yu H, Kim SH, Noh MY, Lee S, Park Y. Relationship between dietary fiber intake and the prognosis of amytrophic lateral sclerosis in Korea. *Nutrients.* (2020) 12:3420. doi: 10.3390/nu12113420

14. Zhang YJ, Liu Q, Zhang WM, Zhang ZJ, Wang WL, Zhuang S. Gastrointestinal microbial diversity and short-chain fatty acid production in pigs fed different fibrous diets with or without cell wall-degrading enzyme supplementation. *Livestock Ence.* (2018) 207:105–16. doi: 10.1016/j.livsci.2017.11.017

15. Louis P, Hold GL, Flint HJ. The gut microbiota, bacterial metabolites and colorectal cancer. *Nat Rev Microbiol.* (2014) 12:661–72. doi: 10.1038/nrmicro3344

16. Sheridan OP, Martin JC, Lawley TD, Browne HP, Harris HMB, Bernalier-Donadille A, et al. Polysaccharide utilization loci and nutritional specialization in a dominant group of butyrate-producing human colonic firmicutes. *Microb Genom.* (2016) 2: e000043. doi: 10.1099/mgen.0.000043

17. Kaiko G, Ryu S, Koues O, Collins P, Solnica-Krezel L, Pearce E, et al. The colonic crypt protects stem cells from microbiota-derived metabolites. *Cell.* (2016) 16:1708–20. doi: 10.1016/j.cell.2016.05.018

18. Dai Z, Wu G, Zhu W. Amino acid metabolism in intestinal bacteria: links between gut ecology and host health. *Frontiers Biosci.* (2011) 16:1768–86. doi: 10.2741/3820

19. Zhang Z, Mu X, Shi Y, Zheng H. Distinct roles of honeybee gut bacteria on host metabolism and neurological processes. *Microbiol Spect.* (2022) 10:e0243821. doi: 10.1128/spectrum.02438-21

20. Liu Y, Wang X, Hu CA. Therapeutic potential of amino acids in inflammatory bowel disease. *Nutrients.* (2017) 9:920. doi: 10.3390/nu9090920

21. Duca F, Waise T, Peppler W, Lam T. The metabolic impact of small intestinal nutrient sensing. *Nat Commun.* (2021) 12:903. doi: 10.1038/s41467-021-21235-y

22. Agus A, Planchais J, Sokol H. Gut microbiota regulation of tryptophan metabolism in health and disease - sciencedirect. *Cell Host Microbe.* (2018) 23:716. doi: 10.1016/j.chom.2018.05.003

23. Jochems P, Garssen J, van Keulen A, Masereeuw R, Jeurink P. Evaluating human intestinal cell lines for studying dietary protein absorption. *Nutrients.* (2018) 10:3022. doi: 10.3390/nu10030322

24. Metges CC. Contribution of microbial amino acids to amino acid homeostasis of the host. *J Nutr.* (2000) 130:1857S. doi: 10.1093/jn/130.7.1857S

25. Wu C, Lyu W, Hong Q, Zhang X, Yang H, Xiao Y. Gut microbiota influence lipid metabolism of skeletal muscle in pigs. *Front Nutr.* (2021) 8:675445. doi: 10.3389/fnut.2021.675445

26. Zhao G, Xiang Y, Wang X, Dai B, Zhang X, Ma L, et al. Exploring the possible link between the gut microbiome and fat deposition in pigs. *Oxid Med Cell Longev.* (2022) 2022:1098892. doi: 10.1155/2022/1098892

27. Lyu W, Xiang Y, Wang X, Li J, Yang C, Yang H, et al. Differentially expressed hepatic genes revealed by transcriptomics in pigs with different liver lipid contents. *Oxid Med Cell Longev.* (2022) 2022:2315575. doi: 10.1155/2022/2315575

28. Yang H, Huang X, Fang S, He M, Zhao Y, Wu Z, et al. Unraveling the fecal microbiota and metagenomic functional capacity associated with feed efficiency in pigs. *Front Microbiol.* (2017) 8:1555. doi: 10.3389/fmicb.2017.01555

29. Berry SE, Valdes AM, Long HN, Segata N. Microbiome connections with host metabolism and habitual diet from 1,098 deeply phenotyped individuals nature. *Medicine.* (2021) 27:321–32. doi: 10.1038/s41591-020-01183-8

30. Singh RK, Chang HW, Yan D, Lee KM, Ucmak D, Wong K, et al. Influence of diet on the gut microbiome and implications for human health. *J Transl Med.* (2017) 15:73. doi: 10.1186/s12967-017-1175-y

31. Wang X, Tsai T, Zuo B, Wei X, Deng F, Li Y, et al. Donor age and body weight determine the effects of fecal microbiota transplantation on growth performance, and fecal microbiota development in recipient pigs. *J Anim Sci Biotechnol.* (2022) 13:49. doi: 10.1186/s40104-022-00696-1

32. Tilocca B, Burbach K, Heyer C, Hoelzle L, Mosenthin R, Stefanski V, et al. Dietary changes in nutritional studies shape the structural and functional composition of the pigs' fecal microbiome-from days to weeks. *Microbiome.* (2017) 5:144. doi: 10.1186/s40168-017-0362-7

33. Lee S, Kang K. Omega-3 fatty acids modulate cyclophosphamide induced markers of immunosuppression and oxidative stress in pigs. *Sci Rep.* (2019) 9:2684. doi: 10.1038/s41598-019-39458-x

34. Chang HW, Mcnulty NP, Hibberd MC, O'Donnell D, Gordon JI. Gut microbiome contributions to altered metabolism in a pig model of undernutrition. *Proc Natl Acad Sci U S A.* (2021) 118:e2024446118. doi: 10.1073/pnas.2024446118

35. Lunney J, Van Goor A, Walker K, Hailstock T, Franklin J, Dai C. Importance of the pig as a human biomedical model. *Sci Trans Med.* (2021) 13:eabd5758. doi: 10.1126/scitranslmed.abd5758

36. Lawley B, Tannock GW. Analysis of 16s Rrna gene amplicon sequences using the qiime software package. *Methods Molecular Biol.* (2017) 1537:153. doi: 10.1007/978-1-4939-6685-1_9

37. Tanja M. Steven, Salzberg. Flash: fast length adjustment of short reads to improve genome assemblies. *Bioinformatics.* (2011) 27:2957–63. doi: 10.1093/bioinformatics/btr507

38. Wang Q, Garrity GM, Tiedje JM, Cole JR. Naïve bayesian classifier for rapid assignment of Rrna sequences into the new bacterial taxonomy. *Appl Environ Microbiol.* (2007) 73:5261–7. doi: 10.1128/AEM.00062-07

39. Segata N, Izard J, Waldron L, Gevers D. Metagenomic biomarker discovery and explanation. *Genome Biol.* (2011) 12:R60. doi: 10.1186/gb-2011-12-6-r60

40. Xiao Y, Li K, Yun X, Zhou W, Hua Y. The fecal microbiota composition of boar duroc, yorkshire, landrace and hampshire pigs. *Asian-Australas J Anim Sci.* (2017) 30:1456–63. doi: 10.5713/ajas.16.0746

41. Du X, Xiang Y, Lou F, Tu P, Zhang X, Hu X, et al. Microbial community and short-chain fatty acid mapping in the intestinal tract of quail. *Animals.* (2020) 10:1006. doi: 10.3390/ani10061006

42. AOAC. *Official Methods of Analysis*. Arlington, VA: Association of Official Analytical Chemists, Inc (2000).

43. Sarita A, Sushma D. Tracking the spread of Covid-19 in India via social networks in the early phase of the pandemic. *J Travel Med.* (2020) 27:130. doi: 10.1093/jtm/taaa130

44. Dai D, Yang Y, Yu J, Dang T, Qin W, Teng L, et al. Interactions between gastric microbiota and metabolites in gastric cancer. *Cell Death Dis.* (2021) 12:1104. doi: 10.1038/s41419-021-04396-y

45. Xiao Y, Kong F, Xiang Y, Zhou W, Wang J, Yang H, et al. Comparative biogeography of the gut microbiome between Jinhua and landrace pigs. *Rep.* (2018) 8:5985. doi: 10.1038/s41598-018-24289-z

46. Ma L, Shen Q, Lyu W, Lv L, Wang W, Yu M, et al. Clostridium Butyricum and its derived extracellular vesicles modulate gut homeostasis and ameliorate acute experimental colitis. *Microbiol Spectrum*. (2022) 10:e0136822. doi: 10.1128/spectrum.01368-22

47. Cignarella F, Cantoni C, Ghezzi L, Salter A, Dorsett Y, Chen L, et al. Intermittent fasting confers protection in Cns autoimmunity by altering the gut microbiota. *Cell Metabolism.* (2018) 27:1222–35.e6. doi: 10.1016/j.cmet.2018.05.006

48. Xiao Y, Zou H, Li J, Song T, Lv W, Wang W, et al. Impact of quorum sensing signaling molecules in gram-negative bacteria on host cells: current understanding and future perspectives. *Gut Microbes.* (2022) 14:2039048. doi: 10.1080/19490976.2022.2039048

49. Vigors S, Sweeney T, O'Shea C, Kelly A, O'Doherty J. Pigs that are divergent in feed efficiency, differ in intestinal enzyme and nutrient transporter gene expression, nutrient digestibility and microbial activity. *Animal.* (2016) 10:1848–55. doi: 10.1017/S1751731116000847

50. Xiao L, Estellé J, Kiilerich P, Ramayo-Caldas Y, Xia Z, Feng Q, et al. A reference gene catalogue of the pig gut microbiome. *Nature Microbiol.* (2016) 1:16161. doi: 10.1038/nmicrobiol.2016.161

51. Yang H, Huang X, Fang S, Xin W, Huang L, Chen C. Uncovering the composition of microbial community structure and metagenomics among three gut locations in pigs with distinct fatness. *Sci Rep.* (2016) 6:27427. doi: 10.1038/srep27427

52. Tropini C, Earle K, Huang K, Sonnenburg J. The gut microbiome: connecting spatial organization to function. *Cell Host Microbe.* (2017) 21:433–42. doi: 10.1016/j.chom.2017.03.010

53. Wang C, Wei S, Chen N, Xiang Y, Wang Y, Jin M. Characteristics of gut microbiota in pigs with different breeds, growth periods and genders. *Microb Biotechnol.* (2022) 15:793–804. doi: 10.1111/1751-7915.13755

54. Li N, Zuo B, Huang S, Zeng B, Han D, Li T, et al. Spatial heterogeneity of bacterial colonization across different gut segments following inter-species microbiota transplantation. *Microbiome.* (2020) 8:161. doi: 10.1186/s40168-020-00917-7

55. Albenberg L, Esipova TV, Judge CP, Bittinger K, Wu GD. Correlation between intraluminal oxygen gradient and radial partitioning of intestinal microbiota in humans and mice. *Gastroenterology.* (2014) 147:1055–63.e8. doi: 10.1053/j.gastro.2014.07.020

56. Wang Y, Song W, Wang J, Wang T, Xiong X, Qi Z, et al. Single-cell transcriptome analysis reveals differential nutrient absorption functions in human intestine. *J Experiment Med.* (2020) 217(2). doi: 10.1084/jem.20191130

57. Spiga L, Winter M, Furtado de Carvalho T, Zhu W, Hughes E, Gillis C, et al. An oxidative Central metabolism enables salmonella to utilize microbiota-derived succinate. *Cell Host Microbe.* (2017) 22:291–301.e6. doi: 10.1016/j.chom.2017.07.018

58. Faith JJ, Guruge JL, Charbonneau M, Subramanian S, Seedorf H, Goodman AL, et al. The long-term stability of the human gut microbiota. *Science.* (2013) 341:1237439. doi: 10.1126/science.1237439

59. James KR, Gomes T, Elmentaite R, Kumar N, Teichmann SA. Distinct microbial and immune niches of the human colon. *Nat Immunol.* (2020) 21:343–53. doi: 10.1038/s41590-020-0602-z

60. Roura E, Koopmans S, Lallès J, Le Huerou-Luron I, de Jager N, Schuurman T, et al. Critical review evaluating the pig as a model for human nutritional physiology. *Nutr Res Rev.* (2016) 29:60–90. doi: 10.1017/S0954422416000020

61. Zhang J, Sun J, Chen X, Nie C, Zhao J, Guan W, et al. Clostridium butyricumcombination of and corn bran optimized intestinal microbial fermentation using a weaned pig model. *Front Microbiol.* (2018) 9:3091. doi: 10.3389/fmicb.2018.03091

62. Xu E, Yang H, Ren M, Wang Y, Xiao Y. Identification of enterotype and its effects on intestinal butyrate production in pigs. *Animals.* (2021) 11:730. doi: 10.3390/ani11030730

63. Tan FPY, Beltranena ET, Zijlstra R. Resistant starch: implications of dietary inclusion on gut health and growth in pigs: a review. *J Animal Sci Biotechnol.* (2022) 13:613–27. doi: 10.1186/s40104-021-00644-5

64. Macfarlane S, Macfarlane GT. Regulation of short-chain fatty acid production. *Proceedings Nutr Soc.* (2003) 62:67–72. doi: 10.1079/PNS2002207

65. Li W, Liu Y, Jiang W, Yan X. Proximate composition and nutritional profile of rainbow trout (oncorhynchus mykiss) heads and skipjack Tuna (katsuwonus pelamis) heads. *Molecules.* (2019) 24:3189. doi: 10.3390/molecules24173189

66. Pakroo S, Tarrah A, Duarte V, Corich V, Giacomini A. Microbial diversity and nutritional properties of persian "yellow curd" (Kashk Zard), a promising functional fermented food. *Microorganisms.* (2020) 8:1658. doi: 10.3390/microorganisms8111658

67. Skrypnik K, Suliburska J. Association between the gut microbiota and mineral metabolism. *J Sci Food Agric.* (2018) 98:2449–60. doi: 10.1002/jsfa.8724

68. Tsukuda N, Yahagi K, Hara T, Watanabe Y, Matsuki T. Key bacterial taxa and metabolic pathways affecting gut short-chain fatty acid profiles in early life. *ISME J.* (2021) 15:1–17. doi: 10.1038/s41396-021-00937-7

69. Kelly J. Daly, Kristian, Moran, Andrew W, et al. Composition and diversity of mucosa-associated microbiota along the entire length of the pig gastrointestinal tract; dietary influences. *Environ Microbiol.* (2017) 19:1425–38. doi: 10.1111/1462-2920.13619

70. Mehta S, Huey SL, McDonald D, Knight R, Finkelstein JL. Nutritional interventions and the gut microbiome in children. *Annu Rev Nutr.* (2021) 41:479–510. doi: 10.1146/annurev-nutr-021020-025755

71. Martinez-Guryn K, Hubert N, Frazier K, Urlass S, Musch M, Ojeda P, et al. Small intestine microbiota regulate host digestive and absorptive adaptive responses to dietary lipids. *Cell Host Microbe.* (2018) 23:458–69.e5. doi: 10.1016/j.chom.2018.03.011

72. Wassie T, Duan X, Xie C, Wang R, Wu X. Dietary enteromorpha polysaccharide-zn supplementation regulates amino acid and fatty acid metabolism by improving the antioxidant activity in chicken. *J Anim Sci Biotechnol.* (2022) 13:878–96. doi: 10.1186/s40104-021-00648-1

frontiers | Frontiers in Nutrition

TYPE Original Research
PUBLISHED 05 October 2022
DOI 10.3389/fnut.2022.1013899

OPEN ACCESS

EDITED BY
Hui Han,
Chinese Academy of Sciences (CAS), China

REVIEWED BY
Wenjian Xie,
Hong Kong Baptist University, Hong Kong SAR, China
Hongbin Si,
Guangxi University, China

*CORRESPONDENCE
Ran Li
wwwlr@163.com
Tao Xie
xt39911159@163.com

†These authors have contributed equally to this work

SPECIALTY SECTION
This article was submitted to Nutrition and Microbes, a section of the journal Frontiers in Nutrition

RECEIVED 08 August 2022
ACCEPTED 12 September 2022
PUBLISHED 05 October 2022

CITATION
Chen S-Y, Zhou QY-J, Chen L, Liao X, Li R and Xie T (2022) The *Aurantii Fructus Immaturus* flavonoid extract alleviates inflammation and modulate gut microbiota in DSS-induced colitis mice.
Front. Nutr. 9:1013899.
doi: 10.3389/fnut.2022.1013899

The *Aurantii Fructus Immaturus* flavonoid extract alleviates inflammation and modulate gut microbiota in DSS-induced colitis mice

Si-Yuan Chen[1†], Qing Yi-Jun Zhou[2,3†], Lin Chen[3], Xin Liao[3], Ran Li[4,5*] and Tao Xie[6*]

[1]The First Hospital of Hunan University of Chinese Medicine, Hunan University of Chinese Medicine, Changsha, China, [2]Science and Technology Innovation Center, Hunan University of Chinese Medicine, Changsha, China, [3]Institute of Chinese Materia Medica, Hunan Academy of Chinese Medicine, Changsha, China, [4]Guangdong Provincial Key Laboratory of Utilization and Conservation of Food and Medicinal Resources in Northern Region, Shaoguan University, Shaoguan, China, [5]Hunan Yueyang Maternal & Child Health-Care Hospital, Yueyang, China, [6]Changsha Traditional Chinese Medicine Hospital, Changsha, China

Inflammatory bowel disease (IBD) is a chronic, relapsing immune-mediated disease that always leads to a progressive loss of intestinal function. Therefore, it is important to find potential therapeutic drugs. This study was conducted to elucidate the effect of *Aurantii Fructus immaturus* flavonoid extract (AFI, 8% neohesperidin, 10% naringin) on DSS-induced intestinal inflammation and the gut microbiome. To explore the mechanism of action by which AFI protects against intestinal inflammation, a total of 50 mice were randomly divided into 5 groups [CG (control group), MG (model group), AFI low dose, AFI middle dose, and AFI high dose] and received 2.5% DSS for 7 days. Then, mice in the AFI groups were orally administered different doses of AFI for 16 days. The results showed that, compared with the MG group, the food intake and body weight were increased in the AFI groups, but the water intake was lower. Additionally, AFI significantly alleviated DSS-induced colitis symptoms, including disease activity index (DAI), and colon pathological damage. The levels of IL-6, IL-1β and TNF-α in serum and colon tissue were significantly decreased. The diversity and abundance of the intestinal microbiota in the AFI group were decreased. The relative abundance of Bacteroidota was increased, and the relative abundance of Firmicutes was decreased. AFI plays an important role in alleviating DSS-induced intestinal inflammation and regulating Oscillospira, Prevotellaceae and Lachnospiraceae in the intestine at low, medium and high doses, respectively. This report is a pioneer in the assessment of AFI. This study not only demonstrated the anti-inflammatory activity of AFI but also identified the microbiota regulated by different concentrations of AFI.

KEYWORDS

***Aurantii Fructus Immaturus*, intestinal flora, anti-inflammatory, neohesperidin, naringin**

Introduction

Inflammatory bowel disease (IBD) is a type of chronic, relapsing immune-mediated disease that always leads to the progressive loss of intestinal function (1). IBD has long been a huge challenge and burden on the public health care system (2, 3). In fact, IBD is caused by multiple pathogens and multiple pathogens, and there is no effective treatment (4). Therefore, finding a useful drug has become an urgent problem that needs to be solved.

Aurantii Fructus Immaturus (Chinese name Zhishi) is the dried unripe fruit of *Citrus aurantium* L. or its cultivars or *Citrus sinensis Osbeck* that is collected from May to June. For a long time, the processed unripe fruits of Bittet Orange, possesses homology of medicine and food characteristic, which is regarded to be health promotion effect in digestive tract system. Additionally, *Aurantii Fructus Immaturus* has been used as a single Chinese medicine and compound to treat gastrointestinal diseases, such as diarrhea, gasteremphraxis and uterine prolapse. The active ingredients of *Citrus aurantium,* such as flavonoids, alkaloids, volatile oils and coumarins, have antifungal (5), anti-anxiety (6), antioxidant (7), anticancer (8), anti-inflammatory (9), gastric mucosa protective (10), anticoagulation, intestinal motility regulatory (11), nerve protective (12) and other effects. In previous studies, some single compound extracted from *Aurantii Fructus Immaturus*, such as neohesperidin and naringin have reported can relieve inflammation (13).

In the present study, we investigated the effects of *Aurantii Fructus immaturus* flavonoid extract (AFI, neohesperidin 8%, naringin 10%) on dextran sulfate sodium (DSS)-induced intestinal inflammation and the gut microbiome. We demonstrate that AFI treatment alleviates DSS-induced gut inflammation and suggest that it is related to the regulation of the intestinal microbiota. These findings thus demonstrate that AFI represents a potential agent for the treatment of intestinal inflammation.

Materials and methods

Chemicals and reagents

The *Aurantii Fructus Immaturus* flavonoid extract (neohesperidin 8% and naringin 10%) was purchased from Kanglu Biotechnology Co., Ltd. (Hunan Province, China). Mouse interleukin 6 (IL-6) (#MM-0163M1), tumor necrosis factor (TNF-α) (#MM-0132M1) and interleukin 1β (IL-1β) (#MM-0040M1) enzyme-linked immunosorbent assay (ELISA) kits were obtained from Jiangsu Meimian Industrial Co. Ltd. (Jiangsu, China). The RNA extraction kit was obtained from Aidlab Biotechnologies Co. Ltd. (Beijing, China). The iScript cDNA synthesis kit and SYBR Green master mix were obtained from Bio-Rad Laboratories, Inc. (Hercules, CA, USA).

Animals and drug administration

The animal research was conducted according to the Guidelines for Animal Experimentation of Hunan University of Chinese Medicine (Changsha, China) and was approved by the Animal Ethics Committee of Hunan University of Chinese Medicine. A total of 50 C57BL/6J male mice (8 weeks old and 18 to 20 g) were obtained from Hunan SJA Laboratory Animal Co., Ltd. (Hunan, China). The mice were acclimated for 1 week. During this time, the mice were fed standard food and given free access to water. Then, they were randomly divided into 5 groups [CG (control group), MG (model group), AFIL (AFI low dose at 50 mg/kg), AFIM (AFI middle dose at 100 mg/kg), and AFIH (AFI high dose at 200 mg/kg); n = 10/group], and the mice received 2.5% DSS in their drinking water for 7 days. All doses of AFIs (AFIL, AFIM and AFIH) were administered by gavage once a day, starting from the 8th day of the experiment. The MG and CG mice were gavaged with saline. Moreover, we used the DAI data which presented as an average score of the diarrhea of stool, body weight loss, and the extent of blood in the feces to evaluated the severity of colitis by this scoring system (14). On the 23rd day, the mice were sacrificed with CO2, and blood was collected via the cardiac puncture method. All mice were observed once a day, and the food intake and water intake by body weight were recorded. The colon samples embedded in paraffin were cut into 4 μm slices. Sections were stained with hematoxylin and eosin (H&E). Histological damage of the colons was observed in H&E-stained sections using a light mi- croscope, and histopathological scores were evaluated according to the scoring system (15). Then, the colon tissue and serum were collected for subsequent qRT-PCR experiments. The intestinal contents were collected, snap-frozen in liquid nitrogen and then stored at −80°C for further analysis.

Real-time quantitative polymerase chain reaction

Total RNA of the colon tissues was extracted using TRIzol reagent (Life Technologies, USA) according to the manufacturer's instructions. Then, the total RNA concentrations were equalized (1 μg) and converted to cDNA using the iScript cDNA synthesis kit according to the manufacturer's protocol. Gene expression was measured by quantitative polymerase chain reaction (qPCR) using SYBR Green Master Mix (Roche, Basel, Switzerland) on a CFX96 Real-Time PCR system from Bio-Rad. Gene expression was measured by qPCR (Roche, Basel, Switzerland) using SYBR Green (Roche, Basel, Switzerland). GAPDH or β-actin was used for gene expression normalization in animal tissue or cells, respectively. The relative expression levels of genes were calculated using the $2^{-\Delta\Delta Ct}$ method. The primers are listed in the **Supplementary material** (**Supplementary Table 1**).

Gut microbiota profiling 16S rDNA amplicon sequencing

Genomic DNA was extracted from the intestinal content samples using the E.Z.N. Stool DNA kit. The hypervariable region V3-V4 of the bacterial 16S rRNA gene was amplified with primer pair 338F (5'-ACTCCTACGGGAGGCAGC AG-3'). The genomic DNA from the fecal samples was extracted using a DNA kit (TIANGEN Biotech Co. Ltd., Beijing, China) and quantified using a Qubit 2.0 fluorometer (Invitrogen, Carlsbad, CA, USA). DNA (30 to 50 ng) was used to generate amplicons using a MetaVx Library Preparation kit. The V3 and V4 hypervariable regions of prokaryotic 16S rDNA were selected for generating amplicons and subsequent taxonomy analysis. DNA libraries were validated by an Agilent 2100 Bioanalyzer (Agilent Technologies, Palo Alto, CA, USA) and quantified by Qubit 2.0 Fluorometer. DNA libraries were multiplexed and loaded on an Illumina MiSeq instrument according to the manufacturer's instructions (Illumina, San Diego, CA, USA). Sequencing was performed by Majorbio Bio-Pharm Technology using paired-end configuration; image analysis and base-calling were conducted by the MiSeq Control Software (MCS) embedded in the MiSeq instrument.

The raw 16S rRNA gene sequencing reads were demultiplexed, quality-filtered by fastp version 0.20.0 (16) and merged by FLASH version 1.2.7 (17) with the following criteria: (i) the 300 bp reads were truncated at any site receiving an average quality score of <20 over a 50 bp sliding window, and the truncated reads shorter than 50 bp were discarded, reads containing ambiguous characters were also discarded; (ii) only overlapping sequences longer than 10 bp were assembled according to their overlapped sequence. The maximum mismatch ratio of overlap region is 0.2. Reads that could not be assembled were discarded; (iii) Samples were distinguished according to the barcode and primers, and the sequence direction was adjusted, exact barcode matching, 2 nucleotide mismatch in primer matching. Operational taxonomic units (OTUs) with 97% similarity cutoff (18, 19) were clustered using UPARSE version 7.1 (19), and chimeric sequences were identified and removed. The taxonomy of each OTU representative sequence was analyzed by RDP Classifier version 2.2 (20) against the 16S rRNA database using confidence threshold of 0.7.

Statistical analysis

The data are presented as the means ± SDs, and statistical analysis was performed using GraphPad Prism (USA). Datasets that involved more than two groups were assessed by one-way or two-way analysis of variance (ANOVA) followed by Tukey's multiple comparison test. The Wilcoxon rank sum test and Tukey's test were used to analyze the differences in species diversity between groups.

Results

Aurantii Fructus immaturus flavonoid extract ameliorates colitis induced by dextran sulfate sodium

The body weight of mice was remarkably reduced after DSS induction. However, this loss was reversed by AFI, and the colitis induced by DSS treatment was ameliorated (**Figure 1A**). We monitored the body weight, food intake and water intake of mice in the CG, MG, AFIL, AFIM, and AFIH groups. In the MG, AFIL, AFIM, and AFIH groups, the food intake and body weight gain were significantly decreased after 7 days of treatment with 2.5% DSS compared to the CG group; however, the water intake of mice was increased. After 16 days of AFI treatment, the body weight, food intake and water intake returned to levels close to those of the CG group and compared to those of the MG group (**Figures 1B–D**). In addition, the DAI scores of AFI groups were significantly decreased compared to the MG group (**Figure 1E**).

The effect of *Aurantii Fructus immaturus* flavonoid extract on serum inflammatory factors

We found that the serum concentrations of IL1-β, IL-6 and TNF-α in the MG group were significantly higher than those in the CG and AFIL groups ($p < 0.001$; **Figures 2A–C**). Additionally, the serum IL1-β ($p < 0.001$; **Figure 2A**), IL-6 ($p < 0.001$; **Figure 2A**) and TNF-α ($p < 0.05$; **Figure 2A**) contents in the AFIM group were also significantly lower than those in the MG group. The levels of IL1-β ($p < 0.005$, **Figure 2A**), IL-6 ($p < 0.01$, **Figure 2B**) and TNF-α ($p < 0.05$, **Figure 2C**) in the serum of the AFIH group were significantly lower than those in the MG groups.

The effect of *Aurantii Fructus immaturus* flavonoid extract on intestinal inflammatory factors

We used the H&E staining to evaluated the histopathologic changes, and semiquantitative analysis of histopathologic damage in the colon was performed (**Figures 3A,B**). These results of CG group showed that there were no histological abnormalities. However, obvious tissue damage and inflammation were observed in the colons of the MG group. Additionally, the damage and inflammatory cell infiltration were ameliorated by AFI treatments. Then, qPCR assays were used to examine the expression of inflammatory cytokines in colon. The results showed that

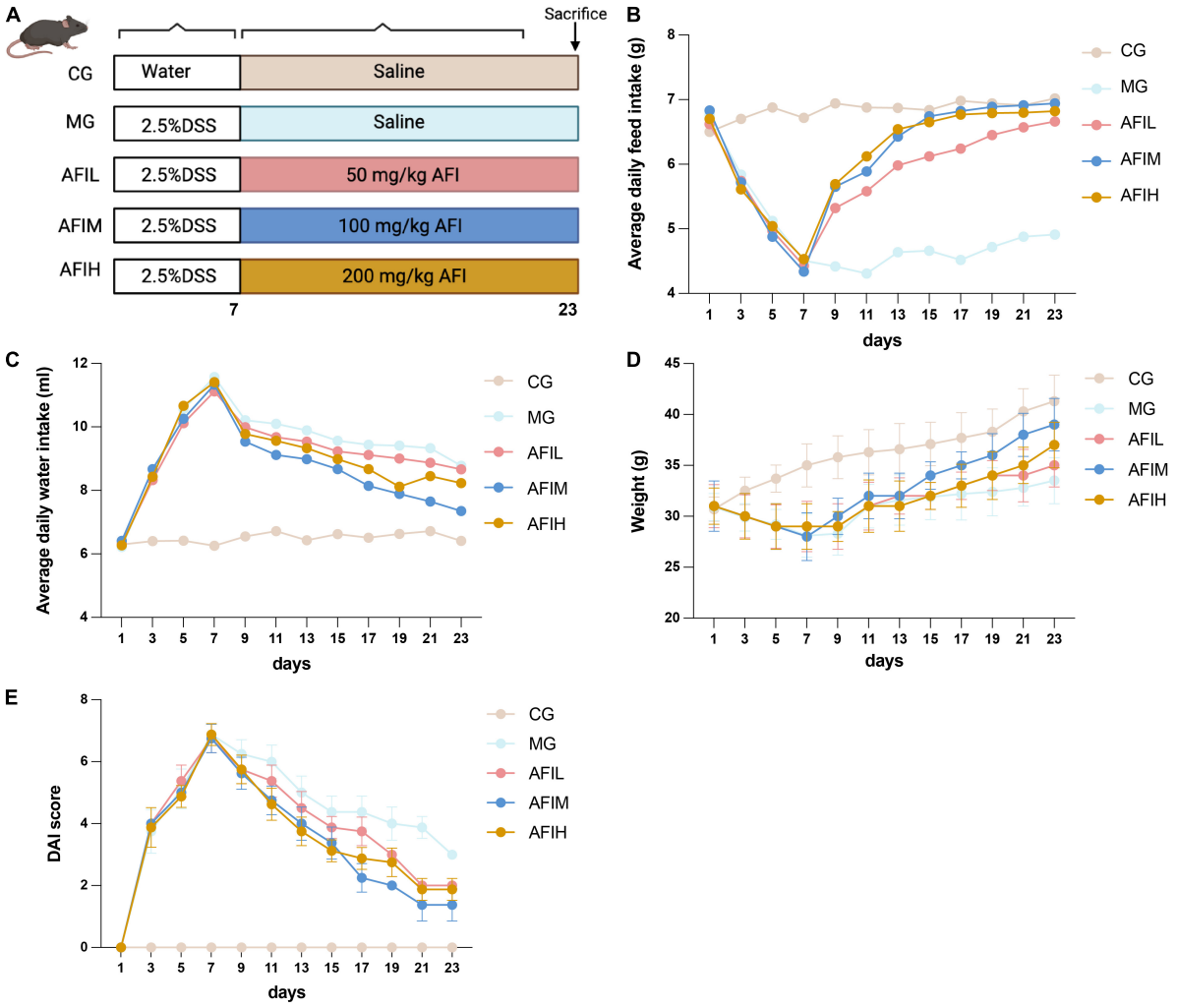

FIGURE 1
The effects of AFI on mice. **(A)** The experimental design, **(B)** food intake, **(C)** water intake, **(D)** body weights and **(E)** DAI scores for all mice.

2.5% DSS stimulated the expression of the cytokines IL-6, TNF-α, and IL1-β in the MG group (Figure 3D). However, these inflammatory factors were significantly reduced by AFI treatment. Additionally, the correlation heatmap showed the relationship between the bacterial family and intestinal inflammatory factors. At the phylum level, the content of the inflammatory factor IL-6 was negatively correlated with Firmicutes and positively correlated with Proteobacteria and Campilobacterota (Supplementary Figure 1). At the family level, Lactobacillaceae showed a significant negative correlation with IL-6. Bacteroidaceae, Tannerellaceae, Helicobacteraceae, Prevotellaceae and Marinifilaceae showed a significant positive correlation with IL-6. Butyricicoccaceae, Enterococcaceae and Enterobacteriaceae demonstrated a significant positive correlation with TNF-α. Corynebacteriaceae and Eggerthellaceae demonstrated a significant positive correlation with TNF and IL-1. Anaerovoracaceae showed a significant positive correlation with IL-1β (Figure 3C).

Alpha diversity and composition of the gut microbiota

The rank-abundance curve was used to explain two aspects of diversity, which were species richness and community evenness. Based our result (Figure 4A), the curve of the AFIH declines gently and extends far, indicating high species diversity. However, the species diversity and richness decreased in the CG and AFIM groups. The Shannon index of the OTU level was set as the vertical axis in the rarefaction curve. The curve tends to flatten, indicating that the sample sequencing volume is sufficient, and no more OTU can be found even with the increase of data (Figure 4B). The ACE index, Chao index and Simpson index were selected for the analysis of diversity among the five groups (CG, MG, AFIL, AFIM, AFIH). Finally, the richness and diversity of the intestinal microbiota showed a tendency to increase in the MG group compared with the CG, AFIL, and AFIH groups and was significantly higher

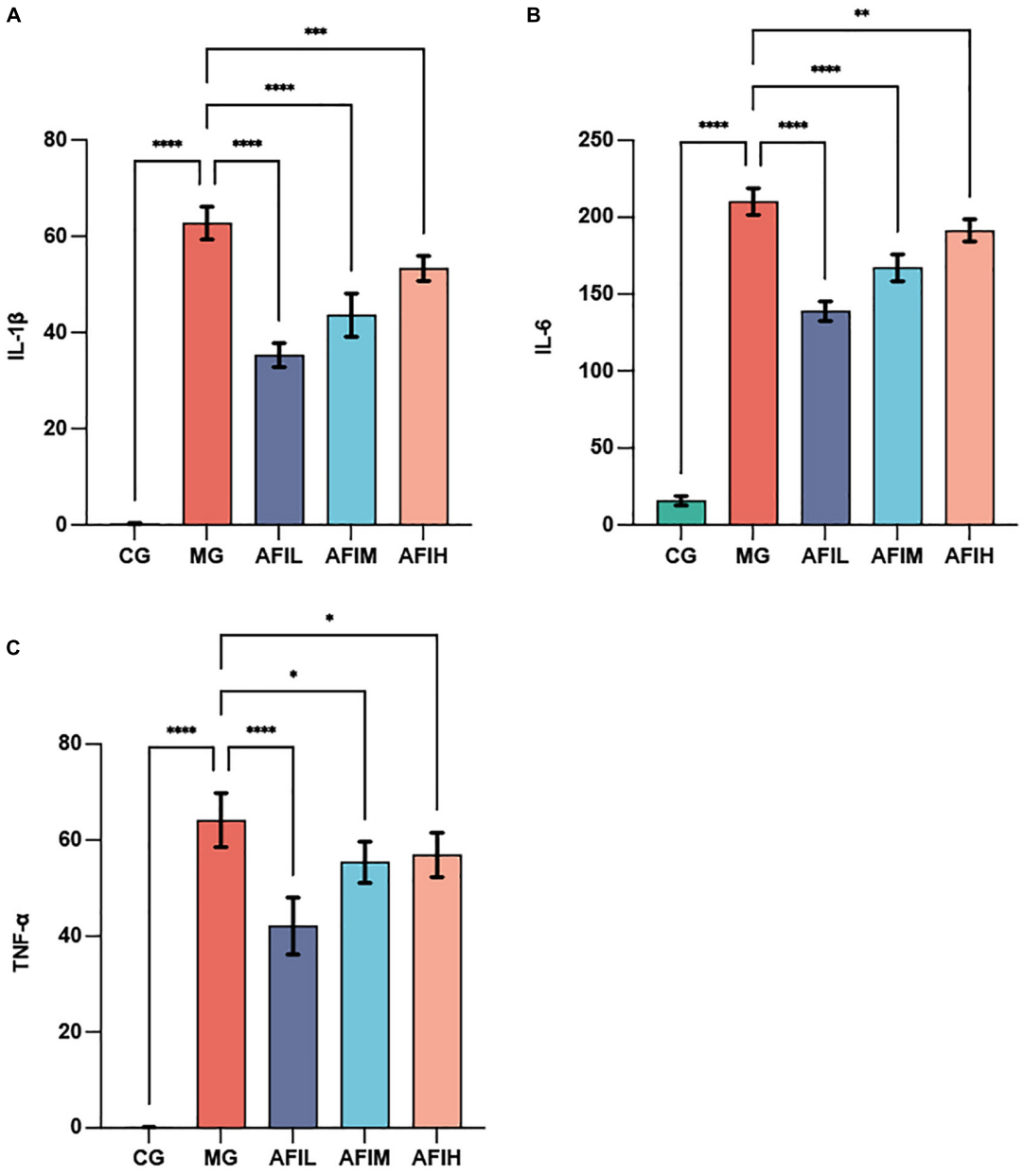

FIGURE 2
The effect of AFI on serum inflammatory factors. Bars represent the mean ± SE (N = 6). **(A)** Serum IL-1β levels. **(B)** Serum IL-6 levels. **(C)** The TNF-α level in the serum. The value of $P < 0.05$ is marked with "*". The value of $P < 0.01$ is marked with "**". The value of $P < 0.005$ is marked with "***". The value of $P < 0.001$ is marked with "****".

than that in the AFIM group (Figures 4C–E). Then, the top 7 dominant phyla and 20 dominant families in all samples were selected to construct a community column chart. This chart revealed that all 20 genera belong to 7 main phyla: Firmicutes, Bacteroidetes, Campilobacterota, Actinobacteriota, Desulfobacterota Proteobacteria, and Deferribacterota. Most of the dominant families in the 5 groups belonged to Firmicutes (44%-70%) and included Lactobacillaceae, Lachnospiraceae, Erysipelotrichaceae, Oscillospiraceae, Ruminococcaceae, Clostridiaceae, Clostridia_UCG-014, and Eubacterium_coprostanoligenes (Figure 4E and Supplementary Tables 2, 3). Lactobacillaceae was the predominant family in the CG group (53%), and the content of this family was much higher than that in the other groups. However, we found that AFI and DSS reduced the abundance of Lactobacillaceae. The second dominant phylum in the 5 groups was Bacteroidetes, and the dominant families included the Muribaculaceae, Bacteroidaceae,

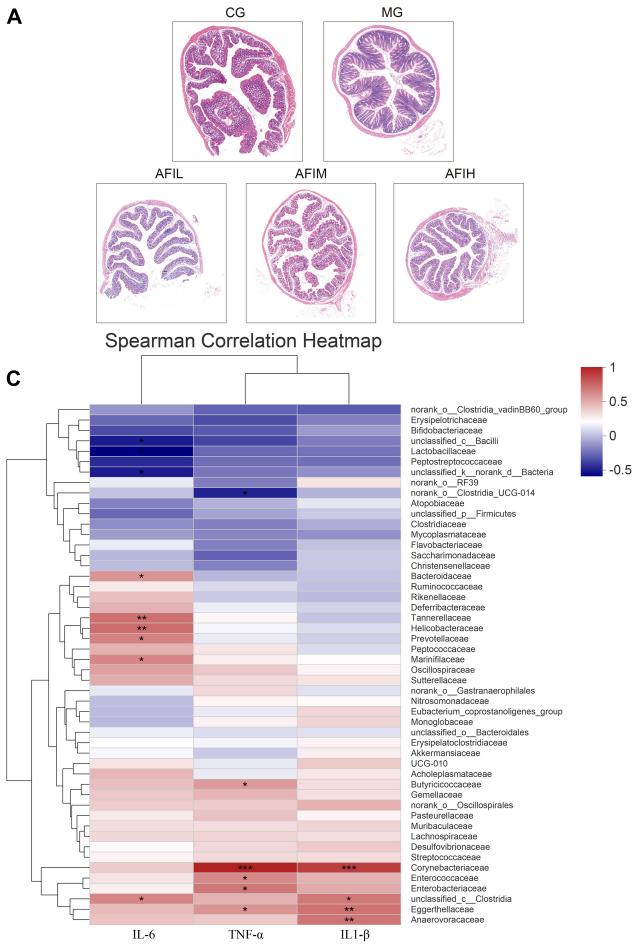

FIGURE 3
Histopathological, Intestinal inflammatory factors and Spearman correlation heatmap in all mice. **(A)** The colons of each group were processed for histological evaluation (H&E staining, 50×). **(B)** Histopathological scores of each group were evaluated. Data are presented as means ± SD (n = 8). ***$p < 0.001$, compared with the control group; * $p < 0.05$ and ** $p < 0.01$, compared with the MG group. **(C)** Correlation heatmap of IL-6, TNF-a, IL-1 and the microbiota. The X and Y axes are the environmental factors and families, respectively. R is shown in different colors. The right side of the legend is the color range of the different R values. The value of $P < 0.05$ is marked with "*". The value of $P < 0.01$ is marked with "**". The value of $P < 0.005$ is marked with "***". The value of $P < 0.001$ is marked with ****. **(D)** IL-6, TNF-α, and IL1-β expression.

Rikenellaceae, Prevotellaceae, and Marinifilaceae families. Muribaculaceae (15.7%) was the predominant family in the CG group and belongs to Bacteroidota. These results show that the abundance of this flora is increased by AFI and DSS intervention.

Beta diversity of the gut microbiota

The beta diversity of the gut microbiota was analyzed to compare the similarity of different samples in species diversity (Figure 5). Partial least squares discriminant analysis (PLS-DA) showed that the gut microbiota of the 3 AFI groups was obviously separated from that of the other two groups, indicating that the composition of the gut microbiota was significantly different between the CG and MG groups. However, the AFIH group was obviously separated from the AFIL and AFIM groups, suggesting that AFI had a different effect on the gut microbial structure when compared with different doses (Figure 5A). The OTU distributions between different treatment groups are shown in Figure 5B. These results showed that the five groups shared the greatest number of different OTUs (363 OTUs) (Figure 5A). Additionally, four groups (AFIL, AFIM, AFIH and MG) shared 73 OTUs. Finally, LEfSe analysis identified the differentially abundant bacterial taxa in the gut microbiota between the five groups. The results showed that MG and AFI mice had lower proportions of the Lactobacillaceae family than CG mice (Supplementary Table 3). The AFI group had higher proportions of the Oscillospiraceae family than the CG and MG groups (Supplementary Table 3). We also found that the effects of different doses of AFI on the gut microbiome were different. MG and AFI mice had lower

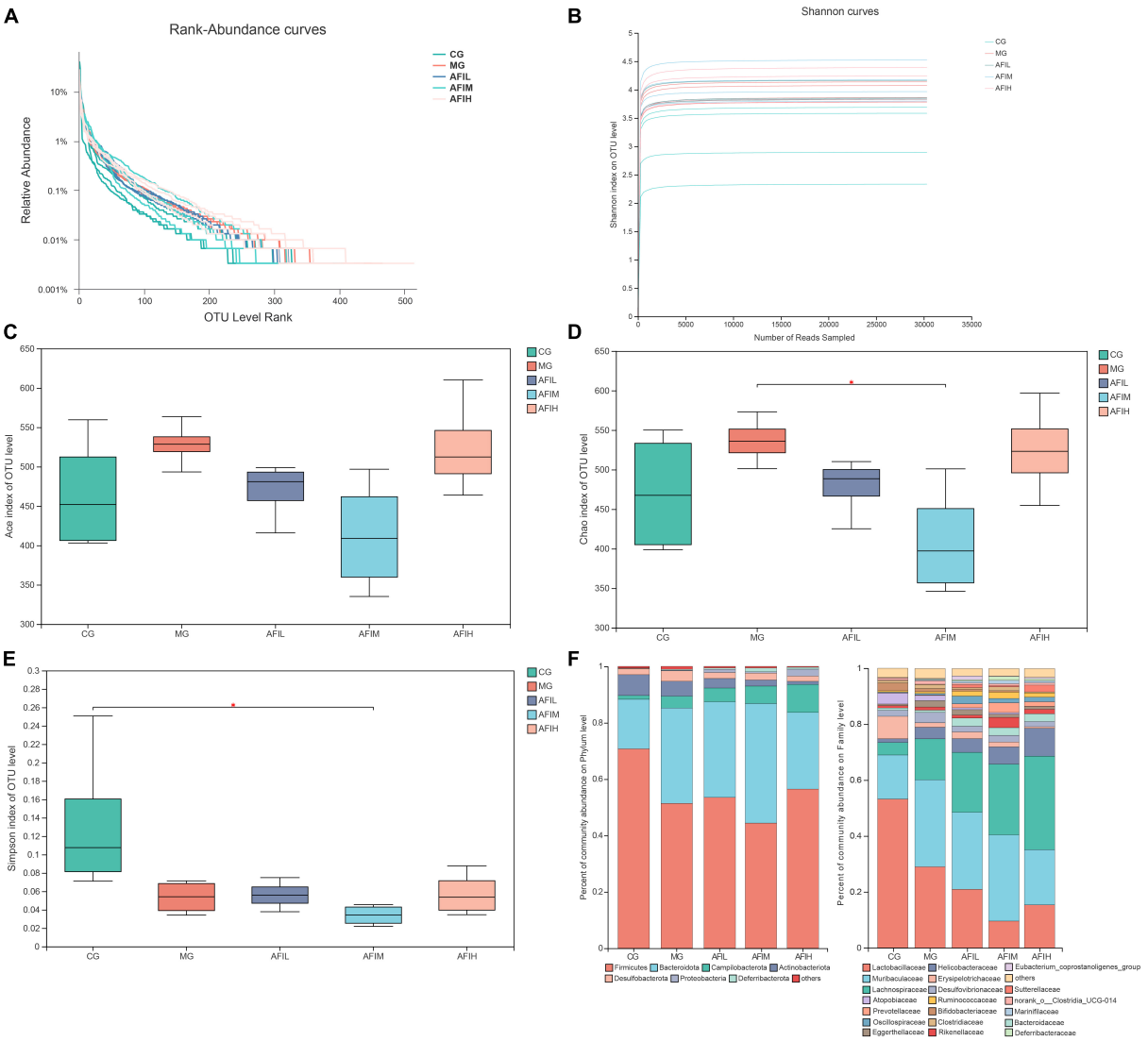

FIGURE 4
Effects of AFI on the intestinal microbiota induced by DSS. **(A)** Rank-Abundance curves of the OUT level. **(B)** Shannon dilution curves. **(C)** ACE. **(D)** Chao. **(E)** Simpson. **(F)** The composition of the gut microbiota and the community bar plot analysis at the phylum and family levels.

proportions of the families Lactobacillaceae than CG mice (Supplementary Table 3). We also found that the effects of different doses of AFI on the gut microbiome were different. At the family level, AFIL mice had higher proportions of Oscillospiraceae than CG and MG mice (Supplementary Table 3). However, Prevotellaceae, Ruminococcaceae, and Marinifilaceae were enriched in the AFIM group, whereas Lachnospiraceae, Lachnospiraceae, Sutterellaceae, and Butyricicoccaceae were more abundant in the AFIH group. At the genus level, Ruminococcus, Blautia, Colidextribacter, Roseburia, GCA-900066575, and Candidatus_Stoquefichus were enriched in the AFIL group. Alloprevotella, Peptococcus, Odoribacter, Prevotellaceae_UCG-001, Tuzzerella, Bilophila, and Lachnospiraceae_FCS020_group were more abundant in the AFM group, and Lachnospiraceae_NK4A136, Parasutterella, Paludicola, Butyricicoccus, and Family_XIII_UCG-001 were enriched in the AFIH group (Figures 5C,D).

Discussion

The results of this study showed that after the mice were given DSS, the food intake and body weight were seriously reduced, the drinking water was increased, the DAI scores were reduced, and the colonic tissue damage were alleviated. Intervention with different concentrations of AFI

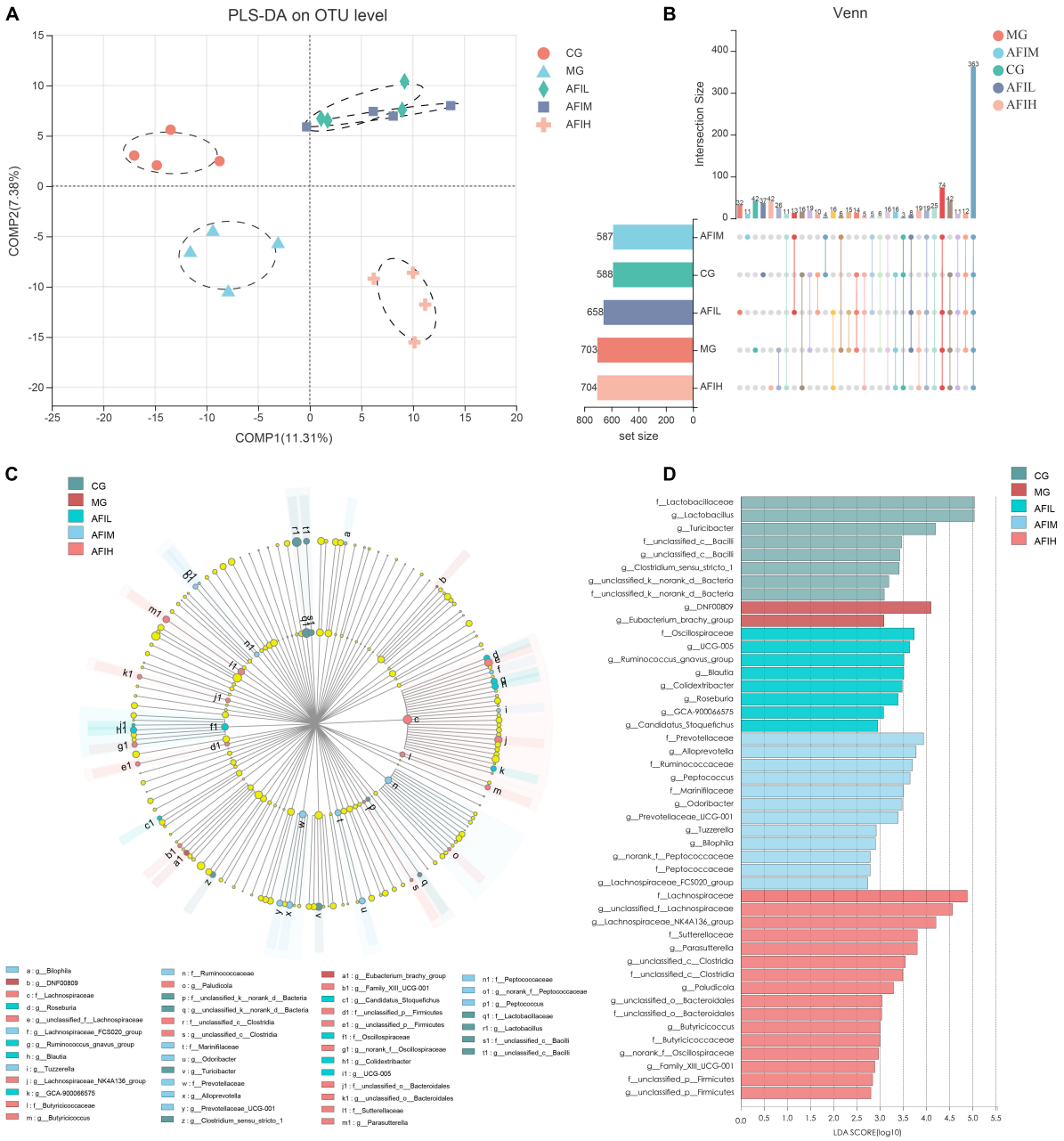

FIGURE 5
The effect of AFI on the intestinal microbiota. **(A)** Partial least squares-discriminant analysis (PLS-DA) of the OTUs in the five groups. **(B)** Advanced venn diagram (UpSet) results for the transcriptome data from the four comparisons. **(C)** Significantly different bacterial taxa at the family to genus levels. **(D)** Significant differences were tested by linear discriminant analysis effect size (LEfSe) analysis, with linear discriminant analysis (LDA) scores of >2 and p values of <0.05. The taxa enriched in the five groups showed positive LDA scores.

significantly improved the physiological state of the mice, indicating that the total amount of AFI can improve the adverse reactions caused by DSS. Low-dose AFI had the best effect in reducing serum and intestinal inflammation. Decreasing NF-κB expression suppresses local inflammatory processes in the intestines. Various proinflammatory and anti-inflammatory cytokines are known to be regulated at least in part by the transcription activator NF-κB. Blocking NF-κB activation could suppress its downstream inflammatory mediators, such as IL-1β, TNF-α and IL-6, to contribute to the resolution of inflammation (21, 22). Additionally, TNF-α not only induces inflammation but also participates in regulating other immune responses in both innate and adaptive immunity, including apoptosis and cell proliferation. The present results indicated

that AFI could inhibit extensive immune responses, including the inflammatory response.

Then, we examined whether the effect of AFI treatment on the mitigation of DSS-induced inflammation is related to the gut microbiota. We found that treatment with different doses of AFI partially shifted the β-diversity of the gut microbiota of DSS-treated mice, and the α-diversity (OTUs) was weakly decreased. Furthermore, both DSS and AFI treatment decreased the abundance of Firmicutes, especially the number of Lactobacillaceae. In fact, previous studies demonstrated that Lactobacillaceae, a type of probiotic, are effective inhibitors against inflammatory bowel disease development, including ulcerative colitis (23). However, the reduction in Lactobacillus abundance after AFI treatment suggests that Lactobacillus is not a key group of bacteria that play a role in AFI mitigation of inflammation. The gut microbiota results showed that the relative abundance of Oscillospira was significantly increased in the AFL group. A previous study showed that the abundance of Oscillospira is decreased in inflammatory diseases (24, 25), possibly because Oscillospira produces the short-chain fatty acid butyrate (26). Additionally, Oscillospira has been shown to produce secondary bile acids for protection against Clostridium difficile infection (27). Therefore, Oscillospira may be the key bacteria for the ability of the low-dose AFI to reduce inflammation. Additionally, the abundance of Oscillospira was also increased in the AFIM and AFIH groups compared to the CG group (**Supplementary Table 3**). However, Oscillospira has not been isolated and cultured (26). This study is the first to find a correlation between AFI and Oscillospira. We also noticed that the abundance of Prevotellaceae and Lachnospiraceae was significantly increased in the AFIM and AFIH groups, respectively. In fact, Prevotellaceae, a butyric acid-producing probiotic, is thought to be associated with anti-inflammatory and antioxidant activities (1, 28, 29). In addition, based on Spearman correlation analysis of intestinal inflammatory factors and intestinal microbiota, we found positive and negative correlations between the abundance of some bacteria and inflammation. The bacteria of Lachnospiraceae impact their hosts by producing short-chain fatty acids and converting primary bile acids to secondary bile acids to induce resistance against intestinal pathogens (30). The main active ingredients in AFI are neohesperidin and naringin, and previous studies have demonstrated that AFI prevents colorectal tumorigenesis by altering the gut microbiota (31, 32). In conclusion, AFI can effectively alleviate DSS-induced intestinal mucositis by inhibiting proinflammatory cytokines and regulating the overall structure and composition of the intestinal microbiota.

Data availability statement

The data presented in the study are deposited in the NCBI repository, https://www.ncbi.nlm.nih.gov/, accession no. PRJNA866702.

Ethics statement

The animal study was reviewed and approved by the Animal Ethics Committee of Hunan University of Chinese Medicine.

Author contributions

RL and TX designed this experiment and edited the manuscript. S-YC and QZ carried out animal trial and collected samples. QZ and LC detected the samples and analyzed the data. RL and XL guided the experiment and revised the manuscript. All authors have read and approved the final manuscript.

Funding

This work was supported by The Special Funds for Development of Local Science and Technology from Central Government (2021SF5045), Natural Science Foundation of Hunan province (2022JJ30041 and 2022JJ40460), Clinical Innovation Leading Scientific Research Projects of Hunan Science and Technology Department (No. 2020SK52603), and Hunan Provincial Clinical Medical Technology Demonstration Base Project (No. 2020SK4025).

Conflict of interest

The authors declare that the research was conducted in the absence of any commercial or financial relationships that could be construed as a potential conflict of interest.

Publisher's note

Supplementary material

The Supplementary Material for this article can be found online at: https://www.frontiersin.org/articles/10.3389/fnut.2022.1013899/full#supplementary-material

References

1. Cignarella F, Cantoni C, Ghezzi L, Salter A, Dorsett Y, Chen L, et al. Intermittent fasting confers protection in CNS autoimmunity by altering the gut microbiota. *Cell Metab.* (2018) 27:1222. doi: 10.1016/j.cmet.2018.05.006

2. Kaplan GG. The global burden of IBD: from 2015 to 2025. *Nat Rev Gastroenterol Hepatol.* (2015) 12:720–7. doi: 10.1038/nrgastro.2015.150

3. Ng SC, Shi HY, Hamidi N, Underwood FE, Tang W, Benchimol EI, et al. Worldwide incidence and prevalence of inflammatory bowel disease in the 21st century: a systematic review of population-based studies. *Lancet.* (2017) 390:2769–78. doi: 10.1016/S0140-6736(17)32448-0

4. Loubet PS, Dias TO, Reis VHDT, Moya AMTM, Dos Santos EF, Cazarin CBB. Feed your gut: functional food to improve the pathophysiology of inflammatory bowel disease. *J Funct Foods.* (2022) 93:105073.

5. Viuda-Martos M, Ruiz-Navajas Y, Fernandez-Lopez J, Perez-Alvarez J. Antifungal activity of lemon (*Citrus lemon* L.), mandarin (*Citrus reticulata* L.), grapefruit (*Citrus paradisi* L.) and orange (*Citrus sinensis* L.) essential oils. *Food Control.* (2008) 19:1130–8.

6. Pultrini Ade M, Galindo LA, Costa M. Effects of the essential oil from *Citrus aurantium* L. in experimental anxiety models in mice. *Life Sci.* (2006) 78:1720–5. doi: 10.1016/j.lfs.2005.08.004

7. Yu J, Wang L, Walzem RL, Miller EG, Pike LM, Patil BS. Antioxidant activity of citrus limonoids, flavonoids, and coumarins. *J Agric Food Chem.* (2005) 53:2009–14.

8. Manthey JA, Guthrie N. Antiproliferative activities of citrus flavonoids against six human cancer cell lines. *J Agric Food Chem.* (2002) 50:5837–43. doi: 10.1021/jf020121d

9. Kim JA, Park HS, Kang SR, Park KI, Lee DH, Nagappan A, et al. Suppressive effect of flavonoids from Korean *Citrus aurantium* L. on the expression of inflammatory mediators in L6 skeletal muscle cells. *Phytother Res.* (2012) 26:1904–12. doi: 10.1002/ptr.4666

10. Takase H, Yamamoto K, Hirano H, Saito Y, Yamashita A. Pharmacological profile of gastric mucosal protection by marmin and nobiletin from a traditional herbal medicine, Aurantii Fructus Immaturus. *Jpn J Pharmacol.* (1994) 66:139–47. doi: 10.1254/jjp.66.139

11. Tan WX, Li Y, Wang Y, Zhang ZJ, Wang T, Zhou Q, et al. Anti-coagulative and gastrointestinal motility regulative activities of Fructus Aurantii Immaturus and its effective fractions. *Biomed Pharmacother.* (2017) 90:244–52. doi: 10.1016/j.biopha.2017.03.060

12. Nakajima A, Yamakuni T, Haraguchi M, Omae N, Song SY, Kato C, et al. Nobiletin, a citrus flavonoid that improves memory impairment, rescues bulbectomy-induced cholinergic neurodegeneration in mice. *J Pharmacol Sci.* (2007) 105:122–6. doi: 10.1254/jphs.sc0070155

13. Cao R, Wu X, Guo H, Pan X, Huang R, Wang G, et al. Naringin exhibited therapeutic effects against DSS-induced mice ulcerative colitis in intestinal barrier-dependent manner. *Molecules.* (2021) 26:6604. doi: 10.3390/molecules26216604

14. Hu J, Huang H, Che Y, Ding C, Zhang L, Wang Y, et al. Qingchang Huashi formula attenuates DSS-induced colitis in mice by restoring gut microbiota-metabolism homeostasis and goblet cell function. *J Ethnopharmacol.* (2021) 266:113394. doi: 10.1016/j.jep.2020.113394

15. Cooper HS, Murthy SN, Shah RS, Sedergran DJ. Clinicopathologic study of dextran sulfate sodium experimental murine colitis. *Lab Invest.* (1993) 69:238–49.

16. Chen S, Zhou Y, Chen Y, Gu J. fastp: an ultra-fast all-in-one FASTQ preprocessor. *Bioinformatics.* (2018) 34:i884–90. doi: 10.1093/bioinformatics/bty560

17. Magoc T, Salzberg SL. FLASH: fast length adjustment of short reads to improve genome assemblies. *Bioinformatics.* (2011) 27:2957–63. doi: 10.1093/bioinformatics/btr507

18. Stackebrandt E, Goebel BM. Taxonomic note: a place for DNA-DNA reassociation and 16S rRNA sequence analysis in the present species definition in bacteriology. *Int J Syst Evol Microbiol.* (1994) 44:846–9.

19. Edgar RC. UPARSE: highly accurate OTU sequences from microbial amplicon reads. *Nat Methods.* (2013) 10:996–8. doi: 10.1038/nmeth.2604

20. Wang Q, Garrity GM, Tiedje JM, Cole JR. Naive Bayesian classifier for rapid assignment of rRNA sequences into the new bacterial taxonomy. *Appl Environ Microbiol.* (2007) 73:5261–7. doi: 10.1128/AEM.00062-07

21. Lawrence T, Bebien M, Liu GY, Nizet V, Karin M. IKKalpha limits macrophage NF-kappaB activation and contributes to the resolution of inflammation. *Nature.* (2005) 434:1138–43. doi: 10.1038/nature03491

22. Taniguchi K, Karin M. NF-kappaB, inflammation, immunity and cancer: coming of age. *Nat Rev Immunol.* (2018) 18:309–24. doi: 10.1038/nri.2017.142

23. Dordevic D, Jancikova S, Vitezova M, Kushkevych I. Hydrogen sulfide toxicity in the gut environment: meta-analysis of sulfate-reducing and lactic acid bacteria in inflammatory processes. *J Adv Res.* (2021) 27:55–69. doi: 10.1016/j.jare.2020.03.003

24. Zhu L, Baker SS, Gill C, Liu W, Alkhouri R, Baker RD, et al. Characterization of gut microbiomes in nonalcoholic steatohepatitis (NASH) patients: a connection between endogenous alcohol and NASH. *Hepatology.* (2013) 57:601–9. doi: 10.1002/hep.26093

25. Walters WA, Xu Z, Knight R. Meta-analyses of human gut microbes associated with obesity and IBD. *FEBS Lett.* (2014) 588:4223–33.

26. Konikoff T, Gophna U. Oscillospira: a central, enigmatic component of the human gut microbiota. *Trends Microbiol.* (2016) 24:523–4. doi: 10.1016/j.tim.2016.02.015

27. Keren N, Konikoff FM, Paitan Y, Gabay G, Reshef L, Naftali T, et al. Interactions between the intestinal microbiota and bile acids in gallstones patients. *Environ Microbiol Rep.* (2015) 7:874–80. doi: 10.1111/1758-2229.12319

28. Huang P, Jiang A, Wang X, Zhou Y, Tang W, Ren C, et al. NMN maintains intestinal homeostasis by regulating the gut microbiota. *Front Nutr.* (2021) 8:714604. doi: 10.3389/fnut.2021.714604

29. Teng T, Clarke G, Maes M, Jiang Y, Wang J, Li X, et al. Biogeography of the large intestinal mucosal and luminal microbiome in cynomolgus macaques with depressive-like behavior. *Mol Psychiatry.* (2022) 27:1059–67. doi: 10.1038/s41380-021-01366-w

30. Sorbara MT, Littmann ER, Fontana E, Moody TU, Kohout CE, Gjonbalaj M, et al. Functional and genomic variation between human-derived isolates of Lachnospiraceae reveals inter- and intra-species diversity. *Cell Host Microbe.* (2020) 28:134. doi: 10.1016/j.chom.2020.05.005

31. Powell F, Rothwell L, Clarkson M, Kaiser P. Development of reagents to study the Turkey's immune response: cloning and characterisation of two Turkey cytokines, interleukin (IL)-10 and IL-13. *Vet Immunol Immunopathol.* (2012) 147:97–103. doi: 10.1016/j.vetimm.2012.03.013

32. Gong Y, Dong R, Gao X, Li J, Jiang L, Zheng J, et al. Neohesperidin prevents colorectal tumorigenesis by altering the gut microbiota. *Pharmacol Res.* (2019) 148:104460. doi: 10.1016/j.phrs.2019.104460

frontiers | Frontiers in Nutrition

TYPE Original Research
PUBLISHED 13 October 2022
DOI 10.3389/fnut.2022.934294

OPEN ACCESS

EDITED BY
Jie Yin,
Hunan Agricultural University, China

REVIEWED BY
David Rios-Covian,
Institut National de Recherche pour l'Agriculture, l'Alimentation et l'Environnement (INRAE), France
Danyue Daisy Zhao,
Hong Kong Polytechnic University, Hong Kong SAR, China

*CORRESPONDENCE
Xiang Fang
fxiang@scau.edu.cn
Hong Wei
weihong63@mail.sysu.edu.cn

†These authors share first authorship

SPECIALTY SECTION
This article was submitted to Nutrition and Microbes, a section of the journal Frontiers in Nutrition

RECEIVED 02 May 2022
ACCEPTED 28 July 2022
PUBLISHED 13 October 2022

CITATION
Dong S, Wu C, He W, Zhong R, Deng J, Tao Y, Zha F, Liao Z, Fang X and Wei H (2022) Metagenomic and metabolomic analyses show correlations between intestinal microbiome diversity and microbiome metabolites in ob/ob and ApoE$^{-/-}$ mice. *Front. Nutr.* 9:934294. doi: 10.3389/fnut.2022.934294

Metagenomic and metabolomic analyses show correlations between intestinal microbiome diversity and microbiome metabolites in ob/ob and ApoE$^{-/-}$ mice

Sashuang Dong[1,2,3†], Chengwei Wu[1†], Wencan He[1], Ruimin Zhong[3], Jing Deng[2], Ye Tao[4], Furong Zha[4], Zhenlin Liao[2], Xiang Fang[2*] and Hong Wei[1*]

[1]Precision Medicine Institute, The First Affiliated Hospital, Sun Yat-sen University, Guangzhou, China, [2]College of Food Science, South China Agricultural University, Guangzhou, China, [3]Guangdong Provincial Key Laboratory of Utilization and Conservation of Food and Medicinal Resources in Northern Region, Shaoguan University, Shaoguan, China, [4]Shanghai Biozeron Biotechnology Co., Ltd., Shanghai, China

Obesity and atherosclerosis are the most prevalent metabolic diseases. ApoE$^{-/-}$ and ob/ob mice are widely used as models to study the pathogenesis of these diseases. However, how gut microbes, gut bacteriophages, and metabolites change in these two disease models is unclear. Here, we used wild-type C57BL/6J (Wt) mice as normal controls to analyze the intestinal archaea, bacteria, bacteriophages, and microbial metabolites of ob/ob and ApoE$^{-/-}$ mice through metagenomics and metabolomics. Analysis of the intestinal archaea showed that the abundances of *Methanobrevibacter* and *Halolamina* were significantly increased and decreased, respectively, in the ob/ob group compared with those in the Wt and ApoE$^{-/-}$ groups ($p < 0.05$). Compared with those of the Wt group, the relative abundances of the bacterial genera *Enterorhabdus*, *Alistipes*, *Bacteroides*, *Prevotella*, *Rikenella*, *Barnesiella*, *Porphyromonas*, *Riemerella*, and *Bifidobacterium* were significantly decreased ($p < 0.05$) in the ob/ob mice, and the relative abundance of *Akkermansia* was significantly decreased in the ApoE$^{-/-}$ group. The relative abundances of *A. muciniphila* and *L. murinus* were significantly decreased and increased, respectively, in the ob/ob and ApoE$^{-/-}$ groups compared with those of the Wt group ($p < 0.05$). *Lactobacillus_ prophage_ Lj965* and *Lactobacillus _ prophage _ Lj771* were significantly more abundant in the ob/ob mice than in the Wt mice. Analysis of the aminoacyl-tRNA biosynthesis metabolic pathway revealed that the enriched compounds of phenylalanine, glutamine, glycine, serine, methionine, valine, alanine, lysine, isoleucine, leucine, threonine, tryptophan, and tyrosine were downregulated in the ApoE$^{-/-}$ mice compared with those of the ob/ob mice. Aminoacyl-tRNA synthetases are considered

10.3389/fnut.2022.934294

manifestations of metabolic diseases and are closely associated with obesity, atherosclerosis, and type 2 diabetes. These data offer new insight regarding possible causes of these diseases and provide a foundation for studying the regulation of various food nutrients in metabolic disease models.

KEYWORDS

ob/ob mice, ApoE$^{-/-}$ mice, metagenomic, metabolomic, gut microbe

Introduction

The intestinal microbiota is composed of trillions of bacteria, archaea, and viruses forming complex ecosystems and is regarded as a modulator of host health (1). Bacterial species commonly serve as a commensal ecosystem that benefits host health by facilitating host metabolism, ameliorating immune cells, and providing barrier protection (2). However, ecological disorders can occur if the gut microenvironment is unbalanced (3). Although causality between intestinal dysbacteriosis and metabolic diseases (e.g., obesity and atherosclerosis) has been extensively reported (4), the mechanism of the pathogenesis remains unclear. Accumulating studies have shown that intestinal dysbacteriosis is associated with key tripartite interaction between bacteriophages and their bacterial and human hosts (5).

Atherosclerosis, a chronic inflammatory disease thought to result from intestinal flora disorders, is becoming prevalent globally (6). The relative abundances of Enterobacteriaceae, *Streptococcus*, *Clostridium*, and other microorganisms are significantly increased in the intestinal tracts of patients with coronary atherosclerosis, thus inhibiting enrichment of beneficial intestinal bacteria. Additionally, the abundances of *Streptococcus* and Enterobacteriaceae are positively correlated with blood pressure and myocardial indices, respectively (7, 8). Although the exact pathogenesis of atherosclerosis is

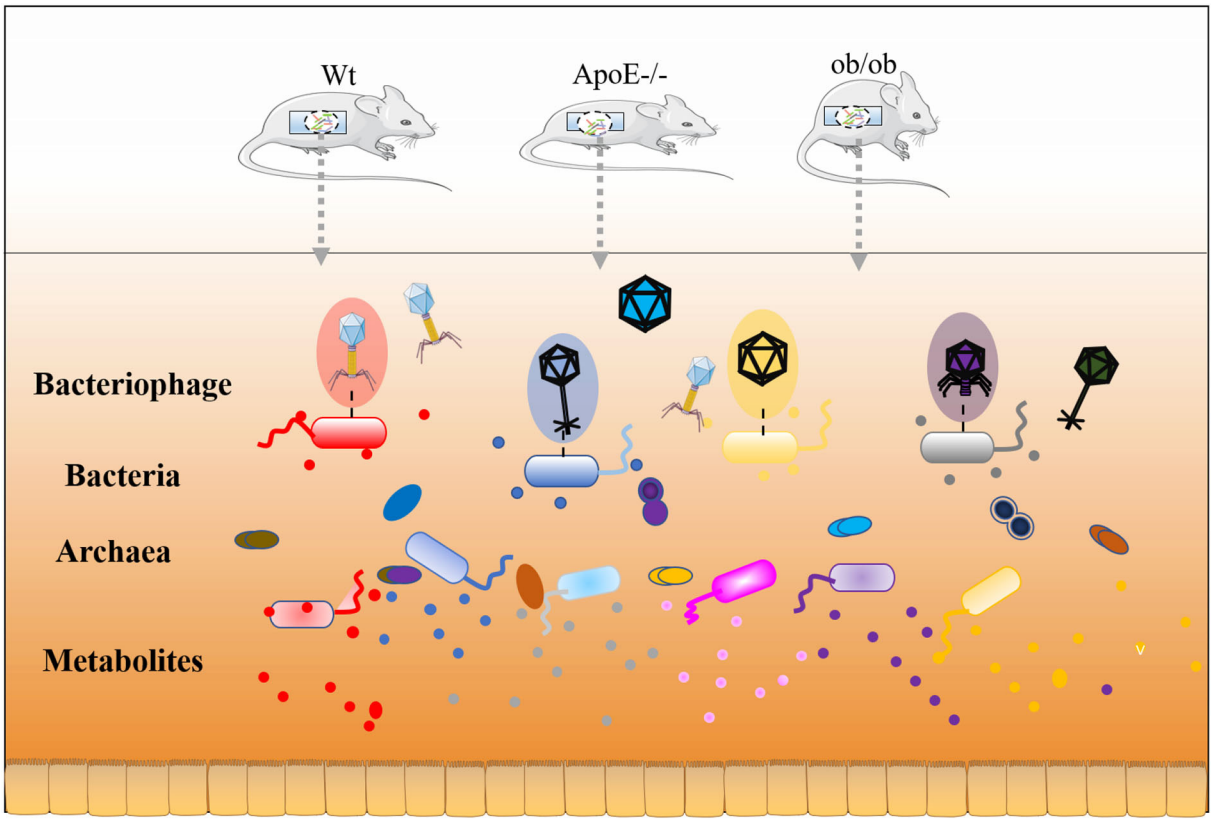

GRAPHICAL ABSTRACT
Overall experimental design.

complex and unclear, inflammation, especially the release of proinflammatory cytokines by macrophages infiltrated by atherosclerotic plaques, is believed to be pivotal (4). ApoE$^{-/-}$ and ob/ob mice are often used as animal models to study the pathogenesis of metabolic diseases (7). Epidemiological studies have shown that the microbial compositions of ApoE$^{-/-}$and ob/ob mice differ significantly from those of normal controls and are characterized by low abundances of butyrate-producing bacteria and increased opportunistic pathogens (4, 9). Leptin is the main metabolite of adipocytes, which regulates energy homeostasis, bone growth, and immune responses. Moreover, leptin-impaired signal transduction is closely related to metabolic diseases, including obesity and type 2 diabetes (10). Researchers have used ob/ob mice as metabolic disease models to study how probiotics regulate the intestinal flora and determine whether improvements in the intestinal flora are related to amelioration of lipid and glucose metabolism (9, 11).

ApoE$^{-/-}$ and ob/ob mice are commonly used as model organisms to clarify the roles of dietary practices in obesity and atherosclerosis treatment. Several studies revealed that dietary intake can relieve these metabolic diseases by modulating the composition and structure of the host's gut microbiota (12–14). However, changes in intestinal bacteria, bacteriophages, and metabolomics of mice with metabolic diseases remain unclear (15, 16). Here, we used metagenomic and metabolomic methods to study the composition and structures of intestinal bacteria and phages and the intestinal metabolomic changes in ob/ob and ApoE$^{-/-}$ mice compared with those of wild-type (Wt) mice. Our results provide insight for further studying the pathophysiology and pharmacology of metabolic diseases such as obesity and atherosclerosis.

Materials and methods

Experimental design

Thirty-six-week-old homozygous male mice were purchased from GemPharmatech Co., Ltd. (Jiangsu, China): ten *ApoE*-deficient mice (B6/JGpt-Apoeem1Cd82/Gpt; ApoE$^{-/-}$ group), ten obese leptin-deficient mice (B6/JGpt-Lepem1Cd25/Gpt; ob/ob group), and ten Wt mice (C57BL/6JGpt; Wt group). Body weight and blood glucose levels differed significantly among the three groups ($p < 0.05$; Supplementary Figure S1). The normal animal diet (D12450J) was prepared by Jiangsu Xietong Pharmaceutical Bioengineering Co., Ltd. (Supplementary Table S1). All animal experiments were performed in the Animal Center of South China Agricultural University. Mice were fed the D12450J diet for 1 week of dietary acclimation, before exposure to a 7-day D12450J feeding. Three or four mice were grouped and fed in a cage with poplar bedding under controlled conditions (temperature: 23 ± 2°C, humidity: 70–75%, and a 12-h/12-h light-dark cycle). Poplar bedding and drinking water were refreshed every 2 days. Water/food consumption and changes in body weight were monitored three times per week. Animal experiments were conducted under National Institute of Health (NIH) guidelines (NIH Publication No. 85-23 Rev. 1985) under supervision of the Animal Experimentation Ethics Review Committee of South China Agricultural University (Guangzhou, China).

Sample collection, DNA extraction, and sequencing

Fecal samples were collected from all mice 2 weeks after feeding and immediately frozen at −80°C for experimentation. DNA was extracted from the fecal samples using the E.Z.N.A.® stool DNA kit (Omega Bio-tek, Norcross, GA, USA) per the manufacturer's protocols. Briefly, DNA buffer was added to the sample for viral capsid lysis and purified through spin-column. The extracted DNA was eluted with TE buffer. The DNA concentration and purity were determined using a Nanodrop 2000 (Thermo Scientific, USA) and stored at −80°C until sequencing. Metagenomic shotgun sequencing libraries were constructed and sequenced at Shanghai Biozeron Biological Technology Co., Ltd. The sequencing libraries were constructed using a Nextera XT DNA Library Preparation kit (Illumina). High-sensitivity double-stranded DNA kits were used to determine the concentrations of all libraries on a Qubit Fluorometer (Thermo Fisher Scientific). After sequencing in the Illumina NovoSeq instrument in pair-end 150-bp (PE150) mode, quality control was performed using Trimmomatic (http://www.usadellab.org/cms/uploads/supplementary/Trimmomatic) on raw sequence reads to remove adaptor contaminants and low-quality reads. Using the BWA mem algorithm with M-k 32 -t 16 parameters (http://bio-bwa.sourceforge.net/bwa.shtml), quality-control reads were mapped to the mouse genome (NCBI). After removing host-genome contaminants and low-quality data, the clean reads were used for further analysis.

Reads-bases phylogenetic annotation

According to the default database downloaded from Broad Institute (min-score-identity = 0.90, identity margin = 0.02), taxonomy of the clean reads for each sample was measured through the PathSeq pipeline distributed in GATK v4.1.3 (https://github.com/usadellab/Trimmomatic) (17). By default, alignments were discarded in PathSeq once two read pairs did not point to the same organism. All bacteriophage, archaeal, and bacterial genome sequences in the NCBI RefSeq database were consistent with those in the taxonomy database. All reads were then classified into seven phylogenetic levels: domain,

phylum, class, order, family, genus, and species or unclassified. Annotations generated in PathSeq were used to construct the host-genome and phage relationships.

Alpha- and beta-diversity analyses

To determine the diversity indices, including the richness and Shannon diversity indices, rarefaction analysis was performed using Mothur v.1.21.1. Beta-diversity analysis was conducted through the community ecology package, *vegan*, in R. Bray-Curtis distance matrices with 999 permutations was applied to measure the virome community similarity using *vegan* in R. Based on a Spearman's rank correlation coefficient >0.6 and $p < 0.05$, correlations between the virus and other elements (other species and metabolites) were determined in R. The relationships were visualized using a correlation heatmap and network diagrams constructed in Gephi (https://gephi.org).

Metabolomic profiling analysis

Targeted metabolomic analysis of the fecal samples was performed using Metabo-Profile (Shanghai, China). The metabolites were detected according to previously published references (18). The sample preparation procedures were performed as per previously published methods with minor modifications (19). UPLC-MS/MS (ACQUITY UPLC-Xevo TQ-S, USA) was used to quantify the microbial metabolites (20). Reserve solutions of all 164 representative reference chemicals of the microbial differential metabolites were prepared in methanol, ultrapure water, or sodium hydroxide solution as per the internal standards (Supplementary Table S2). Internal standards were added to the samples to monitor data quality and compensate for matrix effects (21). After generating raw data files from the UPLC-MS/MS, peak integration, calibration, and quantitation were performed for each metabolite using MassLynx software (v4.1, Waters, Milford, MA, USA) (22). The iMAP platform (v1.0; Metabo-Profile, Shanghai, China) was used for statistical analysis. Principal component analysis (PCoA) and orthogonal partial least square discriminant analysis (OPLS-DA) (23) were used to visualize the metabolic differences among the experimental groups. The biological patterns, functions, and pathways of the differentially expressed metabolites were analyzed using the Matabo Analyst online tool (version 4.0) (24).

Fecal metabolomic analysis

Thawed fecal samples (5 mg) were dispersed in 25 μL of water and homogenate with zirconium oxide beads for 3 min, before metabolite extraction with 120 μL of a mixture of methanol and internal standard. The homogenate process was repeated once, then the mixture was centrifuged at 18000 × *g* for 20 min. Next, 20 μL of supernatant was transferred to a 96-well plate. The subsequent procedures were performed on an Eppendorf epMotion Workstation (Eppendorf Inc., Humburg, Germany). The plate was sealed, and derivatization was performed at 30°C for 60 min. Next, 330 μL of ice-cold 50% methanol solution was added to dilute the sample. The plate was then stored at −20°C for 20 min, then centrifuged at 4000 × *g* at 4°C for 30 min. The supernatant (135 μL) was then transferred to a new 96-well plate with 10 μL of internal standards in each well. The derivatized stock standards were then serially diluted.

Correlation analysis

Spearman's rank correlations and their significances were calculated using the cor and cor.test functions in R, respectively (25). The correlation (*r*-value) was calculated and is shown in yellow to blue, representing positive and negative correlations, respectively (Figure 1).

Statistical analysis

GraphPad Prism 8.3 (GraphPad Software, La Jolla, CA, USA) and TBtools software (26) were used to construct the graphs. All data are expressed as means ± standard deviation. A two-tailed Wilcoxon's rank-sum test was used to identify statistically significant differences between two groups using SPSS (version 23.0, Chicago, IL, USA). $P < 0.05$ was considered statistically significant.

Results

Overall intestinal microbiota diversity in the ApoE$^{-/-}$, ob/ob, and Wt Mice

The intestinal microbiotas composed of archaea, bacteria, and bacteriophages were characterized by metagenomic sequencing. Alpha diversity (e.g., richness and Shannon indices) was used to characterize variations in the gut microbiotas. Archaeal, bacterial, and bacteriophage diversity did not differ significantly between the ApoE$^{-/-}$, ob/ob, and Wt mice ($p > 0.05$; Figures 2A–F).

Next, we further analyzed the differences in species distributions among the three mouse groups. Figures 2G–I show the differences in species abundance compositions among groups. The β-diversity data are shown through PCoA plot of the weighted UniFrac distance. Analysis of the intestinal microbial archaea, bacteria, and bacteriophages of the three groups showed that as the sample points became closer on the

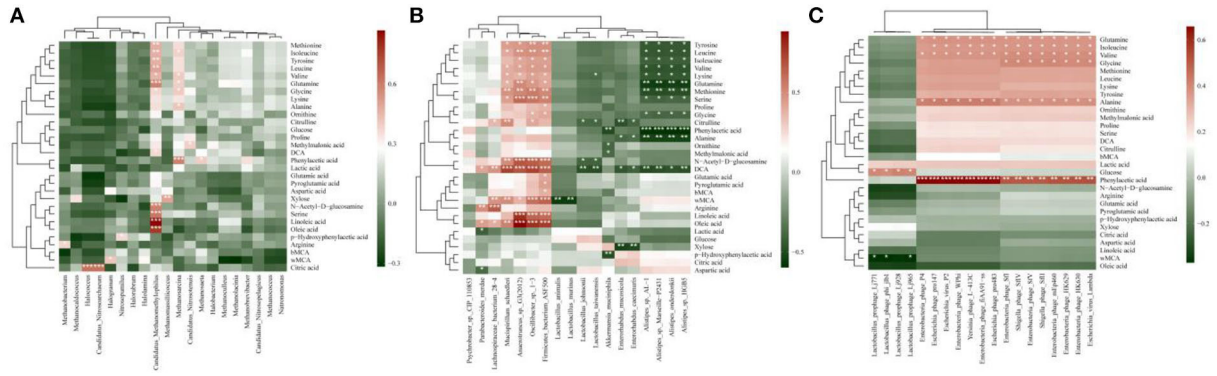

FIGURE 1
Correlation analysis of differential metabolites and intestinal microorganisms. Correlation analyses of differential metabolites with abundances >1% and archaea **(A)**, bacteria **(B)**, and bacteriophages **(C)** with relative abundances >1%. The correlation (*r*-value) was calculated and is shown in red to green, representing positive and negative correlations, respectively.

coordinate axis, the species abundance compositions among the samples became more similar in the corresponding dimension. Archaeal principal components 1 and 2 explained 55.26 and 31.68% of the changes, respectively (Figure 2G). Bacterial principal components 1 and 2 explained 68.67 and 14.66% of the changes, respectively (Figure 2H). Bacteriophage principal components 1 and 2 explained 60.42 and 25.17% of the changes, respectively (Figure 2I).

Overall, these data have shown that the diversity of Archaeal, bacterial, and bacteriophage were no significant difference, but there were differences in species composition in the ApoE$^{-/-}$, ob/ob, and Wt mice, indicating that ApoE-deficient and obese leptin-deficient have certain effects on the composition of gut microbes.

Gut archaeal compositions in the ApoE$^{-/-}$, ob/ob, and Wt mice

Thirty stool samples were shotgun sequenced through the Illumina MiSeq platform and analyzed using metagenomics (Figure 3). Intestinal archaea were mainly composed of the phyla Euryarchaeota and Thaumarchaeota (Supplementary Figure S2A) in all three groups. The relative Euryarchaeota abundances were 97.40 ± 2.36%, 99.66 ± 0.69% and 98.16 ± 3.34% for the Wt, ob/ob and ApoE$^{-/-}$ groups, respectively. Supplementary Figures S2B,C shows the relative abundances of the top six gut archaea at the genus and species levels. *Methanosarcina*, *Methanobrevibacter,* and *Halolamina* were the dominant intestinal archaeal genera in the Wt, ob/ob, and ApoE$^{-/-}$ groups, with relative abundances of 82.19 ± 8.30%, 90.77 ± 10.27%, and 76.47 ± 12.51%; 5.46 ± 4.55%, 1.01 ± 1.47, and 5.71 ± 3.82%; and 4.18 ± 4.33%, 0.13 ± 0.24%, and 0.68 ± 2.16%, respectively (Figure 3A). The relative abundance of *Methanosarcina* was significantly increased in the ob/ob group compared with that of the ApoE$^{-/-}$ group ($p < 0.05$). The relative abundance of *Methanobrevibacter* was significantly decreased in the ob/ob group compared with that of the Wt and ApoE$^{-/-}$ groups ($p < 0.05$), and the relative abundance of *Halolamina* was significantly decreased in the ob/ob group compared with that of the Wt group (Figure 3A). Figure 3B shows the intestinal archaeal species compositions with relative abundances of >1%. Five species belonged to Euryarchaeota, of which, *Methanobrevibacter_smithii* and *Halolamina_sediminis* were significantly decreased in the ob/ob group compared with those of the Wt group; *Methanoculleus_chikugoensis* and *Methanolacinia_paynteri* were significantly increased in the ApoE$^{-/-}$ group compared with those of the Wt group, and *Methanosarcina_mazei* was significantly decreased in the ob/ob group compared with that of the ApoE$^{-/-}$ group (Figure 3B). One species from Thaumarchaeota, *Candidatus_Nitrosopumilus_salaria*, was significantly decreased in the ob/ob group compared with that of the Wt group (Figure 3B).

Overall, compared with that of the ApoE$^{-/-}$ group, the relative abundance of Methanosarcina was significantly increased in the ob/ob group, which indicated that this Methanosarcina is related to obese leptin-deficient.

Gut bacterial compositions in the ApoE$^{-/-}$, Ob/ob, and Wt mice

Supplementary Figures S3A–C show the intestinal bacterial compositions at the phylum, genus, and species levels to illustrate the specific changes in microbial communities in the ApoE$^{-/-}$ and ob/ob mice compared with those of the Wt mice. At the phylum level, the relative abundances of Firmicutes, Bacteroidetes, and Verrucomicrobia did not significantly differ

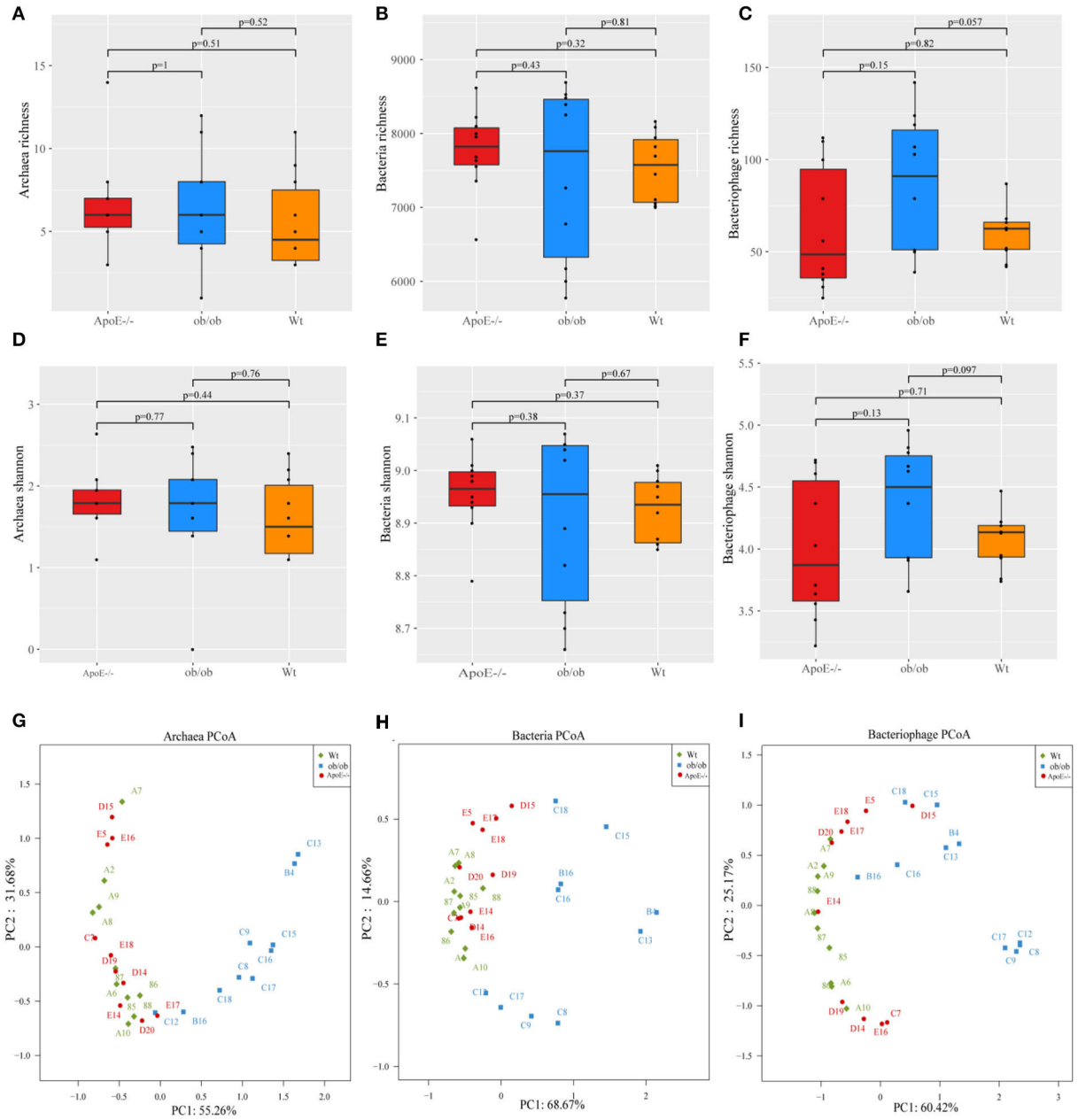

FIGURE 2
Microbiome alpha- and beta-diversity indices. **(A–C)** Archaeal, bacterial, and bacteriophage richness; **(D–F)** Shannon indexes for archaea, bacteria, and bacteriophages; **(G–I)** Scatter plot of principal component (PC) analysis. PC1 and PC2 clusterings for each group.

among the groups ($p > 0.05$; Figure 3C). The relative abundance of Proteobacteria was significantly increased in the ob/ob group compared with that in the ApoE$^{-/-}$ and Wt groups ($p < 0.05$). The relative abundance of Actinobacteria was significantly decreased in the ob/ob group compared with that of the Wt group, and the relative abundance of Deferribacteres in the ob/ob mice was significantly decreased compared with that of the ApoE$^{-/-}$ group ($p < 0.05$). Figure 3D shows the top 20 dominant bacterial genera (relative abundance >1.00%). At the genus level, the relative abundances of *Lactobacillus* and *Akkermansia* were predominant. Compared with the Wt group, the relative abundances of *Enterorhabdus*, *Alistipes*, *Bacteroides*, *Prevotella*, *Rikenella*, *Barnesiella*, *Porphyromonas*, *Riemerella*, and *Bifidobacterium* were significantly decreased ($p < 0.05$) in the ob/ob group, and the relative abundance of *Akkermansia* was significantly decreased in the ApoE$^{-/-}$

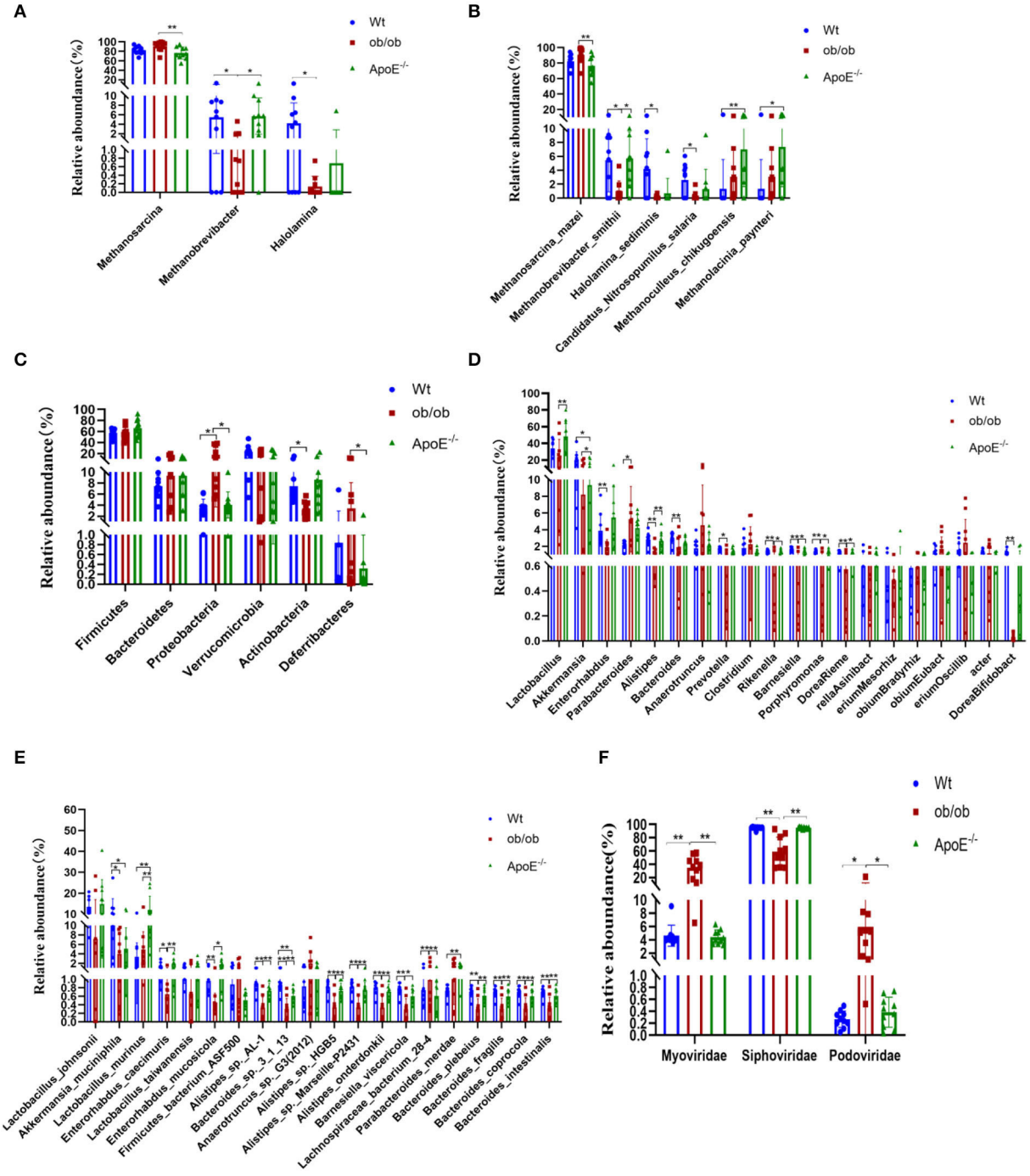

FIGURE 3
Relative abundances of archaea, bacteria and bacteriophages at the phylum, family, genus and species levels and their significantly different compositions in Wt, ob/ob, and ApoE$^{-/-}$ mice. **(A,B)** Relative abundances of archaea at the genus and species levels. **(C)** Relative abundances of bacteria at the phylum level. **(D,E)** Relative abundances of bacteria at the genus and species levels. **(F)** Relative abundances of bacteriophages at the family level.

group. Compared with the ob/ob group, the relative abundances of *Lactobacillus*, *Akkermansia*, *Alistipes*, *Rikenella*, *Barnesiella*, *Porphyromonas,* and *Riemerella* were significantly higher in the ApoE$^{-/-}$ group (Figure 3D). Figure 3E shows the compositions of the top 20 species, including six species from Firmicutes, 11 from Bacteroidetes, two from Actinobacteria, and one from Verrucomicrobia. *Lactobacillus_murinus* (*L. murinus*) and *Akkermansia_muciniphila* (*A. muciniphila*) had the highest

relative abundances in the three groups (Figure 3E). Compared with the Wt group, the relative abundances of *A. muciniphila* and *L. murinus* were significantly decreased and increased ($p < 0.05$) in the ob/ob and ApoE$^{-/-}$ groups, respectively. These species may be the key species of metabolic diseases (Figure 3E).

Overall, these data have shown that the gut dominant microbiota have changed after knockout of ApoE-deficient and obese leptin-deficient, which may be closely associated with metabolic diseases.

Gut bacteriophage composition and associations between phages and their bacterial host in ApoE$^{-/-}$, ob/ob, and Wt mice

Supplementary Figures S4A,B shows the differences in intestinal bacteriophage community structures among the three mouse groups. At the family level, the most common bacteriophages were Siphoviridae (94.85 ± 2.08%, 58.85 ± 21.92% and 4.43 ± 1.06%), Myoviridae (4.62 ± 1.59%, 34.44 ± 17.63% and 94.90 ± 1.33%), and Podoviridae (0.27 ± 0.14%, 5.98 ± 6.02% and 0.39 ± 0.25%) in the Wt, ob/ob, and ApoE$^{-/-}$ groups, respectively (Figure 3F). Compared with the Wt group, the relative abundances of Myoviridae and Podoviridae were significantly increased, and the relative abundance of Siphoviridae was significantly decreased in the ob/ob and ApoE$^{-/-}$ mice (Figure 3F). Compared with the ob/ob group, the relative abundances of Myoviridae and Podoviridae were significantly increased, and the relative abundance of Siphoviridae was significantly decreased in the ApoE$^{-/-}$ mice (Figure 3F).

We summarized the bacteriophage species according to their known bacterial hosts. The relative abundances of the predominant bacteriophage species *Lactobacillus_ prophage_ Lj965* and *Lactobacillus _ prophage _ Lj771* in the Wt and ApoE$^{-/-}$ mice were significantly higher than those in the ob/ob mice. *Escherichia_virus_Lambda*, *Enterobacteria_phage_HK630*, *Enterobacteria_ phage_HK629*, *Escherichia_virus_24B*, *Shigella_phage_SfII*, *Shigella_phage_SfIV*, *Enterobacteria_phage_SfV*, *Enterobacteria_phage_SfI*, *Escherichia_phage_pro147*, *Enterobacteria_phage_fiAA91-ss*, *Escherichia_virus_P2*, *Escherichia_phage_pro483*, *Yersinia_phage_L-413C*, *Enterobacteria_phage_WPhi*, *Escherichia_virus_ADB2*, *Escherichia_virus_T1,* and *Shigella_virus_ PS* were the predominant intestinal phages in the ob/ob mice (relative abundance >1%). These species had relative abundances of <0.3 and 0.6% in the Wt and ApoE$^{-/-}$ mice, respectively (Figure 4A).

The heatmap of the bacteriophages and their host bacteria shows the relative abundances of the 21 most abundant bacteriophages in the three groups (Figure 4B). The bacteriophage/bacteria relationship was characterized by high abundances of some phages and decreased bacterial host abundances in others. Compared with those of the Wt mice, *Shigella_phages*, *Enterobacter_phages*, *Enterococcus_phages,* and *Klebsiella_phages* had lower abundances, and *Shigella*, *Enterobacter*, *Enterococcus,* and *Klebsiella* had higher abundances in the ob/ob mice (Figure 4B). *Ralstonia_phages* and *Propionibacterium_phages* were highly abundant, but the corresponding *Ralstonia* and *Propionibacterium* bacteria had low abundances in the ApoE$^{-/-}$ mice (Figure 4B). *Escherichia* and *Escherichia_phages* had less stringent relationships in only a few ob/ob mice, and *Staphylococcus* and *Staphylococcus_phages* had less stringent relationships in only a few ApoE$^{-/-}$ mice (Figure 4B).

Our study showed that the relative abundance of intestinal phage Podoviridae, *Lactobacillus_prophage_Lj965,* and *Lactobacillus_prophage_Lj771* were significantly elevated in ob mice, which are closely associated with metabolic diseases, such as ulcerative colitis and type 2 diabetes.

Compositions and differential analyses of targeted fecal metabolites in Wt, ob/ob, and ApoE$^{-/-}$ mice

Targeted UPLC-MS/MS analyses of the feces from Wt, ob/ob, and ApoE$^{-/-}$ mice revealed 163 metabolites, mainly including carbohydrates (7.36%), amino acids (21.47%), secondary bases (13.5%), organic acids (14.11%), fatty acids (19.63%), short-chain fatty acids (5.52%), phenols (2.45%), benzenoids (2.45%), benzoic acids (3.07%), phenylpropanoic acids (2.45%), and indoles (3.07%; Figure 5A). Supplementary Figure S5 shows the relative abundance of each metabolite class in each group. The abundance patterns of the metabolites differed significantly among the groups by PCoA analysis (Figure 5B). Compared with those of the Wt mice, acetoacetic acid, 3-hydroxybutyric acid, xylulose, ribulose, tartaric acid, and 3-hydroxyphenylacetic acid-3 were significantly upregulated in the ApoE$^{-/-}$ mice (Figure 5C), and deoxycholic acid (DCA), lithocholic acid (LCA), glycodeoxycholic acid (GDCA), glutamine, α-ketoisovaleric acid, and butyric acid were significantly upregulated in the ob/ob mice (Figure 5D). Compared with those of the ob/ob mice, lysine, citrulline, DCA, eicosapentaenoic acid (EPA), GDCA and glutamine were downregulated in the ApoE$^{-/-}$ mice (Figure 5E).

Overall, these data have shown that the key metabolites in intestinal microorganisms of ApoE-deficient and obese leptin-deficient mice with metabolic diseases may play causal roles in the pathophysiology of metabolic diseases.

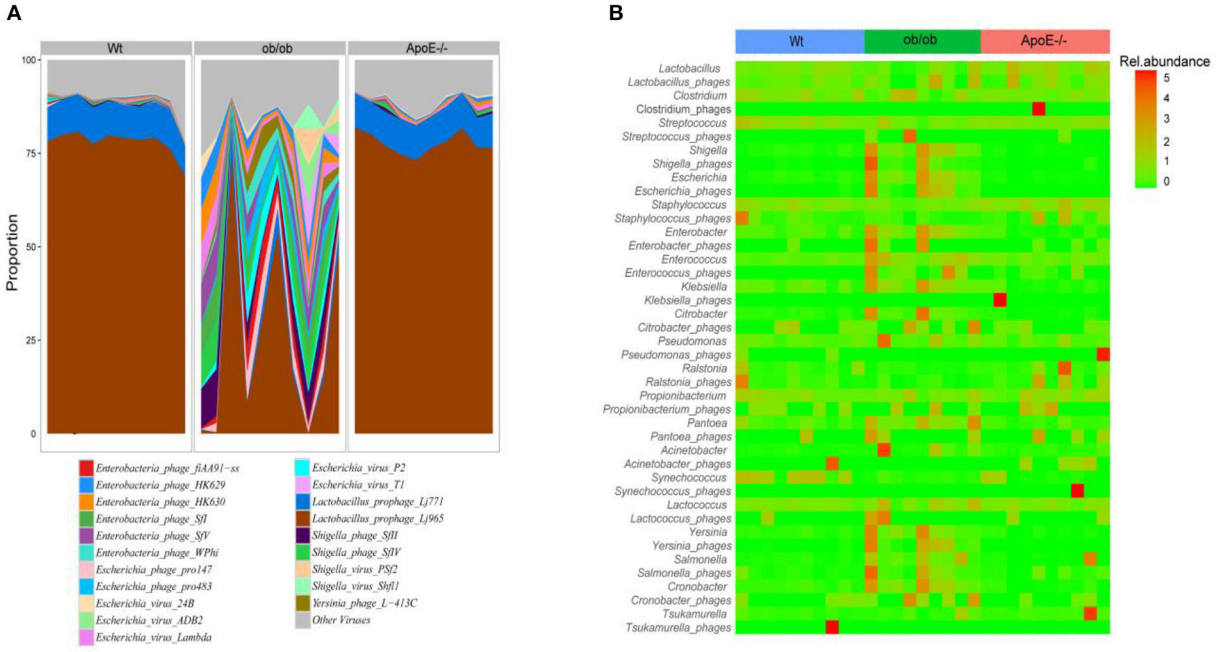

FIGURE 4
Proportions of bacteriophage species and matched alignments with their bacterial hosts and association predictions between the bacteriophages and bacteria. **(A)** The main bacteriophages were classified according to annotation results. The average relative abundances of these aggregated bacteriophages were calculated in phage reads with known bacterial hosts. **(B)** Abundance heatmap of bacteriophages and their host bacteria, showing the relative abundances of the 21 most abundant bacteriophages in the three mouse groups.

Metabolites potential biomarkers and metabolic pathway analysis

Figure 6A shows the top nine differential potential biomarker metabolites ($p < 0.05$). The common metabolites among the Wt, ApoE$^{-/-}$, and ob/ob mice were DCA, LCA, lysine, citrulline, EPA, GDCA, glutamine, methionine, and phenylalanine.

A pathway-associated metabolite sets library pathway enrichment analysis was conducted for the three groups. The metabolite pathway analysis suggested that these pathways were mainly involved in aminoacyl-tRNA biosynthesis; valine, leucine, and isoleucine biosynthesis; phenylalanine, tyrosine, and tryptophan biosynthesis; phenylalanine metabolism; valine, leucine, and isoleucine degradation; ubiquinone and other terpenoid-quinone biosynthesis; alanine, aspartate, and glutamate metabolism; synthesis and degradation of ketone bodies; cyanoamino acid metabolism; glycine, serine, and threonine metabolism; butanoate metabolism and biosynthesis of unsaturated fatty acids (Figure 6B, Supplementary Figure S6). Differential expressions in the synthesis and degradation of ketone bodies pathways in the Wt and ApoE$^{-/-}$ mice showed that acetoacetic acid was significantly upregulated in the ApoE$^{-/-}$ mice (Supplementary Figure S7A). The Kyoto Encyclopedia of Genes and Genomes (KEGG) metabolites pathway of aminoacyl-tRNA biosynthesis was differentially regulated in the Wt and ob/ob mice (Supplementary Figure S7B). Asparagine, histidine, phenylalanine, glutamine, serine, methionine, valine, alanine, lysine, leucine, threonine, and tyrosine were significantly upregulated, and aspartic acid was downregulated in the ob/ob mice. Comparing the aminoacyl-tRNA biosynthesis metabolic pathways showed that the enriched compounds of phenylalanine, glutamine, glycine, serine, methionine, valine, alanine, lysine, isoleucine, leucine, threonine, tryptophan, and tyrosine were downregulated in ApoE$^{-/-}$ mice compared with those of the ob/ob mice (Supplementary Figure S7C).

Microbiota correlation analysis of the Wt, ob/ob, and ApoE$^{-/-}$ mice

We performed correlation analyses of the archaebacteria, bacteria and bacteriophages, and metabolites. *Candidatus_Nitrosoarchaeum* and *Halococcus* were significantly positively correlated with citric acid ($p < 0.05$), and *Candidatus_Methanomethylophilus* was significantly positively correlated with oleic acid, linoleic acid, and serine ($p < 0.05$; Figure 1A). *Lachnospiraceae_bacterium_28-4* was significantly correlated with arginine ($p < 0.05$).

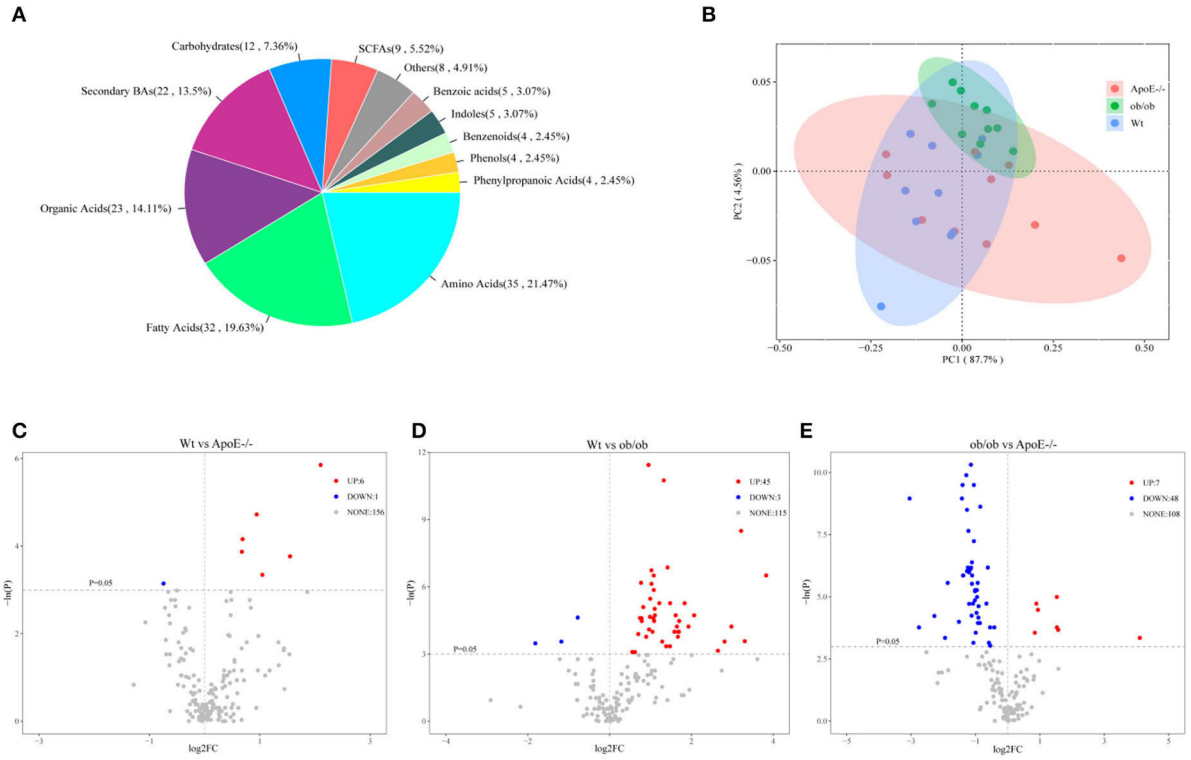

FIGURE 5
Targeted fecal metabolomics analysis of the Wt, ApoE$^{-/-}$, and ob/ob mice. **(A)** Metabolite divisions among the three mouse groups. **(B)** Scatter plot of the principal component (PC) analysis. PC1 and PC2 clusterings for each group. **(C–E)** Volcano plot of differentially expressed genes for Wt vs ApoE$^{-/-}$ **(C)**, Wt vs ob/ob **(D)**, and ob/ob vs ApoE$^{-/-}$ **(E)**, with $p < 0.05$ and log2 fold-change >0. Each point represents a metabolite. Red and blue dots indicate upregulation and downregulation, respectively; gray dots indicate no statistical difference.

Anaerotruncus_sp._G3(2012) was significantly positively correlated with DCA, serine, oleic acid, linoleic acid, and N-acetyl-D glucosamine. *Firmicutes_bacterium_ASF500* was significantly positively correlated with α-muricholic acid (α-MCA), DCA, serine, oleic acid, linoleic acid, and N-acetyl-D-glucosamine. *Lachnospiraceae_bacterium_28-4* was significantly positively correlated with arginine. *Mucispirillum_schaedleri* was significantly positively correlated with DCA and oleic acid. *Oscillibacter_sp._1-3* was significantly positively correlated with oleic acid, linoleic acid, N-acetyl-D-glucosamine, wMCA, DCA, serine, and methionine ($p < 0.05$).

Significant negative correlations were found between *Lactobacillus_animalis* and wMCA; *Lactobacillus_murinus* and wMCA; *Enterorhabdus_mucosicola* and xylose; *Alistipes_sp._AL-1* and phenylacetic acid, glutamine and alanine; *Alistipes_sp._MarseilleP2431* and phenylacetic acid, glutamine and alanine; *Alistipes_onderdonkii* and phenylacetic acid, alanine and glutamine; and *Alistipes_sp._HGB5* and glutamine, alanine and phenylacetic acid ($p < 0.05$; Figure 1B). *Enterobacteria_phage_fiAA91-ss*, *Enterobacteria_phage_P4*, *Enterobacteria_phage_WPhi*, *Escherichia_phage_pro147*, *Escherichia_phage_pro483*, *Escherichia_virus_P2*, and *Yersinia_phage_L-413C* were significantly positively correlated with phenylacetic acid (Figure 1C).

Correlations between intestinal microbes and metabolites in Wt, ob/ob, and ApoE$^{-/-}$mice

To further examine extended network links, we evaluated archaeal, bacterial, and bacteriophage abundances for associations with key metabolite levels. The resulting network contained 30 nodes and 43 edges, representing significant correlations among archaea, bacteria, bacteriophages, and metabolites (Figure 7). *Alistipes_onderdonkii*, *Alistipes_sp._AL-1*, *Alistipes_sp._HGB5*, and *Alistipes_sp._Marseille-P2431* were significantly negatively correlated with 7-KetoLCA ($p < 0.05$). Significant positive correlations were found between *Anaerotruncus_sp._G3(2012)* and DCA, asparagine and GDCA; *Firmicutes_bacterium_ASF500* and asparagine, acetoacetic acid, bHDCA and GDCA; and *Oscillibacter_sp._1-3* and 3-DHCA, asparagine, DCA, acetoacetic acid, bHDCA, and GDCA; *Candidatus_Nitrosopumilus_salaria* and asparagine and DCA; *Methanoculleus_chikugoensis* and acetoacetic acid

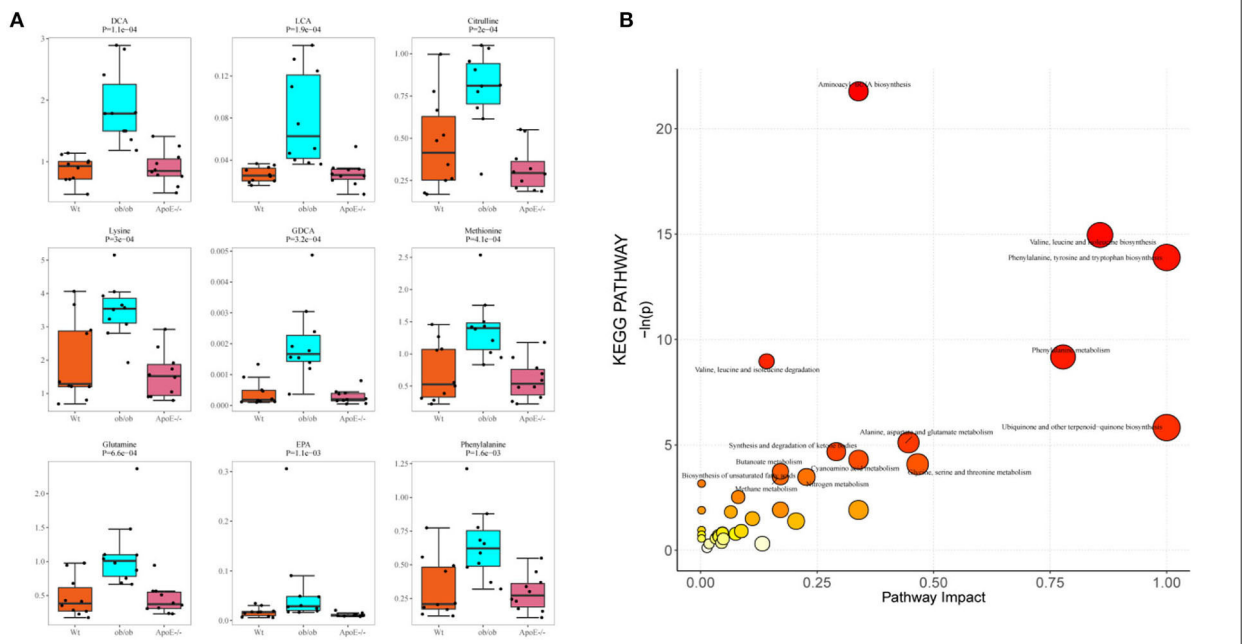

FIGURE 6
Potential biomarker metabolites and KEGG pathway analysis. **(A)** Box-scatter plot of potential biomarker metabolites of the top 9 differential metabolites ordered by *p*-value; **(B)** Bubble plot of enriched KEGG pathways. Bubble size represents the number of metabolites enriched in the pathway.

and bHDCA; *Methanolacinia_paynteri* and acetoacetic acid, bHDCA, asparagine, and GDCA; *Methanosarcina_mazei* and 7KetoLCA; and *Methanoculleus_chikugoensis* and asparagine and GDCA ($p < 0.05$). *Enterobacteria_phage_fiAA91ss*, *Enterobacteria_phage_P4*, *Enterobacteria_phage_WPhi*, *Escherichia_phage_pro147*, *Escherichia_phage_pro483*, *Escherichia_virus_P2*, and *Yersinia_phage_L-413C* were significantly positively correlated with 7-KetoLCA ($p < 0.05$).

In summary, our multi-omics analysis provides fundamental data for investigating the causal relationship of key microbial species and their metabolites in the occurrence and development of metabolic diseases, especially obesity. Metabolite pathway analysis showed that these metabolite pathways were mainly involved in the biosynthesis of aminoacyl-tRNA and were widely present in organisms. These data offer new insights regarding possible causes of these diseases and provide a foundation for studying the regulation of various food nutrients in metabolic disease models.

Discussion

ApoE$^{-/-}$ and ob/ob mice are widely used to study the pharmacology and pathogeneses of metabolic diseases (4). Here, we measured the weight and blood glucose levels of the three mouse groups and found significant differences in ob/ob and ApoE$^{-/-}$ mice compared with those of Wt mice (Supplementary Figure S1), indicating that gene knockout strongly affects the weight and blood glucose levels of mice. We described the structure and compositions of the gut archaea, bacteria, bacteriophages, and metabolites in the ob/ob and ApoE$^{-/-}$ mice compared with those of the Wt mice. To our knowledge, this is the first study to focus on the gut archaea, bacteria, bacteriophages, and metabolites of ob/ob and ApoE$^{-/-}$ mice. These data enable better understanding obesity, cardiovascular disease, diabetes, and their related treatments.

Our results showed no significant differences in microbial diversity among ob/ob and ApoE$^{-/-}$ mice compared with those of Wt mice ($p > 0.05$), likely because the ob/ob and ApoE$^{-/-}$ mice were still young and showed early subtle pathological symptoms (Figures 2A–F). The relative abundance of *Methanosarcina* was significantly increased in the ob/ob group compared with that of the ApoE$^{-/-}$ group ($p < 0.05$). Studies have increasingly focused on the metabolism of *Methanosarcina* fermentation products (methane) in the intestines, mainly focusing on the relationship between *Methanosarcina* and intestinal dysfunction. The number of intestinal methanogens in patients with irritable bowel syndrome is often less than that of the normal population. Intestinal methanogens have also been associated with obesity (27).

Compared with the Wt group, the relative abundances of *A. muciniphila* and *L. murinus* were significantly decreased and increased ($p < 0.05$) in the ob/ob and ApoE$^{-/-}$ groups,

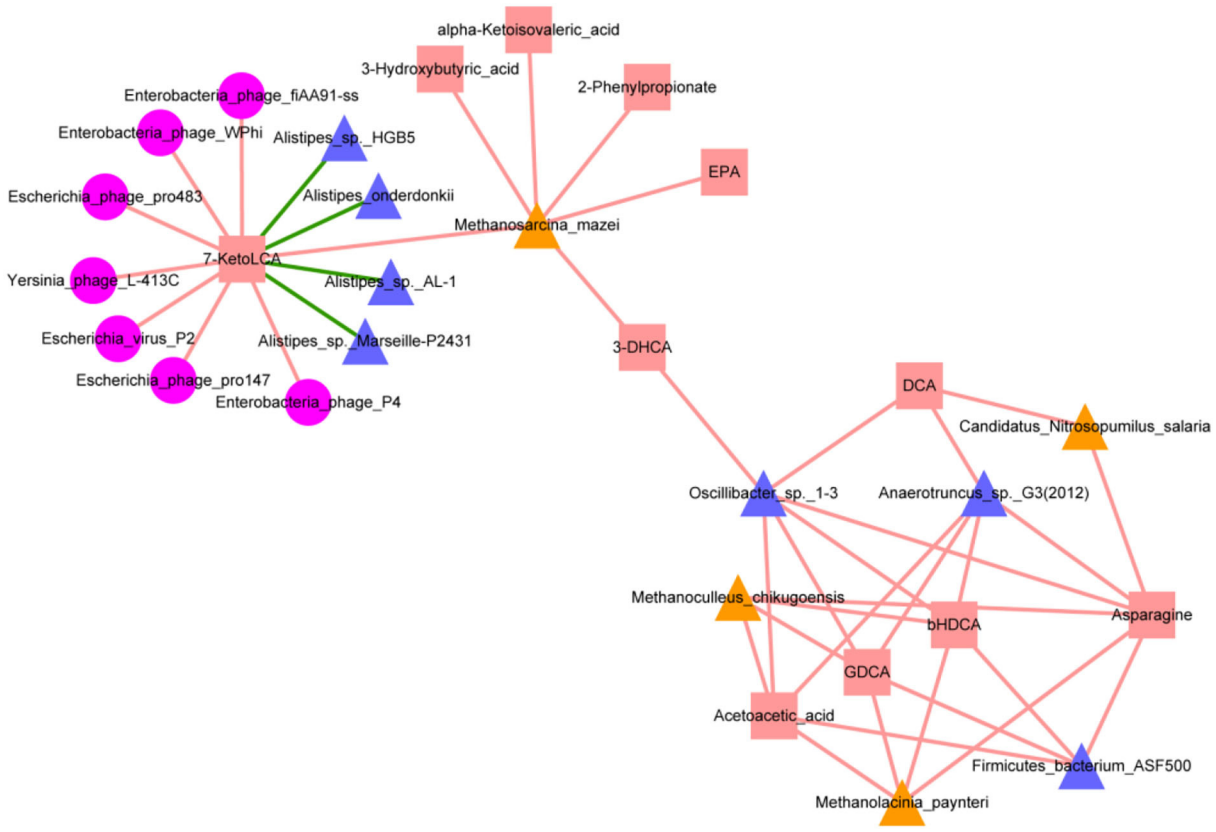

FIGURE 7
Interaction network of metagenomic and metabolomic features for mice with metabolic diseases (ApoE$^{-/-}$ and ob/ob) groups and wild-type (Wt) control group. Red squares represent metabolites; yellow triangles represent archaea; pink circles represent bacteriophages; blue-purple triangles represent bacteria. Red and green lines represent positive and negative correlations, respectively. Interactions were visualized using Cytoscape.

respectively. These may be key species in metabolic diseases (Figure 3E). *A. muciniphila* is a typical species of intestinal bacteria. *Akkermansia* belongs to the Verrucomicrobia phylum (28) and human intestinal mucin-degrading bacteria (29). Decreased abundances of intestinal *Akkermansia* in metabolic diseases may be related to diet-induced obesity, type 2 diabetes, liver injury, and other metabolic disorders (23, 30). Previous studies have shown decreased abundances of *A. muciniphila* in the guts of patients with ulcerative colitis and metabolic disorders, suggesting that *A. muciniphila* may have potential anti-inflammatory properties (31). When ApoE$^{-/-}$ mice were treated with *A. muciniphila* for 8 weeks after consuming a western-type diet, their lipid metabolism did not change, but the expressions of proinflammatory cytokines and intercellular adhesion molecule 1 (ICAM-1) in the aorta decreased, and infiltration of macrophages into aortic atherosclerosis decreased (7, 32). These results suggest that *A. muciniphila* can positively regulate the intestinal microflora (33), improve intestinal barrier functions, and protect against obesity and atherosclerosis (34). However, further research is needed to explore the correlation between *A. muciniphila* and ulcerative colitis and metabolic diseases, especially in humans. Studies have demonstrated that *L. murinus* can reduce inflammation associated with aging in calorie-restricted mice (35), and its abundance is significantly decreased in the intestinal tracts of cirrhotic rats (36). However, the *L. murinus* abundance is high in obese and atherosclerotic mice. Studies have found that antibiotic-induced ecological disorders, especially excessive growth of *L. murinus*, can impair intestinal metabolic functions and lead to the development of alopecia. Additionally, high salt intake has been linked to depletion of *L. murinus*, which has been associated with increased CD4^{+}Rorγt^{+}TH17 cells and blood pressure (31, 37, 38).

We next analyzed the most abundant members of Myoviridae, Siphoviridae, and Podoviridae in the microbial community structure of bacteriophages. Compared with those of Wt and ApoE$^{-/-}$mice, the relative abundances of Podoviridae, Myoviridae, and Siphoviridae were significantly increased and decreased, respectively, in the intestinal tracts of ob/ob mice. Podoviridae has been associated with

ulcerative colitis and type 2 diabetes and can aggravate these diseases (39). Myoviridae abundances are significantly increased ($p < 0.05$) in patients with type 2 diabetes, although the mechanism remains unclear (40, 41). Additionally, *Lactobacillus_ prophage_ Lj965* and *Lactobacillus _ prophage _ Lj771* abundances were significantly higher in ob/ob mice than in Wt mice. Studies have shown that *Lactobacillus* is significantly positively associated with Parkinson's disease (11, 42). The intestinal microbial composition is closely related to glucose homeostasis in the blood of obese mice (34), and a sugar-rich diet can induce *Lactobacillus* prophage lysis, which can profoundly impact the intestinal microbial community (43). Further study is needed to determine how gut microbes regulate glucose homeostasis in patients with metabolic diseases and provide microbial resources for developing new therapies for obesity and related metabolic disorders (44–46).

Herein, we have shown that the key microbial species in intestinal microorganisms of mice with metabolic diseases may play causal roles in the pathophysiology of metabolic diseases (47). To further support a potential causal relationship, the characteristics of intestinal metabolites must be analyzed to achieve similar metabolic disease characteristics and show a significant correlation with intestinal microorganisms. Additionally, in the ob/ob mouse model, the levels of several landmark metabolites, including short-chain fatty acids, DCA, LCA, GDCA, and glutamine, were altered. These microbial metabolites are related to the main intestinal microorganisms, i.e., *Lactobacillus*, *Bifidobacterium*, and *Enterobacter*, which promote lipid absorption, which affects triglycerides, cholesterol, glucose, and energy homeostasis (48, 49). *Lactobacillus* promotes the growth of pancreatic ductal carcinoma by activating tumor-associated macrophages through tryptophan in metabolic foods (37, 50). Our multi-omics analysis provides basic data to research the causal relationship between key microbial species and their metabolites in the occurrence and development of metabolic diseases, especially obesity.

Metabolite pathways analysis suggested that these metabolite pathways were mainly involved in aminoacyl-tRNA biosynthesis and are widely present in organisms. With the development of genome and exon sequencing technology and the discovery of new clinical cases, aminoacyl-tRNA synthetases (ARSs) are considered manifestations of metabolic diseases and are closely associated with obesity, atherosclerosis, and type 2 diabetes (3, 14, 51). The classic function of ARSs is to provide raw materials for protein biosynthesis (51). Increasing evidence suggests that ARSs play important roles in controlling inflammation, immune response (15, 48), tumorigenesis, and other important physiological and pathological processes. The availability of intracellular amino acids is closely related to the regulation of various cellular processes (44, 52). However, further work is needed to determine which gut bacteriophages, bacteria, and metabolites can be used as targets for metabolic diseases to develop nutritional interventions for obesity and atherosclerosis-related diseases.

Data availability statement

The datasets presented in this study can be found in online repositories. The names of the repository/repositories and accession number(s) can be found in the article/Supplementary material. Ultra-deep metagenomic sequencing of the fecal samples was performed at Shanghai Biozeron Biotechnology Co., Ltd. The NCBI accession number for the metagenomic sequences reported herein is PRJNA755346.

Ethics statement

The animal study was reviewed and approved by the animal experiments were carried out under NIH guidelines (NIH Publication No. 85-23 Rev. 1985) with supervision of Animal Experimentation Ethics Review Committee of South China Agricultural University (Guangzhou, China).

Author contributions

XF and HW conceived and designed the research framework. SD performed the experiment, analyzed and interpreted the data, and prepared the original draft of the manuscript. CW revised the grammar of the manuscript and supplemented the discussion. YT and FZ analyzed the bioinformatics and constructed the bioinformatics graphs. JD assisted in the animal experiments. WH, RZ, and ZL revised and edited the manuscript. All authors contributed to the article and approved the submitted version.

Funding

This work was supported by the National Natural Science Foundation of China (31871790, 31671855, and 81770434), the National Key Research and Development Program of China (2018YFC1313802), and the Key-Area Research and Development Program of Guangdong Province (2018B020205002).

Conflict of interest

Authors YT and FZ were employed by the company Shanghai Biozeron Biotechnology Co., Ltd.

The remaining authors declare that the research was conducted in the absence of any commercial or financial relationships that could be construed as a potential conflict of interest.

Publisher's note

Supplementary material

The Supplementary Material for this article can be found online at: https://www.frontiersin.org/articles/10.3389/fnut.2022.934294/full#supplementary-material

SUPPLEMENTARY FIGURE S1
Body weight and blood glucose levels in the three mouse groups. **(A)** Changes in body weight in the t 31.68% of the changes, respectively hree mouse groups; **(B)** Changes in blood glucose in the three mouse groups. The same letter indicates no significant difference; different letters indicate significant differences.

SUPPLEMENTARY FIGURE S2
Proportions of gut archaea at the phylum, genus and species levels. **(A)** Proportions of gut archaea at the phylum level; **(B)** Proportions of gut archaea at the genus level; **(C)** Proportions of gut archaea at the species level.

SUPPLEMENTARY FIGURE S3
Proportions of gut bacteria at the phylum, genus and species levels. **(A)** Proportions of gut bacteria at the phylum level; **(B)** Proportions of gut bacteria at the genus level; **(C)** Proportions of gut bacteria at the species level.

SUPPLEMENTARY FIGURE S4
Proportions of gut bacteriophages at the family and species levels. **(A)** Proportions of gut bacteriophages at the family level; **(B)** Proportions of gut bacteriophages at the species level.

SUPPLEMENTARY FIGURE S5
Composition of intestinal metabolites in the three groups of mice.

SUPPLEMENTARY FIGURE S6
Bubble plot of the enriched KEGG pathways. Bubble size represents the number of metabolites enriched in the pathway.

SUPPLEMENTARY FIGURE S7
Differential expressions in the intestinal metabolic KEGG pathways in the three mouse groups. **(A)** Differential expressions in the synthesis and degradation of the ketone bodies pathways in the Wt and ApoE$^{-/-}$ mice; **(B)** The KEGG metabolites pathway of aminoacyl tRNA biosynthesis was differentially regulated in the Wt and ob/ob mice; **(C)** Comparing the aminoacyl-tRNA biosynthesis metabolic pathways in ApoE$^{-/-}$ and ob/ob mice. Red reflects upregulation; blue reflects downregulation.

References

1. Wahida A, Tang F, Barr JJ. Rethinking phage-bacteria-eukaryotic relationships and their influence on human health. *Cell Host Microbe.* (2021) 29:681–8. doi: 10.1016/j.chom.2021.02.007

2. Oh TG, Kim SM, Caussy C, Fu T, Guo J, Bassirian S, et al. Universal gut-microbiome-derived signature predicts cirrhosis. *Cell Metab.* (2020) 32:878–88. doi: 10.1016/j.cmet.2020.06.005

3. Yan Y, Ren S, Duan Y, Lu C, Niu Y, Wang Z, et al. Microbiota and metabolites of alpha-synuclein transgenic monkey models with early stage of Parkinson's disease. *NPJ Biofilms Microb.* (2021) 7:69. doi: 10.1038/s41522-021-00242-3

4. Yamauchi T, Kamon J, Waki H, Imai Y, Shimozawa N, Hioki K, et al. Globular adiponectin protected ob/ob mice from diabetes and ApoE-deficient mice from atherosclerosis. *J Biol Chem.* (2003) 278:2461–8. doi: 10.1074/jbc.M209033200

5. Manrique, P., Zhu, Y., Van der Oost, J., Herrema, H., Nieuwdorp, M., Vos de W. M., et al. (2021). Gut bacteriophage dynamics during fecal microbial transplantation in subjects with metabolic syndrome. *Gut Microbes.* 13, 1–15. doi: 10.1080/19490976.2021.1897217

6. Yang S, Zhang Y, Li W, You B, Yu J, Huang X, et al. Gut microbiota composition affects procyanidin A2-attenuated atherosclerosis in ApoE(-/-) mice by modulating the bioavailability of its microbial metabolites. *J Agric Food Chem.* (2021) 69:6989–99. doi: 10.1021/acs.jafc.1c00430

7. Menu P, Pellegrin M, Aubert JF, Bouzourene K, Tardivel A, Mazzolai L, et al. Atherosclerosis in ApoE-deficient mice progresses independently of the NLRP3 inflammasome. *Cell Death Dis.* (2011) 2:e137. doi: 10.1038/cddis.2011.18

8. Jie Z, Xia H, Zhong SL, Feng Q, Li S, Liang S, et al. The gut microbiome in atherosclerotic cardiovascular disease. *Nat Commun.* (2017) 8:845. doi: 10.1038/s41467-017-00900-1

9. Liu X, Wang S, You Y, Meng M, Zheng Z, Dong M, et al. Brown adipose tissue transplantation reverses obesity in Ob/Ob mice. *Endocrinology.* (2015) 156:2461–9. doi: 10.1210/en.2014-1598

10. Yang M, Liu Y, Xie H, Wen Z, Zhang Y, Wu C, et al. Gut microbiota composition and structure of the Ob/Ob and Db/Db mice. *Int J Endocrinol.* (2019) 19:1394097. doi: 10.1155/2019/1394097

11. Park JM, Shin Y, Kim SH, Jin M, Choi JJ. Dietary epigallocatechin-3-gallate alters the gut microbiota of obese diabetic db/db mice: lactobacillus is a putative target. *J Med Food.* (2020) 23:1033–42. doi: 10.1089/jmf.2020.4700

12. Boling L, Cuevas DA, Grasis JA, Kang HS, Knowles B, Levi K, et al. Dietary prophage inducers and antimicrobials: toward landscaping the human gut microbiome. *Gut Microbes.* (2020) 11:721–34. doi: 10.1080/19490976.2019.1701353

13. Dong S, Zeng B, Hu L, Zhang Y, Xiong J, Deng J, et al. Effect of a humanized diet profile on colonization efficiency and gut microbial diversity in human flora-associated mice. *Front Nutr.* (2021) 8:633738. doi: 10.3389/fnut.2021.633738

14. Hezaveh K, Shinde RS, Klotgen A, Halaby MJ, Lamorte S, Ciudad MT, et al. (2022). Tryptophan-derived microbial metabolites activate the aryl hydrocarbon receptor in tumor-associated macrophages to suppress anti-tumor immunity. *Immunity.* 55, 324–340. doi: 10.1016/j.immuni.2022.01.006

15. Oppi S, Luscher TF, Stein S. Mouse models for atherosclerosis research-which is my line? *Front Cardiovasc Med.* (2019) 6:46. doi: 10.3389/fcvm.2019.00046

16. Kennedy AJ, Ellacott KL, King VL, Hasty AH. Mouse models of the metabolic syndrome. *Dis Model Mech.* (2010) 3:156–66. doi: 10.1242/dmm.003467

17. Kostic AD, Ojesina AI, Pedamallu CS, Jung J, Verhaak RG, Getz G, et al. PathSeq: software to identify or discover microbes by deep

sequencing of human tissue. *Nat Biotechnol.* (2011) 29:393–6. doi: 10.1038/nbt.1868

18. Nicholson JK, Holmes E, Kinross J, Burcelin R, Gibson G, Jia W, et al. Host-gut microbiota metabolic interactions. *Science.* (2012) 336:1262–7. doi: 10.1126/science.1223813

19. Xie G, Wang L, Chen T, Zhou KW. A metabolite array technology for precision medicine. *Anal Chem.* (2021) 14:5709–17. doi: 10.1021/acs.analchem.0c04686

20. Gao JX, Wei W, Li R, Hu K, et al. The association of fried meat consumption with the gut microbiota and fecal metabolites and its impact on glucose homoeostasis, intestinal endotoxin levels, and systemic inflammation: a randomized controlled-feeding trial. *Am Diab Assoc.* [2021] 44:1–10. doi: 10.2337/dc21-0099

21. Zhou Q, Deng J, Liang X, Bai Y. Gut microbiome mediates the protective effects of exercise after myocardial infarction. *Microbiome.* (2022) 10:82–101. doi: 10.1186/s40168-022-01271-6

22. Ungaro F, Massimino L, Furfaro F, Rimoldi V, Peyrin-Biroulet L, D'Alessio S, et al. Metagenomic analysis of intestinal mucosa revealed a specific eukaryotic gut virome signature in early-diagnosed inflammatory bowel disease. *Gut Microbes.* (2019) 10:149–58. doi: 10.1080/19490976.2018.1511664

23. Everard A, Belzer C, Geurts L, Ouwerkerk JP, Druart C, Bindels LB, et al. Cross-talk between Akkermansia muciniphila and intestinal epithelium controls diet-induced obesity. *Proc Natl Acad Sci USA.* (2013) 110:9066–71. doi: 10.1073/pnas.1219451110

24. Ijaz MU, Ahmed MI, Zou X, Hussain M, Zhang M, Zhao F, et al. Casein, and soy proteins differentially affect lipid metabolism, triglycerides accumulation and gut microbiota of high-fat diet-Fed C57BL/6J mice. *Front Microbiol.* (2018) 9:2200. doi: 10.3389/fmicb.2018.02200

25. Dong SZ, He W, Zhang Y, Xiong J. Correlation between the regulation of intestinal bacteriophages by green tea polyphenols and the flora diversity in SPF mice. *Food Funct.* (2022) 5:2952–65. doi: 10.1039/D1FO03694G

26. Chen C, Chen H, Zhang Y, Thomas HR, Frank MH, He Y, et al. TBtools: an integrative toolkit developed for interactive analyses of big biological data. *Mol Plant.* (2020) 13:1194–202. doi: 10.1016/j.molp.2020.06.009

27. Chaudhary PP, Conway PL, Schlundt J. Methanogens in humans: potentially beneficial or harmful for health. *Appl Microbiol Biotechnol.* (2018) 102:3095–104. doi: 10.1007/s00253-018-8871-2

28. Derrien, M., Collado, M. C., Ben-Amor, K., Salminen, S., and Vos de W. M. (2008). The Mucin degrader Akkermansia muciniphila is an abundant resident of the human intestinal tract. *Appl Environ Microbiol.* 74, 1646–1648. doi: 10.1128/AEM.01226-07

29. Collado, M. C., Derrien, M., Isolauri, E., Vos, D. E., and Salminen, W. M. (2007). Intestinal integrity and Akkermansia muciniphila, a mucin-degrading member of the intestinal microbiota present in infants, adults, and the elderly. *Appl Environ Microbiol.* 73, 7767–7770. doi: 10.1128/AEM.01477-07

30. Derrien, M., and Belzer, C., and Vos de W. M. (2017). Akkermansia muciniphila and its role in regulating host functions. *Microb Pathog.* 106, 171–181. doi: 10.1016/j.micpath.2016.02.005

31. Ascher S, Reinhardt C. The gut microbiota: an emerging risk factor for cardiovascular and cerebrovascular disease. *Eur J Immunol.* (2018) 48:564–75. doi: 10.1002/eji.201646879

32. Li J, Lin S, Vanhoutte PM, Woo CW, Xu A. Akkermansia muciniphila protects against atherosclerosis by preventing metabolic endotoxemia-induced inflammation in Apoe-/- mice. *Circulation.* (2016) 133:2434–46. doi: 10.1161/CIRCULATIONAHA.115.019645

33. Cox LM, Yamanishi S, Sohn J, Alekseyenko AV, Leung JM, Cho I, et al. Altering the intestinal microbiota during a critical developmental window has lasting metabolic consequences. *Cell.* (2014) 158:705–21. doi: 10.1016/j.cell.2014.05.052

34. Rasmussen TS, Mentzel CMJ, Kot W, Castro-Mejia JL, Zuffa S, Swann JR, et al. Faecal virome transplantation decreases symptoms of type 2 diabetes and obesity in a murine model. *Gut.* (2020) 69:2122–30. doi: 10.1136/gutjnl-2019-320005

35. Pan F, Zhang L, Li M, Hu Y, Zeng B, Yuan H, et al. Predominant gut Lactobacillus murinus strain mediates anti-inflammaging effects in calorie-restricted mice. *Microbiome.* (2018) 6:54. doi: 10.1186/s40168-018-0440-5

36. Wang G, Xu X, Yao X, Zhu Z, Yu L, Chen L, et al. Latanoprost effectively ameliorates glucose and lipid disorders in db/db and ob/ob mice. *Diabetologia.* (2013) 56:2702–12. doi: 10.1007/s00125-013-3032-8

37. Yuan T, Wang J, Chen L, Shan J, Lactobacillus DIL. Murinus improved the bioavailability of orally administered glycyrrhizic acid in rats. *Front Microbiol.* (2020) 11:597. doi: 10.3389/fmicb.2020.00597

38. Oerlemans, M. M. P., Akkerman, R., Ferrari, M., Walvoort, M. T. C., and Vos de P. (2021). Benefits of bacteria-derived exopolysaccharides on gastrointestinal microbiota, immunity and health. *J Func Foods.* (2021) 76, 104289. doi: 10.1016/j.jff.2020.104289

39. Zuo T, Lu XJ, Zhang Y, Cheung CP, Lam S, Zhang F, et al. Gut mucosal virome alterations in ulcerative colitis. *Gut.* (2019) 68:1169–79. doi: 10.1136/gutjnl-2018-318131

40. Ma Y, You X, Mai G, Tokuyasu T, Liu CA. human gut phage catalog correlates the gut phageome with type 2 diabetes. *Microbiome.* (2018) 6:24. doi: 10.1186/s40168-018-0410-y

41. Wu Z, Huang S, Li T, Li N, Han D, Zhang B, et al. Gut microbiota from green tea polyphenol-dosed mice improves intestinal epithelial homeostasis and ameliorates experimental colitis. *Microbiome.* (2021) 9:184. doi: 10.1186/s40168-021-01115-9

42. Barichella M, Severgnini M, Cilia R, Cassani E, Bolliri C, Caronni S, et al. Unraveling gut microbiota in Parkinson's disease and atypical parkinsonism. *Mov Disord.* (2019) 34:396–405. doi: 10.1002/mds.27581

43. Zhao Y, Jiang Q. Roles of the polyphenol-gut microbiota interaction in alleviating colitis and preventing colitis-associated colorectal cancer. *Adv Nutr.* (2021) 12:546–65. doi: 10.1093/advances/nmaa104

44. Camarillo-Guerrero LF, Almeida A, Rangel-Pineros G, Finn RD, Lawley TD. (2021). Massive expansion of human gut bacteriophage diversity. *Cell.* 184, 1098–1109. doi: 10.1016/j.cell.2021.01.029

45. Vemuri R, Shankar EM, Chieppa M, Eri R, Kavanagh K. Beyond just bacteria: functional biomes in the gut ecosystem including virome mycobiome archaeome and helminths. *Microorganisms.* (2020) 8:483. doi: 10.3390/microorganisms8040483

46. Liang G, Conrad MA, Kelsen JR, Kessler LR, Breton J, Albenberg LG, et al. Dynamics of the stool virome in very early-onset inflammatory bowel disease. *J Crohns Colitis.* (2020) 14:1600–10. doi: 10.1093/ecco-jcc/jjaa094

47. Fujimoto K, Kimura Y, Shimohigoshi M, Satoh T, Sato S, Tremmel G, et al. (2020). Metagenome data on intestinal phage-bacteria associations aids the development of phage therapy against pathobionts. *Cell Host Microbe*. 28, 380–389. doi: 10.1016/j.chom.2020.06.005

48. Ahmad A, Ali T, Kim MW, Khan A, Jo MH, Rehman SU, et al. Adiponectin homolog novel osmotin protects obesity/diabetes-induced NAFLD by upregulating AdipoRs/PPARalpha signaling in ob/ob and db/db transgenic mouse models. *Metabolism.* (2019) 90:31–43. doi: 10.1016/j.metabol.2018.10.004

49. Chang H, Meng HY, Liu SM, Wang Y, Yang XX, Lu F, et al. Identification of key metabolic changes during liver fibrosis progression in rats using a urine and serum metabolomics approach. *Sci Rep.* (2017) 7:11433. doi: 10.1038/s41598-017-11759-z

50. Zhang N, Zhou L, Yang Z, Gu J. Effects of food changes on intestinal bacterial diversity of wintering hooded cranes (*Grus monacha*). *Animals.* (2021) 11:433. doi: 10.3390/ani11020433

51. Zou Y, Yang Y, Fu X, He X, Liu M, Zong T, et al. The regulatory roles of aminoacyl-tRNA synthetase in cardiovascular disease. *Mol Ther Nucleic Acids.* (2021) 25:372–87. doi: 10.1016/j.omtn.2021.06.003

52. Shkoporov AN, Clooney AG, Sutton TDS, Ryan FJ, Daly KM, Nolan JA, et al. The human gut virome is highly diverse, stable, and individual specific. *Cell Host Microbe.* (2019) 26:527–41. doi: 10.1016/j.chom.2019.09.009

frontiers | Frontiers in Nutrition

TYPE Original Research
PUBLISHED 03 November 2022
DOI 10.3389/fnut.2022.1024722

OPEN ACCESS

EDITED BY
Balamurugan Ramadass,
All India Institute of Medical Sciences Bhubaneswar, India

REVIEWED BY
Xin Wu,
Chinese Academy of Sciences (CAS), China
Tongxing Song,
Huazhong Agricultural University, China

*CORRESPONDENCE
Minyi Luo
156313593@qq.com
Siting Xia
siting_hsia@stu.hunau.edu.cn

SPECIALTY SECTION
This article was submitted to Nutrition and Microbes, a section of the journal Frontiers in Nutrition

RECEIVED 22 August 2022
ACCEPTED 10 October 2022
PUBLISHED 03 November 2022

CITATION
Wang K, Ma J, Li Y, Han Q, Yin Z, Zhou M, Luo M, Chen J and Xia S (2022) Effects of essential oil extracted from *Artemisia argyi* leaf on lipid metabolism and gut microbiota in high-fat diet-fed mice. *Front. Nutr.* 9:1024722. doi: 10.3389/fnut.2022.1024722

Effects of essential oil extracted from *Artemisia argyi* leaf on lipid metabolism and gut microbiota in high-fat diet-fed mice

Kaijun Wang[1,2], Jie Ma[1], Yunxia Li[1], Qi Han[1], Zhangzheng Yin[1], Miao Zhou[1], Minyi Luo[3]*, Jiayi Chen[4] and Siting Xia[1]*

[1]Animal Nutritional Genome and Germplasm Innovation Research Center, College of Animal Science and Technology, Hunan Agricultural University, Changsha, Hunan, China, [2]State Key Laboratory for Conservation and Utilization of Subtropical Agro-Bioresources, College of Animal Science and Technology, Guangxi University, Nanning, Guangxi, China, [3]Agricultural Service Center, Zhongshan, Guangdong, China, [4]Academician Workstation, Changsha Medical University, Changsha, Hunan, China

Artemisia argyi leaf is a well-known species in traditional Chinese medicine, and its essential oil (AAEO) has been identified to exert various physiological activities. The aim of this study was to investigate the effects of AAEO on lipid metabolism and the potential microbial role in high-fat diet (HFD)-fed mice. A total of 50 male mice were assigned to five groups for feeding with a control diet (Con), a high-fat diet (HFD), and the HFD plus the low (LEO), medium (MEO), and high (HEO) doses of AAEO. The results demonstrated that dietary HFD markedly increased the body weight gain compared with the control mice ($p < 0.05$), while mice in the HEO group showed a lower body weight compared to the HFD group ($p < 0.05$). The weight of fatty tissues and serum lipid indexes (TBA, HDL, and LDL levels) were increased in response to dietary HFD, while there was no significant difference in AAEO-treated mice ($p < 0.05$). The jejunal villus height was dramatically decreased in HFD-fed mice compared with the control mice, while HEO resulted in a dramatically higher villus height than that in the HFD group ($p < 0.05$). Microbial α-diversity was not changed in this study, but β-diversity indicated that microbial compositions differed in control, HFD, and EO subjects. At the genus level, the relative abundance of *Bacteroides* was greater ($p < 0.05$) in the feces of the Con group when compared to the HFD and EO groups. On the contrary, the abundance of *Muribaculum* was lower in the Con group compared to the HFD and EO groups ($p < 0.05$). Although the *Muribaculum* in the EO group was lower than that in the HFD group, there was no statistically notable difference between the HFD and EO groups ($p > 0.05$). Simultaneously, the relative abundance of *Alistipes* ($p < 0.05$) and *Rikenella* ($p < 0.05$) was also dramatically higher in the Con group than in the HFD and EO groups. The abundance of *norank_f__norank_o__Clostridia_UCG-014* was lower in the

HFD or EO group than in the Con group ($p < 0.05$). In conclusion, the results suggested that HEO could affect body weight and lipid metabolism without gut microbes in ICR mice, and it was beneficial for the structure of the jejunal epithelial tissue.

KEYWORDS

***Artemisia argyi*, high fat, lipid, gut, microbiota**

Introduction

Obesity is a nutritional disorder caused by an imbalance between energy intake and expenditure (1). As economic development increased in developing countries, obesity and metabolic syndrome became more prevalent, primarily due to accelerated urbanization and nutritional changes; declining physical activity and genetics also played a role (2, 3). The prevalence of childhood obesity has increased by approximately 5% per decade over the past 50 years, not only among adults but also children (4). As fat accumulated in the body, dyslipidemia and metabolic syndrome would develop. An elevated level of lipids was associated with an increased risk of atherosclerosis and cardiovascular diseases (5). Atherosclerosis was closely associated with lipids and lipid-containing substances in the blood, of which cholesterol played the most important role (6). In humans, losing weight was a major way to reduce the risk of diabetes (7). It has been demonstrated that some anti-obesity drugs, such as orlistat and lorcaserin, as well as sustained-release tablets of phentermine/topiramate and naltrexone/bupropion are effective at reducing weight (8, 9). However, anti-obesity drugs may also cause gastrointestinal problems, weakness, mental disorders, and cardiovascular diseases, among others (10). Therefore, many experts predicted that natural products will provide hypolipidemic active factors that will intervene in obesity and its complications, as well as direct drug treatment.

There was a need for effective weight loss strategies and effective methods to prevent weight gain due to the current global obesity epidemic. A variety of gut microbial metabolites were necessary for gut microbiota to regulate host lipid metabolism, including short-chain fatty acids, secondary bile acids, and trimethylamine (11). Animal health depended on gut microbiota which were involved in digestion, metabolism, immunity, and defense against pathogens (12, 13). A better understanding of the interactions between host and gut microbes was crucial to study the complex relationship between host and microbiota. With the development of gene sequencing technology, we can explore the impact of changes in animal diet on the structure and function of intestinal microorganisms (14, 15). The molecules involved in this interaction could be measured, especially the microbiota-produced metabolites that were available to the host.

Looking for effective traditional Chinese medicine extracts is critical for obesity prevention, and it is still unclear how they impact the gut microenvironment. The leaves of *Artemisia argyi* were part of the Compositae family and were herbaceous perennial plants (16). It is well known that *A. argyi* leaves were the original source of Moxa floss (made from ground *A. argyi* leaves) in Moxibustion. The technique was widely known for its ability to diminish inflammation, relieve pain, promote blood circulation, and remove obstructions in channels through acupuncture and moxibustion therapy (17). *A. argyi* was beneficial for improving egg quality and increasing polyunsaturated fatty acids in egg yolk (18). Additionally, *A. argyi* leaf was used for preparing medical products, such as capsules and aerosols containing Moxa essential oil (16). Several studies had shown that *A. argyi* leaves were the main source of essential oil; it has antihistamine, phlegm-eliminating properties, cough-relieving properties, antifungal, and antiviral properties (19–21). Additionally, an analysis of the chemical composition, extraction yield, and quality evaluation of the essential oils extracted from *A. argyi* leaves (AAEO) has been conducted (22–24). Although AAEO was a geo-authentic medicine, there was relatively little research on it. The objective of this study was to investigate the effect of AAEO on lipid metabolism, body fat distribution, and gut microbes in a diet-induced obesity mouse model. Moreover, we also examined whether AAEO levels at different concentrations improved lipid metabolism. A systematic study was conducted using ICR mice to determine the effect of AAEO levels on fat metabolism and whether the effects were harmful or beneficial to the structure of the gastrointestinal tract.

Materials and methods

Animals and treatments

Animal experiments were conducted in accordance with the Hunan Agricultural University Institutional Animal Care and Use Committee (202105). Six-week-old male ICR mice were purchased from SLAC Laboratory Animal Central (Changsha, China). The mice were housed in a controlled environment after

a 1-week adaptation period. AAEO was purchased from Jiangxi Hairui Natural Plant Co., Ltd., Jian, China.

A total of 50 male mice (29.40 ± 1.23 g) were divided into 5 groups at random, with 10 repetitions in each group. Mice were fed the control diet (Con), the high-fat diet (HFD), and the HFD-fed mice with the low (LEO), medium (MEO), and high (HEO) doses of AAEO. AAEO was dissolved in 4% Tween 80. In the LEO, MEO, and HEO groups, mice received 0.20, 0.40, and 0.80 ml/kg AAEO, respectively. The Con and HFD groups were given the same amount of physiological saline by oral gavage.

Fecal samples were obtained and kept at −80°C for examination. The mice were sacrificed under anesthesia. Finally, blood, subcutaneous adipose tissue (SAT), abdominal adipose tissue (AAT), epididymal adipose tissue (EAT), perirenal adipose tissue (PEAT), brown adipose tissue (BAT), liver, and jejunal tissue were collected for further examination.

Analyzing blood samples for biochemical parameters

Serum extracted from blood samples using 3,000 rpm for 10 min at 4°C. Biochemical parameters of serum were tested using an automatic biochemistry analyzer (25), the index included total bile acid (TBA), glucose (Glu), total cholesterol (TC), triglycerides (TG), low-density lipoprotein (LDL), and high-density lipoprotein (HDL).

Histological analysis

The jejunal tissue was removed and fixed in a 4% paraformaldehyde solution, then the fixed tissue was paraffin-embedded, and the jejunal tissue block was cut approximately 4-μm thick using a microtome and stained with hematoxylin and eosin (H&E) (26). The villus height was the distance from the villus tip to the crypt mouth, and crypt depth was the distance from the crypt mouth to the base of the crypt (27, 28).

DNA extraction and microbiota analysis

As previously reported, DNA extraction and 16S ribosomal RNA amplification were carried out (29). Fecal samples were extracted for DNA with an E.Z.N.A.® soil DNA kit (Omega Biotek, Norcross, GA, USA) on the basis of the standard protocol. Using universal primers targeting the V3-V4 region 338F/806R, 16S rRNA from bacteria was amplified and sampled for sequencing using an Illumina Miseq PE300 platform (Illumina, SD, USA) (30). Sequence reads from the original sequence were uploaded to NCBI's Sequence Read Archive. The 16S rRNA amplicon sequences have been deposited in the National Center for Biotechnology Information (NCBI) Sequence Read Archive (SRA)[1] under accession number PRJNA861869.

Statistical analyses

Statistical analyses between the means of each group were analyzed using one-way ANOVA (one-way analysis of variance) followed by Duncan comparison range tests through SPSS 22.0. The statistical significance level was set at $p < 0.05$.

Results

Body weight and organ index

As described in **Figure 1A**, the HFD group mice markedly raised the body weight compared to the Con group ($p < 0.05$). An 8-week treatment with HEO markedly decreased body weight compared to the HFD group ($p < 0.05$), but medium and low doses of AAEO did not affect body weight in ICR mice ($p > 0.05$). As described in **Figure 1B**, the low, medium, and high doses of AAEO did not markedly change SAT, AAT, EAT, PEAT, and BAT weight in ICR mice ($p > 0.05$). Although HFD markedly promoted liver weight compared to the control group ($p < 0.05$), the addition of high, medium, and low doses of AAEO did not dramatically affect liver weight in the HFD group ($p > 0.05$).

Indicator of serum lipid metabolism

As demonstrated in **Figure 2**, the HFD, LEO, MEO, and HEO raised serum TBA levels compared to the Con ($p < 0.05$). However, the addition of low, medium, and high doses of AAEO did not dramatically affect TBA level compared to the HFD group ($p > 0.05$). In addition, the HFD, LEO, MEO, and HEO declined in TG level compared to the Con ($p < 0.05$). However, the addition of low, medium, and high doses of AAEO did not dramatically affect TG levels compared to the HFD group ($p > 0.05$). There was no remarkable difference in Glu concentration in Con, HFD, and AAEO groups ($p > 0.05$). Although LEO- and MEO-fed ICR mice had no remarkable difference in TC level from the HFD group ($p > 0.05$), the HEO markedly enhanced the level of TC in blood compared with the HFD group ($p < 0.05$). All the AAEO treatments markedly raised the level of TC in blood compared with the Con group ($p < 0.05$). Meanwhile, the HFD, LEO, MEO, and HEO raised HDL levels compared to the Con ($p < 0.05$). However, the addition of low, medium, and high doses of AAEO showed no

1 https://dataview.ncbi.nlm.nih.gov/object/PRJNA861869

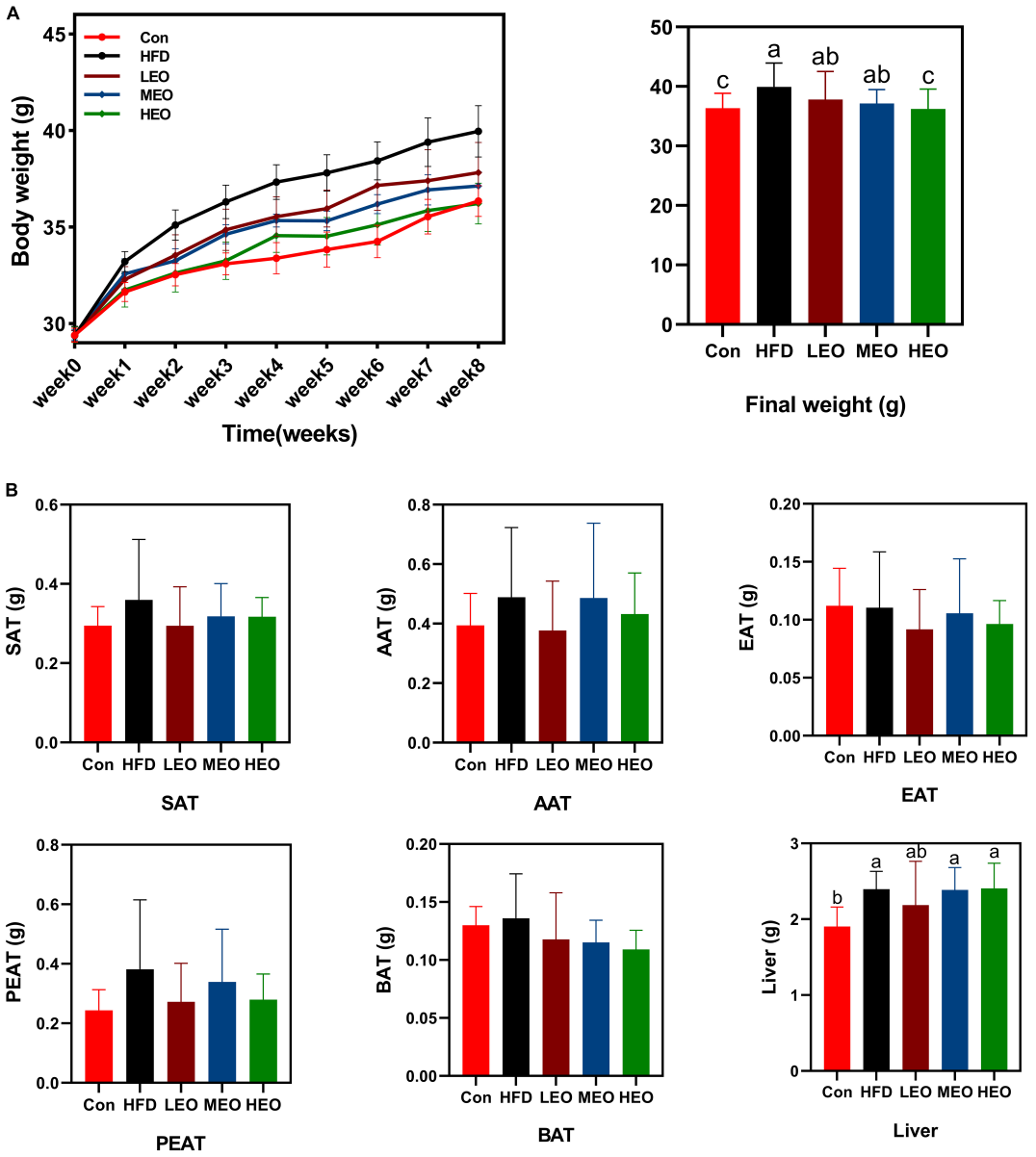

FIGURE 1
Effects of *Artemisia argyi leaves* (AAEO) on **(A)** body weight and **(B)** organ index in mice.

remarkable effect on HDL levels compared to the HFD group ($p > 0.05$). The HFD markedly raised LDL levels in ICR mice with or without AAEO supplementation ($p < 0.05$), and there was no remarkable effect on blood LDL levels between high, medium, and low doses of AAEO ($p > 0.05$).

Histomorphological analysis of jejunum

Figure 3A shows the morphology of jejunal tissue under Con, HFD, and HEO treatments in ICR mice. In this study, jejunal villus height notably declined with the high-fat group compared to the Con diet-fed to ICR mice as described in Figure 3B ($p < 0.05$), but a high dose of AAEO induced a notably higher jejunal villus height than HFD in mice ($p < 0.05$). In ICR mice, the HFD fed to mice did not notably increase crypt depth in the jejunum compared to the Con group ($p > 0.05$), and there was no noteworthy change between the HEO, Con, and HFD groups ($p > 0.05$). With the high-fat diet fed to mice, the VH/CD declined in ICR mice compared to the Con diet ($p < 0.05$), and the VH/CD of the HFD group was notably lower than that of the AAEO group ($p < 0.05$). No matter the control

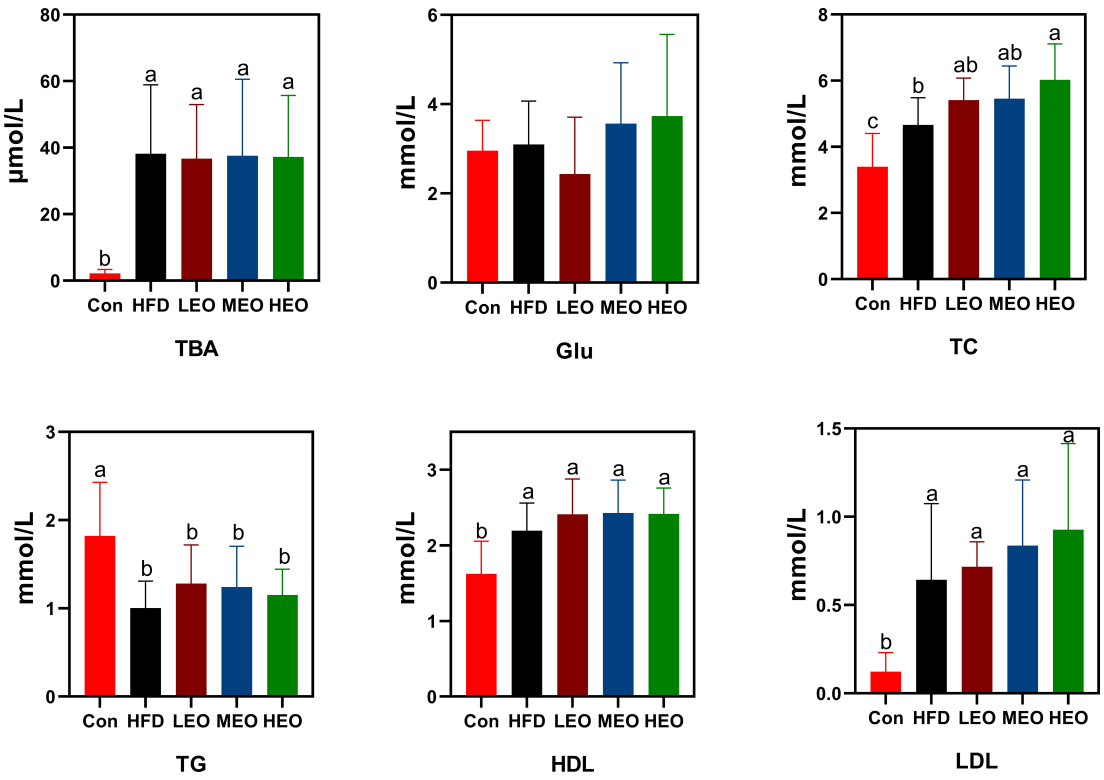

FIGURE 2
Effects of AAEO on serum lipid levels in mice.

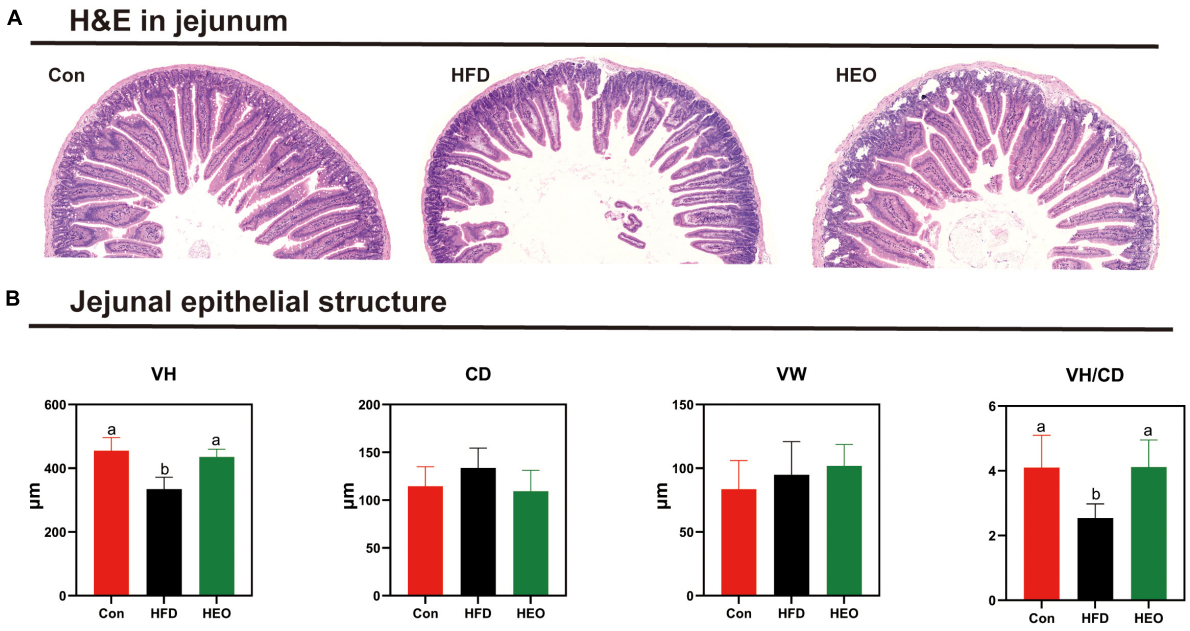

FIGURE 3
Effects of AAEO on the morphology of jejunal epithelial tissue in mice. **(A)** Light microscopy cross-section of the jejunal tissue. **(B)** The structure of the jejunal epithelial tissue.

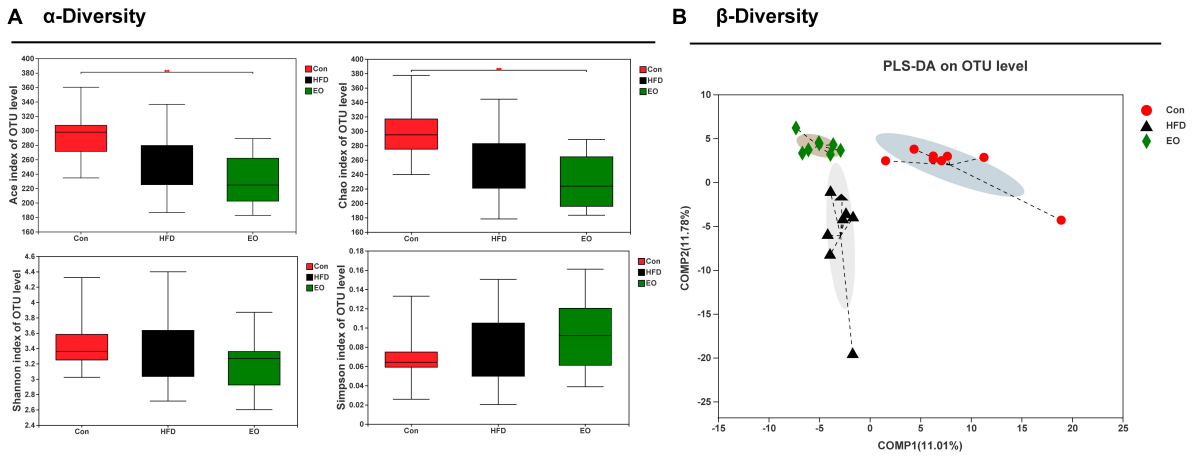

FIGURE 4
Effects of AAEO on **(A)** α diversity and **(B)** β diversity in the fecal microbiota of mice.

group, high-fat group, or AAEO group, there was no noteworthy effect on the jejunal villus width of ICR mice ($p > 0.05$).

Bacterial diversity in feces

Based on three dietary treatments, Figure 4A shows the differences in fecal bacterial diversity among ICR mice. The study demonstrated that the EO fed to mice remarkably decreased the ACE index of OTU levels compared with the Con diet ($p < 0.05$). The three treatments did not affect fecal Shannon index of OTU levels in ICR mice ($p > 0.05$). Although the addition of EO in the diet had no marked effect on the HFD group on Chao index, while EO group remarkably decreased the Chao index compared with the Con group ($p < 0.05$). There was no notable change on the Simpson index of OTU level between the three different dietary treatments ($p > 0.05$). As demonstrated in Figure 4B, the male mice affected by the three dietary treatments produced significant segregation of PLS-DA on an OTU level.

Fecal microbial composition

Figure 5 shows how the three treatments affected mice's fecal microbiota at the phylum level (>1%). *Bacteroidota*, *Firmicutes*, *Actinobacteriota*, and *Proteobacteria* were the main phyla in the feces of mice, accounting for more than 98% of the total number of fecal bacteria. At the dominant phylum level, no differences were found in fecal bacteria from mice ($p > 0.05$). As described in Figure 6, *norank_f__Muribaculaceae*, *Lactobacillus*, *Bacteroides*, *Faecalibaculum*, and *norank_f__Erysipelotrichaceae* were major bacteria in the Con, HFD, and EO groups at the genus level. There were marked changes in 5 of the top 40 genera throughout the whole stage. The relative abundance of *Bacteroides* was greater ($p < 0.05$) in the feces from the Con diet when compared to the HFD and EO diets. On the contrary, the abundance of *Muribaculum* was lower in the Con diet than in the HFD and EO diets ($p < 0.05$). In the meantime, the relative abundance of *Alistipes* ($p < 0.05$) and *Rikenella* ($p < 0.05$) were also notably higher in the Con diet than in the HFD and EO diets. The abundance of *norank_f__norank_o__Clostridia_UCG-014* was lower in the HFD or EO diet than in the Con diet ($p < 0.05$). Although the abundance of *Muribaculum* in the EO diet was lower than that in the HFD diet, there was no notable difference ($p > 0.05$).

Discussion

At present, the research in traditional Chinese medicine (TCM) focuses more on polysaccharides and flavonoids (31, 32). Researchers have demonstrated that a variety of dietary components can be used to treat obesity, including polysaccharides, polyphenols, terpenes, and alkaloids (33, 34). In addition, dietary amino acids and uridine can also affect body fat catabolism (35–37). The anti-obesity mechanisms usually included appetite suppression, fat absorption reduction, lipolysis enhancement, lipolysis reduction, and modification of the gut microbiota (38, 39). The leaf of *A. argyi* was widely used in TCM for its antimicrobial properties, relief from itching, and improvement of blood circulation. Compositae plants had a strong aromatic smell that attracted researchers to investigate their volatile composition (16). This study examined the effects of AAEO on fat deposition, blood lipid metabolism, fecal microbiota, and epithelial structure of jejunum in ICR mice. The HFD remarkably raised the final weight of the mice than their basal diet, while HEO restored the mice's weight to the

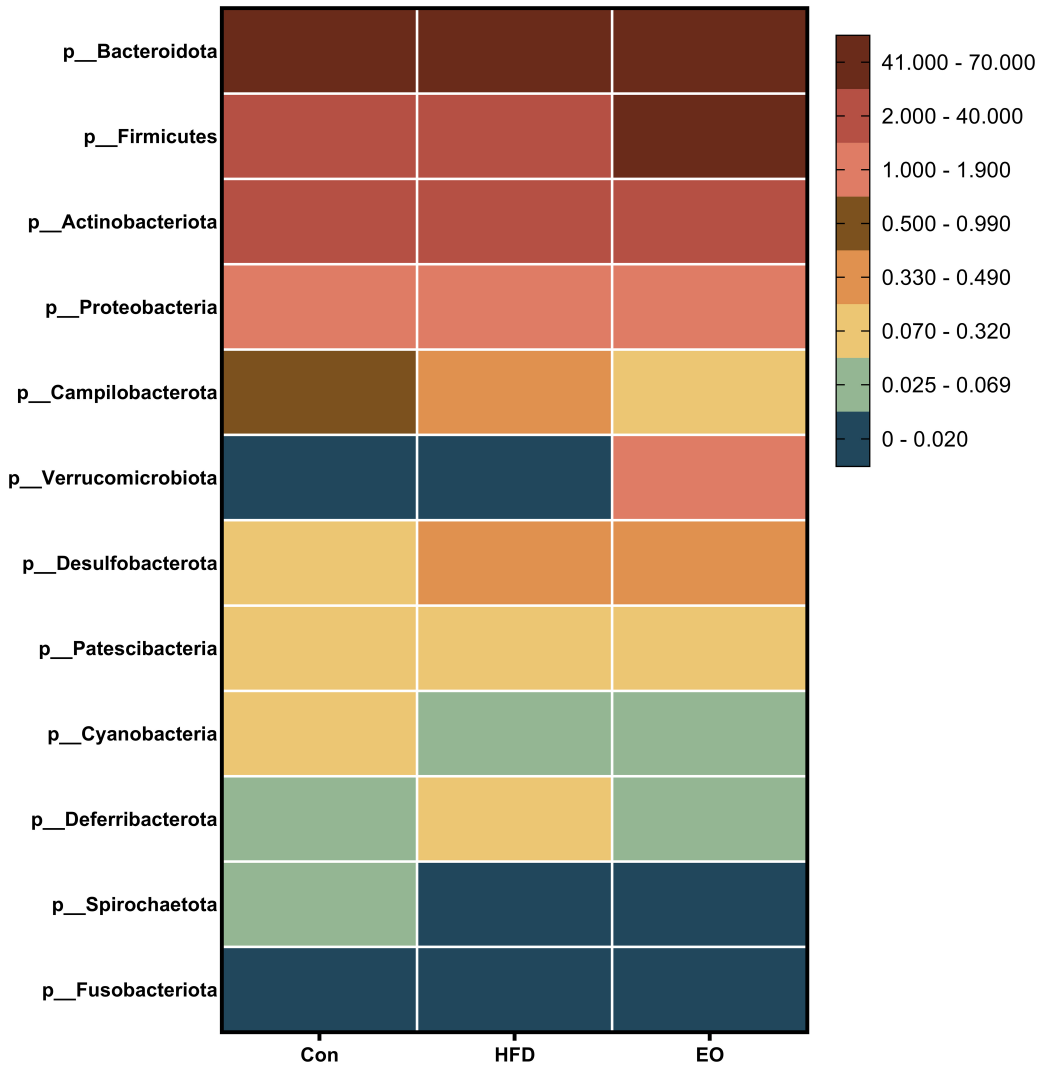

FIGURE 5
Effects of AAEO on phylum-level bacteria in the fecal microbiota of mice.

level of their basal diet. It showed that AAEO had a certain alleviating effect on obesity in mice. According to the results of fat deposition in this experiment, AAEO did not affect the fat weight of ICR mice, but AAEO did affect the weight of the liver, and the mechanism needed further experiments to clarify.

The blood biochemical indexes of the host not only provide information about the health and immune function of the body but also reveal their biological characteristics (40). There was a correlation between hypertrophymia and TC levels in the blood. Compared with LDL, HDL is more likely to cause hypertrophymia (41). In this experiment, AAEO did not change the concentrations of TBA, Glu, TG, HDL, and LDL in the blood of HFD mice; the high concentration of AAEO only raised the concentration of TC in the blood of HFD fed to mice. This indicated that AAEO had little effect on blood lipid metabolism in ICR mice.

Physical, chemical, microbiological, and immunological barriers make up the gut barrier (42). Dietary nutrients can modulate the small intestinal tissue morphology and digestive function of animals, and the gut barrier function is very critical to the host (43, 44). Nutrients were absorbed primarily through the small intestine. In evaluating small intestine digestion and absorption, villi height and crypt depth were key indicators. Deeper crypts reflected faster cell formation, whereas shallower crypts indicated accelerated maturation and improved secretion. It was possible to determine the functioning state of the gut by measuring the villus height and crypt depth (45). In recent years, physical barriers have been extensively examined in HFD resulting in increased intestinal permeability, which greatly increased the translocation of endotoxins from the gut to the blood circulation (46, 47). Throughout the intestine, tightly connected epithelial cells form a dynamic permeability

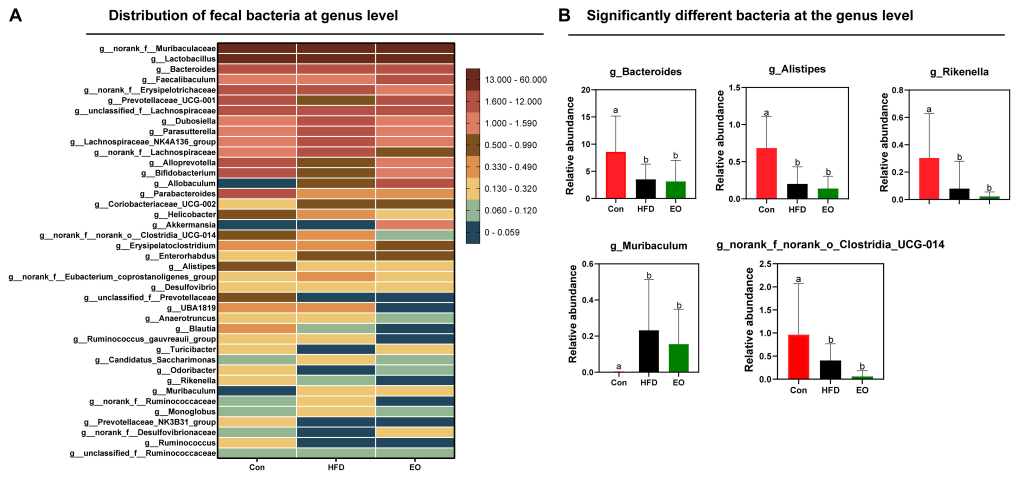

FIGURE 6
Effects of AAEO on **(A)** genus-level bacteria distribution and **(B)** significantly different bacteria at the genus level in the fecal microbiota of mice.

barrier that prevents potentially harmful substances and allows nutrients into the blood circulation (42). In this study, HFD reduced villus length and increased crypt depth in mice, suggesting a disruption of the physical barrier of the jejunum. Meanwhile, HFD decreased the VH/CD in the jejunum of mice, but AAEO restored it, so the effect of AAEO on jejunal function may be positive.

The study of fecal microbiota is very necessary for the growth and health of animals (25, 30). Blood lipids are closely associated with gut microbiota, and normal gut microbiota may regulate blood lipid levels (48). Therefore, the main phylum-level flora of the mouse gut in this study was not affected by AAEO, corresponding to the same unaffected blood lipids in the experiment. To achieve nutrient absorption and deposition, the intestinal structures and microbiota must remain intact in order to induct chemicals and maintain digestive functions. The intestinal bacterial community was considered to have an important role in preserving intestinal function (49, 50). There were more than 100 trillion microorganisms in the ecosystem, most of which were bacteria (51). Microbiota composition and activity in the intestine were affected by many factors, including age, environment, and diet, with diet being the most crucial of these (52–54). Gut microbiota colonization and gut microbiota-mediated immunity are both influenced by diet (55). We explored the effect of AAEO on the bacteria community in feces. Based on the findings of the current study, HFD mice had lower bacterial diversity than ICR mice on a basal diet. Due to the high variability between and within species in the gut microbiome, it was difficult to define a healthy gut microorganism in terms of specifications (56, 57). Despite this, gut microbes and metabolites may be relatively stable (57, 58). According to previous studies, the ratio of Firmicutes to Bacteroides was increased in obese host (59) and correlated with host energy intake (60, 61). We found that 5 of the top 40 genera were notably altered over the course of the entire stage. The relative abundance of Bacteroides, Alistipes, Rikenella, and norank_f__norank_o__Clostridia_UCG-014 was lower in the HFD fed to ICR male mice in comparison with the control diet given to the mice. However, the addition of AAEO had no effect on these four bacteria. Simultaneously, the abundance of Muribaculum was higher after feeding HFD than after feeding the control diet, but adding AAEO on the basis of HFD had no effect on Muribaculum. This proved that AAEO had little effect on the main microbiota of mouse feces. So, we inferred that AAEO will not broadly regulate the intestinal microbial community.

Conclusion

This study demonstrated that HFD could alter lipid metabolism and gut microbiota in ICR mice. Simultaneously, the gut barrier was weakened by HFD, which may impair the ability of nutrient absorption and digestion for the host. Although AAEO did not affect lipid deposition in mice, AAEO improved intestinal tissue morphology in mice. This study, which comprehensively investigated lipid metabolism, intestinal barrier, and the microbial response of AAEO in mice, indicated that AAEO was mainly beneficial to the intestinal barrier of mice.

Data availability statement

The data presented in the study are deposited in the NCBI Sequence Read Archive (SRA) repository, accession number PRJNA861869.

Ethics statement

The animal experiments were conducted in accordance with the Hunan Agricultural University Institutional Animal Care and Use Committee (202105).

Author contributions

KW and ML designed the experiment. KW conducted the experiment and wrote the manuscript. KW, SX, JM, YL, QH, ZY, MZ, and JC collected and analyzed the data. SX revised the manuscript. All authors contributed to the article and approved the submitted version.

Funding

We acknowledge the financial support received from the Young Elite Scientists Sponsorship Program by CAST (2019QNRC001) and the Natural Science Foundation of Hunan Province for Outstanding Young Scholars (2020JJ3023).

Conflict of interest

The authors declare that the research was conducted in the absence of any commercial or financial relationships that could be construed as a potential conflict of interest.

Publisher's note

References

1. Ren W, Xia Y, Chen S, Wu G, Bazer FW, Zhou B, et al. Glutamine metabolism in macrophages: a novel target for obesity/type 2 diabetes. *Adv Nutr.* (2019). 10:321–30. doi: 10.1093/advances/nmy084

2. Hingorani AD, Finan C, Schmidt AF. Obesity causes cardiovascular diseases: adding to the weight of evidence. *Eur Heart J.* (2020) 41:227–30. doi: 10.1093/eurheartj/ehz569

3. Misra A, Khurana L. Obesity and the metabolic syndrome in developing countries. *J Clin Endocrinol Metab.* (2008) 93(11 Suppl 1):S9–30. doi: 10.1210/jc.2008-1595

4. Sabin MA, Kiess W. Childhood obesity: current and novel approaches. *Best Pract Res Clin Endocrinol Metab.* (2015) 29:327–38. doi: 10.1016/j.beem.2015.04.003

5. Heymsfield SB, Wadden TA. Mechanisms, pathophysiology, and management of obesity. *N Engl J Med.* (2017) 376:254–66. doi: 10.1056/NEJMra1514009

6. Ference BA, Ginsberg HN, Graham I, Ray KK, Packard CJ, Bruckert E, et al. Low-density lipoproteins cause atherosclerotic cardiovascular disease. 1. Evidence from genetic, epidemiologic, and clinical studies. A consensus statement from the European Atherosclerosis Society Consensus Panel. *Eur Heart J.* (2017) 38:2459–72. doi: 10.1093/eurheartj/ehx144

7. Hamman RF, Wing RR, Edelstein SL, Lachin JM, Bray GA, Delahanty L, et al. Effect of weight loss with lifestyle intervention on risk of diabetes. *Diabetes Care.* (2006) 29:2102–7. doi: 10.2337/dc06-0560

8. Kakkar AK, Dahiya N. Drug treatment of obesity: current status and future prospects. *Eur J Intern Med.* (2015) 26:89–94. doi: 10.1016/j.ejim.2015.01.005

9. Khera R, Murad MH, Chandar AK, Dulai PS, Wang Z, Prokop LJ, et al. Association of pharmacological treatments for obesity with weight loss and adverse events: a systematic review and meta-analysis. *Jama.* (2016) 315:2424–34. doi: 10.1001/jama.2016.7602

10. Kim GW, Lin JE, Blomain ES, Waldman SA. Antiobesity pharmacotherapy: new drugs and emerging targets. *Clin Pharmacol Ther.* (2014) 95:53–66. doi: 10.1038/clpt.2013.204

11. Schoeler M, Caesar R. Dietary lipids, gut microbiota and lipid metabolism. *Rev Endocr Metab Disord.* (2019) 20:461–72. doi: 10.1007/s11154-019-09512-0

12. Cani P, Delzenne N. The role of the gut microbiota in energy metabolism and metabolic disease. *Curr Pharm Des.* (2009) 15:1546–58. doi: 10.2174/138161209788168164

13. Wang K, Peng X, Lv F, Zheng M, Long D, Mao H, et al. Microbiome-metabolites analysis reveals unhealthy alterations in the gut microbiota but improved meat quality with a high-rice diet challenge in a small ruminant model. *Animals.* (2021) 11:2306. doi: 10.3390/ani11082306

14. He B, Zhu R, Yang H, Lu Q, Wang W, Song L, et al. Assessing the impact of data preprocessing on analyzing next generation sequencing data. *Front Bioeng Biotechnol.* (2020) 8:817. doi: 10.3389/fbioe.2020.00817

15. Wang K, Yan Q, Ren A, Zheng M, Zhang P, Tan Z, et al. Novel linkages between bacterial composition of hindgut and host metabolic responses to SARA induced by high-paddy diet in young goats. *Front Vet Sci.* (2021) 8:791482. doi: 10.3389/fvets.2021.791482

16. Ge Y-B, Wang Z-G, Xiong Y, Huang X-J, Mei Z-N, Hong Z-G. Anti-inflammatory and blood stasis activities of essential oil extracted from *Artemisia argyi* leaf in animals. *J Nat Med.* (2016) 70:531–8. doi: 10.1007/s11418-016-0972-6

17. Deng H, Shen X. The mechanism of moxibustion: ancient theory and modern research. *Evid Based Complement Alternat Med.* (2013) 2013:379291. doi: 10.1155/2013/379291

18. Chen J, Chen F, Peng S, Ou Y, He B, Li Y, et al. Effects of *Artemisia argyi* powder on egg quality, antioxidant capacity, and intestinal development of roman laying hens. *Front Physiol.* (2022) 13:902568. doi: 10.3389/fphys.2022.902568

19. Edris AE. Pharmaceutical and therapeutic potentials of essential oils and their individual volatile constituents: a review. *Phytother Res.* (2007) 21:308–23. doi: 10.1002/ptr.2072

20. Huang HC, Wang HF, Yih KH, Chang LZ, Chang TM. Dual bioactivities of essential oil extracted from the leaves of *Artemisia argyi* as an antimelanogenic versus antioxidant agent and chemical composition analysis by GC/MS. *Int J Mol Sci.* (2012) 13:14679–97. doi: 10.3390/ijms131114679

21. Hu Y, Yang Y, Ning Y, Wang C, Tong Z. Facile preparation of *Artemisia argyi* oil-loaded antibacterial microcapsules by hydroxyapatite-stabilized Pickering emulsion templating. *Colloids Surf B Biointerfaces.* (2013) 112:96–102. doi: 10.1016/j.colsurfb.2013.08.002

22. Wenqiang G, Shufen L, Ruixiang Y, Yanfeng H. Comparison of composition and antifungal activity of *Artemisia argyi* Lévl. et Vant inflorescence essential oil extracted by hydrodistillation and supercritical carbon dioxide. *Nat Prod Res.* (2006) 20:992–8. doi: 10.1080/14786410600921599

23. He ZY, Zhang YH, Wei D, Yu RH, Yuan HH, Lan MB. Chemical composition of essential oil from fresh and dried Folium *Artemisia argyi* from Hubei Province. *Chin Tradit Patent Med.* (2009) 31:1079–82.

24. Li N, Mao Y, Deng C, Zhang X. Separation and identification of volatile constituents in *Artemisia argyi* flowers by GC-MS with SPME and steam distillation. *J Chromatogr Sci.* (2008) 46:401–5. doi: 10.1093/chromsci/46.5.401

25. Wang K, Peng X, Yang A, Huang Y, Tan Y, Qian Y, et al. Effects of diets with different protein levels on lipid metabolism and gut microbes in the host of different genders. *Front Nutr.* (2022) 9:940217. doi: 10.3389/fnut.2022.940217

26. Chen C, Wang Z, Li J, Li Y, Huang P, Ding X, et al. Dietary vitamin E affects small intestinal histomorphology, digestive enzyme activity, and the expression of nutrient transporters by inhibiting proliferation of intestinal epithelial cells within jejunum in weaned piglets1. *J Anim Sci.* (2019) 97:1212–21. doi: 10.1093/jas/skz023

27. Deng Q, Shao Y, Wang Q, Li J, Li Y, Ding X, et al. Effects and interaction of dietary electrolyte balance and citric acid on growth performance, intestinal histomorphology, digestive enzyme activity and nutrient transporters expression of weaned piglets. *J Anim Physiol Anim Nutr.* (2021) 105:272–85. doi: 10.1111/jpn.13491

28. Yin L, Li J, Wang H, Yi Z, Wang L, Zhang S, et al. Effects of vitamin B6 on the growth performance, intestinal morphology, and gene expression in weaned piglets that are fed a low-protein diet1. *J Anim Sci.* (2020) 98:skaa022. doi: 10.1093/jas/skaa022

29. Wang K, Yang A, Peng X, Lv F, Wang Y, Cui Y, et al. Linkages of various calcium sources on immune performance, diarrhea rate, intestinal barrier, and post-gut microbial structure and function in piglets. *Front Nutr.* (2022) 9:921773. doi: 10.3389/fnut.2022.921773

30. Wang H, Hu C, Cheng C, Cui J, Ji Y, Hao X, et al. Unraveling the association of fecal microbiota and oxidative stress with stillbirth rate of sows. *Theriogenology.* (2019) 136:131–7. doi: 10.1016/j.theriogenology.2019.06.028

31. Ma W, Wei S, Peng W, Sun T, Huang J, Yu R, et al. Antioxidant effect of *Polygonatum sibiricum* Polysaccharides in D-galactose-induced heart aging mice. *Biomed Res Int.* (2021) 2021:6688855. doi: 10.1155/2021/6688855

32. Zhong WJ, Luo YJ, Li J, Wu YP, Gao YJ, Luo HJ, et al. Polymethoxylated flavonoids from *Citrus reticulata* Blanco. *Biochem Syst Ecol.* (2016) 68:11–4. doi: 10.1016/j.bse.2016.02.031

33. Zhang WL, Zhu L, Jiang JG. Active ingredients from natural botanicals in the treatment of obesity. *Obes Rev.* (2014) 15:957–67. doi: 10.1111/obr.12228

34. Li J, Pang B, Shao D, Jiang C, Hu X, Shi J. Artemisia sphaerocephala Krasch polysaccharide mediates lipid metabolism and metabolic endotoxaemia in associated with the modulation of gut microbiota in diet-induced obese mice. *Int J Biol Macromol.* (2020) 147:1008–17. doi: 10.1016/j.ijbiomac.2019.10.069

35. Liu Y, Zhang Y, Yin J, Ruan Z, Wu X, Yin Y. Uridine dynamic administration affects circadian variations in lipid metabolisms in the liver of high-fat-diet-fed mice. *Chronobiol Int.* (2019) 36:1258–67. doi: 10.1080/07420528.2019.1637347

36. Zhou X, He L, Zuo S, Zhang Y, Wan D, Long C, et al. Serine prevented high-fat diet-induced oxidative stress by activating AMPK and epigenetically modulating the expression of glutathione synthesis-related genes. *Biochim Biophys Acta Mol Basis Dis.* (2018) 1864:488–98. doi: 10.1016/j.bbadis.2017.11.009

37. Zhou X, He L, Wan D, Yang H, Yao K, Wu G, et al. Methionine restriction on lipid metabolism and its possible mechanisms. *Amino Acids.* (2016) 48:1533–40. doi: 10.1007/s00726-016-2247-7

38. Mohamed GA, Ibrahim SRM, Elkhayat ES, El Dine RS. Natural anti-obesity agents. *Bull Faculty Pharm Cairo Univ.* (2014) 52:269–84. doi: 10.1016/j.bfopcu.2014.05.001

39. Cuevas-Sierra A, Ramos-Lopez O, Riezu-Boj JI, Milagro FI, Martinez JA. Diet, gut microbiota, and obesity: links with host genetics and epigenetics and potential applications. *Adv Nutr.* (2019) 10(Suppl_1):S17–30. doi: 10.1093/advances/nmy078

40. Chen C, Yang B, Zeng Z, Yang H, Liu C, Ren J, et al. Genetic dissection of blood lipid traits by integrating genome-wide association study and gene expression profiling in a porcine model. *BMC Genomics.* (2013) 14:848. doi: 10.1186/1471-2164-14-848

41. Abd El-Gawad IA, El-Sayed EM, Hafez SA, El-Zeini HM, Saleh FA. The hypocholesterolaemic effect of milk yoghurt and soy-yoghurt containing bifidobacteria in rats fed on a cholesterol-enriched diet. *Int Dairy J.* (2005) 15:37–44. doi: 10.1016/j.idairyj.2004.06.001

42. Cui Y, Wang Q, Chang R, Zhou X, Xu C. Intestinal barrier function-non-alcoholic fatty liver disease interactions and possible role of gut microbiota. *J Agric Food Chem.* (2019) 67:2754–62. doi: 10.1021/acs.jafc.9b00080

43. Li J, Yin L, Wang L, Li J, Huang P, Yang H, et al. Effects of vitamin B6 on growth, diarrhea rate, intestinal morphology, function, and inflammatory factors expression in a high-protein diet fed to weaned piglets1. *J Anim Sci.* (2019) 97:4865–74. doi: 10.1093/jas/skz338

44. Wu J, He C, Bu J, Luo Y, Yang S, Ye C, et al. Betaine attenuates LPS-induced downregulation of Occludin and Claudin-1 and restores intestinal barrier function. *BMC Vet Res.* (2020) 16:75. doi: 10.1186/s12917-020-02298-3

45. Rieger J, Janczyk P, Hünigen H, Neumann K, Plendl J. Intraepithelial lymphocyte numbers and histomorphological parameters in the porcine gut after *Enterococcus faecium* NCIMB 10415 feeding in a *Salmonella* Typhimurium challenge. *Vet Immunol Immunopathol.* (2015) 164:40–50. doi: 10.1016/j.vetimm.2014.12.013

46. Zhao R, Long X, Yang J, Du L, Zhang X, Li J, et al. Pomegranate peel polyphenols reduce chronic low-grade inflammatory responses by modulating gut microbiota and decreasing colonic tissue damage in rats fed a high-fat diet. *Food Funct.* (2019) 10:8273–85. doi: 10.1039/c9fo02077b

47. Ghosh SS, Wang J, Yannie PJ, Ghosh S. Intestinal barrier function and metabolic/liver diseases. *Liver Res.* (2020) 4:81–7. doi: 10.1016/j.livres.2020.03.002

48. Tang ML. Probiotics and prebiotics: immunological and clinical effects in allergic disease. *Nestlé Nutr Institute Workshop Ser.* (2009) 64:219–35.

49. Sczesnak A, Segata N, Qin X, Gevers D, Petrosino JF, Huttenhower C, et al. The genome of Th17 cell-inducing segmented filamentous bacteria reveals extensive auxotrophy and adaptations to the intestinal environment. *Cell Host Microbe.* (2011) 10:260–72. doi: 10.1016/j.chom.2011.08.005

50. Chen J, Li Y, Tian Y, Huang C, Li D, Zhong Q, et al. Interaction between microbes and host intestinal health: modulation by dietary nutrients and gut-brain-endocrine-immune axis. *Curr Protein Pept Sci.* (2015) 16:592–603. doi: 10.2174/1389203716666150630135720

51. Collins SM, Surette M, Bercik P. The interplay between the intestinal microbiota and the brain. *Nat Rev Microbiol.* (2012) 10:735–42. doi: 10.1038/nrmicro2876

52. Fan P, Li L, Rezaei A, Eslamfam S, Che D, Ma X. Metabolites of dietary protein and peptides by intestinal microbes and their impacts on gut. *Curr Protein Pept Sci.* (2015) 16:646–54. doi: 10.2174/1389203716666150630133657

53. Sonnenburg ED, Smits SA, Tikhonov M, Higginbottom SK, Wingreen NS, Sonnenburg JL. Diet-induced extinctions in the gut microbiota compound over generations. *Nature.* (2016) 529:212–5. doi: 10.1038/nature16504

54. Ma N, Tian Y, Wu Y, Ma X. Contributions of the interaction between dietary protein and gut microbiota to intestinal health. *Curr Protein Pept Sci.* (2017) 18:795–808. doi: 10.2174/1389203718666170216153505

55. Saresella M, Mendozzi L, Rossi V, Mazzali F, Piancone F, LaRosa F, et al. Immunological and clinical effect of diet modulation of the gut microbiome in multiple sclerosis patients: a pilot study. *Front Immunol.* (2017) 8:1391. doi: 10.3389/fimmu.2017.01391

56. Nguyen, TL, Vieira-Silva S, Liston A, Raes J. How informative is the mouse for human gut microbiota research? *Dis Models Mech.* (2015) 8:1–16. doi: 10.1242/dmm.017400

57. Sender R, Fuchs S, Milo R. Revised estimates for the number of human and bacteria cells in the body. *PLoS Biol.* (2016) 14:e1002533. doi: 10.1371/journal.pbio.1002533

58. McCoy KD, Geuking MB, Ronchi F. Gut microbiome standardization in control and experimental mice. *Curr Protoc Immunol.* (2017) 117:21–3. doi: 10.1002/cpim.25

59. Bäckhed F, Ding H, Wang T, Hooper LV, Koh GY, Nagy A, et al. The gut microbiota as an environmental factor that regulates fat storage. *PNAS.* (2004) 101:15718–23. doi: 10.1073/pnas.0407076101

60. Cottenie K. Integrating environmental and spatial processes in ecological community dynamics. *Ecol Lett.* (2005) 8:1175–82. doi: 10.1111/j.1461-0248.2005.00820.x

61. Ley RE, Turnbaugh PJ, Klein S, Gordon JI. Human gut microbes associated with obesity. *Nature.* (2006) 444:1022–3. doi: 10.1038/4441022a

frontiers | Frontiers in Nutrition

TYPE Review
PUBLISHED 07 November 2022
DOI 10.3389/fnut.2022.1019430

OPEN ACCESS

EDITED BY
Hui Han,
Chinese Academy of Sciences (CAS), China

REVIEWED BY
Lingbing Zeng,
Yangtze River Fisheries Research Institute (CAFS), China
Sweta Ghosh,
University of Louisville, United States
Qingyun Yan,
Sun Yat-sen University, China

*CORRESPONDENCE
Jianguo Xiang
2507467211@qq.com

SPECIALTY SECTION
This article was submitted to Nutrition and Microbes, a section of the journal Frontiers in Nutrition

RECEIVED 15 August 2022
ACCEPTED 21 October 2022
PUBLISHED 07 November 2022

CITATION
Hou J, Xiang J, Li D, Liu X and Pan W (2022) Gut microbial response to host metabolic phenotypes. *Front. Nutr.* 9:1019430. doi: 10.3389/fnut.2022.1019430

Gut microbial response to host metabolic phenotypes

Jinliang Hou[1], Jianguo Xiang[1]*, Deliang Li[1], Xinhua Liu[1] and Wangcheng Pan[2]

[1]College of Animal Science and Technology, Hunan Agricultural University, Changsha, China, [2]Changde Dabeinong Feed Co. Ltd., Changde, China

A large number of studies have proved that biological metabolic phenotypes exist objectively and are gradually recognized by humans. Gut microbes affect the host's metabolic phenotype. They directly or indirectly participate in host metabolism, physiology and immunity through changes in population structure, metabolite differences, signal transduction and gene expression. Obtaining comprehensive information and specific identification factors associated with gut microbiota and host metabolic phenotypes has become the focus of research in the field of gut microbes, and it has become possible to find new and effective ways to prevent or treat host metabolic diseases. In the future, precise treatment of gut microbes will become one of the new therapeutic strategies. This article reviews the content of gut microbes and carbohydrate, amino acid, lipid and nucleic acid metabolic phenotypes, including metabolic intermediates, mechanisms of action, latest research findings and treatment strategies, which will help to understand the relationship between gut microbes and host metabolic phenotypes and the current research status.

KEYWORDS

metabolic phenotype, gut microbiome, nutrient metabolism, disease control, microbial metabolites

Introduction

Biological metabolic phenotype is based on the analysis of cell types, biological fluids and biological tissues, and uses a variety of parameters to approximately describe the organism in a specific physiological state (1). Johnson et al. (2) included genetic, environmental and gut microbial information into the biological metabolic phenotype for the first time in 2012. This new concept can describe the biological metabolic phenotype more accurately. The so-called biological metabolic phenotype is mainly determined by the organism's genome, intestinal flora, its environment (including stress, diet, and lifestyle) and its intake of foreign substances (including drugs, cosmetics, environmental pollution, and food) (2). It is commonly described by four indexes, including the presence or absence of metabolites, the concentration of metabolites, the ratio between metabolites, and the overall information of metabolites (1).

Gut microbes are one of the important factors that determine the biological metabolic phenotype. Their metabolites and components directly affect the host's nutrient absorption and development, and affect the host's health by promoting the development of the host's epithelial tissue and the immune system (3). In turn, the host's living environment, nutrient levels, developmental stage and health status influence the composition of the gut microbiome.

The types, concentrations, ratios and overall information of metabolites vary with the composition of gut microbes. Different microbial metabolites play different metabolic roles, and thus make the host present different metabolic phenotypes. For example, *Faecalibacterium prausnitzii* and *Eubacterium rectale* produce butyrate; Probiotics such as *Lactobacillus* and *Bifidobacterium*, and 7α-dehydroxybacteria such as *Clostridium*, exhibit bile acid resistance associated with glycolytic activation; Gram-positive bacteria are more sensitive to bile acids than Gram-negative bacteria; Bile acids directly and rapidly affect the metabolism of bacteria, including membrane damage, disruption of amino acid, nucleotide and carbohydrate metabolism, and short-term exposure to bile acids significantly affects host metabolism by altering bacterial community structure (4). Some studies have changed the relative abundance of *Escherichia*, *Romboutsia*, *Intestinibacter,* and *Clostridium* in the gut through the intervention of external drugs (metformin), which leads the alterations of the concentrations of metabolites such as carbohydrates, amino acids, and fatty acids in the gut (5). The metformin also affects energy metabolism, gluconeogenesis, and branched-chain amino acid metabolism, hindering host hypoglycemic-related metabolic pathways (5). Therefore, to study the impact of gut microbes on host metabolic phenotypes, high attention should be paid to comprehensive information on gut microbiota composition and its specific metabolites.

The gut microbiota regulates host metabolism, including carbohydrate, amino acid, lipid and nucleic acid metabolism. So far, there have been a lot of researches on the influence of gut microbes on host metabolism, but most of them focus on the dominant flora and its metabolites. Therefore, comprehensive information about the metabolic phenotype of gut microbiota to the host yet to be fully explored.

Gut microbes influence host metabolic phenotype through metabolites

The metabolites of gut microbes are very rich, such as a variety of short-chain fatty acids (acetate, propionate, and butyrate, etc.), alcohol, carbon dioxide, and hydrogen. They can utilize their respective metabolites to ensure gut viability and influence the development of the host immune system, homeostasis, and function through nutrient- and metabolite-dependent mechanisms (**Table 1**) (6). For example, *Blautia* spp. can convert carbon dioxide plus hydrogen to acetate; *Methanobrevibacter* convert carbon dioxide plus hydrogen to methane; *Desulfovibrio* convert sulfate to hydrogen sulfide (7, 8). These metabolites directly or indirectly affect the response of host immune and promote or delay the occurrence of their own diseases.

Fiber and bacterial metabolites affect host and gut health by modulating inflammation, glucose and lipid metabolism (9). For example, bacterial metabolites short-chain fatty acids have anti-inflammatory effects: Butyrate produced by *Clostridium butyricum* (10) stimulates intestinal epithelial cells and antigen presentation to produce cytokines such as TGF-β, IL-10, IL-18, (11) and reduces mild inflammation, glucose metabolism imbalance and insulin resistance in the host (12); Propionate can fight lipogenesis, lower cholesterol (13), inhibit colon cancer cell proliferation (14, 15) and induce T cells to differentiate into T regulatory cells (16). At the same time, it can control weight by stimulating satiety (17), and be absorbed by intestinal epithelial cells to improve the integrity of host intestinal epithelial cells (18). Propionate alone also reduces intra-abdominal tissue hyperplasia and lipid content in liver cells in overweight adults (19). Studies have confirmed that gut microbes can produce propionate by metabolizing carbohydrates such as L-*rhamnose*, D-*tagatose*, *Resistant starch*, *Inulin*, *Polydextrose*, *Arabinoxylans*, *Arabinoxylan oligosaccharides*, *Mannooligosaccharides,* and *Laminarans* (17); Acetate and propionate can inhibit Toll-like receptor (TLR4) stimulation to mediate the production of proinflammatory cytokines (16, 20), and the ratio of propionate to acetate determines whether propionate inhibits the conversion of acetate to cholesterol and fat (21, 22); Pyruvate mainly comes from carbohydrate metabolism, and can be further metabolized by the microbiota into succinic acid, lactic acid or acetyl-CoA to produce short-chain fatty acids, which provide energy for the normal functioning of the body (16, 18).

When the metabolites interacting with the intestinal flora are disordered, it also leads to increased intestinal permeability, bacterial endotoxin and increased harmful substances absorbed into the liver through the portal system, thereby affecting the metabolism of carbohydrates and lipids in the liver and exacerbating the imbalance between pro-inflammatory factors and anti-inflammatory effectors (23–25). Eventually, it leads to the development of metabolic fatty liver disease, infectious diseases and certain neurological diseases (26–29). For example, The deconjugation, oxidation/epimerization, (7-α-) dehydroxylation and esterification of bile acids (30) by the intestinal microbiota can dramatically change their physicochemical properties and subsequently affect their microbial toxicity and intestinal absorption (31). In addition, the metabolites enhance intestinal reabsorption by uncoupling BAs through microbial bile salt hydrolase (32); Some probiotic

TABLE 1 Gut bacteria and the metabolites they contribute.

Metabolites	Related bacteria	Potential biological functions	References
Short-chain fatty acids: propionate, butyrate, acetate, hexanoate, valerate	*Faecalibacterium prausnitzii*, *Eubacterium rectale*, *Clostridium butyricum, Blautia* spp., *Bifidobacterium*, *lactobacillus*, *Allobaculum*, *Roseburia*, *Butyrivibrio*, *Dorea*, and *Blautia genera*	Provides energy for body functions and is associated with cholesterol synthesis, inflammation, obesity, imbalances in glucose metabolism, colorectal cancer and insulin resistance.	(7, 8, 13, 16–18, 20–22, 187, 214)
Bile acids	*Lactobacillus*, *Bifidobacteria*, *Clostridium*, *Clostridioides*, *Lactobacillus rhamnosus*, *Akkermansia muciniphila*, *Bifidobacteria*, *Enterobacter*	Regulates the balance of triglyceride, cholesterol and glucose metabolism, maintains intestinal barrier function and promotes lipid metabolism and absorption.	(4, 30, 34, 180)
Phenolic, benzoyl, and phenyl derivatives: 5-hydroxytryptophan, phenylalanine, tyrosine	*Lactobacillus*, *Some species of the genera Clostridium*, *Rumenococcus and Eubacterium.*	Related to tryptophan metabolism, brain-gut axis.	(174–176, 197, 206)
Indole derivatives: indoleacetate, indole, melatonin, serotonin, 5-hydroxyindole	*Lactococcus*, *Lactobacillus*, *Streptococcus*, *Escherichia coli, and Klebsiella*	Implicated in gastrointestinal pathologies, brain-gut axis, and a few neurological conditions.	(137, 179, 180)
Lipids: triglycerides, cholesterol, Lipopolysaccharide	*Lactiplantibacillus*, *Lactobacillus rhamnosus*, *Akkermansia muciniphila*, *Bifidobacterium*, *Klebsiella*, *Lactobacillus*	Cholesterol is the basis for sterol and bile acid production. Lipopolysaccharide induces chronic systemic inflammation; Regulate carbohydrate and lipid metabolism.	(21, 22, 35, 38, 39, 62, 75, 76, 101)

bacteria such as *Lactobacillus* and *Bifidobacterium* and 7α-dehydroxylating bacteria such as *Clostridium scindens* show bile acid resistance that is associated with activation of glycolysis (4).

The use of antibiotics can disrupt the gut microbiota structure and the formation of microbial metabolites, eventually affecting the host health. For example, the antibiotics can disrupt the commensal microbiota that converts primary bile acids into secondary bile acids (33–35), and the gradual accumulation of primary bile acids promotes the germination of *Clostridioides difficile spores* (a spore-forming Gram-positive bacterium and the causative agent of antibiotic-associated diarrhea), bacterial replication and the production of colitis-mediating enterotoxins, which induce host diarrhea and enteritis (31). Importantly, the gut microbial metabolites are one of the important components of host immune system. A large number of studies have shown that the metabolic phenotype of most hosts could be observed during the changes of intestinal microorganisms and their metabolites.

Gut microbial responses to carbohydrate metabolism phenotypes

Many gut microbes can directly metabolize carbohydrates. *Lactobacillus plantarum* presents a stronger carbohydrate utilization capability (36–39), which also plays a certain role in maintaining the balance of gastrointestinal flora, improving self-immunity of host, promoting effective absorption of nutrients, reducing cholesterol content, and alleviating lactose intolerance (40). In addition to metabolizing exogenous carbohydrates by gut microbes, endogenous carbohydrates released in the gut mucus are also a constant source of nutrients for the microbiota, which are decomposed and used as components for synthesizing bacterial cell walls, thereby affecting host mucosal immunity (41); Host intestinal epithelial cells also obtain nutrients from microbial metabolism. When nutrients are deficient, microbes undergo autophagy, and some bacteria have evolved a sugar-decomposing lifestyle to escape competition (18). This direct metabolism can not only supply the growth and development needs of the host, but also enhance the disease resistance of the host to a certain extent.

Gut microbes are one of the important sources of carbohydrate metabolizing enzymes. Carbohydrate metabolizing enzymes are highly correlated with the abundance of certain gut flora (e.g., *Bacteroides*, *Prevotella*) (42). Studies have reported that a large number of carbohydrate-activating enzymes are found in the human gut flora, such as *Bacteroides thetaiotaomicron*, which has 260 glycoside hydrolases in its genome (43, 44). Human cells rarely produce these enzymes, which rely on gut microbes for energy production from remaining complex carbohydrates (45, 46). Gut microbes are not only dependent on the host, but also influence the balance of the host gut microbial ecology. Intestinal microorganisms produce metabolic enzymes that improve the host's ability to digest complex carbohydrates and promote the growth and reproduction of the corresponding flora.

The structure, metabolites and derived metabolites of the host gut flora are altered by the ingestion of different types and levels of carbohydrates, which in turn produce different metabolic phenotypes. The gut microbiota is very sensitive to the subtle structural differences between insoluble (47) and soluble (48) plant fibers, and different fiber structures correspond to specific microbial taxa (49). Shi et al. (50) found

that supplementation with microbially available carbohydrates ameliorated cognitive impairment in obese mice induced by chronic high-fat and fiber-deficient diets. Low-fiber diets cause increased by-products of proteolytic fermentation, resulting in altered microbiota and its derived metabolites (increased fecal branched-chain amino acids and decreased short-chain fatty acids), impaired colonic epithelium and intestinal mucosal detoxification, and increased inflammation (51, 52). The long-term low-carbohydrate diet in traditional Western societies has led to changes in the composition of the intestinal flora. The production of short-chain fatty acids in the metabolites of the intestinal flora is less, which cannot meet the requirements of reducing inflammation, and the incidence of diseases is significantly increased (53). Increasing the content of resistant starch (RS) in the diet increases the content of short-chain fatty acids in the human gut and feces, and the gut microbiota also changes (54, 55). For example, adding RS2 can increase the abundance of *Eubacterium rectale* and *Ruminococcus bromii* (56, 57); RS3 can alter the abundance of *Lachnospiraceae*, *Faecalibacterium*, *Alistipes*, and *Bifidobacterium*; RS4 can increase the relative numbers of *R. bromii* L2-63, *Parabacteroides distasonis* 8503, *E. rectale* 17629, and *B. adolescentis* IVS-1 (47); RS5 has potential prebiotic activity, and addition of RS5 significantly increases the relative abundance of *Bifidobacterium*, *Dialister*, *Collinsella*, *Romboutsia*, and *Megamonas* (58). Recent evidence from molecular ecology has also shown that the amount and type of non-digestible carbohydrates (e.g., resistant starch, non-starch polysaccharides, and prebiotics) influences the species composition of the intestinal microbiota both in short-term dietary interventions and in response to habitual long-term dietary intake (59). For example, supplementation of the diet with specific polysaccharides can promote the growth of *Bifidobacteria*, *Lactobacilli*, or butyric acid-producing bacteria, short-chain fatty acids production, lowering pH, and lead to inhibitory effects toward pathogens (9); A diet with low fermentable oligosaccharides, disaccharides, monosaccharides and polyols (FODMAP) diet can enrich a large amount of sugar catabolizing bacteria, reduce the frequency of abdominal pain, and treat intestinal allergies (60); Study has also shown that gut microbiome biomarkers might be associated with low FODMAP diet efficacy (42). Different types of carbohydrates select the corresponding intestinal dominant flora for the host, producing different metabolites that affect the host's development and immune system. Resistant starch can reduce the proportion of pathogenic bacteria to a certain extent and enhance the host's resistance to disease, which is promising in cultivating intestinal probiotics and regulating host immunity.

The latest research reports that the link between the genes encoding carbohydrate-active enzymes and the host can be used as a tool to predict whether carbohydrates can be metabolized, and guide the restoration of the ecological balance of the host's intestinal flora, transplantation of flora and supplementation of probiotics (61). The correlation analysis between the expressions of regulatory genes and sugar metabolism genes showed that some regulatory genes were correlated with most of the sugar metabolism genes, suggesting that some two-component systems might be involved in the regulation of sugar metabolism (62). Jia et al. (12) also found that individuals with type 2 diabetes (T2D) also had altered gut microbiota. And the detection of genes related to sugar and amino acid metabolism in their gut microbiota found that the abundance of related genes was significantly reduced, indicating that the abundance of these depleted genes can be used as potential biomarkers to identify obese individuals at high risk of developing T2D (12).

Gut microbial responses to lipid metabolism phenotypes

Lipid metabolism includes four categories: triglyceride metabolism, phospholipid metabolism, cholesterol metabolism and blood lipid metabolism, and one of the metabolic pathways is blocked, it can cause lipid metabolism disorders (63). Disorders of lipid metabolism can cause damage to host vascular endothelial cells, abnormal proliferation of smooth muscle cells, enhanced coagulation activity, inhibition of the fibrinolytic system (64), and excessive levels of total cholesterol or triglycerides in serum (65). The most intuitive phenotypes of lipid metabolism disorders in host are obesity and hyperlipidemia (64), which induce thrombosis and complications such as atherosclerosis, coronary heart disease and other cardiovascular and cerebrovascular diseases (66).

The role of gut microbes in host lipid metabolism is irreplaceable. It regulates the absorption and metabolism of lipids in the host, mainly by affecting bile acid metabolism, producing short-chain fatty acids and regulating the enteroendocrine system. Clinical studies have found that *Lactobacillus rhamnosus* is a classic probiotic, which can improve metabolism-related fatty liver disease by regulating intestinal flora, improving intestinal mucosal barrier and lowering cholesterol (67). Oral *Akkermansia muciniphila* supplementation can significantly improve insulin sensitivity and reduce insulinemia and total plasma cholesterol (68); Abnormal levels of one or both of *Bifidobacterium* and *Bacteroidetes* in the intestinal flora can cause hyperlipidemia (69–71); With the decreasing abundance of probiotics such as *Bifidobacterium*, *Lactobacillus* and *Faecalibacterium* genus in the intestines of most patients with hyperlipidemia and the increasing content of *Enterobacteriaceae* family and *Enterococcus* genus the lipopolysaccharide in the body will accumulate due to increased secretion or slowed metabolism (66, 72). Then, a part of the accumulated lipopolysaccharide enters the blood to cause endotoxemia and inflammatory response, and the inflammatory response also aggravates the symptoms of lipid metabolism disorder, resulting in a vicious

circle (66, 72); Most diabetic patients have intestinal flora imbalance, and it will affect lipid metabolism and promote the occurrence and development of diabetes (73–75); Pig gut bacteria *Prevotella* is the core microbe that dominates fat deposition. Its abundance is positively correlated with feed intake, and significantly negatively correlated with pig carcass lean meat percentage. Induced by a high-fat diet, mice colonized with *Prevotelle* developed severe adipose tissue deposition (76). Studies have shown that *Prevotelle* can induce chronic inflammation in the body by activating Toll-like receptor 4 and mammalian target protein signaling pathway of rapamycin, hindering the normal operation of the body's physiological metabolism, thereby aggravating fat inflammation and deposition (77). Lipid metabolism is an important and complex biochemical reaction in the host. Gut microbes can play a role in regulating lipid metabolism, both directly by breaking down lipids and through the production of other metabolites.

Prebiotics or probiotics can modulate lipid metabolism to improve metabolic syndrome and treat diseases such as obesity and diabetes associated with dysbiosis of the gut microbiome (78, 79). Prebiotics can promote the growth of beneficial bacteria such as *Bifidobacteria* and *Lactobacillus*, which are metabolized into lactic acid and short-chain fatty acids in the large intestine, improving host physiology, especially gastrointestinal health (80–82); Studies by Cani et al. (83) have shown that the regulation of intestinal flora by prebiotics such as *Fructooligosaccharides* can increase the content of *Bifidobacteria* in the host intestine and prevent hyperlipidemia-induced metabolic diseases such as diabetes and obesity.

The lipid structure of the diet affects the composition of the gut microbiota, which in turn affects lipid metabolism and host health. High-fat diet has been recognized as a major determinant of obesity, and the gut microbiota plays an important role in this phenotype (84). High-fat diet can induce enrichment of opportunistic pathogens such as *Betaproteobacteria* (85), *Clostridium bolteae*, *Desulfovibrio* sp. (86), and *Enterobacter cloacae* (87); Regular consumption of functional foods rich in fiber, polyphenols and polysaccharides can reduce the risk of cardiometabolic diseases, and their metabolites may inhibit pathogenic bacteria and stimulate the growth of beneficial bacteria (88); Caesar et al. (89) validated that pro-inflammatory *Bilophila wadsworthia* thrived on a lard-based diet, while *Lactobacillus* and *Akkermansia muciniphila* thrived on a fish oil-based diet; Feeding Auricularia auricula polysaccharid can increase the abundance of intestinal flora in rats, such as Parabacteroides (90), and Auricularia auricula polysaccharid can also play a role by inhibiting the absorption of external fat and enhancing the metabolism of liver fat (91); Lesel et al. (92) fed rainbow trout with low-fat and high-fat diets and found that the main bacterial groups in the feces of the low-fat group were only *Acinetobacter* spp. and *Enterobacteria*, while the high-fat group had higher bacterial diversity, mainly including *Acinetobacter* spp., *Enterobacteria*, *Flavobacterium* spp., *Pseudomonas* spp., and *Coryneforms*; In the high-fat-fed mice, the content of *Bacteroidetes* increased significantly at 1 week, and the ratio of *Firmicutes* to *Bacteroidetes* changed from 0.86 to 1.77 after 8 weeks. At the same time, fat deposition and intestinal dysbiosis were also found, the content of *Verrucobacterium* was significantly increased, while the *E. coli* was significantly decreased (93); Recent studies have shown that fasting can reduce host serum lipid levels and improve hepatic steatosis by reducing the ratio of *Firmicutes* to *Bacteroidetes* and increasing the abundance of *Allobaculum* in the host, resulting in improving metabolic disorders and intestinal flora imbalance caused by high-fat diet (94). The effects of an imbalance in the host's flora reflect the problems caused by an imbalance in diet, and a balanced diet is one of the ways in which the host can ensure that all of its physiological functions are functioning properly. Too high or too low a lipid intake will eventually upset the existing balance.

External environmental conditions affect the structure of gut microbiota, which in turn affects host lipid metabolism. Some studies have found that the structure of the intestinal flora of carp exposed to copper has changed significantly, and the abundance of some short-chain fatty acid-producing species (such as *Allobaculum*, *Blautia*, etc.) has decreased significantly (95). Moreover, liver fat synthesis genes were significantly down-regulated, and the expression of lipolysis-related genes was significantly increased. It can be inferred that there is a significant correlation between changes in intestinal flora structure and lipid metabolism (95); Under chronic hypoxia, the intestinal microbiota composition and mucosal morphology of *Macrobrachium nipponense* are changed, which affects the metabolic enzyme activity of liver, reduces the content of intestinal short-chain fatty acids, affects the immune enzyme activity and inhibits the immune response, thus affecting the intestinal health (96).

Artificial regulation of intestinal flora structure can effectively improve host lipid metabolism and control obesity. Serum lipid levels in patients with hyperlipidemia are significantly correlated with changes in intestinal dominant flora, suggesting that adjusting the structure of intestinal dominant flora can improve serum lipid levels in patients (66). Antibiotics have been reported to disrupt gut microbial structure and gut immune cell composition, resulting in abnormal lipid metabolism. This reflects the importance of promoting antibiotic-free farming in modern farming, which is the ultimate choice in microbial treatment strategies. *Monascus vinegar* can lower body weight, total cholesterol, and triglycerides as well as ameliorating hyperlipidemia by regulating Peroxisome proliferator-activated α (PPARα)-, Nuclear factor-E2-related factor 2 (Nrf2)-, and Nuclear factor κB (NF-κB)-mediated signals and modulating the gut microbiota composition in hyperlipidemia rats (97); *Octylphenol* is a widely distributed endocrine disruptor, which

can affect the expression level of genes related to fat digestion and absorption, and change the structure of intestinal flora, gradually reduce the ratio of Firmicutes/Bacteroidetes, and destroy lipid metabolism (98). The artificial addition of biological agents to alter the microbiological structure of the gut to improve disease is increasingly recognized. The ratio of *Firmicutes* to *Bacteroidetes* in the gut microbiota of patients with type 2 diabetes is altered to absorb higher energy for insulin resistance (45, 46); Regulating the content of glucagon and insulin in blood can also improve lipid metabolism disorder and intestinal flora structure, effectively preventing and treating type 2 diabetes (99). Currently, diabetes is treated with extracorporeal insulin injections. Finding insulin-secreting microorganisms and colonizing them in the gut would be a historic advance in the fight against diabetes.

Gut microbial responses to amino acid metabolic phenotypes

Intestinal microorganisms can extensively metabolize a variety of amino acids, such as Histidine, Lysine, Threonine, Arginine, Glutarnine, Leucine, Isoleucine, and Valine, etc., with a metabolic rate of more than 50% (100, 101). When the host metabolizes amino acids, gut microbes secrete enzymes to assist amino acid metabolism, while amino acid metabolites of some microorganisms [e.g., histamine; immunomodulatory signaling; alpha-aminobutyric acid (102); putrescine] can also be involved in immunity, anti-inflammatory and other pathological mechanisms (such as improving obesity, diabetes) (103). The metabolize of amino acids by gut microbes also contribute to the survival and value-added of the microbiota and the further synthesize bacterial components (104).

Gut microbes can synthesize a variety of amino acids. Dietary amino acids can be absorbed and metabolized by intestinal cells for life activities and protein synthesis, and can also be metabolized and decomposed by intestinal microbes to maintain the ecology of intestinal microbes, meet the host's amino acid requirements, and regulate the host's inflammation and immune levels. Gut microbes such as *Streptococcus bovis, Selenomonas ruminantium,* and *Prevotella bryantii* can synthesize amino acids at physiological peptide concentrations and integrate them into host proteins (105, 106); The most abundant BCAAs, valine, isoleucine and leucine, are essential amino acids synthesized by plants, fungi and bacteria, particularly by members of the gut microbiota (107); Gut bacteria can produce aspartic-, cysteine-, serine-, and metallo-proteases, in a typical fecal sample, these bacterial enzymes are far outnumbered by proteases arising from human cells (108).

The difference in the amount of essential amino acids measured by N balance method and tracer-derived statistics also indicates that in addition to diet, the gastrointestinal microbiota can also synthesize essential amino acids to meet host requirements (109). Gut microbes synthesize amino acids not only to deliver energy but also to maintain a reduced cofactor cycle (109).

Amino acids and their metabolites are integral components of host nutrition and synthetic immunity, and they play a role in maintaining mammalian homeostasis by regulating protein synthesis, glucose and lipid metabolism, insulin resistance, hepatocyte proliferation, and immunity (107). For example, L-tryptophan (Trp) is an important component of protein, and can be converted into a variety of substances (such as serotonin, melatonin, indole, kynurenine) as a metabolic substrate. It plays an important role in the onset of neurological diseases and immune regulation such as intestinal tolerance, balance between intestinal microbiota, hinder depression, chronic fatigue syndrome and physical mobility disorder (110–113); Endogenous Trp metabolites (kynurenines, serotonin, and melatonin), and bacterial Trp metabolites (indole, indolic acid, skatole, and tryptamine) also have profound effects on gut microbial composition, microbial metabolism, the host's immune system, the host-microbiome interface, and host immune system–intestinal microbiota interactions (114); Aromatic amino acids are metabolized by gut microbes and their products can serve as signaling molecules in host physiology (115).

Try metabolism has a central role in host health. Host genes can directly or indirectly modulate the production of microbial Trp metabolites and affect the composition and function of the gut microbiota (114). Shotgun metagenomics data shows that host hepatic steatosis and metabolism are associated with an imbalance in aromatic and branched-chain amino acid metabolism (116). The phenotype of host metabolic disturbances in the gut microbiota has been found preclinically and clinically to be a reduced ability of microorganisms to metabolize tryptophan as an aromatic hydrocarbon agonist (117). When the activation of the aromatic hydrocarbon pathway is defective, host GLP-1 and IL-22 production is reduced, intestinal permeability is altered, and lipopolysaccharide translocation is promoted, leading to host inflammation, insulin resistance, and hepatic steatosis (118). When changes in host tissue homeostasis require an immune response, gut microbiota can directly or indirectly activate host aryl hydrocarbon receptors and pregnane X receptors through derivatives produced by tryptophan metabolism (indole and its compounds) (119). A tryptophan-rich diet increases Aryl Hydrocarbon Receptor (AhP) mRNA expression and activates AhP (114). AhR can mediate exogenous metabolism, rely on IL-22 activation in the gut, and influence the balance between immunity and microbiota by modulating microbial composition through antimicrobial peptides (120–122). On a low-tryptophan diet, tryptophan metabolites were reduced, and mice or piglets were prone to inflammation (123). After adequate supplementation, metabolites were increased, inflammation was significantly reduced, and the degree of

dextran sodium sulfate-induced colitis was reduced (121, 124, 125).

In turn, the composition of microbiota can influence the production of Trp microbiota-derived metabolites, affect the host's intestinal homeostasis and lead to the loss of intestinal homeostasis and intestinal inflammation (114). Specific gut bacteria determines the availability of Trp to the host and then regulates serotonin and subsequent melatonin synthesis (126). Serotonin is a monoamine neurotransmitter involved in the regulation of central nervous system transmission and intestinal physiological functions, while tryptophan is the only precursor for serotonin production. Melatonin, a powerful anti-inflammatory factor, is also produced through tryptophan metabolism and can alleviate increase gut permeability and immune activation caused by *Escherichia coli* (127–130).

Various preclinical experimental strategies emphasize that both tryptophan availability and 5-HT signaling are profoundly affected by gut microbiota composition (131), and intervention targeting the microbiota can modulate the tryptophan metabolites kynurenine, tryptamine, indole, serotonin, and melatonin, which has important implications for the treatment of brain-gut axis diseases (127, 129). Gut microbiota derivatives reduce the ratio of kynurenine to tryptophan in blood in the regulation of tryptophan metabolism, suggesting that lack of gut microbiota reduces the activity of host Indoleamine 2,3-dioxygenase, which affects color kynurenine pathway of amino acid (118, 132). Gut microbiota can also influence tryptophan degradation and tryptophan cycling in the host through kynurenine pathway (131), and mitigate the adverse effects of aging on the central nervous system (133–136).

The dietary structure of amino acids affects the host gut microbial structure, which in turn affects host metabolism and health. Studies have shown that the foul odor of pig excrement is produced by intestinal microorganisms metabolizing amino acids (137). The level of amino acids in a balanced diet can change the abundance of pig intestinal microbes, thereby improving fermentation and reducing odor-causing compounds in pig excrement (137). An increase in branched-chain amino acids induces changes in the abundance of certain gut flora, such as increased abundance of *Akkermansia* and *Bifidobacterium* in mice supplemented with a mixture of branched-chain amino acids (138). The accumulation of branched-chain amino acids is positively correlated with insulin resistance. The number of bacteria that absorb branched-chain amino acids (such as *Butyrivibrio crossotus* and *Eubacterium siraeum*) gradually decreases in insulin-resistant patients, resulting in the accumulation of branched-chain amino acids and an insulin-resistant phenotype (139). Metabolism of proline is associated with disturbances in host emotional expression. Proline is the dietary factor that has the greatest impact on depression, and individual depression levels are enhanced with increased proline intake and plasma proline levels, which are not significantly associated with antidepressants (140). The higher the proline content in plasma, the lower the proline recycling-involved in glutamate, gamma-aminobutyric acid receptor activation, synaptic interactions, and axon guidance pathways. Likewise, the higher abundance of *Parabacteroides* and *Acidaminococcus* species and lower abundance of Bifidobacterium and short-chain fatty acid-producing species (such as *Roseburia*, *Butyrivibrio*, *Dorea*, and *Blautia genera*) in the gut (140). If mice are fed with a diet deficient in tryptophan, the gut microbiota will be dysregulated and gut immunity will be compromised (130).

Gut microbes can affect host health by affecting protease activity. The protease activity in the intestine is not only affected by the environment such as temperature and pH, but also restricted by microorganisms such as *Bacteroides*, *Clostridium*, *Propionibacterium*, *Fusobacterium*, *Streptococcus*, and *Lactobacillus* (141). Affected by various factors such as heredity, diet, medication, the host has respective characteristic of intestinal flora. Under normal circumstances, intestinal flora and host can benefit from this kind of dynamic balance. Once this balance is broken, the body of the peroxidase proliferation of activated receptors (PPARs) signaling pathway and amp activated protein kinase (AMPK) path are blocked (142, 143). The lack of proteases in the host will lead to increased susceptibility to disease, such as lack of angiotensin I-converting enzyme 2 (Ace2), which will lead to increased susceptibility to intestinal inflammation caused by intestinal epithelial cells (123).

Gut microbial responses to nucleic acid metabolic phenotypes

Nucleic acids in food mostly exist in the form of nucleoproteins, which are broken down into nucleic acids and proteins in the stomach. Nucleotide is the basic unit of nucleic acid. Its main functions are the raw material for nucleic acid synthesis, the utilization form of energy in the body, the participation in metabolism and physiological regulation, the component of coenzyme, the intermediate product of activation, etc. The assembly of nucleotides has a high metabolic demand and requires substances such as glucose, aspartic acid, serine, glycine, CO_2, and glutamine for synthesis. These substances supplement the carbon and nitrogen sources for nucleotide synthesis through major pathways such as glycolysis, the serine-glycine pathway, the glutamine aminotransferase reaction, the Krebs cycle without or with anaplerotic inputs, and the pentose phosphate pathway (144).

Nucleic acid substances are considered to be an very important class of molecules in organisms because they have function of heredity, mediating and catalyzing biochemical reactions, providing or transferring energy, etc. (145). Lack of nucleotides in food can damage the host liver (146, 147), gut (148–151) and immune system (152, 153). Exogenous addition

can promote the maturation, activation and proliferation of lymphocytes, improve the phagocytosis of macrophages (154, 155), promote the balance of intestinal flora (such as increasing the proportion of *Bifidobacteria*), and reduce the proportion of pathogenic bacteria (145). Exogenous nucleotides have an important impact on maintaining the normal function of the host immune system, intestinal function, improving the structure of the intestinal flora and lipid metabolism, and will have a broad prospect and development space in the field of medical and health care.

The intestinal flora is one of the important "organs" for the host to absorb and utilize nucleic acids. For example, the nucleosidase produced by *Ochrobactrum anthropi* in the human intestine can decompose purine nucleosides in food, and also promote other enzymatic reactions (156–158). *Escherichia coli* and baker's yeast (dietary nucleotides) can convert glucose to 2-deoxyribose 5-phosphate and generate the desired substrate for 2-deoxyribose 5-phosphate, respectively (159).

Nucleotides and nucleosides strongly dose-dependently modulate infant gut microbiota composition and metabolic activity. Nucleotide and nucleoside are added in the infant formula, increasing the amount of the anaerobic bacteria, gastrointestinal bacteria, *Fusobacterium*, *Lactobacillus*, *Staphylococcus*, *Leuconostoc*, increased levels of bacteria and bacteria related to nucleotide and metabolism of sulfur and iron transcription content will increase, and decreasing the biosynthesis of *Salmonella*, total factor and vitamin (160). Yeast extract (dietary nucleotides) can increase the number of *Lactobacilli* and *Bifidobacteria*, thereby increasing butyrate production to stabilize and promote the gut microbiota in the elderly (161). Numerous studies have also demonstrated that the addition of exogenous nucleotides can increase the proportion of beneficial bacteria in the host gut microflora and play a positive regulatory role.

Signaling roles of gut microbes in host metabolism

In recent years, the gut microbiota has attracted much attention as a key mediator of brain-gut axis signaling. Brain-gut interactions are mainly divided into neural, endocrine and immune pathways. There is growing evidence that the influence of the gut microbiota extends beyond the gut, which modulates brain function and subsequent behavior through the brain-gut axis (162–164). Dysregulation of the microbiota-gut-brain axis leads to neuroinflammation and synaptic damage that contribute to obesity-related cognitive decline (50). Preclinical and clinical studies have also shown that the gut microbiota influences central nervous system physiology, anxiety, depression, social behavior, cognitive function and visceral pain (134). For example, high-fat diet-induced changes in gut microbiota can lead to cognitive impairment in mice; Mice transplanted with microbiota from obese humans also showed reduced memory scores. Moreover, RNA sequencing of the medial prefrontal cortex showed that short-term memory was associated with aromatic amino acid pathways, inflammatory genes, and bacterial communities (165). Among them, *Clostridium*, *Ruminococcus* and *Eubacterium* genera in *Firmicutes* phylum, as well as *Selenomonas* family are positively correlated with memory score, while *Bacteroidetes* phylum and *Proteobacteria* phylum species are negatively correlated with memory score (165). This suggests that gut microbes can talk to the brain through neural interactions and influence host cognition and behavior.

Gut microbiota imbalance affects hippocampal brain and nerve development by activating microglia (32). Brain-gut interactions play a role in functional GI disorders [e.g., irritable bowel syndrome (IBS)] (166), organic GI disorders to a lesser extent [e.g., inflammatory bowel disease (IBD)], and other disorders that may be associated with dysregulation of brain-gut communication (e.g., obesity and anorexia nervosa), but the specific mechanisms of the interaction are not well understood (167).

In the study of the host brain-gut axis, it was found that tryptophan and 5-hydroxytryptophan metabolic systems are involved in all levels of the brain-gut-microbiome axis. For example, germ-free mice show different social novelty preferences than normal mice (132, 168, 169); Bacterial colonization of germ-free mice after weaning normalizes this phenomenon (132, 169, 170); More importantly, bacterial colonization of weaned germ-free mice normalizes circulating tryptophan availability and kynurenine pathway metabolism (132, 171). *Lactococcus*, *Lactobacillus*, *Streptococcus*, *Escherichia coli,* and *Klebsiella* can directly use tryptophan to synthesize serotonin (127, 131). Serotonin is widely present in the gut, which can cross the blood-brain barrier and act directly on the central nervous system. At present, tryptophan treatment strategies have focused on direct regulation of the 5-hydroxytryptophan (5-HT) metabolic system, but due to the heterogeneous of the disease and the diversification of 5-HT effects, these strategies are only partially effective in distinct patient subsets with stress-related brain-gut axis disorders (131).

The gut-liver axis is another pathway by which the host controls and shapes the gut microbe to protect the gut barrier. The gut microbiome, liver inflammation and metabolism are connected by the gut-liver axis, and the important mediators between the two are the gut microbiota and microbiota metabolites (172). Gut-derived compounds, such as short-chain fatty acids, bile acids, methylamine, amino acid derivatives, and related microbial molecular patterns stimulate host energy metabolism, food intake, and regulate signaling and metabolic pathways in key tissues by sensing signals, enhancing host–gut microbiota interactions (173). Another example is that microbial tryptophan metabolites are directly involved in hepatic immune responses in liver disease, or indirectly affect

function by modulating gut barrier function and signaling along the gut-liver axis (117, 174). The link between the gut and liver directly influences the composition of the gut flora and the integrity of the barrier, and is an important factor in liver function. An imbalance on either side will lead to a decrease in immunity and even disease.

In the brain-gut axis and gut-liver axis, the gut microbes directly participate in or indirectly regulate the metabolic functions of key tissues such as the brain and liver through signal transduction, thereby affecting the health of the host. At present, although the key mediators and specific mechanisms of brain-gut axis and gut-liver axis signaling are still poorly understood, it is of great significance to pay close attention to the signaling of gut microbes.

Prospects for the study of gut microbes and host metabolic phenotypes

Various chemicals produced or modified by the gut microbiota trigger responses in various physiological functions of the host, including immune, neurological, and metabolic (175). A large number of studies have proved that the occurrence of host diseases is closely related to the diversity of intestinal flora, the difference of main representative flora, and the abundance and ratio of different flora, mainly affecting host metabolism and metabolites (144). The role and status of intestinal flora and its metabolites in monitoring host health and disease prevention and control is becoming more and more important. Furthermore, the monitoring of key indicators and the mining of therapeutic factors will be another great progress in the history of human disease prevention and control.

Gut microbes and their metabolites may be important markers for disease screening

Numerous studies have demonstrated that changes in the abundance of gut microbiota are a common marker of neoplastic diseases, such as *Fusobacterium nucleatum*, *Escherichia coli*, *Bacteroides fragilis*, and *Aspergillus* are associated with carcinogenesis (176, 177); By comparing the gut flora of gestational diabetes patients and healthy people, it was found that gestational diabetes patients had abundant OTUs of *Lachnospiraceae* family, and decreased OTUs of *Enterobacteriaceae* and *Ruminococcaceae* families (178); Obese patients are often complicated by diabetes, and the abundances of *Ruminococcus gnavus*, different *Bacteroidetes* and *Enterobacter* species in the gut tend to increase compared with insulin resistance and obesity (179, 180); Compared with healthy people, patients with primary sclerosing cholangitis had significantly reduced gut microbiota but significantly enriched *Clostridium* species with reduced *Eubacterium* spp. and *Ruminococcus obeum* (181); And then a further study of its gut microbial genes showed that the genes related to the synthesis of vitamin B6 and branched-chain amino acid cores in gut microbes were significantly reduced (181).

Different microbial metabolites in blood can reflect different healthy aging (age) states with unique gut microbiota. In the study of the intestinal flora of physiologically aging people, the core flora of the gut microbiota of the elderly is attenuated, and the results at the genus level show that Bacteroides are mainly reduced (182). Studies have also confirmed that there are key families of microorganisms in the gut microbiota with potential therapeutic effects (183–185).

The structure of the gut microbiota and its metabolites are also markers of many diseases. Elevated ratio of Firmicutes to Bacteroidetes is regarded as a microbial marker of obesity (186); The profiles of gut microbiota and serum metabolites are potential diagnostic markers for lung cancer. Compared with healthy individuals, the feces of patients with lung cancer showed significant differences in *Megasphaera*, *Clostridioides*, *Erysipelotrichaceae,* and *Phascolarctobacterium*, which the diversity of intestinal flora in patients with lung cancer was higher. Moreover, the serum levels of certain glycerophospholipids (e.g., LysoPE, LysoPC, LysoPC), AcylGlcADG, AcylGlcADG, Acylcarnitine and hypoxanthine can be used to distinguish lung cancer patients from normal individuals (187); Microbial metabolic imbalance of aromatic and branched-chain amino acids is a metabolic hallmark that accompanies liver inflammation (188). Aromatic amino acid metabolites can be used as signal molecules in host physiology (116). For example, phenylalanine (189) metabolism can be used as a stage-specific marker for colorectal cancer, because it can be seen that the genes that metabolize Phe in the intestinal flora of patients with colorectal cancer are increased, and it is significantly increased in the gut (116); Tyrosine and tryptophan metabolism and valine, leucine, and isoleucine degradation are significantly associated with identified gut microbiota markers and osteoporosis. Ling et al. (190) found that the relative abundances of *Actinobacillus*, *Blautia*, *Oscillospira*, *Bacteroides*, and *Phascolarctobacterium* were positively correlated with osteoporosis, while some of genera of *Veillonellaceae*, *Ruminococcaceae*, and *Collinsella* were negatively associated with the presence of osteoporosis. However, further confirmation in animal or *in vitro* experiments is required as a diagnostic or therapeutic marker (190).

Inflammatory cytokines are key factors for the expression of indoleamine 2, 3-dioxygenase (IDO1) and tryptophan 2, 3-dioxygenase (TDO) (131). Moreover, it has been proposed as markers of gastrointestinal diseases in the study of mucosal inflammation and colon cancer (131).

Different types of carbohydrate-active enzymes may provide markers for the screening of certain diseases. For example, glycosyltransferases can catalyze the synthesis of glycoconjugates, including the inflammatory factor lipopolysaccharide-a common feature of many diseases. Comparing differences in carbohydrate-active enzymes in health and disease suggests that microbial carbohydrate metabolism can be a good basis for optimizing pre-selected, pro- and synergistic biological candidates (61). Most disease changes are associated with changes in gut microbial abundance, while further research is needed to prove whether differential bacteria can be used as indicators. The clarification of indicator species will provide new ideas for therapeutic strategies.

Improving gut microbes will become an effective means of disease prevention and treatment

Gut microbes are an important factor in regulating various physiological functions, immune system, cardiovascular system, intestinal function, digestion and absorption of nutrients and their metabolites (191). Once the healthy balance of the host's intestinal flora is disrupted, the host will become ill. On the contrary, adjusting the balance of the host's intestinal flora will help the host maintain a healthy state. Direct supplementation of beneficial microorganisms modulates host hepatic and systemic lipid metabolism (192), energy stabilization (193), and glycemic control (194). Meanwhile, it reduces the risk of diet-induced obesity, insulin resistance, and type 2 diabetes (195).

Transplanting fecal microbiota can effectively treat some recurrent *Clostridium difficile* infections in small trial in metabolic syndrome and obesity (196); Gavage of mice with *Bacteroides thetaiotaomicron* reduced plasma glutamate concentrations and attenuated diet-induced weight gain and obesity in mice, suggesting the possibility of targeting the gut microbiota to intervene in obesity (197); In mouse experiments, it was found that *Prevotella copri* and *Bacteroides vulgatus* are the key species driving branched chain amino acids (BCAAs) biosynthesis and insulin resistance (139). In addition, using *Prevotella copri* to interfere with the intestinal flora of mice can induce insulin resistance, aggravate glucose intolerance and increase BCAAs circulation level (139). Kato et al. (198) found that oral administration of *Porphyromonas gingivalis* could alter the composition of the host gut microbiota, thereby impeding or altering the metabolic function of host amino acids, altering immune regulation and gut barrier function, and mediating systemic diseases.

Nutritional stress caused by an unbalanced diet can lead to changes in the host gut microbiome, which is one of the important factors in the occurrence of metabolic diseases such as hypertension, abnormal lipid metabolism, and vascular dysfunction (191). This makes dietary guidelines for the population, based on regional differences, particularly important. Dietary and lifestyle interventions to supplement carbohydrates needed by microorganisms can enhance the ability of intestinal microbiota to metabolize carbohydrates, reduce body weight (199), and reduce metabolic diseases caused by intestinal microbiota metabolism in overweight and obese patients. An unbalanced diet not only adds to the metabolic stress of the host's metabolic organs, but also disrupts the balance of the intestinal microbial ecology.

More and more data suggest that host health is associated with dietary microbial and carbohydrate-induced changes in microbiota composition and diversity (53). Breast milk contains a variety of complex oligosaccharides that are not easily digested but are essential for the composition of the neonatal gut microbiota (200). The microbiota that colonize an infant's gut are directly related to its ability to grow and develop normally in later life and to the strength of its immune system. Compared with formula, breastfed infants had higher levels of *Bifidobacteria* and lactic acid bacteria as well as lower levels of potential pathogens. By contrast, formula-fed infants had a more diverse gut flora, mainly *Staphylococcus*, *Bacteroides*, *Clostridium*, *Enterococcus*, *Enterobacter*, and *Atopobium* (201). During weaning, the phyla *Proteobacteria* and *Actinobacteria* are replaced by *Firmicutes* and *Bacteroidetes* as the dominant members of the infant microbiome due to the complementary introduction of a variety of novel food substances and nutrients (202, 203). Tanes et al. (204) found that unbalanced dietary nutrition can lead to an imbalance of gut microbiota, and dietary fiber plays an important role in the restoration of gut microbiota, but the mechanism remains unclear. Flint found that both the amount and type of indigestible carbohydrates (such as resistant starch, non-starch polysaccharides, and prebiotics) affected the species composition of the gut microbiota during both short-term dietary interventions and long-term dietary habits (59). Different geographic regions have different dietary habits, and there are also significant differences in the composition of gut microbes. Compared with Europeans, Africans consume approximately twice as much dietary fiber, have a higher diversity of gut microbes, produce more short-chain fatty acids, and are more abundant in *Bacteroidetes* relative to *Firmicutes* (179, 205).

It is clear that differences in food culture also reflect the consistency of nutritional needs from the dietary guidelines of different countries[1]. All guidelines recommend limiting or avoiding foods with high added sugar, salt, and saturated fat (206).

1 http://www.fao.org/nutrition/education/food-based-dietary-guidelines

Some countries specifically mention avoiding processed, ultra-processed and/or packaged foods (206).

Conclusion

The metabolic phenotype of organisms exists objectively (207), and is gradually being recognized and deciphered by humans. Gut microbes are the second digestive organ in the host and one of the key factors determining the host's metabolic phenotype (2). They directly or indirectly participate in the host's metabolism, physiology, and immunity through population structure changes, metabolite differences, signal transduction, and gene expression, helping the host to resist disease and maintain health. A large number of studies have confirmed that finding new and effective ways to prevent or treat host metabolic diseases through the association of gut microbiota with host metabolic phenotypes is not only feasible and will be a historic step in the study of gut microbiota.

But gut microbiota composition and function are also influenced by host genetics (208), diet (209), age (210, 211), mode of birth (212), geography (210), host immune status (213), travel (214), and drug use (215, 216). How to obtain comprehensive information on the impact of gut microbes on host metabolic phenotypes? What are the mechanisms underlying the role of gut microbes in host metabolic phenotypes? Can we find the key regulators and indicators that gut microbes regulate host metabolism? These issues would be the focuses of future research on gut microbes.

The gut microbiota and metabolites are not only the monitors of host disease, but also the guardians of maintaining and stabilizing host health. Although the existing researches still focus on the simple flora structure and the level of a few influencing factors, the theoretical concept that gut microbes affects the host's metabolic phenotype provides a good research idea for the systematic study of metabolic diseases caused by gut microbes. As more and more new discoveries about the metabolic phenotypes of gut microbes on the host are published, it is about to become possible to use gut microbes to maintain the metabolic health of life.

Author contributions

JH and JX conceived the manuscript. JH wrote the manuscript. JX, DL, XL, and WP edited the manuscript. All authors read and approved the final version of the manuscript.

Funding

This research was supported by the Hunan Province Modern Agricultural Industrial Technology System Project (Xiangnongfa [2019] No. 105) and the School-Enterprise Horizontal Project (5026401/0319085).

Acknowledgments

We thank the reviewers for their constructive and valuable comments and the editor for their assistance in refining this article.

Conflict of interest

Author WP was employed by Changde Dabeinong Feed Co. Ltd.

The remaining authors declare that the research was conducted in the absence of any commercial or financial relationships that could be construed as a potential conflict of interest.

Publisher's note

References

1. Zhou XW, Zhong RM. Review on metabotype. *J Food Sci Biotechnol.* (2015) 34:673–8.

2. Johnson CH, Patterson AD, Idle JR, Gonzalez FJ. Xenobiotic metabolomics: major impact on the metabolome. *Ann Rev Pharmacol.* (2012) 52:37–56. doi: 10.1146/annurev-pharmtox-010611-134748

3. Eckburg PB, Bik EM, Bernstein CN, Purdom E, Dethlefsen L, Sargent M. Diversity of the human intestinal microbial flora. *Science.* (2005) 308:1635–8. doi: 10.1126/science.1110591

4. Tian Y, Gui W, Koo I, Smith PB, Allman EL, Nichols RG, et al. The microbiome modulating activity of bile acids. *Gut Microbes.* (2020) 11:979–96.

5. Lee Y, Kim AH, Kim E, Lee S, Yu KS, Jang IJ, et al. Changes in the gut microbiome influence the hypoglycemic effect of metformin through the altered metabolism of branched-chain and nonessential amino acids. *Diabetes Res Clin.* (2021) 178:108985. doi: 10.1016/j.diabres.2021.108985

6. Brestoff JR, Artis D. Commensal bacteria at the interface of host metabolism and the immune system. *Nat Immunol.* (2013) 14:676–84. doi: 10.1038/ni.2640

7. Krajmalnik-Brown R, Ilhan ZE, Kang DW, DiBaise JK. Effects of gut microbes on nutrient absorption and energy regulation. *Nutr Clin Pract.* (2012) 27:201–14. doi: 10.1177/0884533611436116

8. Wolf PG, Biswas A, Morales SE, Greening C, Gaskins HR. H2 metabolism is widespread and diverse among human colonic microbes. *Gut Microbes.* (2016) 7:235–45. doi: 10.1080/19490976.2016.1182288

9. Chassard C, Lacroix C. Carbohydrates and the human gut microbiota. *Curr Opin Clin Nutr.* (2013) 16:453–60. doi: 10.1097/MCO.0b013e3283619e63

10. Chen DF, Jin DC, Huang SM, Wu J, Xu M, Liu T, et al. Clostridium butyricum, a butyrate-producing probiotic, inhibits intestinal tumor development through modulating Wnt signaling and gut microbiota. *Cancer Lett.* (2020) 469:456–67. doi: 10.1016/j.canlet.2019.11.019

11. Lee WJ, Hase K. Gut microbiota-generated metabolites in animal health and disease. *Nat Chem Biol.* (2014) 10:416–24. doi: 10.1038/nchembio.1535

12. Jia RK, Huang M, Qian LC, Yan X, Lv Q, Ye H, et al. The depletion of carbohydrate metabolic genes in the gut microbiome contributes to the transition from central obesity to type 2 diabetes. *Front Endocrinol.* (2021) 12:747646. doi: 10.3389/fendo.2021.747646

13. Delzenne NM, Williams CM. Prebiotics and lipid metabolism. *Curr Opin Lipidol.* (2002) 13:61–7. doi: 10.1097/00041433-200202000-00009

14. Jan G, Belzacq AS, Haouzi D, Rouault A, Métivier D, Kroemer G. Propionibacteria induce apoptosis of colorectal carcinoma cells via short-chain fatty acids acting on mitochondria. *Cell Death Differ.* (2002) 9:179–88. doi: 10.1038/sj.cdd.4400935

15. Li CJ, Elsasser TH. Butyrate-induced apoptosis and cell cycle arrest in bovine kidney epithelial cells: involvement of caspase and proteasome pathways. *J Anim Sci.* (2005) 83:89–97. doi: 10.2527/2005.83189x

16. Koh A, De Vadder F, Kovatcheva-Datchary P, Bäckhed F. From dietary fiber to host physiology: short-chain fatty acids as key bacterial metabolites. *Cell.* (2016) 165:1332–45. doi: 10.1016/j.cell.2016.05.041

17. Hosseini E, Grootaert C, Verstraete W, Van de Wiele T. Propionate as a health-promoting microbial metabolite in the human gut. *Nutr Rev.* (2011) 69:245–58. doi: 10.1111/j.1753-4887.2011.00388.x

18. Oliphant K, Allen-Vercoe E. Macronutrient metabolism by the human gut microbiome: major fermentation by-products and their impact on host health. *Microbiome.* (2019) 7:91. doi: 10.1186/s40168-019-0704-8

19. Chambers ES, Viardot A, Psichas A, Morrison DJ, Murphy KG, Zac-Varghese SEK, et al. Effects of targeted delivery of propionate to the human colon on appetite regulation, body weight maintenance and adiposity in overweight adults. *Gut.* (2015) 64:1744–54. doi: 10.1136/gutjnl-2014-307913

20. den Besten G, van Eunen K, Groen AK, Venema K, Reijngoud DJ, Bakker BM. The role of short-chain fatty acids in the interplay between diet, gut microbiota, and host energy metabolism. *J Lipid Res.* (2013) 54:2325–40. doi: 10.1194/jlr.R036012

21. Morrison DJ, Preston T. Formation of short chain fatty acids by the gut microbiota and their impact on human metabolism. *Gut Microbes.* (2016) 7:189–200. doi: 10.1080/19490976.2015.1134082

22. Nishina PM, Freedland RA. Effects of propionate on lipid biosynthesis in isolated rat hepatocytes. *J Nutr.* (1990) 120:668–73. doi: 10.1093/jn/120.7.668

23. Kolodziejczyk AA, Zheng DP, Shibolet O, Elinav E. The role of the microbiome in NAFLD and NASH. *Embo Mol Med.* (2019) 11:e9302. doi: 10.15252/emmm.201809302

24. Passos M, Moraes-Filho JP. Intestinal microbiota in digestive diseases. *Arq Gastroenterol.* (2017) 54:255–62. doi: 10.1590/S0004-2803.201700000-31

25. Xie C, Halegoua-DeMarzio D. Role of probiotics in non-alcoholic fatty liver disease: does gut microbiota matter? *Nutrients.* (2019) 11:2837. doi: 10.3390/nu11112837

26. Beilharz JE, Kaakoush NO, Maniam J, Morris MJ. The effect of short-term exposure to energy-matched diets enriched in fat or sugar on memory, gut microbiota and markers of brain inflammation and plasticity. *Brain Behav Immun.* (2016) 57:304–13. doi: 10.1016/j.bbi.2016.07.151

27. de Clercq NC, Frissen MN, Groen AK, Nieuwdorp M. Gut microbiota and the gut-brain axis: new insights in the pathophysiology of metabolic syndrome. *Psychosom Med.* (2017) 79:874–9. doi: 10.1097/PSY.0000000000000495

28. Hand TW. The role of the microbiota in shaping infectious immunity. *Trends Immunol.* (2016) 37:647–58. doi: 10.1016/j.it.2016.08.007

29. Marques C, Meireles M, Faria A, Calhau C. High-fat diet-induced dysbiosis as a cause of neuroinflammation. *Biol Psychiatry.* (2016) 80:e3–4. doi: 10.1016/j.biopsych.2015.10.027

30. Rabinowitz T, Polsky A, Golan D, Danilevsky A, Shapira G, Raff C, et al. Bayesian-based noninvasive prenatal diagnosis of single-gene disorders. *Genome Res.* (2019) 29:428–38. doi: 10.1101/gr.235796.118

31. Gruner N, Mattner J. Bile acids and microbiota: multifaceted and versatile regulators of the liver-gut axis. *Int J Mol Sci.* (2021) 22:1397. doi: 10.3390/ijms22031397

32. Erny D, de Angelis ALH, Jaitin D, Wieghofer P, Staszewski O, David E, et al. Host microbiota constantly control maturation and function of microglia in the CNS. *Nat Neurosci.* (2015) 18:965–77. doi: 10.1038/nn.4030

33. Giel JL, Sorg JA, Sonenshein AL, Zhu J. Metabolism of bile salts in mice influences spore germination in *Clostridium difficile*. *PLoS One.* (2010) 5:e8740. doi: 10.1371/journal.pone.0008740

34. Sorg JA, Sonenshein AL. Inhibiting the initiation of clostridium difficile spore germination using analogs of chenodeoxycholic acid, a bile acid. *J Bacteriol.* (2010) 192:4983–90. doi: 10.1128/JB.00610-10

35. Weingarden AR, Chen C, Bobr A, Yao D, Lu Y, Nelson VM, et al. Microbiota transplantation restores normal fecal bile acid composition in recurrent *Clostridium difficile* infection. *Am J Physiol Gastr.* (2014) 306:G310–9. doi: 10.1152/ajpgi.00282.2013

36. Buntin N, Hongpattarakere T, Ritari J, Douillard FP, Paulin L, Boeren S. An inducible operon is involved in inulin utilization in lactobacillus plantarum strains, as revealed by comparative proteogenomics and metabolic profiling. *Appl Environ Microb.* (2017) 83:e2402–16. doi: 10.1128/AEM.02402-16

37. Fuhren J, Rosch C, ten Napel M, Schols HA, Kleerebezem M. Synbiotic matchmaking in *Lactobacillus plantarum*: substrate screening and gene-trait matching to characterize strain-specific carbohydrate utilization. *Appl Environ Microb.* (2020) 86:e1081–1020. doi: 10.1128/AEM.01081-20

38. Mao BY, Yin RM, Li XS, Cui S, Zhang H, Zhao J. Comparative genomic analysis of *Lactiplantibacillus plantarum* isolated from different niches. *Genes Basel.* (2021) 12:241. doi: 10.3390/genes12020241

39. Siezen RJ, Tzeneva VA, Castioni A, Wels M, Phan HT, Rademaker JL, et al. Phenotypic and genomic diversity of *Lactobacillus plantarum* strains isolated from various environmental niches. *Environ Microbiol.* (2010) 12:758–73. doi: 10.1111/j.1462-2920.2009.02119.x

40. Seddik HA, Bendali F, Gancel F, Fliss I, Spano G, Drider D, et al. *Lactobacillus plantarum* and its probiotic and food potentialities. *Probiotics Antimicro.* (2017) 9:111–22. doi: 10.1007/s12602-017-9264-z

41. Weiss GA, Grabinger T, Garzon JG. Intestinal inflammation alters mucosal carbohydrate foraging and monosaccharide incorporation into microbial glycans. *Cell Microbiol.* (2021) 23:e13269. doi: 10.1111/cmi.13269

42. Aakko J, Pietila S, Toivonen R, Rokka A, Mokkala K, Laitinen K, et al. A carbohydrate-active enzyme (CAZy) profile links successful metabolic specialization of prevotella to its abundance in gut microbiota. *Sci Rep.* (2020) 10:12411. doi: 10.1038/s41598-020-69241-2

43. Singh RK, Chang HW, Yan D, Ucmak D. Influence of diet on the gut microbiome and implications for human health. *J Transl Med.* (2017) 15:73. doi: 10.1186/s12967-017-1175-y

44. Xu J, Bjursell MK, Himrod J, Deng S, Carmichael LK, Chiang HC, et al. A genomic view of the human-*Bacteroides thetaiotaomicron* symbiosis. *Science.* (2003) 299:2074–6. doi: 10.1126/science.1080029

45. Bhattacharya T, Ghosh TS, Mande SS. Global profiling of carbohydrate active enzymes in human gut microbiome. *PLoS One.* (2015) 10:e0142038. doi: 10.1371/journal.pone.0142038

46. Wong JMW, Jenkins DJA. Carbohydrate digestibility and metabolic effects. *J Nutr.* (2007) 137:2539s–46s. doi: 10.1093/jn/137.11.2539S

47. Deehan EC, Yang C, Perez-Munoz ME, Nguyen NK, Cheng CC, Triador L, et al. Precision microbiome modulation with discrete dietary fiber structures directs short-chain fatty acid production. *Cell Host Microbe.* (2020) 27:389–404e6. doi: 10.1016/j.chom.2020.01.006

48. Tuncil YE, Thakkar RD, Arioglu-Tuncil S, Hamaker BR, Lindemann SR. Subtle variations in dietary-fiber fine structure differentially influence the composition and metabolic function of gut microbiota. *Msphere.* (2020) 5:e180–120. doi: 10.1128/mSphere.00180-20

49. Cantu-Jungles TM, Hamaker BR. Erratum for cantu-jungles and hamaker, "new view on dietary fiber selection for predictable shifts in gut microbiota". *mBio.* (2020) 11:e747–720. doi: 10.1128/mBio.00747-20

50. Shi H, Wang Q, Zheng M, Hao S, Lum JS, Chen X, et al. Supplement of microbiota-accessible carbohydrates prevents neuroinflammation and cognitive decline by improving the gut microbiota-brain axis in diet-induced obese mice. *J Neuroinflammation.* (2020) 17:77. doi: 10.1186/s12974-020-01760-1

51. Blachier F, Beaumont M, Portune KJ, Steuer N, Lan A, Audebert M, et al. High-protein diets for weight management: interactions with the intestinal microbiota and consequences for gut health. A position paper by the my new gut study group. *Clin Nutr.* (2019) 38:1012–22. doi: 10.1016/j.clnu.2018.09.016

52. Hernandez MAG, Canfora EE, Blaak EE. Faecal microbial metabolites of proteolytic and saccharolytic fermentation in relation to degree of insulin resistance in adult individuals. *Beneficial Microbes.* (2021) 12:259–66. doi: 10.3920/Bm2020.0179

53. Sonnenburg ED, Sonnenburg JL. Starving our microbial self: the deleterious consequences of a diet deficient in microbiota-accessible carbohydrates. *Cell Metab.* (2014) 20:779–86. doi: 10.1016/j.cmet.2014.07.003

54. Duan YF, Wang Y, Liu QS. Changes in the intestine microbial, digestion and immunity of *Litopenaeus vannamei* in response to dietary resistant starch. *Sci Rep.* (2019) 9:6464. doi: 10.1038/s41598-019-42939-8

55. Muegge BD, Kuczynski J, Knights D, Clemente JC, González A, Fontana L, et al. Diet drives convergence in gut microbiome functions across mammalian phylogeny and within humans. *Science.* (2011) 332:970–4. doi: 10.1126/science.1198719

56. Abell GCJ, Cooke CM, Bennett CN, Conlon MA, McOrist AL. Phylotypes related to *Ruminococcus bromii* are abundant in the large bowel of humans and increase in response to a diet high in resistant starch. *Fems Microbiol Ecol.* (2008) 66:505–15. doi: 10.1111/j.1574-6941.2008.00527.x

57. Martinez I, Wallace G, Zhang CM, Legge R, Benson AK, Carr TP, et al. Diet-induced metabolic improvements in a hamster model of hypercholesterolemia are strongly linked to alterations of the gut microbiota. *Appl Environ Microb.* (2009) 75:4175–84. doi: 10.1128/AEM.00380-09

58. Qin RB, Wang J, Chao C. RS5 produced more butyric acid through regulating the microbial community of human gut microbiota. *J Agr Food Chem.* (2021) 69:3209–18. doi: 10.1021/acs.jafc.0c08187

59. Flint HJ. The impact of nutrition on the human microbiome. *Nutr Rev.* (2012) 70:S10–3. doi: 10.1111/j.1753-4887.2012.00499.x

60. Chumpitazi BP, Cope JL, Hollister EB, Tsai CM, McMeans AR, Luna RA, et al. Randomised clinical trial: gut microbiome biomarkers are associated with clinical response to a low FODMAP diet in children with the irritable bowel syndrome. *Aliment Pharmacol Ther.* (2015) 42:418–27. doi: 10.1111/apt.13286

61. Onyango SO, Juma J, De Paepe K, Van de Wiele T. Oral and gut microbial carbohydrate-active enzymes landscape in health and disease. *Front Microbiol.* (2021) 12:653448. doi: 10.3389/fmicb.2021.653448

62. Cui Y, Wang M, Zheng Y, Miao K, Qu X. The carbohydrate metabolism of *Lactiplantibacillus plantarum*. *Int J Mol Sci.* (2021) 22:13452. doi: 10.3390/ijms222413452

63. Tang FL, Wang F, Su XJ. Effects of deep eutectic solvents on the properties and antioxdant activity of polysaccharides from *Polygonatum cyrtonema* hua. *Food Ferment Indust.* (2021) 47:151–7. doi: 10.13995/j.cnki.11-1802/ts.026440

64. Furino VO, Alves JM, Marine DA, Sene-Fiorese M, Rodrigues CNDS, Arrais-Lima C, et al. Dietary intervention, when not associated with exercise, upregulates Irisin/FNDC5 while reducing visceral adiposity markers in obese rats. *Front Physiol.* (2021) 12:564963. doi: 10.3389/fphys.2021.564963

65. Bordoloi J, Ozah D, Bora T, Kalita J, Manna P. Gamma-glutamyl carboxylated Gas6 mediates the beneficial effect of vitamin K on lowering hyperlipidemia via regulating the AMPK/SREBP1/PPARalpha signaling cascade of lipid metabolism. *J Nutr Biochem.* (2019) 70:174–84. doi: 10.1016/j.jnutbio.2019.05.006

66. Xiong JF. Correlations between gut predominant bacteria and serum lipids in patients with hyperlipidemia. *Chin J Microecol.* (2013) 25:1282–5. doi: 10.13381/j.cnki.cjm.2013.11.028

67. Li MY, Liu Y. Research progress of *Lactobacillus rhamnosus* intervenrion on intestinal flora and lipid metabolism in the treatment of metabolic associated fatty liver disease. *Chin J Gastroenterol Hepatol.* (2022) 31:141–5.

68. Depommier C, Everard A, Druart C, Plovier H, Van Hul M, Vieira-Silva S, et al. Supplementation with *Akkermansia muciniphila* in overweight and obese human volunteers: a proof-of-concept exploratory study. *Nat Med.* (2019) 25:1096–103. doi: 10.1038/s41591-019-0495-2

69. Alessandri G, van Sinderen D, Ventura M. The genus bifidobacterium: from genomics to functionality of an important component of the mammalian gut microbiota running title: bifidobacterial adaptation to and interaction with the host. *Comput Struct Biotechnol J.* (2021) 19:1472–87. doi: 10.1016/j.csbj.2021.03.006

70. Bernini LJ, Simao AN, Alfieri DF, Lozovoy MA, Mari NL. Beneficial effects of *Bifidobacterium lactis* on lipid profile and cytokines in patients with metabolic syndrome: a randomized trial. Effects of probiotics on metabolic syndrome. *Nutrition.* (2016) 32:716–9. doi: 10.1016/j.nut.2015.11.001

71. Guo ZT, Hu B, Wang HX. Supplementation with nanobubble water alleviates obesity-associated markers through modulation of gut microbiota in high-fat diet fed mice. *J Funct Foods.* (2020) 67:130820. doi: 10.1016/j.jff.2020.103820

72. Wang WH. Study on the effect and mechanism of strengthening spleen and expectorating phlegm in improving dyslipidemia by regulating intestinal flora and bile acid metabolism. *Liaoning Univ Tradit Chin Med.* (2020) 2020:28. doi: 10.27213/d.cnki.glnzc.2020.000028

73. Li QW, Zhao YH, Gao F, Zhang K, Tian J. Research progress of regulatory key factors involved in cholesterol metabolism by lactic acid bacteria. *J Chin Instit Food Sci Technol.* (2021) 21:341–50. doi: 10.16429/j.1009-7848.2021.01.041

74. Wu JX. *The Effects of Mussel Polysaccharide a-D-Glucan(MP-A) on Non-Alcoholic Fatty Liver Disease Based on Gut Microbiota and Related Gut-Liver Axis Signaling Pathways*. Jinan: Shandong University (2019).

75. Zheng LS, Tai W, Lan DB, Li P, Wang M, Wang T, et al. Research progress on traditional Chinese medicine against diabetes based on intestinal flora new targets. *Drug Evaluat Res.* (2017) 40:1173–81. doi: 10.1007/s11655-017-2811-3

76. Yang H, Yang M, Fang SM, Huang X, He M, Ke S, et al. Evaluating the profound effect of gut microbiome on host appetite in pigs. *BMC Microbiol.* (2018) 18:215. doi: 10.1186/s12866-018-1364-8

77. Chen CY, Fang SM, Wei H, He M, Fu H, Xiong X, et al. Prevotella copri increases fat accumulation in pigs fed with formula diets. *Microbiome.* (2021) 9:175. doi: 10.1186/s40168-021-01110-0

78. He MQ, Shi BY. Gut microbiota as a potential target of metabolic syndrome: the role of probiotics and prebiotics. *Cell Biosci.* (2017) 7:54. doi: 10.1186/s13578-017-0183-1

79. Yang JY, Kweon MN. The gut microbiota: a key regulator of metabolic diseases. *BMB Rep.* (2016) 49:536–41. doi: 10.5483/bmbrep.2016.49.10.144

80. Azmi AFMN, Mustafa S, Hashim DM, Manap YA. Prebiotic activity of polysaccharides extracted from *Gigantochloa levis* (buluh beting) shoots. *Molecules.* (2012) 17:1635–51. doi: 10.3390/molecules17021635

81. Deville C, Gharbi M, Dandrifosse G. Study on the effects of laminarin, a polysaccharide from seaweed, on gut characteristics. *J Sci Food Agr.* (2007) 87:1717–25. doi: 10.1002/jsfa.2901

82. Zaporozhets TS, Besednova NN, Kuznetsova TA, Zvyagintseva TN, Makarenkova ID. The prebiotic potential of polysaccharides and extracts of seaweeds. *Russian J Mar Biol.* (2014) 40:1–9. doi: 10.1134/S1063074014010106

83. Cani PD, Neyrinck AM, Fava F, Knauf C, Burcelin RG, Tuohy KM, et al. Selective increases of bifidobacteria in gut microflora improve high-fat-diet-induced diabetes in mice through a mechanism associated with endotoxaemia. *Diabetologia.* (2007) 50:2374–83. doi: 10.1007/s00125-007-0791-0

84. Gao J, Ding GQ, Li Q, Gong L, Huang J, Sang Y, et al. Tibet kefir milk decreases fat deposition by regulating the gut microbiota and gene expression of Lpl and Angptl4 in high fat diet-fed rats. *Food Res Int.* (2019) 121:278–87. doi: 10.1016/j.foodres.2019.03.029

85. Larsen N, Vogensen FK, van den Berg FWJ, Nielsen DS, Andreasen AS, Pedersen BK, et al. Gut microbiota in human adults with type 2 diabetes differs from non-diabetic adults. *PLoS One.* (2010) 5:9085. doi: 10.1371/journal.pone.0009085

86. Qin JJ, Li YR, Cai ZM. A metagenome-wide association study of gut microbiota in type 2 diabetes. *Nature.* (2012) 490:55–60. doi: 10.1038/nature11450

87. Fei N, Zhao LP. An opportunistic pathogen isolated from the gut of an obese human causes obesity in germfree mice. *Isme J.* (2013) 7:880–4. doi: 10.1038/ismej.2012.153

88. Lyu M, Wang YF, Fan GW, Wang XY, Xu SY, Zhu Y, et al. Balancing herbal medicine and functional food for prevention and treatment of cardiometabolic diseases through modulating gut microbiota. *Front Microbiol.* (2017) 8:2146. doi: 10.3389/fmicb.2017.02146

89. Caesar R, Tremaroli V, Kovatcheva-Datchary P, Cani PD, Bäckhed F. Crosstalk between gut microbiota and dietary lipids aggravates WAT inflammation through TLR signaling. *Cell Metab.* (2015) 22:658–68. doi: 10.1016/j.cmet.2015.07.026

90. Zhang TT, Zhao WY, Xie BZ. Effects of *Auricularia auricula* and its polysaccharide on diet-induced hyperlipidemia rats by modulating gut microbiota. *J Funct Foods.* (2020) 72:104038. doi: 10.1016/j.jff.2020.104038

91. Luo Y, Chen G, Li B, Ji B. Evaluation of antioxidative and hypolipidemic properties of a novel functional diet formulation of Auricularia auricula and Hawthorn. *Innov Food Sci Emerg.* (2009) 10:215–21.

92. Lésel R, Choubert G. Fecal bacterial flora of rainbow trout under antibiotic treatment: effect of the number of pyloric caeca and the lipid content of food. *IMIS.* (1989) 1:897–903.

93. Davis CD. The gut microbiome and its role in obesity. *Nutr Today.* (2016) 51:167–74. doi: 10.1097/NT.0000000000000167

94. Deng Y, Liu WJ, Wang JQ, Yu J, Yang LQ. Intermittent fasting improves lipid metabolism through changes in gut microbiota in diet-induced obese mice. *Med Sci Monitor.* (2020) 26:e926789. doi: 10.12659/MSM.926789

95. Meng XL, Li S, Qin CB, Zhu ZX, Hu WP, Yang LP, et al. Intestinal microbiota and lipid metabolism responses in the common carp (*Cyprinus carpio* L.) following copper exposure. *Ecotox Environ Safe.* (2018) 160:257–64. doi: 10.1016/j.ecoenv.2018.05.050

96. Sun SM, Yang M, Fu HT. Altered intestinal microbiota induced by chronic hypoxia drives the effects on lipid metabolism and the immune response of oriental river prawn *Macrobrachium nipponense*. *Aquaculture.* (2020) 526:735431. doi: 10.1016/j.aquaculture.2020.735431

97. Song J, Zhang JJ, Su Y. Monascus vinegar-mediated alternation of gut microbiota and its correlation with lipid metabolism and inflammation in hyperlipidemic rats. *J Funct Foods.* (2020) 74:104152. doi: 10.1016/j.jff.2020.104152

98. Liu R, Zhang YH, Gao JS, Li X. Effects of octylphenol exposure on the lipid metabolism and microbiome of the intestinal tract of rana chensinensis tadpole by RNAseq and 16s amplicon sequencing. *Ecotox Environ Safe.* (2020) 197:110650. doi: 10.1016/j.ecoenv.2020.110650

99. Zhang J. Gut microflora induce type 2diabetes mellitus: progress in researches. *Chin J Microecol.* (2016) 28:113–6.

100. Dai ZL, Li XL, Xi PB, Zhang J, Wu G, Zhu WY, et al. Metabolism of select amino acids in bacteria from the pig small intestine. *Amino Acids.* (2012) 42:1597–608. doi: 10.1007/s00726-011-0846-x

101. Dai ZL, Zhang J, Wu G, Zhu WY. Utilization of amino acids by bacteria from the pig small intestine. *Amino Acids.* (2010) 39:1201–15. doi: 10.1007/s00726-010-0556-9

102. Verberkmoes NC, Russell AL, Shah M, Godzik A, Rosenquist M, Halfvarson J, et al. Shotgun metaproteomics of the human distal gut microbiota. *Isme J.* (2009) 3:179–89. doi: 10.1038/ismej.2008.108

103. Devaraj S, Hemarajata P, Versalovic J. The human gut microbiome and body metabolism: implications for obesity and diabetes. *Clin Chem.* (2013) 59:617–28. doi: 10.1373/clinchem.2012.187617

104. Libao-Mercado AJ, Zhu CL, Cant JP, Lapierre H, Thibault JN, Sève B, et al. Dietary and endogenous amino acids are the main contributors to microbial protein in the upper gut of normally nourished pigs. *J Nutr.* (2009) 139:1088–94. doi: 10.3945/jn.108.103267

105. Ciarlo E, Heinonen T, Herderschee J, Fenwick C, Mombelli M, Le Roy D, et al. Impact of the microbial derived short chain fatty acid propionate on host susceptibility to bacterial and fungal infections in vivo. *Sci Rep.* (2016) 6:37944. doi: 10.1038/srep37944

106. Hullar MA, Fu BC. Diet, the gut microbiome, and epigenetics. *Cancer J.* (2014) 20:170–5. doi: 10.1097/PPO.0000000000000053

107. Tajiri K, Shimizu Y. Branched-chain amino acids in liver diseases. *Transl Gastroenterol Hepatol.* (2018) 3:47. doi: 10.21037/tgh.2018.07.06

108. Vergnolle N. Protease inhibition as new therapeutic strategy for GI diseases. *Gut.* (2016) 65:1215–24. doi: 10.1136/gutjnl-2015-309147

109. Metges CC. Contribution of microbial amino acids to amino acid homeostasis of the host. *J Nutr.* (2000) 130:1857S–64S. doi: 10.1093/jn/130.7.1857S

110. Maes M, Leonard BE, Myint AM, Kubera M, Verkerk R. The new '5-HT' hypothesis of depression: cell-mediated immune activation induces indoleamine 2,3-dioxygenase, which leads to lower plasma tryptophan and an increased synthesis of detrimental tryptophan catabolites (TRYCATs), both of which contribute to the onset of depression. *Prog Neuropsychopharmacol Biol Psychiatry.* (2011) 35:702–21. doi: 10.1016/j.pnpbp.2010.12.017

111. Maes M, Rief W. Diagnostic classifications in depression and somatization should include biomarkers, such as disorders in the tryptophan catabolite (TRYCAT) pathway. *Psychiatry Res.* (2012) 196:243–9. doi: 10.1016/j.psychres.2011.09.029

112. Morris G, Berk M, Carvalho A, Caso JR, Sanz Y, Walder K, et al. The role of the microbial metabolites including tryptophan catabolites and short chain fatty acids in the pathophysiology of immune-inflammatory and neuroimmune disease. *Mol Neurobiol.* (2017) 54:4432–51. doi: 10.1007/s12035-016-0004-2

113. Nguyen NT, Nakahama T, Le DH, Van Son L, Chu HH, Kishimoto T, et al. Aryl hydrocarbon receptor and kynurenine: recent advances in autoimmune disease research. *Front Immunol.* (2014) 5:551. doi: 10.3389/fimmu.2014.00551

114. Gao J, Xu K, Liu HN, Liu G, Bai M, Peng C, et al. Impact of the gut microbiota on intestinal immunity mediated by tryptophan metabolism. *Front Cell Infect Mi.* (2018) 8:13. doi: 10.3389/fcimb.2018.00013

115. Liu YL, Hou YL, Wang GJ, Zheng X, Hao H. Gut microbial metabolites of aromatic amino acids as signals in host-microbe interplay. *Trends Endocrin Met.* (2020) 31:818–34. doi: 10.1016/j.tem.2020.02.012

116. Hoyles L, Fernandez-Real JM, Federici M. Molecular phenomics and metagenomics of hepatic steatosis in non-diabetic obese women. *Nat Med.* (2018) 24:1070–80. doi: 10.1038/s41591-018-0061-3

117. Natividad JM, Agus A, Planchais J. Impaired aryl hydrocarbon receptor ligand production by the gut microbiota is a key factor in metabolic syndrome. *Cell Metab.* (2018) 28:737–749.e4. doi: 10.1016/j.cmet.2018.07.001

118. Taleb S. Tryptophan dietary impacts gut barrier and metabolic diseases. *Front Immunol.* (2019) 10:2113. doi: 10.3389/fimmu.2019.02113

119. Grifka-Walk HM, Jenkins BR, Kominsky DJ. Amino acid trp: the far out impacts of host and commensal tryptophan metabolism. *Front Immunol.* (2021) 12:653208–653208. doi: 10.3389/fimmu.2021.653208

120. Behnsen J, Jellbauer S, Wong CP. The cytokine IL-22 promotes pathogen colonization by suppressing related commensal bacteria. *Immunity.* (2014) 40:262–73. doi: 10.1016/j.immuni.2014.01.003

121. Zelante T, Iannitti RG, Cunha C, De Luca A, Giovannini G, Pieraccini G, et al. Tryptophan catabolites from microbiota engage aryl hydrocarbon receptor and balance mucosal reactivity via interleukin-22. *Immunity.* (2013) 39:372–85. doi: 10.1016/j.immuni.2013.08.003

122. Zenewicz LA, Yin X, Wang G, Elinav E, Hao L, Zhao L, et al. IL-22 deficiency alters colonic microbiota to be transmissible and colitogenic. *J Immunol.* (2013) 190:5306–12. doi: 10.4049/jimmunol.1300016

123. Hashimoto T, Perlot T, Rehman A, Trichereau J, Ishiguro H, Paolino M, et al. ACE2 links amino acid malnutrition to microbial ecology and intestinal inflammation. *Nature.* (2012) 487:477–81. doi: 10.1038/nature11228

124. Etienne-Mesmin L, Chassaing B, Gewirtz AT. Tryptophan: a gut microbiota-derived metabolites regulating inflammation. *World J Gastrointest Pharmacol Ther.* (2017) 8:7–9. doi: 10.4292/wjgpt.v8.i1.7

125. Kim CJ, Kovacs-Nolan JA, Yang C. l-tryptophan exhibits therapeutic function in a porcine model of dextran sodium sulfate (DSS)-induced colitis. *J Nutr Biochem.* (2010) 21:468–75. doi: 10.1016/j.jnutbio.2009.01.019

126. Sun X, Shao Y, Jin Y, Huai J, Zhou Q, Huang Z, et al. Melatonin reduces bacterial translocation by preventing damage to the intestinal mucosa in an experimental severe acute pancreatitis rat model. *Exp Ther Med.* (2013) 6:1343–9. doi: 10.3892/etm.2013.1338

127. Gao K, Mu CL, Farzi A, Zhu WY. Tryptophan metabolism: a link between the gut microbiota and brain. *Adv Nutr.* (2020) 11:709–23. doi: 10.1093/advances/nmz127

128. George A, Maes M. The gut-brain axis: the role of melatonin in linking psychiatric, inflammatory and neurodegenerative conditions. *Adv Int Med.* (2015) 2:31–7. doi: 10.1016/j.aimed.2014.12.007

129. Gheorghe CE, Martin JA, Manriquez FV, Dinan TG, Cryan JF, Clarke G, et al. Focus on the essentials: tryptophan metabolism and the microbiome-gut-brain axis. *Curr Opin Pharmacol.* (2019) 48:137–45. doi: 10.1016/j.coph.2019.08.004

130. Wikoff WR, Anfora AT, Liu J. Metabolomics analysis reveals large effects of gut microflora on mammalian blood metabolites. *Proc Natl Acad Sci USA.* (2009) 106:3698–703. doi: 10.1073/pnas.0812874106

131. O'Mahony SM, Clarke G, Borre YE, Dinan TG, Cryan JF. Serotonin, tryptophan metabolism and the brain-gut-microbiome axis. *Behav Brain Res.* (2015) 277:32–48. doi: 10.1016/j.bbr.2014.07.027

132. Clarke G, Grenham S, Scully P, Fitzgerald P, Moloney RD, Shanahan F, et al. The microbiome-gut-brain axis during early life regulates the hippocampal serotonergic system in a sex-dependent manner. *Mol Psychiatr.* (2013) 18:666–73. doi: 10.1038/mp.2012.77

133. Claesson MJ, Jeffery IB, Conde S. Gut microbiota composition correlates with diet and health in the elderly. *Nature.* (2012) 488:178–84. doi: 10.1038/nature11319

134. Kennedy PJ, Cryan JF, Dinan TG, Clarke G. Kynurenine pathway metabolism and the microbiota-gut-brain axis. *Neuropharmacology.* (2017) 112:399–412. doi: 10.1016/j.neuropharm.2016.07.002

135. Oxenkrug GF. Genetic and hormonal regulation of tryptophan kynurenine metabolism: implications for vascular cognitive impairment, major depressive disorder, and aging. *Ann N Y Acad Sci.* (2007) 1122:35–49. doi: 10.1196/annals.1403.003

136. Prenderville JA, Kennedy PJ, Dinan TG, Cryan JF. Adding fuel to the fire: the impact of stress on the ageing brain. *Trends Neurosci.* (2015) 38:13–25. doi: 10.1016/j.tins.2014.11.001

137. Recharla N, Kim K, Park J, Jeong J, Jeong Y, Lee H, et al. Effects of amino acid composition in pig diet on odorous compounds and microbial characteristics of swine excreta. *J Anim Sci Technol.* (2017) 59:28. doi: 10.1186/s40781-017-0153-5

138. Yang Z, Huang S, Zou D, Dong D, He X, Liu N, et al. Metabolic shifts and structural changes in the gut microbiota upon branched-chain amino acid supplementation in middle-aged mice. *Amino Acids.* (2016) 48:2731–45. doi: 10.1007/s00726-016-2308-y

139. Pedersen HK, Gudmundsdottir V, Nielsen HB. Human gut microbes impact host serum metabolome and insulin sensitivity. *Nature.* (2016) 535:376–81. doi: 10.1038/nature18646

140. Mayneris-Perxachs J, Castells-Nobau A, Arnoriaga-Rodriguez M. Microbiota alterations in proline metabolism impact depression. *Cell Metab.* (2022) 34:681–701e10. doi: 10.1016/j.cmet.2022.04.001

141. Dalmasso G, Nguyen HT, Yan Y. Butyrate transcriptionally enhances peptide transporter PepT1 expression and activity. *PLoS One.* (2008) 3:e2476. doi: 10.1371/journal.pone.0002476

142. Chen XP, Zhang F. Effect of forsythin on lipid metabolism and intestinal flora imbalance in obese rats through PPARs signaling pathway. *J Chin Med Mater.* (2022) 2022:949–54. doi: 10.13863/j.issn1001-4454.2022.04.031

143. Park H, Kaushik VK, Constant S. Coordinate regulation of malonyl-CoA decarboxylase, sn-glycerol-3-phosphate acyltransferase, and acetyl-CoA carboxylase by AMP-activated protein kinase in rat tissues in response to exercise. *J Biol Chem.* (2002) 277:32571–7. doi: 10.1074/jbc.M201692200

144. Bordignon V, Cavallo I, D'Agosto G, Trento E, Pontone M, Abril E, et al. Nucleic acid sensing perturbation: how aberrant recognition of self-nucleic acids may contribute to autoimmune and autoinflammatory diseases. *Int Rev Cel Mol Bio.* (2019) 344:117–37. doi: 10.1016/bs.ircmb.2018.09.001

145. Liang XG, Li Q, Huang LL. Reasearchs on nucleic acid metabolism and nutrition and their development. *Period Ocean Univ China.* (2019) 49:064–078.

146. Lopez-Navarro A, Gil A, Sanchez-Pozo A. Age-related effect of dietary nucleotides on liver nucleic acid content in rats. *Ann Nutr Metab.* (1997) 41:324–30. doi: 10.1159/000177963

147. Valdes R, Ortega MA, Casado FJ. Nutritional regulation of nucleoside transporter expression in rat small intestine. *Gastroenterology.* (2000) 119:1623–30. doi: 10.1053/gast.2000.20183

148. Che LQ, Hu L, Liu Y. Dietary nucleotides supplementation improves the intestinal development and immune function of neonates with intra-uterine growth restriction in a pig model. *PLoS One.* (2016) 11:e0157314. doi: 10.1371/journal.pone.0157314

149. Meng Y, Ma R, Ma J. Dietary nucleotides improve the growth performance, antioxidative capacity and intestinal morphology of turbot (*Scophthalmus maximus*). *Aquacult Nutr.* (2017) 23:585–93. doi: 10.1111/anu.12425

150. Miao X, Cao JJ, Xu W, Zhang L, Lin F. Effects of dietary nucleotides on growth performance,intestinal morphology and anti-oxidative capacities of large yellow croaker(*Larimichthys crocea*). *J Fish China.* (2014) 38:1140–8.

151. Xu L, Ran C, He S. Effects of dietary yeast nucleotides on growth, non-specific immunity, intestine growth and intestinal microbiota of juvenile hybrid tilapia *Oreochromis niloticus* female symbol x *Oreochromis aureus* male symbol. *Anim Nutr.* (2015) 1:244–51. doi: 10.1016/j.aninu.2015.08.006

152. Hess JR, Greenberg NA. The role of nucleotides in the immune and gastrointestinal systems: potential clinical applications. *Nutr Clin Pract.* (2012) 27:281–94. doi: 10.1177/0884533611434933

153. Hester SN. *Impact of Formula Additives on Immune and Gastrointestinal Development in the Piglet*. Chicago, IL: Natritional Sciences in the Graduate College, University of Illinois at Urbana-Champaign (2012).

154. Gil A. Modulation of the immune response mediated by dietary nucleotides. *Eur J Clin Nutr.* (2002) 56:S1–4. doi: 10.1038/sj.ejcn.1601475

155. Xu M, Zhao M, Yang R. Effect of dietary nucleotides on immune function in Balb/C mice. *Int Immunopharmacol.* (2013) 17:50–6. doi: 10.1016/j.intimp.2013.04.032

156. Edwards NL, Fox IH. Disorders associated with purine and pyrimidine metabolism. *Spec Top Endocrinol Metab.* (1984) 6:95–140.

157. Krenitsky TA, Koszalka GW, Tuttle JV. Purine nucleoside synthesis, an efficient method employing nucleoside phosphorylases. *Biochemistry.* (1981) 20:3615–21. doi: 10.1021/bi00515a048

158. Ogawa J, Takeda S, Xie SX. Purification, characterization, and gene cloning of purine nucleosidase from *Ochrobactrum anthropi*. *Appl Environ Microbiol.* (2001) 67:1783–7. doi: 10.1128/AEM.67.4.1783-1787.2001

159. Horinouchi N, Ogawa J, Sakai T, Kawano T, Matsumoto S, Sasaki M, et al. Construction of deoxyriboaldolase-overexpressing *Escherichia coli* and its application to 2-deoxyribose 5-phosphate synthesis from glucose and acetaldehyde for 2'-deoxyribonucleoside production. *Appl Environ Microbiol.* (2003) 69:3791–7. doi: 10.1128/AEM.69.7.3791-3797.2003

160. Doo EH, Chassard C, Schwab C. Effect of dietary nucleosides and yeast extracts on composition and metabolic activity of infant gut microbiota in PolyFermS colonic fermentation models. *Fems Microbiol Ecol.* (2017) 93:88. doi: 10.1093/femsec/fix088

161. Doo EH, Schwab C, Chassard C. Cumulative effect of yeast extract and fructooligosaccharide supplementation on composition and metabolic activity of elderly colonic microbiota in vitro. *J Funct Foods.* (2019) 52:43–53. doi: 10.1016/j.jff.2018.10.020

162. Cryan JF, Dinan TG. Mind-altering microorganisms: the impact of the gut microbiota on brain and behaviour. *Nat Rev Neurosci.* (2012) 13:701–12. doi: 10.1038/nrn3346

163. Mayer EA, Knight R, Mazmanian SK. Gut microbes and the brain: paradigm shift in neuroscience. *J Neurosci.* (2014) 34:15490–6. doi: 10.1523/JNEUROSCI.3299-14.2014

164. Sampson TR, Mazmanian SK. Control of brain development, function, and behavior by the microbiome. *Cell Host Microbe.* (2015) 17:565–76. doi: 10.1016/j.chom.2015.04.011

165. Arnoriaga-Rodriguez M, Mayneris-Perxachs J, Burokas A, Contreras-Rodríguez O, Blasco G, Coll C, et al. Obesity impairs short-term and working memory through gut microbial metabolism of aromatic amino acids. *Cell Metab.* (2020) 32:548–560e7. doi: 10.1016/j.cmet.2020.09.002

166. Mayer EA, Aziz Q, Coen S, Labus JS, Lane R, Kuo B, et al. Brain imaging approaches to the study of functional GI disorders: a rome working team report. *Neurogastroent Motil.* (2009) 21:579–96. doi: 10.1111/j.1365-2982.2009.01304.x

167. Schellekens H, Finger BC, Dinan TG, Cryan JF. Ghrelin signalling and obesity: at the interface of stress, mood and food reward. *Pharmacol Therapeut.* (2012) 135:316–26. doi: 10.1016/j.pharmthera.2012.06.004

168. Arentsen T, Raith H, Qian Y, Forssberg H, Diaz Heijtz R. Host microbiota modulates development of social preference in mice. *Microb Ecol Health Dis.* (2015) 26:29719. doi: 10.3402/mehd.v26.29719

169. Desbonnet L, Clarke G, Shanahan F, Dinan TG, Cryan JF. Microbiota is essential for social development in the mouse. *Mol Psychiatr.* (2014) 19:146–8. doi: 10.1038/mp.2013.65

170. O'Hara AM, Shanahan F. The gut flora as a forgotten organ. *Embo Rep.* (2006) 7:688–93. doi: 10.1038/sj.embor.7400731

171. El Aidy S, van Baarlen P, Derrien M, Lindenbergh-Kortleve DJ, Hooiveld G, Levenez F, et al. Temporal and spatial interplay of microbiota and intestinal mucosa drive establishment of immune homeostasis in conventionalized mice. *Mucosal Immunol.* (2012) 5:567–79. doi: 10.1038/mi.2012.32

172. Lee K, Jayaraman A. Interactions between gut microbiota and non-alcoholic liver disease: the role of microbiota-derived metabolites. *Pharmacol Res.* (2019) 142:314–314. doi: 10.1016/j.phrs.2019.02.013

173. Ringseis R, Gessner DK, Eder K. The gut-liver axis in the control of energy metabolism and food intake in animals. *Ann Rev Anim Biosci.* (2020) 8:295–319. doi: 10.1146/annurev-animal-021419-083852

174. Krishnan S, Ding Y, Saedi N, Choi M, Sridharan GV, Sherr DH. Gut microbiota-derived tryptophan metabolites modulate inflammatory response in hepatocytes and macrophages. *Cell Rep.* (2018) 23:1099–111. doi: 10.1016/j.celrep.2018.03.109

175. Fan Y, Pedersen O. Gut microbiota in human metabolic health and disease. *Nat Rev Microbiol.* (2021) 19:55–71. doi: 10.1038/s41579-020-0433-9

176. Garrett WS. Cancer and the microbiota. *Science.* (2015) 348:80–6. doi: 10.1126/science.aaa4972

177. Schwabe RF, Jobin C. The microbiome and cancer. *Nat Rev Cancer.* (2013) 13:800–12. doi: 10.1126/science.abc4552

178. Wang X, Liu HL, Li YF, Huang S, Zhang L, Cao C, et al. Altered gut bacterial and metabolic signatures and their interaction in gestational diabetes mellitus. *Gut Microbes.* (2020) 12:1–13. doi: 10.1080/19490976.2020.1840765

179. Ley RE, Turnbaugh PJ, Klein S, Gordon JI. Microbial ecology: human gut microbes associated with obesity. *Nature.* (2006) 444:1022–3. doi: 10.1038/4441022a

180. Org E, Parks BW, Joo JWJ, Emert B, Schwartzman W, Kang EY, et al. Genetic and environmental control of host-gut microbiota interactions. *Genome Res.* (2015) 25:1558–69. doi: 10.1101/gr.194118.115

181. Kummen M, Thingholm LB, Ruhlemann MC. Altered gut microbial metabolism of essential nutrients in primary sclerosing cholangitis. *Gastroenterology.* (2021) 160:1784–98. doi: 10.1053/j.gastro.2020.12.058

182. Wilmanski T, Diener C, Rappaport N. Gut microbiome pattern reflects healthy ageing and predicts survival in humans (vol 3, pg 274, 2021). *Nat Metab.* (2021) 3:586–586. doi: 10.1038/s42255-021-00377-9

183. de Groot P, Scheithauer T, Bakker GJ. Donor metabolic characteristics drive effects of faecal microbiota transplantation on recipient insulin sensitivity, energy expenditure and intestinal transit time. *Gut.* (2020) 69:502–12. doi: 10.1136/gutjnl-2019-318320

184. Kootte RS, Levin E, Salojarvi J, Smits LP, Hartstra AV, Udayappan SD, et al. Improvement of insulin sensitivity after lean donor feces in metabolic syndrome is driven by baseline intestinal microbiota composition. *Cell Metab.* (2017) 26:611–619e6. doi: 10.1016/j.cmet.2017.09.008

185. Yu EW, Gao L, Stastka P, Cheney MC, Mahabamunuge J, Torres Soto M, et al. Fecal microbiota transplantation for the improvement of metabolism in obesity: the FMT-TRIM double-blind placebo-controlled pilot trial. *PLoS Med.* (2020) 17:e1003051. doi: 10.1371/journal.pmed.1003051

186. Wu CF, Lyu WT, Hong QH. Gut microbiota influence lipid metabolism of skeletal muscle in pigs. *Front Nutr.* (2021) 8:675445. doi: 10.3389/fnut.2021.675445

187. Zhao F, An R, Wang LQ, Shan J, Wang X. Specific gut microbiome and serum metabolome changes in lung cancer patients. *Front Cell Infect Mi.* (2021) 11:725284. doi: 10.3389/fcimb.2021.725284

188. Yachida S, Mizutani S, Shiroma H. Metagenomic and metabolomic analyses reveal distinct stage-specific phenotypes of the gut microbiota in colorectal cancer. *Nat Med.* (2019) 25:968–76. doi: 10.1038/s41591-019-0458-7

189. Pearson RG, Raxworthy CJ, Nakamura M, Peterson AT. ORIGINAL ARTICLE: predicting species distributions from small numbers of occurrence records: a test case using cryptic geckos in madagascar. *J Biogeogr.* (2007) 34:102–17. doi: 10.1111/j.1365-2699.2006.01594.x

190. Ling CW, Miao ZL, Xiao ML, Zhou H, Jiang Z, Fu Y, et al. The association of gut microbiota with osteoporosis is mediated by amino acid metabolism: multiomics in a large cohort. *J Clin Endocr Metab.* (2021) 106:e3852–64. doi: 10.1210/clinem/dgab492

191. Duttaroy AK. Role of gut microbiota and their metabolites on atherosclerosis, hypertension and human blood platelet function: a review. *Nutrients.* (2021) 13:144. doi: 10.3390/nu13010144

192. Christ B, Bruckner S, Winkler S. The therapeutic promise of mesenchymal stem cells for liver restoration. *Trends Mol Med.* (2015) 21:673–86. doi: 10.1016/j.molmed.2015.09.004

193. Backhed F, Manchester JK, Semenkovich CF. Mechanisms underlying the resistance to diet-induced obesity in germ-free mice. *Proc Natl Acad Sci USA.* (2007) 104:979–84. doi: 10.1073/pnas.0605374104

194. Mazloom Z, Yousefinejad A, Dabbaghmanesh MH. Effect of probiotics on lipid profile, glycemic control, insulin action, oxidative stress, and inflammatory markers in patients with type 2 diabetes: a clinical trial. *Iran J Med Sci.* (2013) 38:38–43.

195. Lin R, Liu WT, Piao MY, Zhu H. A review of the relationship between the gut microbiota and amino acid metabolism. *Amino Acids.* (2017) 49:2083–90. doi: 10.1007/s00726-017-2493-3

196. Agus A, Clement K, Sokol H. Gut microbiota-derived metabolites as central regulators in metabolic disorders. *Gut.* (2021) 70:1174–82. doi: 10.1136/gutjnl-2020-323071

197. Liu RX, Hong J, Xu XQ, Feng Q, Zhang D, Gu Y, et al. Gut microbiome and serum metabolome alterations in obesity and after weight-loss intervention. *Nat Med.* (2017) 23:859. doi: 10.1038/nm.4358

198. Kato T, Yamazaki K, Nakajima M. Oral administration of *Porphyromonas gingivalis* alters the gut microbiome and serum metabolome. *Msphere.* (2018) 3:e460–418. doi: 10.1128/mSphere.00460-18

199. Muniz Pedrogo DA, Jensen MD, Van Dyke CT. Gut microbial carbohydrate metabolism hinders weight loss in overweight adults undergoing lifestyle intervention with a volumetric diet. *Mayo Clin Proc.* (2018) 93:1104–10. doi: 10.1016/j.mayocp.2018.02.019

200. Zivkovic AM, German JB, Lebrilla CB, Zhang Y, Zhong H, Liu R, et al. Human milk glycobiome and its impact on the infant gastrointestinal microbiota. *Proc Natl Acad Sci USA.* (2011) 108:4653–8. doi: 10.1073/pnas.1000083107

201. Milani C, Duranti S, Bottacini F, Casey E, Turroni F, Mahony J, et al. The first microbial colonizers of the human gut: composition, activities, and health implications of the infant gut microbiota. *Microbiol Mol Biol.* (2017) 81:17. doi: 10.1128/MMBR.00036-17

202. Fallani M, Amarri S, Uusijarvi A, Adam R, Khanna S, Aguilera M, et al. Determinants of the human infant intestinal microbiota after the introduction of first complementary foods in infant samples from five European centres. *Microbiol Sgm.* (2011) 157:1385–92. doi: 10.1099/mic.0.042143-0

203. Koenig JE, Spor A, Scalfone N, Fricker AD. Succession of microbial consortia in the developing infant gut microbiome. *Proc Natl Acad Sci USA.* (2011) 108:4578–85. doi: 10.1073/pnas.1000081107

204. Tanes C, Bittinger K, Gao Y, Friedman ES, Nessel L, Paladhi UR, et al. Role of dietary fiber in the recovery of the human gut microbiome and its metabolome. *Cell Host Microbe.* (2021) 2:394–407.e5. doi: 10.1016/j.chom.2020.12.012

205. Ley RE, Backhed F, Turnbaugh P, Lozupone CA, Knight RD, Gordon JI, et al. Obesity alters gut microbial ecology. *Proc Natl Acad Sci USA.* (2005) 102:11070–5. doi: 10.1073/pnas.0504978102

206. Armet AM, Deehan EC, O'Sullivan AF, Mota JF, Field CJ, Prado CM, et al. Rethinking healthy eating in light of the gut microbiome. *Cell Host Microbe.* (2022) 30:764–85. doi: 10.1016/j.chom.2022.04.016

207. Assfalg M, Bertini I, Colangiuli D, Luchinat C, Schäfer H, Schütz B. Evidence of different metabolic phenotypes in humans. *Proc Natl Acad Sci USA.* (2008) 105:1420–4. doi: 10.1073/pnas.0705685105

208. Blekhman R, Goodrich JK, Huang K, Sun Q, Bukowski R, Bell JT, et al. Host genetic variation impacts microbiome composition across human body sites. *Genome Biol.* (2015) 16:191. doi: 10.1186/s13059-015-0759-1

209. Graf D, Di Cagno R, Fak F, Flint HJ, Nyman M, Saarela M, et al. Contribution of diet to the composition of the human gut microbiota. *Microb Ecol Health Dis.* (2015) 26:26164. doi: 10.3402/mehd.v26.26164

210. Yatsunenko T, Rey FE, Manary MJ, Trehan I, Dominguez-Bello MG, Contreras M, et al. Human gut microbiome viewed across age and geography. *Nature.* (2012) 486:222–7. doi: 10.1038/nature11053

211. Odamaki T, Kato K, Sugahara H, Hashikura N, Takahashi S, Xiao JZ, et al. Age-related changes in gut microbiota composition from newborn to centenarian: a cross-sectional study. *BMC Microbiol.* (2016) 16:90. doi: 10.1186/s12866-016-0708-5

212. Nagpal R, Tsuji H, Takahashi T. Ontogenesis of the gut microbiota composition in healthy, full-term, vaginally born and breast-fed infants over the first 3 years of life: a quantitative bird's-eye view. *Front Microbiol.* (2017) 8:1388. doi: 10.3389/fmicb.2017.01388

213. Fiebiger U, Bereswill S, Heimesaat MM. Dissecting the interplay between intestinal microbiota and host immunity in health and disease: lessons learned from germfree and gnotobiotic animal models. *Eur J Microbiol Immunol.* (2016) 6:253–71. doi: 10.1556/1886.2016.00036

214. Riddle MS, Connor BA. The traveling microbiome. *Curr Infect Dis Rep.* (2016) 18:29. doi: 10.1007/s11908-016-0536-7

215. Cho I, Yamanishi S, Cox L. Antibiotics in early life alter the murine colonic microbiome and adiposity. *Nature.* (2012) 488:621–6. doi: 10.1038/nature11400

216. Hasan N, Yang HY. Factors affecting the composition of the gut microbiota, and its modulation. *Peerj.* (2019) 7:e7502. doi: 10.7717/peerj.7502

frontiers | Frontiers in Nutrition

TYPE Original Research
PUBLISHED 07 November 2022
DOI 10.3389/fnut.2022.1021215

OPEN ACCESS

EDITED BY
Jie Yin,
Hunan Agricultural University, China

REVIEWED BY
Gloria Solano-Aguilar,
Agricultural Research Service (USDA), United States
Zhi Peng Li,
Institute of Special Animal and Plant Sciences (CAAS), China
Ruiyang Zhang,
Shenyang Agricultural University, China

*CORRESPONDENCE
Daiwen Chen
dwchen@sicau.edu.cn
Yuheng Luo
luoluo212@126.com

SPECIALTY SECTION
This article was submitted to Nutrition and Microbes, a section of the journal Frontiers in Nutrition

RECEIVED 17 August 2022
ACCEPTED 11 October 2022
PUBLISHED 07 November 2022

CITATION
Li J, Chen D, Yu B, He J, Huang Z, Zheng P, Mao X, Li H, Yu J, Luo J, Yan H and Luo Y (2022) Batch and sampling time exert a larger influence on the fungal community than gastrointestinal location in model animals: A meaningful case study.
Front. Nutr. 9:1021215.
doi: 10.3389/fnut.2022.1021215

Batch and sampling time exert a larger influence on the fungal community than gastrointestinal location in model animals: A meaningful case study

Jiayan Li, Daiwen Chen*, Bing Yu, Jun He, Zhiqing Huang, Ping Zheng, Xiangbing Mao, Hua Li, Jie Yu, Junqiu Luo, Hui Yan and Yuheng Luo*

Key Laboratory for Animal Disease-Resistance Nutrition of Ministry of Education of China, Key Laboratory for Animal Disease-Resistance Nutrition and Feed of Ministry of Agriculture of China, Key Laboratory of Animal Disease-Resistant Nutrition of Sichuan Province, Animal Nutrition Institute, Sichuan Agricultural University, Chengdu, China

Fungi play a fundamental role in the intestinal ecosystem and health, but our knowledge of fungal composition and distribution in the whole gastrointestinal tract (GIT) is very limited. The physiological similarity between humans and pigs in terms of digestive and associated metabolic processes places, the pig in a superior position over other non-primate models. Here, we aimed to characterize the diversity and composition of fungi in the GIT of pigs. Using high-throughput sequencing, we evaluated the fungal community in different locations of GIT of 11 pigs with 128.41 ± 1.25 kg body weight acquired successively. Among them, five pigs are sacrificed in April 2019 (Batch 1) and the other six are sacrificed in January 2020 (Batch 2). All subjects with similar genetic backgrounds, housing, management, and diet. Finally, no significant difference is found in the α-diversity (Richness) of the fungal community among all intestinal segments. Basidiomycota and Ascomycota are the two predominant fungal phyla, but Batch 1 harbored a notably high abundance of Basidiomycota and Batch 2 harbored a high abundance of Ascomycota. Moreover, the two batches harbored completely different fungal compositions and core fungal genera. FUNGuild (Fungal Functional Guild) analysis revealed that most of the fungal species present in the GIT are saprotroph, plant pathogen, and animal endosymbiont. Our study is the first to report that even under the same condition, large variations in fungal composition in the host GIT still occur from batch-to-batch and sampling time. The implications of our observations serve as references to the development of better models of the human gut.

KEYWORDS

model animal, gastrointestinal tract, fungi, different batch, sampling time

Introduction

The gastrointestinal tract (GIT) is the home of gut microbiota, with trillions of colonizing and transient microorganisms, including bacteria, archaea, fungi, viruses, and protozoa (1). Accumulating evidence indicates that microbiota plays a critical role in many physiological processes of the host, such as digestion, metabolism, immune development, and resistance to pathogens (2–5). To date, many studies have focused on the bacterial community and function in GIT, while fungi received much less attention. The fungi referred to as the "mycobiota" comprise 1–2% of the microbial biomass in the gut ecosystem of humans and monogastric animals (6). Our understanding of fungi has changed over the last decade with the advances in sequencing technologies and the deciphering of the microbiome. More and more studies have demonstrated the importance of fungi to intestinal nutrition and immune function (1, 7–9). It is noteworthy that the size of a typical fungal cell is much larger than a typical bacterial cell, suggesting that fungi may contribute to intestinal microbial metabolism and provide a substantial mass of surface area for host-microbe interactions (10).

To explore the fungal community in the GIT, increased studies have been conducted in humans and mice. Despite the large individual variations, most of the intestinal fungi are considered to belong to the phyla Ascomycota and Basidiomycota, with *Candida, Saccharomyces, and Cladosporium* spp. as the three most abundant genera in the gut of humans and mice (10–12). A Pig is regarded as an ideal animal model to study the composition and function of the microbiome in GIT due to its anatomy and physiology being highly similar to humans (13). The pig has already been used in many studies as an animal model for humans to assess the gut microbiota, due to similarities in GIT functions and anatomical structure, metabolism, and nutritional requirements, but also due to similar major bacteria phyla occurring in the GIT of pigs (Firmicutes and Bacteroidetes) (14). However, with considerable large individual variations in fungal composition, experiments are needed to assess whether pigs can serve as a good model of human gut fungi. The critical role of gut bacteria in the metabolism and health of animals is gradually revealed, but the role of gut fungi remains to be assessed. A typical role of gut fungi may be the degradation of plant cell walls, which has been shown in many studies on ruminants (15, 16). As carbohydrates are the main source of energy for humans and animals, future studies are vital to understanding the role of commensal fungi and the utilization of dietary nutrients.

In this study, we investigated the fungal community along different locations of the GIT (from the stomach to the colon) in growing-finishing pigs with similar genetic backgrounds. These pigs are fed with a basal corn-soybean diet and selected from two successive batches under the same feeding condition. A high-throughput sequencing targeting the internal transcribed spacer 1 (ITS1) and FUNGuild is used to reveal the fungal composition and potential function in the GIT. The implications of our observation are scrutinizing the efficient use of pigs in research directed to serve human needs.

Materials and methods

All experimental procedures and animal care were performed following the Guide for the Care and Use of Laboratory Animals prepared by the Institutional Animal Care and Use Committee of Sichuan Agricultural University, and all animal protocols were approved by the Animal Care and Use Committee of Sichuan Agricultural University under permit number DKY- B20172008.

Animal feeding management and sample collection

A total of 11 cross-bred (Duroc × Landrace × Yorkshire) growing-finishing male pigs with similar genetic backgrounds and average body weight (128.41 ± 1.25 kg) were selected. These pigs were from the same commercial supplier and successively allocated to one pen with a concrete floor in the same mechanically ventilated room in the experimental farm of the Sichuan Agricultural University for more than three months [Batch 1 (no. 1–5), Batch 2 (no.6–11)]. A basal corn-soybean diet was used and met the nutrient requirement of the National Research Council (17) for 100–135 kg pigs, and the levels of main nutrients in the diet (**Supplementary Table 1**) were analyzed using the standard method recommended by the Association of Official Analytical Chemists (18). The diet was antibiotics and growth promotors free, and no fungal growth promoters or additives were supplemented. All pigs were given *ad libitum* access to fresh water and feed, the room temperature was maintained at 25–28°C and relative humidity was controlled at 55–65%.

Sampling was performed in April 2019 (Batch 1) and January 2020 (Batch 2). The pigs were humanely euthanized by being electrically stunned. The whole GIT was removed from the abdominal cavity and immediately dissected. Approximately 2 g of digesta from each of six GIT regions, the middle stomach, duodenum, jejunum, ileum, cecum, and colon, of each pig was collected into a 2-mL sterilized tube. All pigs were fasted overnight before the sampling day to ensure the homogeneity of all samples, which resulted in the failure to collect a few samples, and the sample information can be found in **Supplementary Table 2**. The collected samples were flash-frozen in liquid nitrogen and stored at −80°C until further processing. Samples were categorized by the GIT region: duodenum, jejunum, and ileum samples were categorized as "Upper GIT," cecum

and colon were categorized as "Lower GIT," and the stomach remained categorized as "Stomach".

DNA extraction and sequencing

All samples were thawed on ice. Approximately 0.2 g of each digesta sample was added to bead-beating tubes with TE buffer, and a lysis buffer was then added for homogenization. The treated sample was then subjected to bead beating at 6.0 m/s for 40 s twice using a FastPrep-24 (MP Biomedicals, Solon, OH, USA). The genomic DNA of each sample was extracted using a QIAamp Fast DNA Stool Mini Kit (Qiagen, Hilden, Germany). DNA concentration and quality were further assessed using a NanoDrop 2000 Spectrophotometer (NanoDrop Technologies, Wilmington, DE). The ITS1 region was sequenced with specific primers (ITS1f, CTTGGTCATTTAG AGGAAGTAA; ITS2r, GCTGCGTTCTTCATCGATGC) (19–21). PCR for each sample was carried out in a 30-μL reaction with 15 μL of Phusion® High-Fidelity PCR Master Mix (New England Biolabs, Massachusetts, United States), 3 μL of forward and reverse primers, and 10 μL of template DNA, as well as 2 μL of H_2O. The thermal cycling was initiated with a denaturation step at 98°C for 1 min, followed by a sequence of 30 cycles of denaturation at 98°C for 10 s, annealing at 50°C for 30 s, elongation at 72°C for 30 s, and finalized with an elongation at 72°C for 5 min. Three parallel PCR reactions were conducted for each sample, and the PCR products were detected with electrophoresis using 2% agarose gel. PCR products for each sample were mixed in equal density ratios and the mixture was then purified with a GeneJET™ Gel Extraction Kit (Thermo Scientific, United States). Sequencing libraries were generated using an Ion Plus Fragment Library Kit 48 rxns (Thermo Scientific) following the manufacturer's recommendations. The library quality was assessed on the Qubit® 2.0 Fluorometer (Thermo Scientific). Finally, the library was sequenced on an Ion S5™ XL platform and 400 bp single-end reads were generated. To minimize the other effects (i.e., DNA extraction kits or equipment), the genomic DNA from all samples was extracted with the same batch of kits and then amplified together on an Ion S5™ XL platform.

Bioinformatics analysis

QIIME2 (2022.2[1]) (22) was used to process and classify raw sequences. Raw reads were denoised with the DADA2 plugin in QIIME2 (23). This plugin produces fine-scale resolution through amplicon sequence variants (ASVs), and its workflow consists of filtering (e.g., primer trimming only for metabarcoding), dereplication, and reference-free chimera detection. In brief, single-end reads were assigned to samples based on their unique barcode and truncated by cutting off the barcode and primer sequences. The truncation was performed based on a quality score of 20 and with a maximum number of expected errors (maxEE) set to 2. We did not truncate the sequences to a fixed length due to the variable length of fungal ITS fragments. The sequences were clustered into ASVs and then filtered for chimeras. The UNITE database (Version 8.3[2]) was trained using the naive Bayesian classifier in QIIME2, and then the taxonomy was assigned to filtered ASVs using a pretrained UNITE database with 99% identity for fungi. The identified taxonomies were then assigned to representative sequences. Finally, the 58 digesta samples yielded a total of 2,277,899 non-chimeric sequence reads. Separate rarefaction curves for digesta samples were produced and visualized using the vegan package in R software (v 4.1.2) to determine minimum sequencing depth, and we rarefied our data to 10,000 reads per sample for downstream analysis (**Supplementary Table 3**).

The α-diversity of each sample was reflected by 4 indices (Richness, Chao1, Shannon, and Good's coverage), which were calculated in QIIME2 and visualized by R (V 4.1.2). R was used to analyze the β-diversity of each sample based on multivariate statistical techniques, including principal coordinate analysis (PCoA) and non-metric multidimensional scaling (NMDS) of Bray-Curtis and unweighted UniFrac distance matrixes. Wilcoxon rank test, adonis permutational multivariate analysis of variance (also called PERMANOVA), and ANOSIM (analysis of similarities) tests were performed with R package vegan. The linear discriminant analysis effect size (LEfSe) analysis was performed using the Galaxy web application.[3] To test the core fungal community in all samples, the compute_core_microbiome.py command in QIIME was used, and the core ASVs were required to be present in at least 80% of the samples based on the data set.

The FUNGuild analysis

The ASVs' taxonomic information was uploaded to the FUNGuild database for functional prediction (trophic modes and guilds) (24), and the sequences were aligned using the PhyDE (Phylogenetic Data Editor). Since the calling of guilds in the FUNGuild is predicated on the confidence of assigned taxonomy, a 93% threshold was chosen to represent a reasonable general cutoff point for ITS-based inputs in this study. For this procedure, we considered all assignments with a confidence score of "probable" or "highly probable." Genera not represented in the database or with a confidence score of "possible" were classified as undetermined.

1 http://qiime.org/

2 https://doi.org/10.15156/BIO/1264708

3 https://huttenhower.sph.harvard.edu/galaxy/

Statistical analysis

Data were analyzed using R (V 4.1.2) and SPSS 23.0 statistical software (SPSS Inc., Chicago, IL, USA). α-diversity and β-diversity data were performed and visualized entirely in R using the ggplot2 package with custom R scripts. The relative abundance of fungal taxa was assessed using the Kruskal-Wallis test, and Dunn's test was applied to conduct multiple comparisons. The linear mixed effect model (R package nlme) was used to analyze the differences in the α-diversity of the fungal community among sampling time, the GIT region, and body weight. Interactions were removed from the model if they were not significant ($p > 0.05$). Differences were considered significant when $p < 0.05$, while the differences were defined as insignificant when $p \geq 0.05$. A significant trend was defined when $0.05 < p < 0.1$.

Results

The diversity of the fungal community in the gastrointestinal tract

There were 39,274 high-quality sequences in each sample on average, and the rarefaction curves showed that a minimum sampling depth of 10,000 sequences was sufficient to capture fungal diversity (Supplementary Figure 1). Indices for Richness, Shannon, Chao 1, and Good's coverage were calculated to measure the α-diversity. The Good's coverage estimates averaged 0.99, indicating a sufficient and representative sequencing depth (Supplementary Table 4). In Batch 1, the Shannon index of the fungal community in the samples from the duodenum was higher than that from other locations ($p < 0.05$, Figure 1B), while no difference in the Richness was found among the samples from different regions (Figure 1A). Meanwhile, the α-diversity of the fungal community showed no difference among diverse gastrointestinal segments in Batch 2 (Figures 1C,D). Based on the mixed model analysis, the Richness and Chao1 indices were significantly affected by sampling time ($p < 0.01$, Table 1), while the GIT region and body weight showed no significant effect on all α-diversity indices. Furthermore, an interaction between the GIT region and sampling time was detected for the Richness and Chao1 indices ($p < 0.05$).

The PCoA plot based on the Bray-Curtis (PERMANOVA: $F = 8.821$, $p = 0.001$, Figure 2A) and unweighted UniFrac (PERMANOVA: $F = 6.456$, $p = 0.001$, Supplementary Figure 2) distance matrices showed that samples from the two batches were clearly divided into two different clusters. To overcome the shortcomings of linear models (PCoA) and better reflect the

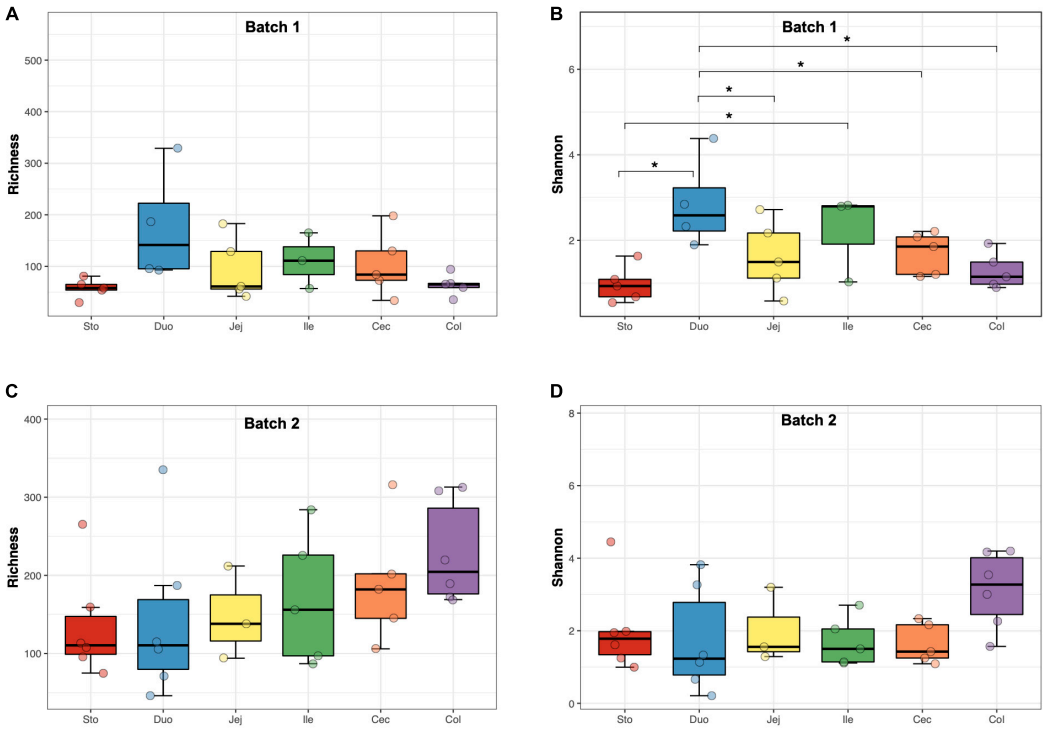

FIGURE 1
The α-diversity of the fungal community in different regions of the gastrointestinal tract in the pigs. **(A)** Richness (batch 1). **(B)** Shannon index (batch 1). **(C)** Richness (batch 2). **(D)** Shannon index (batch 2). Significance is indicated by "*" when $p < 0.05$.

10.3389/fnut.2022.1021215

TABLE 1 Linear mixed effect model analysis of fungal α -diversity.

Item	Sampling time		Region					P-value			
	Batch 1 (2019.4)	Batch 2 (2020.1)	Stomach	Duodenum	Jejunum	Ileum	Cecum	Colon	p_{Time}	p_{Region}	p_{Weight}	$p_{Time*region}$
Richness	98 ± 13[a]	171 ± 15[b]	100 ± 20	157 ± 32	114 ± 2	148 ± 27	147 ± 26	154 ± 30	0.004	0.14	0.59	0.05
shannon	1.70 ± 0.17	2.07 ± 0.20	1.56 ± 0.32	2.19 ± 0.44	1.77 ± 0.31	1.89 ± 0.28	1.68 ± 0.16	2.29 ± 0.38	0.20	0.35	0.69	0.25
Chao1	100.37 ± 12.90[a]	198.68 ± 16.54[b]	110.89 ± 22.32	174.36 ± 33.18	120.26 ± 24.17	164.50 ± 28.54	168.54 ± 31.73	176.56 ± 336.38	0.001	0.08	0.75	0.04

Data are presented as means ± standard error (SEM). Different alphabetical (a, b) superscripts mean significant difference ($p < 0.05$).

non-linear structure, we evaluated the accuracy of the model with NMDS stress values. We confirmed that the stress values of the Bray index were less than 0.2 (Figure 2B), which ensured the reliability of the model. The significance was shown by the Wilcoxon rank sum test further emphasized the difference in the fungal community between the two batches ($p < 0.001$, Figure 2C). The ANOSIM test confirmed that the distance between batches was greater than the distance within batches ($R = 0.419$, $p < 0.05$, Figure 2D). In detail, samples from the stomach and duodenum were clustered to distinguish them from those samples from other intestinal segments in Batch 1 (PERMANOVA: $F = 3.917$, $p = 0.001$, Supplementary Figure 3). However, samples from different intestinal segments showed a high degree of overlap in Batch 2 (PERMANOVA: $F = 1.331$, $p = 0.113$, Supplementary Figure 3).

The community and composition of fungi in the gastrointestinal tract

The predominant taxonomic composition of fungi across the GIT was investigated at the phyla and genera levels. According to the ASVs annotations, a total of 11 known fungal phyla (Ascomycota, Basidiomycota, Mucoromycota, Mortierellomycota, Rozellomycota, Olpidiomycota, Glomeromycota, Aphelidiomycota, Chytridiomycota, Zoopagomycota, and Kickxellomycota) were identified in all samples (Supplementary Figure 4 and Supplementary Tables 5, 6). Ascomycota and Basidiomycota were identified as the two predominant fungal phyla in the GIT, and the most abundant phylum identified in Batch 1 was Basidiomycota, but Ascomycota was the most predominant phylum in Batch 2. The abundance of phyla Ascomycota, Basidiomycota, and Mortierellomycota was different among gastrointestinal locations in Batch 1 ($p < 0.05$), and the abundance of Mucoromycota and Rozellomycota was different between the upper GIT and lower GIT in Batch 2 ($p < 0.05$). Interestingly, we found that the abundance of Basidiomycota and Mucoromycota increased gradually from the stomach and upper GIT to the lower GIT in batches 1 and 2, respectively ($p < 0.05$, Supplementary Figures 4A,B).

At the genus level, all sequences obtained from batches 1 and 2 were affiliated with 230 and 358 known fungal genera, respectively. The fungal composition of samples from all GIT locations in these pigs differs between batches. For example, in Batch 1, *Naganishia, Rhodotorula, Fusarium, Mortierella,* and *Candida* were identified as the top 5 genera across all gastrointestinal segments (Figure 3A, Supplementary Figure 4C, and Supplementary Table 5). Of these genera, the relative abundance of *Naganishia, Rhodotorula, Mortierella,* and *Candida* was different among locations ($p < 0.05$), with an increasing tendency of *Naganishia* and *Rhodotorula* from the stomach and upper GIT to the lower GIT (Figure 3C). Yet, the

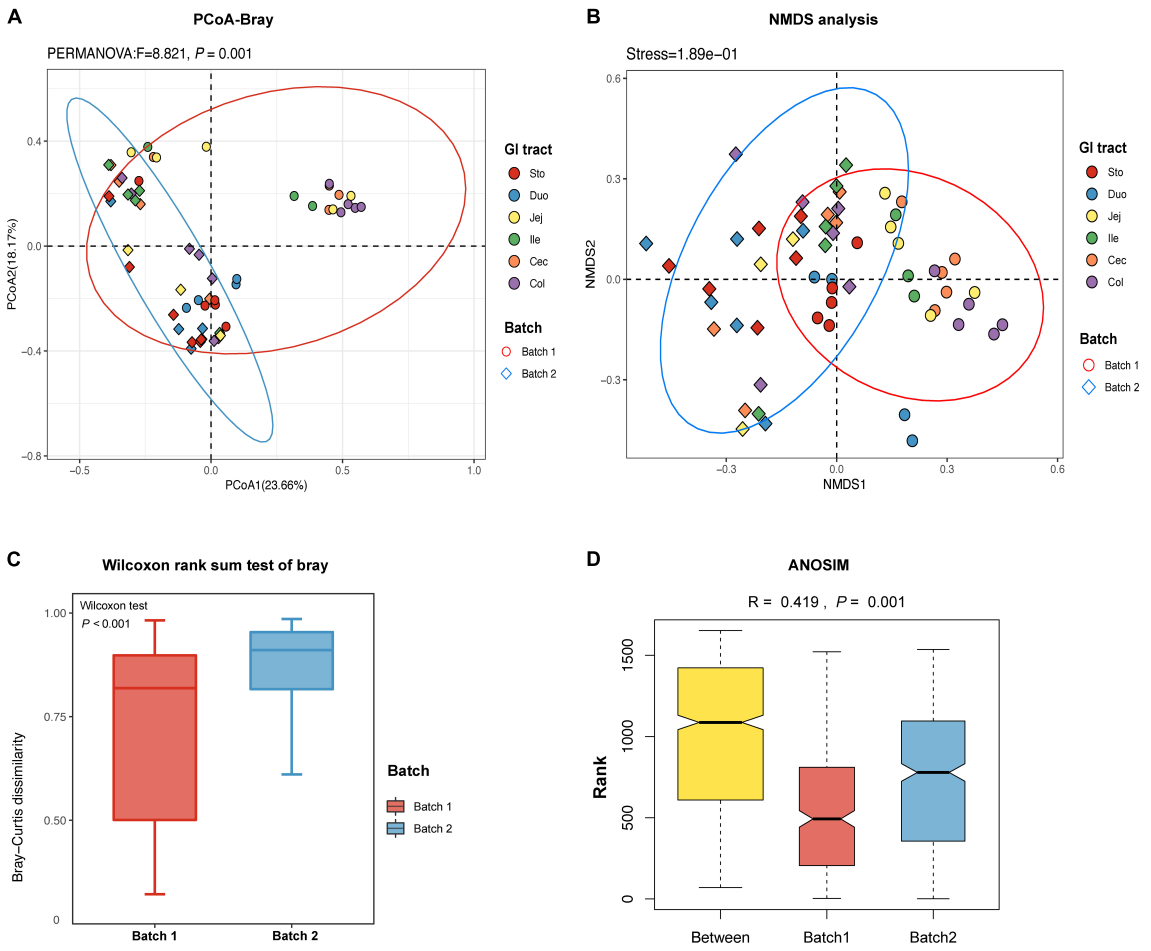

FIGURE 2
The β-diversity of fungal community in different regions of the gastrointestinal tract in the pigs. **(A)** Principal coordinate analysis (PCoA) of Bray-Curtis distances showed the stratification of batch 1 from batch 2 samples by their fungal compositional profiles. **(B)** Non-metric multidimensional scaling (NMDS) analysis showed that fungal profiles formed two clusters. A stress value less than 0.2 indicates that the model grouping is reliable. **(C)** Based on the ASVs feature table and Bray-Curtis distances, the Wilcoxon rank sum test is used to identify the significant difference and the degree of difference in fungal microbiome structure within the groups is compared. **(D)** Based on the distance index ranking, ANOSIM (analysis of similarities) confirmed that the distance between groups is significantly greater than the distance within groups, indicating that the fungal structure of the two batches is significantly different ($R > 0$, $p < 0.05$). Each point represents one sample and colors indicate different GIT regions. Sto: Stomach, Duo: Duodenum, Jej: Jejunum, Ile: Ileum, Cec: Cecum, Col: Colon.

dominant fungal genera in the gut of pigs from Batch 2 were *Kazachstania, Mucor, Trichosporon, Nothophoma,* and *Fusarium* (Figure 3B, Supplementary Figure 4D, and Supplementary Table 6), with a difference in the relative abundance of *Mucor* among intestinal segments (Figure 3C, $p < 0.05$), which showed an increasing tendency from the stomach and upper GIT to the lower GIT.

Using LefSe analysis, we compared the specific fungal taxa in the six different gastrointestinal locations. The results revealed 13 and 4 specific fungal taxa (at genus, family, and order levels) with a significant difference among segments in pigs from Batches 1 and 2, respectively (LDA score > 2.0, $p < 0.05$). Detailly, 5 (*Alternaria, Chaetomiaceae, Agaricales, Thelebolales,* and *Mortierella*), 6 (*Saccharomycetales, Meyerozyma, Cryptococcus, Tremellales, Candida,* and *Mucor*), and 2 (*Naganishia* and *Rhodotorula*) taxa were enriched in the duodenum, ileum, and colon of pigs from Batch 1 (Figure 4A). While for those pigs from Batch 2, *Bionectriaceae* and *Phaeosphaeriaceae* showed enriched in the stomach and ileum, respectively, and *Mucor* and *Glomerellales* were enriched in the colon (Figure 4B).

The core fungal community in the gastrointestinal tract

The core fungal community for each intestinal segment was defined as those taxa found in more than 80% of samples. The

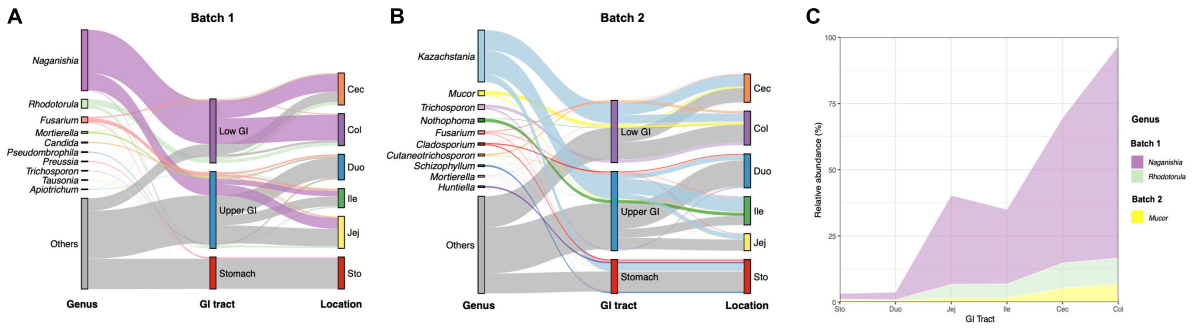

FIGURE 3
Variations of fungal composition in different regions of the gastrointestinal tract at the genus level. Relative abundance of the top 10 abundant genera over intestinal segments (stomach, duodenum, jejunum, ileum, cecum, and colon) are aggregated and colored on a Sankey-stream graph. **(A)** Batch 1, **(B)** Batch 2. Low abundance taxa (except for the 10 most abundant genera) are grouped together as "others". Lines represent associations between indicator genera and intestinal segments, colored by genus taxa. The line width is scaled to reflect the relative abundance. **(C)** Trends in mean relative abundances of significant fungi along the GIT of growing-finishing pigs from two batches.

core gut fungal taxa in Batch 1 consisted of 6 genera including *Naganishia, Rhodotorula, Fusarium, Mortierella, Trichosporon,* and *Alternaria* (Figure 5A). For those pigs from Batch 2, a total of 16 core fungal taxa were identified, with *Kazachstania, Mucor, Fusarium, Trichosporon,* and *Cladosporium* as the five dominant core genera (Figure 5B).

The predicted functional composition of the fungal community

Based on the ASV's taxonomic data, we used FUNGuild to perform the functional classification prediction of the observed fungal communities. For the samples from Batch 1, the fungal taxa were classified into eight trophic modes and 46 ecological guilds except for unassigned. The results indicated that Saprotroph and Pathotroph-Saprotroph were the representatives and dominant predicted functional trophic modes of the fungal community across all segments, with three main fungal guilds named animal endosymbiont, plant pathogens, and undefined saprotroph (Figure 6A). For those samples from Batch 2, the fungal taxa were classified into eight types (most as saprotrophs) and 49 ecological guilds, with animal pathogens, plant pathogens, and undefined saprotrophs as predominant guilds (Figure 6B). The relative abundances of functional trophic modes guilds in different gastrointestinal locations of each batch were summarized in Supplementary Tables 7, 8.

Discussion

Accumulating evidence has shown that gut fungi have an indisputable role in host homeostasis and gut ecosystem, despite its constituting only a small proportion of gut (25, 26). Although gut microbiota research has been given too much attention, studies on fungi are constrained due to technical defects and incomplete databases. To date, little is known about fungal diversity and composition across the whole animal GIT. In addition to limited studies on gut fungi in humans and mice, the fungal community in the gut of a pig, an important model animal, has received increasing attention (27–31). In our previous studies (27, 28, 32), we focused on the fungal community in the gut of pigs with different genetic backgrounds and diets. Here, we reveal unexpected differences in the gut fungal diversity and composition along different locations of GIT between two batches of pigs as model animals.

Unlike what we expected, the difference in the fungal community among the GIT locations appears to be smaller than that between batches. Similar results are observed in chickens, batch-to-batch variations of microbiota are found in the cecum of chickens across three similar trials, represented by individually analyzed samples from 207 birds (33). Another research in two separate shipment batches of 24 Wistar rats also reports differences in the gut microbiota revealed by 16S rRNA amplicon sequencing. It is worth mentioning that these rats are obtained from the same commercial supplier and subjected to the same experimental treatment (34). A study following fungal communities in mice shows that different cages of mice receiving the same treatment also differ in their dominant fungal lineage, and their gut mycobiome varies substantially over time. These findings occur in mice housed in the same animal facility and on a homogeneous diet (35). There is research elaborated with very small numbers of human subjects, demonstrating diurnal changes in the composition of gut microbiota, and more details are described in mice (36, 37). If confirmed, such volatility of gut microbiota would necessitate protocols with standardized stool sampling times (seasons, hours of the day) to support comparisons across studies and allow generalizations to be

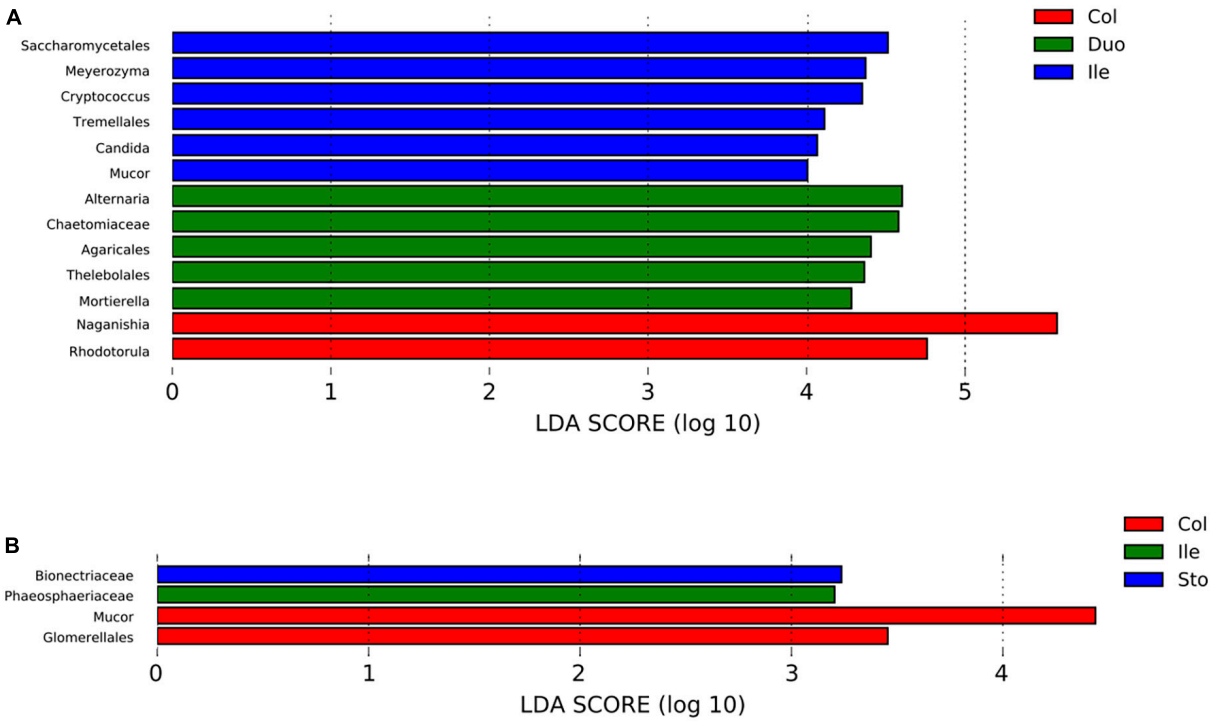

FIGURE 4
Linear discriminant analysis (LDA) effect size (LEfSe) identified the differences in fungal taxa in different regions of the gastrointestinal tract in the pigs (LDA score > 2.0, $p < 0.05$). **(A)** Batch 1, **(B)** Batch 2. Horizontal bars represent the effect size for each taxon. Sto: Stomach, Duo: Duodenum, Jej: Jejunum, Ile: Ileum, Cec: Cecum, Col: Colon.

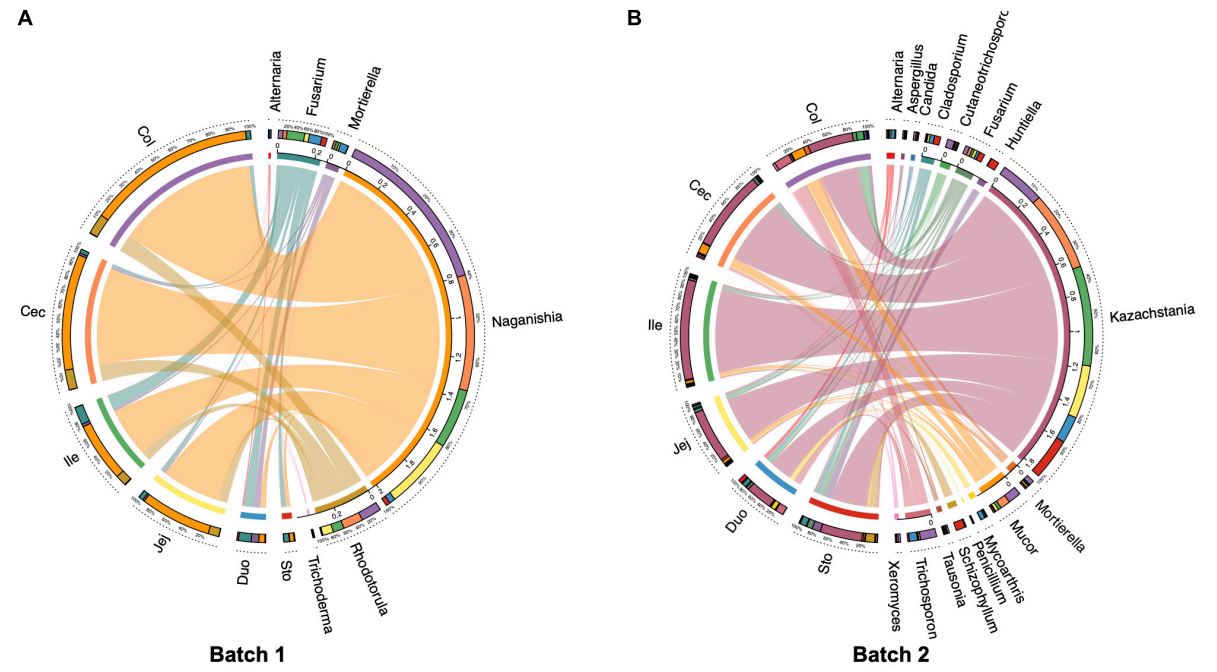

FIGURE 5
Circos plot showing the distributions of core fungal genera in different regions of the gastrointestinal tract in the pigs (present in more than 80% of all digesta samples). **(A)** Batch 1, **(B)** Batch 2.

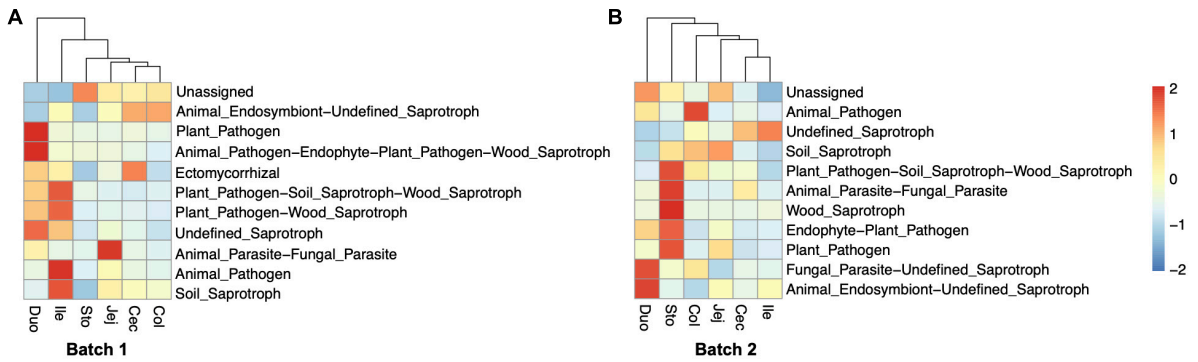

FIGURE 6
Functional prediction of fungal community in different regions of the gastrointestinal tract in the pigs. Heatmap representing the relative abundance of predicted fungal functional guilds. Trophic guild assignments for fungal sequences were analyzed based on the FUNGuild database. **(A)** Bacth1, **(B)** Batch2.

deduced. Although we collected digesta samples from only 11 pigs, the overall comparison showed extensive differences in the fungal community between the two batches, which are consistent with the above studies. Indeed, previous studies identified that season and pen greatly influenced the gut bacterial composition of pigs (38). We have reasons to believe that different sampling times may lead to changes in the fungal community, even if other conditions are the same. The batch-to-batch variation suggests a need for large-number of samples to faithfully reflect the microbial profile investigated, even within one trial, which should be taken into account during experimental design.

Compared with gut bacteria, the biodiversity of the gut fungal community is lower and characterized by greater unevenness, which is consistent with previous studies (39–41). The diversity of gut bacteria is regarded to linearly increase along the GIT of pigs (42). However, we found that the fungal α-diversity of fungi maybe with a completely different presentation. The upper GIT (duodenum) of pigs in Batch 1 harbored higher fungal diversity than that in the hindgut, but a similar phenomenon is not been observed in Batch 2. Generally, fewer numbers and diversity of microorganisms can be found in the stomach and upper GIT compared with the hindgut due to rapid luminal flow and lower pH (43, 44). But several acid-resistant fungi have been found in the stomach, such as *Candida* and *Phialemonium* (40, 45). *Candida albicans*, one of the conditionally pathogenic fungi, is found in 43% of jejunal aspirate/culture at a threshold of at least 10^2 CFU/mL (46), suggesting some gut fungi may be acid-tolerant. These factors may lead to the failure of investigation of clearly fewer fungi in the stomach and foregut. Fungal signaling pathways responding to external pH signals are important components of their cellular machinery. For example, *Candida albicans* is a commensal fungus that commonly colonizes mucosal areas such as the oral, GIT, and vaginal tract of human, the pH in these different organs range from acidic (the stomach and the vaginal tract) to slightly alkaline (oral-pharyngeal tract). To survive pH changes of this magnitude, *C. albicans* depends on pH-sensing pathways (Rim101 pathway) to regulate its pH tolerance (47–49). Thus, we may speculate that the high diversity of fungi in the stomach of pigs in Batch 1 may be due to its greater tolerance in highly acidic environments. However, we cannot find sufficient evidence to infer why pigs in Batch 2 were not observed significantly more fungi in the foregut than in the hindgut.

We found that the predominant fungal phyla in the GIT were Ascomycota and Basidiomycota, which is in line with the results obtained in previous studies on humans and mice (27, 28), indicating that the fungal composition in the GIT of pigs, mice, and human may be homogeneous at the phylum level. Among all classifiable fungal genera, composition and relative abundance varied significantly between the two batches. Unlike humans and mice, the commonly found fungi belonging to genera *Candida* and *Saccharomyces* are either absent or found at a low relative abundance in our study (1, 50). Instead, we found *Naganishia* is a core fungal taxon in pigs from Batch 1 with an increasing trend along the GIT. *Naganishia* (formerly *Cryptococcus*) is a commensal fungus observed in the human gut, skin, oral cavity, and scalp (51, 52). A higher relative abundance of *Naganishia* in the feces is observed in healthy Tibetan piglets when compared with the diarrhea group (53). This is a novel fungal genus known for its ability to utilize a variety of carbon sources including lignocellulosic hydrolysates, complex sugars, and fatty acids (54, 55), and its high abundance in the hindgut probably because the hindgut is the main location for fermentation of complex carbohydrates. Interestingly, the relative abundance of *Naganishia* is found extremely low in pigs from Batch 2 fed the same diet. Instead, we found a group of yeast, *Kazachstania* spp., is enriched in the gut of these pigs. Species *K. slooffiae* is found in most pigs (28, 30, 42) and may positively contribute to the body weight and gut health of piglets (56, 57). Mycobiome instability suggests transient colonization

in the GIT by some fungi due to environmental and dietary exposures. While this may be the case for certain fungal species, various yeasts do stably colonize in the GIT of murine (58, 59), and longitudinal sampling could be used to identify a stable gut mycobiota that might be likely residents. More comprehensive and accurate profiling will be needed to reveal whether the fungal population in the GIT is residents or passers-by.

Different from the huge differences in fungal composition along with the GIT between the two batches, we found that the predicted function of the fungal community in the two batches of pigs may be similar. The high percentage of "undefined saprotrophs" fungal taxa may assist in the breakdown of indigestible dietary fiber and the redistribution of nutrients (60, 61). In soil, saprophytic fungi are well known for producing secondary metabolites, which play a crucial role in the initial destruction of complex organic compounds (62). Although all pigs included are healthy, there is still a small part of intestinal fungi categorized as pathogenic guilds, these fungi may serve as opportunistic pathogens. Plant pathogenic and ectomycorrhizal fungi are naturally found in plants and soil (63, 64), and their presence in the GIT of pigs may be originated from diet or soil. Compared with the upper GIT, the abundance of plant pathogenic fungi in the hindgut is almost absent, which supports the view mentioned above that food-borne fungi may not colonize or inhabit the intestinal tract in the long-term. Unlike humans and model animals, pigs have more opportunities to contact soil, and the habit of digging the earth with their snouts may be another way for the fungi in the soil to enter the pig gut (65). The abundance of animal endosymbiont increased along the GIT, indicating that the hindgut harbored more commensal fungi and can colonize or inhabit the gut for the long-term.

In summary, we provided a comprehensive overview of the fungal composition along the GIT in pig model from two separate batches, as well as new insight into potential functional profiles of gut fungi. Our results demonstrated that the most abundant phyla in the GIT were Ascomycota and Basidiomycota, and gut fungal distribution between the two batches was distinct, indicating gut fungi in healthy pigs is highly variable. In addition, even with the same diet and feeding environment, animals with similar genetic backgrounds and body weights may harbor completely different diversity and composition of fungi along the GIT. These findings emphasize that sampling time or season may be an important factor to be considered in research on intestinal fungi.

Data availability statement

The data presented in this study are deposited in the NCBI repository (www.ncbi.nlm.nih.gov), accession number PRJNA855916.

Ethics statement

The animal study was reviewed and approved by DC and YL, Sichuan Agricultural University. Written informed consent was obtained from the owners for the participation of their animals in this study.

Author contributions

JiL, DC, and YL conceived and designed the experiments. DC and YL administered the project. JiL performed the experiments and collected and analyzed the data. JiL and YL wrote and revised the manuscript. BY, JH, ZH, PZ, XM, HL, JY, JuL, and HY contributed valuable advice on the data analysis and manuscript. All authors reviewed the manuscript and agreed to the published version of the manuscript.

Funding

This work was supported by the National Natural Science Foundation of China (NSFC; grant numbers 32072743, 31730091, 31872369, and 31672436).

Conflict of interest

The authors declare that the research was conducted in the absence of any commercial or financial relationships that could be construed as a potential conflict of interest.

Publisher's note

Supplementary material

The Supplementary Material for this article can be found online at: https://www.frontiersin.org/articles/10.3389/fnut.2022.1021215/full#supplementary-material

References

1. Li J, Chen D, Yu B, He J, Zheng P, Mao X, et al. Fungi in gastrointestinal tracts of human and mice: from community to functions. *Microb Ecol.* (2018) 75:821–9. doi: 10.1007/s00248-017-1105-9

2. Manor O, Dai CL, Kornilov SA, Smith B, Magis AT. Health and disease markers correlate with gut microbiome composition across thousands of people. *Nat Commun.* (2020) 11:5206. doi: 10.1038/s41467-020-18871-1

3. Pilla R, Suchodolski JS. The role of the canine gut microbiome and metabolome in health and gastrointestinal disease. *Front Vet Sci.* (2020) 6:498. doi: 10.3389/fvets.2019.00498

4. Tanes C, Bittinger K, Gao Y, Friedman ES, Nessel L, Paladhi UR, et al. Role of dietary fiber in the recovery of the human gut microbiome and its metabolome. *Cell Host Microbe.* (2021) 29:394–407. doi: 10.1016/j.chom.2020.12.012

5. Wu J, Wang K, Wang X, Pang Y, Jiang C. The role of the gut microbiome and its metabolites in metabolic diseases. *Protein Cell.* (2020) 12:360–73. doi: 10.1007/s13238-020-00814-7

6. Iliev ID, Cadwell K. Effects of intestinal fungi and viruses on immune responses and inflammatory bowel diseases. *Gastroenterology.* (2021) 160:1050–66. doi: 10.1053/j.gastro.2020.06.100

7. Wu X, Xia Y, He F, Zhu C, Ren W. Intestinal mycobiota in health and diseases: from a disrupted equilibrium to clinical opportunities. *Microbiome.* (2021) 9:60. doi: 10.1186/s40168-021-01024-x

8. Chin VK, Yong VC, Chong PP, Amin Nordin S, Basir R, Abdullah M, et al. Mycobiome in the gut: a multiperspective review. *Mediat Inflam.* (2020) 2020:9560684. doi: 10.1155/2020/9560684

9. Mims TS, Abdallah QA, Stewart JD, Watts SP, White CT, Rousselle TV, et al. The gut mycobiome of healthy mice is shaped by the environment and correlates with metabolic outcomes in response to diet. *Commun Biol.* (2021) 4:281. doi: 10.1038/s42003-021-01820-z

10. Underhill DM, Iliev ID. The mycobiota: interactions between commensal fungi and the host immune system. *Nat Rev Immunol.* (2014) 14:405–16. doi: 10.1038/nri3684

11. Hallen-Adams HE, Suhr MJ. Fungi in the healthy human gastrointestinal tract. *Virulence.* (2017) 8:352–8. doi: 10.1080/21505594.2016.1247140

12. Heisel T, Montassier E, Johnson A, Al-Ghalith G, Lin Y-W, Wei L-N, et al. High-fat diet changes fungal microbiomes and interkingdom relationships in the murine gut. *Msphere.* (2017) 2:e00351–17. doi: 10.1128/mSphere.00351-17

13. Heinritz SN, Mosenthin R, Weiss E. Use of pigs as a potential model for research into dietary modulation of the human gut microbiota. *Nutr Res Rev.* (2013) 26:191–209. doi: 10.1017/S0954422413000152

14. Zhang Q, Widmer G, Tzipori S. A pig model of the human gastrointestinal tract. *Gut microbes.* (2013) 4:193–200. doi: 10.4161/gmic.23867

15. Gruninger RJ, Nguyen TTM, Reid ID, Yanke JL, Wang P, Abbott DW, et al. Application of transcriptomics to compare the carbohydrate active enzymes that are expressed by diverse genera of anaerobic fungi to degrade plant cell wall carbohydrates. *Front Microbiol.* (2018) 9:1581. doi: 10.3389/fmicb.2018.01581

16. Wang L, Zhang G, Xu H, Xin H, Zhang Y. Metagenomic analyses of microbial and carbohydrate-active enzymes in the rumen of holstein cows fed different forage-to-concentrate ratios. *Front Microbiol.* (2019) 10:649. doi: 10.3389/fmicb.2019.00649

17. National Research Council [NRC]. *Nutrient Requirements of Swine*. 11th ed. Washington, DC: National Academies Press (2012).

18. Association of Officiating Analytical Chemists [AOAC]. *Official Methods of Analysis*. 18th ed. Washington, DC: Association of Officiating Analytical Chemists (2006).

19. Gardes M, Bruns TD. Its primers with enhanced specificity for basidiomycetes-application to the identification of mycorrhizae and rusts. *Mol Ecol.* (1993) 2:113–8.

20. White TJ, Bruns T, Lee S, Taylor JW. *PCR Protocols: A Guide to Methods and Applications*. New York, NY: Academic Press (1990). p. 315–22.

21. Wiesmann C, Lehr K, Kupcinskas J, Vilchez-Vargas R, Link A. Primers matter: influence of the primer selection on human fungal detection using high throughput sequencing. *Gut Microbes.* (2022) 14:2110638. doi: 10.1080/19490976.2022.2110638

22. Bolyen E, Rideout JR, Dillon MR, Bokulich NA, Abnet CC, Al-Ghalith GA, et al. Reproducible, interactive, scalable and extensible microbiome data science using QIIME 2. *Nat Biotechnol.* (2019) 37:852–7.

23. Callahan BJ, Mcmurdie PJ, Rosen MJ, Han AW, Johnson A, Holmes SP. Dada2: high-resolution sample inference from Illumina amplicon data. *Nat Methods.* (2016) 13:581–3. doi: 10.1038/nmeth.3869

24. Nguyen NH, Song Z, Bates ST, Branco S, Tedersoo L, Menke J, et al. Funguild: an open annotation tool for parsing fungal community datasets by ecological guild. *Fungal Ecol.* (2016) 20:241–8.

25. Iliev ID, Funari VA, Taylor KD, Quoclinh N, Reyes CN, Strom SP, et al. Interactions between commensal fungi and the C-Type lectin receptor Dectin-1 influence colitis. *Science.* (2012) 336:1314–7. doi: 10.1126/science.1221789

26. Christian H, Serena D, Stephanie G, Jun C, Hongzhe L, Wu GD, et al. Archaea and fungi of the human gut microbiome: correlations with diet and bacterial residents. *PLoS One.* (2013) 8:e66019. doi: 10.1371/journal.pone.0066019

27. Li J, Chen D, Yu B, He J, Huang Z, Mao X, et al. The fungal community and its interaction with the concentration of short-chain fatty acids in the faeces of Chenghua, Yorkshire and Tibetan pigs. *Microb Biotechnol.* (2019) 13:509–21. doi: 10.1111/1751-7915.13507

28. Li J, Luo Y, Chen D, Yu B, He J, Huang Z. The fungal community and its interaction with the concentration of short-chain fatty acids in the caecum and colon of weaned piglets. *J Anim Physiol Anim Nutr.* (2020) 104:616–28. doi: 10.1111/jpn.13300

29. Hu J, Nie Y, Chen J, Zhang Y, Wang Z, Fan Q, et al. Gradual changes of gut microbiota in weaned miniature piglets. *Front Microbiol.* (2016) 7:1727. doi: 10.3389/fmicb.2016.01727

30. Summers KL, Frey JF, Ramsay TG, Arfken AM. The piglet mycobiome during the weaning transition: a pilot study. *J Anim Sci.* (2019) 97:2889–900. doi: 10.1093/jas/skz182

31. Arfken AM, Frey JF, Summers KL. Temporal dynamics of the gut bacteriome and mycobiome in the weanling pig. *Microorganisms.* (2020) 8:868. doi: 10.3390/microorganisms8060868

32. Luo Y, Li J, Zhou H, Yu B, He J, Wu A, et al. The nutritional significance of intestinal fungi: alteration of dietary carbohydrate composition triggers colonic fungal community shifts in a pig model. *Appl Environ Microb.* (2021) 87:e00038–21. doi: 10.1128/AEM.00038-21

33. Stanley D, Geier MS, Hughes RJ, Denman SE, Moore RJ. Highly variable microbiota development in the chicken gastrointestinal tract. *PLoS One.* (2013) 8:e84290. doi: 10.1371/journal.pone.0084290

34. Randall D, Kieswich J, Swann J, McCafferty K, Thiemermann C, Curtis M, et al. Batch effect exerts a bigger influence on the rat urinary metabolome and gut microbiota than uraemia: a cautionary tale. *Microbiome.* (2019) 7:127. doi: 10.1186/s40168-019-0738-y

35. Dollive S, Chen YY, Grunberg S, Bittinger K, Hoffmann C, Vandivier L, et al. Fungi of the murine gut: episodic variation and proliferation during antibiotic treatment. *PLoS One.* (2013) 8:e71806. doi: 10.1371/journal.pone.0071806

36. Brüssow H. Problems with the concept of gut microbiota dysbiosis. *Microb Biotechnol.* (2020) 13:423–34. doi: 10.1111/1751-7915.13479

37. Thaiss CA, Zeevi D, Levy M, Zilberman-Schapira G, Suez J, Tengeler AC, et al. Transkingdom control of microbiota diurnal oscillations promotes metabolic homeostasis. *Cell.* (2014) 159:514–29. doi: 10.1016/j.cell.2014.09.048

38. Pajarillo EAB, Chae JP, Balolong MP, Kim HB, Seo K-S, Kang D-K. Pyrosequencing-based analysis of fecal microbial communities in three purebred pig lines. *J Microbiol.* (2014) 52:646–51. doi: 10.1007/s12275-014-4270-2

39. Qin J, Li R, Raes J, Arumugam M, Burgdorf KS, Manichanh C, et al. A human gut microbial gene catalogue established by metagenomic sequencing. *Nature.* (2010) 464:59–65. doi: 10.1038/nature08821

40. Suhr MJ, Hallen-Adams HE. The human gut mycobiome: pitfalls and potentials—a mycologist's perspective. *Mycologia.* (2015) 107:1057–73. doi: 10.3852/15-147

41. Nash AK, Auchtung TA, Wong MC, Smith DP, Gesell JR, Ross MC, et al. The gut mycobiome of the human microbiome project healthy cohort. *Microbiome.* (2017) 5:153. doi: 10.1186/s40168-017-0373-4

42. Arfken AM, Frey JF, Ramsay TG, Summers KL. Yeasts of burden: exploring the mycobiome–bacteriome of the piglet GI tract. *Front Microbiol.* (2019) 10:2286. doi: 10.3389/fmicb.2019.02286

43. Donaldson GP, Lee SM, Mazmanian SK. Gut biogeography of the bacterial microbiota. *Nat Rev Microbiol.* (2016) 14:20–32. doi: 10.1038/nrmicro3552

44. Walter J, Ley R. The human gut microbiome: ecology and recent evolutionary changes. *Annu Rev Microbiol.* (2011) 65:411–29. doi: 10.1146/annurev-micro-090110-102830

45. Von Rosenvinge EC, Song Y, White JR, Maddox C, Blanchard T, Fricke WF. Immune status, antibiotic medication and pH are associated with changes in the stomach fluid microbiota. *ISME J.* (2013) 7:1354–66. doi: 10.1038/ismej.2013.33

46. Erdogan A, Rao SS. Small intestinal fungal overgrowth. *Curr Gastroenterol Rep.* (2015) 17:16. doi: 10.1007/s11894-015-0436-2

47. Davis D, Wilson RB, Mitchell AP. Rim101-dependent and -independent pathways govern pH responses in *Candida Albicans*. *Mol Cell Biol.* (2000) 20:971–8. doi: 10.1128/MCB.20.3.971-978.2000

48. Davis DA. How human pathogenic fungi sense and adapt to pH: the link to virulence. *Curr Opin Microbiol.* (2009) 12:365–70. doi: 10.1016/j.mib.2009.05.006

49. Davis DA, Edwards JE, Mitchell AP, Ibrahim AS. *Candida Albicans* Rim101 pH response pathway is required for host-pathogen interactions. *Infect Immun.* (2000) 68:5953–9. doi: 10.1128/IAI.68.10.5953-5959.2000

50. Qi S, Chang M, Chai L. The fungal mycobiome and its interaction with gut bacteria in the host. *Int J Mol Sci.* (2017) 18:330. doi: 10.3390/ijms18020330

51. Imai T, Inoue R, Kawada Y, Morita Y, Inatomi O, Nishida A, et al. Characterization of fungal dysbiosis in Japanese patients with inflammatory bowel disease. *J Gastroenterol.* (2019) 54:149–59. doi: 10.1007/s00535-018-1530-7

52. O'Connell LM, Santos R, Springer G, Burne RA, Nascimento MM, Richards VP. Site-specific profiling of the dental mycobiome reveals strong taxonomic shifts during progression of early-childhood caries. *Appl Environ Microb.* (2020) 86:e02825–19. doi: 10.1128/AEM.02825-19

53. Kong Q, Liu S, Li A, Wang Y, Zhang L, Iqbal M, et al. Characterization of fungal microbial diversity in healthy and diarrheal Tibetan piglets. *BMC Microbiol.* (2021) 21:204. doi: 10.1186/s12866-021-02242-x

54. Horváth E, Sipiczki M, Csoma H, Miklós I. Assaying the effect of yeasts on growth of fungi associated with disease. *BMC Microbiol.* (2020) 20:320. doi: 10.1186/s12866-020-01942-0

55. Sathiyamoorthi E, Dikshit PK, Kumar P, Kim BS. Co-fermentation of agricultural and industrial waste by *Naganishia albida* for microbial lipid production in fed-batch fermentation. *J Chem Technol Biotechnol.* (2020) 95:813–21. doi: 10.1002/jctb.6271

56. Ramayo-Caldas Y, Prenafeta-Boldú F, Zingaretti LM, Gonzalez-Rodriguez O, Dalmau A, Quintanilla R, et al. Gut eukaryotic communities in pigs: diversity, composition and host genetics contribution. *Anim Microbiome.* (2020) 2:18. doi: 10.1186/s42523-020-00038-4

57. Urubschurov V, Büsing K, Souffrant WB, Schauer N, Zeyner A. Porcine intestinal yeast species, *Kazachstania slooffiae*, a new potential protein source with favourable amino acid composition for animals. *J Anim Physiol Anim Nutr.* (2017) 102:e892–901. doi: 10.1111/jpn.12853

58. Fiers WD, Gao IH, Iliev ID. Gut mycobiota under scrutiny: fungal symbionts or environmental transients?. *Curr Opin Microbiol.* (2019) 50:79–86. doi: 10.1016/j.mib.2019.09.010

59. Gutierrez MW, Arrieta M-C. The intestinal mycobiome as a determinant of host immune and metabolic health. *Curr Opin Microbiol.* (2021) 62:8–13. doi: 10.1016/j.mib.2021.04.004

60. Borruso L, Checcucci A, Torti V, Correa F, Sandri C, Luise D, et al. I like the way you eat it: lemur (*Indri Indri*) gut mycobiome and geophagy. *Microb Ecol.* (2021) 82:215–23. doi: 10.1007/s00248-020-01677-5

61. Hättenschwiler S, Tiunov AV, Scheu S. Biodiversity and litter decomposition in terrestrial ecosystems. *Annu Rev Ecol Evol Syst.* (2005) 36:191–218. doi: 10.1146/annurev.ecolsys.36.112904.151932

62. Bani A, Borruso L, Matthews Nicholass KJ, Bardelli T, Polo A, Pioli S, et al. Site-specific microbial decomposer communities do not imply faster decomposition: results from a litter transplantation experiment. *Microorganisms.* (2019) 7:349. doi: 10.3390/microorganisms7090349

63. Yang T, Tedersoo L, Soltis PS, Soltis DE, Gilbert JA, Sun M, et al. Phylogenetic imprint of woody plants on the soil mycobiome in natural mountain forests of eastern China. *ISME J.* (2019) 13:686–97. doi: 10.1038/s41396-018-0303-x

64. Averill C, Hawkes CV. Ectomycorrhizal fungi slow soil carbon cycling. *Ecol Lett.* (2016) 19:937–47. doi: 10.1111/ele.12631

65. Velie BD, Maltecca C, Cassady JP. Genetic relationships among pig behavior, growth, backfat, and loin muscle area. *J Anim Sci.* (2009) 87:2767–73. doi: 10.2527/jas.2008-1328

frontiers | Frontiers in Nutrition

TYPE Original Research
PUBLISHED 16 November 2022
DOI 10.3389/fnut.2022.1028459

OPEN ACCESS

EDITED BY
Jie Yin,
Hunan Agricultural University, China

REVIEWED BY
Zhiyuan Guan,
Peking University Third Hospital, China
Tao Yang,
Central South University of Forestry and Technology, China

*CORRESPONDENCE
Liqun Liu
liuliqun@csu.edu.cn

SPECIALTY SECTION
This article was submitted to Nutrition and Microbes, a section of the journal Frontiers in Nutrition

RECEIVED 26 August 2022
ACCEPTED 31 October 2022
PUBLISHED 16 November 2022

CITATION
Gong X, Liu L, Li X, Xiong J, Xu J, Mao D and Liu L (2022) Neuroprotection of cannabidiol in epileptic rats: Gut microbiome and metabolome sequencing. *Front. Nutr.* 9:1028459. doi: 10.3389/fnut.2022.1028459

Neuroprotection of cannabidiol in epileptic rats: Gut microbiome and metabolome sequencing

Xiaoxiang Gong[1,2], Lingjuan Liu[1,2], Xingfang Li[1,2], Jie Xiong[1,2], Jie Xu[1,2], Dingan Mao[1,2] and Liqun Liu[1,2]*

[1]Department of Pediatrics, The Second Xiangya Hospital, Central South University, Changsha, Hunan, China, [2]Children's Brain Development and Brain Injury Research Office, The Second Xiangya Hospital, Central South University, Changsha, Hunan, China

Aims: Epilepsy is a neurological disease occurring worldwide. Alterations in the gut microbial composition may be involved in the development of Epilepsy. The study aimed to investigate the effects of cannabidiol (CBD) on gut microbiota and the metabolic profile of epileptic rats.

Materials and methods and results: A temporal lobe epilepsy rat model was established using Li-pilocarpine. CBD increased the incubation period and reduced the epileptic state in rats. Compared to epileptic rats, the M1/M2 ratio of microglia in the CBD group was significantly decreased. The expression of IL-1β, IL-6, and TNF-α in the CBD group decreased, while IL-10, IL-4, and TGF-β1 increased. 16S rDNA sequencing revealed that the ANOSIM index differed significantly between the groups. At the genus level, *Helicobacter*, *Prevotellaceae_UCG-001*, and *Ruminococcaceae_UCG-005* were significantly reduced in the model group. CBD intervention attenuated the intervention effects of Li-pilocarpine. *Roseburia*, *Eubacterium_xylanophilum_group*, and *Ruminococcus_2* were strongly positively correlated with proinflammatory cytokine levels. CBD reversed dysregulated metabolites, including glycerophosphocholine and 4-ethylbenzoic acid.

Conclusion: CBD could alleviate the dysbiosis of gut microbiota and metabolic disorders of epileptic rats. CBD attenuated Epilepsy in rats might be related to gut microbial abundance and metabolite levels.

Significance and impact of study: The study may provide a reliable scientific clue to explore the regulatory pathway of CBD in alleviating Epilepsy.

KEYWORDS

Epilepsy, cannabidiol, gut microbiota, metabolism, neuroprotection

Introduction

Epilepsy is a chronic nervous system disease that affects at least 70 million people worldwide (1). Temporal lobe epilepsy (TLE) is the most common type of focal Epilepsy worldwide. In the TLE model, inflammation is one of the most upregulated biological processes in Epilepsy (2). Inflammatory factors released by immune cells directly or indirectly affect neuronal excitability, thereby regulating the threshold of epileptic seizures (3). Neuroinflammation is considered the main pathological finding of Epilepsy. Microglia are highly adaptable glial cells in the central nervous system (CNS) and play an important role in maintaining CNS homeostasis (4). Epilepsy triggers the rapid activation of nearby microglia. The excess inflammatory mediators produced by activated microglia may promote the inflammatory immune cascade (5, 6). New evidence has shown that neuroinflammation can affect hyperexcitability and promote Epilepsy (7). Meanwhile, M2 microglia polarization could alleviate seizures *via* suppressing neuronal apoptosis and the hyperactivation of M1 microglia (8–10). Therefore, neuroinflammation and M2 microglia polarization may be an important pathophysiological mechanism in the development of TLE.

Cannabidiol (CBD) is the main active ingredient in cannabis. Unlike tetrahydrocannabinol (THC), CBD does not exhibit excitation-inducing properties. CBD has antioxidant and anti-inflammatory activities and could play a neuroprotective role by modulating the biological targets of the brain in neurodegenerative diseases (11). Clinical studies have reported that CBD has a good therapeutic effect in relieving pain and treating Epilepsy (12). Some enzymes, ion channels, receptors, and transporters, including G protein-coupled receptor (GPR), are molecular targets for CBD therapy (13). However, how CBD regulates neuroinflammation in the brain and alleviates the development of Epilepsy and its internal regulatory pathways remain unclear.

Gut microbiota can regulate gut permeability, alter local or peripheral immune responses, and produce essential metabolites and neurotransmitters (14). Moreover, gut microbiota can achieve "gut-brain" communication through endocrine, immune and metabolic pathways (15). There is evidence that the composition of gut microbiota changes during Epilepsy (16), and antiepileptic drugs can affect gut microbiota (17). Recent studies have shown that the anti-inflammatory properties of CBD may be involved in resisting gut inflammation, leakage of the gut vascular barrier caused by dysregulation of the gut microbiome, and subsequent neuroinflammation (18). However, the effects of CBD on gut microbiota during Epilepsy treatment have been rarely reported.

We speculated that CBD might inhibit the overexpression of inflammatory factors in Epilepsy by reducing the activation of microglia. In addition, we will explore whether CBD mediates changes in the composition and function of gut microbiota in epileptic rats. We hope that this study provides preliminary reliable scientific evidence in support of further investigations to explore the regulatory pathway of CBD in alleviating Epilepsy.

Materials and methods

Animal

Fifty Sprague-Dawley male rats were purchased from Hunan SJA Laboratory Animal Co., Ltd., Rats were adaptively fed for 5 days (d) under specific pathogen-free conditions with a controlled 12 h light/dark cycle, temperature (20–25°C), humidity (50–60%), and free access to water and diet. The rats were randomly divided into the following five groups: a control group (control group) (n = 10), an epilepsy model group (n = 10), a low-CBD epilepsy model group (Model + 20 mg/kg CBD group) (n = 10), a high-CBD epilepsy model group (Model + 100 mg/kg CBD group) (n = 10), and a Carbamazepine (CBZ) epilepsy model group (Model + 75 mg/kg CBZ group) (n = 10). CBD and CBZ were purchased from Sigma-Aldrich, St. Louis, MO, USA. We chose a dose of 20 mg/kg based on a previous study demonstrating that this was within the range of anti-inflammatory therapy in rodents and humans (19). A second study also demonstrated that 100 mg/kg of CBD exerted a significant antiepileptic effect in rodent models of Epilepsy (20). CBZ could relieve seizures with CBZ 75 mg/kg injected (21).

Model treatment: The rats were intraperitoneally injected with 127 mg/kg lithium chloride the day before modeling (day 6). After 18–24 h, freshly prepared pilocarpine (1538902, Sigma-Aldrich, St. Louis, MO, USA) was intraperitoneally injected at a ratio of 25 mg/kg. The control group was injected with the same volume of solvent. The rats were subcutaneously injected with 0.1 mg atropine sulfate monohydrate 30 min before the injection of pilocarpine. Seizure severity was graded according to the Racine Scale (22). Rats with recurrent epileptic lasting 30 min were considered to have status epilepticus (SE). Rats with SE were intraperitoneally injected with 10 mg/kg of Diazepam to terminate the attack (23, 24).

The low-CBD group was administered 20 mg/kg CBD by gavage half an hour before modeling. The high-CBD group was administered 100 mg/kg CBD. The CBZ group was injected at 75 mg/kg CBZ half an hour before modeling. The control and model groups were administered the same amount of carrier solution (2% Tween 80 + 98% saline). The rats were treated continuously for 7 days. Under the experimental animal ethics protocol, all rats were intraperitoneally injected with chloral hydrate for euthanasia. Brain tissue and feces were collected. The experiments on rats in this study were approved by the Animal Ethical and Welfare Committee, The Second Xiangya Hospital, Central South University (No. 2021523).

Hematoxylin and eosin staining

Rat brain tissue was collected and fixed with 4% paraformaldehyde for 24 h. After treatment with xylene and graded alcohol, samples were stained with hematoxylin for 10 min. Next, the samples were incubated with eosin staining solution for 5 min. Samples were dehydrated through graded alcohol. Neutral resin was used for sealing. A light microscope was used for observation, and images were obtained.

Immunofluorescence

Rat brains were sectioned and dewaxed. The slices were then dipped in ethylene diamine tetraacetic acid (EDTA) buffer (pH 9.0) for thermal repair. 3% H_2O_2 was used to inactivate endogenous enzymes, and phosphate-buffered saline (PBS) was used for flushing. Primary antibody microglia/macrophage-specific protein IBA1 (MA5-27726, Invitrogen, Carlsbad, CA, USA) was added and diluted at a ratio of 1:100, incubated overnight at 4°C, and washed with PBS. An appropriate amount of anti-mouse-IgG-labeled fluorescent antibody was added, incubated at 37°C for 90 min, and rinsed with PBS. The DAPI working solution was stained at 37°C for 10 min. Buffered glycerin was used to seal the tablets, which were then observed under a fluorescence microscope.

Flow cytometry

Brain tissue was trypsinized to obtain cells. Samples, about 1×10^6 cells per well, were placed in a 1.5 ml centrifuge tube, and the cells were resuspended in 200 μl PBS. The 5 μl of CD45 (12-0461-82, eBioscience, USA) and CD86 (374215, BioLegend, San Diego, CA, USA), or CD45 and CD163 (326511, BioLegend, San Diego, CA, USA) were added to the sample. The mixture was then incubated in the dark for 30 min. The cells were washed twice with 1 ml of PBS. Then cells were resuspended in 200 μl PBS and filtered through a nylon mesh. Flow cytometry was used for detection.

Quantitative real-time PCR

Total RNA was extracted from the temporal lobe cortex using the TRIzol^{TM} method. The TRIzol Reagent was purchased from ThermoFisher scientific. RNA concentration was measured using an ultraviolet spectrophotometer. According to the instructions of the Hifiscript cDNA Synthesis Kit (CW2569M, CWBIO, Beijing, China), a 20 μl reaction system was used for reverse transcription. PCR amplification was performed according to the UltraSYBR Mixture (CW2601, CWBIO, Beijing, China) manual, and the reaction volume was 30 μl. The SYBR method was used for qPCR detection, and the primers were synthesized by Sangon Biotech. Specific primer sequences are as follows: Rat-β-actin, F-ACATCCGTAAAGACCTCTATGCC, R-TACTCCTGCTTGCTGATCCAC, product length 223bp; Rat-IL-1β, F-CAGCAGCATCTCGACAAGAG, R-AAAGAAGGTGCTTGGGTCCT, product length 123bp; Rat-IL-6, F-TCACTATGAGGTCTACTCGG, R-CATATTGCCAGTTCTTCGTA, product length 141bp; Rat-TNF-α, F-CCCCTCTATTTATAATTGCACCT, R-CTGGTAGTTTAGCTCCGTTT, product length 167bp; Rat-IL-10, F-AATAAGCTCCAAGACAAAGGT, R-TCACGTAGGCTTCTATGCAG, product length 79bp; Rat-IL-4, F-ATGCACCGAGATGTTTGTACC, R-GACCGCTGACACCTCTACAGA, product length 185bp; Rat-TGF-β1, F-ACTACGCCAAAGAAGTCACC, R-CACTGCTTCCCGAATGTCT, product length 125 bp. Data were normalized relative to the control group, and β-actin was used as an internal reference. The $2^{-\Delta\Delta\ Ct}$ reflects the ratio of each sample's target gene expression level relative to that of the control group.

Western blotting

The detection of temporal lobe cortex proteins was undertaken as previously described (25). Radio Immunoprecipitation Assay (RIPA) lysate (P0013B, Beyotime, Shanghai, China) was used to extract total protein from temporal lobe cortex tissue. After lysed for 10 min on ice, the tissue homogenate was centrifuged at 12,000 rpm, 4°C for 10 min. The supernatant was boiled in water for 5 min to denature the protein. Denatured proteins were separated on 10% SDS-polyacrylamide gels and transferred to nitrocellulose (NC) membranes. After blocking with non-fat milk, the membranes were incubated with the primary antibody overnight at 4°C. The secondary antibody was incubated for 90 min. Images were obtained using a chemiluminescence imaging system. The antibodies used in this study were as follows: IL-1β (16806-1-AP,1:1000, Proteintech, Chicago, IL, USA), IL-6 (M620,1:1000, Invitrogen, Carlsbad, CA, USA), TNF-α (17590-1-AP,1:500, Proteintech, Chicago, IL, USA), IL-10 (20850-1-AP,1:1000, Proteintech, Chicago, IL, USA), IL-4 (66142-1-Ig,1:1000, Proteintech, Chicago, IL, USA), TGF-β1 (21898-1-AP,1:1000, Proteintech, Chicago, IL, USA), β-actin (60008-1-Ig,1:5000, Proteintech, Chicago, IL, USA), HRP goat anti-mouse IgG (SA00001-1,1:5000, Proteintech, Chicago, IL, USA), and HRP goat anti-rabbit IgG (SA00001-2,1:6000, Proteintech, Chicago, IL, USA).

16S rDNA sequencing

16S rDNA sequencing was performed on fecal samples from 20 rats, with five rats in each group. A NovaSeq

PE250 instrument (Illumina, San Diego, CA, USA) was used for 16S amplicon sequencing to obtain raw data. DADA2 performed low-quality filtering operations, such as adapters, primer removal, de-noising, merging paired-end sequences, and removing chimeras to obtain valid data. The quality control standard was set as truncQ = 2, F maxEE = 5, R maxEE = 2. The sequencing depth was 50,000 reads, and one read was 250 bp. In order to obtain species classification information, according to the silva-132-99 database, the amplification primer Bacterial V3/V4 (341F + 805R) in the V3–V4 region was selected, and the primer sequence was: CCTACGGGNGGCWGCAG GACTACHVGGGTATCTAATCC. Clusters that reached 99% features of the reference genome Silva132 were grouped into the same taxon. QIIME 2 (Qiime2-2020.2) was used to calculate the α-diversity indices of the samples. The R Phyloseq/Vegan package, Deseq2 package, and Jvenn[1] online software were used for visualization.

Untargeted metabolomics analysis

For investigating the effects of CBD on fecal metabolite levels in epileptic rats, 20 fecal samples were analyzed using untargeted metabolomics analysis. The rats were divided into control, model, low-CBD, and high-CBD model groups, with five rats in each group. Samples were quickly pounded using a plastic hammer. A fecal sample (approximately 50 mg) was collected from each rat and weighed. Nine volumes of the extract containing an internal standard of ^{13}C stable isotope were added to each sample. The sample was stored on ice for 15 min to lyse cells fully. The mixture was centrifuged at 16,000 *g* at 4°C for 10 min. The supernatant was transferred to a new centrifuge tube, and nitrogen was used to dry the samples. After rescaling, the supernatant of the extract was used for the injection analysis. A TripleTOF 5600 + MS system (AB Sciex, Framingham, MA, USA) and an Acquity UPLC HSS T3 column (Waters) were used for LC-MS analysis.

Data analyses

Statistical software SPSS 23.0 and GraphPad Prism 8.0.1 were used to analyze the data in this study. Data are presented as the mean ± standard deviation. A Kruskal–Wallis test, one-way ANOVA, and two-way ANOVA were used to compare groups. Metabolomics data analysis was completed online using MetaboAnalyst5.0.[2] Spearman's rank test was used to analyze the correlation between different indicators, and statistical significance was set at $P < 0.05$.

1 http://www.bioinformatics.com.cn/static/others/jvenn/example.html

2 https://www.metaboanalyst.ca/

Results

Cannabidiol alleviates epilepsy in rats

After modeling, we found that the rats in the model group had the earliest seizures, at 15.5 min on average, followed by the low-CBD group at 27.3 min on average, and the slowest in the high-CBD group at 38.0 min on average (**Figure 1A**). Statistics of epileptic rats' seizures within 80 min demonstrated. The model group had grade 4–5 seizures within 30 min, then continued to have grade 3–4 seizures. The rats required anesthesia to stop the seizures forcibly. The low-CBD group had grades 3–4 seizures within 40 min, occasional grades 2–3 seizures within 50–70 min, and occasional grades 1–2 seizures within 70–80 min, and there was no need to terminate the seizures forcibly. The high-CBD group had grades 3–4 within 60 min, and 1–2 seizures occasionally occurred within 60–80 min, without the need for forced termination of seizures (**Figure 1B**). Compared with the CBZ group, the high-CBD group had no significant difference in latency and seizure statistics within 80 min. H&E staining was performed to analyze the pathological morphology of temporal lobe cortex and hippocampus (**Figure 1C**). Compared with the control group, the model group showed significant histopathological changes, including neuronal atrophy and pyknosis. The morphological damage of brain tissue was improved in the CBD group and the CBZ group. From this, we believed that CBD could relieve Epilepsy in rats.

Cannabidiol promotes M2-type polarization in epileptic rats

To explore the effect of CBD on epileptic rats, we applied the CBD treatment on epileptic rats. The IF results of IBA1 demonstrated that the low-and high-CBD groups were significantly lower than the model group (**Figure 2A**). FCM double staining was used to detect the expression of CD45 + CD86 (**Figures 2B,C**) and CD45 + CD163 (**Figures 2D,E**) to identify the content of M1 type and M2 type microglia cells, respectively. M1-type microglia cells were significantly decreased in the low-CBD and high-CBD groups compared to the Model group. However, the expression of M2-type cells was markedly increased. The ratio of M1/M2 was significantly decreased in the low-CBD and high-CBD groups compared with the Model group (**Figure 2F**).

Cannabidiol reduces neuroinflammation in epileptic rats

We subsequently determined the relative levels of proinflammatory factors in the brain tissues of epileptic

10.3389/fnut.2022.1028459

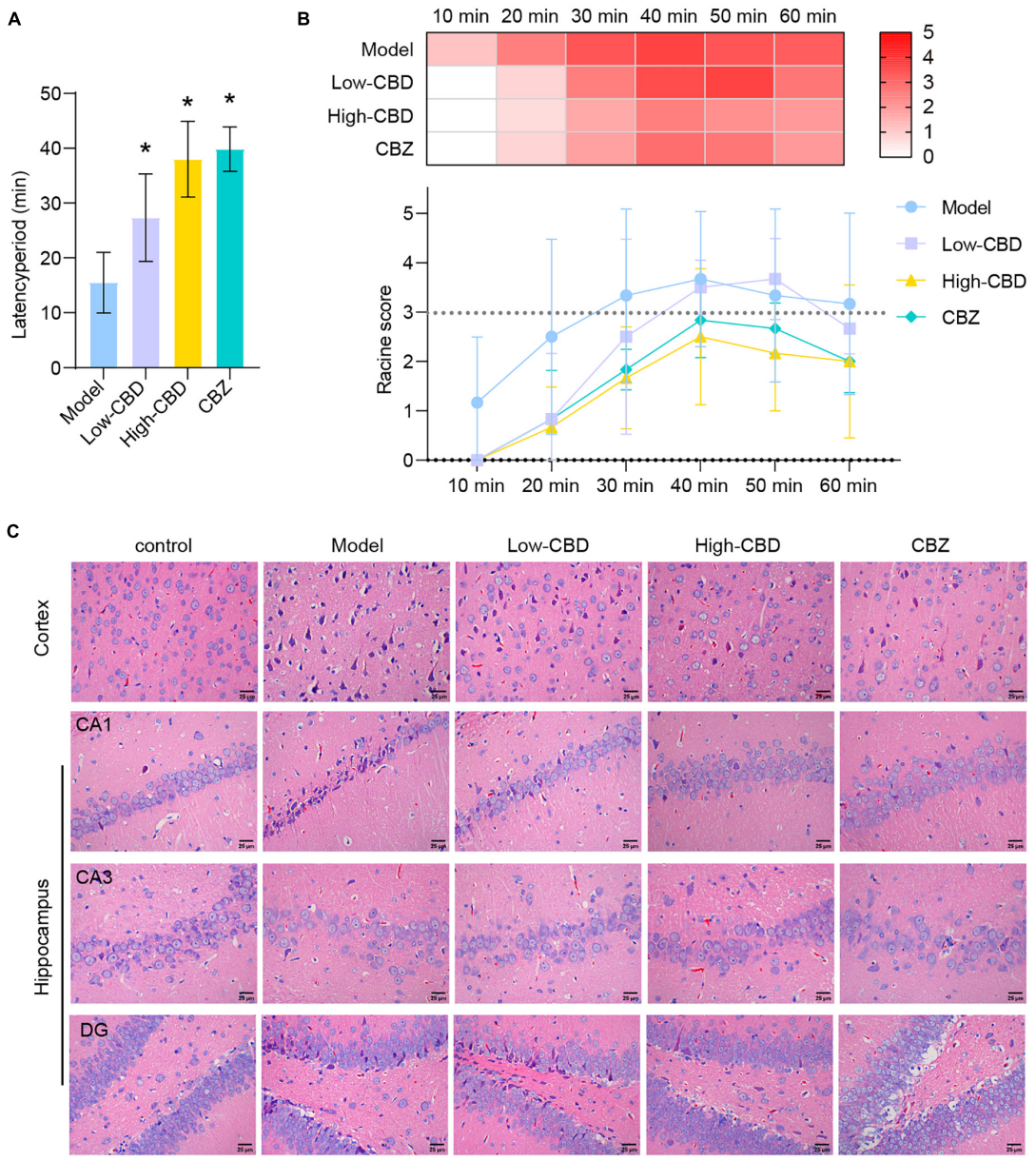

FIGURE 1
Cannabidiol (CBD) alleviates Epilepsy in rats. **(A)** The latency period of epileptic rat. **(B)** The Racine score within 1 h of modeling. **(C)** H&E staining results of the temporal lobe cortex and hippocampus. *Represents significant comparison with the Model group, $P < 0.05$. The darker the red, the higher the Racine score.

rats. The expression levels of IL-1β, IL-6, and TNF-α in the model group were significantly higher than in the control group (Figures 3A–C). Thus, the levels of proinflammatory factors in the brains of epileptic rats were markedly increased. The low- and high-CBD groups were significantly lower than the model group, and the result from Western Blotting further demonstrated this (Figures 3D–F). The expression of IL-1β, IL-6, and TNF-α in the low-CBD and high-CBD groups was significantly lower than that in the model group. Moreover, the gene and protein expression of IL-1β, IL-6, and TNF-α were not significantly different in the CBZ group compared with the high-CBD group (Supplementary Figure 1).

The results of qRT-PCR (Figures 4A–C) and WB (Figures 4D–F) demonstrated the levels of anti-inflammatory factors, including IL-10, IL-4, and TGF-β1, in the brain of rats altered among the four groups. The CBD treatment group was significantly higher than the model group. The high-CBD group was higher than the low-CBD group. IL-10, IL-4, and TGF-β1 were lower in

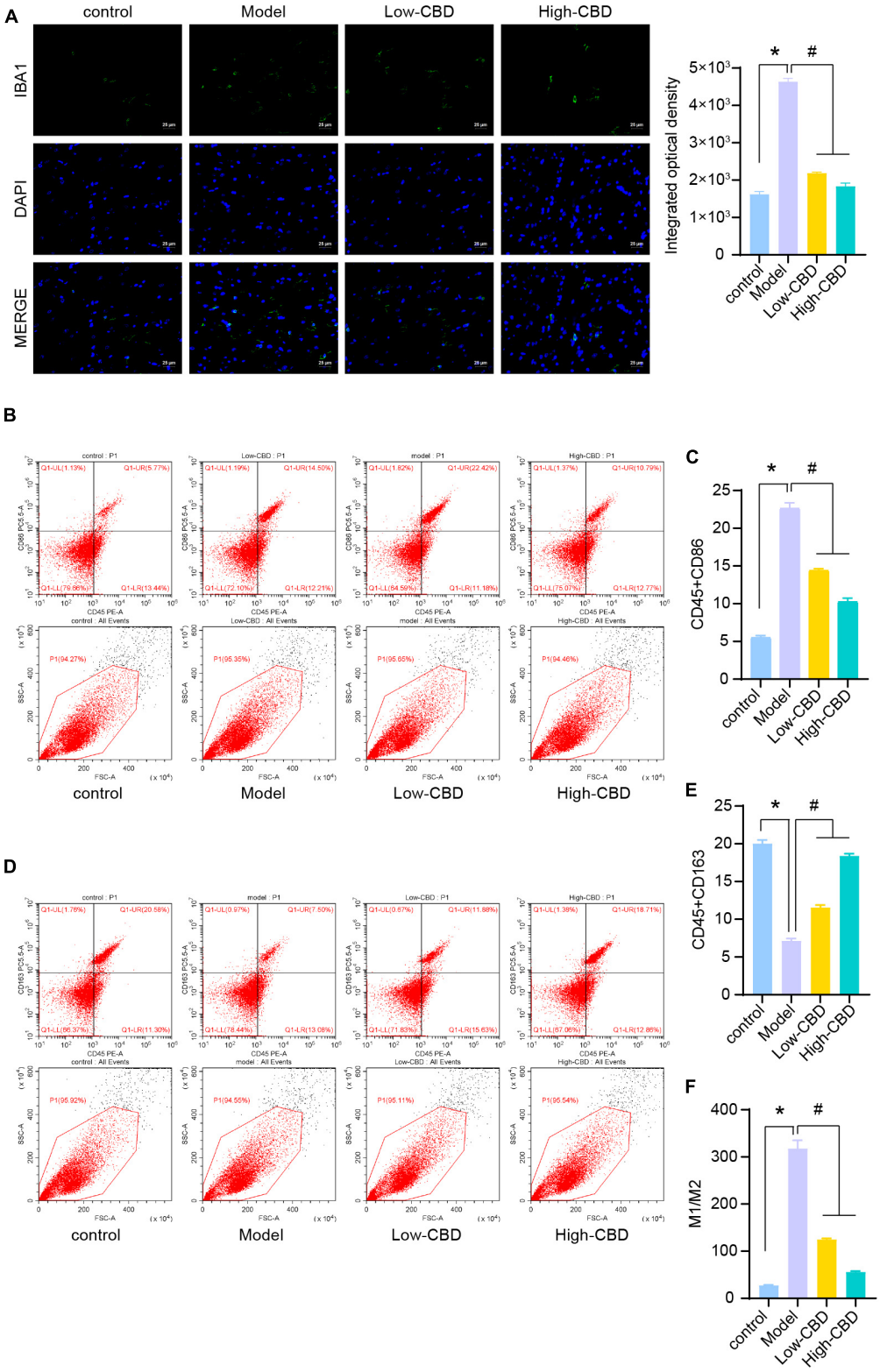

FIGURE 2
Effects of cannabidiol (CBD) on microglia polarization in epileptic rats. **(A)** IBA1 expression was detected by immunofluorescence (IF). **(B,C)** Analysis of M1 type microglia. CD45 + CD86 + double positive cells are expressed as M1 type microglia. **(D,E)** Analysis of M2 type microglia. CD45 + CD163 + double positive cells are expressed as M2 type microglia. **(F)** Statistical graph of M1/M2. *Represents significant comparison with the control group, and #represents significant comparison with the Model group, $P < 0.05$.

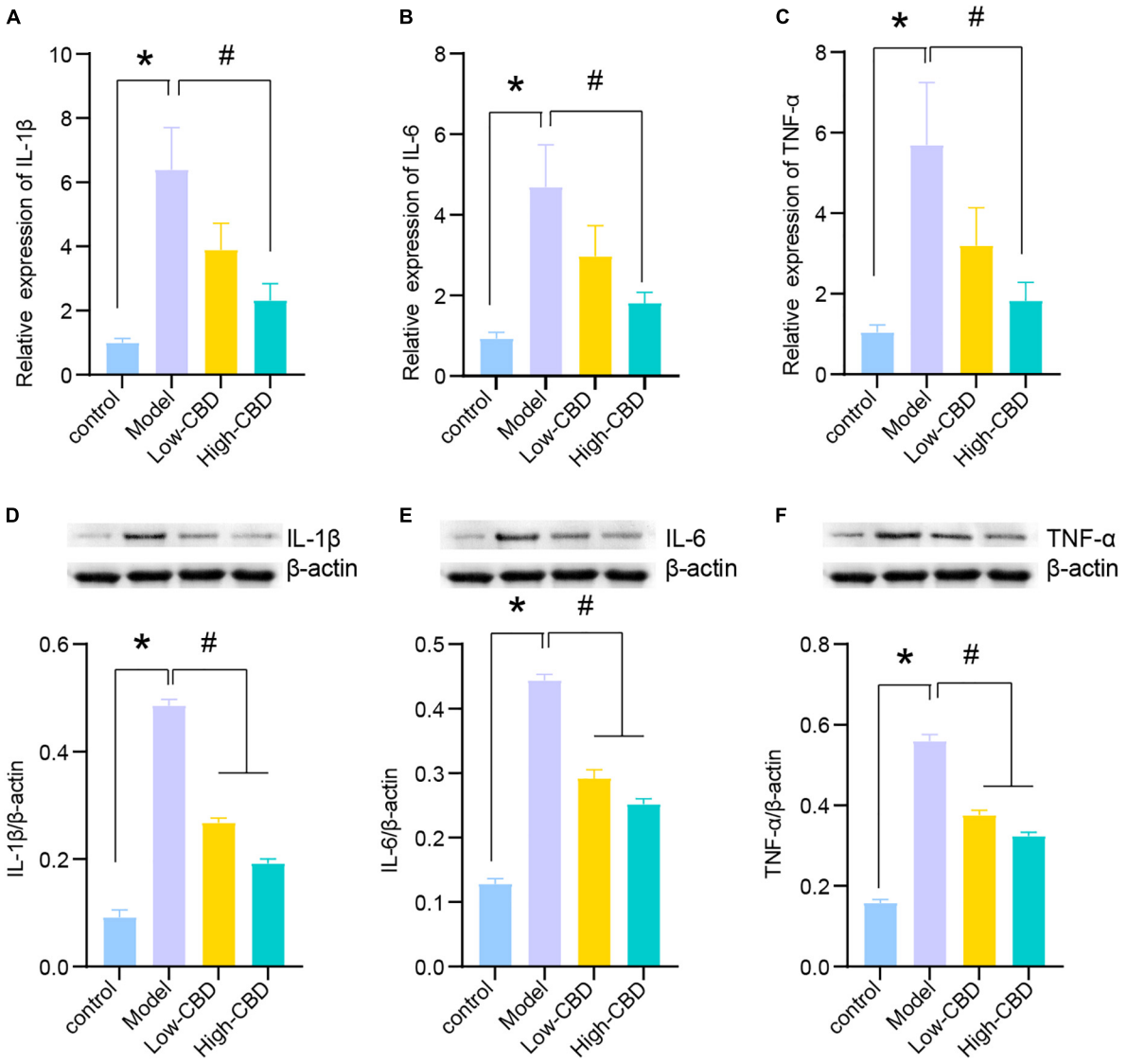

FIGURE 3
Effects of cannabidiol (CBD) on the expression of IL-1β, IL-6, and TNF-α in the temporal lobe cortex of epileptic rats. **(A-C)** IL-1β, IL-6, and TNF-α were detected by qRT-PCR. **(D-F)** IL-1β, IL-6, and TNF-α were detected by western blotting (WB). *Represents significant comparison with the control group, #represents significant comparison with the Model group, $P < 0.05$.

the CBZ than in the high-CBD groups (Supplementary Figure 1).

Cannabidiol partially regulates gut microbiota in epileptic rats

16S rDNA sequencing was performed on rat fecal samples. A Venn diagram was used to visualize the four groups of common and unique amplicon sequence variants (ASVs) (Figure 5A). ASVs were used to identify species characteristics. 89 ASVs were common among the four groups. There were 64 unique ASVs in the control group, 84 in the model group, 91 in the low-CBD group, and 155 unique ASVs in the high-CBD group. There were no significant differences among all groups' Chao1, Shannon, and Simpson indices. The results suggested no significant difference in the α-diversity of the gut microbiota of rats receiving different treatments (Figure 5B). However, ANOSIM analysis showed that the *R*-value was 0.33 and the *P*-value was 0.001 (Figure 5C), demonstrating that the intergroup difference exceeded the intragroup difference, and the grouping was meaningful. A Heat Map was used to visualize the classification information and relative abundance of the top 20 ASVs (Figure 5D).

10.3389/fnut.2022.1028459

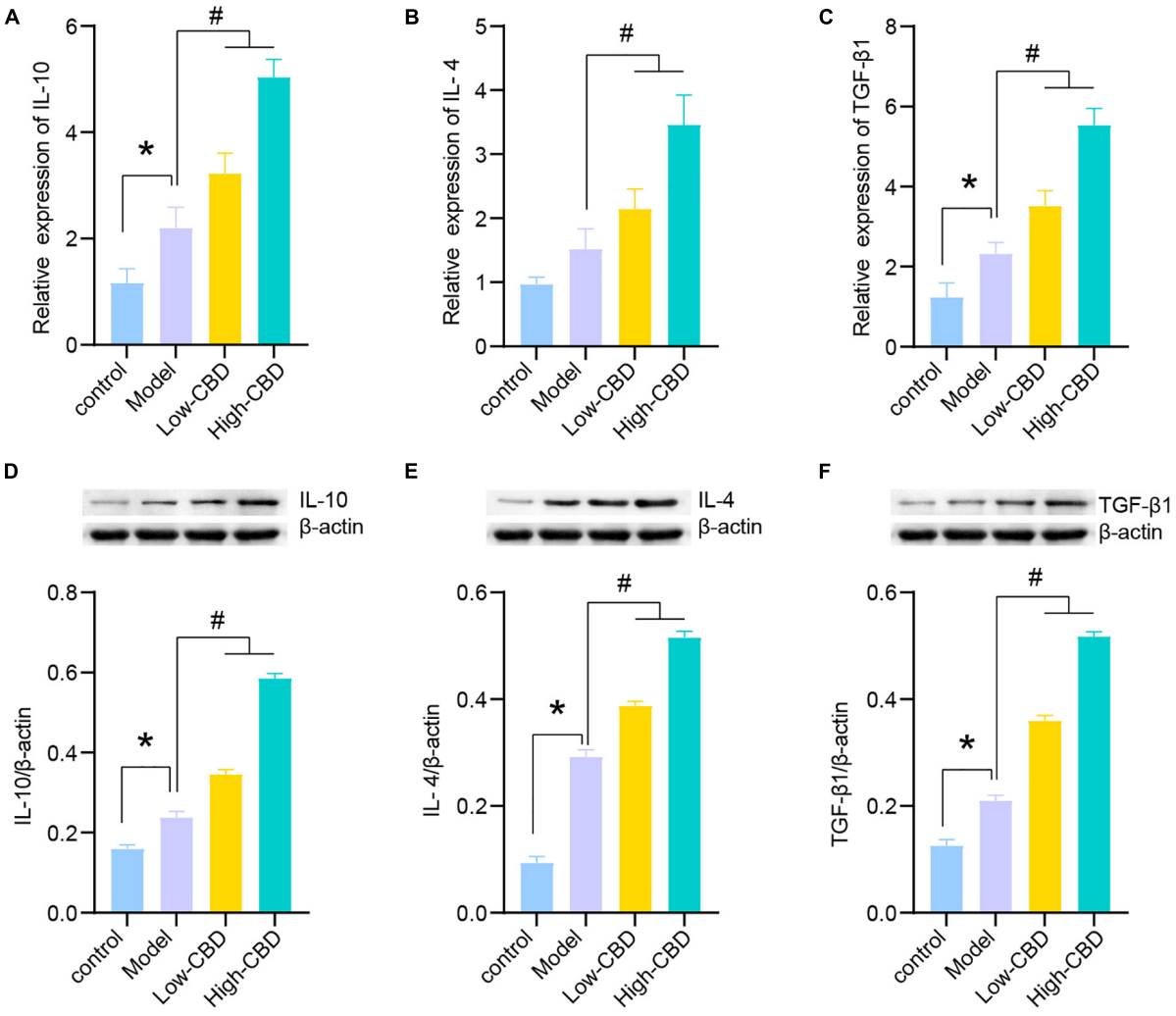

FIGURE 4
Effects of cannabidiol (CBD) on the expression of IL-10, IL-4, and TGF-β1 in the temporal lobe cortex of epileptic rats. **(A-C)** IL-10, IL-4, and TGF-β1 were detected by qRT-PCR. **(D-F)** IL-10, IL-4, and TGF-β1 were detected by western blotting (WB). *Represents significant comparison with the control group, #represents significant comparison with the Model group, $P < 0.05$.

We conducted a different analysis of gut microbiota at different levels to further clarify the influence of CBD on the abundance of specific microbiota in epileptic rats. At the genus level (Figures 6A–F), the abundance of *Helicobacter*, *Roseburia*, *Eubacterium_xylanophilum_group*, *Prevotellaceae_UCG-001*, *Ruminococcaceae_UCG-005*, and *Ruminococcus_2* were significantly different in the model group compared with the control group. However, the abundance of gut microbiota in epileptic rats was altered after the CBD intervention. Spearman's rank correlation coefficient showed a significant correlation between the abundance of gut microbiota and inflammatory factors (Figure 6G). Furthermore, the abundances of *Prevotellaceae_UCG-001* were negatively correlated with proinflammatory and anti-inflammatory factors. The abundances of *Helicobacter* and *Ruminococcaceae_UCG-005* were negatively correlated with proinflammatory factors, and *Roseburia*, *Eubacterium_xylanophilum_group*, and *Ruminococcus_2* were positively correlated with proinflammatory factors. Consequently, we conclude that the structure of gut microbiota of epileptic rats is dysregulated, and CBD could promote gut microbiota remodeling or rebalance to some extent.

Cannabidiol partially mediates gut microbiota metabolism in epileptic rats

Finally, to explore whether CBD has an effect on the metabolism of rats with Epilepsy, we performed an untargeted

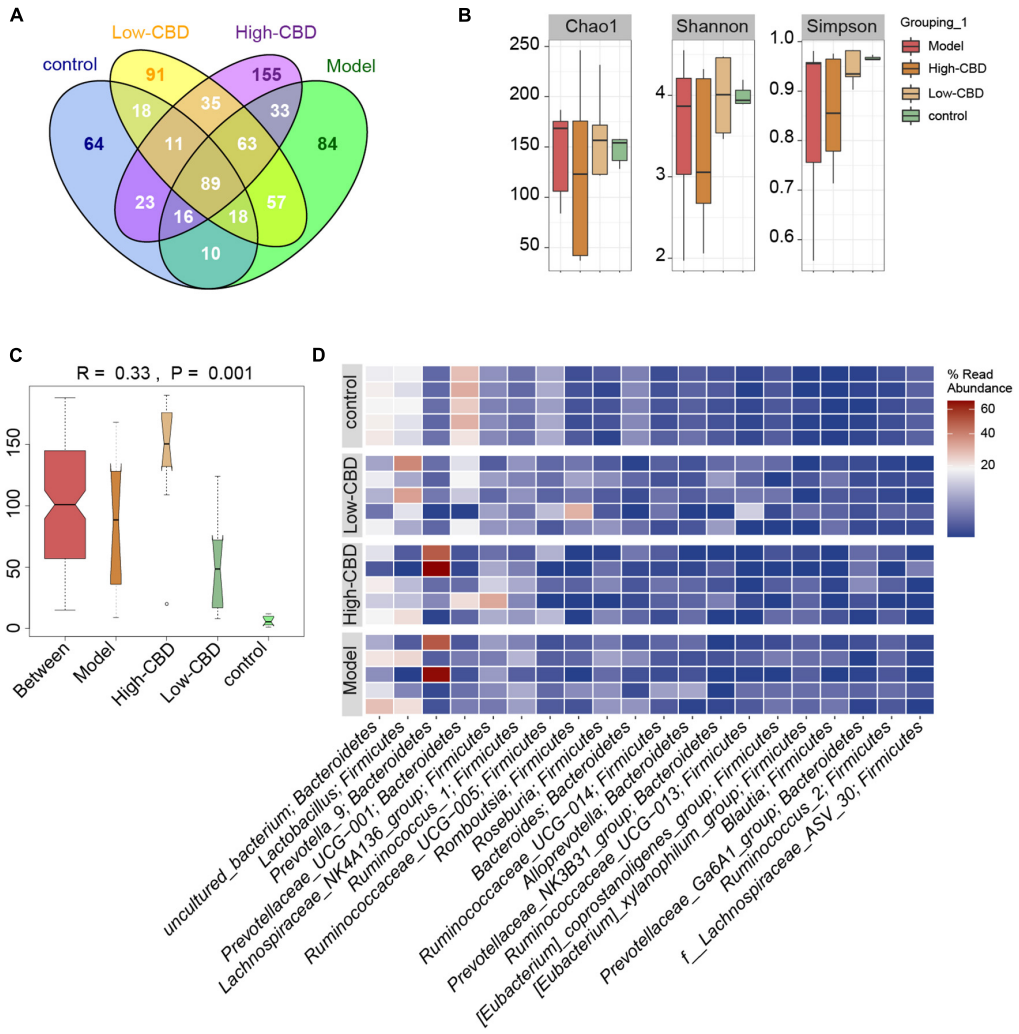

FIGURE 5
Effects of cannabidiol (CBD) on the gut microbiota structure in epileptic rats. **(A)** Venn diagram. **(B)** α-diversity analysis. **(C)** ANOSIM analysis. **(D)** The Heat Map visualization of the abundance and classification information of the top 20 ASVs. A color change from blue to red represents higher abundance.

metabolomics analysis of fecal samples from rats. A Heat Map was used to visualize the top 100 differential metabolites (Figure 7). It was clear that the abundance of metabolites differed among the four groups.

The results of partial least squares discriminant analysis (pLSDA) (Figure 8A) and sparse partial least squares discriminant analysis (spLSDA) (Figure 8B) showed that the sample points of the control and model groups were far from each other. In the pLSDA, the sample points of the low-CBD and high-CBD groups were far from those of the model group. In the spLSDA, the low-CBD and high-CBD sample points were far apart. The results demonstrated that the four groups of samples were separated. A bubble diagram was used to visualize the different metabolic pathways enriched in the top 25 (Figure 8C). Among these, the functional pathways of metabolism and genetic information processing at the L1 level were altered. The D-glutamine and D-glutamate metabolism; valine, leucine, and isoleucine biosynthesis; aminoacyl-tRNA biosynthesis; arginine biosynthesis; phenylalanine, tyrosine, and tryptophan biosynthesis; and phenylalanine metabolism were significantly different at the L3 level. We then analyzed the levels of metabolites (Figures 9A–H). Glycerophosphocholine (Figure 9B) was lower in the model and low-CBD groups compared with the control group but increased significantly in the high-CBD group. The levels of several metabolites, including 4-ethylbenzoic acid (Figure 9C), glycochenodeoxycholate (Figure 9E), indole-3-methyl acetate (Figure 9F), inosine (Figure 9G) and methylthioadenosine (Figure 9H) were significantly increased in the model group compared with those in the control group, while the levels

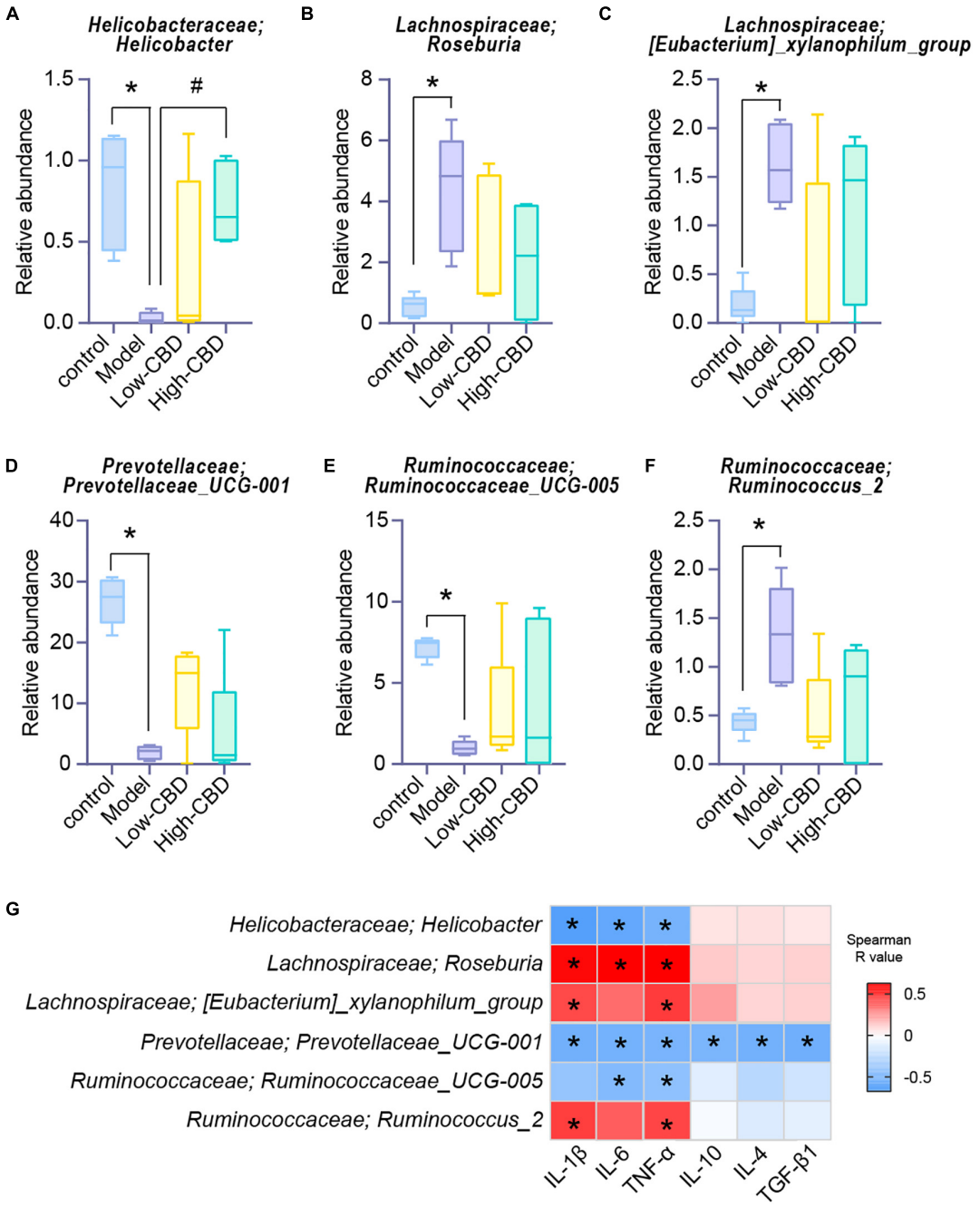

FIGURE 6
Effects of cannabidiol (CBD) on the changes of the abundance of gut microbiota in rats with Epilepsy. **(A-F)** At the genus level, the abundance of *Helicobacter*, *Roseburia*, *[Eubacterium]_xylanophilum_group*, *Prevotellaceae_UCG-001*, *Ruminococcaceae_UCG-005*, and *Ruminococcus_2*. *Represents significant comparison with the control group, #represents significant comparison with the Model group, $P < 0.05$. **(G)** Correlation analysis of gut bacteria and cytokines. Blue represents negative correlation, and red represents positive correlation; The larger the absolute value of R, the stronger the correlation; *indicates significant correlation.

of metabolites in the CBD treatment group were significantly lower compared to those in the model group.

The abundance of *Helicobacter*, *Roseburia*, *[Eubacterium]_xylanophilum_group*, and *Ruminococcus_2* was significantly associated with multiple metabolites at the genus level (Figure 9I). Among them, the levels of the metabolites glycerophosphocholine, butyrylcarnitine (C4), glycochenodeoxycholate, indole-3-methyl acetate, and methylthioadenosine were correlated with different bacterial communities.

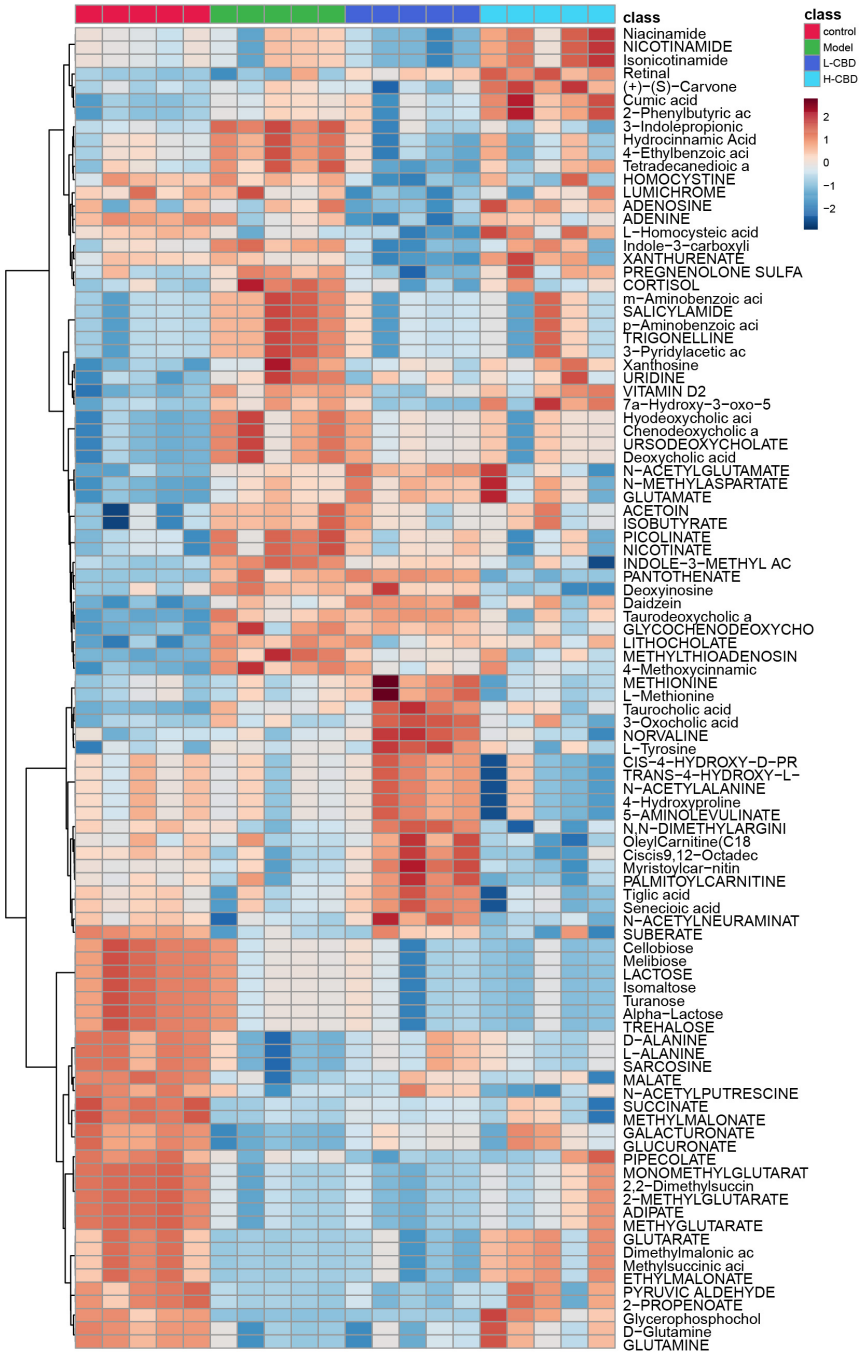

FIGURE 7
Differential metabolites abundance analysis. A change from blue to red indicates an increase in the levels of metabolite.

Discussion

Cannabidiol (CBD), a major non-psychoactive compound derived from cannabis, can potentially treat neuropsychiatric diseases (26). In this study, CBD treatment alleviated neuroinflammation in brain tissues of epileptic rats, reduced M1/M2 and played a neuroprotective role. In addition, we found that CBD may play a role in treating epileptic rats by regulating the gut microbiota and related metabolism.

The role of CBD in alleviating Epilepsy is well-known (27). Mori et al. found that CBD plays a neuroprotective role by reducing glial cell responses (28). This finding is consistent with the results of our study, where the number of microglial cells and proinflammatory M1 type positive cells

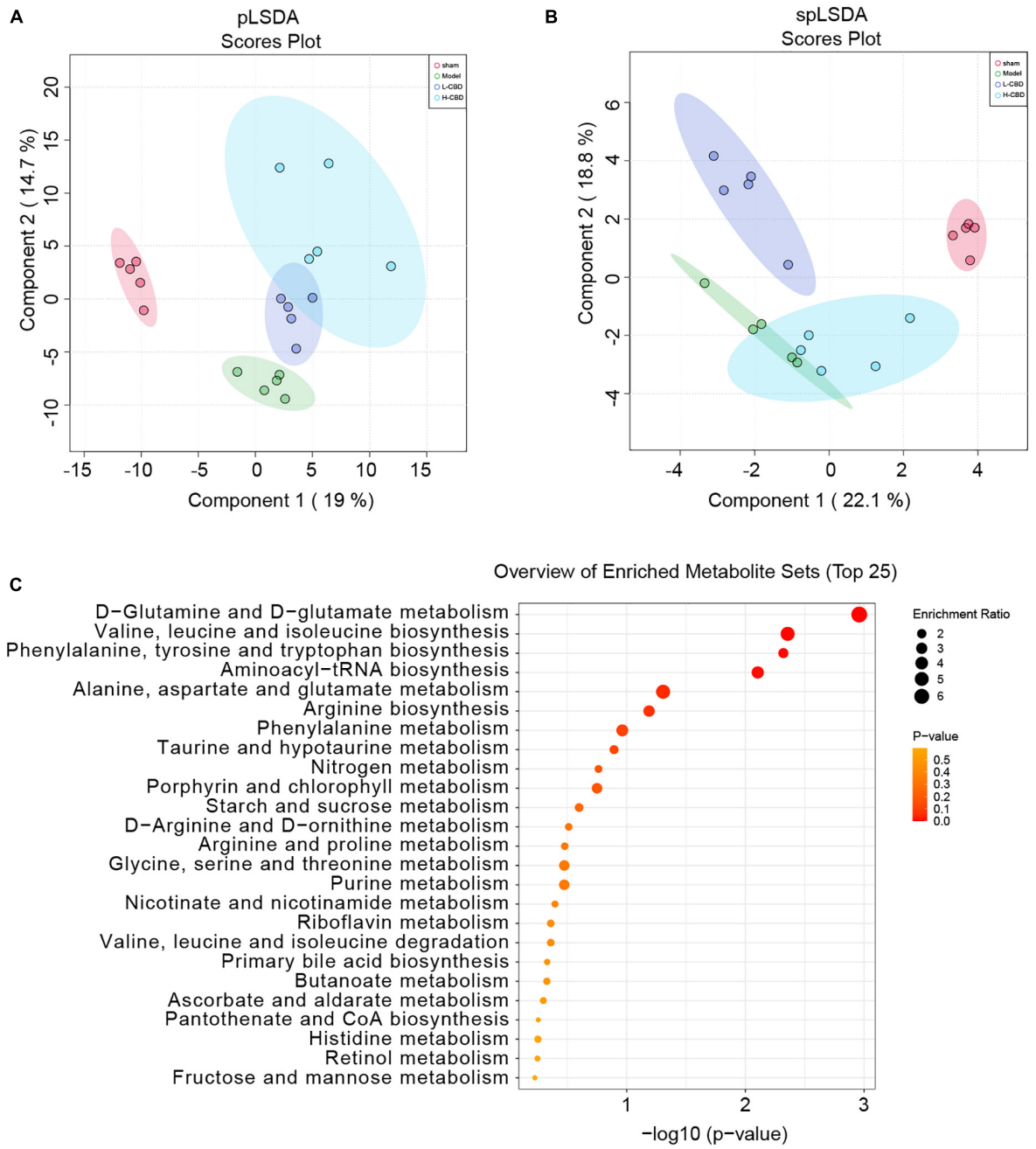

FIGURE 8
Effects of cannabidiol (CBD) on fecal metabolism in epileptic rats. **(A)** partial least squares discriminant analysis (pLSDA) analysis. **(B)** sparse partial least squares discriminant analysis (spLSDA) analysis. **(C)** Enrichment of the differential metabolic pathways. A color change from yellow to red represents the lower of the *P* value.

decreased, and the number of anti-inflammatory M2 type positive cells increased in epileptic rats treated with CBD. This suggests that CBD promotes microglial polarization into the M2 type. Furthermore, the expression of proinflammatory factors, including IL-6 and TNF-α, can be reduced to alleviate neuronal injury and play a neuroprotective role (29). We also found that the levels of IL-1β, IL-6, and TNF-α decreased, and levels of anti-inflammatory cytokines IL-10, TGF-β1, and IL-4 [regulatory factor with adaptive immunity (30)] increased. These confirmed the effectiveness of CBD in anti-neuroinflammation in rats with Epilepsy.

The gut microbiota plays an important role in maintaining the stability of the gut barrier and resisting pathogen invasion (31). Several studies have found that gut microbiota plays

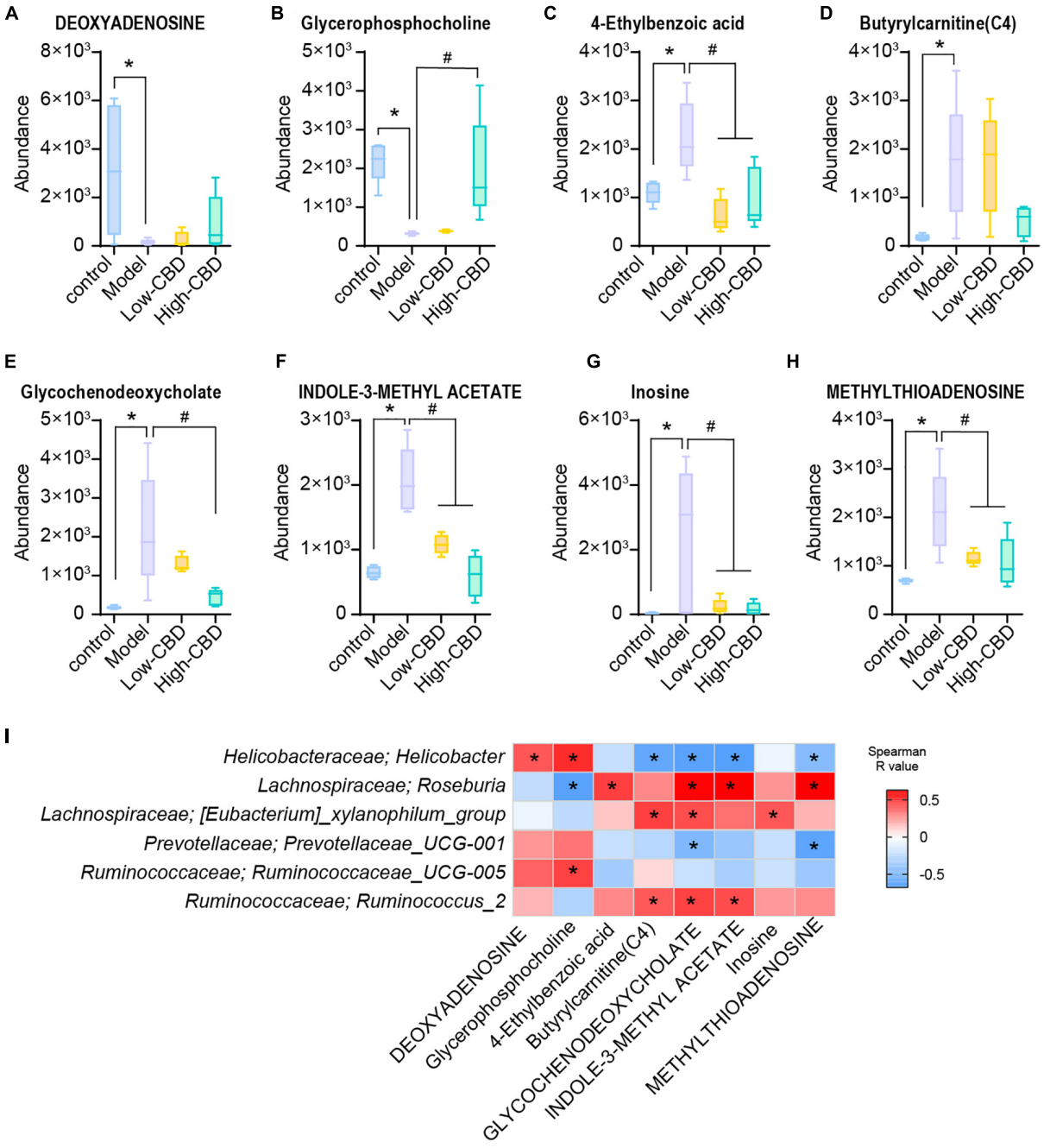

FIGURE 9
Effects of cannabidiol (CBD) on the changes of the levels of metabolites in rats with Epilepsy. **(A-H)** Relative abundance of deoxyadenosing, glycerophosphocholine, 4-ethylbenzoic acid, butyrylcarnitine (C4), glycochenodeoxycholate, indole-3-methyl acetate, inosine, and methylthioadenosine. *Indicates a significant difference compared with the control group and #indicates a significant difference compared with the model group, $P < 0.05$. **(I)** The relationship between the gut bacteria and the different metabolites. Blue represents negative correlation and red represents positive correlation. The larger the absolute value of R, the stronger the correlation; *indicates significant correlation.

an important role in the pathophysiology of nervous system diseases, including spinal cord injury (SCI) (32), neuromyelitis Optica (NMO) (33), Alzheimer's disease (AD) (34), and multiple sclerosis (MS) (35). şafak et al. demonstrated that dysregulation of gut microbiota could affect the development of Epilepsy (36). In our study, the abundance of *Helicobacter*, *Prevotellaceae_UCG-001*, and *Ruminococcaceae_UCG-005* was significantly decreased in epileptic rats, whereas the abundance of *Roseburia*, *[Eubacterium]_xylanophilum_group*, and *Ruminococcus_2* was significantly increased. Exposure to

various compounds, including drugs for Epilepsy, can positively or negatively alter the gut microbiota and reduce or exacerbate seizures (37). Although some antiepileptic drugs affect the growth and metabolism of gut bacteria, for example, lamotrigine suppresses ribosome biogenesis in *E. coli*, and thus may restrain its growth (38), there is little evidence of direct interaction between antiepileptic drugs and the gut microbiome. In our study, we found that the composition of the gut microbiota of epileptic rats was disordered. CBD treatment was beneficial for the restoration of at least part of the gut bacterial abundance in epileptic rats, such as *Prevotellaceae_UCG-001*. To the best of our knowledge, *Prevotellaceae UCG-001* is an SCFA-producing bacterium that plays an anti-inflammatory role in immune cells and inhibits the growth of invasive pathogens (39). This is an encouraging finding, suggesting that CBD may improve Epilepsy through beneficial gut bacteria.

Moreover, study has found that the gut microbiome can affect the occurrence and development of epilepsy by regulating the polarization of microglia (40). Activation of the M2 phenotype could suppress subsequent inflammation in epilepsy (40). Combined with the above analysis, microglia M2 polarization might be involved in the process of gut microbiome affecting epileptic seizures. Recent study has found that modulating the microbiome can affect the expression of IL-1β, IL-6, and TNF-α (41). Transplantation of a disturbed gut microbiome exacerbates inflammatory damage, including stimulating the expression of pro-inflammatory factors IL-1β, IL-6, and TNF-α, and reducing the levels of anti-inflammatory IL-10, IL-4, and TGF-β (42). From this, we could speculate that the gut microbiome might affect epileptic seizures by regulating the expression of inflammatory factors while regulating M2 polarization.

Gut microbiota produces a variety of substances that alter the excitation-inhibitory balance of the nervous system, including metabolites that act as neuromodulators (37). Correlation analysis showed that glycochenodeoxycholate levels were significantly correlated with different gut microbiota. Glycochenodeoxycholate is an important component of bile acids and is involved in steatosis and poor glucose tolerance (43). Gut microbiota can produce bioactive metabolites that directly or indirectly affect host physiology and metabolic balance (44). Dysfunctional glutamate metabolism in astrocytes can directly lead to neuronal over-excitation, which plays an important role in the pathogenesis of Epilepsy (45). Administration of valine, leucine, isoleucine, and branched-chain amino acids to epileptic rats increases the average latency period of epileptic seizures (46). In addition, mitochondrial aminoacyl-tRNA synthetases (AaRSs) provide amino acids homologous to tRNAs and regulate a variety of cellular processes. One study showed that mutations in human mitochondrial AaRSs cause epilepsy in infants (47). Acute supplementation of branched-chain amino acids (valine, leucine, and isoleucine) reduced seizures, whereas long-term oral supplementation with branched-chain amino acids led to worsening seizures (48). We also found a statistical difference in different groups' enrichment of D-glutamine and D-glutamate metabolism, valine, leucine, isoleucine biosynthesis, and aminoacyl-tRNA biosynthesis. Hence, we hypothesized that CBD might be involved in regulating the metabolic function of the gut microbiota of epileptic rats. Furthermore, the composition of the gut microbiome and the levels of IL-10, IL-4, and TNF-α were altered in mice after drug intervention, and regulation of SCFAs, microbial metabolites, could affect the expression of IL-6 (49). Combined with the above analysis, we could speculate that the gut microbiome is involved in the process of CBD alleviating epilepsy, which might be mediated by microbial metabolites regulating inflammatory factors.

There were some limitations to our study. Although there are some network and neurochemical similarities between human TLE and Li-pilocarpine models, including increased neurotrophins and cognitive and memory disorders (50, 51), because these models have not been fully validated clinically, they cannot predict clinical responses to all treatment strategies. In addition, owing to the inherent limitations of the Li-pilocarpine model, the frequency and severity of induced spontaneous seizures vary, which may lead to unavoidable systematic errors. Therefore, in the selection of samples and sample size, the CBD group alone could be set, relevant clinical samples could be supplemented, and the number of samples could be increased. Furthermore, animal behavioral tests, untargeted metabolic analysis of blood, and targeted analysis of related metabolites could be supplemented to obtain more comprehensive data. In the future, we intend to combine clinical samples and fecal microbiota transplantation (FMT) to further study the mechanism of CBD and gut microbiota in Epilepsy.

Conclusion

In conclusion, CBD could effectively inhibit neuroinflammation in epileptic rats. Furthermore, CBD might have a tendency to promote gut microbiota remodeling and altered the metabolic pathways in the gut of epileptic rats. It is not yet clear whether CBD manipulates the gut microbiota to improve the symptoms of Epilepsy. We hypothesized that the improvement of CBD in Epilepsy might be through changes induced in the gut microbiota and will continue to explore this area in further research.

Data availability statement

The datasets presented in this study can be found in online repositories. The names of the repository/repositories and accession number(s) can be found below: https://www.ncbi.nlm.nih.gov/, PRJNA735800.

Ethics statement

This animal study was reviewed and approved by the Animal Ethical and Welfare Committee and The Second Xiangya Hospital, Central South University (No. 2021523).

Author contributions

LqL and DM conceived and designed the experiments. LjL and XL analyzed the data. JXu and JXi prepared the figures. XG performed the experiments and drafted the work or revised it critically for important content. All authors contributed to manuscript revision, read, and approved the submitted version.

Funding

This research was supported by Natural Science Foundation of Hunan province (No. 2022JJ40684).

Acknowledgments

Special thanks to the staff within the Second Xiangya Hospital, Central South University who provide technical assistance to us.

Conflict of interest

The authors declare that the research was conducted in the absence of any commercial or financial relationships that could be construed as a potential conflict of interest.

Publisher's note

Supplementary material

The Supplementary Material for this article can be found online at: https://www.frontiersin.org/articles/10.3389/fnut.2022.1028459/full#supplementary-material

SUPPLEMENTARY FIGURE 1
After cannabidiol (CBD) and carbamazepine (CBZ) treatment, gene and protein expression of IL-1β, IL-6, TNF-α, IL-10, IL-4, and TGF-β1 was determined. *Represents significant comparison with the control group, #represents significant comparison with the Model group, and represents significant comparison with the high-CBD group, $P < 0.05$.

References

1. Thijs RD, Surges R, O'Brien TJ, Sander JW. Epilepsy in adults. *Lancet.* (2019) 393:689–701. doi: 10.1016/S0140-6736(18)32596-0

2. Gorter JA, van Vliet EA, Aronica E, Breit T, Rauwerda H, Lopes da Silva FH, et al. Potential new antiepileptogenic targets indicated by microarray analysis in a rat model for temporal lobe Epilepsy. *J Neurosci.* (2006) 26:11083–110. doi: 10.1523/JNEUROSCI.2766-06.2006

3. Webster KM, Sun M, Crack P, O'Brien TJ, Shultz SR, Semple BD. Inflammation in epileptogenesis after traumatic brain injury. *J Neuroinflamm.* (2017) 14:10. doi: 10.1186/s12974-016-0786-1

4. Nayak D, Roth TL, McGavern DB. Microglia development and function. *Annu Rev Immunol.* (2014) 32:367–402. doi: 10.1146/annurev-immunol-032713-120240

5. Vezzani A, French J, Bartfai T, Baram TZ. The role of inflammation in Epilepsy. *Nat Rev Neurol.* (2011) 7:31–40. doi: 10.1038/nrneurol.2010.178

6. Leal B, Chaves J, Carvalho C, Rangel R, Santos A, Bettencourt A, et al. Brain expression of inflammatory mediators in mesial temporal lobe Epilepsy patients. *J Neuroimmunol.* (2017) 313:82–8. doi: 10.1016/j.jneuroim.2017.10.014

7. Hodges SL, Lugo JN. Therapeutic role of targeting mtor signaling and neuroinflammation in Epilepsy. *Epilepsy Res.* (2020) 161:106282. doi: 10.1016/j.eplepsyres.2020.106282

8. Liu L, Xu Y, Dai H, Tan S, Mao X, Chen Z. Dynorphin activation of kappa opioid receptor promotes microglial polarization toward M2 phenotype Via Tlr4/Nf-Kb pathway. *Cell Biosci.* (2020) 10:42. doi: 10.1186/s13578-020-00387-2

9. Yu T, Huo L, Lei J, Sun JJ, Wang H. Modulation of microglia M2 polarization and alleviation of hippocampal neuron injury by Mir-106b-5p/Rgma in a mouse model of status epilepticus. *Inflammation.* (2022): [Epub ahead of print]. doi: 10.1007/s10753-022-01686-1

10. Liu JT, Wu SX, Zhang H, Kuang F. Inhibition of Myd88 signaling skews microglia/macrophage polarization and attenuates neuronal apoptosis in the hippocampus after status epilepticus in mice. *Neurotherapeutics.* (2018) 15:1093–111. doi: 10.1007/s13311-018-0653-0

11. Mannucci C, Navarra M, Calapai F, Spagnolo EV, Busardo FP, Cas RD, et al. Neurological aspects of medical use of cannabidiol. *CNS Neurol Disord Drug Targets.* (2017) 16:541–53. doi: 10.2174/1871527316666170413114210

12. VanDolah HJ, Bauer BA, Mauck KF. Clinicians' guide to cannabidiol and hemp oils. *Mayo Clin Proc.* (2019) 94:1840–51. doi: 10.1016/j.mayocp.2019.01.003

13. Leo A, Russo E, Elia M. Cannabidiol and Epilepsy: rationale and therapeutic potential. *Pharmacol Res.* (2016) 107:85–92. doi: 10.1016/j.phrs.2016.03.005

14. De Caro C, Iannone LF, Citraro R, Striano P, De Sarro G, Constanti A, et al. Can we 'Seize' the gut microbiota to treat Epilepsy? *Neurosci Biobehav Rev.* (2019) 107:750–64. doi: 10.1016/j.neubiorev.2019.10.002

15. Grenham S, Clarke G, Cryan JF, Dinan TG. Brain-gut-microbe communication in health and disease. *Front Physiol.* (2011) 2:94. doi: 10.3389/fphys.2011.00094

16. Lum GR, Olson CA, Hsiao EY. Emerging roles for the intestinal microbiome in Epilepsy. *Neurobiol Dis.* (2020) 135:104576. doi: 10.1016/j.nbd.2019.104576

17. Iannone LF, Gomez-Eguilaz M, Citaro R, Russo E. The potential role of interventions impacting on gut-microbiota in Epilepsy. *Expert Rev Clin Pharmacol.* (2020) 13:423–35. doi: 10.1080/17512433.2020.1759414

18. Al-Ghezi ZZ, Busbee PB, Alghetaa H, Nagarkatti PS, Nagarkatti M. Combination of cannabinoids, Delta-9-Tetrahydrocannabinol (THC) and cannabidiol (CBD), mitigates experimental autoimmune encephalomyelitis (EAE) by altering the gut microbiome. *Brain Behav Immun.* (2019) 82:25–35. doi: 10.1016/j.bbi.2019.07.028

19. Nichols JM, Kaplan BLF. Immune responses regulated by cannabidiol. *Cannabis Cannabinoid Res.* (2020) 5:12–31. doi: 10.1089/can.2018.0073

20. Jones NA, Glyn SE, Akiyama S, Hill TD, Hill AJ, Weston SE, et al. Cannabidiol exerts anti-convulsant effects in animal models of temporal lobe and partial seizures. *Seizure.* (2012) 21:344–52. doi: 10.1016/j.seizure.2012.03.001

21. Barzroodi Pour M, Bayat M, Navazesh A, Soleimani M, Karimzadeh F. Exercise improved the anti-epileptic effect of carbamazepine through gaba enhancement in epileptic rats. *Neurochem Res.* (2021) 46:2112–30. doi: 10.1007/s11064-021-03349-3

22. Racine RJ. Modification of seizure activity by electrical stimulation. Ii. motor seizure. *Electroencephalogr Clin Neurophysiol.* (1972) 32:281–94. doi: 10.1016/0013-4694(72)90177-0

23. Zeng X, Hu K, Chen L, Zhou L, Luo W, Li C, et al. The effects of ginsenoside compound K against Epilepsy by enhancing the gamma-aminobutyric acid signaling pathway. *Front Pharmacol.* (2018) 9:1020. doi: 10.3389/fphar.2018.01020

24. Shen Y, Peng W, Chen Q, Hammock BD, Liu J, Li D, et al. Anti-inflammatory treatment with a soluble epoxide hydrolase inhibitor attenuates seizures and Epilepsy-associated depression in the licl-pilocarpine post-status epilepticus rat model. *Brain Behav Immun.* (2019) 81:535–44. doi: 10.1016/j.bbi.2019.07.014

25. Sun Z, Gao C, Gao D, Sun R, Li W, Wang F, et al. Reduction in pericyte coverage leads to blood-brain barrier dysfunction via endothelial transcytosis following chronic cerebral hypoperfusion. *Fluids Barriers CNS.* (2021) 18:21. doi: 10.1186/s12987-021-00255-2

26. Elsaid S, Kloiber S, Le Foll B. Effects of cannabidiol (CBD) in neuropsychiatric disorders: a review of pre-clinical and clinical findings. *Prog Mol Biol Transl Sci.* (2019) 167:25–75. doi: 10.1016/bs.pmbts.2019.06.005

27. Patra PH, Barker-Haliski M, White HS, Whalley BJ, Glyn S, Sandhu H, et al. Cannabidiol reduces seizures and associated behavioral comorbidities in a range of animal seizure and Epilepsy models. *Epilepsia.* (2019) 60:303–14. doi: 10.1111/epi.14629

28. Mori MA, Meyer E, Soares LM, Milani H, Guimaraes FS, de Oliveira RMW. Cannabidiol reduces neuroinflammation and promotes neuroplasticity and functional recovery after brain ischemia. *Prog Neuropsychopharmacol Biol Psychiatry.* (2017) 75:94–105. doi: 10.1016/j.pnpbp.2016.11.005

29. Castillo A, Tolon MR, Fernandez-Ruiz J, Romero J, Martinez-Orgado J. The neuroprotective effect of cannabidiol in an in vitro model of newborn hypoxic-ischemic brain damage in mice is mediated by Cb(2) and adenosine receptors. *Neurobiol Dis.* (2010) 37:434–40. doi: 10.1016/j.nbd.2009.10.023

30. Shimabukuro-Vornhagen A, Godel P, Subklewe M, Stemmler HJ, Schlosser HA, Schlaak M, et al. Cytokine release syndrome. *J Immunother Cancer.* (2018) 6:56. doi: 10.1186/s40425-018-0343-9

31. Zhang YJ, Li S, Gan RY, Zhou T, Xu DP, Li HB. Impacts of gut bacteria on human health and diseases. *Int J Mol Sci.* (2015) 16:7493–519. doi: 10.3390/ijms16047493

32. Gungor B, Adiguzel E, Gursel I, Yilmaz B, Gursel M. Intestinal microbiota in patients with spinal cord injury. *PLoS One.* (2016) 11:e0145878. doi: 10.1371/journal.pone.0145878

33. Cree BA, Spencer CM, Varrin-Doyer M, Baranzini SE, Zamvil SS. Gut microbiome analysis in neuromyelitis optica reveals overabundance of clostridium perfringens. *Ann Neurol.* (2016) 80:443–7. doi: 10.1002/ana.24718

34. Li B, He Y, Ma J, Huang P, Du J, Cao L, et al. Mild cognitive impairment has similar alterations as Alzheimer's disease in gut microbiota. *Alzheimers Dement.* (2019) 15:1357–66. doi: 10.1016/j.jalz.2019.07.002

35. Cosorich I, Dalla-Costa G, Sorini C, Ferrarese R, Messina MJ, Dolpady J, et al. High frequency of intestinal Th17 cells correlates with microbiota alterations and disease activity in multiple sclerosis. *Sci Adv.* (2017) 3:e1700492. doi: 10.1126/sciadv.1700492

36. Safak B, Altunan B, Topcu B, Eren Topkaya A. The gut microbiome in Epilepsy. *Microb Pathog.* (2020) 139:103853. doi: 10.1016/j.micpath.2019.103853

37. Amlerova J, Sroubek J, Angelucci F, Hort J. Evidences for a role of gut microbiota in pathogenesis and management of Epilepsy. *Int J Mol Sci.* (2021) 22:5576. doi: 10.3390/ijms22115576

38. Stokes JM, Davis JH, Mangat CS, Williamson JR, Brown ED. Discovery of a small molecule that inhibits bacterial ribosome biogenesis. *Elife.* (2014) 3:e03574. doi: 10.7554/eLife.03574

39. Zhou X, Zhang B, Zhao X, Lin Y, Wang J, Wang X, et al. Chlorogenic acid supplementation ameliorates hyperuricemia, relieves renal inflammation, and modulates intestinal homeostasis. *Food Funct.* (2021) 12:5637–49. doi: 10.1039/d0fo03199b

40. Ding X, Zhou J, Zhao L, Chen M, Wang S, Zhang M, et al. Intestinal flora composition determines microglia activation and improves epileptic episode progress. *Front Cell Infect Microbiol.* (2022) 12:835217. doi: 10.3389/fcimb.2022.835217

41. Yun SW, Kim JK, Han MJ, Kim DH. Lacticaseibacillus Paracasei Nk112 mitigates *Escherichia Coli*-induced depression and cognitive impairment in mice by regulating Il-6 expression and gut microbiota. *Benef Microbes.* (2021) 12:541–51. doi: 10.3920/bm2020.0109

42. Rong Z, Huang Y, Cai H, Chen M, Wang H, Liu G, et al. Gut microbiota disorders promote inflammation and aggravate spinal cord injury through the Tlr4/Myd88 signaling pathway. *Front Nutr.* (2021) 8:702659. doi: 10.3389/fnut.2021.702659

43. Sun L, Pang Y, Wang X, Wu Q, Liu H, Liu B, et al. Ablation of gut microbiota alleviates obesity-induced hepatic steatosis and glucose intolerance by modulating bile acid metabolism in hamsters. *Acta Pharm Sin B.* (2019) 9:702–10. doi: 10.1016/j.apsb.2019.02.004

44. Tang WHW, Li DY, Hazen SL. Dietary metabolism, the gut microbiome, and heart failure. *Nat Rev Cardiol.* (2019) 16:137–54. doi: 10.1038/s41569-018-0108-7

45. Boison D, Steinhauser C. Epilepsy and astrocyte energy metabolism. *Glia.* (2018) 66:1235–43. doi: 10.1002/glia.23247

46. Skeie B, Petersen AJ, Manner T, Askanazi J, Steen PA. Effects of valine, leucine, isoleucine, and a balanced amino acid solution on the seizure threshold to picrotoxin in rats. *Pharmacol Biochem Behav.* (1994) 48:101–3. doi: 10.1016/0091-3057(94)90504-5

47. Almalki A, Alston CL, Parker A, Simonic I, Mehta SG, He L, et al. Mutation of the human Mitochondrial Phenylalanine-Trna synthetase causes Infantile-Onset Epilepsy and Cytochrome C Oxidase Deficiency. *Biochim Biophys Acta.* (2014) 1842:56–64. doi: 10.1016/j.bbadis.2013.10.008

48. Gruenbaum SE, Dhaher R, Rapuano A, Zaveri HP, Tang A, de Lanerolle N, et al. Effects of branched-chain amino acid supplementation on spontaneous seizures and neuronal viability in a model of mesial temporal lobe Epilepsy. *J Neurosurg Anesthesiol.* (2019) 31:247–56. doi: 10.1097/ANA.0000000000000499

49. Chun J, Lee SM, Ahn YM, Baek MG, Yi H, Shin S, et al. Modulation of the gut microbiota by sihocheonggan-tang shapes the immune responses of atopic dermatitis. *Front Pharmacol.* (2021) 12:722730. doi: 10.3389/fphar.2021.722730

50. Kandratavicius L, Balista PA, Lopes-Aguiar C, Ruggiero RN, Umeoka EH, Garcia-Cairasco N, et al. Animal models of Epilepsy: use and limitations. *Neuropsychiatr Dis Treat.* (2014) 10:1693–705. doi: 10.2147/NDT.S50371

51. Grone BP, Baraban SC. Animal models in Epilepsy research: legacies and new directions. *Nat Neurosci.* (2015) 18:339–43. doi: 10.1038/nn.3934

frontiers | Frontiers in Nutrition

TYPE Original Research
PUBLISHED 16 November 2022
DOI 10.3389/fnut.2022.1018026

OPEN ACCESS

EDITED BY
Hui Han,
Chinese Academy of Sciences (CAS), China

REVIEWED BY
Md. Abul Kalam Azad,
Institute of Subtropical Agriculture (CAS), China
Wuyundalai Bao,
Inner Mongolia Agricultural University, China

*CORRESPONDENCE
Peihua Zhang
peiqin41-@163.com
Jie Ma
Jie_Ma2022@stu.hunau.edu.cn

SPECIALTY SECTION
This article was submitted to Nutrition and Microbes, a section of the journal Frontiers in Nutrition

RECEIVED 12 August 2022
ACCEPTED 31 October 2022
PUBLISHED 16 November 2022

CITATION
Wang K, Zhou M, Gong X, Zhou Y, Chen J, Ma J and Zhang P (2022) Starch–protein interaction effects on lipid metabolism and gut microbes in host.
Front. Nutr. 9:1018026.
doi: 10.3389/fnut.2022.1018026

Starch–protein interaction effects on lipid metabolism and gut microbes in host

Kaijun Wang[1,2], Miao Zhou[1], Xinyu Gong[1], Yuqiao Zhou[1], Jiayi Chen[3], Jie Ma[1]* and Peihua Zhang[1]*

[1]Animal Nutritional Genome and Germplasm Innovation Research Center, College of Animal Science and Technology, Hunan Agricultural University, Changsha, Hunan, China, [2]College of Animal Science and Technology, State Key Laboratory for Conservation and Utilization of Subtropical Agro-Bioresources, Guangxi University, Nanning, Guangxi, China, [3]Academician Workstation, Changsha Medical University, Changsha, Hunan, China

The purpose of this experiment was to investigate the effects of different starch and protein levels on lipid metabolism and gut microbes in mice of different genders. A total of 160 male mice were randomly assigned to sixteen groups and fed a 4 × 4 Latin square design with dietary protein concentrations of 16, 18, 20, and 22%, and starch concentrations of 50, 52, 54, and 56%, respectively. The results of the study showed that different proportions of starch and protein had obvious effects on the liver index of mice, and there was a significant interaction between starch and protein on the liver index ($p = 0.005$). Compared with other protein ratio diets, 18% protein diet significantly increased the serum TBA concentration of mice ($p < 0.001$), and different starch ratio diets had no effect on serum TBA concentration ($p = 0.442$). It was proved from the results of ileal tissue HE staining that the low protein diet and the low starch diet were more favorable. There was a significant interaction between diets with different starch and protein levels on *Bacteroidetes*, *Firmicutes* and *Proteobacteria* abundance in feces of mice ($p < 0.001$). Compared with 16 and 18% protein ratio diets, both 20 and 22% protein diets significantly decreased the *Parabacteroides* and *Alistipes* abundance in feces of mice ($p < 0.05$), and 52% starch ratio diet significantly decreased the *Parabacteroides* and *Alistipes* abundance than 50% starch ratio diet of mice ($p < 0.05$). There was a significant interaction between diets with different starch and protein levels on *Parabacteroides* ($p = 0.014$) and *Alistipes* ($p = 0.001$) abundance in feces of mice. Taken together, our results suggest that a low protein and starch diet can alter lipid metabolism and gut microbes in mice.

KEYWORDS

starch, protein, lipid, gut, microbes

Introduction

According to the World Health Organization, more than 1 billion people worldwide are obese—650 million adults in 2022, which represents a health risk (1). Obesity is a nutritional disorder caused by an imbalance between energy intake and expenditure (2). Over the last few decades, obesity, cardiovascular disease, and type 2 diabetes have been on the rise worldwide, in order to prevent those diseases, numerous studies have attempted to reduce starch digestion and glycemic index through human diets (3–5). Recent years have seen a growing interest in developing healthy food ingredients that may enhance their protein, fiber, and nutraceutical qualities (6). Therefore, macro- and micronutrients with high participation in the diet, such as starch and protein, need to be studied and in order to develop functional foods, nutritional value and technological function had to be balanced correctly (7–9).

Historically, starch has been a major source of carbohydrates in human diets, which was absorbed as monosaccharides in the digestive tract, different functions were performed by foods depending on their chemical properties, their susceptibility to amylase, and their rate of glucose release and absorption in the gastrointestinal tract (10, 11). In order to maintain a high level of protein, new raw materials, such as soya, amaranth grain, or buckwheat, have been used as well as improved the final product's nutritional quality and functional properties (12). Additionally, it may reduce the glycemic index (GI) of starch-based foods and prevent diabetic complications. By obstructing enzyme binding sites, protein interferes with nutritional properties and facilitates starch malabsorption in the study on starch hydrolysis (13). Animals depended on dietary protein to function physiologically. The benefits of low-protein diets in terms of resource conservation and reducing nitrogen emissions have received considerable attention in recent years. Researchers have found that reducing dietary protein levels by 3 percentage points can enhance lipid metabolism in skeletal muscle without affecting growth in pigs, while the performance of growth would be adversely affected by protein reduction of exceeding 4 percentage points (14, 15). There was ample evidence that optimum nitrogen utilization for protein accretion can be achieved by reducing protein intake in the diet and simultaneously supplementing crystalline amino acids (16).

To coordinate body health, the host developed a huge microbiota at birth. The abundance of microbes also changed and played different roles at different stages (17, 18). A better understanding of the interactions between host and gut microbes was crucial to study the complex relationship between host and microbiota. The molecules involved in this interaction could be measured, especially the microbiota produced metabolites that were available to the host. Animal health depended on gut microbiota, which were involved in digestion, metabolism, immunity, and defense against pathogens (19–21). Diet, environment, and age all influenced gut microbiota composition and activity, but diet played the largest role among them (22–24). Besides affecting the composition of the gut microbiota, diet also influenced the state of the immune system (25).

Starch and protein were thermodynamically incompatible to form complexes, but the interaction between them can also affect their respective physicochemical property (26, 27). Protein can also interact with lipid through hydrophobic or electrostatic interaction to affect their property (28, 29). These various binary interactions have been studied extensively, but to gain a better understanding of factors that can affect the quality of food product interaction between starch, protein and lipid need to be examined in detail (27, 30). There was currently little knowledge of how a low-protein diet affected the gut micro-environment and how it can solve environmental problems. The purpose of this study was to investigate the effect of different dietary protein and starch levels on lipid metabolism in mice. Moreover, we examined whether improvements in lipid metabolism also affected intestinal microbiota at different proteins and starches levels. Using male mice as a model, it was possible to systematically study the importance of different protein and starch levels on fat metabolism in mice, and to evaluate the possible harmful or beneficial effect of different levels of these two substances on the structure of the gastrointestinal tract.

Materials and methods

Animals and dietary treatments

This experiment was approved by the Hunan Agricultural University Institutional Animal Care and Use Committee (202105). The male C57 mice were 4 weeks old and purchased from SLAC Laboratory Animal Central (Changsha, China). The mice were housed in a controlled environment (temperature: 25 ± 2°C, relative humidity: 45–60%, and a 12-h light–dark cycle) after one week adaptation period, with free access to food and water during the experiment. The diet of mice was mainly composed of corn, soybean meal, beer yeast, casein and lard. And the diets used in the experiment as described in **Table 1**. The experiment lasted for four weeks.

A total of 160 male mice (13. 85 ± 0.27 g) were randomly divided into 16 groups with 10 repetitions in each group. Mice were fed a 4 × 4 Latin square design with dietary protein concentrations of 16, 18, 20, and 22%, and starch concentrations of 50, 52, 54, and 56%, respectively. Mice were weighed on a weekly basis. Fecal samples were obtained and kept at −80°C for further examination. The 160 mice were sacrificed by cervical dislocation with 1% pentobarbital sodium (50 mg/kg)

TABLE 1 Composition and nutrients levels of the diet.

Items	CP:TS (16:50)	CP:TS (16:52)	CP:TS (16:54)	CP:TS (16:56)	CP:TS (18:50)	CP:TS (18:52)	CP:TS (18:54)	CP:TS (18:56)	CP:TS (20:50)	CP:TS (20:52)	CP:TS (20:54)	CP:TS (20:56)	CP:TS (22:50)	CP:TS (22:52)	CP:TS (22:54)	CP:TS (22:56)
Ingredients																
Corn	73.5	72	65	53.5	65.5	53	49	40	72.5	68	57	41.5	64	54	43.5	33.5
Corn starch	1	3	8	13.5	5	12.4	15	18	1.5	3	9	15.5	4.5	9	14	18
Bran	2	3.5	6	12	4	8.6	11	17.5	1	5	10	18	4	9.5	15	21
Casein	5	5	5	5	5	5.5	5.5	5	8.5	10	10	10	11	11	11	11
Soybean meal	6.5	6.5	7	7	12	11.5	11.5	11.5	9	6	6	6	9	9	9	9
Fish meal	4	4	4	4	4	4	4	4	4	4	4	4	4	4	4	4
Lard	6	4	2	2	2.5	3	2	2	1.5	2	2	3	1.5	1.5	1.5	1.5
Soybean oil	1	1	2	2	1	1	1	1	1	1	1	1	1	1	1	1
Premixture	1	1	1	1	1	1	1	1	1	1	1	1	1	1	1	1
Total	100	100	100	100	100	100	100	100	100	100	100	100	100	100	100	100
Nutrient levels																
GE	4405	4298	4238	4222	4260	4270	4212	4193	4256	4279	4263	4294	4291	4278	4264	4252
CP	16.1	16.2	16.3	16.3	18.2	18.1	18.2	18.0	20.1	20.3	20.2	20.2	22.1	22.1	22.1	22.2
TS	50.4	52.3	54.1	56.4	50.3	52.4	54.0	56.1	50.0	52.0	54.2	56.3	50.1	52.0	54.1	56.0

CP, crude protein; TS, starch.

anesthesia, and every effort was made to minimize suffering. Finally, blood, abdominal adipose tissue (AAT), liver, ileal tissue, and feces were collected for further examination.

Analysis of biochemical parameters in blood samples

Serum extracted form blood samples using 845 rcf (g) for 10 min at 4°C. The total bile acid (TBA), total cholesterol (TC), high density lipoprotein (HDL), low density lipoprotein (LDL), triglycerides (TG), and glucose (GLU) were detected according to the standard protocol by an automatic biochemical instrument (KHB 450, Shanghai Kehua bio-engineering co., Ltd, Shanghai, China) (31).

Histology analysis

The ileal tissues were removed and fixed in 4% paraformaldehyde solution, then hematoxylin and eosin were used to stain the paraffin-embedded and cut tissue sections. Light microscopes with computer-assisted morphometric systems were used to measure villus height and crypt depth in each section. The villus height was the distance from the villus tip to the crypt mouth, and crypt depth was the distance from the crypt mouth to the base of the crypt (32, 33).

Microbiota analysis

DNA extraction and 16S ribosomal RNA amplification were conducted as previously reported (34). Briefly, DNA was extracted from each fecal sample with an E.Z.N.A. ® soil DNA Kit (Omega Biotek, Norcross, GA, USA) according to the standard protocol. The thermal cycling programing was performed as follows: initial denaturation step, 95°C, 3 min; denaturation, 27 cycles, 95°C, 30 s; annealing, 55°C, 30 s; elongation, 72°C, 45 s; and final extension, 72°C, 10 min. The bacterial 16S rRNA was amplified using the universal primers targeting the V3-V4 region 338F/806R and sample sequenced by an Illumina Miseq PE300 platform (Illumina, SD, USA) according to the standard scheme (35). Quality filters were applied to trim raw sequences according to the following criteria: (i) reads with average quality score <20 over a 10-bp sliding window were removed, and truncated reads shorter than 150 bp were discarded. (ii) Truncated reads containing homopolymers longer than 8 nucleotides, more than 0 base in barcode matching, or more than 2 different bases to the primer were removed from the dataset. The possible chimeras were checked and removed via USEARCH using the ChimeraSlayer "gold" database as described by Edgar et al. (36). Operational taxonomic units (OTUs) with 97% similarity cutoff were clustered using USEARCH (37).

Statistical analyses

Two-tailed Student's *t*-test was used to compare two groups and ANOVA (one-way analysis of variance) and Tukey's *post-hoc* analysis was used to compare more than two groups through SPSS 22.0. The data was expressed as the means ± standard errors of the means (SEM). Statistical significance was set at $p < 0.05$.

Results

Body weight and organ index

In order to study whether dietary starch and protein can affect the lipid metabolism of the body, we used mice fed diets with different concentrations of starch and protein as models. As shown in **Figure 1**, the four different ratios of starch had no significant effect on the final body weight of male mice ($p = 0.307$), while the 22% protein group significantly decreased the final body weight of the mice than other protein ratio groups ($p < 0.05$). At the same time, starch and protein had no significant interaction effect on body weight ($p = 0.246$). Different proportions of starch and protein had obvious effects on the liver index of mice, and there was a significant interaction between starch and protein on the liver index ($p = 0.005$). Although different ratios of starch and protein had no significant effect on abdominal adipose weight in mice separately, there was a significant interaction between different starch and protein ratios on abdominal adipose weight ($p < 0.001$). Different proportions of starch have significant effect on the weight of the small intestine of male mice ($p = 0.005$), and the different protein level diet fed the male mice has a very significant difference in the weight of the small intestine ($p = 0.001$). The small intestine weight of mice with 18% protein in the diet was significantly higher than that of other diet groups with 3 protein ratios ($p < 0.05$). In addition, the small intestine of male mice fed the 50% starch diet was much heavier than the 52, 54, and 56% starch diets ($p < 0.05$). Correspondingly, there was a significant interaction between different starch and protein ratios on intestinal weight ($p < 0.001$). Diets with different protein levels had no effect on the length of the small intestine of the mice ($p = 0.435$), however, the 52% starch diet significantly reduced the small intestine length of mice compared with other starch ratio diets ($p = 0.018$). At the same time, the ratio of starch and protein had no significant interaction on the length of the small intestine ($p > 0.05$). Ultimately, different levels of protein had a significant effect on the ratio of small intestine weight to length ($p < 0.05$), but different levels of starch had no such effect. There was a significant interaction between starch and protein on the ratio of small intestine weight to length ($p < 0.05$).

Influence of the interaction between protein and starch on serum biochemical indexes

Variation of biochemical index in the serum of male mice was shown in **Figure 2**. Compared with other protein ratio diets, 18% protein diet significantly increased the serum TBA concentration of mice ($p < 0.001$), and different starch ratio diets had no effect on serum TBA concentration ($p = 0.442$). Compared with the 18 and 20% protein diets, the 16% protein diet significantly increased the serum TC concentration in mice ($p < 0.05$), and the different starch ratio diets had no effect on the serum TC concentration ($p = 0.301$). There was a significant interaction between diets with different starch and protein levels on serum TC in mice ($p = 0.004$). Compared with the 18 and 20% protein diets, the 16 and 22% protein diets significantly increased the serum HDL concentration in mice ($p < 0.05$), and the different starch ratio diets had no effect on the serum HDL concentration ($p > 0.05$). There was a significant interaction between diets with different starch and protein levels on serum HDL in mice ($p = 0.012$), and the combination of 16% protein and 56% starch diets increased serum HDL concentrations in mice. Compared with the 20 and 22% protein diets, the 16% protein diet significantly increased the serum GLU concentration of mice ($p < 0.05$), and the different starch ratio diets had no effect on the serum GLU concentration ($p > 0.05$). There was a significant interaction between diets with different starch and protein levels on the serum GLU of mice ($p = 0.003$), and the GLU concentration in serum was highest in mice fed a combination of 16% protein and 56% starch than other protein and starch diets. There was a significant interaction between diets with different starch and protein levels on serum TG in mice ($p = 0.003$), and the TG concentration in serum of mice fed with 18% protein and 50% starch diets was significantly higher than that of 22% protein and 50, 52, 56% starch diet combination ($p < 0.05$). Different starch ratio diets had no effect on the serum TG concentration of mice ($p = 0.714$). During the experiment, the serum LDL concentration of mice in each group was also affected by diets with different protein levels ($p = 0.006$), but not affected by different starch ratio diets ($p = 0.854$). Diets with different starch and protein levels also had a significant interaction on serum LDL in mice ($p < 0.001$). The LDL concentration in the serum of mice fed the 16% protein and 56% starch diet was significantly higher than that of the 22% protein and 52, 54, and 56% starch diets ($p < 0.05$).

Intestinal histomorphology analysis

The ileal tissue morphology under different starch and protein treatments was shown in **Figure 3**. It was proved from the pictures of ileal tissue HE staining that the low protein diet

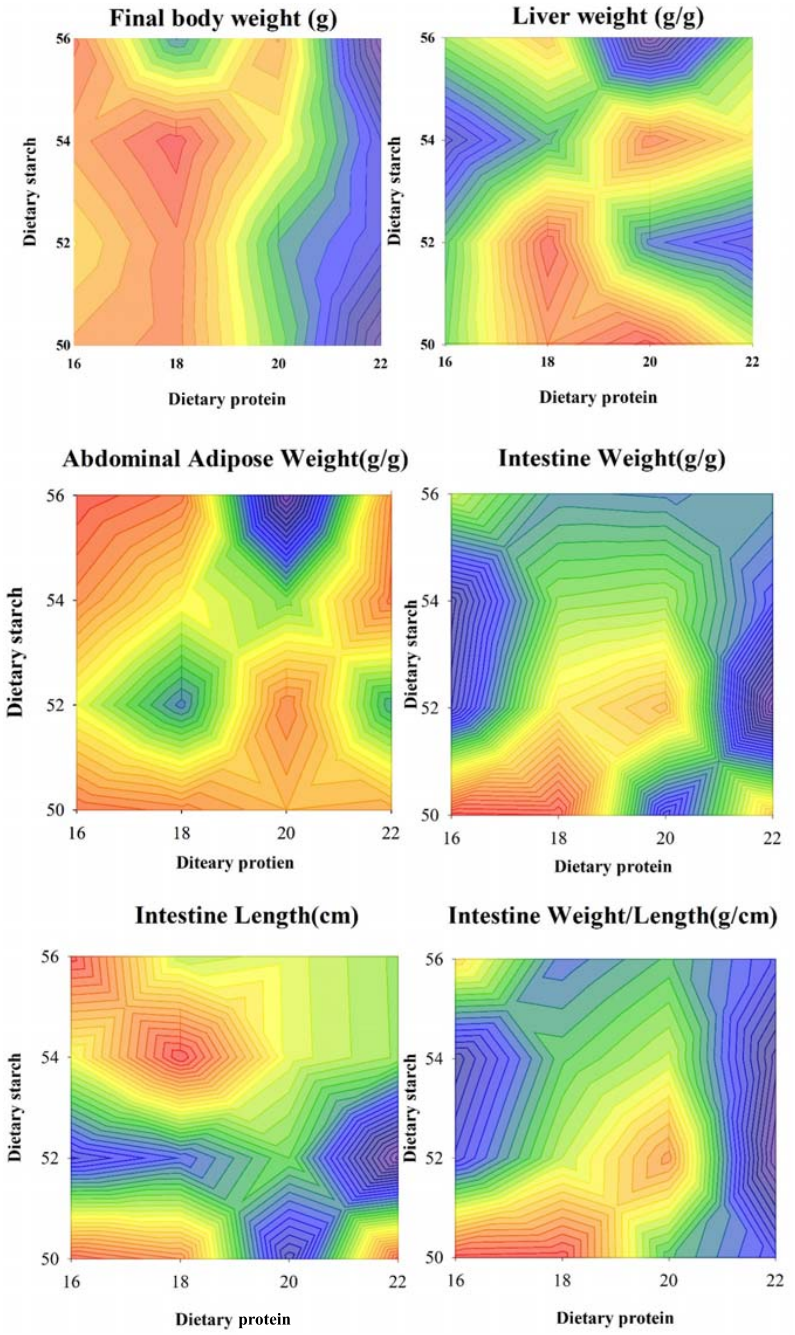

FIGURE 1
Effects of different ratios of starch and protein in diet on final weight and organ index of mice. The value increases with the deepening of red and decreases with the deepening of blue.

and the low starch diet were more favorable. The measurement results for ileal tissue were shown in Figure 4, the ileal villus height in the diet tended to decrease with the increase of protein concentration (p = 0.059), and different proportions of starch had no effect on the ileal villus height ($p > 0.05$). Different levels of protein and starch also had significant interaction effects on ileal villus height (p = 0.044). Diets with different protein and starch ratios had no significant effect on ileal crypt depth in male mice ($p > 0.05$), and there was no interaction effect ($p > 0.05$). The ileal villus width was not affected by the dietary starch ratio (p = 0.461); however, the 22% protein diet significantly increased the ileal villus width compared with the other protein ratio diets ($p < 0.05$), and finally different starch and protein ratios had no interaction effect on ileal villus width (p = 0.114). The

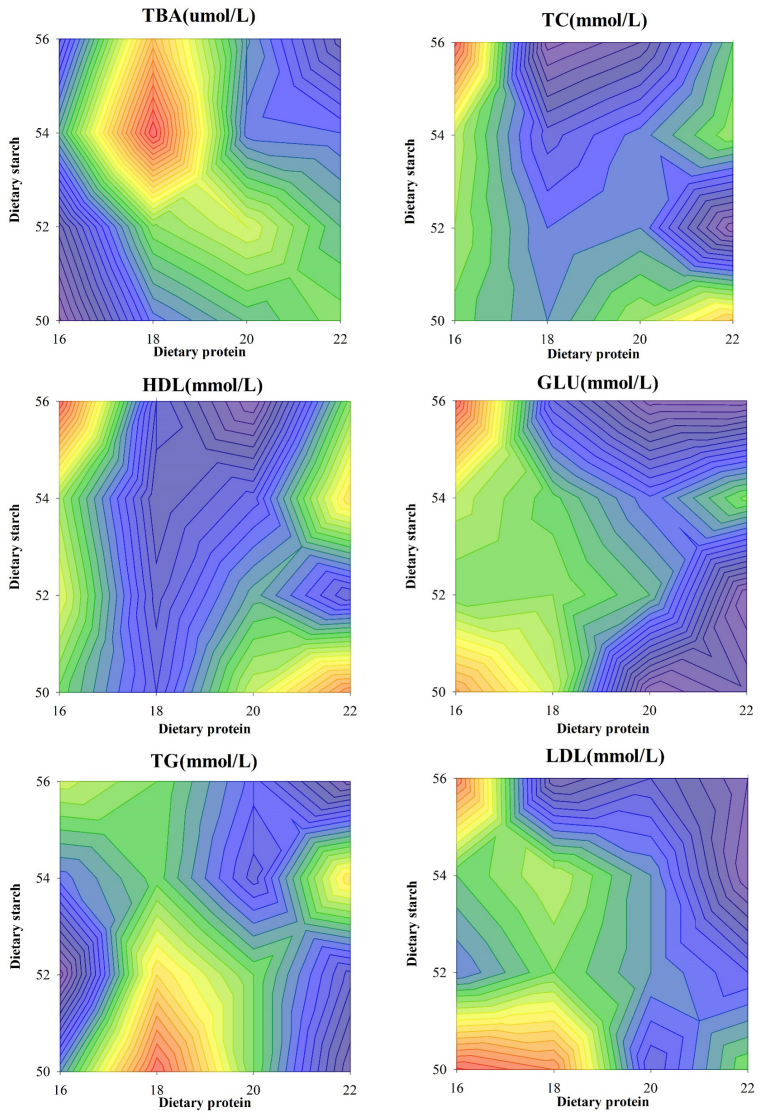

FIGURE 2
Effects of different ratios of starch and protein in diet on serum lipid levels in mice. The value increases with the deepening of red and decreases with the deepening of blue.

ratio of ileal villus height to crypt depth in mice was affected by different dietary protein and starch content, and the ratio of ileal villus height to crypt depth in mice with 16% protein diet was significantly higher than that of 18, 20, and 22% protein diet ($p = 0.009$). The ratio of villus height to crypt depth was significantly higher in the 50% starch diet than in male mice fed the 54% starch diet ($p < 0.05$). Different dietary protein and starch contents had significant interaction effects on the ratio of ileal villus height to crypt depth in mice ($p = 0.006$). The effects of different dietary protein and starch contents on mice ileal villus area were similar to the effects on the ratio of villus height and crypt depth. And the ratio of ileal villus area in mice with 16% protein diet was significantly higher than other protein ratio diets ($p = 0.001$). The ratio of villus height to crypt depth was significantly higher in the 50% starch diet than in male mice fed the 54% starch diet ($p < 0.05$). The number of goblet cells in the ileum of mice increased significantly with increasing dietary protein content ($p < 0.05$), while the number of ileal goblet cells was not affected by dietary starch content ($p > 0.05$). Different dietary protein and starch levels had significant interaction effects on the ileal number of goblet cells in mice ($p = 0.007$).

Fecal bacterial diversity and similarity

The results of different protein and starch diets on the fecal microbial α-diversity of male mice were shown in Figure 5.

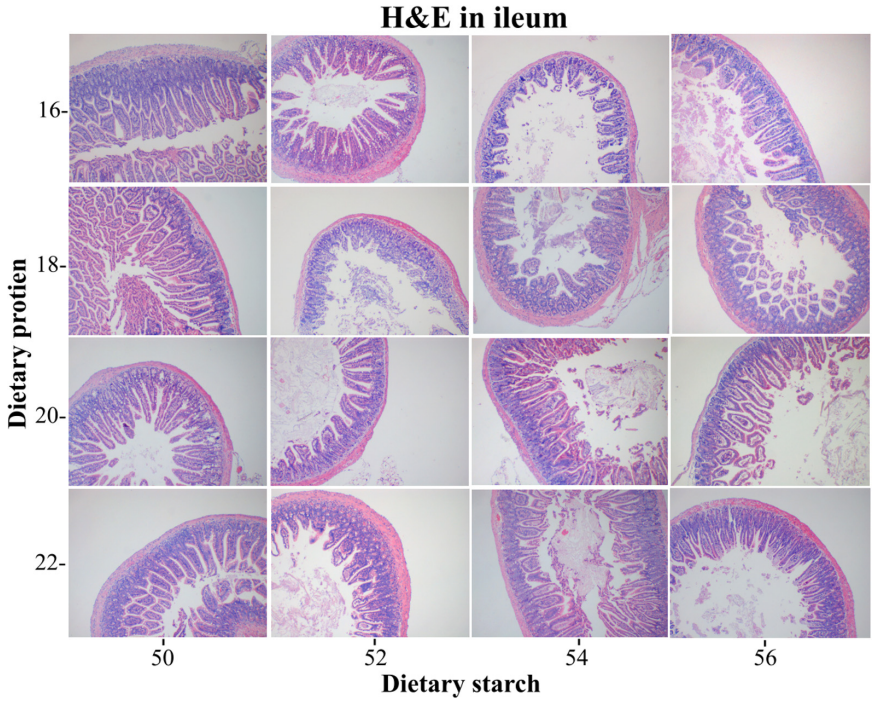

FIGURE 3
Light microscopy cross-section of ileal tissue by different ratios of starch and protein in diet.

The observed species in feces of mice was affected by different dietary protein and starch content, the 16% protein diet significantly increased observed species in the feces compared to other protein levels ($p < 0.05$), and the observed species was significantly higher in mice with 50% starch diet than in mice with 52% starch diet ($p < 0.05$). Different dietary protein and starch contents had significant interaction effects on the observed species in feces of mice ($p < 0.01$). Diet with 16% protein fed to mice significantly increased Shannon index in feces than other different protein level diet ($p < 0.05$), and 50% starch diet fed to mice also significantly increased Shannon index in feces than other starch protein level diet ($p < 0.05$). Different dietary protein and starch levels had significant interaction effects on Shannon index in mice ($p < 0.01$). For the Simpson index in fecal microbiota, the 16% protein diet fed to mice significantly improved the Simpson index in the feces compared to the other protein concentration diets ($p < 0.05$), and the 50% starch diet fed to mice also significantly improved the Simpson index in the feces compared to the other starch concentration diets ($p < 0.05$). Dietary protein and starch concentrations had a significant interaction effect on the Simpson index in mouse feces ($p < 0.05$). The effects of diets with different protein and different starch concentrations on the chao1 index of mouse feces were similar to the Simpson index, both the 16% protein diet and 50% starch diet fed to mice significantly increased the chao1 index than other groups in mouse feces ($p < 0.05$), and dietary protein and starch concentrations had a very significant interaction effect on the chao1 index in mouse feces ($p < 0.05$). The ACE index in feces of mice was affected by different dietary protein and starch content, and the ACE index in feces with 16% protein diet was significantly higher than that of 18, 20, and 22% protein diet ($p < 0.01$). The ACE index was significantly lower in the 52% starch diet than in male mice fed the 50, 54, and 56% starch diet ($p < 0.05$). Different dietary protein and starch contents had a very significant interaction effect on the ACE index in feces of mice ($p < 0.001$). The 16% protein diet significantly increased PD_whole_tree in the feces compared to 18% protein levels ($p < 0.05$), and the PD_whole_tree was significantly higher in mice with 50% starch diet than in mice with 52% starch diet ($p < 0.05$). Different dietary protein and starch contents had a significant interaction effect on the PD_whole_tree in feces of mice ($p < 0.01$).

Intestinal bacterial community structure

Variation of phylum-level composition (>1%) on the fecal bacterial community of mice fed different starch and protein ratio diets was shown in Table 2, *Bacteroidetes*, *Firmicutes*, *Verrucomicrobia* and *Proteobacteria* were dominant phyla in the feces of mice, accounting for more than 95% of the fecal total bacterial community. Compared with 16 and 22% protein

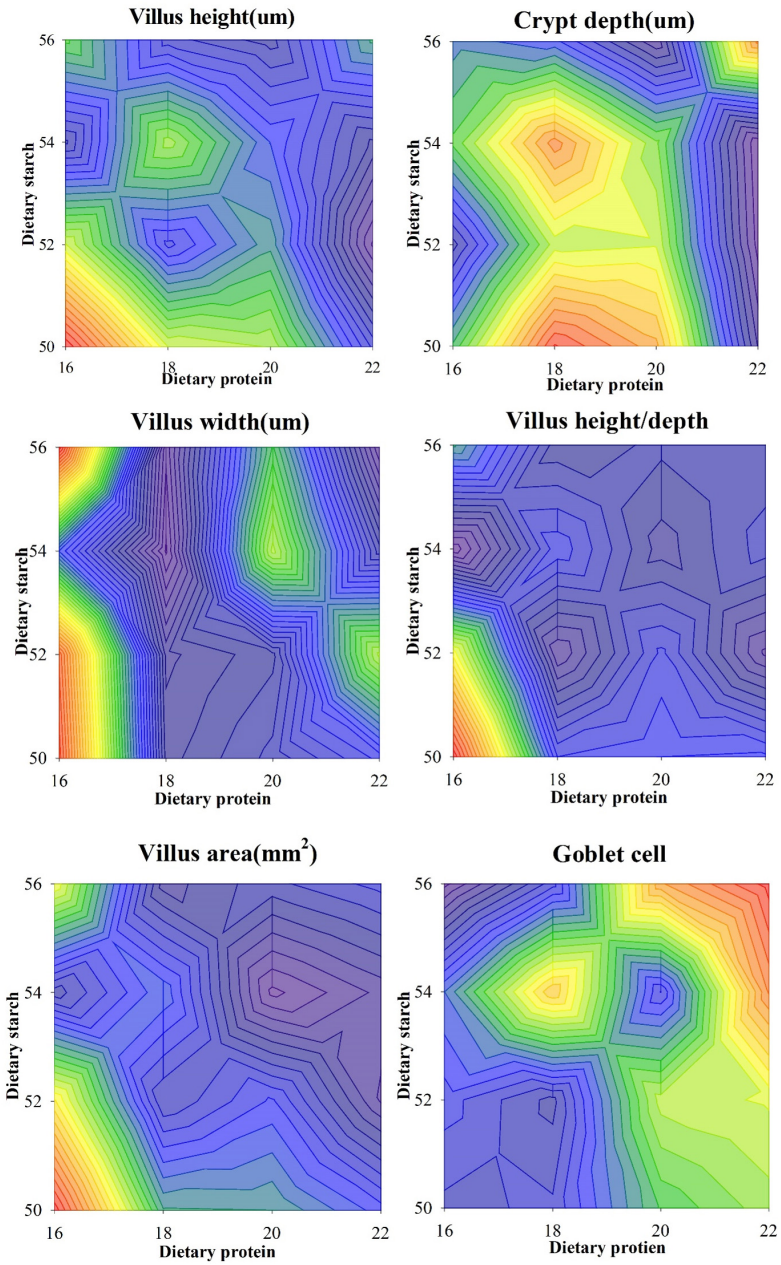

FIGURE 4
Effects of different ratios of starch and protein in diet on the structure of ileal epithelium in mice. The value increases with the deepening of red and decreases with the deepening of blue.

ratio diets, both 18 and 20% protein diets significantly increased the *Bacteroidetes* abundance in feces of mice ($p < 0.05$), and 52% starch ratio diet significantly increased the *Bacteroidetes* abundance than other starch ratio diets of mice ($p < 0.05$). There was a significant interaction between diets with different starch and protein levels on *Bacteroidetes* abundance in feces of mice ($p < 0.001$). Compared with the 18, 20, and 22% protein diets, the 16% protein diet significantly increased the *Firmicutes* abundance in mice ($p < 0.05$), and the 50% starch ratio diet significantly increased the *Firmicutes* abundance than 52 and 56% starch diet in feces of mice ($p < 0.05$). There was a significant interaction between diets with different starch and protein levels on *Firmicutes* abundance in mice ($p < 0.001$). Although *Verrucomicrobia* of phyla proportion varied with the different starch level added to the diet, there was no significant difference on *Verrucomicrobia* abundance in the feces of different starch level ($p = 0.045$). Both of the 16 and 18% protein diets fed to mice decreased *Verrucomicrobia* abundance in feces

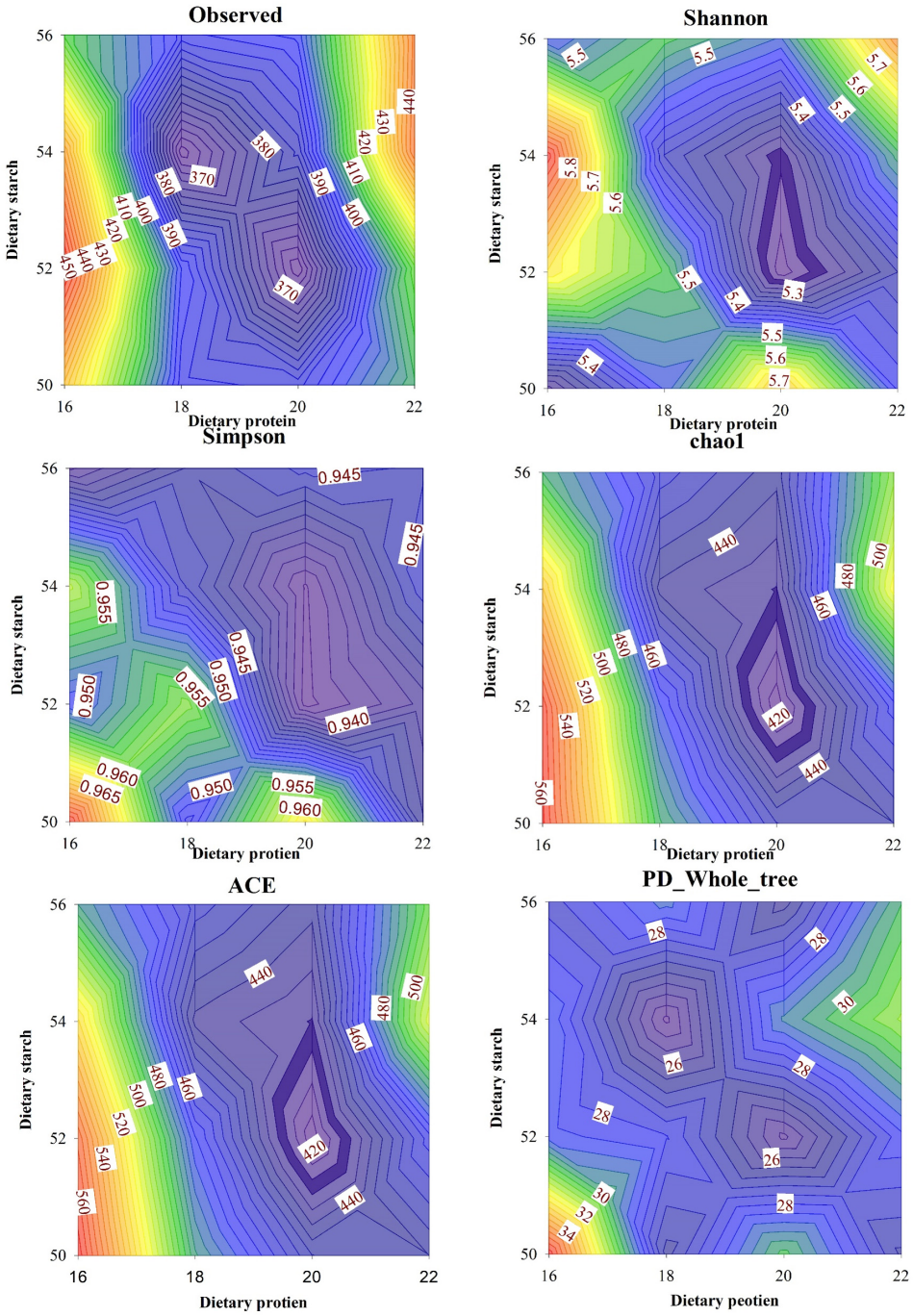

FIGURE 5
Effects of different ratios of starch and protein in diet on α diversity in the fecal microbiota of mice. The value increases with the deepening of red and decreases with the deepening of blue.

than 20 and 22% protein diets ($p < 0.05$). Different dietary protein and starch contents had a significant interaction effect on the *Verrucomicrobia* abundance in feces of mice ($p < 0.001$). Compared with the 18 and 22% protein diets, the 16% protein diet significantly decreased the *Proteobacteria* abundance in feces of mice ($p < 0.05$), and the 52% starch ratio diet fed to mice increased *Proteobacteria* abundance significantly in feces than other starch ratio diets ($p < 0.05$). There was a significant interaction between diets with different starch and protein levels on *Proteobacteria* abundance in mice ($p < 0.001$).

Downward to genus levels, *Helicobacter*, *Alloprevotella*, *Akkermansia*, *Parasutterella*, and *Bacteroides* were the

10.3389/fnut.2022.1018026

TABLE 2 Phylum-level composition (>1%) on the fecal bacterial community of mice fed different starch and protein ratio diets.

Diets		*Bacteroidetes*	*Firmicutes*	*unidentified_Bacteria*	*Verrucomicrobia*	*Proteobacteria*
CP	**TS**					
16	50	50.9	37.5	5.90	3.30	2.12
16	52	58.0	23.5	1.10	14.5	2.69
16	54	58.8	30.5	6.05	1.68	2.74
16	56	75.3	13.9	5.37	1.14	3.88
18	50	70.6	14.1	3.66	4.79	3.98
18	52	77.5	10.2	3.92	1.64	6.28
18	54	81.2	11.3	1.76	1.14	3.76
18	56	70.5	17.8	3.33	1.82	3.71
20	50	68.2	22.9	2.44	2.40	3.24
20	52	80.4	7.60	1.11	5.29	5.41
20	54	68.2	13.9	0.81	13.5	2.05
20	56	69.4	14.5	2.60	11.0	1.80
22	50	72.0	14.5	6.41	3.86	2.19
22	52	69.9	14.2	4.29	5.64	5.49
22	54	61.5	17.4	7.14	8.41	4.95
22	56	55.0	22.1	11.4	8.83	2.20
Univariate analysis						
16	–	61.1^{b}	27.6^{a}	5.63^{a}	2.49^{b}	2.87^{c}
18	–	74.3^{a}	14.0^{b}	3.00^{b}	2.65^{b}	4.00^{a}
20	–	71.3^{a}	15.2^{b}	1.89^{b}	7.73^{a}	3.16^{bc}
22	–	64.7^{b}	17.0^{b}	7.27^{a}	6.65^{a}	3.74^{ab}
–	50	65.4^{b}	22.5^{a}	4.60^{ab}	3.59	2.90^{b}
–	52	74.3^{a}	11.6^{c}	2.82^{b}	5.54	5.40^{a}
–	54	66.9^{b}	18.8^{ab}	4.36^{ab}	5.72	3.52^{b}
–	56	67.5^{b}	17.0^{b}	5.64^{a}	6.06	2.88^{b}
SEM		0.010	0.009	0.005	0.005	0.002
CP *P*-value		<0.001	<0.001	<0.001	<0.001	0.007
TS *P*-value		0.360	0.006	0.200	0.045	0.001
CP × TS *P*-value		<0.001	<0.001	0.457	<0.001	<0.001

CP, crude protein; TS, starch; Each group contains 10 samples; SEM, standard error of the mean. In the same column, values with no letter or the same letter superscripts mean no significant difference ($p > 0.05$), while with different small letter superscripts mean significant difference ($p < 0.05$).

predominant genera in feces of sixteen groups. As shown in Table 3, the different starch ratio diets had no effect on the relative abundance of *Akkermansia* and *Bacteroides* in feces of mice ($p > 0.05$). But 20 and 22% protein diets significantly increased the *Akkermansia* abundance than 16 and 18% protein diets fed to mice ($p < 0.05$), and 18% protein diet significantly increased the *Bacteroides* abundance than other three protein diets fed to mice ($p < 0.05$). Diets with different starch and protein levels had a very significant interaction on the relative abundance of *Akkermansia* ($p < 0.001$) and *Bacteroides* in feces of mice ($p = 0.001$). The different starch diets did not change significantly the *Helicobacter* abundance in mice ($p = 0.360$), but 22% protein diet significantly increased the *Helicobacter* abundance than 18 and 20% protein diets fed to mice ($p < 0.05$). There was no significant interaction between diets with different starch and protein levels on *Helicobacter* abundance in mice ($p = 0.483$). Compared with the 18 and 20% protein diets, the 16% protein diet significantly increased the relative abundance of *unidentified_Lachnospiraceae* and *unidentified_Ruminococcaceae* in feces of mice ($p < 0.05$), and the 50% starch ratio diet significantly increased the *unidentified_Lachnospiraceae* and *unidentified_Ruminococcaceae* abundance than 52% starch fed to mice in feces ($p < 0.05$). There was a very significant interaction between diets with different starch and protein levels on the *unidentified_Lachnospiraceae* abundance ($p = 0.012$) and *unidentified_Ruminococcaceae* abundance of mice ($p = 0.001$). Compared with 16 and 18% protein ratio diets, both 20 and 22% protein diets significantly decreased the *Parabacteroides* and *Alistipes* abundance in feces of mice ($p < 0.05$), and 52% starch ratio diet significantly decreased the *Parabacteroides* and *Alistipes* abundance than 50% starch ratio diet of mice ($p < 0.05$). There was a very significant interaction between diets with different starch and protein levels on *Parabacteroides* ($p = 0.014$) and *Alistipes* ($p = 0.001$) abundance in feces of mice. The *Alloprevotella* abundance in feces was highest to mice fed a combination of 16% protein and 56% starch than other protein and starch diets fed to mice. There was a significant

TABLE 3 Genus-level composition (>1%) on the fecal bacterial community of mice fed different starch and protein ratio diets.

Diets		*Helicobacter*	*Alloprevotella*	*Akkermansia*	*unidentified_ Lachnospiraceae*	*Parasutterella*	*Parabacteroides*	*Bacteroides*	*unidentified_ Ruminococcaceae*	*Alistipes*
CP	**TS**									
16	50	5.85	2.33	3.30	4.33	0.69	0.71	0.94	3.00	1.05
16	52	1.09	4.47	14.50	2.92	2.04	0.50	0.47	1.20	1.63
16	54	6.02	6.07	1.68	3.36	1.28	1.53	1.83	2.01	1.13
16	56	5.28	14.37	1.14	0.95	2.85	1.42	1.32	2.13	1.11
18	50	3.60	3.41	4.79	1.34	3.46	1.88	0.95	2.20	1.28
18	52	3.86	4.99	1.64	1.33	5.47	0.62	1.25	1.48	0.70
18	54	1.71	11.61	1.14	1.03	2.64	1.23	2.13	1.30	0.47
18	56	3.23	2.90	1.82	2.39	2.89	0.68	2.62	1.86	1.12
20	50	2.39	4.74	2.40	2.74	2.19	0.73	1.84	2.33	1.08
20	52	1.01	8.33	5.29	0.89	5.01	0.26	1.29	0.92	0.31
20	54	0.77	3.38	13.53	3.04	2.20	0.44	0.82	1.02	0.42
20	56	2.58	5.52	10.96	2.03	1.56	0.36	0.89	0.99	0.74
22	50	6.37	4.91	3.86	2.94	1.62	0.36	1.00	1.04	0.24
22	52	4.26	3.84	5.64	2.27	3.56	0.45	1.17	1.11	0.40
22	54	7.11	6.21	8.41	2.72	2.28	0.91	1.34	1.11	0.58
22	56	11.22	2.56	8.83	3.13	0.31	0.46	0.45	1.10	0.81
Univariate analysis										
16	–	5.58^{a}	7.26^{a}	2.49^{b}	2.97^{a}	1.62^{c}	1.19^{a}	1.34^{b}	1.76^{b}	1.12^{a}
18	–	2.93^{b}	5.93^{ab}	2.65^{b}	1.54^{b}	3.21^{a}	1.27^{a}	1.83^{a}	1.39^{c}	0.96^{a}
20	–	1.83^{b}	5.57^{ab}	7.73^{a}	2.16^{b}	2.66^{ab}	0.46^{b}	1.22^{b}	1.09^{d}	0.68^{b}
22	–	7.21^{a}	4.44^{b}	6.65^{a}	2.77^{a}	1.95^{bc}	0.55^{b}	1.01^{b}	2.37^{a}	0.50^{b}
–	50	4.55^{ab}	3.85^{b}	3.59	2.84^{a}	2.04^{b}	0.92^{a}	1.17	1.48^{b}	0.92^{a}
–	52	2.76^{b}	5.78^{ab}	5.54	1.66^{b}	4.25^{a}	0.39^{b}	1.19	1.09^{c}	0.46^{b}
–	54	4.32^{ab}	7.07^{a}	5.72	2.54^{ab}	2.08^{b}	1.06^{a}	1.57	1.38^{b}	0.68^{b}
–	56	5.56^{a}	6.41^{a}	6.06	2.15^{ab}	1.87^{b}	0.72^{ab}	1.29	2.14^{a}	0.93^{a}
SEM		0.005	0.005	0.005	0.002	0.002	0.001	0.001	0.005	<0.001
CP *P*-value		<0.001	0.302	<0.001	0.038	<0.001	0.004	0.032	<0.001	<0.001
TS *P*-value		0.360	0.015	0.050	0.211	0.001	0.121	0.284	<0.001	0.024
CP × TS *P*-value		0.483	<0.001	<0.001	0.012	0.004	0.014	0.001	0.001	0.001

CP, crude protein; TS, starch; Each group contains 10 samples; SEM, standard error of the mean. In the same column, values with no letter or the same letter superscripts mean no significant difference ($p > 0.05$), while with different small letter superscripts mean significant difference ($p < 0.05$).

10.3389/fnut.2022.1018026

interaction between diets with different starch and protein levels on *Alloprevotella* abundance in mice ($p < 0.001$). The *Parasutterella* abundance in feces of mice fed with 22% protein and 56% starch diets was lowest than other protein and starch diets fed to mice. Different starch or protein ratio diets had effect on the *Parasutterella* abundance of mice and a very significant interaction between diets with different starch and protein levels on *Parasutterella* abundance in feces of mice ($p = 0.004$).

Discussion

Interactions between starch and protein have been increasingly appreciated during the last few years, for example in combined system of protein and starch for formulation of novel functional foods such as bakery products, infant foods, dessert and snack foods (4, 38–40), owing to their rich functionality, superior nutritional value and significant bioactivity. In this study, male mice were used as an experimental model to investigate the effects of different levels of protein and starch diets on fat deposition, fecal microbiota, and small intestinal tissue structure in mice. Studies have shown that dietary protein and starch played a role in regulating lipid biological synthesis.

The high protein diet reduced liver fat more effectively than the low protein diet (41). For example, in mice and human research, the high protein diet has proven to increase energy consumption, reduce blood glucose levels, promote fat oxidation, thereby supporting weight loss, and reducing liver fat (42–45). The relatively lower carbohydrate content in the high protein diet may also be part of the cause of new fat production and reduced intrahepatic fat. In addition, compared with fat-generating genes, in several rats' research, protein intake in diet has not changed the expression of genes related to lipid oxidation or substrate oxidation (46, 47). Our results showed that the 22% protein group significantly decreased the final body weight of the mice than other protein ratio groups, and 20% protein with 56% starch fed to mice got the lowest abdominal adipose weight than others group. The reason may be that the fat intake and lipid biological synthesis may be inhibited. The liver is one of the important organs for host lipid metabolism, including lipid assembly and transportation (48). Meanwhile, the absorption and transport of lipids in the small intestine also determines the fate of lipid metabolism (49), and a two-way effect occurs with intestinal microbes and metabolites (50, 51). In this study, different starch and protein diets had less effect on the final liver and abdominal adipose weight in male mice, which may also be due to the shorter experimental period.

The biochemical indicators of the blood could not only feedback the health of the host and the strength of immune function, but also revealed the biological characteristics of different hosts (52). Jenkins et al. (53) studied the effect of the starch–protein complex interaction in wheat-based food, founding that the presence of protein in white flour produced a reduction in the digestibility rate of starch *in vitro* and had a direct relationship with the decrease of the glycemic response *in vivo*, which may be relevant in the effect of food on the gastrointestinal tract. In the present study, feeding male mice with a 22% high-protein diet reduced blood Glu level, while starch ratio had no significant effect on Glu concentrations. This showed that the Glu level in blood was easily affected by the protein in the diet, and the Glu concentration in the blood increased with the lower the protein content. The study demonstrated that plasma lipoprotein, especially HDL, can be combined with LPS and preferentially shunt liver cells away from liver macrophages, thereby increasing LPS excretion through the bile and preventing immune responses (54). When the level of TC in the host's blood rises, hypertrophymia will occur. Compared with LDL, HDL level may lead to this situation (55). Some researchers have compared the influence of high and low diets on obesity and their related diseases. One of the main discoveries in the system summary was that the HP solution had a favorable impact on TG and HDL (56). Our study confirmed that the protein in the dietary formula affected the indicators of blood lipid metabolism in mice, and these indicators were hardly affected by the proportion of starch in the diet. These data were very important for preventing hyperlipidemia and heart and liver disease (57).

Dietary nutrients can modulate the small intestinal tissue morphology and digestive function of animals, and the intestinal barrier function was very important to the host (58–60). Villus height and crypt depth are important indicators to measure the digestion and absorption function of the small intestine. The depth of the crypts reflects the rate of cell formation, while shallower crypts indicate an increased rate of cell maturation and enhanced secretory function. The height of villi and the depth of crypts can comprehensively reflect the functional status of the small intestine (34, 61). In our study, the ileal crypt depth was not affected significantly by the ratio of dietary protein and starch. Since the intestinal surface area represented by the tight packing and long projections of villi showed the maximal absorption of nutrients allowed (62), the decreased ratio of villi height to crypt depth in the ileum of the 22% CP group showed reduced nutrient absorption. In the present study, although the increased dietary protein concentration did not significantly alter the villus height and crypt depth of the small intestine, the ratio of villus height to crypt depth decreased, and the villus area was also reduced, so the high concentration of protein in the diet impaired the mucosal morphology of the small intestine resulting in underdevelopment of the small intestine, and dietary starch has a negligible effect on intestinal morphology.

The integrity of the intestinal structure and dynamic balance of intestinal microbiota guarantee the chemical induction and digestive functions of the gut, which is the premise for nutrient absorption, metabolism, and deposition. With the development of gene sequencing technology, we can explore the impact of

changes in animal diet on the structure and function of intestinal microorganisms (63, 64). The *Bacteroidetes* and *Firmicutes* were dominant phyla in the feces of mice in this study. The decline of *Streptococcus* and *Escherichia-Shigella* in the ileum when dietary protein concentration decreased by 3 percentage points suggested the positive effect (65). In this study, the abundance of *Streptococcus* and *Escherichia-Shigella* was less than 1%, both of them responsed to the diet were negligible. Recently, altered gut microbiome has been shown to be associated with host lipid metabolism through dietary structure (49, 66, 67). Germ-free mice demonstrated that the changes of the gut microbiota community including decreased relative abundance of *Lachnospiraceae* and an enhanced occurrence of *Desulfovibrionaceae*, *Clostridium lactatifermentans* and *Flintibacter butyricus* were associated with impaired glucose metabolism, lowered counts of enteroendocrine cells, fatty liver, and elevated amounts of hepatic triglycerides, cholesteryl esters, and monounsaturated fatty acids by high-fat diet (68). In the present study, the content of *unidentified_Lachnospiraceae* in mouse feces was higher and affected by the interaction between protein and starch in the diet, and the effect of protein was greater than that of starch. However, the content of *Desulfovibrionaceae*, *Clostridium lactatifermentans* and *Flintibacter butyricus* in mouse feces was very low, so it was not investigated. Furthermore, gut microbiota-mediated cholesterol metabolism via a microbial cholesterol dehydrogenase played an important role in host cholesterol homeostasis (69). Interestingly, there may be a bridge between gut microbes and metabolites and lipid levels, and several relevant genes regulated the concentration of lipids. A study has found that theabrownin reduced liver cholesterol and decreased lipogenesis by the gut microbe-bile acid-FXR-FGF15 signaling pathway (50). In our study, the concentration of TBA in blood was the highest when the diet contained 18% protein, and the ratio of dietary starch had no significant effect on TBA. Therefore, dietary protein may regulate host lipid metabolism through some bacteria, which required more follow-up research.

Futher, the microbial composition, along with a wide range of microbial metabolites, played a complex role in various host processes, such as resistance to autoimmunity (70). For the ileal microbiota in pigs, when dietary protein dropped by 3 percentage points, the decreased *Enterobacteriaceae* within the *Proteobacteria* phyla has been considered to contain many pathogenic bacteria (71), indicating the potential for inhibiting pathogens with moderate dietary protein restriction. In general, the abundance of *Proteobacteria* in mouse feces was the highest when the diet contained 56% starch in this study. Therefore, the increase of dietary starch content was harmful to the health of mice from the perspective of microorganisms. In the colon, when dietary protein concentration declined, the abundance of *Firmicutes* increased while *Bacteroidetes*, *Spirochaetae,* and *Verrucomicrobia* decreased (65). Consistent with previous research, the abundance of *Firmicutes* in mouse feces decreased with the increase of dietary protein, while the abundance of *Bacteroides* and *Verrucomicrobia* decreased conversely in this study. Since microorganisms were greatly affected by dietary formulation, starch and protein had obvious interaction effect on the main dominant bacterial genera, which provided insights for future exploration of the effects of specific microorganisms on dietary formulation.

Conclusion

In conclusion, our results showed that the 22% protein group significantly decreased the final body weight of the mice than other protein ratio groups, and 20% protein with 56% starch fed to mice got the lowest abdominal adipose weight than others group. The gut microbial abundance was altered by different starch and protein fed to male mice. Our study provided a more comprehensive understanding of mouse fecal microbial responses to different starch and protein diets, including lipid metabolism and gut barrier.

Data availability statement

This original contributions presented in this study are included in the article/supplementary material, further inquiries can be directed to the corresponding authors.

Ethics statement

This animal study was reviewed and approved by Hunan Agricultural University Institutional Animal Care and Use Committee (202105). Written informed consent was obtained from the owners for the participation of their animals in this study.

Author contributions

JM and PZ designed the experiment. PZ supported the funding. JM and KW conducted the experiment. KW, JM, MZ, XG, and YZ collected and analyzed data. KW wrote the manuscript. PZ, JC, and JM revised the manuscript. All authors contributed to the article and approved the submitted version.

Funding

The authors wish to acknowledge the financial support received from the Young Elite Scientists Sponsorship Program by CAST (2019QNRC001) and the Natural Science

Foundation of Hunan Province for outstanding Young Scholars (2020JJ3023).

Conflict of interest

The authors declare that the research was conducted in the absence of any commercial or financial relationships that could be construed as a potential conflict of interest.

Publisher's note

References

1. World Health Organization [WHO]. *World Obesity Day 2022 – Accelerating Action to Stop Obesity*. Geneva: World Health Organization (2022).

2. Ren W, Xia Y, Chen S, Wu G, Bazer FW, Zhou B, et al. Glutamine metabolism in macrophages: a novel target for obesity/type 2 diabetes. *Adv Nutr.* (2019) 10:321–30. doi: 10.1093/advances/nmy084

3. Dunn KL, Yang L, Girard A, Bean S, Awika JM. Interaction of sorghum tannins with wheat proteins and effect on in vitro starch and protein digestibility in a baked product matrix. *J Agric Food Chem.* (2015) 63:1234–41. doi: 10.1021/jf504112z

4. Giuberti G, Gallo A, Cerioli C, Fortunati P, Masoero F. Cooking quality and starch digestibility of gluten free pasta using new bean flour. *Food Chem.* (2015) 175:43–9. doi: 10.1016/j.foodchem.2014.11.127

5. Vujić L, Vitali Čepo D, Šebečić B, Dragojević I. Effects of pseudocereals, legumes and inulin addition on selected nutritional properties and glycemic index of whole grain wheat-based biscuits. *J Food Nutr Res.* (2014) 53:152–61.

6. Carbonaro M, Maselli P, Nucara A. Structural aspects of legume proteins and nutraceutical properties. *Food Res Int.* (2015) 76:19–30. doi: 10.1016/j.foodres.2014.11.007

7. Huerta-Abrego A, Campos M, Guerrero L. Changes in the functional properties of three starches by interaction with lima bean proteins. *Food Technol Biotechno.* (2010) 48:36–41.

8. Bravo-Núñez Á, Garzón R, Rosell CM, Gómez M. Evaluation of starch¯protein interactions as a function of pH. *Foods.* (2019) 8:155. doi: 10.3390/foods8050155

9. Yang C, Zhong F, Douglas Goff H, Li Y. Study on starch-protein interactions and their effects on physicochemical and digestible properties of the blends. *Food Chem.* (2019) 280:51–8. doi: 10.1016/j.foodchem.2018.12.028

10. Fernandes JM, Madalena DA, Vicente AA, Pinheiro AC. Influence of the addition of different ingredients on the bioaccessibility of glucose released from rice during dynamic in vitro gastrointestinal digestion. *Int J Food Sci Nutr.* (2021) 72:45–56. doi: 10.1080/09637486.2020.1763926

11. Mann J, Cummings JH, Englyst HN, Key T, Liu S, Riccardi G, et al. FAO/WHO scientific update on carbohydrates in human nutrition: conclusions. *Eur J Clin Nutr.* (2007) 61(Suppl 1.):S132–7. doi: 10.1038/sj.ejcn.1602943

12. Filipčev B, Šimurina O, Sakač M, Sedej I, Jovanov P, Pestorić M, et al. Feasibility of use of buckwheat flour as an ingredient in ginger nut biscuit formulation. *Food Chem.* (2011) 125:164–70. doi: 10.1016/j.foodchem.2010.08.055

13. Oates CG. Towards an understanding of starch granule structure and hydrolysis. *Trends Food Sci Technol.* (1997) 8:375–82. doi: 10.1016/S0924-2244(97)01090-X

14. Herrero M, Henderson B, Havlik P, Thornton PK, Conant RT, Smith P, et al. Greenhouse gas mitigation potentials in the livestock sector. *Nat Clim Change.* (2016) 6:452–61. doi: 10.1038/NCLIMATE2925

15. Wood JD, Lambe NR, Walling GA, Whitney H, Jagger S, Fullarton PJ, et al. Effects of low protein diets on pigs with a lean genotype. 1. Carcass composition measured by dissection and muscle fatty acid composition. *Meat Sci.* (2013) 95:123–8. doi: 10.1016/j.meatsci.2013.03.001

16. Zhou L, Fang L, Sun Y, Su Y, Zhu W. Effects of the dietary protein level on the microbial composition and metabolomic profile in the hindgut of the pig. *Anaerobe.* (2016) 38:61–9. doi: 10.1016/j.anaerobe.2015.12.009

17. Errington J, Scazzocchio C. Growth and development. Microbial development–regulation in space and time. *Curr Opin Microbiol.* (2003) 6:531–3. doi: 10.1016/j.mib.2003.10.017

18. Robertson RC, Manges AR, Finlay BB, Prendergast AJ. The human microbiome and child growth - first 1000 days and beyond. *Trends Microbiol.* (2019) 27:131–47. doi: 10.1016/j.tim.2018.09.008

19. Cani P, Delzenne N. The role of the gut microbiota in energy metabolism and metabolic disease. *Curr Pharm Des.* (2009) 15:1546–58. doi: 10.2174/138161209788168164

20. Wang K, Ren A, Zheng M, Jiao J, Yan Q, Zhou C, et al. Diet with a high proportion of rice alters profiles and potential function of digesta-associated microbiota in the ileum of goats. *Animals.* (2020) 10:1261. doi: 10.3390/ani10081261

21. Wang K, Peng X, Lv F, Zheng M, Long D, Mao H, et al. Microbiome-metabolites analysis reveals unhealthy alterations in the gut microbiota but improved meat quality with a high-rice diet challenge in a small ruminant model. *Animals.* (2021) 11:2306. doi: 10.3390/ani11082306

22. Ma N, Tian Y, Wu Y, Ma X. Contributions of the interaction between dietary protein and gut microbiota to intestinal health. *Curr Protein Peptide Sci.* (2017) 18:795–808. doi: 10.2174/1389203718666170216153505

23. Sonnenburg, Smits SA, Tikhonov M, Higginbottom SK, Wingreen NS, Sonnenburg JL. Diet-induced extinctions in the gut microbiota compound over generations. *Nature.* (2016) 529:212–5. doi: 10.1038/nature16504

24. Fan P, Li L, Rezaei A, Eslamfam S, Che D, Ma X. Metabolites of dietary protein and peptides by intestinal microbes and their impacts on gut. *Curr Protein Peptide Sci.* (2015) 16:646–54. doi: 10.2174/1389203716666150630133657

25. Saresella M, Mendozzi L, Rossi V, Mazzali F, Piancone F, LaRosa F, et al. Immunological and clinical effect of diet modulation of the gut microbiome in multiple sclerosis patients: a pilot study. *Front Immunol.* (2017) 8:1391. doi: 10.3389/fimmu.2017.01391

26. Bakar J, Saeed M, Abbas K, Abdul Rahman R, Karim R, Hashim D. Protein-starch interaction and their effect on thermal and rheological characteristics of a food system: a review. *J. Food Agric. Environ.* (2009) 7:169–74.

27. Wang S, Chao C, Cai J, Niu B, Copeland L, Wang S. Starch–lipid and starch–lipid–protein complexes: a comprehensive review. *Compr Rev Food Sci Food Saf.* (2020) 19:1056–79. doi: 10.1111/1541-4337.12550

28. Ioffe VM, Gorbenko GP, Deligeorgiev T, Gadjev N, Vasilev A. Fluorescence study of protein–lipid complexes with a new symmetric squarylium probe. *Biophys Chem.* (2007) 128:75–86. doi: 10.1016/j.bpc.2007.03.007

29. Zhang G, Hamaker BR. Sorghum (*Sorghum bicolor* L. Moench) flour pasting properties influenced by free fatty acids and protein. *Cereal Chem.* (2005) 82:534–40. doi: 10.1094/CC-82-0534

30. Parada J, Santos JL. Interactions between starch, lipids, and proteins in foods: microstructure control for glycemic response modulation. *Crit Rev Food Sci Nutr.* (2016) 56:2362–9. doi: 10.1080/10408398.2013.840260

31. Wang K, Peng X, Yang A, Huang Y, Tan Y, Qian Y, et al. Effects of diets with different protein levels on lipid metabolism and gut microbes in the host of different genders. *Front Nutr.* (2022) 9:940217. doi: 10.3389/fnut.2022.940217

32. Deng Q, Shao Y, Wang Q, Li J, Li Y, Ding X, et al. Effects and interaction of dietary electrolyte balance and citric acid on growth performance, intestinal histomorphology, digestive enzyme activity and nutrient transporters expression of weaned piglets. *J Anim Physiol Anim Nutr.* (2021) 105:272–85. doi: 10.1111/jpn.13491

33. Yin L, Li J, Wang H, Yi Z, Wang L, Zhang S, et al. Effects of vitamin B6 on the growth performance, intestinal morphology, and gene expression in

weaned piglets that are fed a low-protein diet1. *J Anim Sci.* (2020) 98:skaa022. doi: 10.1093/jas/skaa022

34. Wang K, Yang A, Peng X, Lv F, Wang Y, Cui Y, et al. Linkages of various calcium sources on immune performance, diarrhea rate, intestinal barrier, and post-gut microbial structure and function in piglets. *Front Nutr.* (2022) 9:921773. doi: 10.3389/fnut.2022.921773

35. Wang H, Hu C, Cheng C, Cui J, Ji Y, Hao X, et al. Unraveling the association of fecal microbiota and oxidative stress with stillbirth rate of sows. *Theriogenology.* (2019) 136:131–7. doi: 10.1016/j.theriogenology.2019.06.028

36. Edgar RC, Haas BJ, Clemente JC, Quince C, Knight R. UCHIME improves sensitivity and speed of chimera detection. *Bioinformatics.* (2011) 27:2194–200. doi: 10.1093/bioinformatics/btr381

37. Edgar RC. UPARSE: highly accurate OTU sequences from microbial amplicon reads. *Nat Methods.* (2013) 10:996–8. doi: 10.1038/nmeth.2604

38. Sarabhai S, Prabhasankar P. Influence of whey protein concentrate and potato starch on rheological properties and baking performance of Indian water chestnut flour based gluten free cookie dough. *LWT Food Sci Technol.* (2015) 63:1301–8. doi: 10.1016/j.lwt.2015.03.111

39. Colombo A, León AE, Ribotta PD. Rheological and calorimetric properties of corn-, wheat-, and cassava- starches and soybean protein concentrate composites. *Starch Stärke.* (2011) 63:83–95. doi: 10.1002/star.201000095

40. Yang N, Liu Y, Ashton J, Gorczyca E, Kasapis S. Phase behaviour and in vitro hydrolysis of wheat starch in mixture with whey protein. *Food Chem.* (2013) 137:76–82. doi: 10.1016/j.foodchem.2012.10.004

41. Xu C, Markova M, Seebeck N, Loft A, Hornemann S, Gantert T, et al. High-protein diet more effectively reduces hepatic fat than low-protein diet despite lower autophagy and FGF21 levels. *Liver Int.* (2020) 40:2982–97. doi: 10.1111/liv.14596

42. Arslanow A, Teutsch M, Walle H, Grünhage F, Lammert F, Stokes CS. Short-term hypocaloric high-fiber and high-protein diet improves hepatic steatosis assessed by controlled attenuation parameter. *Clin Transl Gastroenterol.* (2016) 7:e176. doi: 10.1038/ctg.2016.28

43. Markova M, Pivovarova O, Hornemann S, Sucher S, Frahnow T, Wegner K, et al. Isocaloric diets high in animal or plant protein reduce liver fat and inflammation in individuals with type 2 diabetes. *Gastroenterology.* (2017) 152:571–85.e8. doi: 10.1053/j.gastro.2016.10.007

44. Bortolotti M, Maiolo E, Corazza M, Van Dijke E, Schneiter P, Boss A, et al. Effects of a whey protein supplementation on intrahepatocellular lipids in obese female patients. *Clin Nutr.* (2011) 30:494–8. doi: 10.1016/j.clnu.2011.01.006

45. Benjaminov O, Beglaibter N, Gindy L, Spivak H, Singer P, Wienberg M, et al. The effect of a low-carbohydrate diet on the nonalcoholic fatty liver in morbidly obese patients before bariatric surgery. *Surg Endosc.* (2007) 21:1423–7. doi: 10.1007/s00464-006-9182-8

46. Chaumontet C, Even PC, Schwarz J, Simonin-Foucault A, Piedcoq J, Fromentin G, et al. High dietary protein decreases fat deposition induced by high-fat and high-sucrose diet in rats. *Br J Nutr.* (2015) 114:1132–42. doi: 10.1017/s000711451500238x

47. Stepien M, Gaudichon C, Fromentin G, Even P, Tomé D, Azzout-Marniche D. Increasing protein at the expense of carbohydrate in the diet down-regulates glucose utilization as glucose sparing effect in rats. *PLoS One.* (2011) 6:e14664. doi: 10.1371/journal.pone.0014664

48. Zhao Y, Zhao MF, Jiang S, Wu J, Liu J, Yuan XW, et al. Liver governs adipose remodelling via extracellular vesicles in response to lipid overload. *Nat Commun.* (2020) 11:719. doi: 10.1038/s41467-020-14450-6

49. Ko CW, Qu J, Black DD, Tso P. Regulation of intestinal lipid metabolism: current concepts and relevance to disease. *Nat Rev Gastroenterol Hepatol.* (2020) 17:169–83. doi: 10.1038/s41575-019-0250-7

50. Huang F, Zheng X, Ma X, Jiang R, Zhou W, Zhou S, et al. Theabrownin from Pu-erh tea attenuates hypercholesterolemia via modulation of gut microbiota and bile acid metabolism. *Nat Commun.* (2019) 10:4971. doi: 10.1038/s41467-019-12896-x

51. Martinez-Guryn K, Hubert N, Frazier K, Urlass S, Musch MW, Ojeda P, et al. Small intestine microbiota regulate host digestive and absorptive adaptive responses to dietary lipids. *Cell Host Microbe.* (2018) 23:458–69.e5. doi: 10.1016/j.chom.2018.03.011

52. Chen C, Yang B, Zeng Z, Yang H, Liu C, Ren J, et al. Genetic dissection of blood lipid traits by integrating genome-wide association study and gene expression profiling in a porcine model. *BMC Genomics.* (2013) 14:848. doi: 10.1186/1471-2164-14-848

53. Jenkins DJ, Thorne MJ, Wolever TM, Jenkins AL, Rao AV, Thompson LU. The effect of starch-protein interaction in wheat on the glycemic response and rate of in vitro digestion. *Am J Clin Nutr.* (1987) 45:946–51. doi: 10.1093/ajcn/45.5.946

54. Baumberger C, Ulevitch RJ, Dayer JM. Modulation of endotoxic activity of lipopolysaccharide by high-density lipoprotein. *Pathobiology.* (1991) 59:378–83. doi: 10.1159/000163681

55. Abd El-Gawad IA, El-Sayed EM, Hafez SA, El-Zeini HM, Saleh FA. The hypocholesterolaemic effect of milk yoghurt and soy-yoghurt containing bifidobacteria in rats fed on a cholesterol-enriched diet. *Int Dairy J.* (2005) 15:37–44. doi: 10.1016/j.idairyj.2004.06.001

56. Santesso N, Akl EA, Bianchi M, Mente A, Mustafa R, Heels-Ansdell D, et al. Effects of higher- versus lower-protein diets on health outcomes: a systematic review and meta-analysis. *Eur J Clin Nutr.* (2012) 66:780–8. doi: 10.1038/ejcn.2012.37

57. Abdel-Maksoud M, Sazonov V, Gutkin SW, Hokanson JE. Effects of modifying triglycerides and triglyceride-rich lipoproteins on cardiovascular outcomes. *J Cardiovasc Pharmacol.* (2008) 51:331–51. doi: 10.1097/FJC.0b013e318165e2e7

58. Chen C, Wang Z, Li J, Li Y, Huang P, Ding X, et al. Dietary vitamin E affects small intestinal histomorphology, digestive enzyme activity, and the expression of nutrient transporters by inhibiting proliferation of intestinal epithelial cells within jejunum in weaned piglets1. *J Anim Sci.* (2019) 97:1212–21. doi: 10.1093/jas/skz023

59. Li J, Yin L, Wang L, Li J, Huang P, Yang H, et al. Effects of vitamin B6 on growth, diarrhea rate, intestinal morphology, function, and inflammatory factors expression in a high-protein diet fed to weaned piglets1. *J Anim Sci.* (2019) 97:4865–74. doi: 10.1093/jas/skz338

60. Wu J, He C, Bu J, Luo Y, Yang S, Ye C, et al. Betaine attenuates LPS-induced downregulation of occludin and claudin-1 and restores intestinal barrier function. *BMC Vet Res.* (2020) 16:75. doi: 10.1186/s12917-020-02298-3

61. Rieger J, Janczyk P, Hünigen H, Neumann K, Plendl J. Intraepithelial lymphocyte numbers and histomorphological parameters in the porcine gut after *Enterococcus faecium* NCIMB 10415 feeding in a *Salmonella Typhimurium* challenge. *Vet Immunol Immunopathol.* (2015) 164:40–50. doi: 10.1016/j.vetimm.2014.12.013

62. Shyer AE, Huycke TR, Lee C, Mahadevan L, Tabin CJ. Bending gradients: how the intestinal stem cell gets its home. *Cell.* (2015) 161:569–80. doi: 10.1016/j.cell.2015.03.041

63. He B, Zhu R, Yang H, Lu Q, Wang W, Song L, et al. Assessing the impact of data preprocessing on analyzing next generation sequencing data. *Front Bioeng Biotechnol.* (2020) 8:817. doi: 10.3389/fbioe.2020.00817

64. Wang KJ, Yan QX, Ren A, Zheng ML, Zhang PH, Tan ZL, et al. Novel linkages between bacterial composition of hindgut and host metabolic responses to sara induced by high-paddy diet in young goats. *Front Vet Sci.* (2022) 8:791482. doi: 10.3389/fvets.2021.791482

65. Chen X, Song P, Fan P, He T, Jacobs D, Levesque CL, et al. Moderate dietary protein restriction optimized gut microbiota and mucosal barrier in growing pig model. *Front Cell Infect Microbiol.* (2018) 8:246. doi: 10.3389/fcimb.2018.00246

66. Canibe N, O'Dea M, Abraham S. Potential relevance of pig gut content transplantation for production and research. *J Anim Sci Biotechnol.* (2019) 10:55. doi: 10.1186/s40104-019-0363-4

67. Kim Y, Hwang SW, Kim S, Lee YS, Kim TY, Lee SH, et al. Dietary cellulose prevents gut inflammation by modulating lipid metabolism and gut microbiota. *Gut Microbes.* (2020) 11:944–61. doi: 10.1080/19490976.2020.1730149

68. Just S, Mondot S, Ecker J, Wegner K, Rath E, Gau L, et al. The gut microbiota drives the impact of bile acids and fat source in diet on mouse metabolism. *Microbiome.* (2018) 6:134. doi: 10.1186/s40168-018-0510-8

69. Kenny DJ, Plichta DR, Shungin D, Koppel N, Hall AB, Fu B, et al. Cholesterol metabolism by uncultured human gut bacteria influences host cholesterol level. *Cell Host Microbe.* (2020) 28:245–57. doi: 10.1016/j.chom.2020.05.013

70. He L, Han M, Farrar S, Ma X. Impacts and regulation of dietary nutrients on gut microbiome and immunity. *Protein Peptide Lett.* (2017) 24:380–1. doi: 10.2174/0929866524051705102147 15

71. Lv LX, Fang DQ, Shi D, Chen DY, Yan R, Zhu YX, et al. Alterations and correlations of the gut microbiome, metabolism and immunity in patients with primary biliary cirrhosis. *Environ Microbiol.* (2016) 18:2272–86. doi: 10.1111/1462-2920.13401

frontiers | Frontiers in Nutrition

TYPE Review
PUBLISHED 01 December 2022
DOI 10.3389/fnut.2022.1008514

OPEN ACCESS

EDITED BY
Hui Han,
Chinese Academy of Sciences (CAS), China

REVIEWED BY
Guangtian Cao,
China Jiliang University, China
Kai Wang,
Chinese Academy of Agricultural Sciences (CAAS), China

*CORRESPONDENCE
Shuai Chen
chenshuai@mail.com

†These authors have contributed equally to this work

SPECIALTY SECTION
This article was submitted to Nutrition and Microbes, a section of the journal Frontiers in Nutrition

RECEIVED 31 July 2022
ACCEPTED 07 November 2022
PUBLISHED 01 December 2022

CITATION
Long J, Wang J, Li Y and Chen S (2022) Gut microbiota in ischemic stroke: Where we stand and challenges ahead. *Front. Nutr.* 9:1008514. doi: 10.3389/fnut.2022.1008514

Gut microbiota in ischemic stroke: Where we stand and challenges ahead

Jiaxin Long[1,2†], Jinlong Wang[1†], Yang Li[1] and Shuai Chen[1*]

[1]Key Laboratory of Systems Health Science of Zhejiang Province, School of Life Science, Hangzhou Institute for Advanced Study, University of Chinese Academy of Sciences, Hangzhou, China, [2]College of Pharmacy, Hunan University of Chinese Medicine, Changsha, China

Gut microbiota is increasingly recognized to affect host health and disease, including ischemic stroke (IS). Here, we systematically review the current understanding linking gut microbiota as well as the associated metabolites to the pathogenesis of IS (e.g., oxidative stress, apoptosis, and neuroinflammation). Of relevance, we highlight that the implications of gut microbiota-dependent intervention could be harnessed in orchestrating IS.

KEYWORDS

gut microbiota, microbial metabolites, ischemic stroke, oxidative stress, inflammation, apoptosis

Introduction

Stroke ranks among the top three fatal diseases in developed countries and has even more lethality in developing countries (1, 2). The stroke is classified to ischemic stroke (IS) and hemorrhagic stroke. The IS is responsible for 87% of stroke (3). Except for population growth and aging, non-negligible risk factors such as high body mass index, environmental particulate pollution, high fasting blood glucose, high systolic blood pressure, alcohol consumption, low physical activity, renal insufficiency, and high temperature also exacerbate the prevalence of IS (4). Clinically, thrombolysis is an early treatment for IS. Recombinant tissue plasminogen activator (rtPA), an effective thrombolytic drug, is the only Food and Drug Administration (FDA)-approved medicine for acute IS. However, the bleeding risk and short treatment window (3–4.5 h after onset) of rtPA limits its clinical use (5). Considering that postischemic neuroprotective therapy can prolong the time window of thrombolytic treatment, it is urgent to develop neuroprotective strategies to protect brain cells from ischemia and reperfusion injury (6–8).

Gut microbiota enables bidirectional communication between the gut and the brain through the "microbial-gut-brain axis", associated with immune, endocrine, and neuromodulatory mechanisms (9, 10). Cytokines and chemokines produced in the brain could be released into the systemic circulation after IS, potentially impacting gut microbiota imbalance. Clinical studies showed that the diversity of gut microbiota in the IS population is significantly reduced, among which *Escherichia*, *Megamonas*, *Bacillus*, *Bifidobacterium*, and *Ruminococcus* are increased significantly, while *Parabacteroides*, *Ekmanella*, *Prevotella*, and *Faecalibacterium* burden are decreased in IS population compared to the healthy people (11, 12).

Likewise, Yamashiro et al. studied the intestinal microbiota of 41 IS patients and 40 healthy people and confirmed the significant differences of gut microbiota between them. In the middle cerebral artery occlusion (MCAO) mouse model, the gut microbiota could cross the intestinal barrier and migrate to various organs through the blood to induce inflammatory responses (13, 14). These findings suggest that gut microbiota might be used as a neuroprotective strategy for IS (15, 16). Interestingly, studies on animal experiments demonstrated that fecal microbiota transplantation from healthy donors could restore the gut microbiota imbalance caused by IS and consequently improved neural function (17). Moreover, gut microbial metabolites were found to regulate the IS process. For example, trimethylamine oxide (TMAO), a metabolite of Gammaproteobacteria, can promote atherosclerosis and cerebral vascular embolism by affecting cholesterol reverse transport and metabolism (18). The immunogenic endotoxin lipopolysaccharide (LPS) may promote neuroinflammation by inducing the migration of peripheral immune cells to the brain (19). Short-chain fatty acids (SCFAs) can reduce the severity of neuroinflammation, protect brain tissue, and reduce neuronal damage in IS patients (17).

This review aims to elucidate the mechanism of gut microbiota in the pathological process of IS and provide new ideas for IS treatment.

IS pathogenesis and microbiota

IS is associated with the interruption of cerebral blood flow induced by thrombotic or embolic occlusion of a cerebral artery. The pathological change of brain cell damage in IS is a dynamic developmental process of complex spatiotemporal cascade reactions in the penumbra area involving oxidative stress, inflammation, and apoptosis (20–22). Acute reduction or deprivation of cerebral blood flow limits glucose and oxygen access to brain tissue, and the limitation of glucose and oxygen reduces adenosine triphosphate (ATP) production and further induces bioenergetic failure, acidotoxicity, and excitotoxicity in brain cells (23). ATP consumption also causes the depolarization of neuronal plasma membrane and dysfunction of ATP-dependent ion pumps, further disrupting sodium, potassium, and calcium (Ca) ionic balance and leading to anoxic depolarization in neurons and glial cells (23, 24). Neuronal cell bioenergetic failure and depolarization lead to cellular sodium and Ca^{2+} accumulation, inducing mitochondria dysfunction and catabolic enzyme activation to promote reactive oxygen species (ROS) and oxidative intermediates generation, resulting in endogenous redox disbalance and oxidative severe stress damage (cell apoptosis and necrosis) (25). Furthermore, complex triggers such as bioenergetic failure, ROS, and cell necrosis initiate brain cell immune response characterized by the activation of glial cells, the infiltration of monocytes/macrophage and leukocytes, and the production of pro-inflammatory cytokines and chemokines (26) (Figure 1).

Numerous studies have reported the role of gut microbiota in oxidative stress, inflammation, and apoptosis (Figure 2), indicating its potential protective effects in IS (27–30).

Oxidative stress and microbiota

Oxidative stress (OS) induced by the excess generation of ROS attacks cellular lipids, proteins, and nucleic acid, causing cell apoptosis, death, or even necrosis (25). OS also promotes the release of cytochrome C (Cytc) and the activation of astrocytes and microglia, inducing early inflammation and cell apoptosis (31). Of note, the transcription factor NF-E2-related factor (Nrf2)/antioxidant response element (ARE) signaling pathway is recognized as the central player in the antioxidant system (32). By binding to its inhibitor Kelch-like epichlorohydrin-associated protein-1 (Keap1) under normal conditions, Nrf2 mainly exists in the cytoplasm as an inactive state but would be rapidly degraded following ubiquitin protease activation, maintaining the regular and low transcriptional activity of Nrf2 (33). When free sulfhydryl groups (i.e., Nrf2 or electrophilic stress sensors) are oxidized by ROS, Nrf2 is activated and translocated into the nucleus to interact with AREs, resulting in the gene expression of phase II antioxidants and detoxification enzymes (Figure 1).

The gut microbiota can affect the ROS level. Both commensal and pathogenic bacteria in the gut can alter intracellular ROS by modulating mitochondrial activity, which may be related to Keap1/Nrf2/ARE signaling pathway (34, 35) (Figure 1). For example, some Lactobacilli can stimulate cells to produce ROS through specific membrane components or secreted factors (36); in addition, LPS from gram-negative bacteria can increase the sensitivity of neurons to OS (37). Indeed, IS and microbiota dysbiosis often occurs simultaneously in patients and animal models (38, 39). Interestingly, ROS generated in IS stimulates IL-6 and other inflammatory factors production by activating the nuclear factor κB (NF-κB) pathway, indirectly increasing the abundance of facultative anaerobic bacteria (mainly Enterobacteriaceae) and promoting microbiota dysbiosis (40, 41). These studies suggest that targeting gut microbiota is an effective method to regulate OS and further prevent IS.

Apoptosis and microbiota

Neurons and glial cells in the penumbra undergo apoptosis in the hours to days following IS (42). Apoptosis is an ATP-dependent programmed cell death characterized by the early degradation of DNA and intact cell membrane without cellular contents efflux. Ca^{2+} overload and mitochondrial dysfunction in IS are the main inducers of neuronal apoptosis, which

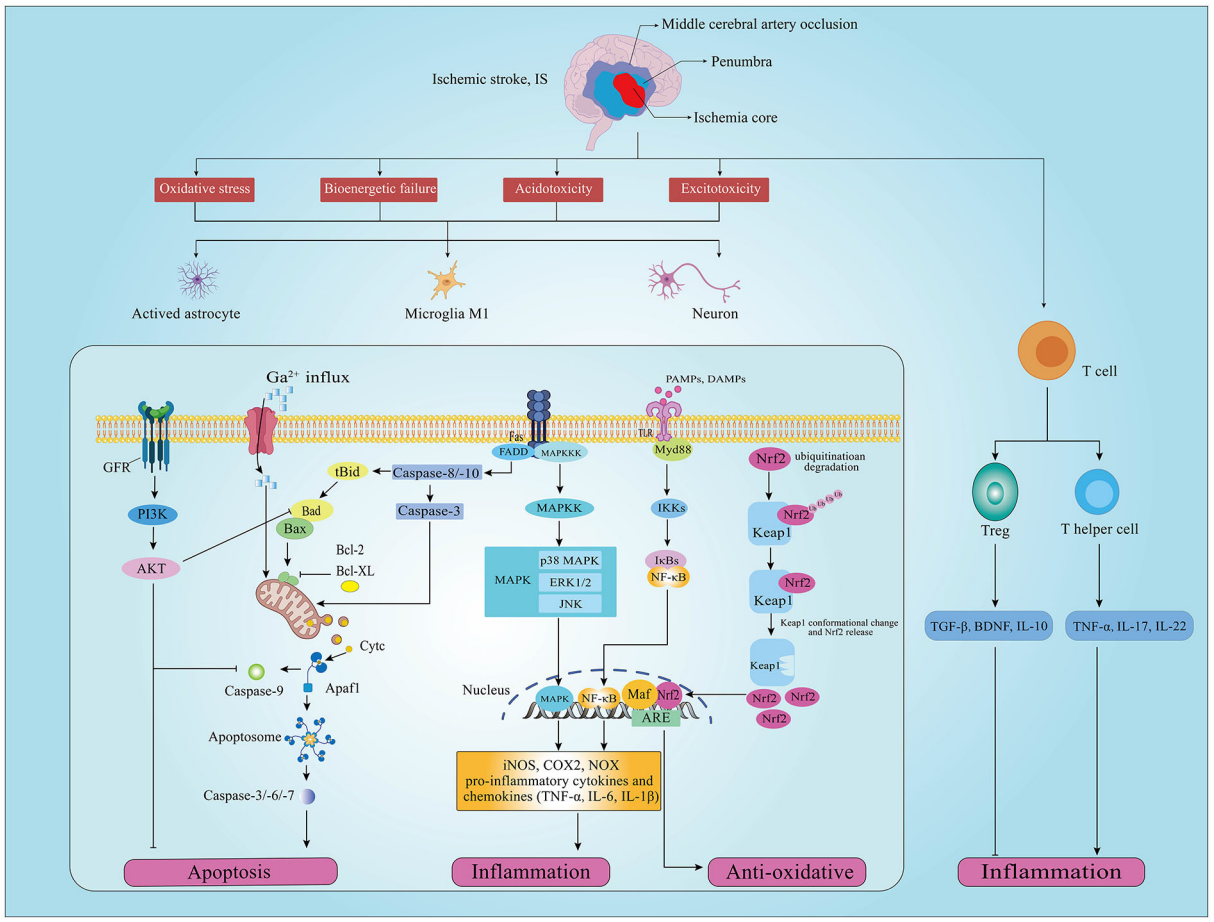

FIGURE 1
Schematic diagram of oxidative stress, apoptosis, and inflammation signaling pathways involved in ischemic stroke (IS). Oxidative stress, inflammation and apoptosis occur in neurons of the penumbra after IS, which are regulated by different upstream pathways. (GFR, growth factor receptor; PI3K, phosphatidylinositol 3-kinase; AKT, protein kinase B; Bad, Bcl2 associated agonist of cell death; Bcl-2, B-cell lymphoma-2; Bcl-XL, B-cell lymphoma-extra large; Bax, Bcl-2-associated X; Cytc, cytochrome c; Apafl, apoptotic protease activating factor-1; TGF-β, transforming growth factor beta; BDNF, brain-derived neurotrophic factor; Keapl, Kelch-like ECH-associated protein 1; Nrf2, nuclear factor E2 related factor 2; Ub, ubiquitination; ARE, adenylate Uridylate-rich element; Maf, macrophage activating factor; TLR4, toll-like receptor 4; Myd88, myeloid differentiation primary response 88; Ikks, I-κB kinase; NF-κB, nuclear factor kappa B; IL-1β, interleukin 1 beta; MAPK, mitogen-activated protein kinases; JNK, c-Jun N-terminal kinase; ERK, extracellular regulated protein kinases; iNOS, inducible NO synthase; COX2, cyclooxygenase 2, COX2; NOX, nitrogen oxide; TNF-α, tumor necrosis factor alpha; Treg, regulatory T cell).

consist of two principal pathways: the endogenous apoptosis (or mitochondrial) pathway and the exogenous apoptosis (or death receptor) pathways (43). The endogenous apoptosis pathway is induced by the release of key apoptosis-related proteins in mitochondria, and the exogenous apoptosis pathway is triggered by the combination of surface death receptors and their ligands (43) (Figure 1).

Apoptosis stimuli such as Ca^{2+} overload and ROS mediate endogenous apoptosis. Excessive Ca^{2+} ions influx at the pre-synaptic terminal causes uncontrolled glutamate release to the synaptic terminal, activating ionotropic N-methyl-d-aspartate receptors (NMDAR) and resulting in Ca^{2+} further influx (44). Abnormal aggregation of Ca^{2+} leads to calpain activation to split the Bcl-2 interaction domain (BID) into truncated BID (tBID), together with caspase-8 cleavage. tBID interacts with the Bad-Bax for opening the mitochondrial transition pore (MTP) and promoting the release of mitochondrial Cytc, endonuclease G, and apoptosis-inducing factors (AIFs) (45, 46). Cytc binds to the apoptotic protease activating factor 1 (Apaf-1) and pro-caspase-9 to form apoptosomes, activating caspase-9 and inducing downstream effector caspase-3. Activation of caspase-3 leads to mitochondrial membrane permeabilization, chromatin condensation, DNA fragmentation, and ultimately cell death (47). Bax, Bad, and BH3 protein polymers can bind on the outer membrane of mitochondria to promote MTP formation, while Bcl-2 family inhibitors could inhibit MTP formation by competitively binding with Bax and Bad (48). The exogenous apoptosis pathway is activated by the binding of cell

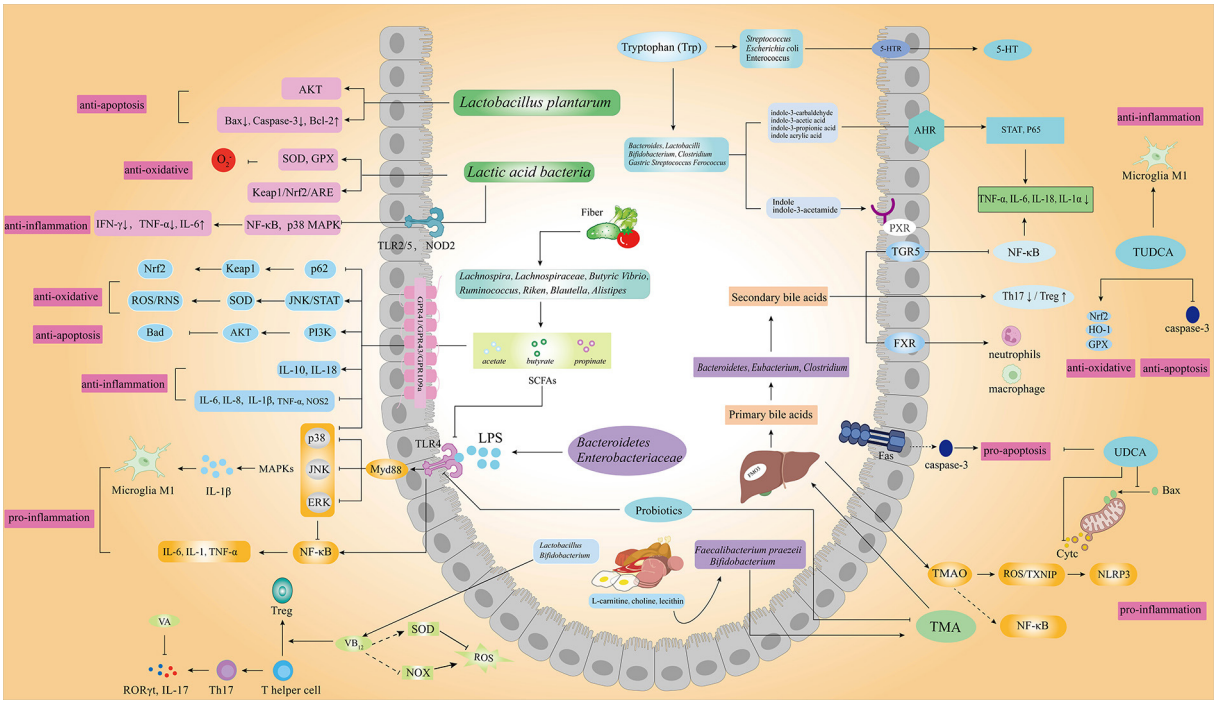

FIGURE 2
Gut microbiota and its metabolic products associated with IS. Gut microbiota and the metabolism of SCFAs, tryptophan, bile acids, TMAO, LPS, and vitamins play important roles in oxidative stress, inflammation, and apoptosis of IS through different signaling pathways. (AKT, protein kinase B; Bax, Bcl2-associated X; Bcl-2, B-cell lymphoma-2; SOD, superoxide dismutase; GPX, glutathione peroxidase; Keapl, kelch-like ECH-associated protein 1; Nrf2, nuclear factor E2 related factor 2; Ub, ubiquitination; ARE, adenylate uridylate-rich element; IFN-γ, interferon gamma; IL-6, interleukin 6; IL-17, interleukin 17; IL-18, interleukin 18; IL-1α, interleukin 1 alpha; Treg, regulatory T cell; Th17, helper T 17 cell; RORγt, retinoic acid related orphan nuclear receptor γt; IL-10, interleukin 10; iNOS, inducible NO synthase; COX2, cyclooxygenase 2; NOX, nitrogen oxide; NOS2, nitric oxide synthase 2; GPR43/GPR41, G protein-coupled receptors 43/41; MAPK, mitogen-activated protein kinases; JNK, c-Jun N-terminal kinase; ERK, extracellular regulated protein kinases; TMA, trimethylamine; TMAO, trimethylamine oxide; TXNIP, thioredoxin-interacting protein; FMO3, flavin-containing monooxygenase 3; FXR, farnesoid X receptor; TNF-α, tumor necrosis factor alpha; PI3K, phosphatidylinositol 3-kinase; STAT, signal transducer and activator of transcription; TUDCA, tauroursodeoxycholic acid; UDCA, ursodeoxycholic acid; HO-1, heme oxygenase-1; PXR, pregnane X receptors; AHR, aryl hydrocarbon receptors; 5-HT, 5-hydroxytryptamine; 5-HTR, 5-hydroxytryptamine receptor).

surface death receptors such as TNF receptor 1 (TNFR-1), Fas receptor (FasR), p75 neurotrophin receptor (p75NTR), and their corresponding ligands (49). The combination of legends, such as TNF-α and Fas ligand (FasL), and death receptors leads to the activation of caspase-8 and caspase-10, which in turn activate downstream effector, finally leading to neuronal death (50, 51). Although reversing the necrotic neurons in the infarcted area is difficult, targeted interfering upstream apoptosis signals is a potential neuroprotective strategy to rescue the damaged neurons (52) (Figure 1).

Gut microbiota is reported to regulate the apoptosis of multiple cells from the intestine, kidney, and brain (53, 54). Liu et al. demonstrated that the intestinal probiotic *Clostridium butyricum* could phosphorylate protein kinase B (AKT) by regulating the protein expression levels of brain-derived neurotrophic factor (BDNF), Bcl-2, and Bax to prevent neuronal apoptosis in cerebral I/R injury diabetic mice (55). SCFAs are found reduced in IS mice model, within which the butyric acid showed the highest negative correlation with IS parameter (56). Ursodeoxycholic acid (UDCA) and taurine deoxycholic acid (TUDCA) could be produced by microbiota and are also reported to play important roles in regulating neuronal apoptosis (57, 58). Collectively, these studies indicate that gut microbiota could be a potential strategy for targeting apoptosis in IS therapy.

Inflammation and microbiota

The activation of inflammatory cells, like microglia, astrocyte, and T cell, is the hallmark of the inflammatory response in IS (59). After IS onset, insufficient oxygen, glucose, and energy production result in the accumulation of some toxic metabolites, such as excitotoxic products, acidic metabolites, and inflammatory mediators, and cause extensive neuron and glial cell death. These dead cells induce innate immune inflammatory

responses by releasing damage-associated molecular patterns (DAMPs) [e.g., ATP, high mobility histone B (HMGB1), and hypoxia-inducible factor 1α (HIF-1α)] (23). Indeed, microglia activation releases danger signals to activate the innate immune response in lesions, promoting tumor necrosis factor-alpha (TNF-α), interleukin-1β (IL-1β), interleukin-6 (IL-6), and other potentially cytotoxic molecules such as prostaglandins, ROS, and nitric oxide (NO) (60). Activated astrocytes also release inflammatory factors, such as inducible nitric oxide synthase (iNOS), cyclooxygenase-2 (COX2), and NADPH oxidase (NOX) (61). Cytokines produced by microglia and astrocytes play critical roles in IS pathology (62). Proinflammatory cytokines (e.g., TNF-α, IL-1β, and IL-6) and chemokines exacerbate brain damage, while anti-inflammatory cytokines [e.g., IL-10 and transforming growth factor beta (TGF-β)] are neuroprotective (63, 64) (Figure 1).

Toll-like receptors (TLRs) expressed in astrocytes and microglias play essential roles in DAMPs/pathogen-associated molecular pattern (PAMPs) recognization and inflammatory responses (65). For example, TLR4 activated by DAMPs through the downstream myeloid differentiation factor 88 (MyD88)-dependent pathway can mediate NF-κB translocation to the nucleus for initiating the transcription of inflammatory cytokines and the following inflammatory response cascades, thereby inducing vascular damage (66). Mitogen-activated protein kinases (MAPKs) is also the critical signaling molecules associated with inflammatory responses by regulating multiple extracellular kinases, including extracellular signal-regulated protein kinase (ERK)1/2, p38MAP Kinase (p38), c-Jun N-terminal kinases (JNK) (67). MAPK signaling pathway affects the balance of pro-inflammatory and anti-inflammatory responses by regulating the production of TNF-α, IL-1, IL-6, and IL-12 (68). Moreover, T cells are recruited to the injured brain tissue within the first days after stroke and play a decisive role in secondary neuroinflammation in IS (69–71). The helper T (Th) cell subpopulations have differential effects on IS outcomes. Pro-inflammatory such as Th1 and Th17 promote inflammatory damage, worsing IS outcomes, whereas regulatory T cells (Tregs) have been shown to suppress an excess neuroinflammatory reaction to brain injury (72, 73) (Figure 1). Therefore, it could effectively alleviate the inflammation injury of IS by targeting the inflammation-related cells and cytokines.

Gut microbiota could affect the central neuron system (CNS) and brain function by interacting with the immune system (74). IS is associated with decreased SCFAs and SCFAs-producing bacteria such as Bacteroidaceae, Ruminococcaceae, and *Faecalibacterium* and also associated with increased fecal valeric acid, which is positively correlated with inflammatory marker levels (e.g., high-sensitivity C-reactive protein and white blood cell counts) (38, 75, 76). Numerous studies have demonstrated gut microbiota is a key regulator of IS-related immune cells (77, 78). For example, *Group B Streptococcus* and *Listeria monocytogenes* could stimulate the differentiation of effector T cell, increase T cell infiltration to the brain, and disrupt the integrity of the blood-brain barrier (BBB), consequently inducing neuroimmune inflammatory responses (79). The gut microbiota is also associated with inflammation-associated mediators. Germ-free (GF) mice recolonized with microbiota from IS mice showed higher IL-17 and IFN-γ expression and Th17 cell infiltration in hemispheres in the context of IS, than those received the health mouse microbiota (15). Moreover, in the experimental IS mouse model, antibiotics-induced "GF" mice show moderate brain injury than those mice with normal microbiota (80). Together, it is reasonable that gut microbiota may be a key target for the effective management and treatment of IS therapy.

Microbiota, microbial metabolites, and IS

Probiotics

Probiotics such as *Lactobacillus*, *Bacillus subtilis*, and *Bifidobacterium* have positive effects on anti-oxidative, immune modulation, and pathogen antagonism (81). Probiotic fermented milk showed significant antioxidant capacity *in vitro* and *vivo* as a dietary source (82, 83). Lactic acid bacteria (LAB) could be autolyzed under stress, such as low pH conditions, and release intracellular antioxidant substances *in vitro* (84). I*n vivo*, LAB like *Lactobacillus plantarum* was reported to have salutary effects against exogenous insults *via* the Nrf2/ARE signaling pathway in mice and drosophila (85). Cheon et al. found that LAB KU200793 in fermented foods showed high antioxidant activity and protected human neuroblastoma cell SH-SY5Y from 1-methyl-4-phenyl pyridine-induced damage (86). The modulatory role of probiotics in immunity and inflammation has long been investigated, although the precise mechanisms are still not fully understood (87, 88).

In terms of apoptosis, Sirin, S. et al. found that *Bulgarian bacterium B3* and *Lactobacillus plantarum GD2* protected amyloid beta-induced mitochondrial dysfunction SH-SY5Y cells from apoptosis (89). *In vivo* experiments showed that probiotic preparations (*Lactobacillus helveticus R0052* and *Bifidobacterium longum R0175*) attenuated LPS-induced apoptosis in rat hippocampus through the gut-brain axis by increasing Bcl-2 and inhibiting Bax and caspase-3 (90). Probiotic cocktail, including bifidobacteria, *lactobacillus*, *laccoccus*, and yeast, showed anti-apoptosis function by activating the AKT signaling pathway of the hippocampus (91). The evidence supports the beneficial effect of probiotics on IS therapy.

Moreover, LAB may trigger natural killer T cells to promote IFN-γ (92) and alleviates intestinal inflammation by regulating the NF-κB and p38 MAPK pathway mediated by TLR2/TLR5 receptors (93) and NOD2 receptors (94). The mechanism might be associated with LAB-secreted

polypeptide, which could inhibit I-κB phosphorylation and the process of NF-κB translocation to the nucleus (95). Studies have also demonstrated the role of microbiota in neuronal function, such as neurogenesis and neuroinflammation (96). Indeed, *Lactobacillus plantarum* showed significant anti-inflammation activity by decreasing IFN-γ, TNF-α, and BBB permeability and increasing IL-10 (97, 98). Other probiotics, such as *Faecalibacterium prausnitzii,* also had anti-inflammatory functions in depression-like and anxiety-like behavior rat model (99) (Figure 2).

Short-chain fatty acids

SCFAs are gut microbiota metabolites that could serve as key signaling molecules in the gut-brain communication (100) and can control neurodevelopment, neurotransmitters, and microglia activation (101, 102). Acetic acid, propionic acid, and butyric acid account for more than 95% of intestinal SCFAs and play important roles in oxidative stress, immune inflammation, and neuronal apoptosis (103). SCFAs, especially butyrate, can regulate oxidative stress. In healthy humans, administration of butyrate at physiological concentrations has been shown to increase the antioxidant glutathione and reduce ROS production (104, 105). Wang et al. showed that sodium butyrate supplementation relieves cerebral ischemia-reperfusion injury *via* increasing superoxide dismutase expression in mice, which was related to the JNK/STAT pathway (106). Also, sodium butyrate could improve brain damage in mice by reducing the oxidative stress of neurons *via* the Keap1/Nrf2/HO-1 pathway (99). Butyrate-producing *Clostridium butyricum* resists oxidative damage by regulating the p62-Keap1-Nrf2 signaling pathway (107).

The regulatory role of SCFAs on cell apoptosis mainly focuses on the intestinal cell (108–110). Some studies reveal the anti-apoptosis role of SCFAs in IS. For example, butyrate was reported against neuronal apoptosis *via* up-regulating histone H3 acetylation, heat shock protein 70 (HSP70), and p-Akt and down-regulating p53 in ischemic brain tissue (111, 112). SCFAs play important roles in regulating neuroinflammation and microglia and could reduce inflammation after IS (113). Oral administration of SCFAs can repair the defective microglia, promote the activation of the anti-inflammatory phenotype of microglia, and increase the expression of tight junction protein to enhance the structural integrity of BBB while reduce the harmful substances invasion of the brain (114, 115). Acetate reduces LPS-induced glial cell activation by activating GPR43 and inhibiting IL-1β expression and MAPK phosphorylation in rats with neuroinflammation (116, 117). Patiala et al. found that sodium butyrate down-regulates pro-inflammatory mediators TNF-α and NOS2 and up-regulates the expression of anti-inflammatory mediator IL-10 in the MCAO mice (118) (Figure 2).

Tryptophan and its derivatives

The level of serum L-Trp in IS patients is increased significantly, suggesting that Trp may be a potential biomarker of IS (119). Wang et al. reported that Trp supplementation affected immunity by regulating the balance of anti-inflammatory cytokines and pro-inflammatory cytokines and signal transducer and activator of transcription 3 (STAT3) and p65 signal transduction (120). 5-hydroxytryptamine (5-HT), the vital metabolite of Trp, serves as the junction of the gut-brain microbiota axis and the suppressor of inflammation (121). Also, Trp can produce indole and indole derivatives (e.g., indole-3-propionic acid), the ligands of pregnane X receptors (PXR) and aryl hydrocarbon receptors (AHR), *via* the gut microbial, such as *Lactobacillus*, *Clostridium,* and *Peptostreptococcus* (122–125). Rothhammer et al. found that indole-3-acetic acid can regulate the inflammatory response of the central nervous system, which might be associated with inhibiting the secretion of pro-inflammatory factors such as TNF-α, IL-1β, and monocyte chemoattractant protein-1 (MCP-1) from macrophages (126, 127). Indole-3-acetaldehyde produced by *Lactobacillus reuteri* can increase the expression level of IL-22 (127) (Figure 2). In conclusion, the function of Trp metabolism for regulating inflammation may provide a therapeutic solution for IS.

Bile acids

BA metabolites are one of the most widely metabolites in host-microbe interactions and may play critical roles in the oxidative stress, apoptosis, and inflammation of IS. Gut microbiota regulates BA synthesis by regulating enzyme Cholesterol 7α-hydroxylase (CYP7A1), CYP7B1, and CYP27A1 and in turn, BA could re-modulate gut microbiota by promoting BA metabolism-microbiota growth and prevent the other microbes (18). For example, *Clostridium* affects the metabolism of BA, inhibits the activation of farnesoid X receptor (FXR), and promotes inflammation (128).

Indeed, a 20-year prospective follow-up study showed decreased BA excretion functioned as an independent risk factor for IS incidence and mortality (129). A clinical study found that total BAs levels were inversely associated with 3-month mortality in patients with acute IS (130). The reason may be partly associated with immunity because the imbalance of Th17/Treg was reported to aggravate IS (131), while BAs could control the host immune response by directly regulating the balance of the Th17/Treg (132, 133). Studies have shown that gut microbiota could affect the occurrence and development of IS *via* metabolizing primary BAs produced by the liver to secondary BAs by *Bacteroides*, *Eubacterium*, and *Clostridium spp*. (134, 135). In recent years, *Nature* has reported that UDCA,

an intestinal bacteria-derived secondary bile acid, showed anti-oxidative activity by reducing the production of ROS and reactive nitrogen production and maintaining the level of GSH (136). UDCA was also reported had an anti-apoptotic activates by maintaining mitochondrial membrane integrity through preventing the transfer of apoptotic Bax from the cytoplasm to mitochondria, the release of Cytc, and the subsequent activation of caspase (57, 137, 138). Furthermore, UDCA could also prevent apoptosis through the Fas-L-induced death receptor pathway (139). TUDCA, a taurine conjugate of UDCA that could pass the BBB (140, 141), was reported to inhibit oxidative stress by enhancing the expression of Nrf2, the antioxidant enzymes heme oxygenase-1(HO-1), and glutathione peroxidase (GPx) (142). TUDCA also plays an anti-inflammatory role by inhibiting the activation of glial cells (143). Rodrigues reported that TUDCA could significantly increase the level of brain bile acid, inhibit mitochondrial swelling and caspase-3 expression, reduce infarct area, and improve neural function (144). Hence, TUDCA showed a neuroprotective effect against apoptosis in the MCAO animal model; the mechanism may be associated with activating PI3K dependent Bad signaling pathway and inhibiting E2F-1/p53/Bax pathway (145–148) (Figure 2). In conclusion, targeting BAs could also be one of the neuroprotective strategies of IS.

Choline metabolites

Choline metabolites mainly include trimethylamine (TMA), dimethylamine, methylamine, dimethylglycine, and other substances. After being absorbed into the blood, TMA is rapidly oxidized to TMAO by liver flavin-containing monooxygenase-3 (FMO-3) or other flavin monooxygenases (FMOs) (149). TMAO could also be produced by microbiota such as *Faecalibacterium praezeii* and *Bifidobacterium* (150). Studies showed that TMAO could accelerate the process of atherosclerosis by enhancing platelet aggregation, inflammation, and oxidative stress (151, 152). Li et al. found that a high concentration of TMAO could promote the expression of TNF-α, IL-1β, and superoxide, inhibit the expression of endothelial nitric oxide synthase (eNOS), and cause vascular inflammation and oxidative stress (153). Mechanistically, TMAO induces oxidative stress and inflammation response *via* the ROS/thioredoxin-interacting protein (TXNIP)/ NOD-, LRR- and pyrin domain-containing protein 3 (NLRP3) signaling pathway (154, 155). Besides, TMAO induces foam cell formation through MAPK/JNK pathway for promoting arterial occlusion (156). Glial scarring and astrogliosis models are widely used to mimic the clinical conditions of the human stroke (157). Recently, it has been demonstrated that TMAO promoted reactive astrogliosis and glial scarring by interacting with the Smad ubiquitination-related factor 2 (Smurf2)/Activity-like kinase 5 (ALK5) pathway, resulting in severer nerve injury after IS (158). Reducing TMAO and its precursor TMA is an important strategy to prevent IS. Some studies have shown that probiotics could reduce plasma TMAO levels and alleviate related diseases. Qiu et al. found *Enterobacter aerogenes* reduced serum TMAO and cecal TMA levels in mice with a high-choline diet (159). And they subsequently found that *Lactobacillus plantarum* could modulate cecal TMA or serum TMAO levels by affecting gut microbiota but not the expression of liver FMO3, which could stimulate the reverse transport of cholesterol against inflammation, finally alleviating atherosclerosis caused by TMAO (160) (Figure 2). These studies indicate promising strategies for preventing and treating IS by reducing the intake of choline-rich diet or using probiotics to inhibit the formation of TMAO.

Lipopolysaccharide

LPS, also known as endotoxin, is present in the outer membrane of Gram-negative bacteria, such as Bacteroidetes and Enterobacteriaceae (161–163). Bacteroides account for approximately 50% of the human gut microbiota (164) and produce a considerable amount of LPS (165, 166). Lehr HA et al. found LPS increased atherosclerosis in hypercholesterolemic and decreased atherosclerosis and plaque in mice lacking TLR4 (167). Clinical research shows that LPS increases the risk of IS, and elevated plasma LPS levels are associated with poorer short-term outcomes of acute IS patients (168). Indeed, LPS significantly increased the infarct volume in MCAO mice, partially *via* TLR4/NF-κB pathway, resulting in the production of pro-inflammatory cytokines such as TNF-α, IL-1, and IL-6 (169). LPS aggravated brain damage, while increasing *Lactobacillus*, *Bifidobacteria,* and butyric acid-producing bacteria were reported to inhibit TLR4 signaling, reduce plasma LPS level, as well as and maintain T cell abundance (for example, reducing Th1 and Th17 cells while increasing Treg cells) (Figure 2).

Vitamins and related compounds

Vitamins, including vitamin A (VA), vitamin B (VB), vitamin K (VK), vitamin H (VH), folic acid, thiamine, and riboflavin, are essential micronutrients that cannot be synthesized in mammals and must be absorbed through the intestine. The gut microbiota is a great source of crucial vitamins. *Lactobacillus* and *Bifidobacterium* are inseparable from VB, VK, and folic acid synthesis (170). VA was reported to regulate intestinal immune response and can maintain gut microbiota homeostasis (171, 172). Studies have shown that VA supplementation can relieve arterial occlusion, which is related to the role of VA in reducing IL-17 and RORγt gene expression and Th17 cells (173, 174). As an essential cofactor for

energy production, VB directly participates in the tricarboxylic acid cycle of cells, promotes ATP production, and provides energy for exercise. VB_{12} is an essential cofactor in amino acid and nucleotide biosynthesis in gut microbiota. It protects against IS by scavenging free radicals to inhibit oxidation-induced damage and resist oxidation neuroinflammation and apoptosis (175, 176). VB_{12} can also change gut immunity by promoting the differentiation of Th cells to Treg, which is crucial in reducing post-stroke neuroinflammation (177). Patients with VB_{12} deficiency showed lower levels of Tregs, while VB_{12} supplementation decreased the inflammatory circulating cytokine profiles (177). Furthermore, VB_{12} promotes SCFA-producing commensal bacteria in the gut (178), indicating it might reduce toxic neuroinflammation after IS by promoting gut SCFA (Figure 2). Therefore, in addition to its potential to prevent IS, VB_{12} is also a therapeutic factor in the acute phase of IS.

Conclusion and future perspectives

In this review, we highlight the role of the gut microbiota and metabolites related to IS. IS results from complex pathophysiological processes, such as oxidative stress, neuroinflammation, and apoptosis. Although several drugs are available to prevent the cascade of events that lead to ischemic injury, limited effective neuroprotective drugs are currently available to improve patient outcomes. In recent years, studies about the relationship between gut microbiota and neurological diseases have become a popular subject, indicating that gut microbiota could also play a vital role in the occurrence, development, and prognosis of IS. Gut microbiota can modulate oxidative stress, inflammation, and apoptosis-related signaling pathways through its constituents (e.g., LPS, peptidoglycan) and metabolites (e.g., SCFAs and BAs). Further, therapies targeting gut microbiota and their metabolites might be promising strategies to prevent or treat IS.

Author contributions

JL wrote the manuscript. JL, JW, and SC designed the review. JW, YL, and SC revised the manuscript. All authors contributed to the article and approved the submitted version.

Funding

This study was supported by the Research Funds of Hangzhou Institute for Advanced Study, University of Chinese Academy of Science (B04006C010006 and B04006C018007).

Conflict of interest

The authors declare that the research was conducted in the absence of any commercial or financial relationships that could be construed as a potential conflict of interest.

Publisher's note

References

1. Collaborators GBDRF. Global burden of 87 risk factors in 204 countries and territories, 1990-2019: a systematic analysis for the Global Burden of Disease Study 2019. *Lancet.* (2020) 396:1223–49. doi: 10.1016/S0140-6736(20)30752-2

2. Krishnamurthi RV, Ikeda T, Feigin VL. Global, regional and country-specific burden of ischaemic stroke, intracerebral haemorrhage and subarachnoid haemorrhage: a systematic analysis of the Global Burden of Disease Study 2017. *Neuroepidemiology.* (2020) 54:171–9. doi: 10.1159/000506396

3. Andrabi SS, Parvez S, Tabassum H. Ischemic stroke and mitochondria: mechanisms and targets. *Protoplasma.* (2020) 257:335–43. doi: 10.1007/s00709-019-01439-2

4. Collaborators GBDV. Five insights from the Global Burden of Disease Study 2019. *Lancet.* (2020) 396:1135–59.

5. Prabhakaran S, Ruff I, Bernstein RA. Acute stroke intervention: a systematic review. *JAMA.* (2015) 313:1451–62. doi: 10.1001/jama.2015.3058

6. Yang Y, Li Q, Ahmad F, Shuaib A. Survival and histological evaluation of therapeutic window of post-ischemia treatment with magnesium sulfate in embolic stroke model of rat. *Neurosci Lett.* (2000) 285:119–22. doi: 10.1016/S0304-3940(00)01048-X

7. Furuichi Y, Katsuta K, Maeda M, Ueyama N, Moriguchi A, Matsuoka N, et al. Neuroprotective action of tacrolimus (FK506) in focal and global cerebral ischemia in rodents: dose dependency, therapeutic time window and long-term efficacy. *Brain Res.* (2003) 965:137–45. doi: 10.1016/S0006-8993(02)04151-3

8. Murata Y, Rosell A, Scannevin RH, Rhodes KJ, Wang X, Lo EH. Extension of the thrombolytic time window with minocycline in experimental stroke. *Stroke.* (2008) 39:3372–7. doi: 10.1161/STROKEAHA.108.514026

9. Bruce-Keller AJ, Salbaum JM, Berthoud HR. Harnessing gut microbes for mental health: getting from here to there. *Biol Psychiatry.* (2018) 83:214–23. doi: 10.1016/j.biopsych.2017.08.014

10. Hooks KB, Konsman JP, O'malley MA. Microbiota-gut-brain research: a critical analysis. *Behav Brain Sci.* (2018) 42:e60. doi: 10.1017/S0140525X18002133

11. Ji W, Zhu Y, Kan P, Cai Y, Wang Z, Wu Z, et al. Analysis of intestinal microbial communities of cerebral infarction and ischemia patients based on high throughput sequencing technology and glucose and lipid metabolism. *Mol Med Rep.* (2017) 16:5413–7. doi: 10.3892/mmr.2017.7227

12. Yamashiro K, Tanaka R, Urabe T, Ueno Y, Yamashiro Y, Nomoto K, et al. Gut dysbiosis is associated with metabolism and systemic inflammation in patients with ischemic stroke. *PLoS ONE.* (2017) 12:e0171521. doi: 10.1371/journal.pone.0171521

13. Caso JR, Hurtado O, Pereira MP, García-Bueno B, Menchén L, Alou L, et al. Colonic bacterial translocation as a possible factor in stress-worsening experimental stroke outcome. *Am J Physiol Regul Integr Comp Physiol.* (2009) 296:R979–985. doi: 10.1152/ajpregu.90825.2008

14. Tascilar N, Irkorucu O, Tascilar O, Comert F, Eroglu O, Bahadir B, et al. Bacterial translocation in experimental stroke: what happens to the gut barrier? *Bratisl Lek Listy.* (2010) 111:194–9.

15. Singh V, Roth S, Llovera G, Sadler R, Garzetti D, Stecher B, et al. Microbiota dysbiosis controls the neuroinflammatory response after stroke. *J Neurosci.* (2016) 36:7428–40. doi: 10.1523/JNEUROSCI.1114-16.2016

16. Spychala MS, Venna VR, Jandzinski M, Doran SJ, Durgan DJ, Ganesh BP, et al. Age-related changes in the gut microbiota influence systemic inflammation and stroke outcome. *Ann Neurol.* (2018) 84:23–36. doi: 10.1002/ana.25250

17. Lee J, D'aigle J, Atadja L, Quaicoe V, Honarpisheh P, Ganesh BP, et al. Gut microbiota-derived short-chain fatty acids promote poststroke recovery in aged mice. *Circ Res.* (2020) 127:453–465. doi: 10.1161/CIRCRESAHA.119.316448

18. Wahlstrom A, Sayin SI, Marschall HU, Backhed F. Intestinal crosstalk between bile acids and microbiota and its impact on host metabolism. *Cell Metab.* (2016) 24:41–50. doi: 10.1016/j.cmet.2016.05.005

19. Lukiw WJ, Cong L, Jaber V, Zhao Y. Microbiome-derived Lipopolysaccharide (LPS) selectively inhibits Neurofilament Light Chain (NF-L) gene expression in Human Neuronal-Glial (HNG) cells in primary culture. *Front Neurosci.* (2018) 12:896. doi: 10.3389/fnins.2018.00896

20. Hachinski V, Donnan GA, Gorelick PB, Hacke W, Cramer SC, Kaste M, et al. Stroke: working toward a prioritized world agenda. *Cerebrovasc Dis.* (2010) 30:127–47. doi: 10.1159/000315099

21. Xu S, Lu J, Shao A, Zhang JH, Zhang J. Glial cells: role of the immune response in ischemic stroke. *Front Immunol.* (2020) 11:294. doi: 10.3389/fimmu.2020.00294

22. Ponsaerts L, Alders L, Schepers M, De Oliveira RMW, Prickaerts J, Vanmierlo T, et al. Neuroinflammation in ischemic stroke: inhibition of cAMP-specific Phosphodiesterases (PDEs) to the rescue. *Biomedicines.* (2021) 9:703. doi: 10.3390/biomedicines9070703

23. Fann DY-W, Lee S-Y, Manzanero S, Chunduri P, Sobey CG, Arumugam TV. Pathogenesis of acute stroke and the role of inflammasomes. *Ageing Res Rev.* (2013) 12:941—66. doi: 10.1016/j.arr.2013.09.004

24. White SH, Brisson CD, Andrew RD. Examining protection from anoxic depolarization by the drugs dibucaine and carbetapentane using whole cell recording from CA1 neurons. *J Neurophysiol.* (2012) 107:2083–95. doi: 10.1152/jn.00701.2011

25. Fukuyama N, Takizawa S, Ishida H, Hoshiai K, Shinohara Y, Nakazawa H. Peroxynitrite formation in focal cerebral ischemia-reperfusion in rats occurs predominantly in the peri-infarct region. *J Cereb Blood Flow Metab.* (1998) 18:123–9. doi: 10.1097/00004647-199802000-00001

26. Qin C, Yang S, Chu Y-H, Zhang H, Pang X-W, Chen L, et al. Correction To: Signaling pathways involved in ischemic stroke: molecular mechanisms and therapeutic interventions. *Signal Transduct Target Ther.* (2022) 7:278. doi: 10.1038/s41392-022-01129-1

27. Marciano F, Vajro P. Oxidative Stress and Gut Microbiota * *Conflict of interest: None. In: *Gastrointestinal Tissue*. Amsterdam: Elsevier (2017).

28. Westfall S, Lomis N, Kahouli I, Dia SY, Singh SP, Prakash S. Microbiome, probiotics and neurodegenerative diseases: deciphering the gut brain axis. *Cell Mol Life Sci CMLS.* (2017) 74:3769–87. doi: 10.1007/s00018-017-2550-9

29. Sun L, Jia H, Li J, Yu M, Yang Y, Tian D, et al. Cecal gut microbiota and metabolites might contribute to the severity of acute myocardial ischemia by impacting the intestinal permeability, oxidative stress, and energy metabolism. *Front Microbiol.* (2019) 10:1745. doi: 10.3389/fmicb.2019.01745

30. Wang K, Wan Z, Ou A, Liang X, Guo X, Zhang Z, et al. Monofloral honey from a medical plant, Prunella Vulgaris, protected against dextran sulfate sodium-induced ulcerative colitis via modulating gut microbial populations in rats. *Food Funct.* (2019) 10:3828–38. doi: 10.1039/C9FO00460B

31. Zhao M, Zhu P, Fujino M, Zhuang J, Guo H, Sheikh I, et al. Oxidative stress in hypoxic-ischemic encephalopathy: molecular mechanisms and therapeutic strategies. *Int J Mol Sci.* (2016) 17. doi: 10.3390/ijms17122078

32. Tu W, Wang H, Li S, Liu Q, Sha H. The anti-inflammatory and anti-oxidant mechanisms of the Keap1/Nrf2/ARE signaling pathway in chronic diseases. *Aging Dis.* (2019) 10:637–51. doi: 10.14336/AD.2018.0513

33. Zenkov NK, Menshchikova EB, Tkachev VO. Keap1/Nrf2/ARE redox-sensitive signaling system as a pharmacological target. *Biochemistry.* (2013) 78:19–36. doi: 10.1134/S0006297913010033

34. Jin W, Wang HD, Hu ZG, Yan W, Chen G, Yin HX. Transcription factor Nrf2 plays a pivotal role in protection against traumatic brain injury-induced acute intestinal mucosal injury in mice. *J Surg Res.* (2009) 157:251–60. doi: 10.1016/j.jss.2008.08.003

35. Zorov DBPlotnikov EY, Silachev DN, Zorova LD, Pevzner IBZorov SD, et al. Microbiota and mitobiota. Putting an equal sign between mitochondria and bacteria. *Biochemistry.* (2014) 79:1017–31. doi: 10.1134/S0006297914100046

36. Jones RM, Mercante JW, Neish AS. Reactive oxygen production induced by the gut microbiota: pharmacotherapeutic implications. *Curr Med Chem.* (2012) 19:1519–29. doi: 10.2174/092986712799828283

37. Cobley JN, Fiorello ML, Bailey DM. 13 reasons why the brain is susceptible to oxidative stress. *Redox Biol.* (2018) 15:490–503. doi: 10.1016/j.redox.2018.01.008

38. Sun H, Gu M, Li Z, Chen X, Zhou J. Gut microbiota dysbiosis in acute ischemic stroke associated with 3-month unfavorable outcome. *Front Neurol.* (2021) 12:799222. doi: 10.3389/fneur.2021.799222

39. Chidambaram SB, Rathipriya AG, Mahalakshmi AM, Sharma S, Hediyal TA, Ray B, et al. The influence of gut dysbiosis in the pathogenesis and management of ischemic stroke. *Cells.* (2022) 11:1239. doi: 10.3390/cells11071239

40. Ershler WB. A gripping reality: oxidative stress, inflammation, and the pathway to frailty. *J Appl Physiol.* (2007) 103:3–5. doi: 10.1152/japplphysiol.00375.2007

41. Winter SE, Lopez CA, Bäumler AJ. The dynamics of gut-associated microbial communities during inflammation. *EMBO Rep.* (2013) 14:319–27. doi: 10.1038/embor.2013.27

42. Uzdensky AB. Apoptosis regulation in the penumbra after ischemic stroke: expression of pro- and antiapoptotic proteins. *Apoptosis.* (2019) 24:687–702. doi: 10.1007/s10495-019-01556-6

43. Sekerdag E, Solaroglu I, Gursoy-Ozdemir Y. Cell death mechanisms in stroke and novel molecular and cellular treatment options. *Curr Neuropharmacol.* (2018) 16:1396–415. doi: 10.2174/1570159X16666180302115544

44. Han Y, Yuan M, Guo YS, Shen XY, Gao ZK, Bi X. Mechanism of endoplasmic reticulum stress in cerebral ischemia. *Front Cell Neurosci.* (2021) 15:704334. doi: 10.3389/fncel.2021.704334

45. Culmsee C, Zhu C, Landshamer S, Becattini B, Wagner E, Pellecchia M, et al. Apoptosis-inducing factor triggered by poly(ADP-ribose) polymerase and Bid mediates neuronal cell death after oxygen-glucose deprivation and focal cerebral ischemia. *J Neurosci.* (2005) 25:10262–72. doi: 10.1523/JNEUROSCI.2818-05.2005

46. Nikoletopoulou V, Markaki M, Palikaras K, Tavernarakis N. Crosstalk between apoptosis, necrosis and autophagy. *Biochim Biophys Acta.* (2013) 1833:3448–59. doi: 10.1016/j.bbamcr.2013.06.001

47. Datta A, Sarmah D, Mounica L, Kaur H, Kesharwani R, Verma G, et al. Cell death pathways in ischemic stroke and targeted pharmacotherapy. *Transl Stroke Res.* (2020) 11:1185–202. doi: 10.1007/s12975-020-00806-z

48. Peña-Blanco A, García-Sáez AJ. Bax, Bak and beyond - mitochondrial performance in apoptosis. *FEBS J.* (2018) 285:416–31. doi: 10.1111/febs.14186

49. Rodríguez-Yáñez M, Castillo J. Role of inflammatory markers in brain ischemia. *Curr Opin Neurol.* (2008) 21:353–7. doi: 10.1097/WCO.0b013e3282ffafbf

50. Namura S, Zhu J, Fink K, Endres M, Srinivasan A, Tomaselli KJ, et al. Activation and cleavage of caspase-3 in apoptosis induced by experimental cerebral ischemia. *J Neurosci.* (1998) 18:3659–68. doi: 10.1523/JNEUROSCI.18-10-03659.1998

51. Kim JY, Barua S, Huang MY, Park J, Yenari MA, Lee JE. Heat shock protein 70 (HSP70) induction: chaperonotherapy for neuroprotection after brain injury. *Cells.* (2020) 9. doi: 10.3390/cells9092020

52. Yuan J. Neuroprotective strategies targeting apoptotic and necrotic cell death for stroke. *Apoptosis.* (2009) 14:469–77. doi: 10.1007/s10495-008-0304-8

53. Chen P, Chen F, Lei J, Wang G, Zhou B. The gut microbiota metabolite Urolithin B improves cognitive deficits by inhibiting Cyt C-mediated apoptosis and promoting the survival of neurons through the PI3K pathway in aging mice. *Front Pharmacol.* (2021) 12:768097. doi: 10.3389/fphar.2021.768097

54. Saiki H, Okano Y, Yasuma T, Toda M, Takeshita A, Abdel-Hamid AM, et al. A microbiome-derived peptide induces apoptosis of cells from different tissues. *Cells.* (2021) 10. doi: 10.3390/cells10112885

55. Liu J, Sun J, Wang F, Yu X, Ling Z, Li H, et al. Neuroprotective effects of clostridium butyricum against vascular dementia in mice via metabolic butyrate. *Biomed Res Int.* (2015) 2015:412946. doi: 10.1155/2015/412946

56. Chen R, Xu Y, Wu P, Zhou H, Lasanajak Y, Fang Y, et al. Transplantation of fecal microbiota rich in short chain fatty acids and butyric acid treat cerebral ischemic stroke by regulating gut microbiota. *Pharmacol Res.* (2019) 148:104403. doi: 10.1016/j.phrs.2019.104403

57. Rodrigues CM, Ma X, Linehan-Stieers C, Fan G, Kren BT, Steer CJ. Ursodeoxycholic acid prevents cytochrome c release in apoptosis by inhibiting mitochondrial membrane depolarization and channel formation. *Cell Death Differ.* (1999) 6:842–54. doi: 10.1038/sj.cdd.4400560

58. Rodrigues CM, Stieers CL, Keene CD, Ma X, Kren BT, Low WC, et al. Tauroursodeoxycholic acid partially prevents apoptosis induced by 3-nitropropionic acid: evidence for a mitochondrial pathway independent of the permeability transition. *J Neurochem.* (2000) 75:2368–79. doi: 10.1046/j.1471-4159.2000.0752368.x

59. Li Q, Barres BA. Microglia and macrophages in brain homeostasis and disease. *Nat Rev Immunol.* (2018) 18:225–42. doi: 10.1038/nri.2017.125

60. Colonna M, Butovsky O. Microglia function in the central nervous system during health and neurodegeneration. *Annu Rev Immunol.* (2017) 35:441–68. doi: 10.1146/annurev-immunol-051116-052358

61. Liu M, Xu Z, Wang L, Zhang L, Liu Y, Cao J, et al. Cottonseed oil alleviates ischemic stroke injury by inhibiting the inflammatory activation of microglia and astrocyte. *J Neuroinflammation.* (2020) 17:270. doi: 10.1186/s12974-020-01946-7

62. Shi K, Tian DC, Li ZG, Ducruet AF, Lawton MT, Shi FD. Global brain inflammation in stroke. *Lancet Neurol.* (2019) 18:1058–66. doi: 10.1016/S1474-4422(19)30078-X

63. Dinarello CA. Overview of the IL-1 family in innate inflammation and acquired immunity. *Immunol Rev.* (2018) 281:8–27. doi: 10.1111/imr.12621

64. Tabares-Guevara JH, Villa-Pulgarin JA, Hernandez JC. Atherosclerosis: immunopathogenesis and strategies for immunotherapy. *Immunotherapy.* (2021) 13:1231–44. doi: 10.2217/imt-2021-0009

65. Fitzgerald KA, Kagan JC. Toll-like receptors and the control of immunity. *Cell.* (2020) 180:1044–66. doi: 10.1016/j.cell.2020.02.041

66. Prakash P, Kulkarni PP, Lentz SR, Chauhan AK. Cellular fibronectin containing extra domain A promotes arterial thrombosis in mice through platelet Toll-like receptor 4. *Blood.* (2015) 125:3164–72. doi: 10.1182/blood-2014-10-608653

67. Jeong JH, Jang S, Jung BJ, Jang KS, Kim BG, Chung DK, et al. Differential immune-stimulatory effects of LTAs from different lactic acid bacteria via MAPK signaling pathway in RAW 264.7 cells. *Immunobiology.* (2015) 220:460–6. doi: 10.1016/j.imbio.2014.11.002

68. Schindler JF, Monahan JB, Smith WG. p38 pathway kinases as anti-inflammatory drug targets. *J Dent Res.* (2007) 86:800–11. doi: 10.1177/154405910708600902

69. Gelderblom M, Leypoldt F, Steinbach K, Behrens D, Choe CU, Siler DA, et al. Temporal and spatial dynamics of cerebral immune cell accumulation in stroke. *Stroke.* (2009) 40:1849–57. doi: 10.1161/STROKEAHA.108.534503

70. Vogelgesang A, May VE, Grunwald U, Bakkeboe M, Langner S, Wallaschofski H, et al. Functional status of peripheral blood T-cells in ischemic stroke patients. *PLoS ONE.* (2010) 5:e8718. doi: 10.1371/journal.pone.0008718

71. Schwartz M, Raposo C. Protective autoimmunity: a unifying model for the immune network involved in CNS repair. *Neuroscientist.* (2014) 20:343–58. doi: 10.1177/1073858413516799

72. Shichita T, Sugiyama Y, Ooboshi H, Sugimori H, Nakagawa R, Takada I, et al. Pivotal role of cerebral interleukin-17-producing gammadeltaT cells in the delayed phase of ischemic brain injury. *Nat Med.* (2009) 15:946–50. doi: 10.1038/nm.1999

73. Gelderblom M, Weymar A, Bernreuther C, Velden J, Arunachalam P, Steinbach K, et al. Neutralization of the IL-17 axis diminishes neutrophil invasion and protects from ischemic stroke. *Blood.* (2012) 120:3793–802. doi: 10.1182/blood-2012-02-412726

74. Stilling RM, Dinan TG, Cryan JF. Microbial genes, brain and behaviour - epigenetic regulation of the gut-brain axis. *Genes Brain Behav.* (2014) 13:69–86. doi: 10.1111/gbb.12109

75. Qadis AQ, Goya S, Yatsu M, Yoshida YU, Ichijo T, Sato S. Effects of a bacteria-based probiotic on subpopulations of peripheral leukocytes and their cytokine mRNA expression in calves. *J Vet Med Sci.* (2014) 76:189–95. doi: 10.1292/jvms.13-0370

76. Tan C, Wu Q, Wang H, Gao X, Xu R, Cui Z, et al. Dysbiosis of gut microbiota and short-chain fatty acids in acute ischemic stroke and the subsequent risk for poor functional outcomes. *JPEN J Parenter Enteral Nutr.* (2021) 45:518–29. doi: 10.1002/jpen.1861

77. Arpaia N, Campbell C, Fan X, Dikiy S, Van Der Veeken J, Deroos P, et al. Metabolites produced by commensal bacteria promote peripheral regulatory T-cell generation. *Nature.* (2013) 504:451–5. doi: 10.1038/nature12726

78. Zhou W, Liesz A, Bauer H, Sommer C, Lahrmann B, Valous N, et al. Postischemic brain infiltration of leukocyte subpopulations differs among murine permanent and transient focal cerebral ischemia models. *Brain Pathol.* (2013) 23:34–44. doi: 10.1111/j.1750-3639.2012.00614.x

79. Logsdon AF, Erickson MA, Rhea EM, Salameh TS, Banks WA. Gut reactions: How the blood-brain barrier connects the microbiome and the brain. *Exp Biol Med.* (2018) 243:159–65. doi: 10.1177/1535370217743766

80. Benakis C, Brea D, Caballero S, Faraco G, Moore J, Murphy M, et al. Commensal microbiota affects ischemic stroke outcome by regulating intestinal γδ T cells. *Nat Med.* (2016) 22:516–23. doi: 10.1038/nm.4068

81. Suez J, Zmora N, Segal E, Elinav E. The pros, cons, and many unknowns of probiotics. *Nat Med.* (2019) 25:716–29. doi: 10.1038/s41591-019-0439-x

82. Sharma R, Kapila R, Kapasiya M, Saliganti V, Dass G, Kapila S. Dietary supplementation of milk fermented with probiotic Lactobacillus fermentum enhances systemic immune response and antioxidant capacity in aging mice. *Nutr Res.* (2014) 34:968–81. doi: 10.1016/j.nutres.2014.09.006

83. Fardet A, Rock E. In vitro and in vivo antioxidant potential of milks, yoghurts, fermented milks and cheeses: a narrative review of evidence. *Nutr Res Rev.* (2018) 31:52–70. doi: 10.1017/S0954422417000191

84. Crow VL, Coolbear T, Gopal PK, Martley FG, Mckay LL, Riepe H. The role of autolysis of lactic acid bacteria in the ripening of cheese. *Int Dairy J.* (1995) 5:855–75. doi: 10.1016/0958-6946(95)00036-4

85. Jones RM, Desai C, Darby TM, Luo L, Wolfarth AA, Scharer CD, et al. Lactobacilli Modulate Epithelial Cytoprotection through the Nrf2 Pathway. *Cell Rep.* (2015) 12:1217–25. doi: 10.1016/j.celrep.2015.07.042

86. Cheon MJ, Lim SM, Lee NK, Paik HD. Probiotic properties and neuroprotective effects of Lactobacillus buchneri KU200793 Isolated from Korean fermented foods. *Int J Mol Sci.* (2020) 21:1227. doi: 10.3390/ijms21041227

87. Doenyas C. Gut microbiota, inflammation, and probiotics on neural development in autism spectrum disorder. *Neuroscience.* (2018) 374:271–86. doi: 10.1016/j.neuroscience.2018.01.060

88. Cristofori F, Dargenio VN, Dargenio C, Miniello VL, Barone M, Francavilla R. Anti-inflammatory and immunomodulatory effects of probiotics in gut inflammation: a door to the body. *Front Immunol.* (2021) 12:578386. doi: 10.3389/fimmu.2021.578386

89. Sirin S, Aslim B. Characterization of lactic acid bacteria derived exopolysaccharides for use as a defined neuroprotective agent against amyloid beta(1-42)-induced apoptosis in SH-SY5Y cells. *Sci Rep.* (2020) 10:8124. doi: 10.1038/s41598-020-65147-1

90. Mohammadi G, Dargahi L, Naserpour T, Mirzanejad Y, Alizadeh SA, Peymani A, et al. Probiotic mixture of Lactobacillus helveticus R0052 and Bifidobacterium longum R0175 attenuates hippocampal apoptosis induced by lipopolysaccharide in rats. *Int Microbiol.* (2019) 22:317–23. doi: 10.1007/s10123-018-00051-3

91. Xu N, Fan W, Zhou X, Liu Y, Ma P, Qi S, et al. Probiotics decrease depressive behaviors induced by constipation via activating the AKT signaling pathway. *Metab Brain Dis.* (2018) 33:1625–33. doi: 10.1007/s11011-018-0269-4

92. Fink LN, Zeuthen LH, Christensen HR, Morandi B, Frokiaer H, Ferlazzo G. Distinct gut-derived lactic acid bacteria elicit divergent dendritic cell-mediated NK cell responses. *Int Immunol.* (2007) 19:1319–27. doi: 10.1093/intimm/dxm103

93. Vizoso Pinto MG, Rodriguez Gómez M, Seifert S, Watzl B, Holzapfel WH, Franz CM. Lactobacilli stimulate the innate immune response and modulate the TLR expression of HT29 intestinal epithelial cells in vitro. *Int J Food Microbiol.* (2009) 133:86–93. doi: 10.1016/j.ijfoodmicro.2009.05.013

94. Macho Fernandez E, Valenti V, Rockel C, Hermann C, Pot B, Boneca IG, et al. Anti-inflammatory capacity of selected lactobacilli in experimental colitis is driven by NOD2-mediated recognition of a specific peptidoglycan-derived muropeptide. *Gut.* (2011) 60:1050–9. doi: 10.1136/gut.2010.232918

95. Chon H, Choi B, Jeong G, Lee E, Lee S. Suppression of proinflammatory cytokine production by specific metabolites of Lactobacillus plantarum 10hk2 via inhibiting NF-κB and p38 MAPK expressions. *Comp Immunol Microbiol Infect Dis.* (2010) 33:e41–49. doi: 10.1016/j.cimid.2009.11.002

96. Sherwin E, Sandhu KV, Dinan TG, Cryan JF. May the force be with you: the light and dark sides of the microbiota–gut–brain axis in neuropsychiatry. *CNS Drugs.* (2016) 30:1019–41. doi: 10.1007/s40263-016-0370-3

97. Dhaliwal J, Singh DP, Singh S, Pinnaka AK, Boparai RK, Bishnoi M, et al. Lactobacillus plantarum MTCC 9510 supplementation protects from chronic unpredictable and sleep deprivation-induced behaviour, biochemical and selected gut microbial aberrations in mice. *J Appl Microbiol.* (2018) 125:257–69. doi: 10.1111/jam.13765

98. Chong Chong HX, Yusoff NAA, Hor YY, Lew LC, Jaafar MH, Choi SB, et al. (2019). Lactobacillus plantarum DR7 alleviates stress and anxiety in adults: a randomised, double-blind, placebo-controlled study. *Benef Microbes.* (2019) 10:355–73. doi: 10.3920/BM2018.0135

99. Hao Z, Wang W, Guo R, Liu H. Faecalibacterium prausnitzii (ATCC 27766) has preventive and therapeutic effects on chronic unpredictable mild stress-induced depression-like and anxiety-like behavior in rats. *Psychoneuroendocrinology.* (2019) 104:132–42. doi: 10.1016/j.psyneuen.2019.02.025

100. O'mahony SM, Clarke G, Borre YE, Dinan TG, Cryan JF. Serotonin, tryptophan metabolism and the brain-gut-microbiome axis. *Behav Brain Res.* (2015) 277:32–48. doi: 10.1016/j.bbr.2014.07.027

101. Yissachar N, Zhou Y, Ung L, Lai NY, Mohan JF, Ehrlicher A, et al. An intestinal organ culture system uncovers a role for the nervous system in microbe-immune crosstalk. *Cell.* (2017) 168:1135–48.e1112. doi: 10.1016/j.cell.2017.02.009

102. Jameson KG, Hsiao EY. Linking the gut microbiota to a brain neurotransmitter. *Trends Neurosci.* (2018) 41:413–4. doi: 10.1016/j.tins.2018.04.001

103. Chambers ES, Morrison DJ, Frost G. Control of appetite and energy intake by SCFA: what are the potential underlying mechanisms? *Proc Nutr Soc.* (2015) 74:328–36. doi: 10.1017/S0029665114001657

104. Hamer HM, Jonkers DM, Bast A, Vanhoutvin SA, Fischer MA, Kodde A, et al. Butyrate modulates oxidative stress in the colonic mucosa of healthy humans. *Clin Nutr.* (2009) 28:88–93. doi: 10.1016/j.clnu.2008.11.002

105. Sacco P, Decleva E, Tentor F, Menegazzi R, Borgogna M, Paoletti S, et al. Butyrate-loaded chitosan/hyaluronan nanoparticles: a suitable tool for sustained inhibition of ROS release by activated neutrophils. *Macromol Biosci.* (2017) 17:1700214. doi: 10.1002/mabi.201700214

106. Wang RX, Li S, Sui X. Sodium butyrate relieves cerebral ischemia-reperfusion injury in mice by inhibiting JNK/STAT pathway. *Eur Rev Med Pharmacol Sci.* (2019) 23:1762–9. doi: 10.26355/eurrev_201902_17138

107. Li H, Shang Z, Liu X, Qiao Y, Wang K, Qiao J. Clostridium butyricum alleviates enterotoxigenic escherichia coli K88-induced oxidative damage through regulating the p62-Keap1-Nrf2 signaling pathway and remodeling the cecal microbial community. *Front Immunol.* (2021) 12:771826. doi: 10.3389/fimmu.2021.771826

108. Tang Y, Chen Y, Jiang H, Nie D. Short-chain fatty acids induced autophagy serves as an adaptive strategy for retarding mitochondria-mediated apoptotic cell death. *Cell Death Differ.* (2011) 18:602–18. doi: 10.1038/cdd.2010.117

109. Donohoe DR, Holley D, Collins LB, Montgomery SA, Whitmore AC, Hillhouse A, et al. A gnotobiotic mouse model demonstrates that dietary fiber protects against colorectal tumorigenesis in a microbiota- and butyrate-dependent manner. *Cancer Discov.* (2014) 4:1387–97. doi: 10.1158/2159-8290.CD-14-0501

110. Tsugawa H, Kabe Y, Kanai A, Sugiura Y, Hida S, Taniguchi S, et al. Short-chain fatty acids bind to apoptosis-associated speck-like protein to activate inflammasome complex to prevent Salmonella infection. *PLoS Biol.* (2020) 18:e3000813. doi: 10.1371/journal.pbio.3000813

111. Li D, Bai X, Jiang Y, Cheng Y. Butyrate alleviates PTZ-induced mitochondrial dysfunction, oxidative stress and neuron apoptosis in mice via Keap1/Nrf2/HO-1 pathway. *Brain Res Bull.* (2021) 168:25–35. doi: 10.1016/j.brainresbull.2020.12.009

112. Zhou Z, Xu N, Matei N, Mcbride DW, Ding Y, Liang H, et al. Sodium butyrate attenuated neuronal apoptosis via GPR41/Gβγ/PI3K/Akt pathway after MCAO in rats. *J Cereb Blood Flow Metab.* (2021) 41:267–81. doi: 10.1177/0271678X20910533

113. Maslowski KM, Vieira AT, Ng A, Kranich J, Sierro F, Yu D, et al. Regulation of inflammatory responses by gut microbiota and chemoattractant receptor GPR43. *Nature.* (2009) 461:1282–6. doi: 10.1038/nature08530

114. Erny D, Hrabe De Angelis AL, Jaitin D, Wieghofer P, Staszewski O, David E, et al. Host microbiota constantly control maturation and function of microglia in the CNS. *Nat Neurosci.* (2015) 18:965–77. doi: 10.1038/nn.4030

115. Garcia-Gutierrez E, Narbad A, Rodríguez JM. Autism spectrum disorder associated with gut microbiota at immune, metabolomic, and neuroactive level. *Front Neurosci.* (2020) 14:578666. doi: 10.3389/fnins.2020.578666

116. Smith MD, Bhatt DP, Geiger JD, Rosenberger TA. Acetate supplementation modulates brain adenosine metabolizing enzymes and adenosine A_2A receptor levels in rats subjected to neuroinflammation. *J Neuroinflammation.* (2014) 11:99. doi: 10.1186/1742-2094-11-99

117. Kobayashi M, Mikami D, Kimura H, Kamiyama K, Morikawa Y, Yokoi S, et al. Short-chain fatty acids, GPR41 and GPR43 ligands, inhibit TNF-α-induced MCP-1 expression by modulating p38 and JNK signaling pathways in human renal cortical epithelial cells. *Biochem Biophys Res Commun.* (2017) 486:499–505. doi: 10.1016/j.bbrc.2017.03.071

118. Patnala R, Arumugam TV, Gupta N, Dheen ST. HDAC inhibitor sodium butyrate-mediated epigenetic regulation enhances neuroprotective function of microglia during ischemic stroke. *Mol Neurobiol.* (2017) 54:6391–411. doi: 10.1007/s12035-016-0149-z

119. Khan A, Shin MS, Jee SH, Park YH. Global metabolomics analysis of serum from humans at risk of thrombotic stroke. *Analyst.* (2020) 145:1695–705. doi: 10.1039/C9AN02032B

120. Wang B, Sun S, Liu M, Chen H, Liu N, Wu Z, et al. Dietary L-tryptophan regulates colonic serotonin homeostasis in mice with dextran sodium sulfate-induced colitis. *J Nutr.* (2020) 150:1966–76. doi: 10.1093/jn/nxaa129

121. Mclean PG, Borman RA, Lee K. 5-HT in the enteric nervous system: gut function and neuropharmacology. *Trends Neurosci.* (2007) 30:9–13. doi: 10.1016/j.tins.2006.11.002

122. Nyangale EP, Mottram DS, Gibson GR. Gut microbial activity, implications for health and disease: the potential role of metabolite analysis. *J Proteome Res.* (2012) 11:5573–85. doi: 10.1021/pr300637d

123. Davila AM, Blachier F, Gotteland M, Andriamihaja M, Benetti PH, Sanz Y, et al. Intestinal luminal nitrogen metabolism: role of the gut microbiota and consequences for the host. *Pharmacol Res.* (2013) 68:95–107. doi: 10.1016/j.phrs.2012.11.005

124. Marsland BJ. Regulating inflammation with microbial metabolites. *Nat Med.* (2016) 22:581–3. doi: 10.1038/nm.4117

125. Dodd D, Spitzer MH, Van Treuren W, Merrill BD, Hryckowian AJ, Higginbottom SK, et al. A gut bacterial pathway metabolizes aromatic amino acids into nine circulating metabolites. *Nature.* (2017) 551:648–52. doi: 10.1038/nature24661

126. Rothhammer V, Mascanfroni ID, Bunse L, Takenaka MC, Kenison JE, Mayo L, et al. Type I interferons and microbial metabolites of tryptophan modulate astrocyte activity and central nervous system inflammation via the aryl hydrocarbon receptor. *Nat Med.* (2016) 22:586–97. doi: 10.1038/nm.4106

127. Nicolas GR, Chang PV. Deciphering the chemical lexicon of host-gut microbiota interactions. *Trends Pharmacol Sci.* (2019) 40:430–45. doi: 10.1016/j.tips.2019.04.006

128. Theriot CM, Bowman AA, Young VB. Antibiotic-induced alterations of the gut microbiota alter secondary bile acid production and allow for clostridium difficile spore germination and outgrowth in the large intestine. *mSphere.* (2016) 1. doi: 10.1128/mSphere.00045-15

129. Charach G, Karniel E, Novikov I, Galin L, Vons S, Grosskopf I, et al. Reduced bile acid excretion is an independent risk factor for stroke and mortality: a prospective follow-up study. *Atherosclerosis.* (2020) 293:79–85. doi: 10.1016/j.atherosclerosis.2019.12.010

130. Huang L, Xu G, Zhang R, Wang Y, Ji J, Long F, et al. Increased admission serum total bile acids can be associated with decreased 3-month mortality in patients with acute ischemic stroke. *Lipids Health Dis.* (2022) 21:15. doi: 10.1186/s12944-021-01620-8

131. Deng P, Wang L, Zhang Q, Chen S, Zhang Y, Xu H, et al. Therapeutic potential of a combination of electroacupuncture and human iPSC-derived small extracellular vesicles for ischemic stroke. *Cells.* (2022) 11:820. doi: 10.3390/cells11050820

132. Hang S, Paik D, Yao L, Kim E, Trinath J, Lu J, et al. Bile acid metabolites control T(H)17 and T(reg) cell differentiation. *Nature.* (2019) 576:143–8. doi: 10.1038/s41586-019-1785-z

133. Paik D, Yao L, Zhang Y, Bae S, D'agostino GD, Zhang M, et al. Human gut bacteria produce T_H17-modulating bile acid metabolites. *Nature.* (2022) 603:907–12. doi: 10.1038/s41586-022-04480-z

134. Franco P, Porru E, Fiori J, Gioiello A, Cerra B, Roda G, et al. Identification and quantification of oxo-bile acids in human faeces with liquid chromatography-mass spectrometry: a potent tool for human gut acidic sterolbiome studies. *J Chromatogr A.* (2019) 1585:70–81. doi: 10.1016/j.chroma.2018.11.038

135. Guzior DV, Quinn RA. Review: microbial transformations of human bile acids. *Microbiome.* (2021) 9:140. doi: 10.1186/s40168-021-01101-1

136. Chun HS, Low WC. Ursodeoxycholic acid suppresses mitochondria-dependent programmed cell death induced by sodium nitroprusside in SH-SY5Y cells. *Toxicology.* (2012) 292:105–12. doi: 10.1016/j.tox.2011.11.020

137. Rodrigues CM, Fan G, Ma X, Kren BT, Steer CJ. A novel role for ursodeoxycholic acid in inhibiting apoptosis by modulating mitochondrial membrane perturbation. *J Clin Invest.* (1998) 101:2790–9. doi: 10.1172/JCI1325

138. Rodrigues CM, Fan G, Wong PY, Kren BT, Steer CJ. Ursodeoxycholic acid may inhibit deoxycholic acid-induced apoptosis by modulating mitochondrial

transmembrane potential and reactive oxygen species production. *Mol Med.* (1998) 4:165–78. doi: 10.1007/BF03401914

139. Azzaroli F, Mehal W, Soroka CJ, Wang L, Lee J, Crispe IN, et al. Ursodeoxycholic acid diminishes Fas-ligand-induced apoptosis in mouse hepatocytes. *Hepatology.* (2002) 36:49–54. doi: 10.1053/jhep.2002.34511

140. Cortez L, Sim V. The therapeutic potential of chemical chaperones in protein folding diseases. *Prion.* (2014) 8:197–202. doi: 10.4161/pri.28938

141. Vang S, Longley K, Steer CJ, Low WC. The unexpected uses of Urso- and tauroursodeoxycholic acid in the treatment of non-liver diseases. *Glob Adv Health Med.* (2014) 3:58–69. doi: 10.7453/gahmj.2014.017

142. Yanguas-Casás N, Barreda-Manso MA, Nieto-Sampedro M, Romero-Ramírez L. TUDCA: an agonist of the bile acid receptor GPBAR1/TGR5 with anti-inflammatory effects in microglial cells. *J Cell Physiol.* (2017) 232:2231–45. doi: 10.1002/jcp.25742

143. Yanguas-Casás N, Barreda-Manso MA, Nieto-Sampedro M, Romero-Ramírez L. Tauroursodeoxycholic acid reduces glial cell activation in an animal model of acute neuroinflammation. *J Neuroinflammation.* (2014) 11:50. doi: 10.1186/1742-2094-11-50

144. Rodrigues CM, Spellman SR, Solá S, Grande AWLinehan-Stieers C, Low WC, et al. Neuroprotection by a bile acid in an acute stroke model in the rat. *J Cereb Blood Flow Metab.* (2002) 22:463–71. doi: 10.1097/00004647-200204000-00010

145. Sola S, Castro RE, Laires PA, Steer CJ, Rodrigues CM. Tauroursodeoxycholic acid prevents amyloid-beta peptide-induced neuronal death via a phosphatidylinositol 3-kinase-dependent signaling pathway. *Mol Med.* (2003) 9:226–34. doi: 10.2119/2003-00042.Rodrigues

146. Castro RE, Sola S, Ramalho RM, Steer CJ, Rodrigues CM. The bile acid tauroursodeoxycholic acid modulates phosphorylation and translocation of bad via phosphatidylinositol 3-kinase in glutamate-induced apoptosis of rat cortical neurons. *J Pharmacol Exp Ther.* (2004) 311:845–52. doi: 10.1124/jpet.104.070532

147. Ramalho RM, Ribeiro PS, Sola S, Castro RE, Steer CJ, Rodrigues CM. Inhibition of the E2F-1/p53/Bax pathway by tauroursodeoxycholic acid in amyloid beta-peptide-induced apoptosis of PC12 cells. *J Neurochem.* (2004) 90:567–75. doi: 10.1111/j.1471-4159.2004.02517.x

148. Kusaczuk M. Tauroursodeoxycholate-bile acid with chaperoning activity: molecular and cellular effects and therapeutic perspectives. *Cells.* (2019) 8:1471. doi: 10.3390/cells8121471

149. Schugar RC, Willard B, Wang Z, Brown JM. Postprandial gut microbiota-driven choline metabolism links dietary cues to adipose tissue dysfunction. *Adipocyte.* (2018) 7:49–56. doi: 10.1080/21623945.2017.1398295

150. Nicholson JK, Holmes E, Kinross J, Burcelin R, Gibson G, Jia W, et al. Host-gut microbiota metabolic interactions. *Science.* (2012) 336:1262–7. doi: 10.1126/science.1223813

151. Zhu W, Gregory JC, Org E, Buffa JA, Gupta N, Wang Z, et al. Gut microbial metabolite TMAO enhances platelet hyperreactivity and thrombosis risk. *Cell.* (2016) 165:111–24. doi: 10.1016/j.cell.2016.02.011

152. Zhu W, Wang Z, Tang WHW, Hazen SL. Gut microbe-generated trimethylamine N-Oxide from dietary choline is prothrombotic in subjects. *Circulation.* (2017) 135:1671–3. doi: 10.1161/CIRCULATIONAHA.116.025338

153. Li T, Chen Y, Gua C, Li X. Elevated circulating trimethylamine N-Oxide levels contribute to endothelial dysfunction in aged rats through vascular inflammation and oxidative stress. *Front Physiol.* (2017) 8:350. doi: 10.3389/fphys.2017.00350

154. Ding C, Zhao Y, Shi X, Zhang N, Zu G, Li Z, et al. New insights into salvianolic acid A action: Regulation of the TXNIP/NLRP3 and TXNIP/ChREBP pathways ameliorates HFD-induced NAFLD in rats. *Sci Rep.* (2016) 6:28734. doi: 10.1038/srep28734

155. Paramel Varghese G, Folkersen L, Strawbridge RJ, Halvorsen B, Yndestad A, Ranheim T, et al. NLRP3 inflammasome expression and activation in human atherosclerosis. *J Am Heart Assoc.* (2016) 5:e003031. doi: 10.1161/JAHA.115.003031

156. Geng J, Yang C, Wang B, Zhang X, Hu T, Gu Y, et al. Trimethylamine N-oxide promotes atherosclerosis via CD36-dependent MAPK/JNK pathway. *Biomed Pharmacother.* (2018) 97:941–7. doi: 10.1016/j.biopha.2017.11.016

157. Hermann DM, Popa-Wagner A, Kleinschnitz C, Doeppner TR. Animal models of ischemic stroke and their impact on drug discovery. *Expert Opin Drug Discov.* (2019) 14:315–26. doi: 10.1080/17460441.2019.1573984

158. Su H, Fan S, Zhang L, Qi H. TMAO aggregates neurological damage following ischemic stroke by promoting reactive astrocytosis and glial scar formation via the Smurf2/ALK5 axis. *Front Cell Neurosci.* (2021) 15:569424. doi: 10.3389/fncel.2021.569424

159. Qiu L, Yang D, Tao X, Yu J, Xiong H, Wei H. Enterobacter aerogenes ZDY01 attenuates choline-induced trimethylamine N-Oxide levels by remodeling gut microbiota in mice. *J Microbiol Biotechnol.* (2017) 27:1491–9. doi: 10.4014/jmb.1703.03039

160. Qiu L, Tao X, Xiong H, Yu J, Wei H. Lactobacillus plantarum ZDY04 exhibits a strain-specific property of lowering TMAO via the modulation of gut microbiota in mice. *Food Funct.* (2018) 9:4299–309. doi: 10.1039/C8FO00349A

161. Lindberg AA, Weintraub A, Zähringer U, Rietschel ET. Structure-activity relationships in lipopolysaccharides of Bacteroides fragilis. *Rev Infect Dis.* (1990) 12 Suppl 2:S133–141. doi: 10.1093/clinids/12.Supplement_2.S133

162. Weiss J. Bactericidal/permeability-increasing protein (BPI) and lipopolysaccharide-binding protein (LBP): structure, function and regulation in host defence against Gram-negative bacteria. *Biochem Soc Trans.* (2003) 31:785–90. doi: 10.1042/bst0310785

163. Siebler J, Galle PR, Weber MM. The gut-liver-axis: endotoxemia, inflammation, insulin resistance and NASH. *J Hepatol.* (2008) 48:1032–4. doi: 10.1016/j.jhep.2008.03.007

164. Wu GD, Compher C, Chen EZ, Smith SA, Shah RD, Bittinger K, et al. Comparative metabolomics in vegans and omnivores reveal constraints on diet-dependent gut microbiota metabolite production. *Gut.* (2016) 65:63–72. doi: 10.1136/gutjnl-2014-308209

165. Quigley EMM. Microbiota-brain-gut axis and neurodegenerative diseases. *Curr Neurol Neurosci Rep.* (2017) 17:94. doi: 10.1007/s11910-017-0802-6

166. Zhao Y, Jaber V, Lukiw WJ. Secretory products of the human GI tract microbiome and their potential impact on Alzheimer's disease (AD): detection of lipopolysaccharide (LPS) in AD hippocampus. *Front Cell Infect Microbiol.* (2017) 7:318. doi: 10.3389/fcimb.2017.00318

167. Lehr HA, Sagban TA, Ihling C, Zähringer U, Hungerer KD, Blumrich M, et al. Immunopathogenesis of atherosclerosis: endotoxin accelerates atherosclerosis in rabbits on hypercholesterolemic diet. *Circulation.* (2001) 104:914–20. doi: 10.1161/hc3401.093153

168. Klimiec E, Pera J, Chrzanowska-Wasko J, Golenia A, Slowik A, Dziedzic T. Plasma endotoxin activity rises during ischemic stroke and is associated with worse short-term outcome. *J Neuroimmunol.* (2016) 297:76–80. doi: 10.1016/j.jneuroim.2016.05.006

169. Doll DN, Engler-Chiurazzi EB, Lewis SE, Hu H, Kerr AE, Ren X, et al. Lipopolysaccharide exacerbates infarct size and results in worsened post-stroke behavioral outcomes. *Behav Brain Funct.* (2015) 11:32. doi: 10.1186/s12993-015-0077-5

170. Engevik MA, Morra CN, Röth D, Engevik K, Spinler JK, Devaraj S, et al. Microbial metabolic capacity for intestinal folate production and modulation of host folate receptors. *Front Microbiol.* (2019) 10:2305. doi: 10.3389/fmicb.2019.02305

171. Cantorna MT, Snyder L, Arora J. Vitamin A and vitamin D regulate the microbial complexity, barrier function, and the mucosal immune responses to ensure intestinal homeostasis. *Crit Rev Biochem Mol Biol.* (2019) 54:184–92. doi: 10.1080/10409238.2019.1611734

172. Pham VT, Dold S, Rehman A, Bird JK, Steinert RE. Vitamins, the gut microbiome and gastrointestinal health in humans. *Nutr Res.* (2021) 95:35–53. doi: 10.1016/j.nutres.2021.09.001

173. Mohammadzadeh Honarvar N, Harirchian MH, Koohdani F, Siassi F, Abdolahi M, Bitarafan S, et al. The effect of vitamin A supplementation on retinoic acid-related orphan receptor γt (RORγt) and interleukin-17 (IL-17) gene expression in Avonex-treated multiple sclerotic patients. *J Mol Neurosci.* (2013) 51:749–53. doi: 10.1007/s12031-013-0058-9

174. Mottaghi A, Ebrahimof S, Angoorani P, Saboor-Yaraghi AA. Vitamin A supplementation reduces IL-17 and RORc gene expression in atherosclerotic patients. *Scand J Immunol.* (2014) 80:151–7. doi: 10.1111/sji.12190

175. Spence JD, Bang H, Chambless LE, Stampfer MJ. Vitamin intervention for stroke prevention trial: an efficacy analysis. *Stroke.* (2005) 36:2404–9. doi: 10.1161/01.STR.0000185929.38534.f3

176. De Queiroz KB, Cavalcante-Silva V, Lopes FL, Rocha GA, D'almeida V, Coimbra RS. Vitamin B(12) is neuroprotective in experimental pneumococcal meningitis through modulation of hippocampal DNA methylation. *J Neuroinflammation.* (2020) 17:96. doi: 10.1186/s12974-020-01763-y

177. Boran P, Yildirim S, Karakoc-Aydiner E, Ogulur I, Ozen A, Haklar G, et al. Vitamin B12 deficiency among asymptomatic healthy infants: its impact on the immune system. *Minerva Pediatr.* (2021) 73:59–66. doi: 10.23736/S2724-5276.16.04274-X

178. Kasubuchi M, Hasegawa S, Hiramatsu T, Ichimura A, Kimura I. Dietary gut microbial metabolites, short-chain fatty acids, and host metabolic regulation. *Nutrients.* (2015) 7:2839–49. doi: 10.3390/nu7042839

Frontiers in Nutrition

Explores what and how we eat in the context of health, sustainability and 21st century food science

A multidisciplinary journal that integrates research on dietary behavior, agronomy and 21st century food science with a focus on human health.

Discover the latest Research Topics

See more →

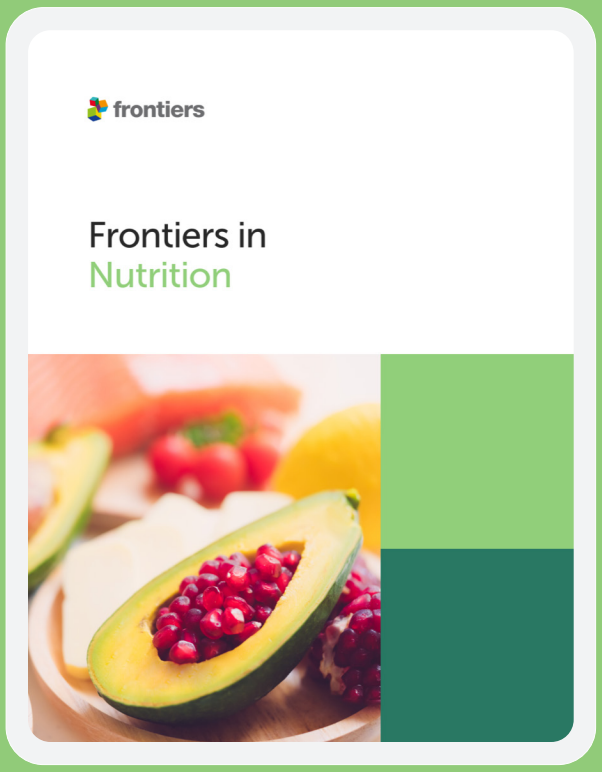

Frontiers

Avenue du Tribunal-Fédéral 34
1005 Lausanne, Switzerland
frontiersin.org

Contact us

+41 (0)21 510 17 00
frontiersin.org/about/contact